

Case Studies of Liquefaction and Lifeline Performance During Past Earthquakes

Volume 1
Japanese Case Studies

Edited by
M. Hamada and T. D. O'Rourke

Technical Report NCEER-92-0001

February 17, 1992

This research was partially supported by the National Science Foundation under Grant No. BCS 90-25010 and the New York State Science and Technology Foundation under Grant No. NEC-91029.



REPORT DOCUMENTATION PAGE	1. REPORT NO. NCEER-92-0001	2.	3. PB92-197243
4. Title and Subtitle Case Studies of Liquefaction and Lifeline Performance During Past Earthquakes - Volume 1 - Japanese Case Studies		5. Report Date February 17, 1992	
7. Author(s) M. Hamada and T.D. O'Rourke		6.	
9. Performing Organization Name and Address		8. Performing Organization Report No.	
		10. Project/Task/Work Unit No.	
		11. Contract(C) or Grant(G) No. (C) BCS 90-25010 (G) NEC-91029	
12. Sponsoring Organization Name and Address National Center for Earthquake Engineering Research State University of New York at Buffalo Red Jacket Quadrangle Buffalo, N.Y. 14261		13. Type of Report & Period Covered Technical Report	
15. Supplementary Notes This research was partially supported by the National Science Foundation under Grant No. BCS 90-25010 and the New York State Science and Technology Foundation under Grant No. NEC-91029.		14.	
16. Abstract (Limit: 200 words) This volume is part of a two-volume compilation of case studies focusing on large, earthquake-induced ground deformations and their effects on lifeline facilities. The two-volume set represents cooperative efforts between the United States and Japan to pool resources, establish a comprehensive database and effect mutual improvement of analytical, experimental, and design methods for lifeline systems. This volume concentrates on earthquake-induced ground deformation in Japan, and consists of case histories of the: 1) 1923 Kanto earthquake, 2) 1948 Fukui earthquake, 3) 1964 Niigata earthquake, 4) 1983 Nihonkai-Chubu earthquake, and 5) 1990 Luzon, Philippines earthquake. These particular earthquakes were chosen because they provide accurate records of permanent ground deformations and their effects upon lifelines, and also because these earthquakes gave rise to extensive investigations into local soil conditions, especially subsurface conditions.			
17. Document Analysis a. Descriptors			
b. Identifiers/Open-Ended Terms EARTHQUAKE ENGINEERING. JAPAN. LIFELINES. SEISMIC PERFORMANCE. GROUND DEFORMATION. CASE STUDIES. GROUND FAILURE. KANTO, JAPAN EARTHQUAKE, SEPTEMBER 1, 1923. FUKUI, JAPAN EARTHQUAKE, JUNE 28, 1948. NIIGATA, JAPAN EARTHQUAKE, JUNE 16, 1964. NIHONKAI-CHUBU, JAPAN EARTHQUAKE, MAY 26, 1983. LUZON, PHILIPPINES EARTHQUAKE, JULY 16, 1990.			
18. Availability Statement Release Unlimited		19. Security Class (This Report) Unclassified	21. No. of Pages: 426
		20. Security Class (This Page) Unclassified	22. Price





**Case Studies of Liquefaction
and Lifeline Performance
During Past Earthquakes**

Volume 1

Japanese Case Studies

Edited by

M. Hamada¹ and T. O'Rourke²

February 17, 1992

Technical Report NCEER-92-0001

NCEER Project Number 90-0038

NSF Master Contract Number BCS 90-25010

and

NYSSTF Grant Number NEC-91029

- 1 Professor, School of Marine Science and Technology, Tokai University, Shimizu, Shizuoka, Japan
- 2 Professor, School of Civil and Environmental Engineering, Cornell University, Ithaca, New York

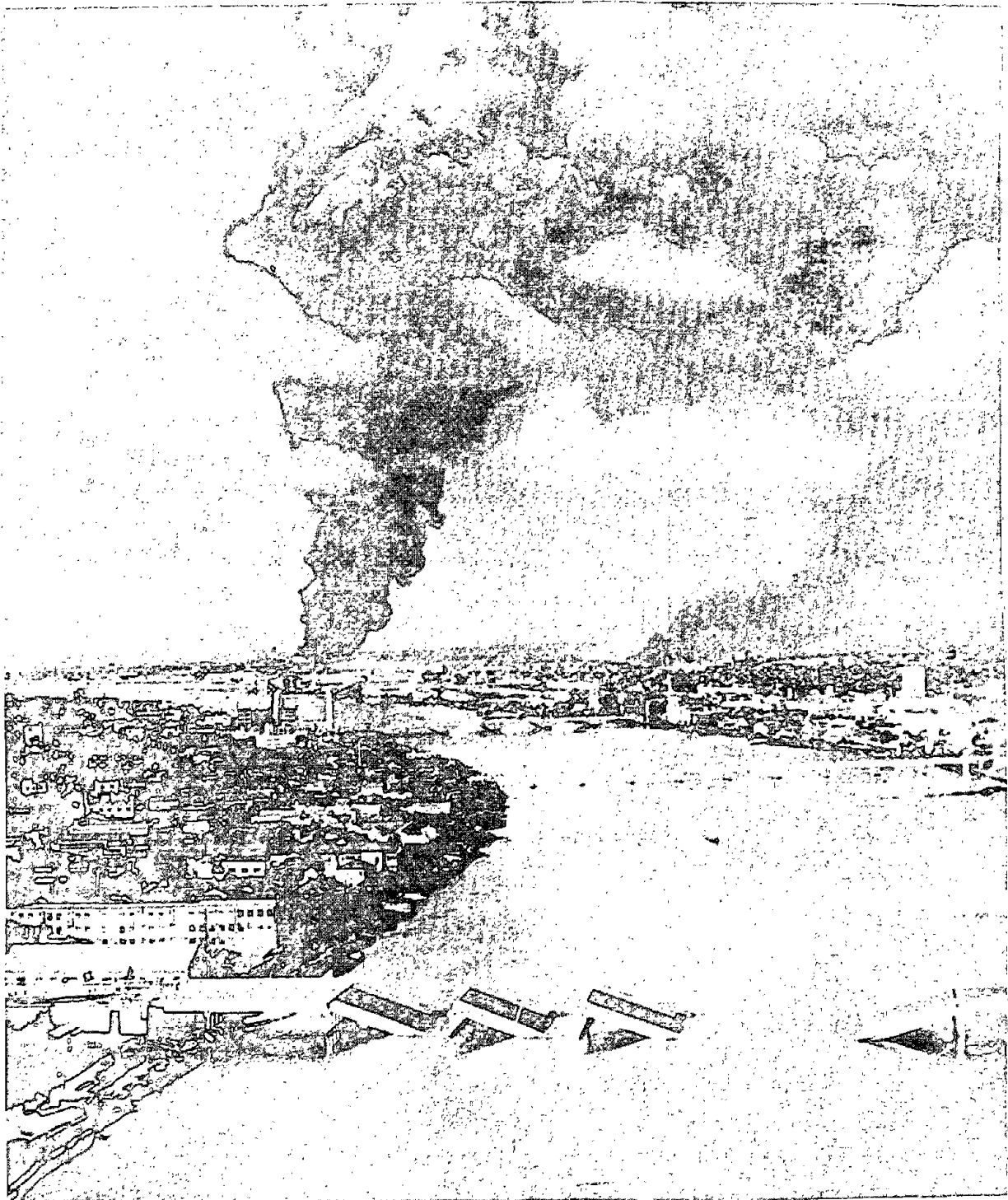
NATIONAL CENTER FOR EARTHQUAKE ENGINEERING RESEARCH
State University of New York at Buffalo
Red Jacket Quadrangle, Buffalo, NY 14261

NOTICE

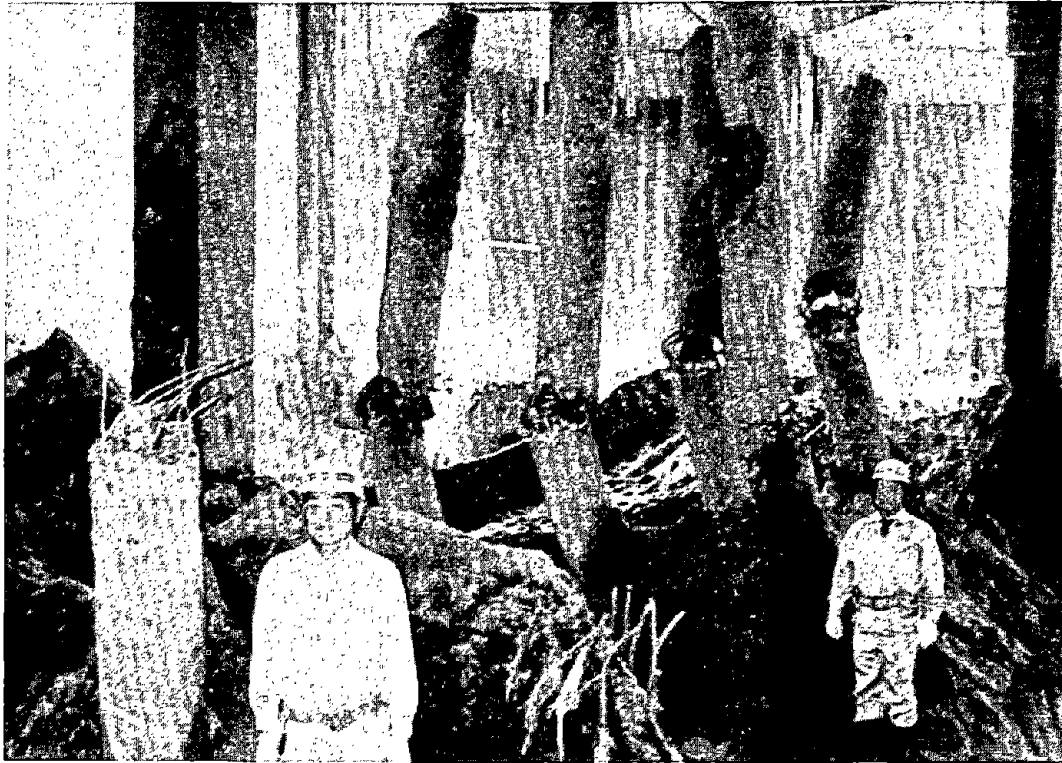
This report was prepared under the auspices of the National Center for Earthquake Engineering Research (NCEER) through grants from the National Science Foundation, the New York State Science and Technology Foundation, and other sponsors. Neither NCEER, associates of NCEER, its sponsors, nor any person acting on their behalf:

- a. makes any warranty, express or implied, with respect to the use of any information, apparatus, method, or process disclosed in this report or that such use may not infringe upon privately owned rights; or
- b. assumes any liabilities of whatsoever kind with respect to the use of, or the damage resulting from the use of, any information, apparatus, method, or process disclosed in this report.

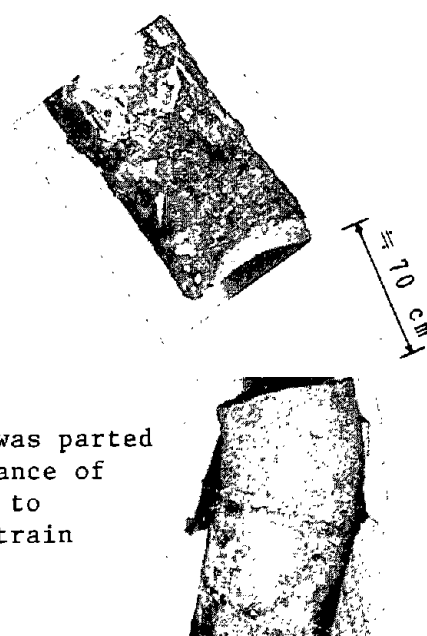
Any opinions, findings, and conclusions or recommendations expressed in this publication are those of the author(s) and do not necessarily reflect the views of NCEER, the National Science Foundation, the New York State Science and Technology Foundation, or other sponsors.



Niigata City suffered severe damage from soil liquefaction during the 1964 earthquake. The Showa Bridge, which had been completed only 3 months prior to the earthquake, collapsed due to liquefaction in the river bed. A number of lifeline facilities, buildings, quaywalls, and oil storage tanks were extensively damaged.



Reinforced concrete piles with a diameter of 35 cm were completely severed due to liquefaction-induced ground displacements in Niigata City. This evidence was discovered about 20 years after the earthquake when the foundation ground was excavated for reconstruction of a building. (S. Kawamura, 1985).



Gas pipe was parted by a distance of 70 cm due to tensile strain

Two broken ends bit into each other due to compressive strain



Welded steel gas pipes with a diameter of 80 mm were severely damaged due to liquefaction-induced ground strain in Noshiro City during the 1983 Nihonkai-Chubu earthquake.



PREFACE

This volume is a part of a two-volume study of large ground deformations induced by earthquakes and their effects on lifeline facilities. The primary emphasis of this work is placed on liquefaction-induced ground deformations and the resultant damage to lifeline facilities. Permanent ground deformations, particularly those generated by soil liquefaction, are now known to be the most troublesome cause of subsurface structural damage and have led to serious disruption of critical lifeline facilities in previous earthquakes.

There has been substantial interest and research in the United States and Japan focused on this subject, and this two-volume compilation of case histories represents an important milestone in cooperative Japanese and U.S. efforts to pool research resources, establish a comprehensive data base, and point the way to improved analytical, testing, design, and planning measures to mitigate the effects of large ground deformations on lifeline systems. Other products of cooperative Japan-U.S. research include the proceedings from joint workshops and bilateral recommendations for improved modeling, siting, design, and construction of buried structures. A brief description of the cooperative research program, supported by the Japanese Association for the Development of Earthquake Prediction and the U.S. National Center for Earthquake Engineering Research, is given in the introductory statement immediately following this preface.

The study of liquefaction-induced ground deformations and lifeline facilities can be viewed as a synthesis of two disciplines within the more general field of earthquake engineering. Soil liquefaction has been an area of substantial importance in geotechnical engineering for over 60 years. The study of earthquake-induced liquefaction can be divided historically into three periods of prominent research and field activities. In the 1960s, earthquakes in Niigata and Alaska focused attention on soil liquefaction. The resulting field and laboratory investigations helped to clarify the factors contributing to soil liquefaction and led to simplified, empirical methodologies for predicting the occurrence of liquefaction. Additional field investigations and laboratory studies in the 1970s and 1980s led to refinements and improvements to the procedures used to determine the susceptibility of soils to liquefaction. Although some significant advances were made in the modeling and prediction of ground deformations resulting from liquefaction, engineering practice during this period emphasized the understanding and identification of soils on the basis of their susceptibility to liquefaction. Furthermore, during this period a considerable amount of research effort was spent on the development of methods to improve soil and to protect structures against soil liquefaction, and these methods were put into practical use. From about the mid-1980s, the emphasis on research and development for practical purposes has been shifting to the consequences of soil liquefaction. It was recognized after the experiences of the Niigata and Alaska earthquakes that there were several distinct consequences of soil liquefaction; these include loss of foundation bearing strength, buoyancy of underground structures, and local subsidence of ground associated with the ejection of soil and water. In addition to these problems, lateral spreading and flow of the liquefied soil, as well as oscillations leading to fissures and compressive ridges in ground overlying

liquefied soil, began to attract attention. The mechanisms of large ground deformations under these circumstances are complex, and a full understanding of them demands a comprehensive and accurate data base for guidance in analytical and physical modeling, site characterization, planning, design, and countermeasures.

The 1970s saw the attention of the earthquake engineering community turn towards the performance of lifeline facilities. Stimulated by the 1971 San Fernando earthquake and the 1978 Miyagiken-oki earthquake, a new area of research and practice evolved, focussing on the performance of lifeline systems. Such systems include water supplies, transportation, gas and liquid fuels, telecommunications, electricity, and wastewater conveyance and treatment. Although the primary emphasis was originally on the response of such lifelines to the seismic waves themselves, by the 1980s it was recognized that permanent ground deformation also played a critical role. In many cases, this is the most important factor affecting lifeline performance following an earthquake.

The study of lifeline performance and large ground deformation, therefore, should be viewed as a logical extension of research and practice-oriented developments associated with soil liquefaction and the emergence of lifeline earthquake engineering. We believe that Japan-U.S. cooperative research has helped to promote and consolidate this merger of lifeline and geotechnical interests, and has led to improved engineering practices.

This volume consists of five case histories: 1) 1923 Kanto earthquake, 2) 1948 Fukui earthquake, 3) 1964 Niigata earthquake, 4) 1983 Nihonkai-Chubu earthquake, and 5) 1990 Luzon, Philippines earthquake. Although the Luzon earthquake did not affect Japan, it nonetheless was investigated extensively by Japanese members of the cooperative research team.

The companion volume reports on the following five U.S. case histories: 1) 1906 San Francisco earthquake, 2) 1964 Alaska earthquake, 3) 1971 San Fernando earthquake, 4) 1979, 1981, and 1987 Imperial Valley earthquakes, and 5) 1989 Loma Prieta earthquake.

These earthquakes were chosen for study on the basis of three principal factors. First, there needed to be accurate records of permanent ground deformation, sufficient in detail to evaluate the magnitude, direction, and areal distribution of ground movements. Second, substantial soil explorations were needed to provide a reliable view of subsurface conditions and soil properties where large ground deformation occurred. Third, accurate records were required of the effects of ground movements on structures, and particularly on lifeline facilities.

A case history represents the real basis for assessing the effects of an earthquake; case histories also establish a baseline of performance with which to verify analytical and physical models, develop design procedures, and guide the planning and siting of facilities. They are also invaluable in developing countermeasures against liquefaction, such as site improvements, strengthening of facilities, and retrofitting existing facilities.

The Japanese and U.S. case histories represent the cumulative observations and analyses of earthquake-induced ground deformations and lifeline response over 84 years. Those described in this volume include the most important earthquakes to have occurred in Japan.

As mentioned previously, it was the 1964 Niigata earthquake in tandem with the Alaska earthquake of the same year, that focused the attention of the engineering community on liquefaction and its devastating effects. These two events should be considered the beginning of modern geotechnical investigations into liquefaction phenomena.

The study of the 1983 Nihonkai-Chubu earthquake was a significant achievement by Japanese researchers working on liquefaction-induced ground displacements and the damage they cause to structures. Large ground displacements of several meters were recorded for the first time through an investigation of damage to buried gas pipes in Noshiro City. The 1923 Kanto earthquake, which severely damaged Metropolitan Tokyo, is one of the most important seismic events in Japanese history. Case histories of the 1923 Kanto and the 1948 Fukui earthquakes provide highly instructive information about liquefaction-induced ground displacement and related structural damage on alluvial plains. This is particularly important since many large Japanese cities are located in similar geological settings. The 1990 Luzon, Philippines earthquake brought soil liquefaction and its related damage to the attention of the Philippino people. In this sense, it was similar to the Japanese situation at the time of the 1964 Niigata earthquake. This earthquake reminded us once again of the severity of liquefaction-induced damage to structures designed and constructed with little or no consideration of such effects.

It is our hope that the information presented in these volumes of case histories will form the basis for future research into liquefaction-induced ground displacement and its effects on lifeline facilities. We also hope that it will be applied to the development of better designs and construction methods, as well as effective measures against earthquakes.

M. Hamada
Professor, Tokai University

T.D. O'Rourke
Professor, Cornell University

JAPAN-U.S. COOPERATIVE RESEARCH PROGRAM

The Japan-U.S. Research Program on Earthquake Resistant Design of Lifeline Facilities and Countermeasures for Soil Liquefaction was initiated formally in November, 1988 with the signing of a Memorandum of Understanding between the Japanese and U.S. sides. The document was signed at a ceremony during a workshop in Tokyo, Japan by K. Kubo, Professor Emeritus of Tokyo University, and M. Shinozuka, Sollenberger Professor of Civil Engineering of Princeton University. Professor Kubo signed on behalf of the Association for the Development of Earthquake Prediction (ADEP), the Japanese sponsoring agency. Professor Shinozuka signed on behalf of Robert L. Ketter, the Director of the National Center for Earthquake Engineering Research (NCEER), the U.S. sponsoring agency. A second Memorandum of Understanding was signed in December, 1990 to continue the cooperative program of research. The signatures were K. Kubo, representing ADEP, and M. Shinozuka, the Director of NCEER.

The products of the research include: 1) case history volumes with assessments of the most important geologic features, siting criteria, and structural features which have influenced lifeline performance in response to soil liquefaction and its induced ground deformation, 2) Japan-U.S. workshops and associated publications covering case history data, analytical modeling, and recommendations for improved practices, and 3) a technical summary and recommendations for improved modeling, siting, design, and construction of buried structures.

Major instruments for collaboration and cooperative exchange are workshops. To date, there have been three workshops. The first was held in Tokyo and Niigata, Japan on November 16-19, 1988. The proceedings of this workshop were published by ADEP, and are available from NCEER. The second workshop was held in Buffalo and Ithaca, N.Y. on September 26-29, 1989. The third workshop was held in San Francisco, Cal. on December 17-19, 1990. The proceedings of both these workshops are available through NCEER. At the time of publication of this volume, a fourth workshop has been planned for Honolulu, Hawaii on May 27-29, 1992.

The cooperative research between Japanese and U.S. earthquake engineers has resulted in significant new findings about the ways in which large ground deformations are caused by soil liquefaction, and their influence on lifelines, and the most effective means of modeling and protecting both soils and structures in the event of a future earthquake. New developments presented and discussed at the workshops include the use of aerial photographs before and after major earthquakes to map ground displacements by photogrammetric techniques, the effects of a large ground deformation on buried pipelines, lateral movement effects on and damage to pile foundations, the most suitable modeling methods for large ground deformation and buried lifeline response, and the countermeasures against liquefaction and its resultant large ground deformation.

It is hoped that the spirit of cooperation fostered by the research program will contribute to a strong and enduring relationship among Japanese and U.S. engineers. It is believed that the accomplishments of this collaborative activity will encourage additional joint projects and lead to improved understanding and mastery in the field of earthquake engineering.

T.D. O'Rourke
Professor, Cornell University

M. Hamada
Professor, Tokai University

ACKNOWLEDGEMENTS

Although acknowledgements are given at the beginning of each case history, as appropriate for those who provided assistance in the execution of the research, special recognition needs to be extended to several people who have been vitally important for the entire Japan-U.S. case history effort. The editors of this volume thank the Association for the Development of Earthquake Prediction (ADEP) and the National Center for Earthquake Engineering Research (NCEER) for sponsoring this project. In particular, thanks are extended to M. Shinozuka, Director of NCEER and K. Kubo, Professor Emeritus of Tokyo University, who provided oversight and support for cooperative activity. We also remember the encouragement and enthusiasm of Dr. Robert L. Ketter, the late Director of NCEER.

We thank the Tokyo Gas Company for providing financial support for the Japanese case study on liquefaction-induced ground deformations which was initiated after the 1983 Nihonkai-Chubu earthquake. In particular, we thank H. Kobayashi, R. Osawa, H. Negishi, and K. Saito for their interest and encouragement.

We extend our sincere thanks to the members of the Japanese team in the Japan-U.S. Cooperative Research, who contributed greatly to the execution of the research. We particularly thank I. Yasudo of Hassu Co., Ltd. for performing the measurements of permanent ground displacements using aerial photographs. Special recognition is extended to M. Koshimizu, M. Ochi, and Y. Kojima, students at Tokai University whose help and support were indispensable for the successful completion of this project.

M. Hamada
Professor, Tokai University

T.D. Rourke
Professor, Cornell University

TABLE OF CONTENTS

Volume 1

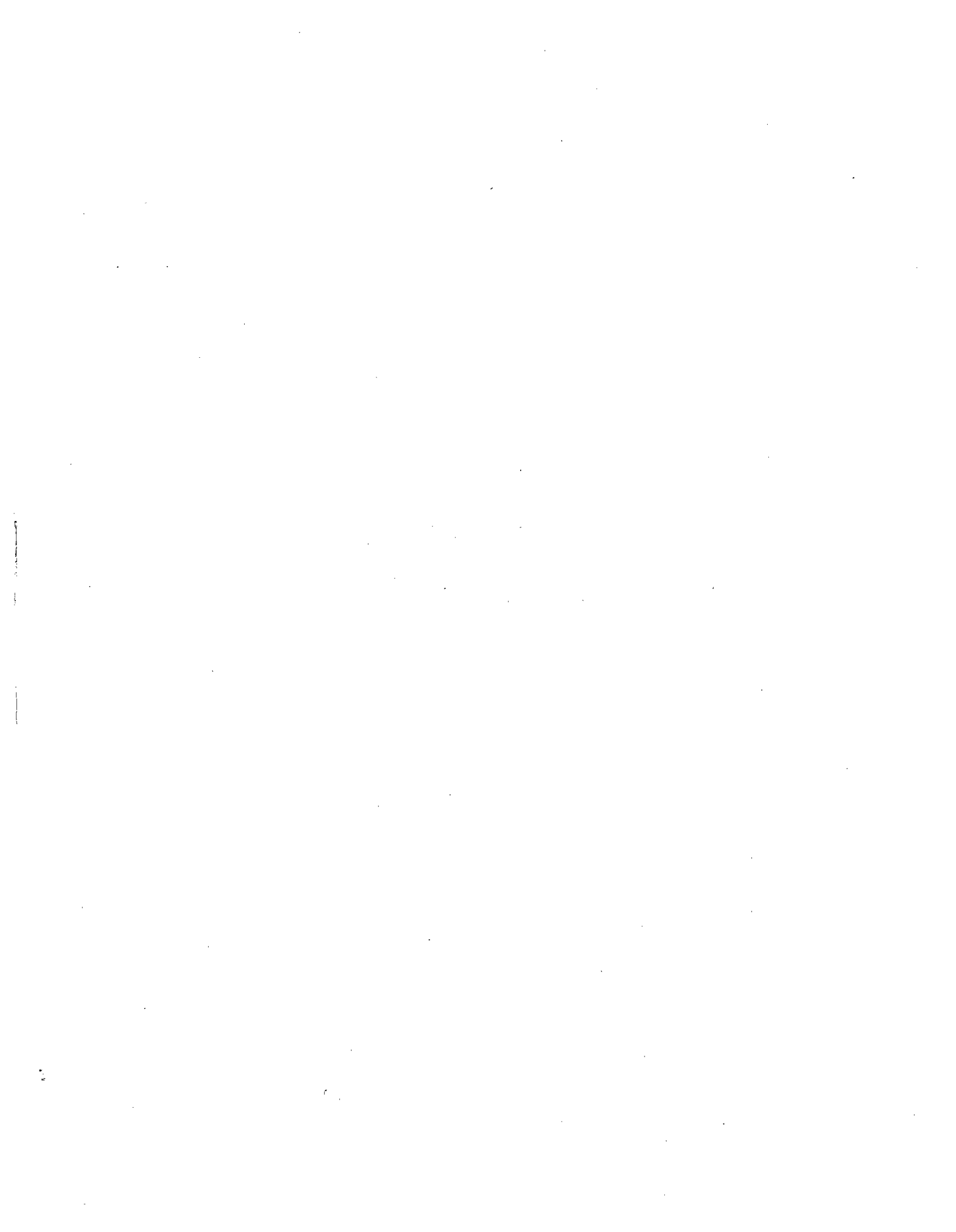
Preface.....	v
Japan - U.S. Cooperative Research Program.....	ix
Acknowledgements.....	xi
Table of Contents.....	xiii
Liquefaction-Induced Ground Deformations During the 1923 Kanto Earthquake <i>M. Hamada, K. Wakamatsu and S. Yasuda</i>	1-i
Large Ground Deformations and Their Effects on Lifelines: 1948 Fukui Earthquake <i>M. Hamada, S. Yasuda and K. Wakamatsu</i>	2-i
Large Ground Deformations and Their Effects on Lifelines: 1964 Niigata Earthquake <i>M. Hamada</i>	3-i
Large Ground Deformations and Their Effects on Lifelines: 1983 Nihonkai- Chubu Earthquake <i>M. Hamada</i>	4-i
Liquefaction-Induced Large Ground Deformations and Their Effects on Lifelines During the 1990 Luzon, Philippines Earthquake <i>K. Wakamatsu, N. Yoshida, N. Suzuki, and T. Tazoh</i>	5-i

Liquefaction-Induced Ground Deformations During the 1923 Kanto Earthquake

*M. Hamada, Professor
School of Marine Science and Technology
Tokai University
Shimizu, Shizuoka, Japan*

*K. Wakamatsu, Research Associate
Science and Engineering Research Laboratory
Waseda University
Tokyo, Japan*

*S. Yasuda, Associate Professor
Faculty of Civil Engineering
Kyushu Institute of Technology
Kitakyushu, Japan*



ABSTRACT

Three case histories of liquefaction-induced ground displacement generated by the 1923 Kanto earthquake are reviewed herein. By re-examining already published damage reports and interviewing local residents, sites of liquefaction-induced ground failure and displacement were identified. The general character and regional extent of these displacement patterns and failures are described, and geomorphological and geotechnical data from displacement sites are examined. Liquefied layers were evaluated by comparing the color and grain size of the vented materials and soil samples taken from bore holes made at each displacement site, and on analytical methods for assessing susceptibility to liquefaction as employed in the Japanese Highway Bridge Code.

The 1923 Kanto earthquake generated horizontal ground displacements in at least three places in Tokyo and its vicinity. The ground displacement generally originated at natural levees and/or abandoned channel bars and terminated at small rivers which were once a large river. The maximum magnitude of the displacement is estimated to be as large as several meters. The gradient of the present ground surface at the displacement sites is very small, under 1%. Recent bore hole data from the three sites revealed that saturated layers of fine to sandy gravel in channel deposits underlie each site at a shallow depth. These deposits were identified as having liquefied during the earthquake.

ACKNOWLEDGEMENTS

The case study of large ground deformations and their related ground failures was conducted by the Japanese team of the U.S.-Japan Cooperative Research on "Liquefaction, Large Ground Deformations and their Effects on Lifeline Facilities," organized by the Association for Development of Earthquake Prediction, Tokyo, Japan. We would like to thank the team members for their assistance and help in discussions. In particular, our gratitude is extended to Prof. K. Kubo who chaired the research committee of the Japanese team. We also would like to express our deep appreciation to Mr. I. Yasuda of Hasshu Inc. for his skillful interpretation of old photographs of the ground cracks in the Nakajima area, Mr. M. Ochi, Mr. Y. Kojima, and other students at Tokai University as well as the Kyushu Institute of Technology for their great contribution to this case study. Finally, our sincere appreciation is extended to Prof. T.D. O'Rourke at Cornell University for his excellent editing of this case study.

TABLE OF CONTENTS

	<u>Page</u>
Acknowledgements	1-v
Table of Contents	1-vii
List of Figures	1-ix
List of Tables	1-xi

<u>Section</u>	<u>Page</u>
1.0 INTRODUCTION	1-1
2.0 OUTLINE OF THE 1923 KANTO EARTHQUAKE	1-2
3.0 COLLECTION AND EVALUATION OF DATA	1-4
4.0 LOCATIONS OF LIQUEFACTION-INDUCED GROUND FAILURES AND DISPLACEMENTS	1-5
5.0 GROUND DISPLACEMENT AT NAKAJIMA AREA IN CHIGASAKI CITY, KANAGAWA PREFECTURE	1-6
5.1 Geographical and Geomorphological Settings	1-6
5.2 Liquefaction-Induced Ground Displacement	1-6
5.3 Damage to Structures as a Result of Ground Displacement	1-10
5.4 Subsurface Conditions and Estimation of the Liquefied Layer	1-12
6.0 GROUND DISPLACEMENT AT THE FURU-SUMIDA CREEK AREA IN TOKYO	1-17
6.1 Geographical and Geomorphological Settings	1-17
6.2 Liquefaction-Induced Ground Displacement	1-17
6.3 Damage to Structures as a Result of Ground Displacement	1-22
6.4 Subsurface Conditions and Estimation of the Liquefied Layer	1-22

<u>Section</u>	<u>Page</u>
7.0 GROUND DISPLACEMENT AT KAWAKUBO AREA IN KASUKABE CITY, SAITAMA PREFECTURE	1-26
7.1 Geographical and Geomorphological Settings	1-26
7.2 Liquefaction-Induced Ground Displacement	1-26
7.3 Damage to Structures	1-30
7.4 Subsurface Conditions and Estimation of Liquefied Layer	1-33
8.0 CONCLUSION	1-35
REFERENCES	1-37

LIST OF FIGURES

<u>Figure</u>	<u>Page</u>
1 Map of Kanto and Chubu Districts Showing Distribution of Seismic Damage Caused by the 1923 Kanto Earthquake (Modified from Usami, 1987) ⁸⁾	1-3
2 Map of Kanto and Chubu Districts Showing Principal Areas Affected by Liquefaction during the 1923 Kanto Earthquake	1-7
3 Geomorphological Land Classification Map of Nakajima and Surrounding Areas	1-7
4 Aerial Photograph of Nakajima Area Taken in 1946	1-8
5 Seven Wooden Piers Which Buoyantly Rose about 1.5 m in a Rice Field during the Kanto Earthquake (Imperial Earthquake Investigation Committee, 1925) ¹¹⁾	1-9
6 Tilting, Rising up and Lateral Movement of Open Caissons of Banyu Bridge over Sagami River (Japan Society of Civil Engineers, 1927) ¹²⁾	1-9
7 Aerial Photograph of Nakajima Area Showing Ground Cracks Caused by the Kanto Earthquake (Looking Southeast) (Association for the Development of National Education, 1926) ¹⁵⁾	1-11
8 Contour Map of Nakajima Showing Locations of Ground Cracks and Ground Deformation Generated by Lateral Ground Movement and Location of Borings and Soundings for the Cross Section A-A' in Figure 12	1-11
9 Damage to Embankment of Tokaido Line and Route 1 Caused by Ground Failure in Nakajima Area (Kanto Headquarters of Martial Law, 1924) ¹⁸⁾	1-13
10 Damage to Bridge over Sagami River (Kanto Headquarters of Martial Law, 1924) ¹⁸⁾	1-13
11 Collapse of Embankment of Tokaido Line in Nakajima Area (Japan Society of Civil Engineers, 1927) ¹²⁾	1-14
12 Cross Section of Sediments at Nakajima Area Showing Geotechnical Features and Estimated Liquefied Layer	1-15
13 Grain Size Distribution Curves from Fine Sand Layer and Sandy Gravel Layer at Nakajima Area	1-14
14 Map of Furu-Sumida Creek Area Showing Geographical and Geomorphological Features and Locations of Surficial Effects of Liquefaction	1-18

<u>Figure</u>	<u>Page</u>
15 Plan View of Kosuge Prison Showing Locations of Ground Cracks and Totally Damaged House (Geological Survey of Japan, 1925) ²⁰	1-18
16 Map of Nishi-Kameari, Tokyo, Showing Geographic Features, Locations of Ground Failures, and Locations of Borings and Soundings for the Cross Section in Figure 18	1-21
17 View of the Furu-Sumida Creek near Kosuge Prison: Photograph Taken in 1989	1-21
18 Cross Section of Sediments at Nishi-Kameari, Tokyo, Showing Geotechnical Features and Estimated Liquefied Layer	1-23
19 Grain Size Distribution Curves from Sand Layer at B-1, Nishi-Kameari, Tokyo	1-25
20 Grain Size Distribution Curves from Sand Layer at B-2, Nishi-Kameari, Tokyo	1-25
21 View of the Furu-Tone River in Kawakubo Area: Photograph Taken in 1989	1-27
22 Map of Reaches of the Furu-Tone River and the Moto-Ara River Showing Locations of Ground Cracks and Sand Boils Caused by the 1923 Kanto Earthquake	1-28
23 Aerial Photograph of Kawakubo and Surrounding Areas Taken in 1947	1-29
24 Ground Cracks and Offset Displacement in Roadway in Kawakubo Area (Geological Survey of Japan, 1925) ²⁰	1-31
25 View of Curved Road Shown in Figure 24: Photograph Taken in 1989 (Looking South)	1-31
26 Geomorphological Land Classification Map of Kawakubo Area Showing Locations of Ground Cracks and Locations of Borings and Soundings for the Cross Section C-C' in Figure 27	1-32
27 Cross Section of Sediments at Kawakubo Showing Geotechnical Features and Estimated Liquefied Layer	1-34
28 Grain Size Distribution Curves from Sand Layer at Kawakubo Area	1-35

LIST OF TABLES

<u>Table</u>		<u>Page</u>
1	Ground Cracks Observed in Kasukabe Town Including Kawakubo Area (Geological Survey of Japan, 1925) ²⁰	1-27

1.0 INTRODUCTION

Recent investigations have revealed that liquefaction generated large-scale ground displacement during several earthquakes in Japan and the United States. These include the 1906 San Francisco earthquake, the 1964 Niigata earthquake, the 1971 San Fernando earthquake, and the 1983 Nihonkai-Chubu earthquake.¹⁾⁻⁷⁾ However, additional case studies are required to identify areas where ground deformations are likely to occur, clarify the mechanisms of ground displacement, and develop an analytical method to assess them.

This study identifies and examines liquefaction-induced ground failures generated during the 1923 earthquake in the Tokyo Metropolitan area, and describes the regional extent of these failures. Sites where ground displacements occurred as a result of liquefaction are identified, and their effects on structures are investigated. Geomorphological and geotechnical conditions of the sites are also studied, and liquefied layers are evaluated.

The Kanto earthquake was selected as the subject of this study for the following reasons: (1) It was the only large earthquake experienced in the Tokyo Metropolitan area in the past 100 years. (2) The Kanto Plain affected by the Kanto earthquake is typical of Japanese alluvial plains, which contain soil deposits associated with deltas, natural levees, and alluvial fans. Large cities, such as Tokyo, Osaka and Nagoya, are located on these types of plains. Therefore, study of the Kanto Plain is important to assess not only the effects of future large earthquakes on the Tokyo Metropolitan area, but also on other large cities.

2.0 OUTLINE OF THE 1923 KANTO EARTHQUAKE

The earthquake occurred on September 1, 1923 at 11:58 a.m. The epicenter was in the Sagami Bay at coordinates 139.5° E and 35.1° N, and the magnitude was measured at 7.9. The earthquake resulted from a slippage in a transform fault between two crustal blocks bounded by the Sagami Trough. Figure 1 shows contours of the damage percentages associated with wooden houses, contours of uplift and subsidence, locations of tsunami and other effects in the most severely affected region.⁸⁾ The source area was estimated as shown in Figure 1 by Ando.⁹⁾ Seismic intensity was estimated at VI on the Japan Meteorological Agency (JMA) scale in the greater part of the region shown in Figure 1. JMA Intensity VI corresponds to approximately Modified Mercalli Intensity IX.

Damage was heaviest in Kanagawa and Tokyo Prefectures. Damage also extended to other areas, such as Shizuoka Prefecture and even as far as Yamanashi and Nagano Prefectures. The death toll in Kanagawa and Tokyo Prefectures was about 97,000 including about 60,000 in Tokyo City. The total number of dead and missing reached about 143,000, and approximately 104,000 people were listed as injured. About 128,000 houses and buildings were destroyed, another 126,000 were heavily damaged, and as many as 447,000 lost to fire. Fire accounted for the majority of houses destroyed in Tokyo, and about 50 percent of houses lost in Kanagawa Prefecture could be attributed to fire.

The earthquake resulted in tsunami which washed away 868 houses in the three prefectures of Shizuoka, Kanagawa and Chiba. Tsunami about 3 m high pounded the southern coast of the Izu Peninsula and others 4-6 m in height hit the coast of Sagami Bay and the southern coast of the Boso Peninsula. Tsunami damage was most conspicuous in the lowland areas around small bays such as Atami, Shizuoka Prefecture, and Ainoama at the tip of the Boso Peninsula. Tokyo Bay only experienced waves of less than one meter in height.

The earthquake was also accompanied by violent crustal movement. The maximum recorded amount of uplift was 2 m at the southern tip of the Boso Peninsula and the coastal area of Sagami Bay. Uplift at the tip of the Miura Peninsula

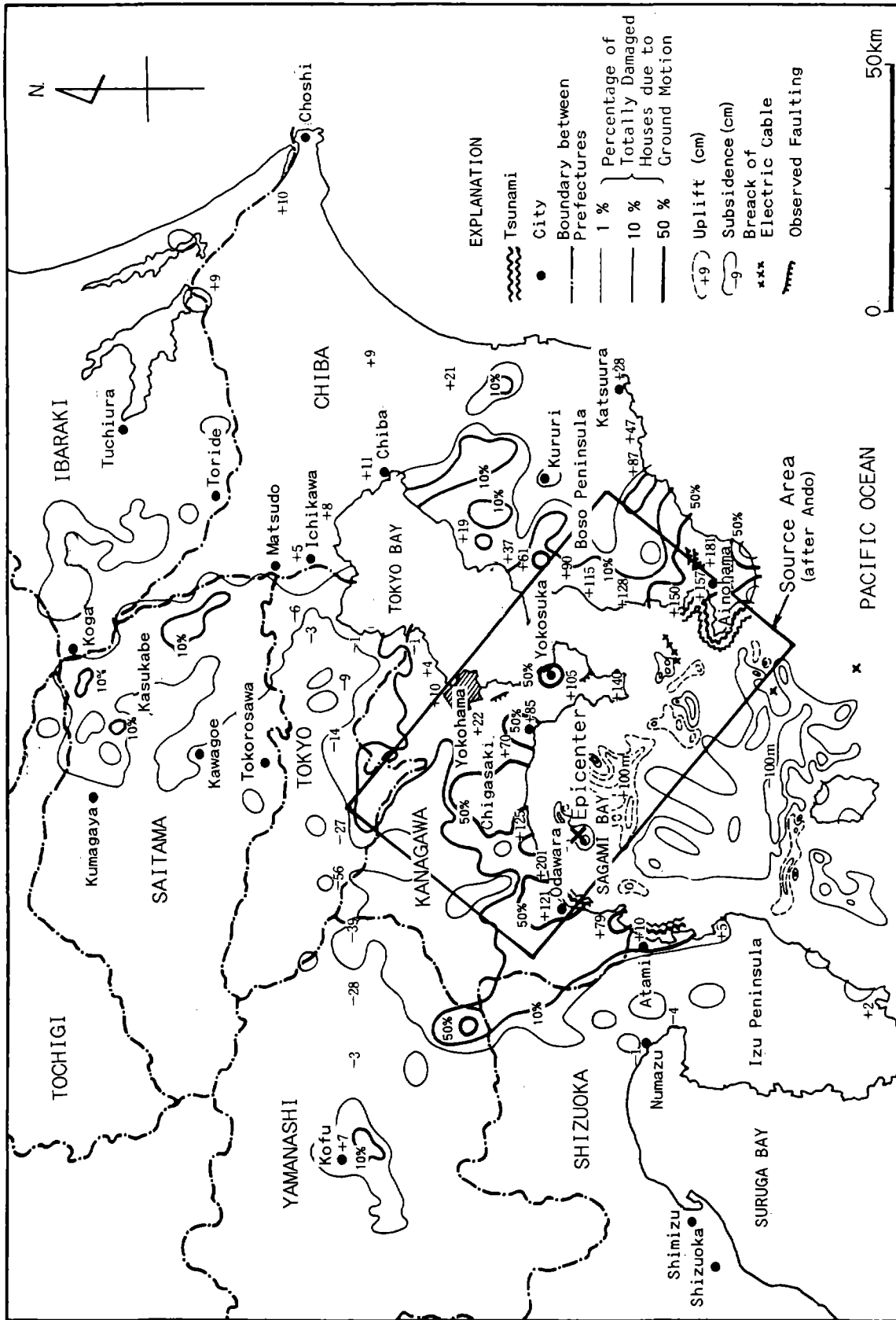


Figure 1 Map of Kanto and Chubu Districts Showing Distribution of Seismic Damage Caused by the 1923 Kanto Earthquake (Modified from Usami, 1987)8)

measured 1.2 m. Most of the changes occurred abruptly at the time of the earthquake, as has been clearly proved by the tide gauge record taken at the Port of Yokosuka.

3.0 COLLECTION AND EVALUATION OF DATA

Aerial photographs taken before and after earthquakes have been used by Hamada et al. to measure ground displacements.^{3),6)} However, unlike the cases of more recent Japanese earthquakes, the authors could find no aerial photographs to enable them to measure photogrammetrically permanent ground displacements generated by the 1923 Kanto earthquake. Although several photos taken immediately after the shock, but covering only very limited areas, were inserted into damage reports, they were not clear enough to estimate ground displacements or deformations. Accurate estimates of displacements could not be made from comparisons of geographic maps compiled before and after the earthquake. The scales of the maps were too small to identify or measure displacements less than several meters. Therefore, eyewitnesses of the 1923 event were personally interviewed with the purpose of surveying those areas where permanent ground displacement may have occurred. Prior to these interviews, published damage reports, books and/or journals were carefully re-examined to search for descriptions of ground failures attributed to liquefaction. Nine sites were selected for interview surveys. Liquefaction effects were particularly pronounced at these nine sites.

At the same time, geomorphological and geotechnical settings were investigated to evaluate site conditions where liquefaction-induced ground failures and displacements took place. Data collected included topographic maps and geographic maps compiled in various periods, geological maps, geomorphological land classification maps, aerial photographs, and existing boring data. In addition, subsurface investigations including borings, standard penetration tests, Swedish weight sounding tests,* and grain size

*See Appendix C of reference 3).

distribution analysis were conducted to establish the geotechnical soil profiles across the displacement sites, and to estimate the location, approximate thickness, and extent of liquefied layers.

The liquefied layers at the sites were estimated and identified in two ways: (1) On the basis of earthquake magnitude, epicentral distance, and appropriate attenuation laws, peak horizontal ground accelerations at ground surface were estimated and used to evaluate liquefaction potential in accordance with the procedure outlined in the Japanese Highway Bridge Code,¹⁰⁾*; and (2) The color and grain size of sand from sand boils identified by the damage report and eyewitnesses were compared with soil samples taken from the bore holes of each displacement site.

4.0 LOCATIONS OF LIQUEFACTION-INDUCED GROUND FAILURES AND DISPLACEMENTS

Figure 2 shows the locations where sand boils were recorded in references on the 1923 earthquake. These locations extended over the whole area of the Kanto Plain and a part of the Kofu Basin, and reached to areas as far as 150 km from the epicenter. Interviews with residents were conducted at sites 1-9 of the figure, where liquefaction effects were particularly pronounced. A total of more than 70 witnesses provided information on ground failures such as ground cracks, sand boils, upheaval or settlement, slope failure of embankments and horizontal ground displacements. Horizontal ground displacements of several meters occurred in three areas within the Kanto Plain. These areas are shown in Figure 2 as: (1) Nakajima area, Chigasaki City (site 1); (2) Furu-Sumida Creek area, Tokyo (site 4); and (3) Kawakubo area, Kasukabe City (site 5).

*See Appendix D of reference 3)

5.0 GROUND DISPLACEMENT AT NAKAJIMA AREA IN CHIGASAKI CITY, KANAGAWA PREFECTURE

5.1 Geographical and Geomorphological Settings

The Nakajima area in Chigasaki City lies on the left bank of the lower reaches of the Sagami River (formerly called the Banyu River) and was located within the earthquake source area (site 1 in Figure 2). The geomorphological features of the Nakajima area are characterized by abandoned braided channels and abandoned channel bars (Figure 3). These channels and bars are covered with alluvial fan deposits. The residential area of Nakajima is located on the bars, which are topographically higher than the abandoned channels. Figure 4 is an aerial photograph of the Nakajima and surrounding areas, taken in 1946, the oldest photograph available of the areas.

5.2 Liquefaction-Induced Ground Displacement

Reports issued shortly after the earthquake documented liquefaction-related damage as follows: (1) Wooden piers, which might have been driven about 700 years ago, surfaced in a rice field at Machiya, site 1 in Figure 4 (Figure 5);¹¹⁾ (2) The open caissons of Banyu Bridge on National Route 1 tilted extremely, rose buoyantly and moved as shown in Figure 6 (site 2 in Figure 4);¹²⁾ and (3) All housing wells in the Suga area, site 3 in Figure 4, filled completely with the deposits of sand.¹³⁾

As a result of the interview survey conducted some 60 years after the earthquake, 110 cases of liquefaction effects were identified in the lower reaches of the Sagami (Banyu) River.¹⁴⁾ According to the survey, the area of the lower reaches of the Sagami River was most affected by liquefaction due to the earthquake. Residents of the area noted that numerous large ground cracks were caused and that the area was flooded with water spurting from the ground, which took two days to recede. Almost all 80 housing wells were filled with deposits of sand boils.¹⁴⁾

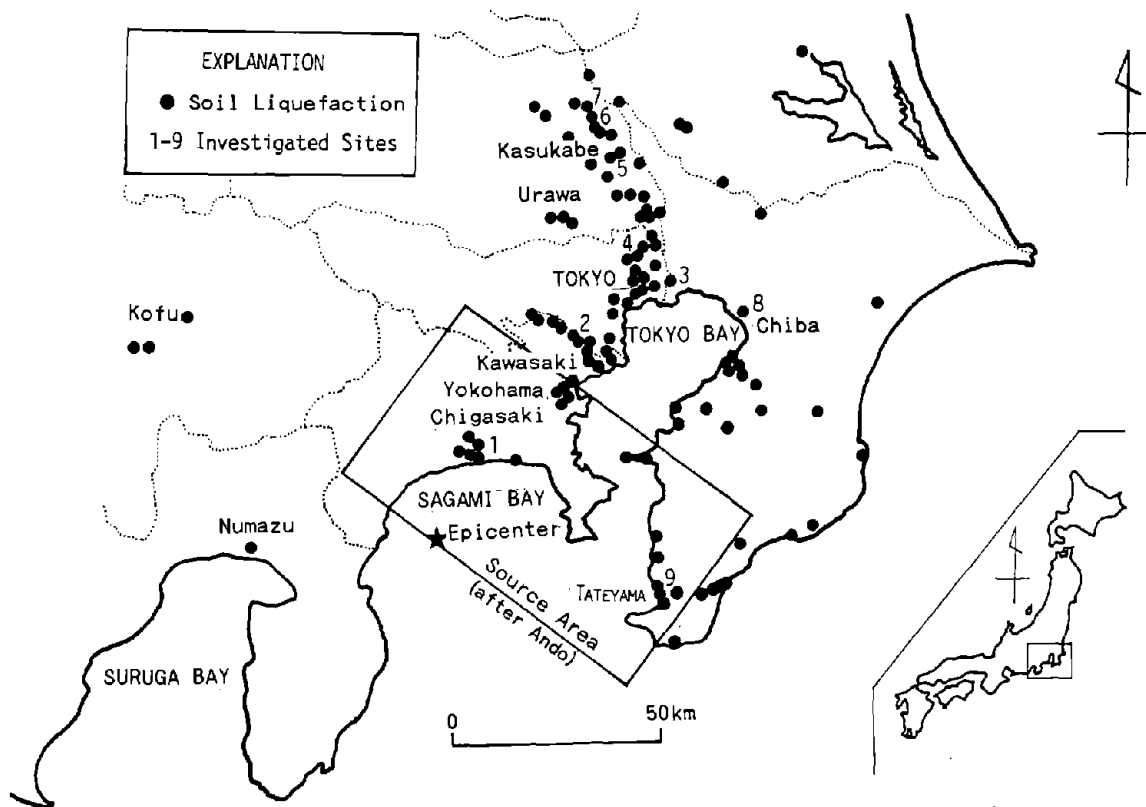


Figure 2 Map of Kanto and Chubu Districts Showing Principal Areas Affected by Liquefaction during 1923 Kanto Earthquake

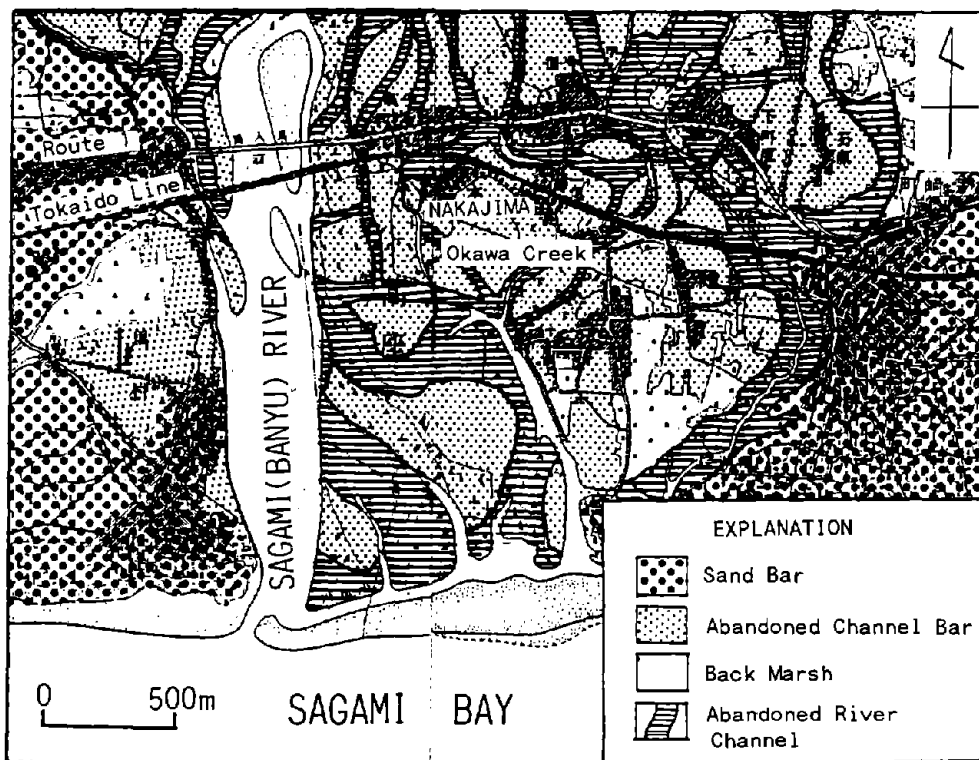


Figure 3 Geomorphological Land Classification Map of Nakajima and Surrounding Areas



Figure 4 Aerial Photograph of Nakajima Area Taken in 1946



Figure 5 Seven Wooden Piers Which Buoyantly Rose about 1.5 m in a Rice Field during the Kanto Earthquake (Imperial Earthquake Investigation Committee, 1925)¹¹⁾

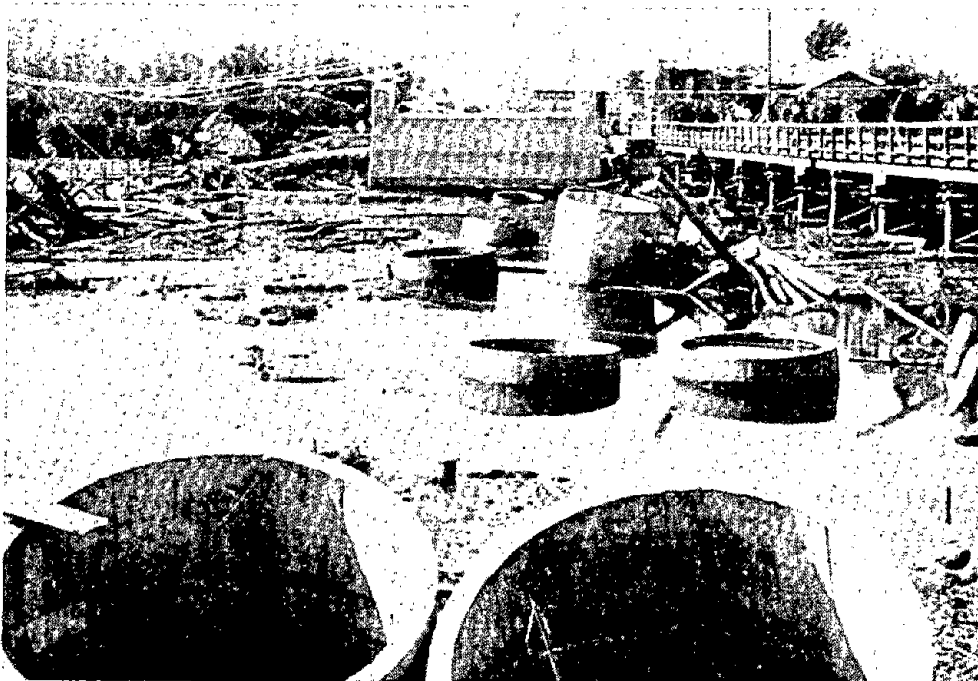


Figure 6 Tilting, Rising up and Lateral Movement of Open Caissons of Banyu Bridge over Sagami River (Japan Society of Civil Engineers, 1927)¹²⁾

An aerial photograph showing ground cracks in the Nakajima area was found in a damage report of the Kanto earthquake (Figure 7).¹⁵⁾ Based on an interpretation of this photo and a field inspection, the locations of ground cracks were drawn onto a topographic map (Figure 8). The contours of the map were delineated by means of stereo pair aerial photos taken in 1946, one of which is shown in Figure 4. The ground cracks occurred on the edge of an abandoned channel bar, where the contours converge to show locally steep relief.

Eyewitnesses reported that Okawa Creek, as it was called by the residents, used to be a river less than 10 m wide and more than 5 m deep, running parallel to the bigger Sagami River. Ground cracks, some of which had vertical offsets, occurred along Okawa Creek. From the cracks considerable amounts of water mixed with sand and fine gravel were expelled. Both the width and depth of the river were reduced to less than half what they were before the earthquake. Currently, the width is about 2.5 m and the stream is completely dry. The areal extent of land in the vicinity of the cracks was found both to have increased and decreased, depending on location (Figure 8). One eyewitness reported that the area of his land increased to 2,500 m² from 2,340 m² because of the earthquake. The magnitude of permanent ground displacement was estimated to be about 3 m toward Okawa Creek, based on the increased area. It can be conjectured that the ground movements may have originated from the abandoned channel bar and proceeded toward Okawa Creek.

5.3 Damage to Structures as a Result of Ground Displacement

Nakajima was a farming area in which about 80 wooden houses, a temple and a shrine existed at the time of the earthquake. No pipelines had been constructed at this site. According to documents of Chigasaki City, as many as 52 houses in this area were completely destroyed by the earthquake.¹⁶⁾

Along the northern boundary of the Nakajima area, runs the Tokaido Line and National Route 1, as shown in Figure 4. They were severely damaged near the



Figure 7 Aerial Photograph of Nakajima Area Showing Ground Cracks Caused by the Kanto Earthquake (Looking Southeast) (Association for the Development of National Education, 1926)¹⁵⁾

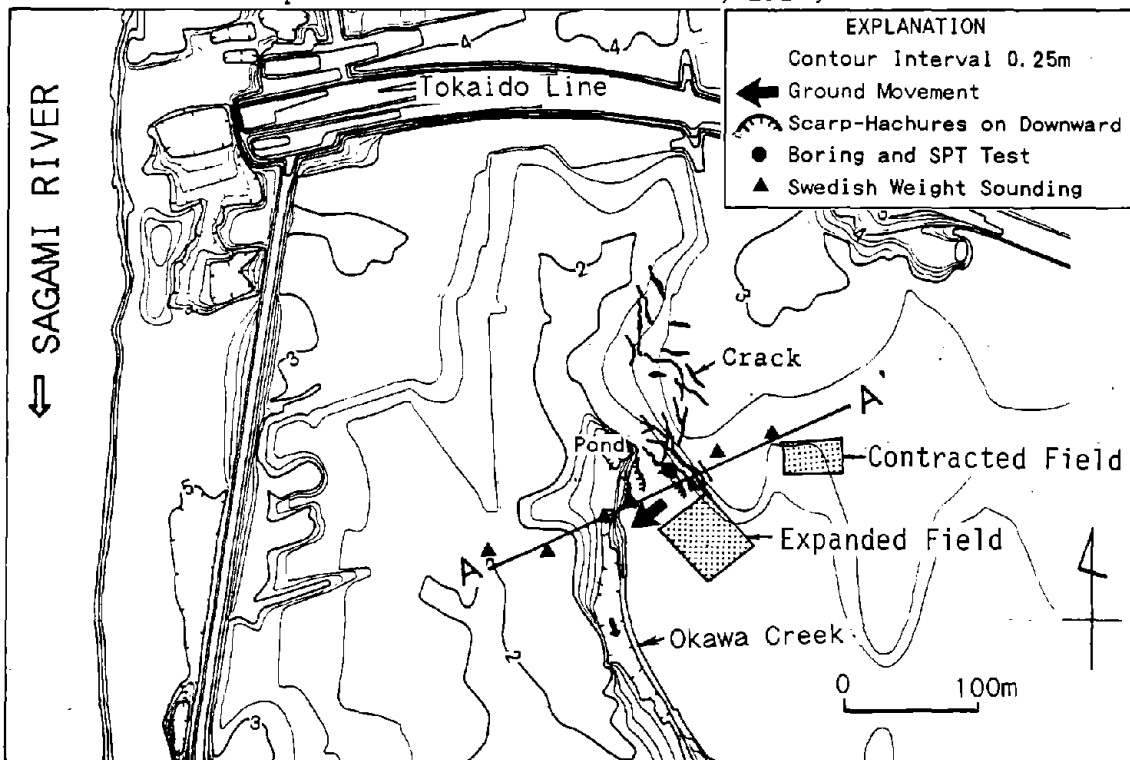


Figure 8 Contour Map of Nakajima Showing Locations of Ground Cracks and Ground Deformation Generated by Lateral Ground Movement and Location of Borings and Soundings for the Cross Section A-A' in Figure 12

Sagami River (Figure 9 and Figure 10). Between Chigasaki Station and the Sagami River, the embankment of the railway cracked, settled, and collapsed due to the earthquake (Figure 11). Abutments of the railway bridge across the Sagami River became inclined and were displaced streamward by 18 cm due to the ground movements. The ground movements also displaced, tilted, and broke twenty-seven piers of the railway bridge, as shown in Figure 10.¹²⁾

Open caissons of the bridge on Route 1, which was under construction at the time of the earthquake, leaned, rose buoyantly, and were displaced as mentioned before (Figure 6). Abutments on both banks tilted toward the river. The inclination of the abutments was about 4 degrees and 12 degrees for the left and right banks, respectively.¹²⁾ The damage to the two bridges indicates that ground displacement occurred in a direction towards the Sagami River in addition to the displacement towards Okawa Creek.

5.4 Subsurface Conditions and Estimation of the Liquefied Layer

Figure 12 shows a geotechnical cross section along line A-A' in Figure 8 as interpreted from the standard penetration test (SPT)* and Swedish weight sounding test (SWS).** The present ground surface is situated 2-3 m above sea level and slopes slightly toward Okawa Creek with a gradient of about 0.5%. The top 1-2 m is composed of agricultural clay fill. Loose fine sand lies beneath the fill, and moderately dense sandy gravel underlies the fine sand. Both of these (gravel and sand) are channel bar or channel deposits. A clay lens containing sand exist over the fine sand layer only at bore holes B-1 and S-4 where ground cracks occurred. The water level at the time of drilling (June, 1989) ranges in depth from 1.3 m-1.9 m. But it is likely that the groundwater level in this area has become appreciably lower since 1923.

*Generally, N-values in U.S. standard are larger than those in Japanese standard, because of the difference in energy transfer efficiency from the hammer to the rod. (See Reference 16)

**See Appendix C of Reference 3).

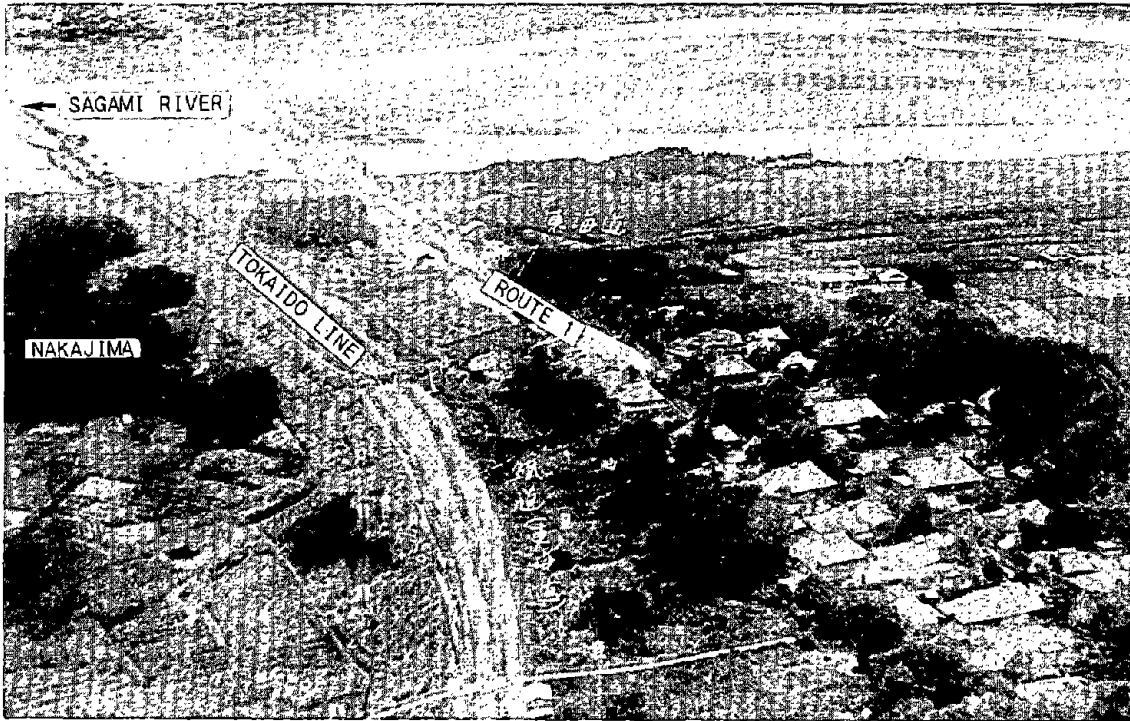


Figure 9 Damage to Embankment of Tokaido Line and Route 1 Caused by Ground Failure in Nakajima Area (Kanto Headquarters of Martial Law, 1924)18)

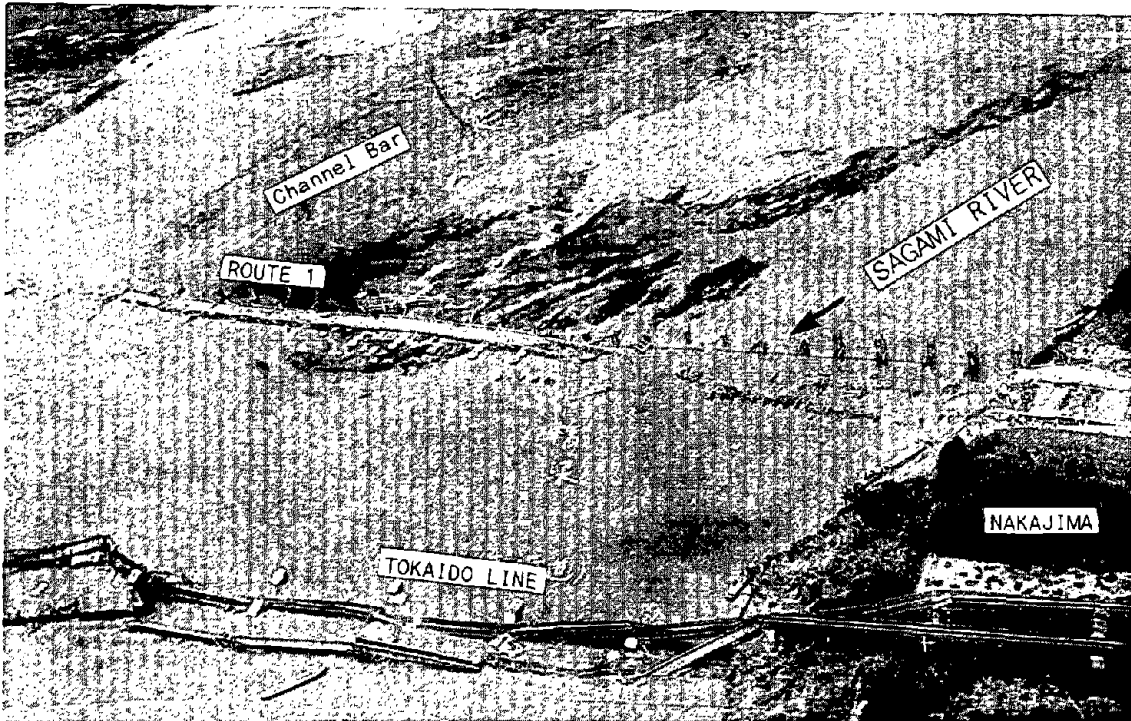


Figure 10 Damage to Bridge over Sagami River (Kanto Headquarters of Martial Law, 1924)18)

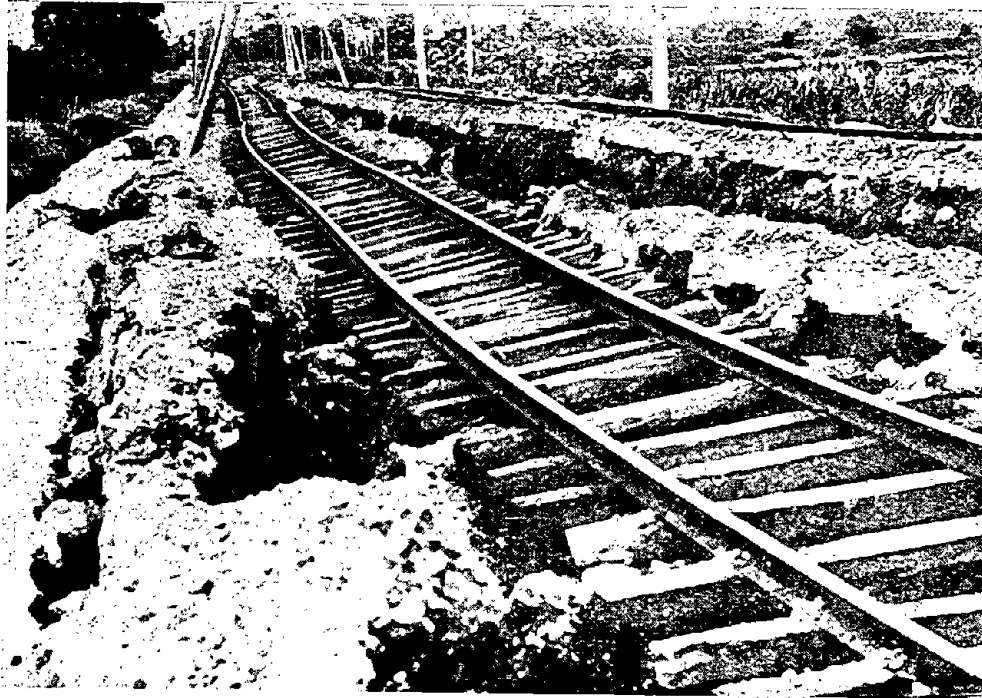


Figure 11 Collapse of Embankment of Tokaido Line in Nakajima Area (Japan Society of Civil Engineers, 1927)¹²⁾

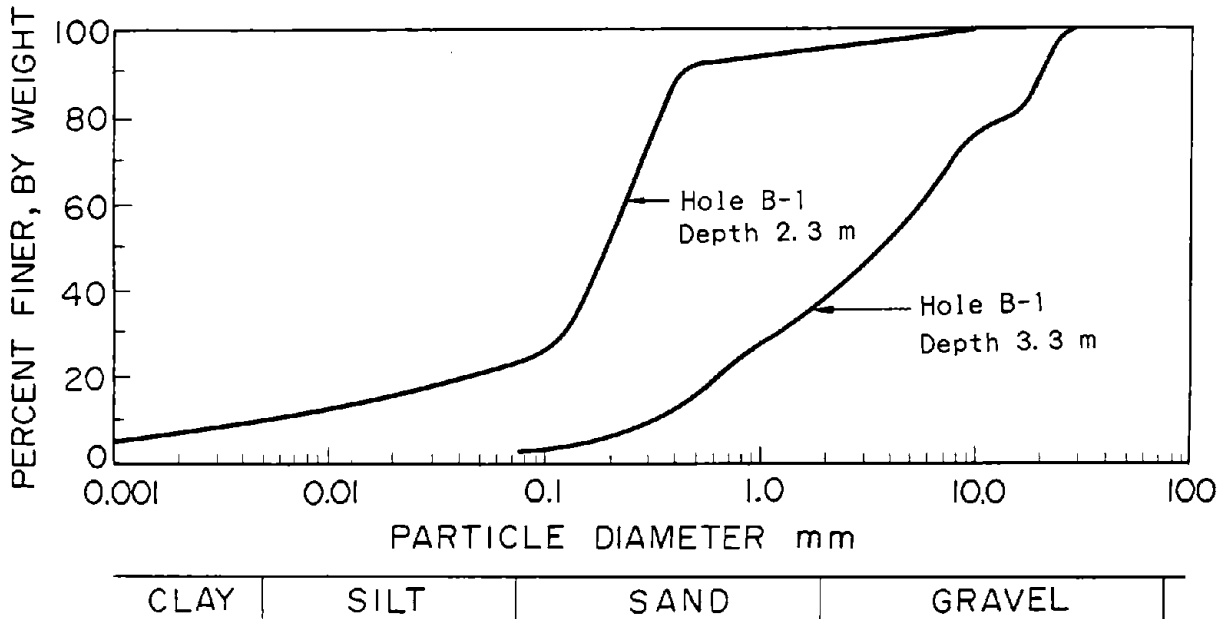


Figure 13 Grain Size Distribution Curves from Fine Sand Layer and Sandy Gravel Layer at Nakajima Area

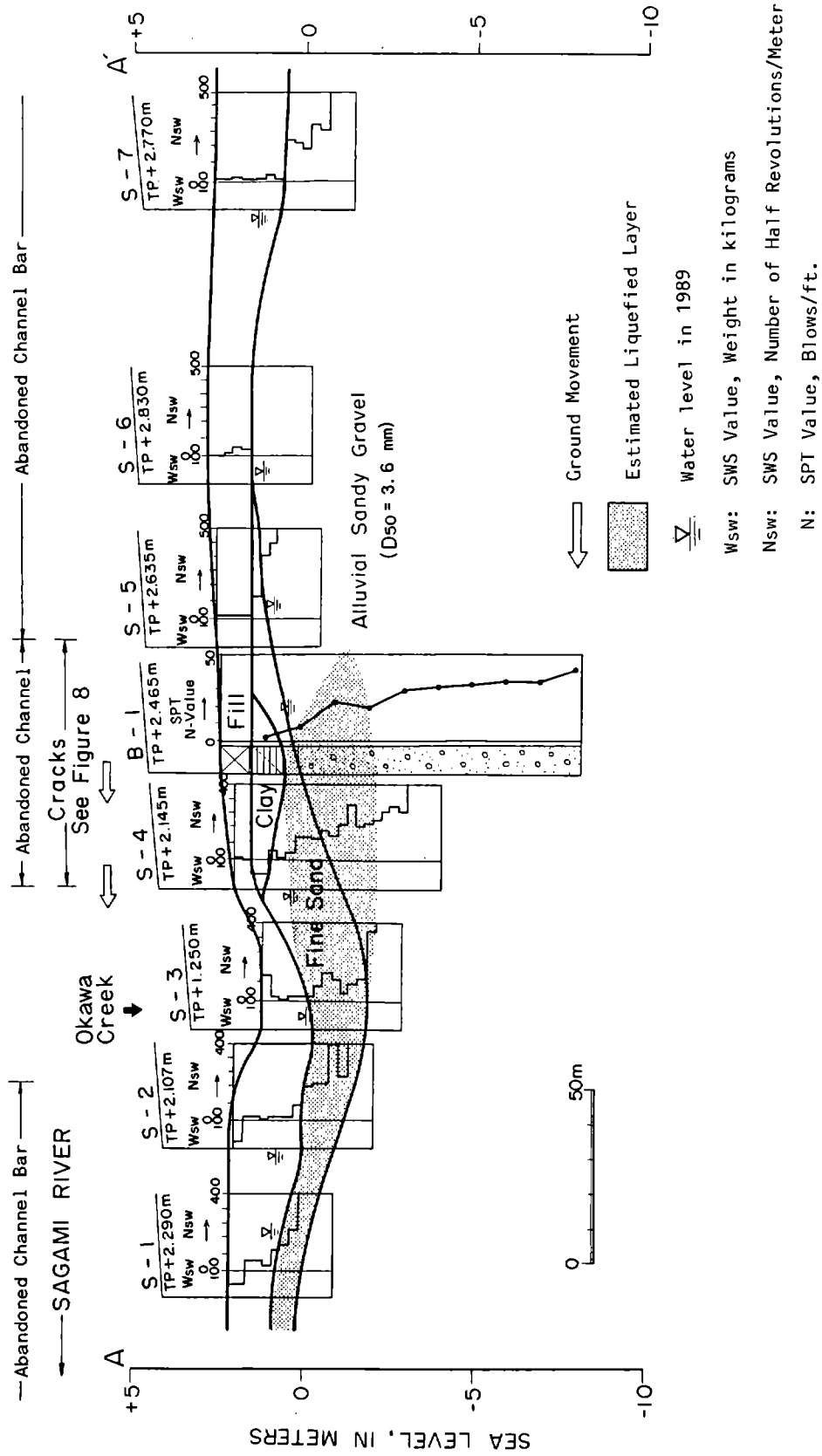


Figure 12 Cross Section of Sediments at Nakajima Area Showing Geotechnical Features and Estimated Liquefied Layer

The grain size distribution curves for samples taken from the sand and gravel layers are plotted in Figure 13. The sediment may be too coarse and well drained to liquefy. However, a feasible explanation for the ground failure in this area is liquefaction of the fine sand and sandy gravel. This assumption is based on the following description given by the residents: "A great quantity of water gushed forth," "the sand boils were composed of coarse sand and a few pebbles." In the case of the Nakajima area, the low permeability of the agricultural clay fill and the clay lens beneath the fill, are likely to have promoted the development of excess pore water pressure in the underlying sand and gravelly deposits.

On the other hand, an estimation of liquefaction was made using both the procedure of the Japanese Highway Bridge Code¹⁰⁾ and that proposed by Kokusho et al.¹⁹⁾ Although no measurements of peak horizontal acceleration are available for this area, peak acceleration at ground surface was estimated as 0.30 g using the empirical formula of the above code. According to the results of the estimation, the whole of the fine sand layer under the water table and part of the gravelly coarse sand layer were susceptible to liquefaction. The liquefaction-susceptible soils are indicated by the shaded portion in Figure 12. The maximum thickness of the estimated liquefied layer is 3 m where ground cracks formed, with a minimum of 1 m, while the thickness decreases from east to west across the site.

6.0 GROUND DISPLACEMENT AT THE FURU-SUMIDA CREEK AREA IN TOKYO

6.1 Geographical and Geomorphological Settings

This area is located in the northeastern part of Tokyo, and was about 80 km northeast of the epicenter (site 4 in Figure 2). Geomorphologically, it belongs in a transitional zone from the delta zone to the natural levee zone of the Kanto Plain. In the area, a small stream called the Furu-Sumida Creek meanders from the northeast to the southwest passing through the Arakawa Canal before finally draining into the Sumida River. The width of the stream was 2.5 m-3 m at the time of the earthquake but was estimated to be more than 50 m several hundred years ago. Prior to 1621, this creek had been the main course of the Tone River which has the largest drainage area of any river in Japan.

Figure 14 shows the geomorphological features of the Furu-Sumida Creek area. The former channel was used as rice fields and was outlined as ploughed fields according to old maps and aerial photographs. Natural levees are well developed along the channel. According to the geological history of the area, about one thousand years ago, it formed part of the coastline.

6.2 Liquefaction-Induced Ground Displacement

Earthquake-induced ground failures in this area were documented in a geological report that included the results of a survey conducted shortly after the event.²⁰⁾ On the basis of this report, sites where ground cracks and sand boils occurred in 1923 were identified, and then the local residents were interviewed. Both the report and the residents' remarks indicated that very large sand boils occurred at various locations along the Furu-Sumida Creek, the general area of which is shown in Figure 14.

According to the Geological Survey of Japan,²⁰⁾ at Kosuge Prison, site C in Figure 14, numerous ground cracks formed on the premises as seen in Figure 15, and sand and water gushed out of these cracks. The water flooded the premises to a depth of about 30 cm. Larger cracks formed in the yard west of the office building.

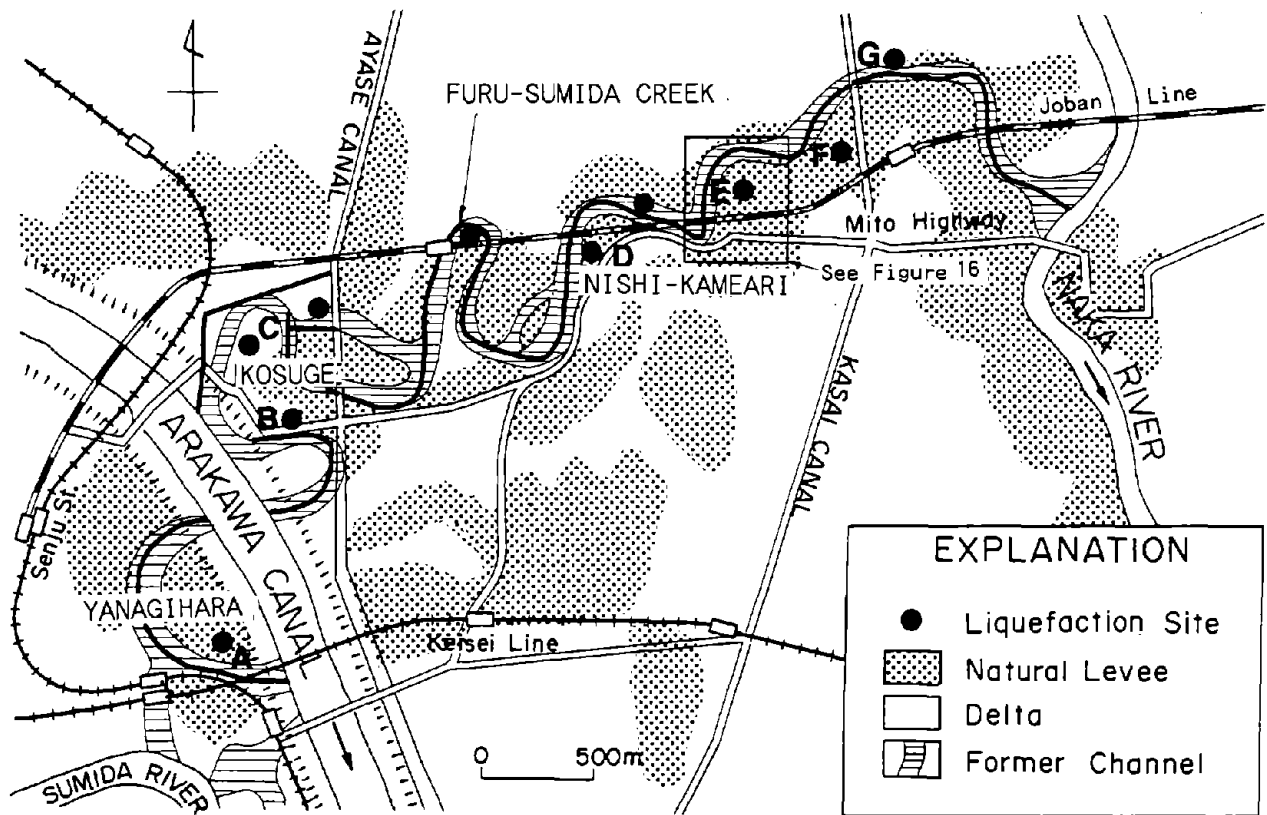


Figure 14 Map of Furu-Sumida Creek Area Showing Geographical and Geomorphological Features and Locations of Liquefaction

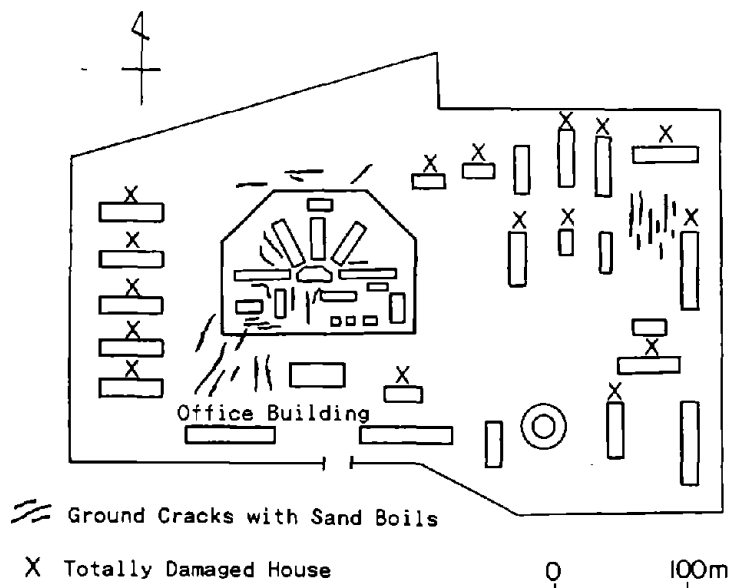


Figure 15 Plan View of Kosuge Prison Showing Locations of Ground Cracks and Totally Damaged House (Geological Survey of Japan, 1925)²⁰⁾

At least three of the cracks measured up of 1 m wide, were deeper than 1 m, and about 30 m in length.

At Nishi-Kameari, site F in Figure 14, extensive ground cracks, 0.3 m wide and several meters long, formed in east-to-west and south-to-north directions, and spewed out a large quantity of blue sand and water, which flooded the area. At Kameari, site G, numerous ground cracks occurred in the residential area and the bed of a creek rose to ground level or higher in a section between site E and site G in Figure 14 after the earthquake.

The interviews with the residents revealed that very large and violent sand boils occurred at several sites in addition to those mentioned above. On Yanagihara, a resident living in site A in Figure 14 told of three cracks with 0.4-0.5 m separations forming parallel to the Furu-Sumida creek in his garden. A considerable amount of water and blue-black clean sand spewed from the cracks and flowed into the adjacent road and field. The road was flooded with the expelled ground water to a depth of about 0.3 m. The floor and wall of his house were rent apart more than 0.5 m by the horizontal movement of the ground. The water well of his house which had been as deep as 11 m before the earthquake was filled with ejected sand and dried up. The depth of the well was measured of 3.6 m after the earthquake. The bottom of a pond and creeks near his house rose to ground level. In contrast, some places experienced large settlements during the earthquake. The 5.5 m high embankment of the Tobu Line experienced cracking in both length-wise and cross-wise directions, and settled about 4 m-5 m. The track became suspended in the air for about 300 m between the front of his house and Horikiri Station.

At Nishi-Kameari, site E in Figure 14, numerous ground cracks of about 0.5 m in width and 1.2 m in depth formed and spewed forth blue sand. Most of the ground surface was covered with boiled sand. No ground failure was observed south of the Joban Line at site E.

Figure 16 shows in detail the features of the ground failures at site E in Figure 14 as reported by the residents. For the area shown in Figure 16,

witnesses reported that there were only seven houses in the neighborhood and the greater part of the area consisted of fields at the time of the earthquake. Two houses were completely destroyed and another two suffered severe subsidence and became tilted. Ground cracks formed in the residential area and non-paddy fields. The cracks spewed forth blue sand, whereas only craters formed in the paddy fields. Numerous ground cracks, as wide as 50 cm, occurred west of the Takagi Shrine, as can be seen in Figure 16. These cracks spewed forth blue sand together with pieces of pumice. Sand boil deposits reached a thickness of 15 cm. In site B-1, two trees about 2 m tall and a wooden bathtub lying in the yard were lost under the ground. The earthen frame of a water well sank almost 1 m. The house settled more than 50 cm, and water came in through the floor boards. The neighborhood was flooded with expelled ground water to a depth of 1 m or more. The residents had to move around by boat for a few days following the earthquake. It took five or six days for the water to recede. These liquefaction effects, including ground cracks and sand boils, were especially pronounced west of the Takagi Shrine and north of site B-2 in Figure 16. Ground movement in the neighborhood was toward the Furu-Sumida Creek (to the west and north) closing the stream channel and pushing its bed up to more than 1 m above ground level after the earthquake. Figure 17 is how the Furu-Sumida River looks now. The channel was re-excavated after the earthquake.

These descriptions by the residents indicate that liquefaction and large horizontal displacements toward the Furu-Sumida River were generated in the areas of Yanagihara (site A in Figure 14), Nishi-Kameari (sites D-F), and Kameari (site G). Ground cracks and sand boils at each site occurred on the gentle slopes of the natural levees and the large cracks formed on the top of the levees, parallel to the river. Sand boils also occurred in the paddy field of the former channel along the Furu-Sumida Creek, but no surface evidence of liquefaction was reported on the delta. The permanent ground displacements of this area originated from the natural levee and moved in a direction toward the Furu-Sumida creek.

In the Furu-Sumida Creek area, ground failures, including ground cracks and sand boils, apparently have occurred during earthquakes in 1855 and 1894.

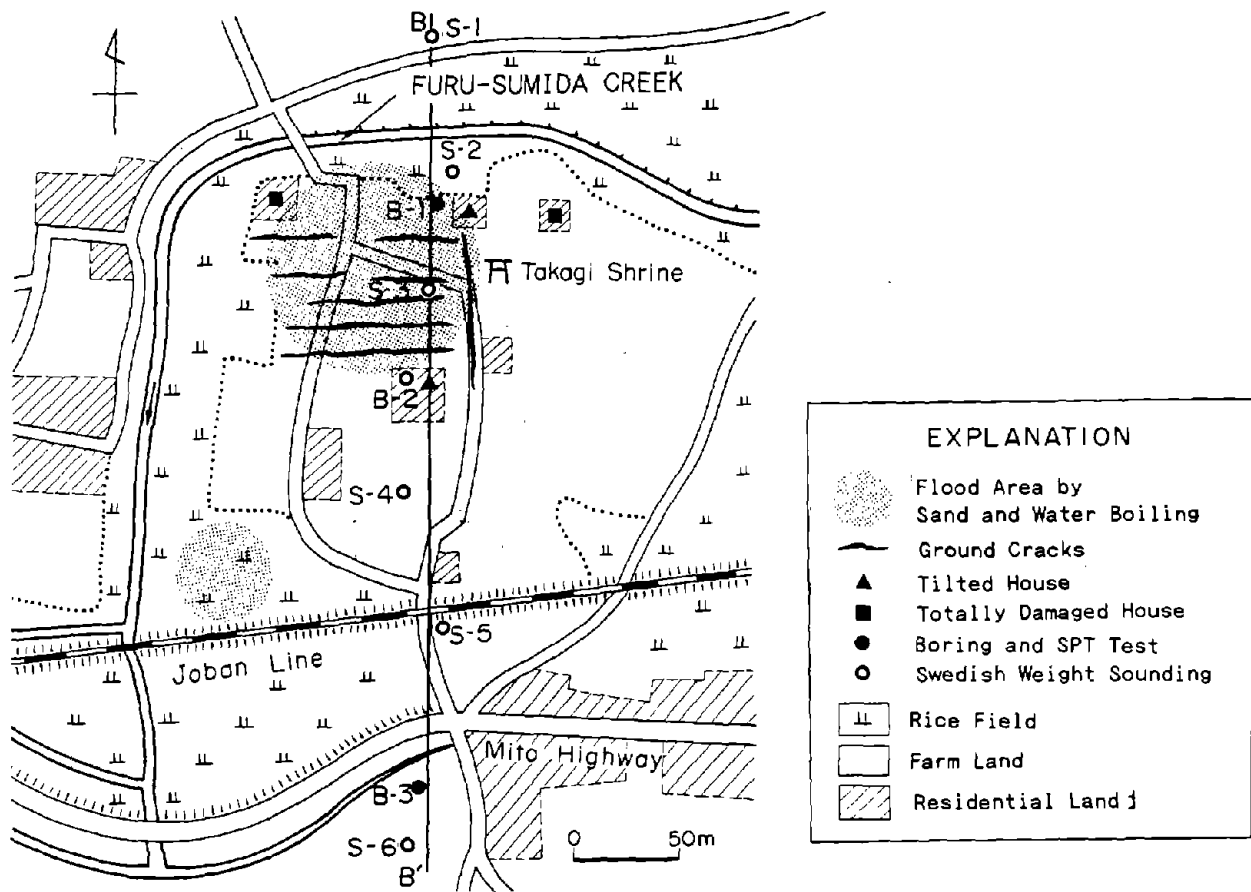


Figure 16 Map of Nishi-Kameari, Tokyo, Showing Geographic Features, Locations of Ground Failures, and Locations of Borings and Soundings for the Cross Section in Figure 18



Figure 17 View of Furu-Sumida Creek near Kosuge Prison: Photograph Taken in 1989

Residents indicated that some of the 1923 sand boils occurred in the same places as during previous earthquakes.

6.3 Damage to Structures as a Result of Ground Displacement

The Furu-Sumida Creek area was a sparsely populated agricultural zone at the time of the Kanto earthquake. There were no major structures except for several wooden houses and railways. According to the Geological Survey of Japan,²⁰⁾ the severest damage to houses was in Kosuge and Yanagihara, and the ratios of completely destroyed houses to the total number of houses in each area were 10.8% and 8.0%, respectively.

A damage report by the Japan Society of Civil Engineers¹²⁾ documented several instances. For example, the railway embankment of the Joban Line sunk a maximum of 0.3 m and cracked over a total distance of 1.6 km at four places in the Furu-Sumida Creek area. The abutments of a bridge over the Arakawa Canal, near site C in Figure 14, settled about 0.9 m on the right bank and 1.2 m on the left bank. A pier on the west bank side was displaced in the downstream direction. The movement of the pier might be a result of the movements in the direction of the Furu-Sumida Creek.

6.4 Subsurface Conditions and Estimation of the Liquefied Layer

Figure 18 shows a geotechnical section along the line B-B' in Figure 16 as interpreted from the bore hole data and Swedish weight sounding tests. The ground surface currently is nearly at sea level and slopes gently toward the Furu-Sumida Creek. The inclination of the ground is only 0.4% now, but it was a little steeper at the time of the earthquake. The difference in ground level was about 2 m between site B-2 and the river according to the residents, whereas, it is now about 0.5 m due to leveling after the earthquake.

The Holocene sediments in this section are about 30 m thick. About a 10 m thick layer of fine sand overlies a soft silty deposit in the northern part of the section. This layer becomes thinner towards the south, where it is

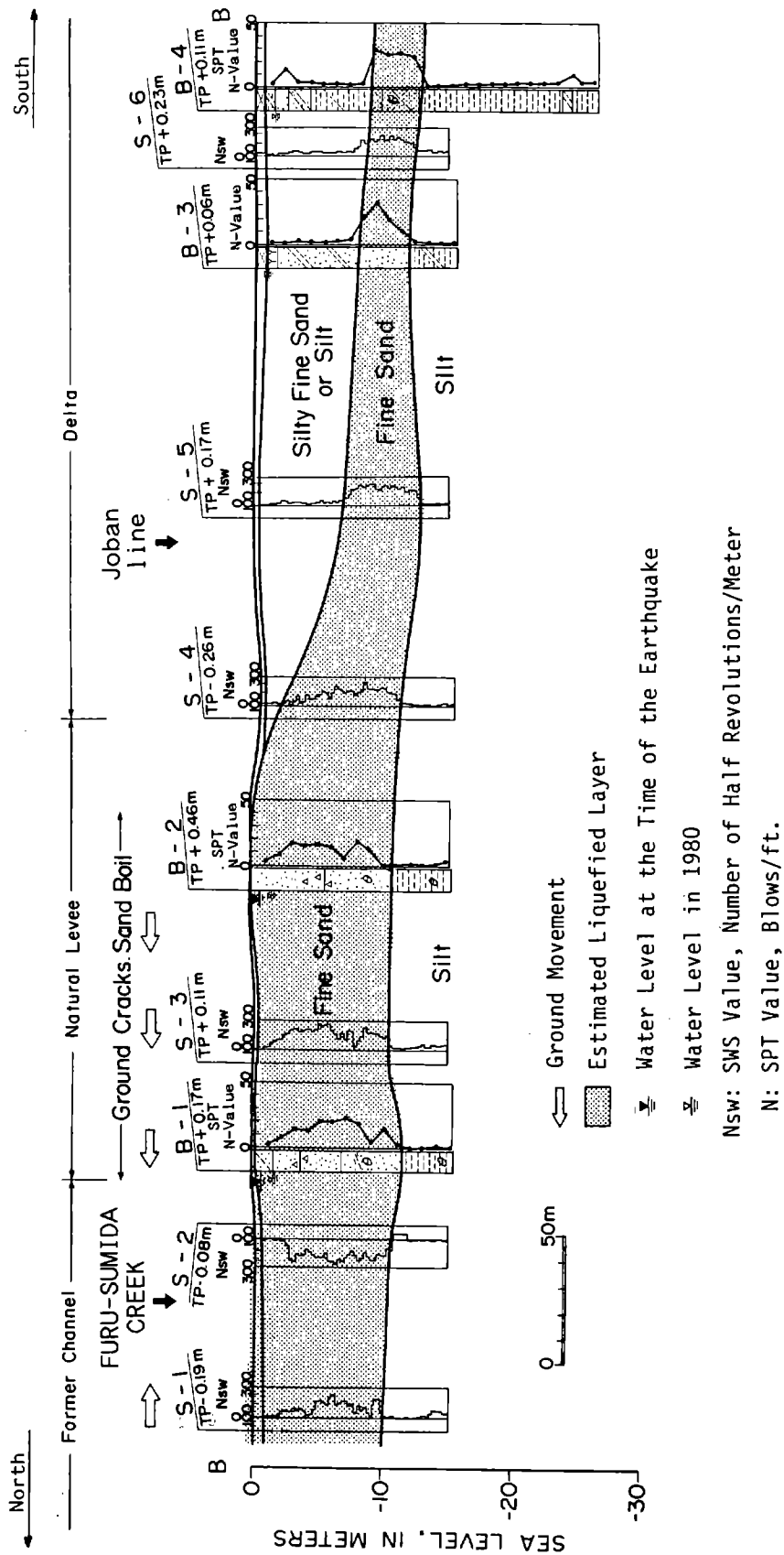


Figure 18 Cross Section of Sediments at Nishi-Kameari, Tokyo, Showing Geotechnical Features and Estimated Liquefied Layer

replaced or covered by a silty layer near S-4. Bore holes B-1 and B-2 encountered pieces of pumice at depths of 3.80-4.50 m and 4.05-6.50 m. This pumice was carried down from the Asama Volcano, which lies upstream of the Tone River. Pieces of shell at depths of 9 m were also encountered. These depositional features suggest the sedimentary environment of the sand layer: the upper part is natural levee deposit, the middle part is channel deposit, and the lower part is delta deposit.

The N-Values of standard penetration tests in the sand layer are less than 20 in the northern part of this section, and range between 20 and 30 blows in the southern part. The water table at the time of drilling (May 1990) was 1.7 m below the ground surface, but was estimated to have been only 0.3 m in 1923 based on the accounts of the residents. Blue sand boil deposits containing pieces of pumice indicate the liquefaction within the fine sand layer of channel deposit.

An estimation of liquefaction was conducted according to the procedures of the Japanese Highway Bridge Code.¹⁰⁾ The peak ground acceleration generated at the site was estimated at 0.25 g, and a 0.3 m water table was assumed. The results of the estimation show that the loose fine sand layer would be completely liquefied as indicated by the shaded portion in Figure 18.

The upper surface of the estimated liquefied layer is slightly inclined toward the river as is the ground surface. The estimated liquefied layer has a maximum thickness of 11 m in the section where severe ground cracks and sand boils occurred. On the contrary, in the section south of the Joban Line where no surficial effects of liquefaction were observed, it is about 3 m in thickness and covered with a 7-9 m thick non-liquefied layer.

Grain size distribution curves for samples taken from the sand layer in bore holes B-1 and B-2 are plotted in Figures 19 and 20, respectively. The sand taken from depths of 3 m and 6 m in bore hole B-1 and that of 3 m in B-2 is very clean and uniform.

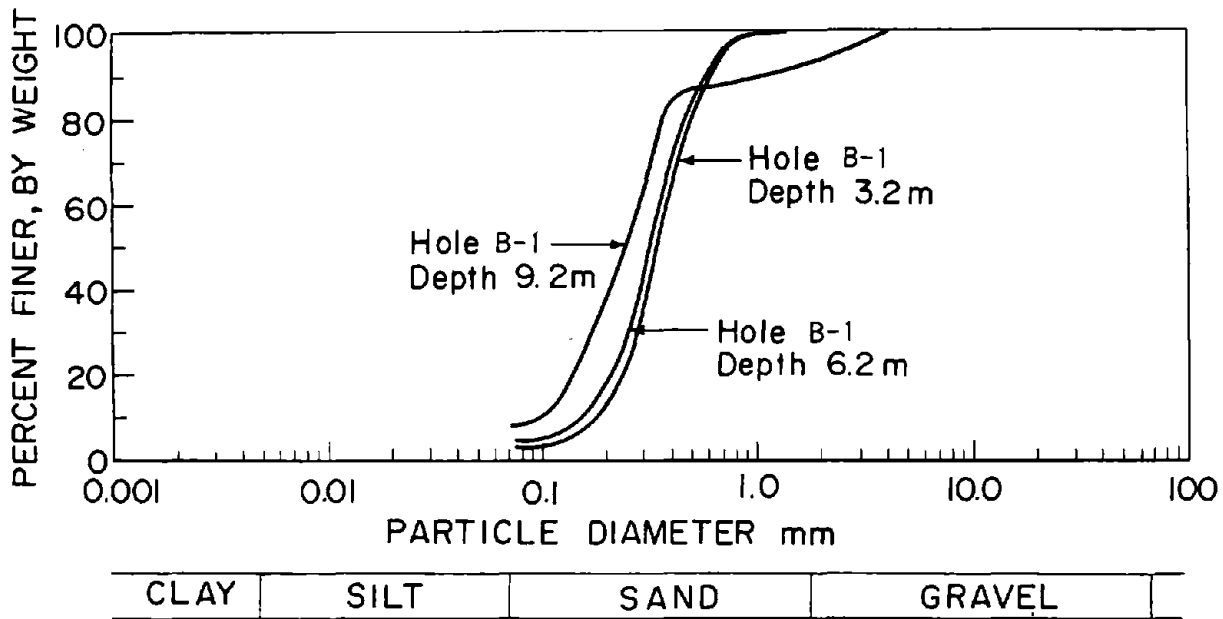


Figure 19 Grain Size Distribution Curves from Sand Layer at B-1, Nishi-Kameari, Tokyo

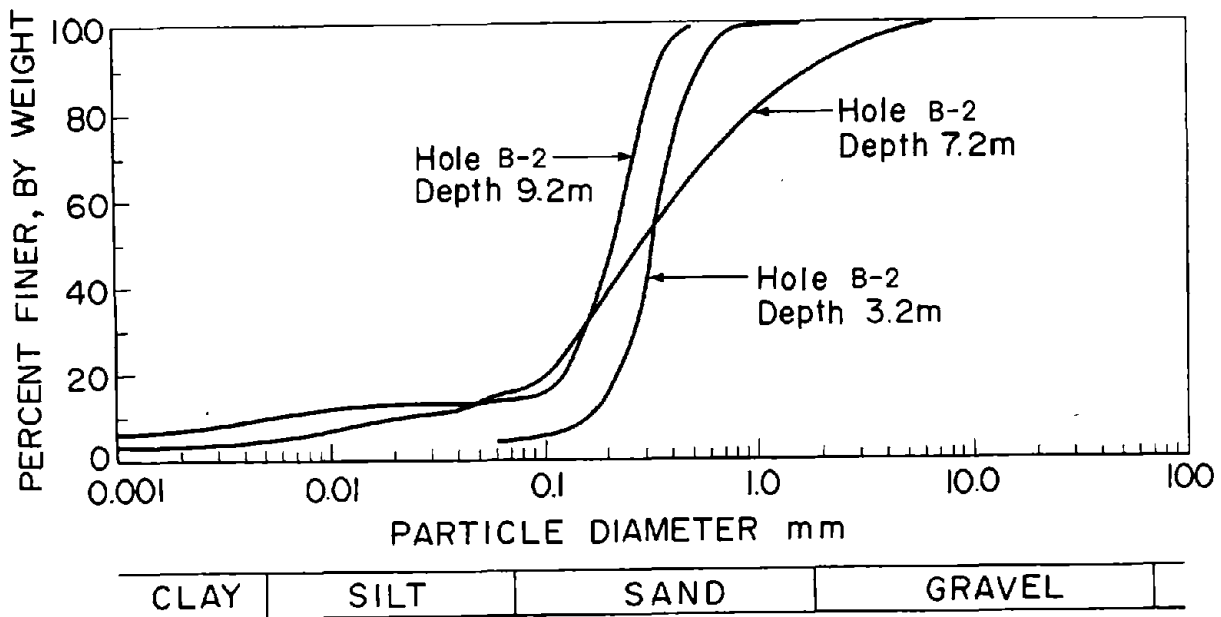


Figure 20 Grain Size Distribution Curves from Sand Layer at B-2, Nishi-Kameari, Tokyo

7.0 GROUND DISPLACEMENT AT KAWAKUBO AREA IN KASUKABE CITY, SAITAMA PREFECTURE

7.1 Geographical and Geomorphological Settings

The Kawakubo area of Kasukabe City is about 100 km northeast of the epicenter (site 5 in Figure 2). This region lies on the right bank of the Furu-Tone River which was the main stream of the Tone River before 1621, as was the Furu-Sumida Creek. Figure 21 shows the Furu-Tone River as it is today. "Furu-Tone" is the current name of the middle stream of the ancient Tone River and "Furu-Sumida" is that of the lower stream of the river. This river has developed typical fluvial geomorphological features that include well developed natural levees, a back marsh and a number of abandoned river channels.

7.2 Liquefaction-Induced Ground Displacement

The Geological Survey of Japan²⁰⁾ gives detailed accounts of numerous ground cracks and sand boils that formed along the Furu-Tone River and the Moto-Ara River during the 1923 earthquake (Figure 22). The characteristics of the ground cracks and sand boils in the Kawakubo area and its vicinity are summarized in Table 1. According to the Geological Survey of Japan,²⁰⁾ lumps of black clay containing pieces of decomposed wood are encountered 1.2 m below the ground surface and this layer is about 0.6 m thick. Pumice is contained in the aquifer lying around 3 m below the ground surface, and housing wells, which drew water from the aquifer, spewed out great quantities of sand.

Figure 23 is an aerial photograph of Kawakubo and surrounding areas, taken in 1947, the oldest photograph available of the areas. In the Kawakubo area, numerous ground cracks developed in residential areas and fields along the Furu-Tone River. These cracks vented large quantities of blue sand with occasional pieces of pumice as big as eggs and lumps of black clay containing rotted pieces of wood. The residential areas were flooded with expelled water up to or above floor level. The vented sands were deposited in the area to a thickness of 10 cm, and a nearby creek was choked with boiled sand.



Figure 21 View of Furu-Tone River in Kawakubo Area: Photograph Taken in 1989

Table 1 Ground Cracks Observed in Kasukabe Town Including Kawakubo Area (Geological Survey of Japan, 1925)²⁰

NAME OF SECTION	GROUND CRACK				AFFECTED AREA	
	Length	Width	Depth	Ejected Material	Land Use	Length or Area
MOTO-SHINJUKU	1440 m	0.3 m	0.3 m	Water, Sand, Pumice	Rice Field	1,915 acres
DOI	540 m	0.45 m	0.45 m	Water, Sand	Plough Field	2,837 acres
KAWAKUBO	1080 m	0.6 m	0.6 m	Water, Sand, Clay with rotten wood	Residential Area	336 acres
		0.9 m	1.8 m		Road	540 m
KAWAKUBO-SHINDEN	1800 m	0.6 m	0.45 m 1.8 m	Water, Sand, Clay with rotten wood	Drain	540 m

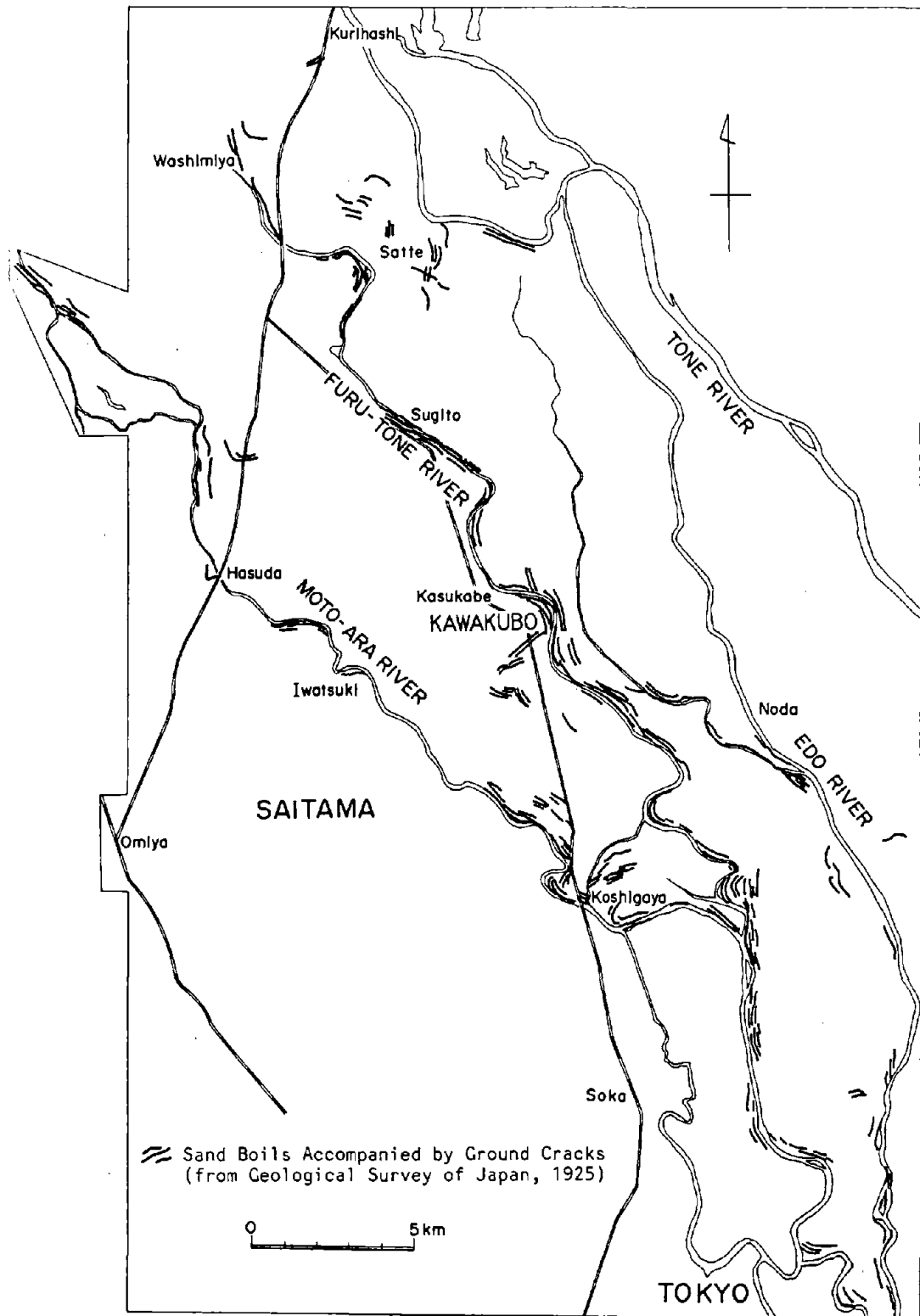


Figure 22 Map of Reaches of the Furu-Tone River and the Moto-Ara River Showing Locations of Ground Cracks and Sand Boils Caused by the 1923 Kanto Earthquake



Figure 23 Aerial Photograph of Kawakubo and Surrounding Areas Taken in 1947

After the earthquake, road running in front of a house cracked and became curved with a maximum displacement of 1.5 m toward the river over a distance of 70 m (Figure 24). Figure 25 shows the road as it is now, still curved. Many residents in this vicinity provided additional information about the ground failures and displacements that occurred during the 1923 event. They identified locations described in the existing damage report.²⁰⁾ The eyewitnesses recalled that the ground cracks reached a maximum of approximately 300 m in length, 2 m in width, with vertical offsets of 1-2 m. A bicycle and a wooden bathtub fell into the cracks and were never found. Many houses partially collapsed because their foundations fractured and split apart due to the ground cracks. The ground in this neighborhood apparently moved in a direction toward the river, and the area along the Furu-Tone River subsided.

Figure 26 shows the geomorphological features and distribution of ground failures in the Kawakubo area as identified by the Geological Survey of Japan²⁰⁾ and the residents. An old stream channel can be seen along the Furu-Tone River. This indicates that the old Furu-Tone River was much wider than that of the current river. Well developed natural levees had formed along the old stream channel. After the river narrowed, new natural levees formed on the former channel in the form of an island. The areas where the road became curved and many houses collapsed are all located within the new levees and the old river channel.

7.3 Damage to Structures

This locality was also an agricultural area in 1923, as were the other two areas. Damage to wooden houses was only documented in the damage report:²⁰⁾ the damage ratios of completely destroyed houses and partially destroyed houses to the total number of houses were 17.7 and 17.4%, respectively, in Kasukabe City including the Kawakubo area. Interviews with the residents revealed that most of the houses in the Kawakubo area were partially destroyed when their foundations were torn apart by ground deformation. Houses in areas, where no prominent ground failures were observed, were completely damaged by seismic shaking.

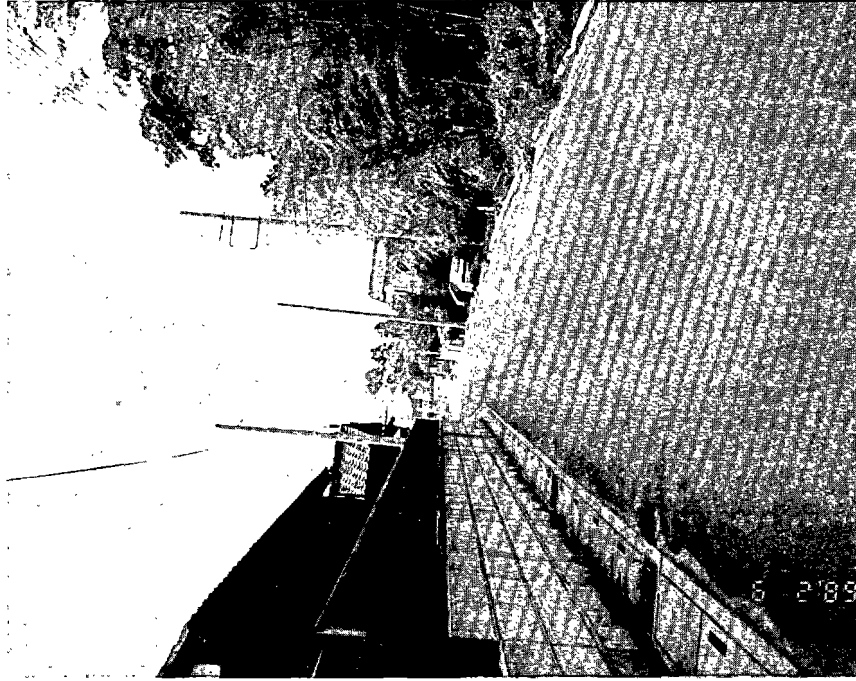


Figure 25 View of Curved Road Shown in Figure 24:
 Photograph Taken in 1989 (Looking South)

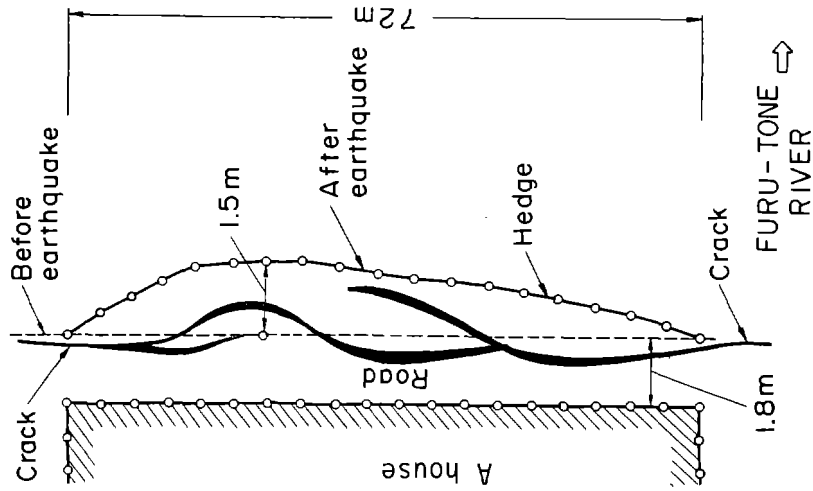


Figure 24 Ground Cracks and Offset Displacement
 in Roadway in Kawakubo Area (Geological
 Survey of Japan, 1925)20)

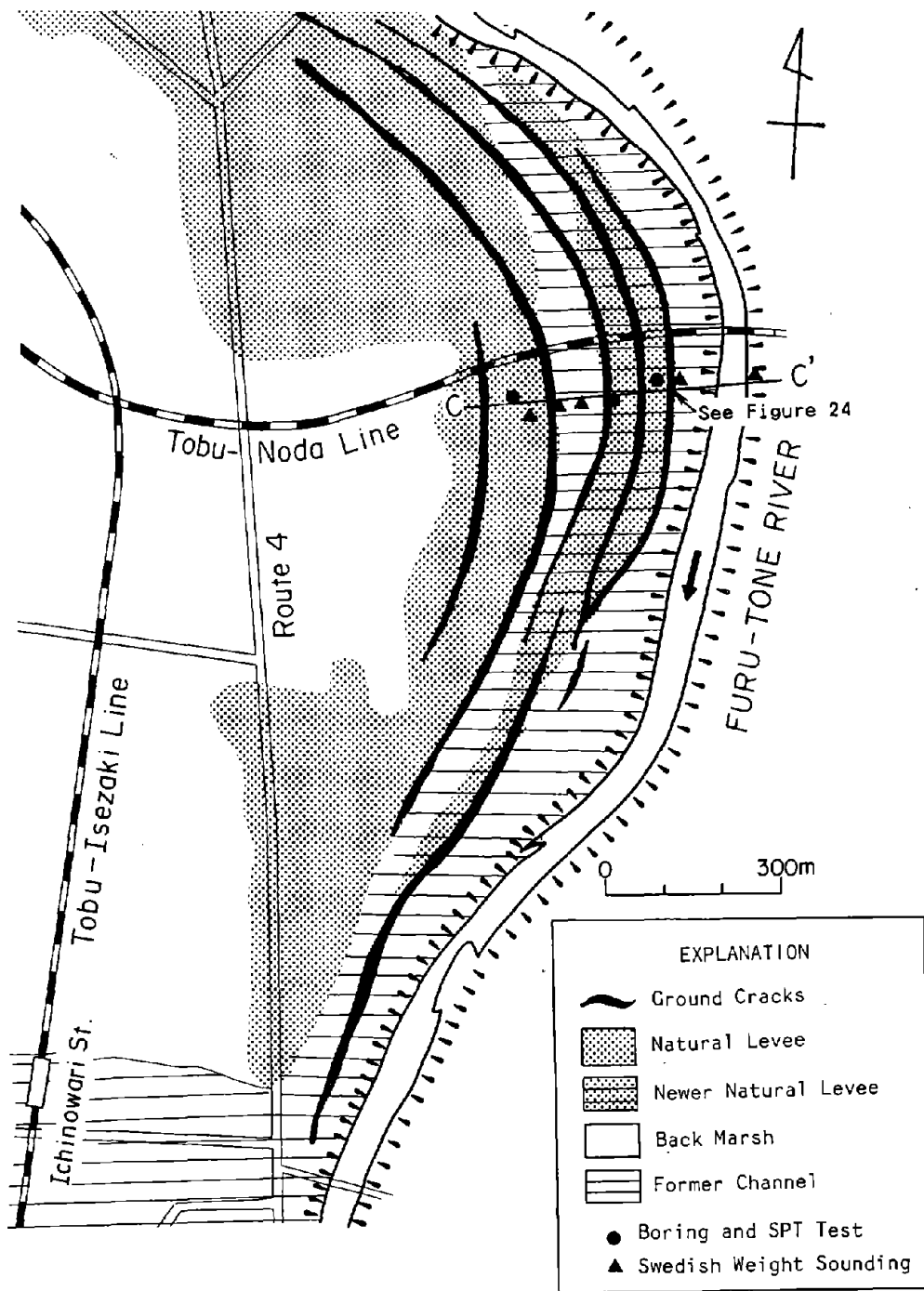


Figure 26 Geomorphological Land Classification Map of Kawakubo Area Showing Locations of Ground Cracks and Locations of Borings and Soundings for the Cross Section C-C' in Figure 27

7.4 Subsurface Conditions and Estimation of Liquefied Layer

Figure 27 is a soil profile along the line C-C' in Figure 26 as interpreted from the bore hole data and Swedish weight sounding data. The present ground surface is 5-7 m above sea level and slopes gently toward the Furu-Tone River with a few undulations. The average slope is only 0.7%, almost the same as the Nakajima area in Chigasaki City. A small mound as high as 1.5 m is present along the boundaries of the natural levees and former river channel.

The Holocene deposits in this area are about as thick as 30 m. The water table in the section at the time of drilling (June 1989) ranged from 0.45 m-2.40 m below the ground surface. The fill, which has a thickness of 0.9-1.8 m, is composed of clay, silt, and sand containing fine gravel, peat or debris, and was probably formed after the 1923 event. Beneath the fill, fine and medium sand layers about 5 m thick overlie very soft marine silt. The sand layers contain no fragments of marine shells, but do contain pieces of pumice originating from the Asama Volcano lying upstream of the ancient Tone River. This indicates that the depositional environment of this sand is natural levee and river channel.

The grain size distribution curves for samples taken from the sand layers in bore holes B-1 and B-2 are plotted in Figure 28. Bore holes B-1 and B-2 are located on the older natural levees and the newer natural levee, respectively. The fines content of the sample from bore hole B-1 is 29%, whereas that from B-2, where the displacement occurred, is less than 10%. The grain size of the samples from bore hole B-2 are uniform, and are very similar to those of the Nishi-Kameari area shown in Figures 19 and 20. It can be conjectured that the fine and medium sand underlying the old river channel liquefied during the earthquake.

An estimation of liquefaction based on the procedure outlined in the Japanese Highway Bridge Code¹⁰⁾ was also conducted, assuming that a peak acceleration of 0.20 g occurred at the site. According to the estimation, the sand layer underlying the areas within the former and present river channels, liquefied as shown by the shaded portion in Figure 27.

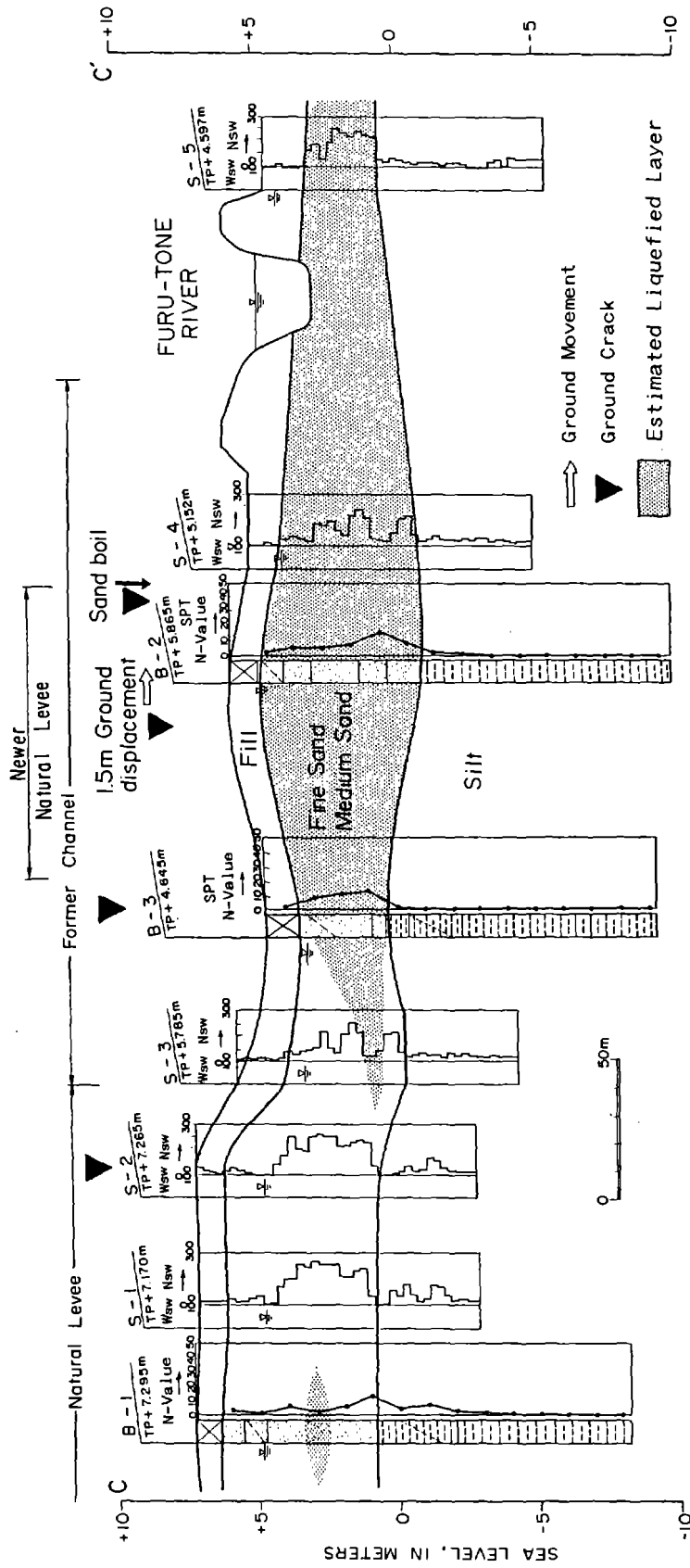


Figure 27 Cross Section of Sediments at Kawakubo Showing Geotechnical Features and Estimated Liquefied Layer

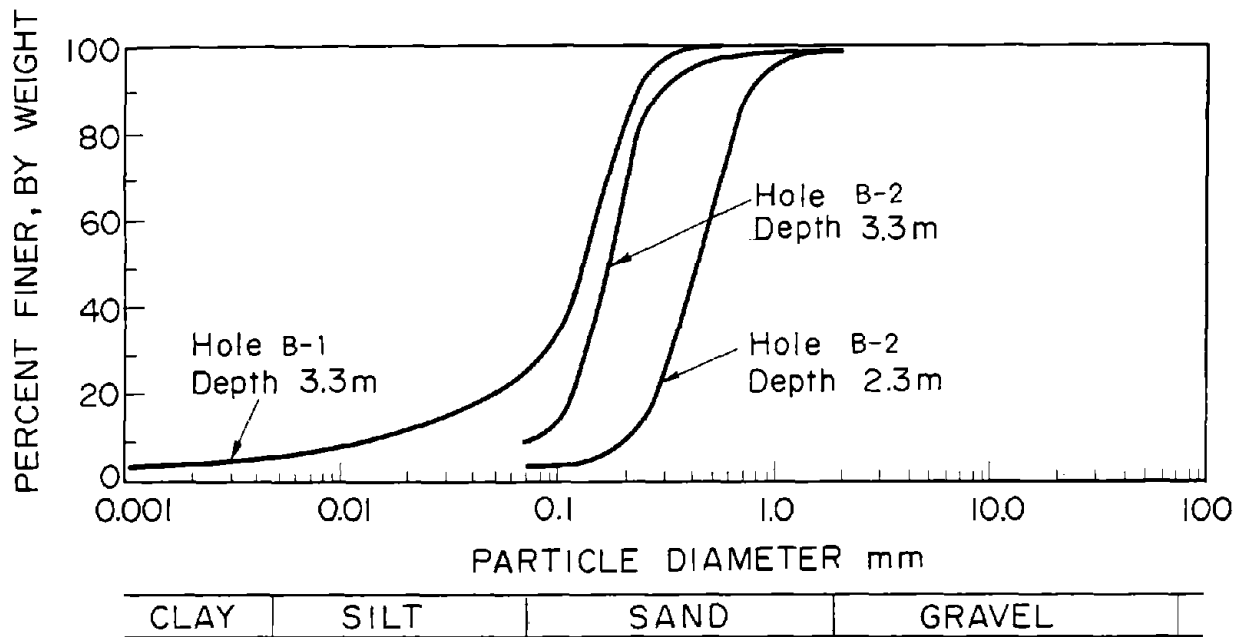


Figure 28 Grain Size Distribution Curves from Sand Layer at Kawakubo Area

8.0 CONCLUSION

The following characteristics can be summarized from the case study of the liquefaction-induced ground failures and their related damage to structures during the 1923 Kanto earthquake:

- (1) Liquefaction-induced ground failures occurred widely in many locations in the Tokyo Metropolitan area during the 1923 Kanto earthquake. The most distant location is about as far away as 150 km northeast of the epicenter.
- (2) Three areas were identified where large horizontal ground displacement had been induced by the earthquake. The magnitude of the permanent displacement was estimated to be as large as several meters.
- (3) The ground displacements occurred from a topographically higher site such as natural levees and former channel bars toward small rivers. These rivers were only several meters wide at the time of the earthquake but had been much wider a few centuries before the earthquake.

(4) Typically, the ground surfaces at displacement sites are inclined slightly toward the direction of ground movements. The surface gradients generally are very small, being less than 1%.

(5) The ground water levels at the sites are 0.5 m-2.0 m below the ground surface, according to recent bore hole data, and are inclined slightly in the direction of observed ground movements.

(6) The depth and extent of the liquefied layers were identified by the procedure of the Japanese Highway Bridge Code as well as a comparison between soil ejected during the earthquake and samples from the bore holes. The characteristics of the liquefied layers can be summarized as follows:

- (i) Upper boundaries of the estimated liquefied soil layers are at a depth 0.3-2 m below the ground surface and are slightly inclined in the direction of observed ground movements, consistent with the inclination of the ground surfaces and ground water levels.
- (ii) The thickness of the estimated liquefied soil layers range from 3 m to a maximum of 11 m.
- (iii) Grain size distribution curves of the samples taken from the Furu-Sumida Creek area and Kawakubo area show that they are clean, uniform and medium to fine sands. However, the samples from the Nakajima area of Chigasaki City are coarse and well drained. In this area, it is probable that the low permeability of the surface sediments promoted the development of excess pore water pressure of the underlying gravelly layers, thereby resulting in liquefaction and ground deformations.

(7) Sand boils recurred in several locations during successive large earthquakes. This fact indicates that sites of past liquefaction are likely to liquefy if soil and groundwater conditions remain unchanged.

REFERENCES

- 1) Youd, T.L. and Hoose, S.N., "Liquefaction during 1906 San Francisco Earthquake," Journal of the Geotechnical Engineering Division, ASCE, Vol. 102, No. GT5, pp. 425-439, 1976
- 2) O'Rourke, T.D., Beaujon, P.A. and Scawthorn, C.R., "Large Ground Deformations and Their Effects on Lifeline Facilities: 1906 San Francisco Earthquake," Technical Report NCEER-91-00002, National Center for Earthquake Engineering Research, Buffalo, N.Y., Feb. 1992.
- 3) Hamada, M., "Large Ground Deformations and Their Effects on Lifelines: 1964 Niigata Earthquake," This volume.
- 4) Youd, T.L., "Landslides in the Vicinity of the Van Norman Lakes," U.S. Department of Commerce, The San Fernando, California Earthquake of Feb. 9, 1971, Geological Survey Professional Paper 733, 1971
- 5) O'Rourke, T.D., Roth, B.L. and Hamada, M., "Large Ground Deformations and Their Effects on Lifeline Facilities: 1971 San Fernando Earthquake," Technical Report NCEER-91-0002, National Center for Earthquake Engineering Research, Buffalo, N.Y., Feb. 1992.
- 6) Hamada, M., "Large Ground Deformations and Their Effects on Lifelines: 1983 Nihonkai-Chubu Earthquake," This volume.
- 7) Hamada, H., Yasuda, S., Isoyama, R. and Emoto, K., "Study on Liquefaction Induced Permanent Ground Displacement," Association for the Development of Earthquake Prediction, Tokyo, Japan, 1986
- 8) Usami, T., "New Edition, Catalogue of Damaging Earthquakes in Japan," Univ. of Tokyo Press., 1987 (in Japanese)
- 9) Ando, M., "Seismo-Tectonics of the Kanto Earthquake," Journal of Physics of the Earth, Vol. 22, pp. 263-277, 1974

- 10) Japan Road Association, "Specifications for Highway Bridges," Part V Earthquake Resistant Design, 1980.
- 11) Imperial Earthquake Investigation Committee, "Reports of the Imperial Earthquake Investigation Committee," Tokyo, Japan, No. 100, Volume B, 1925 (in Japanese)
- 12) Japan Society of Civil Engineers, "Damage Reports on the Kanto Earthquake of 1923," Vol. 1-3, 1927 (in Japanese)
- 13) Ishii, K., "Wells in Katase Kaigan," Journal of Earth Science, Vol. 35, pp.544, 1923 (in Japanese)
- 14) Kotoda, K., Wakamatsu, K. and Watanabe, K., "Ground Damage in the Lower Reaches of the Sagami River due to the Great Kanto Earthquake of 1923," Proceedings, Seventh Japan Earthquake Engineering Symposium, Tokyo, Japan, pp. 43-48, 1986 (in Japanese with English abstract)
- 15) Association for the Development of National Education (Kokumin Kyoiku Fukyukai), "Photo Album of the Great Kanto Earthquake," 1926 (in Japanese)
- 16) Chigasaki City, "History of Chigasaki City," Japan, 1970 (in Japanese)
- 17) Seed, H.B., Tokimatsu, K., Harder, L.F., and Chang, R.M., "Influence of SPT Procedures in Soil Liquefaction Resistance Evaluations," Journal of Geotechnical Engineering, Vol. 111, No. 12, ASCE, New York, N.Y., pp. 1425-1445, 1985
- 18) Kanto Headquarters of Martial Law, "Photo Album of the Great Kanto Earthquake," 1924 (in Japanese)
- 19) Kokusho, T., Yoshida, Y., and Nagasaki, K., "Evaluation of Aseismic Strength of Dense Sand Layer due to Spt N-Value," Proceedings, Japan National Conference on Soil Mechanics and Foundation Engineering, pp. 559-562, The Japanese Society of Soil Mechanics and Foundation Engineering, Tokyo, Japan, 1984 (in Japanese)

- 20) Geological Survey of Japan, "Report on the Kanto Earthquake, Vol. 1 and Vol. 2," 1925 (in Japanese)



Large Ground Deformations and Their Effects on Lifelines: 1948 Fukui Earthquake

*M. Hamada, Professor
School of Marine Science and Technology
Tokai University
Shimizu, Shizuoka, Japan*

*S. Yasuda, Associate Professor
Faculty of Civil Engineering
Kyushu Institute of Technology
Kitakyushu, Japan*

*K. Wakamatsu, Research Associate
Science and Engineering Research Laboratory
Waseda University
Tokyo, Japan*

ACKNOWLEDGEMENTS

This case study of large ground deformations and damage to structures caused by the 1948 Fukui earthquake was conducted by the Japanese research team as part of the U.S.-Japan Cooperative Research on "Liquefaction, Large Ground Deformations, and Their Effects on Lifeline Facilities," organized by the Association for Development of Earthquake Prediction, Tokyo, Japan. Permanent ground displacements were measured at more than 200 points in Morita-cho, Fukui City using aerial photographs taken before and after the earthquake. Besides collecting existing borehole data, 32 Swedish weight sounding tests were conducted in the area where large ground deformations occurred. Furthermore, information about the occurrence of ground failures, such as fissures and sand boils, was collected through interviews with people residing in this area at the time of the earthquake. Existing documentation on the damage to structures caused by liquefaction and associated ground deformation was re-examined.

We wish to express our appreciation to those who provided valuable assistance in carrying out this case study. In particular, thanks are extended to Prof. K. Kubo, who chaired the research committee of the Japanese research team. Existing data on soil conditions and on damage to structures were collected by students of Tokai University, who also undertook the soil surveys in Fukui City. We want to thank Mr. M. Koshimizu, Mr. M. Ochi, Mr. Y. Kojima, and other students at Tokai University for their great contribution to this case study.

Special gratitude is extended to Miss Jane Stoyale, director of the Information Center of the National Center for Earthquake Engineering Research, at Buffalo, N.Y. for her great efforts to collect photographs and other materials about the earthquake, which had been collected by the U.S. Army and preserved in the U.S.A.

Finally, our deepest appreciation to Prof. T.D. O'Rourke at Cornell University for his excellent editing of this case study.

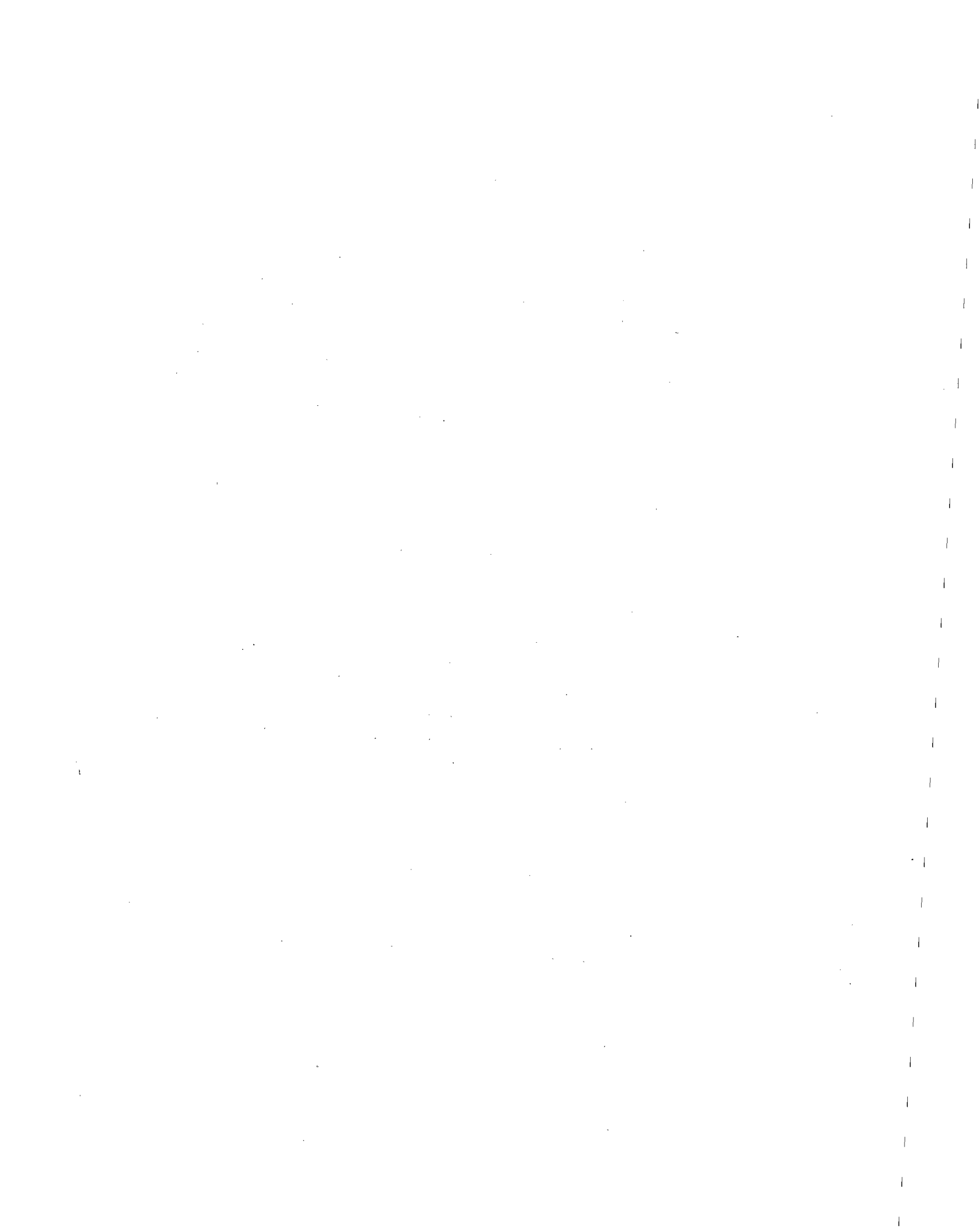


TABLE OF CONTENTS

	<u>Page</u>
Acknowledgements	2-iii
Table of Contents	2-v
List of Figures	2-vii
List of Tables	2-ix
List of Photos	2-xi
 <u>Section</u>	
1.0 INTRODUCTION	2-1
2.0 OUTLINE OF THE 1948 FUKUI EARTHQUAKE	2-3
2.1 Epicenter, Magnitude, and Intensity	2-3
2.2 Strong Motion Data	2-3
2.3 Damage to Houses	2-3
2.4 Liquefaction and Resulting Damage	2-6
2.4.1 Northern Area of The Plain: Takeda, Hyogo, and Tajima River Areas	2-6
2.4.2 Central Area of The Plain: Main Channel Area of Kuzuryu River	2-10
2.4.3 Southern Area of The Plain: Fukui City, and the Asuwa and Hino River Areas	2-14
3.0 LIQUEFACTION-INDUCED GROUND DISPLACEMENTS	2-15
3.1 Measurement of Permanent Ground Displacements	2-15
3.2 Permanent Ground Displacements and Ground Failures	2-17
3.3 Soil Conditions	2-25
4.0 INTERVIEWS WITH EYEWITNESSES OF THE EARTHQUAKE ABOUT GROUND FAILURES AND DAMAGE TO HOUSES	2-28
4.1 Shimomorita-Sakuramachi Area	2-28
4.2 Uenohonmachi Area	2-31
4.3 Summary of Eyewitness Remarks	2-33

	<u>Page</u>
5.0 CONCLUSIONS	2-34
References	2-36
Appendix A Accuracy of Permanent Ground Displacement Measurements in Fukui City	2-38
Appendix B Soil Conditions and Evaluation of Soil Layers Susceptible to Liquefaction	2-39

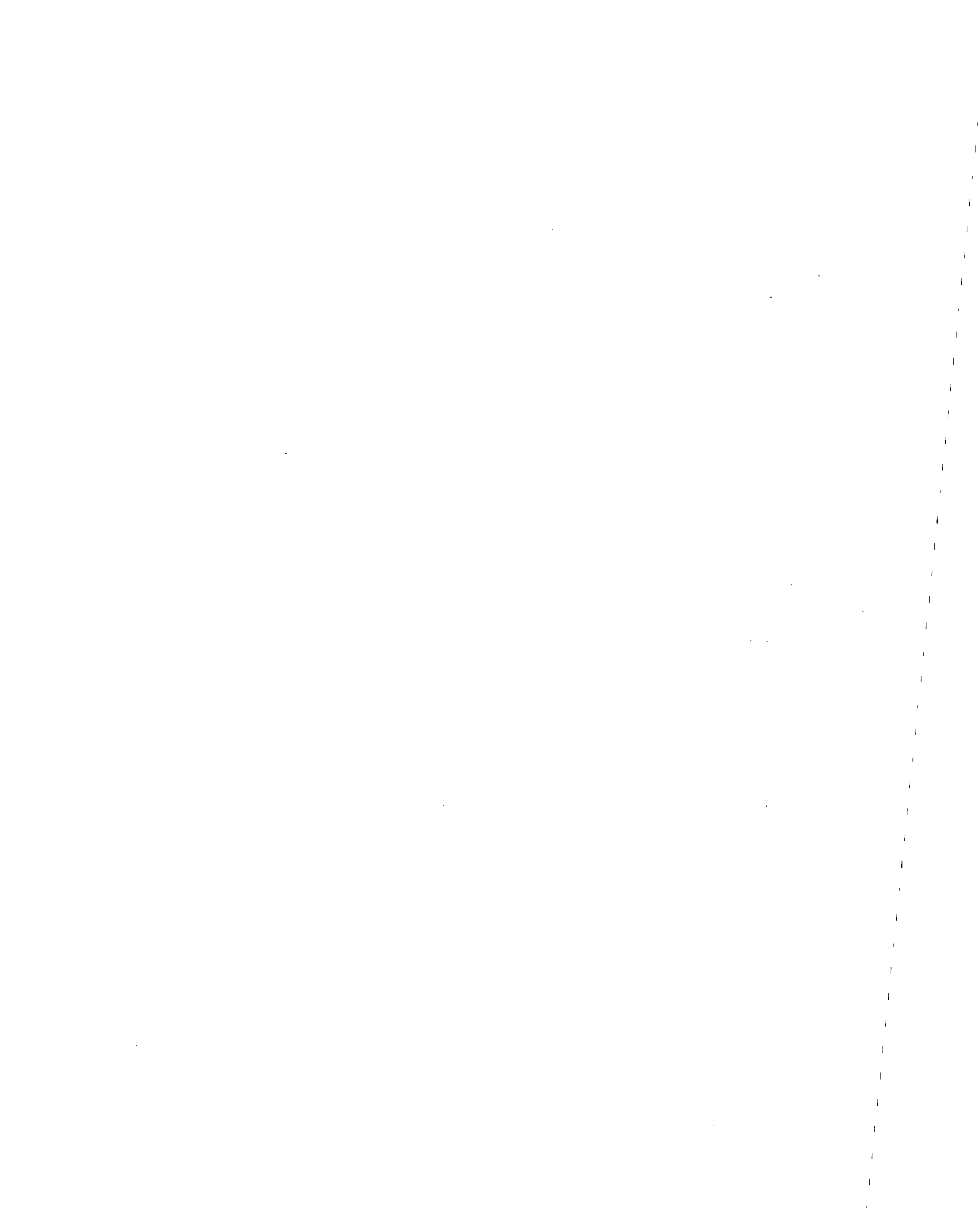
LIST OF FIGURES

<u>Figure</u>		<u>Page</u>
1	Fukui Plain and Epicenter of 1948 Fukui Earthquake	2-4
2	Seismic Intensity on Japan's Honshu Island (JMAI)	2-4
3	Seismogram (Displacement) Recorded at Central Meteorological Observatory in Tokyo	2-5
4	Depth of Alluvial Deposits under Fukui Plain	2-5
5	Ratio of Totally Destroyed Houses on Fukui Plain	2-7
6	Sand Boils and Ground Fissures on Fukui Plain	2-8
7	Damage to Nagaya Bridge (Point ① in Figure 6)	2-9
8	Damage to Nagaune Bridge (Point ② in Figure 6)	
	(a) Sinking of Piers	2-9
	(b) Structure of Piers	2-9
9	Damage to Nakatsuno Bridge (Point ③ in Figure 6)	2-11
10	Damage to the JNR Bridge (Point ④ in Figure 6)	2-12
	(a) Elevation	
	(b) Plan	
	(c) Pier	
11	Inclined Electricity Pylon (Point ⑦ in Figure 6)	2-14
12	Morita-cho and Area for Measurement of Permanent Ground Displacements	2-16
13	Permanent Ground Displacements and Ground Failures	
	(a) West Zone	2-18
	(b) East Zone	2-19
14	Permanent Ground Displacements on Contour Map	
	(a) West Zone	2-20
	(b) East Zone	2-21
15	Correlation between Permanent Ground Displacement and Surface Gradient	2-23
	(a) Case A (Horizontal Distance = 25 m)	
	(b) Case B (Horizontal Distance = 50 m)	

<u>Figure</u>		<u>Page</u>
16	Geographical Features Interpreted from Aerial Photographs	2-23
17	Section Lines for Soil Condition Survey	2-26
18	Soil Condition Profiles	
	(a) Section 4-4'	2-27
	(b) Section 5-5'	2-27
19	Ground Failures in the Vicinity of Hakusan Shrine	2-29
20	Ground Failures in Shimomorita-Sakuramachi and Vicinity	2-29
21	Ground Failures in the Uenohonmachi Area	2-32
B-1	Soil Conditions and Evaluation of Soil Layers Susceptible to Liquefaction	
	(a) Section 1-1'	2-40
	(b) Section 2-2'	2-40
	(c) Section 3-3'	2-41
	(d) Section 4-4'	2-41
	(e) Section 5-5'	2-42

LIST OF TABLES

<u>Table</u>		<u>Page</u>
A-1	Accuracy of Measurement of Permanent Ground Displacements at Morita-cho in Fukui City	2-38



LIST OF PHOTOS

<u>Photo</u>		<u>Page</u>
1	Central Fukui City after the Earthquake	2-7
2	Sand Boils along the Main Channel of the Kuzuryu River	2-8
3	Collapse of Nakatsuno Bridge (Point ③ in Figure 6)	2-11
4	Collapse of the JNR Bridge (Point ④ in Figure 6)	
	(a) Aerial View of Damage	2-12
	(b) Damage to Pier 6	2-13
5	Toppled Locomotive in JNR Fukui Marshalling Yard (Point ⑤ in Figure 6)	2-13
6	Platform Subsidence of Fukui JNR Station (Point ⑥ in Figure 6)	2-13
7	Aerial Photographs Used for Measurement in Morita-cho and Vicinity	
	(a) Before the Earthquake	2-16
	(b) After the Earthquake	2-16
8	Road Curvature due to Permanent Ground Displacement (Point ⑧ in Figure 21)	
	(a) Before the Earthquake	2-32
	(b) After the Earthquake	2-32

1.0 INTRODUCTION

The Fukui earthquake, with an epicenter below the eastern part of the Fukui Plain, occurred at 16:13 on June 28, 1948. The magnitude of the earthquake was 7.1, and the focal depth was 30 km. Figure 1 is a map of the Fukui Plain showing the location of the epicenter.

This earthquake, with its hypocenter directly under a broad alluvial plain, caused severe damage for its magnitude. Claiming more than 5,000 lives and completely destroying about 35,000 houses, it is considered to have been the most disastrous seismic event in Fukui Prefecture's history.

Japan was under occupation at the time. The General Headquarters Far East Command (GHQ) carried out a detailed investigation of the earthquake, and collected an extensive record of aerial photographs taken before and after the event.¹⁾ The newly established Science Council of Japan organized a special committee to investigate the Fukui earthquake,²⁾ and an overall investigation and survey was conducted. In addition, the Meteorological Agency,³⁾ the Geographical Survey Office,^{4),5)} the Japan Society of Civil Engineers,⁶⁾ the Architectural Institute of Japan,⁷⁾ Fukui Prefectural Government,^{8),10)} and many other organizations⁹⁾ recorded valuable information on the basis of field surveys.

Besides re-examining the existing reports by these organizations from the viewpoint of liquefaction-induced ground displacements and the damage to structures caused by them, measurements were made of ground displacements in Morita-cho, Fukui City by using the aerial photographs taken by GHQ before and after the earthquake.

The authors also conducted investigations of soil conditions, both by collecting already existing borehole data and also by performing Swedish weight sounding tests (SWS)¹¹⁾* at about 32 points in the area where

*See Appendix C of reference 11).

permanent ground displacements were observed. Furthermore, interviews were held with eyewitnesses to collect information about the occurrence of ground failures and damage to structures.

2.0 OUTLINE OF THE 1948 FUKUI EARTHQUAKE

2.1 Epicenter, Magnitude, and Intensity

The earthquake occurred at 16:13 on June 28, 1948. It registered magnitude 7.1 and affected the western half of Japan's main Honshu Island. The epicenter was about 10 km northeast of Fukui City at coordinates $36^{\circ}07'N$ and $136^{\circ}15'E$. The focal depth of the earthquake was about 30 km. Because the hypocenter was located directly under an alluvial plain, there were many areas of particularly severe damage. The seismic intensity on the Japanese Meteorological Agency Intensity Scale (JMAI) on the Fukui Plain was VI, which is the second highest level, and is roughly equivalent to IX on the Modified Mercalli Intensity Scale (MMI). Generally, the maximum acceleration at the ground surface in an area of intensity VI (JMAI) is estimated to be in the range 0.25 to 0.40 g. As shown in Figure 2, the area suffering an intensity of IV was extensive, including Kyoto and Nagoya, and the earthquake affected a vast area of Honshu Island.

2.2 Strong Motion Data

In Fukui and neighboring areas no seismogram was recorded. Figure 3 shows the displacement of the ground surface recorded at the Central Meteorological Observatory in Tokyo, about 250 km from the epicenter. The maximum displacement was 4.9 cm in the N-S direction, 2.4 cm E-W, and 2.2 cm vertically.

2.3 Damage to Houses

The Fukui earthquake was very destructive to houses on the Fukui Plain. The large-scale damage can be attributed to four factors. One is that the epicenter was very close to the urbanized areas of Fukui City. Secondly, the earthquake motion appeared to be greatly amplified by the soft deposits of alluvial plain. Figure 4 shows contours of depth for the alluvium in the Fukui Plain. The depths of alluvial sediments range typically from 10 to 60 m. The third factor was the extensive liquefaction which occurred

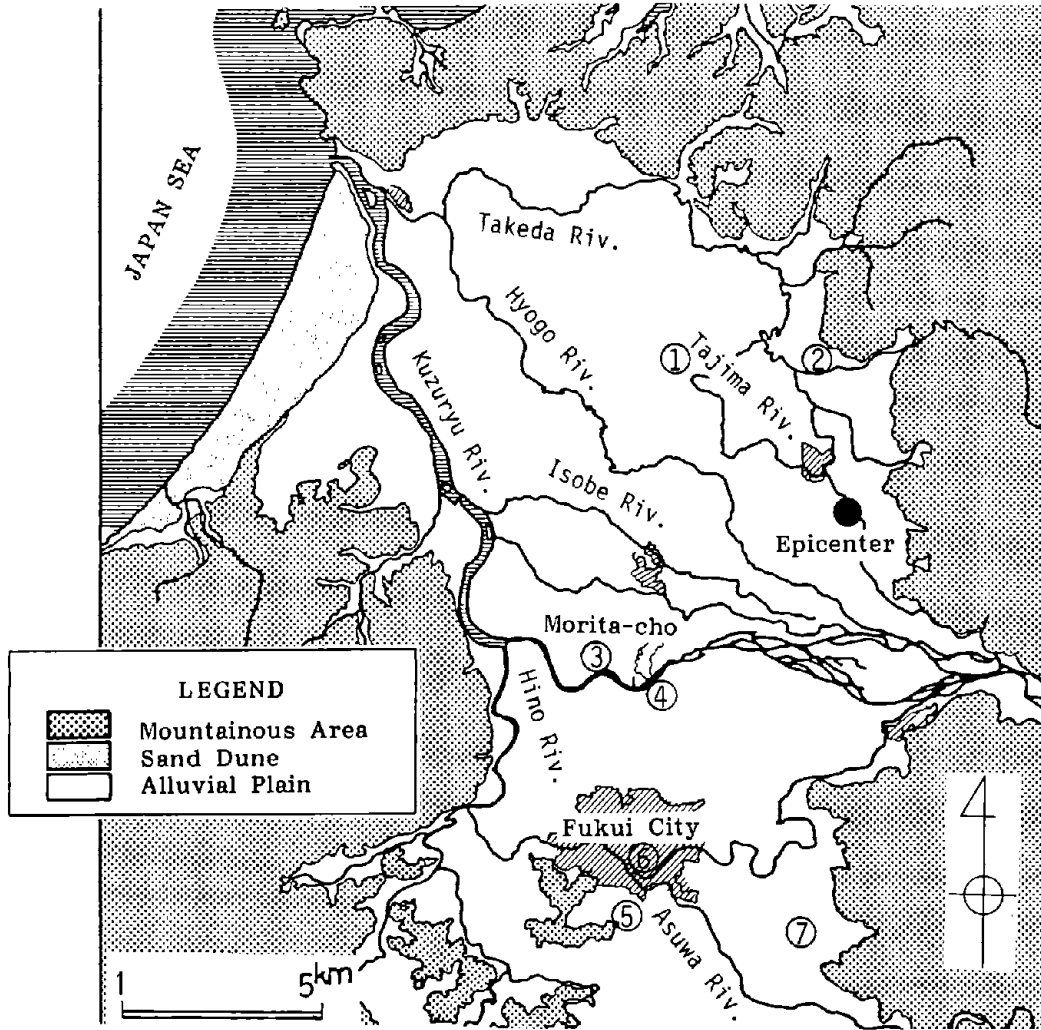


Figure 1. Fukui Plain and Epicenter of 1948 Fukui Earthquake

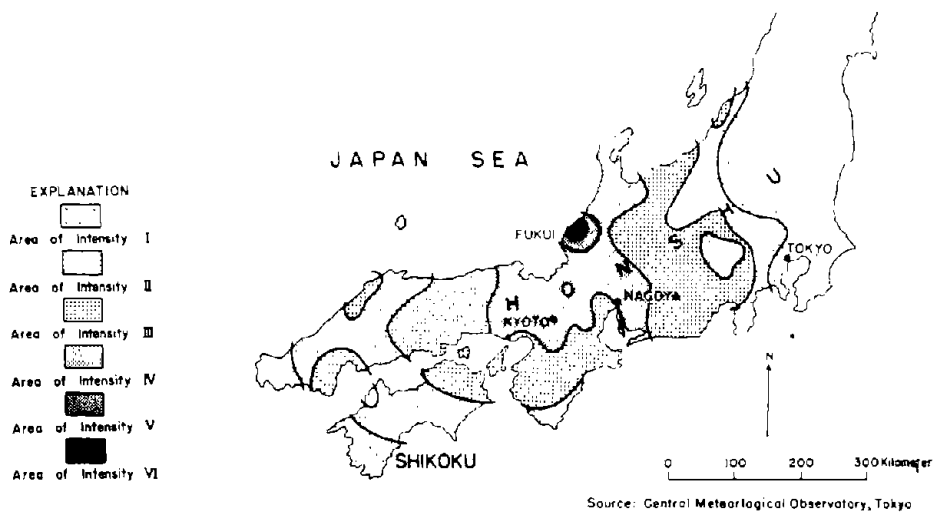


Figure 2. Seismic Intensity on Japan's Honshu Island (Japan Meteorological Agency Intensity Scale)¹⁾

79

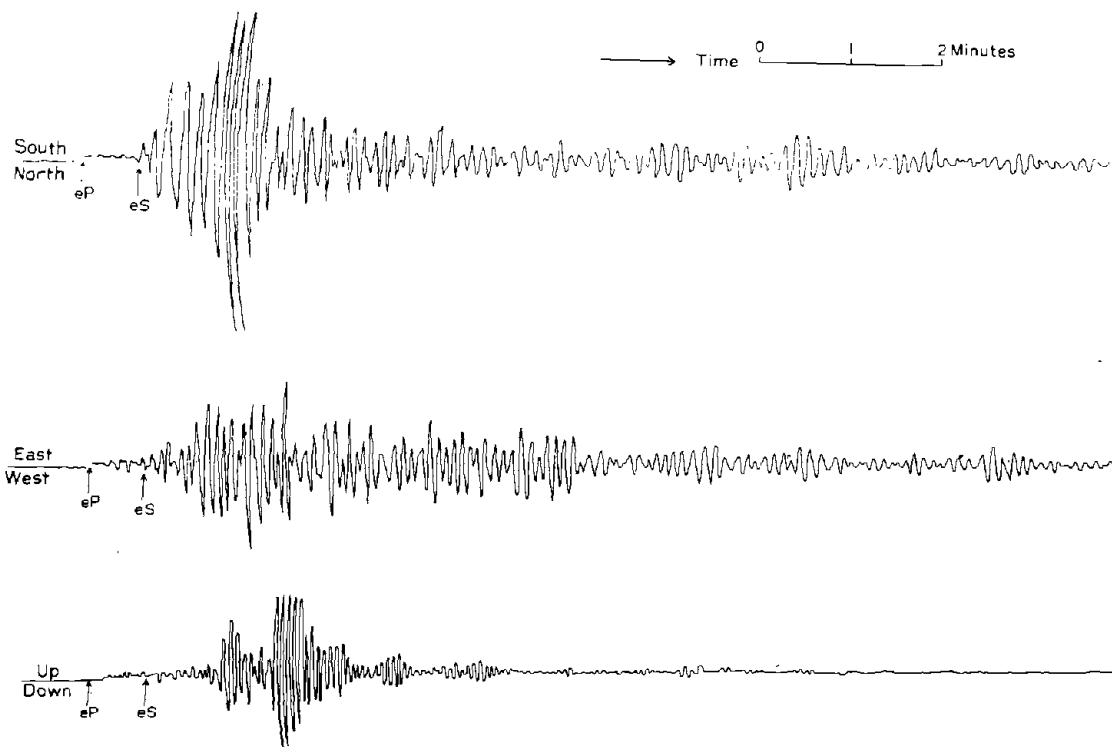


Figure 3. Seismogram (Displacement) Recorded at Central Meteorological Observatory in Tokyo¹⁾

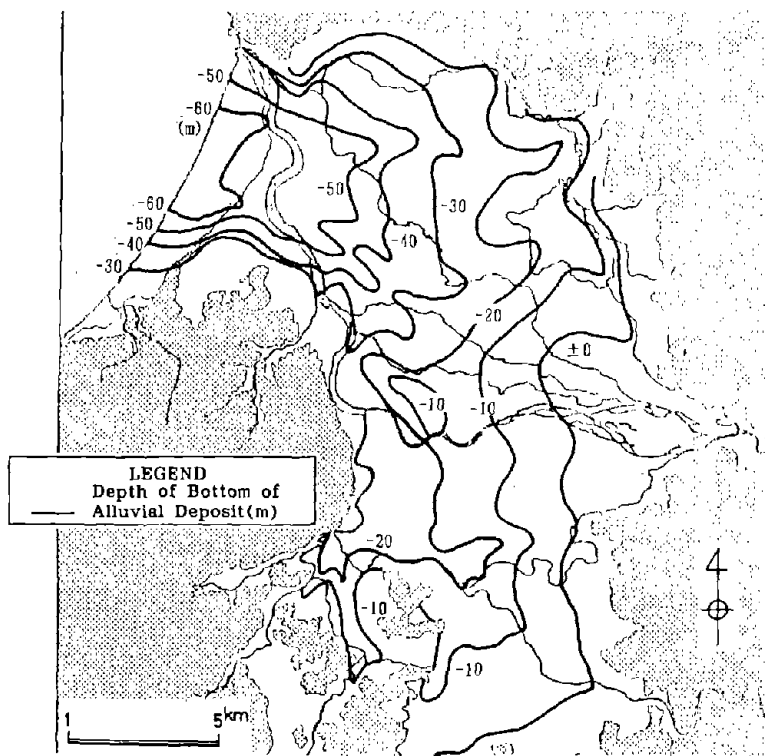


Figure 4. Depth of Alluvial Deposits under Fukui Plain

on the alluvial plain. Finally, the damage was compounded because most of the houses had been constructed poorly just after World War II.

Figure 5 shows the damage rate for houses in the area, which is defined as the ratio of completely collapsed houses to the total number of houses. In most areas of the Fukui Plain, the damage rate exceeded 90%. Photo 1 shows that most of houses were completely destroyed and burnt by post-earthquake fire in the central part of Fukui City immediately after the earthquake.

2.4 Liquefaction and Resulting Damage

Liquefaction occurred extensively in areas along the Kuzuryu River and its tributaries, the Takeda, Hyogo, Hino, and Asuwa Rivers. Figure 6 shows the locations of sand boils on the Fukui Plain, and white-colored area in Photo 2 shows sand, which boiled out of the ground along the Kuzuryu River. In the liquefied area, many bridges, railways, steel electricity pylons, and other structures were critically damaged. Typical examples of liquefaction-caused damage are re-examined below.

2.4.1 Northern Area of the Plain: Takeda, Hyogo, and Tajima River Areas

These areas are now covered by alluvial deposits with maximum thickness of 60 m, and severe spouting of sand and water was experienced. Also gushing of sand and water from wells was reported by many residents.

The Nagaya Bridge is located 5 km from the epicenter at Point ① in Figure 6. Eight spans of reinforced-concrete I-beam over a total length of 58.5 m were supported on concrete piers. Three piers, P5, P6, and P7, sank to ground level due to liquefaction and the beams fell to the ground as shown in Figure 7. It was reported that the piers sank almost vertically.

The Nagaune Bridge, with a total length of 72.2 m, is located about 4 km from the epicenter at Point ② in Figure 6. Eight spans of wooden beams were supported upon timber piers with concrete foundations, as shown in Figure 8. Piers P3 to P6 sank due to loss of bearing capacity in the foundation soils

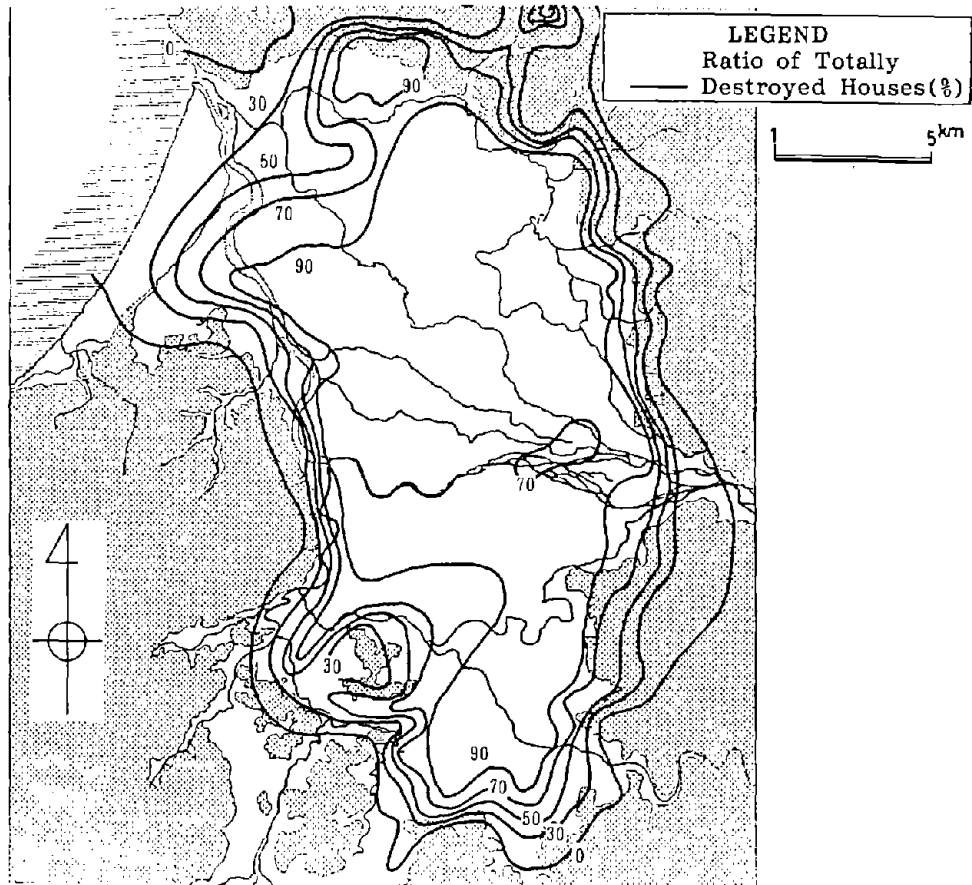


Figure 5.
Ratio of Totally
Destroyed Houses
on Fukui Plain

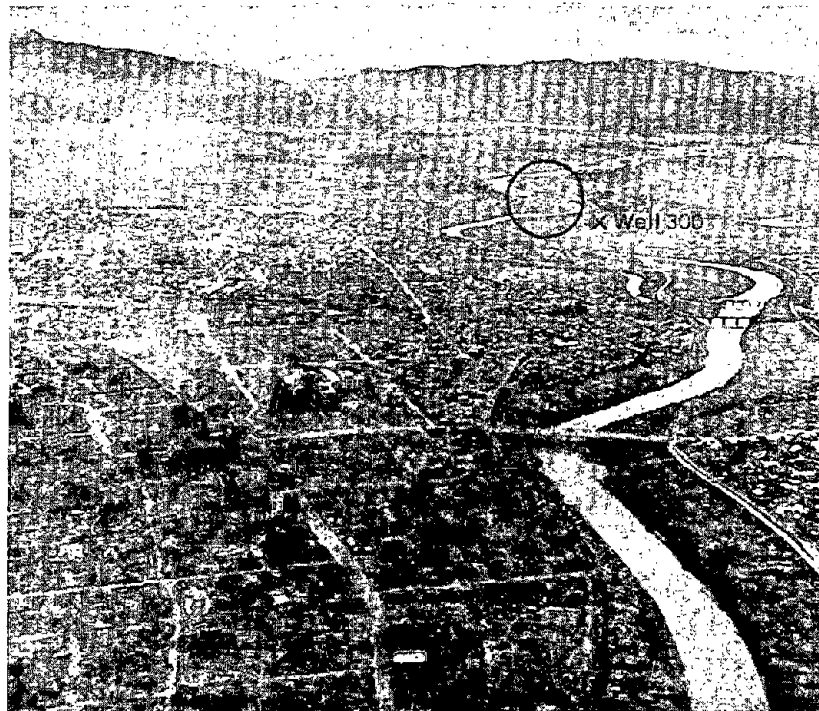


Photo 1
Central Fukui City
after the Earthquake

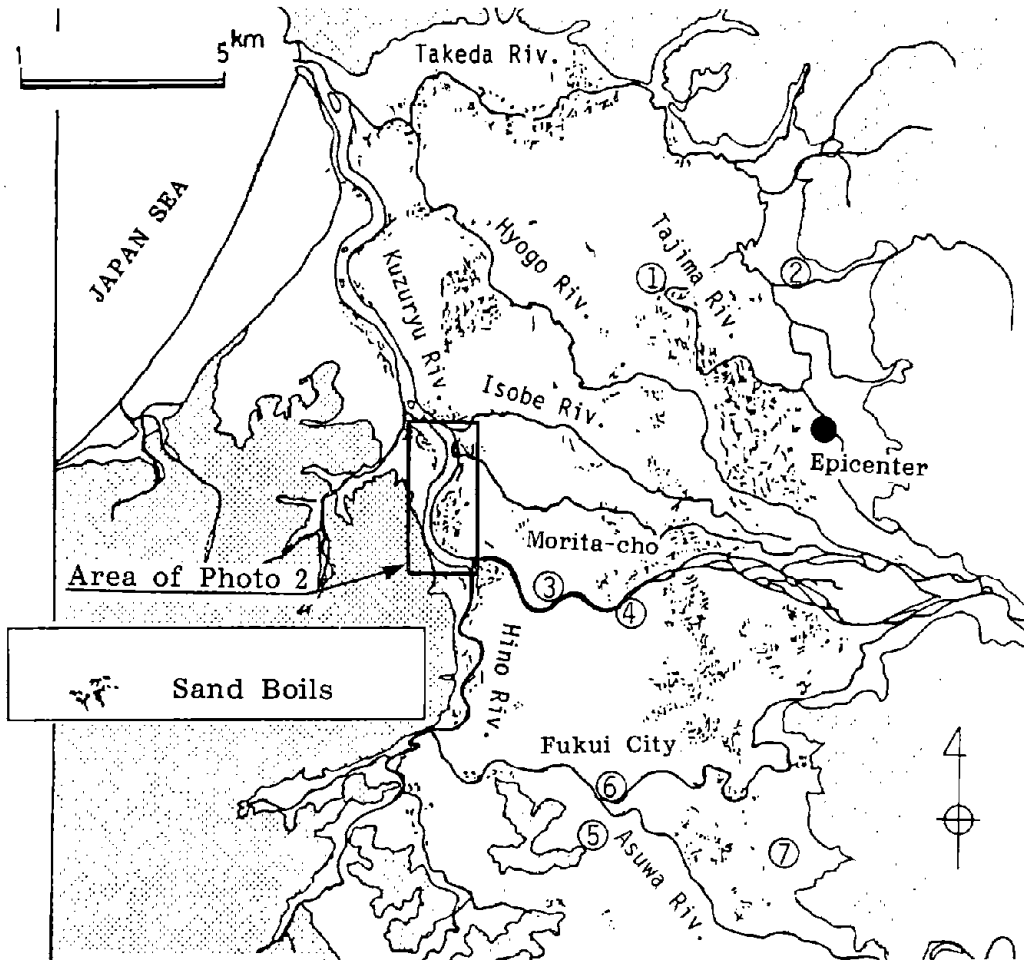


Figure 6. Sand Boils and Ground Fissures on Fukui Plain



Photo 2 Sand Boils along The Main Channel of the Kuzuryu River
(White-colored area shows the sand boiled out of the ground)

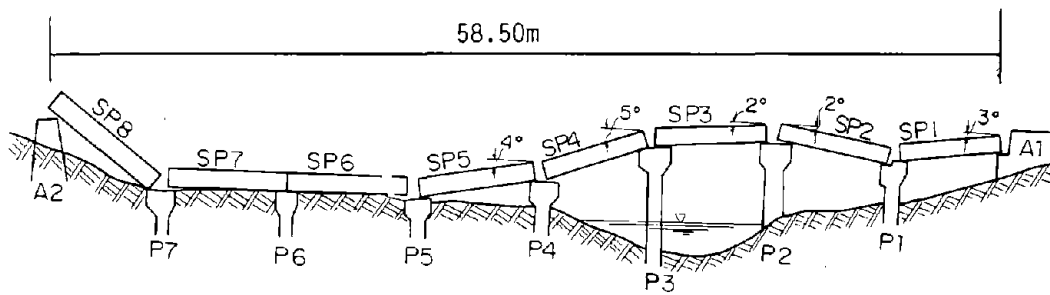
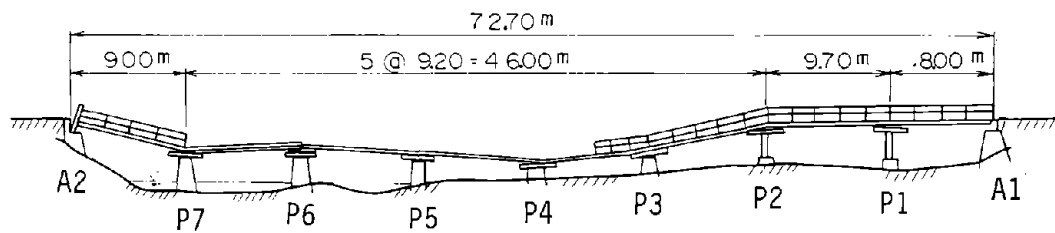
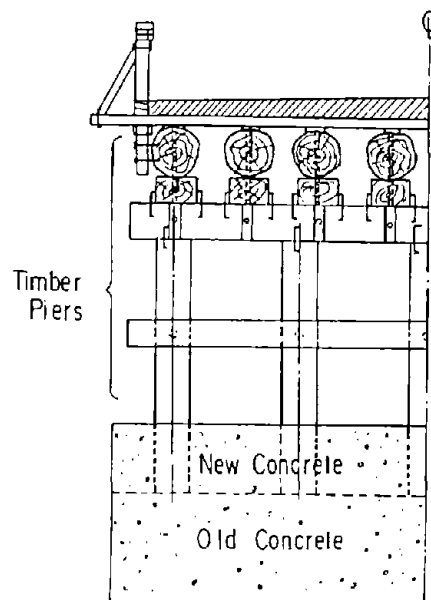


Figure 7. Damage to Nagaya Bridge (Point ① in Figure 6)



(a) Sinking of Piers



(b) Structure of Piers

Figure 8. Damage to Nagaune Bridge (Point ② in Figure 6)

as a result of liquefaction. Two piers in particular, P3 and P4, sank almost to ground level in the same way as those of the Nagaya Bridge.

Both the Nagaya and Nagaune Bridges crossed the Tajima River and its tributary, respectively. It was reported that numerous sand and water boils were observed during the earthquake.

2.4.2 Central Area of the Plain: Main Channel Area of Kuzuryu River

The main channel area of the Kuzuryu River suffered particularly severe damage due to liquefaction. Sand boils downstream from the diversion into the Hino River are shown in Photo 2. Upstream from this diversion, many bridges collapsed during the earthquake. The Nakatsuno Bridge was located at Point ③ in Figure 6. It consisted of 14 spans of I-shaped steel girders with a total length of 259 m. The piers were reinforced concrete columns on open caisson foundations. Figure 9 and Photo 3 show the damage to this bridge. The piers sank, tilted substantially, and collapsed, and the simply-supported girders fell. It was reported that damage to the collapsed girders was comparatively light in spite of the extensive damage to the piers.

The Kuzuryu JNR (Japan National Railway) Bridge was located at Point ④ in Figure 6. The bridge had an overall length of about 260 m, consisting of 11 brick and concrete piers and 12 simply-supported plate girders. Each 19.9 m-high pier had an oval cross section (4.3 m x 2.4 m). The lower portion of each pier consisted of a concrete caisson, with the upper portion constructed of bricks. These two portions were joined by three granite keys. A cross-section and plan view of a typical pier are shown in Figure 10. Of the 11 piers, 9 collapsed and the other 2 were tilted over and sheared off at ground level. Photo 4(a) is an aerial view of the collapsed JNR Bridge, while Photo 4(b) shows Pier 6. Braced by the fallen girders, Pier 6 remained standing in an inclined position. The white-colored zone on the banks in Photo 4(a) represents the sand which boiled out of the ground due to liquefaction.

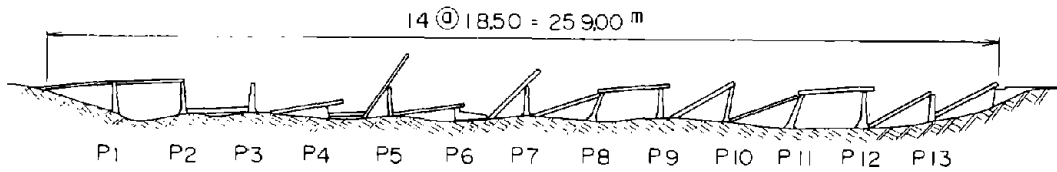


Figure 9. Damage to Nakatsuno Bridge (Point ③ in Figure 6)

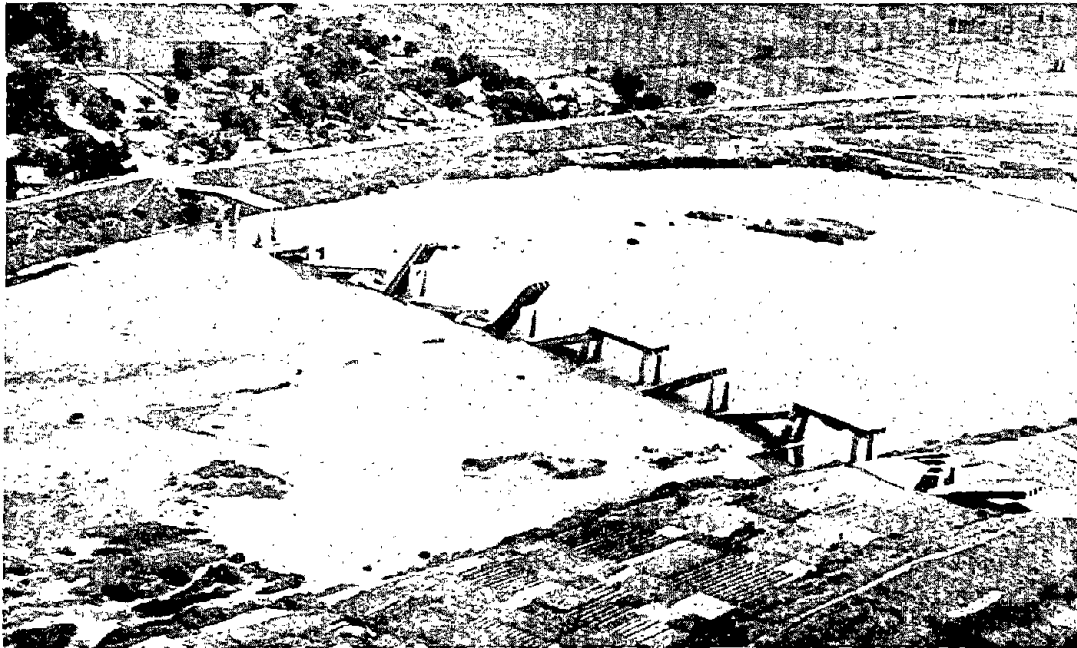
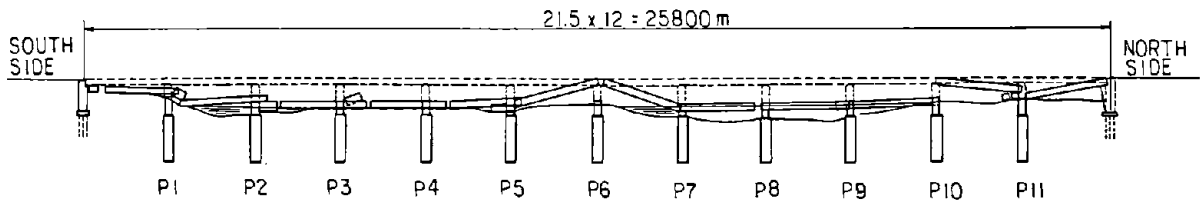
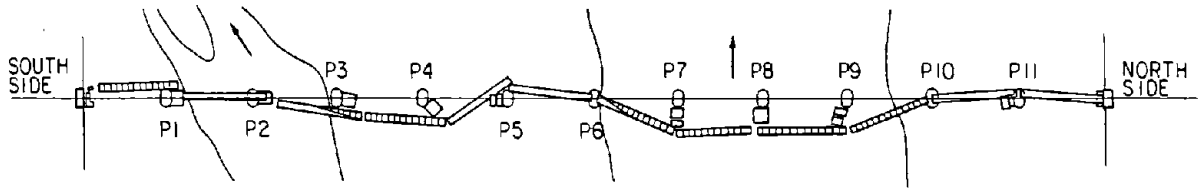


Photo 3 Collapse of Nakatsuno Bridge (Point ③ in Figure 6)¹⁾

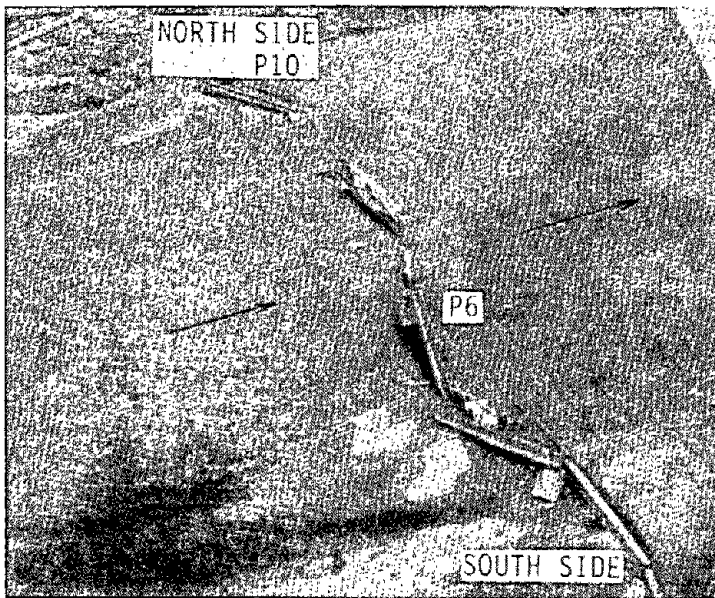


(a) Elevation



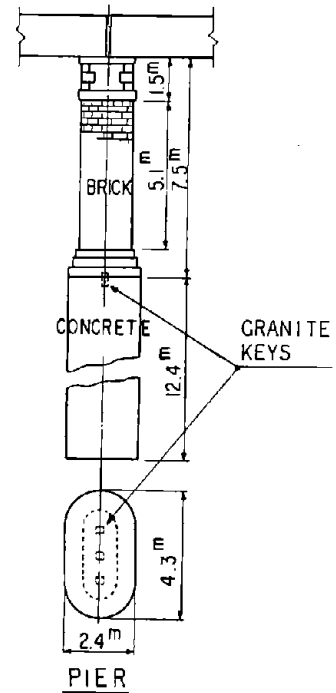
(b) Plan

Figure 10. Damage to the JNR Bridge (Point ④ in Figure 6)1)



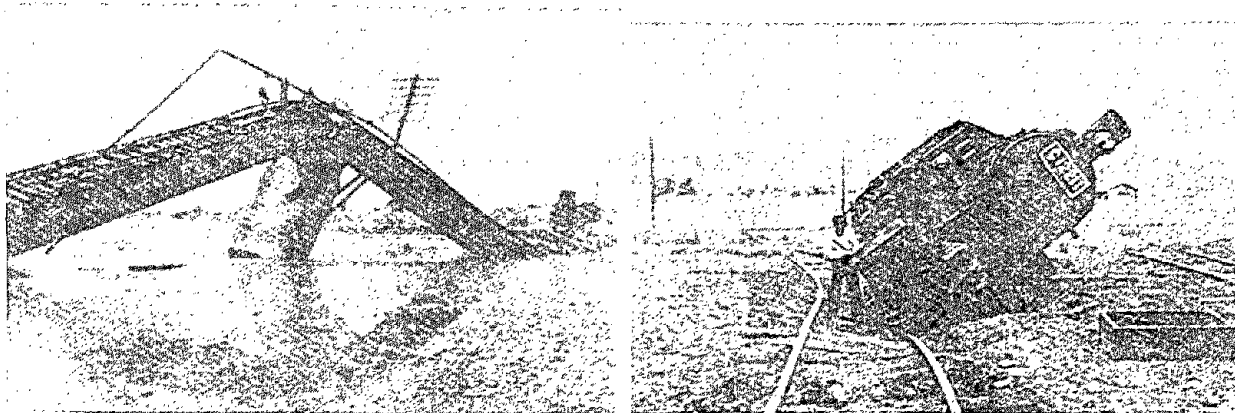
(a) Aerial View of Damage

Photo 4 Collapse of the JNR Bridge (Point ④ in Figure 6)1)



(c) Pier

Figure 10. Damage to the JNR Bridge (Point ④ in Figure 6)1)



(b) Damage to Pier 6

Photo 4 Collapse of the JNR Bridge
(Point ④ in Figure 6)

Photo 5 Toppled Locomotive in JNR
Fukui Marshalling Yard
(Point ⑤ in Figure 6)



Photo 6 Platform Subsidence of Fukui JNR Station (Point ⑥ in Figure 6)

2.4.3 Southern Area of The Plain: Fukui City, and the Asuwa and Hino River Areas

Large ground subsidence and fissures were observed in the Fukui marshalling yard of the JNR Hokuriku Main Line, located at Point ⑤ in Figure 6. The rails were twisted in the horizontal as well as vertical direction and a locomotive was toppled over as a result of the non-uniform subsidence. Furthermore, at Fukui JNR Station, constructed by partial filling of the Fukui Castle moat, a considerable amount of sand and water boiled out. The platforms subsided to a maximum of about 1 m, as shown in Photo 6.

Large inclination of electricity pylons seriously affected electricity supplies after the earthquake. Figure 11 shows one example of the damaged pylons at Point ⑦ in Figure 6. One pylon with a height of 29 m stood on a concrete block foundation in a paddy field. The foundation sank about 10 cm due to liquefaction and the pylon heeled over by about 5°. Many sand boils were found around the foundation.

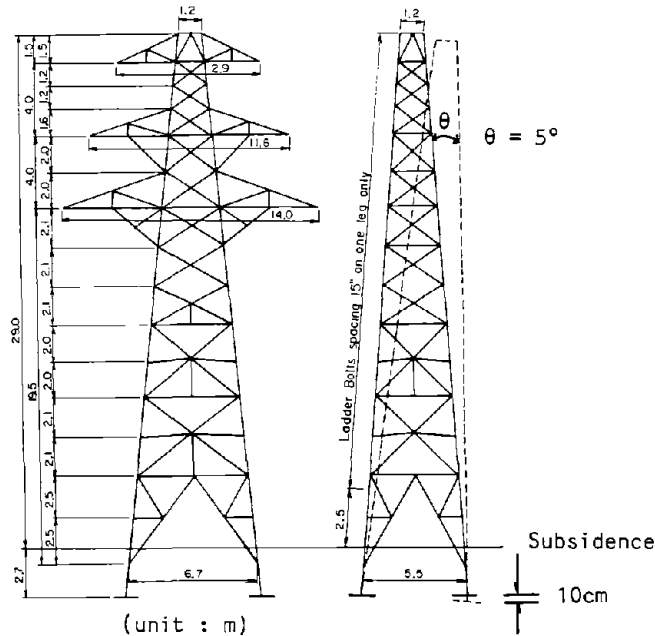


Figure 11. Inclined Electricity Pylon (Point ⑦ in Figure 6)

3.0 LIQUEFACTION-INDUCED GROUND DISPLACEMENTS

Large liquefaction-induced ground displacements were observed over a vast area of the Fukui Plain. The authors conducted measurements of these ground displacements using aerial photographs taken before and after the earthquake. A soil and geological survey was also performed, and the effects of soil type and geological conditions on the occurrence of ground displacements were studied. Furthermore, through interviews with eyewitnesses of the earthquake, data on ground failures and on damage to houses were collected.

3.1 Measurement of Permanent Ground Displacements

Morita-cho, where the measurements were conducted, is located on the north bank of the main Kuzuryu River channel almost centrally on the Fukui Plain as shown in Figures 1 and 6. This area was selected because of the particularly severe liquefaction and related damage it suffered, and because of the good state of preservation of the aerial photographs. In this neighborhood, the Kuzuryu JNR Bridge collapsed as shown in Photo 4 and in Figure 10. The area in which measurements were taken is shown in Figure 12.

The pre-earthquake aerial photos used in the measurements were taken in October 1946 at a scale of 1/12,000 and in October 1947 at a scale of about 1/15,000. The post-earthquake photos were taken on July 28, 1948 and are to a scale of 1/5,400. All aerial photographs were taken by GHQ. Photo 7 shows an example of aerial photographs taken before and after the earthquake. Numerous sand boils and ground fissures can be found in the post-earthquake photograph.

The method used in the study of the 1964 Niigata¹¹⁾ and the Nihonkai-Chubu¹²⁾ earthquakes was adopted for measurement of the permanent ground displacements. The ground displacements were evaluated by subtracting the coordinates of measuring points on the ground in the pre-earthquake photographs from those in the post-earthquake photographs. Triangulation points located on stable hill-tops and sand dunes where no ground failures - including liquefaction and sliding - were found, were selected as the data

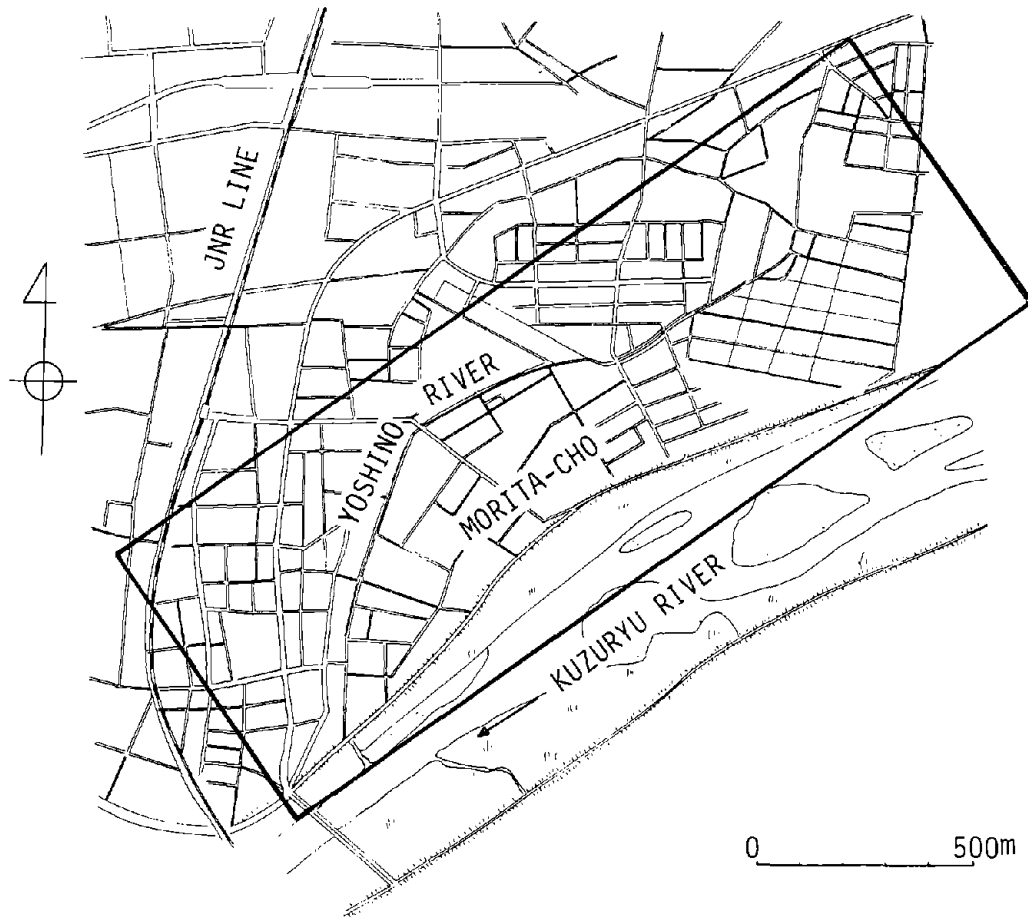


Figure 12. Morita-cho and Area for Measurement of Permanent Ground Displacements



(a) Before the Earthquake

(b) After the Earthquake

Photo 7 Aerial Photographs Used for Measurement in Morita-cho and Vicinity

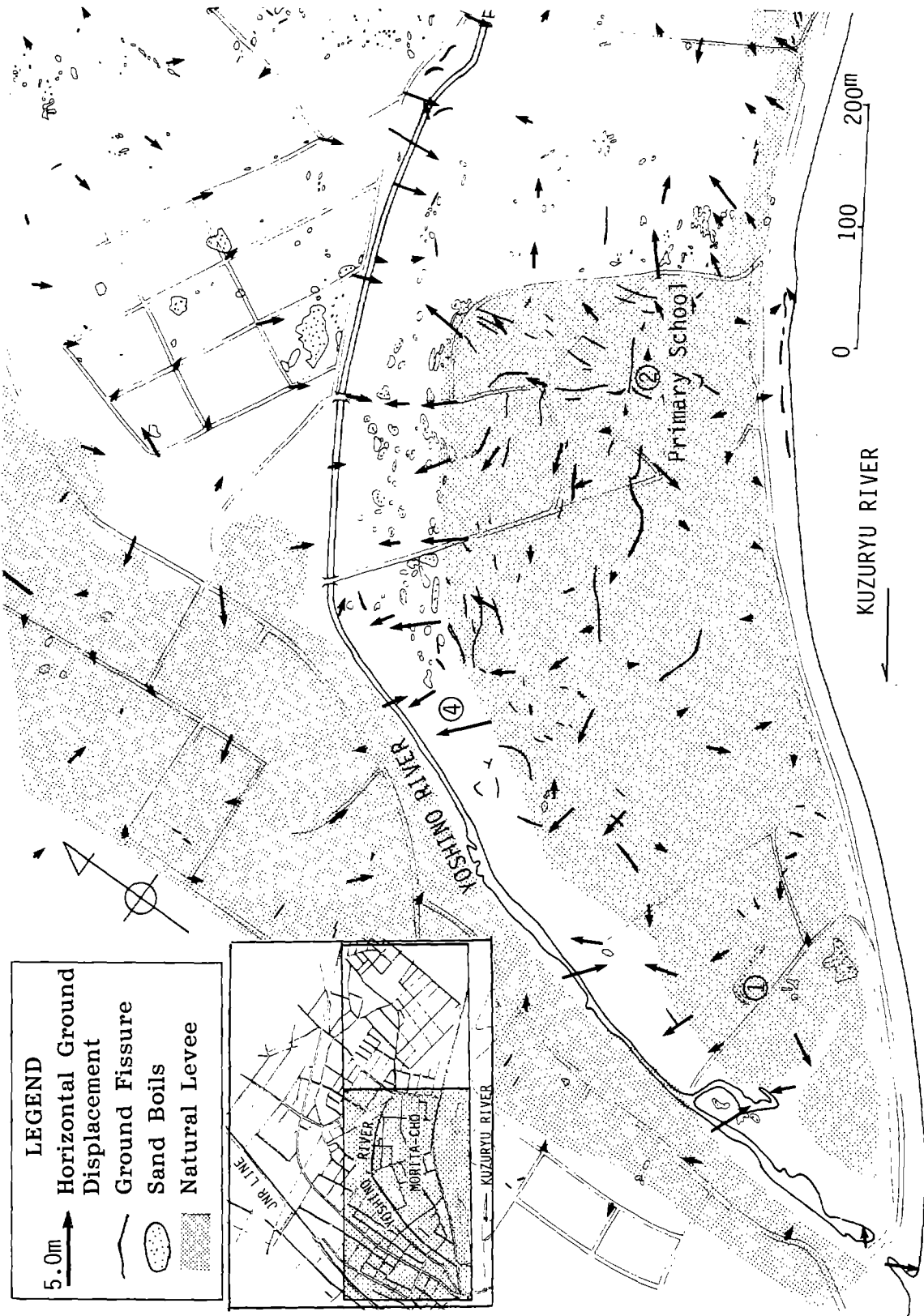
points for the measurements. It can be assumed that no permanent ground displacements resulted from the earthquake at these data points. Objects attached to the ground surface were selected as measuring points, including manholes and corners of drainage channels. Measurements were taken on about 200 points in total.

The accuracy of the measurements depends on the scale of the aerial photographs and human error in reading the coordinates, and is evaluated as the square root of the sum of the squared accuracy of the two aerial surveys before and after the earthquake as described in Appendix A. In the case of the Fukui earthquake the accuracy of the aerial surveys before and after the earthquake was evaluated by a comparison between the coordinates of data points measured by aerial photographs and those taken from topographical maps at a scale of 1/2500. The accuracy estimated in this manner is rather coarse, being ± 1.92 m in the horizontal direction and ± 1.56 m in the vertical direction. The relatively large bounds on the estimated accuracy results in part from errors in the coordinates of the topographical maps. Because vertical displacements with maximum magnitudes less than 1.0 m could not be measured with sufficient accuracy, an evaluation of settlements caused by liquefaction was not pursued. Horizontal displacements, however, were substantially larger than vertical movements, and large enough to exceed the error bounds of the estimated accuracy.

3.2 Permanent Ground Displacements and Ground Failures

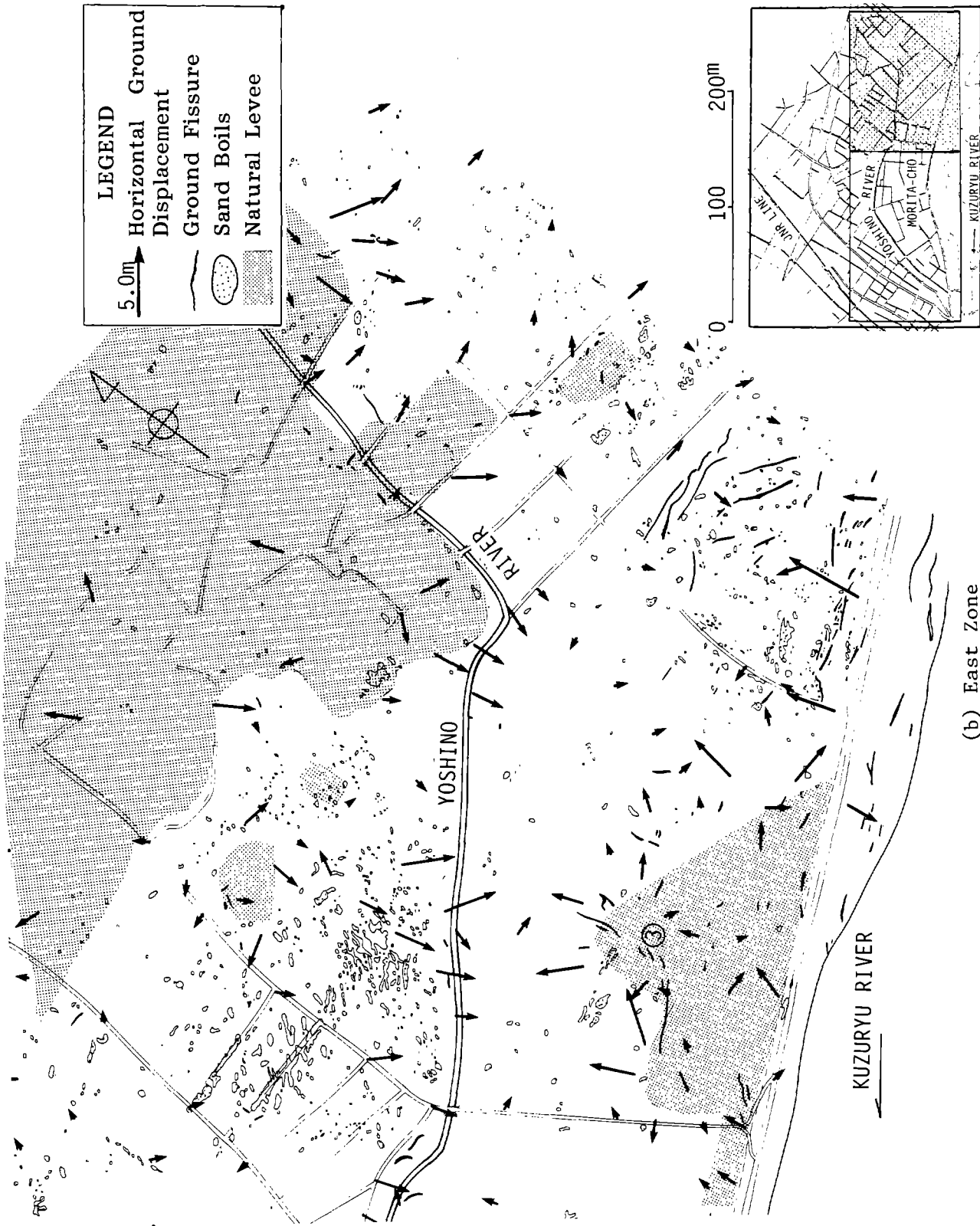
Figure 13 shows the permanent ground displacements in the horizontal direction along with ground failures such as fissures and sand boils. Figure 14 also shows the ground displacements on a contour map, which was drawn up from aerial photographs taken before the earthquake. The numbers in Figure 14 represent the elevation above mean sea level of the contours and specific points (x in the figure).

The Yoshino River flows mostly parallel to the main channel of the Kuzuryu River in Morita-cho. The Yoshino River is a small river with a width of about 5 m, but it had been a major channel of the Kuzuryu River until the



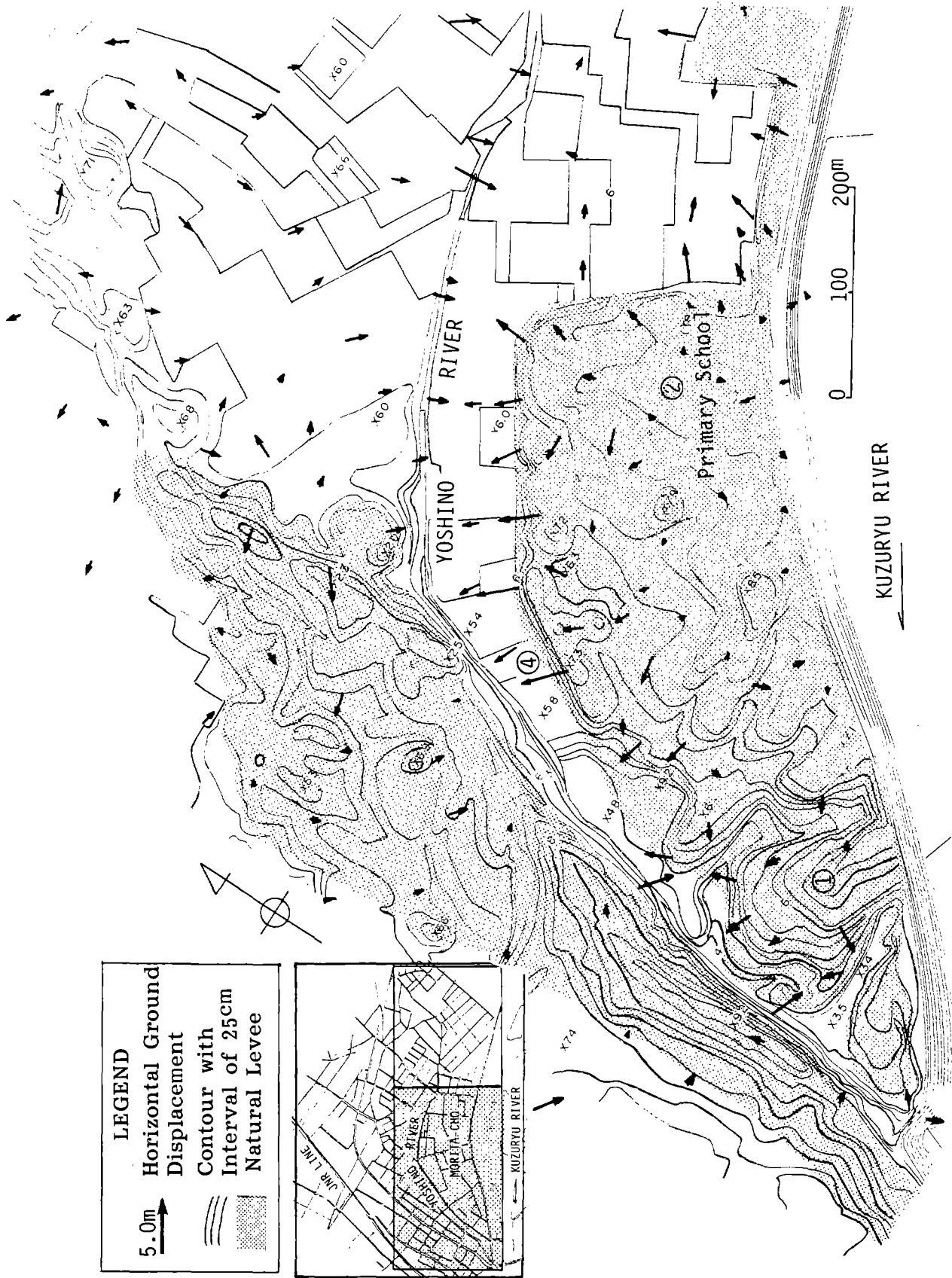
(a) West Zone

Figure 13. Permanent Ground Displacements and Ground Failures

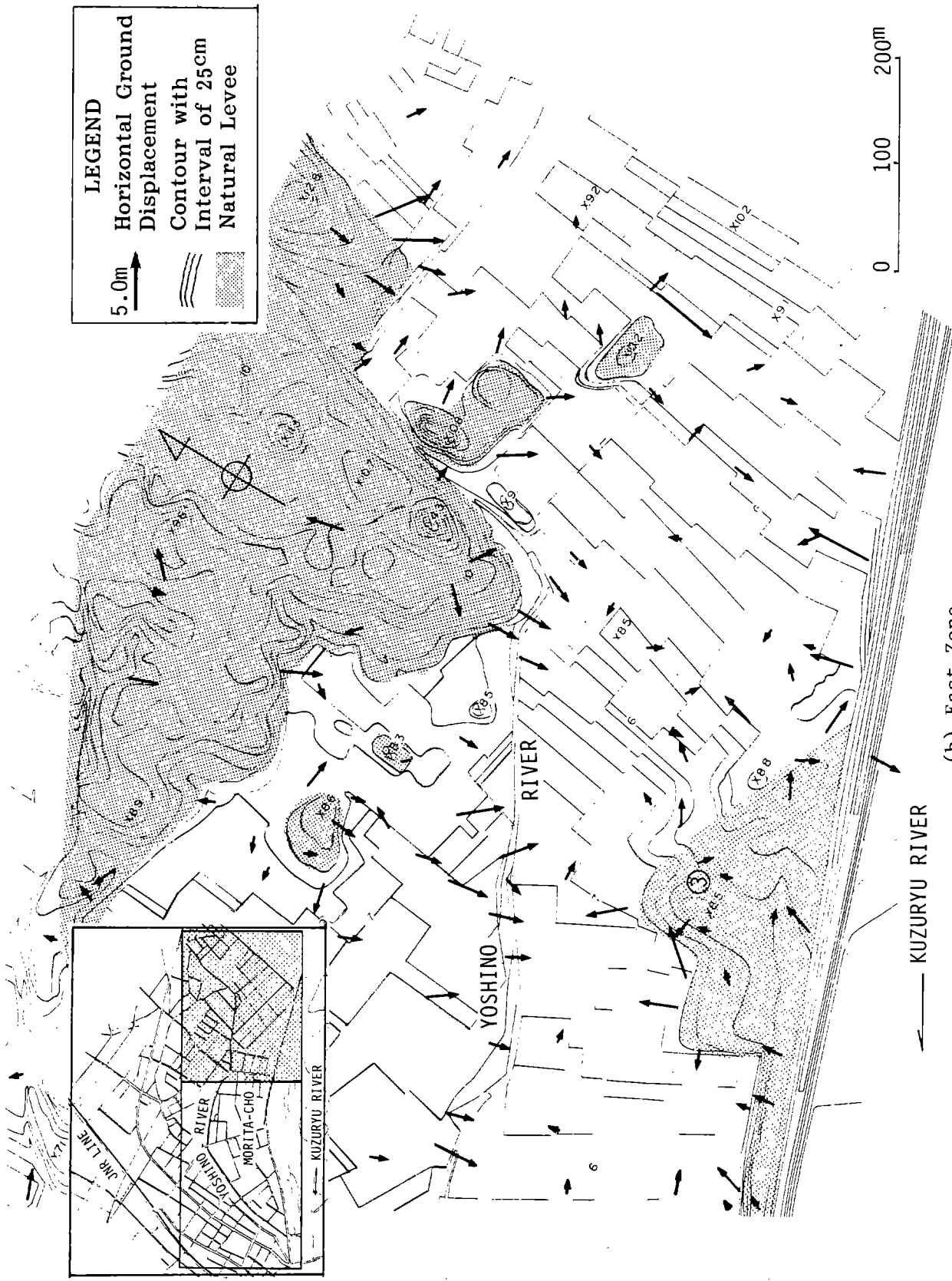


(b) East Zone

Figure 13. Permanent Ground Displacements and Ground Failures



(a) West Zone
 Figure 14. Permanent Ground Displacements on Contour Map (Numbers in the figure represent the elevation above mean sea level of the contours and specific points(x), Unit:m)



(b) East Zone

Figure 14. Permanent Ground Displacements on Contour Map (Numbers in the figure represent the elevation above mean sea level of the contours and specific points(X), Unit:m)

artificial dike along the Kuzuryu River was completed circa 1870. The residential area of Morita-cho is located on the natural levee on the north bank of the Yoshino River and between the Kuzuryu River and the Yoshino River. The flat, low-lying area along the Yoshino River between the natural levees is the old bed of the Kuzuryu River.

Figures 13 and 14 show that the permanent ground displacements were initiated at the natural levee between the Yoshino and Kuzuryu Rivers, Points ①, ②, and ③, and developed mostly in radial directions. In particular, the ground displacements toward the Yoshino River through the low-lying old riverbed are dominant. A large displacement, about 3.5 m in the horizontal direction, was observed at Point ④ in the figures, on a small cliff between the natural levee and the old river-bed.

Many residents stated that the Yoshino River decreased in width as a result of the earthquake, and they had to dredge the riverbed after the earthquake. On the contrary, ground displacements toward the present stream of the Kuzuryu River were comparatively small.

Figure 14 clearly shows that horizontal displacements were directed outward from higher elevations toward lower elevations. However, according to Figure 15, which shows the relationship between the magnitude of the ground displacements in the horizontal direction and the gradient of the ground surface, no statistically significant correlation can be shown, although there is a general trend of increasing displacement with increasing surface gradient. The gradient of the ground surface was determined as a mean value along a section parallel to the direction of the displacements. The horizontal distance over which the gradient was averaged was 25 m and 50 m in cases A and B, respectively.

Similar results were obtained about the correlation of the gradient of ground surface with the magnitude of ground displacement in the studies of the Niigata earthquake¹¹⁾ and the Nihonkai-Chubu earthquake.¹²⁾ In general, permanent ground displacements started in areas of higher elevation and ended in areas of lower elevation, but no clear quantitative correlation could be found between the magnitude of the ground displacements and the gradient of

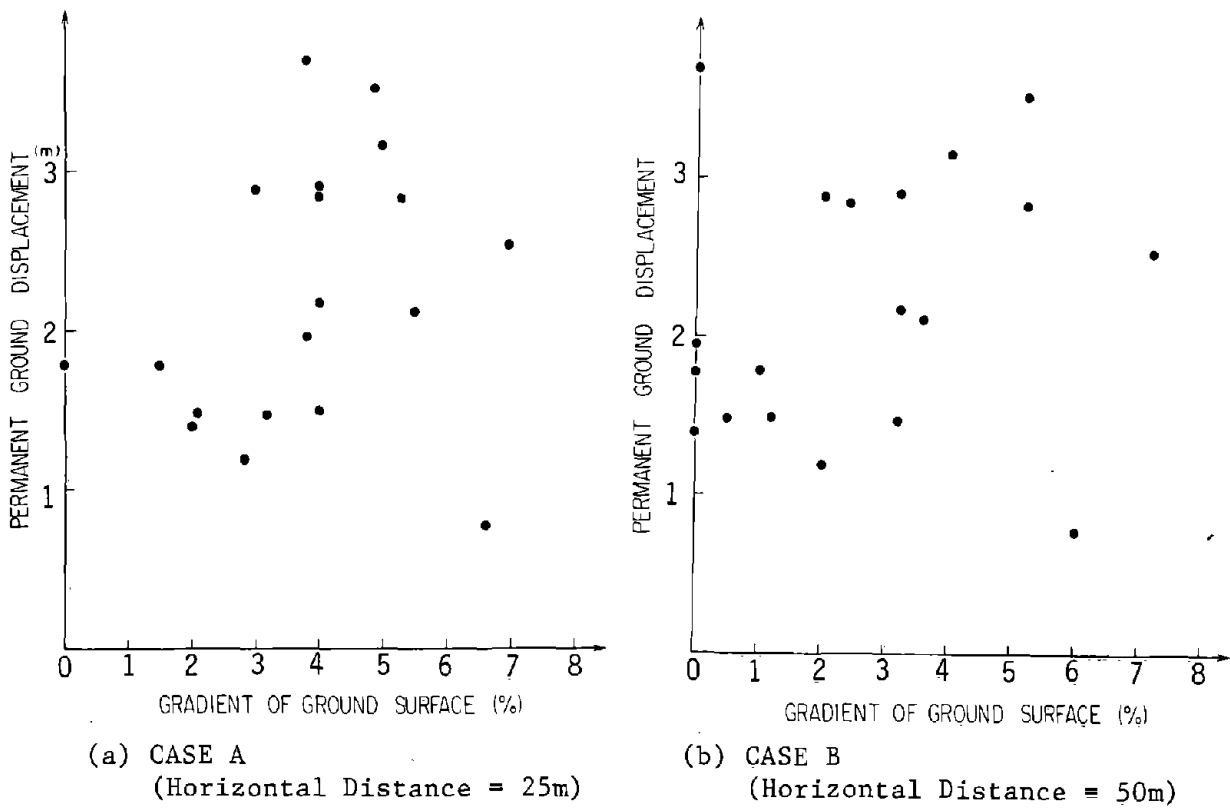


Figure 15. Correlation between Permanent Ground Displacement and Surface Gradient

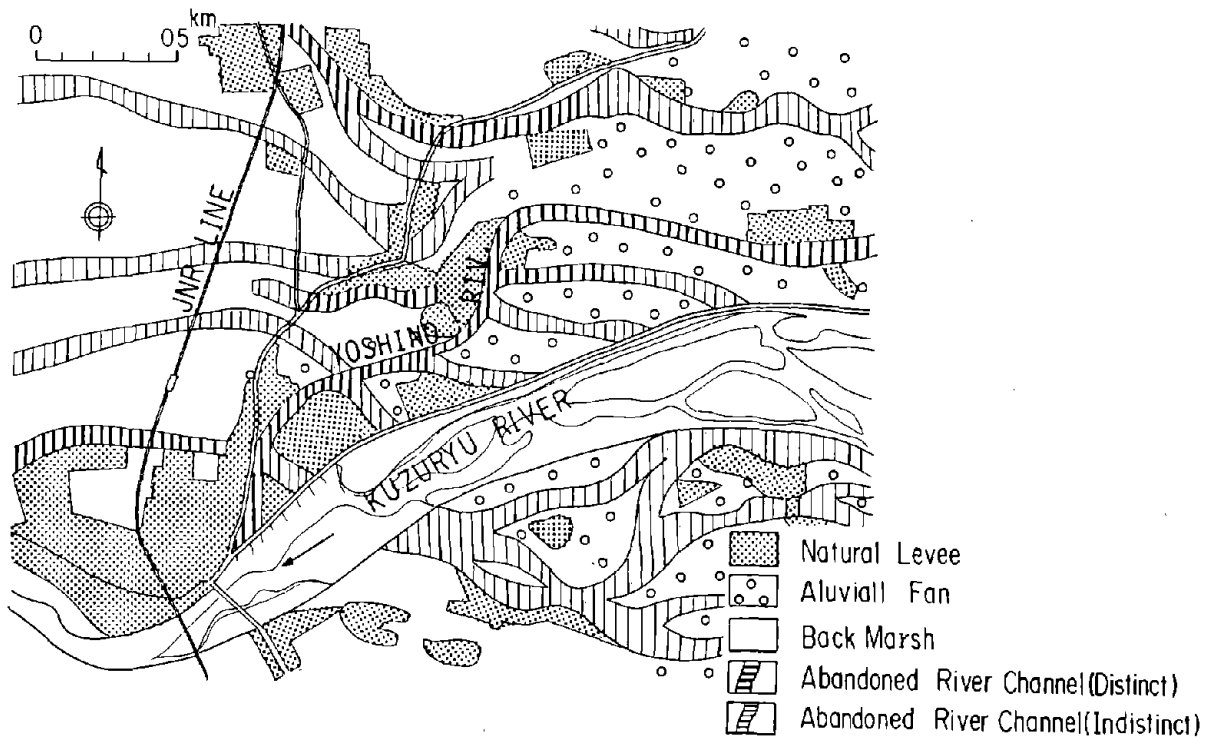


Figure 16. Geographical Features Interpreted from Aerial Photographs

the surface. Thus these results seem to contradict each other. However, the problem can be resolved if it is assumed that the ground displacement is caused by a fluid flow of the liquefied soil. If the liquefied soil behaves as a fluid, the gradient of the surface has little influence on the magnitude of displacement, although it does affect the velocity of the flow.

In the area around Morita Primary School (Point ②) in Figures 13 and 14, where the permanent ground displacements began, many ground fissures were observed. In contrast, numerous sand and water boils were found in the area around the Yoshino River where the ground displacements terminated. Ground displacements in the vertical direction are not available in this case study because of the poor accuracy of the measurements. However, some eyewitnesses stated that the bed of the Yoshino River rose up significantly and that they could cross the river on foot after the earthquake. Accordingly it can be inferred that the ground in the area along the Yoshino River, where the ground displacements terminated, rose up.

The same phenomena were found in the case studies on the 1964 Niigata¹¹⁾ and the 1983 Nihonkai-Chubu¹²⁾ earthquakes. In Ebigase-Ohgata, Niigata City, the liquefaction-induced ground displacements started at a natural levee, and ended near the small Tsusan River in the old bed of the larger Agano River. In the area where the ground displacements started, the ground surface subsided and many ground fissures appeared. In contrast, in the area where the ground displacements ended, the surface rose up and numerous sand boils were found.

Furthermore, on the slopes of sand dunes in Noshiro City during the 1983 Nihonkai-Chubu earthquake, the ground subsided greatly and ground fissures appeared in the area where the horizontal ground displacements started. The ground rose up and sand boils were observed in the area where the horizontal ground displacements terminated. These results suggest that ground displacements in the horizontal direction are caused by a volumetric transfer of liquefied soil.

3.3 Soil Conditions

Figure 16 shows the geographical features of Morita-cho and its surrounding area as interpreted from aerial photographs. The Yoshino River was one of old beds of the Kuzuryu River with much larger width. In addition to the Yoshino River, there were many old riverbeds in Morita-cho and its vicinity. The higher area between the Kuzuryu and Yoshino Rivers formed as a natural levee and alluvial fan. Furthermore, it appears that several old links between the Kuzuryu and Yoshino Rivers existed in this area. As shown in Figure 16, the Kuzuryu River has changed course, such that the geographical features of the Morita-cho area are very complex.

Besides collecting already existing borehole data, Swedish weight sounding tests (SWS)¹¹⁾* were performed at 32 points in Morita-cho. On the basis of these surveys, soil profiles along the 5 section lines shown in Figure 17 were drawn up and estimates were made of the soil which liquefied during the earthquake. The soil conditions along all 5 cross-sections are summarized in Appendix B. The sections were drawn mostly parallel to the dominant direction of permanent ground displacements.

Figure 18 shows the soil profiles along sections 4-4' and 5-5'. The subsurface soils consist of alternate layers of clay, silt, silty sand, sand, and sandy gravel, making soil conditions very complex. The shaded zones were estimated to have liquefied during the earthquake according to the following assumptions:

- (i) The shallow sandy gravel layers liquefied in spite of the high N-values** measured in standard penetration tests because interbedded sand and the sand matrix were considered to be loose.
- (ii) The thin clayey and silty layers between the estimated liquefied sand and gravel layers also liquefied.

*See Appendix C of reference 11).

**Generally, N-values in U.S. standard are larger than those in Japanese standard, because of the difference in energy transfer efficiency from the hammer to the rod (see reference 13)).

Along section 4-4', where the maximum ground displacement in the horizontal direction reached 3.9 m, the liquefied layer was estimated to have a thickness of 7 m to 9 m. The ground surface is mostly flat along this section.* The correlation between the direction of the ground displacements and the inclination of the estimated liquefied layer cannot be discussed in this case because of the lack of reliability of the estimates.

Along section 5-5, where the ground displaced toward the Yoshino River with a maximum magnitude of 3.5 m, the estimated thickness of the liquefied layer was 5 m to 10 m. The ground surface inclined toward the Yoshino River, but no statistically significant correlation could be found between the magnitude of the ground displacements and the gradient of the ground surface, as shown in Figure 15.

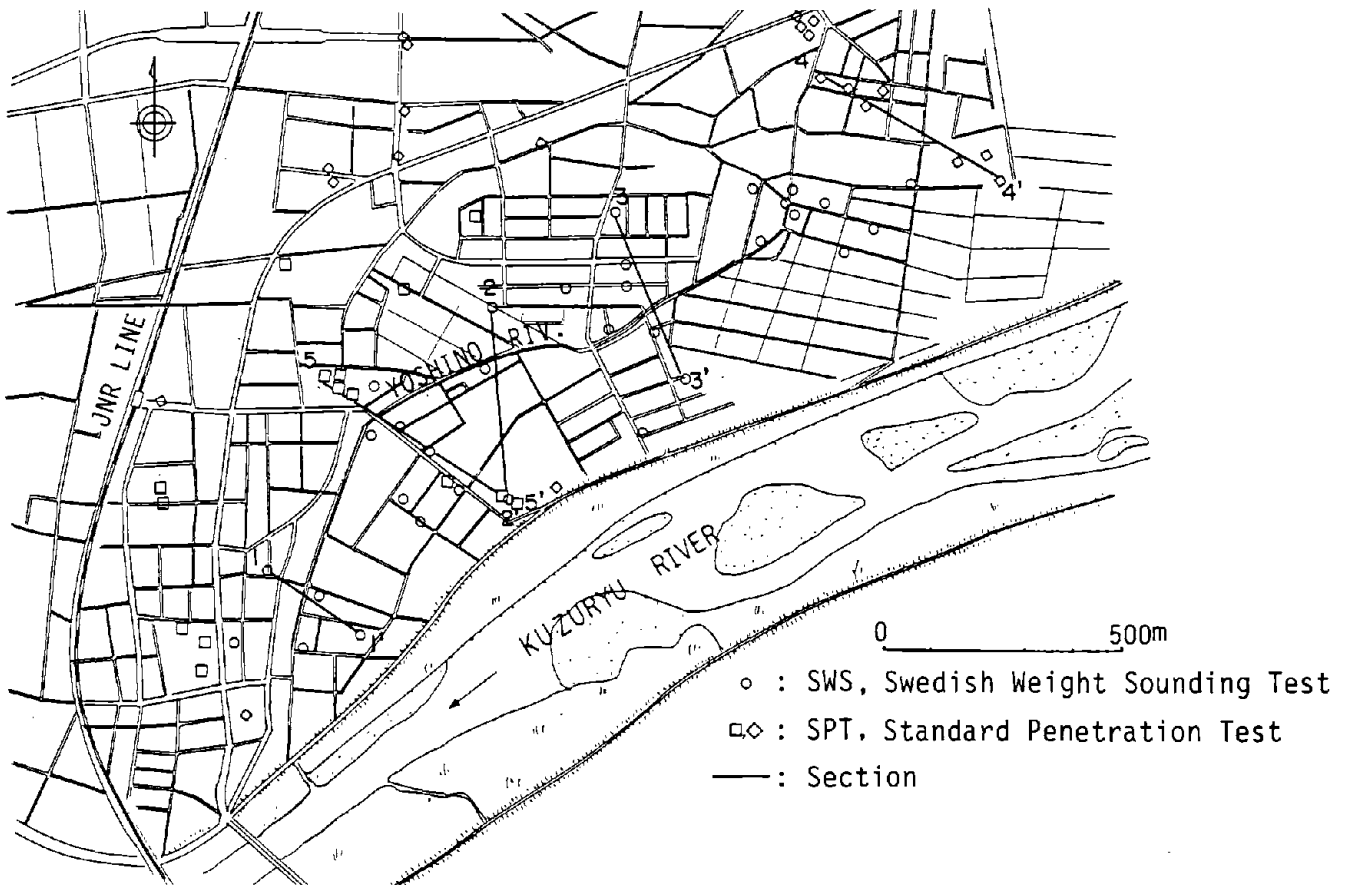
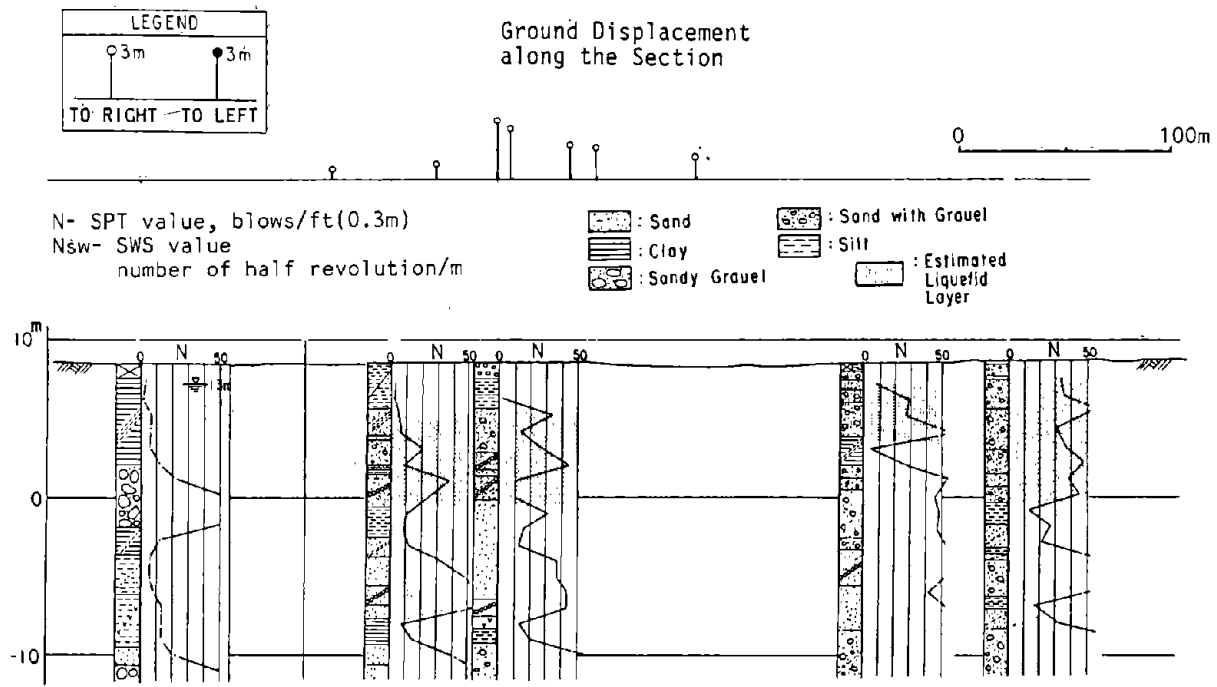
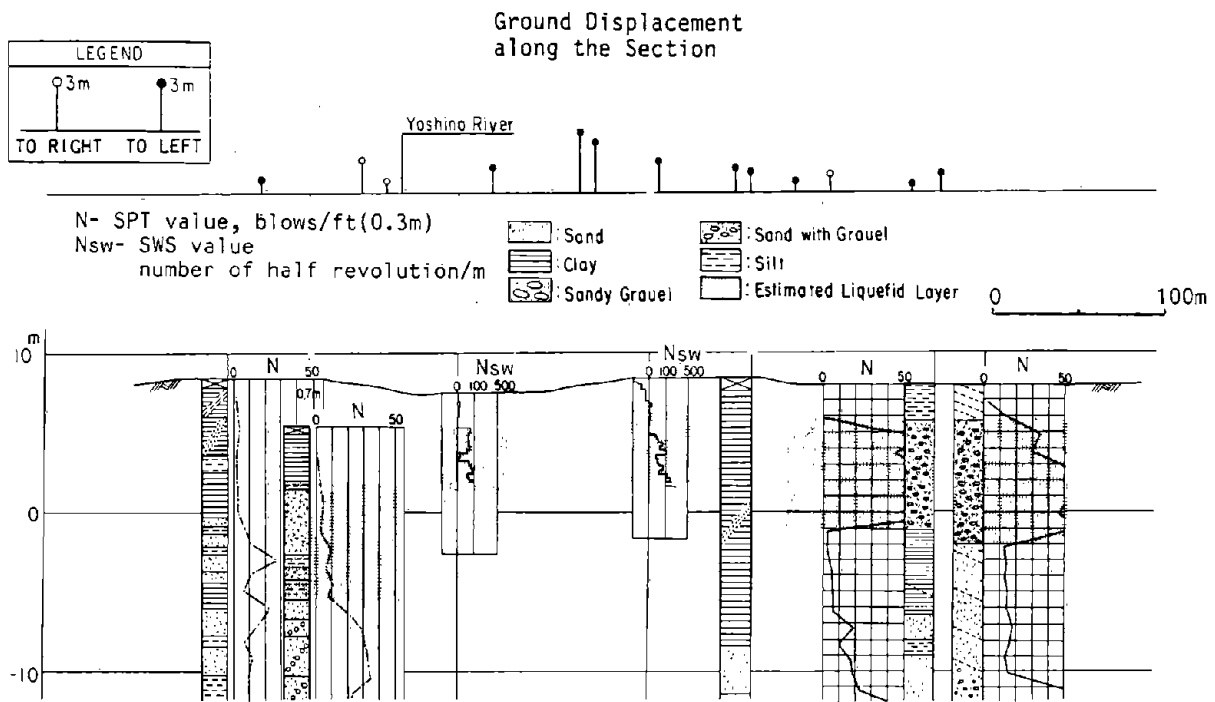


Figure 17. Section Lines for Soil Condition Survey

*It should be noted that the level of the ground surface was measured using the aerial photographs taken before the earthquake.



(a) Section 4-4'



(b) Section 5-5'

Figure 18. Soil Condition Profiles

4.0 INTERVIEWS WITH EYEWITNESSES OF THE EARTHQUAKE ABOUT GROUND FAILURES AND DAMAGE TO HOUSES

In areas where permanent ground displacements were measured, interviews were held with residents to obtain detailed information on the occurrence of ground displacements and related ground failures and damage to houses. A total of 127 testimonies were collected. Some include information with low reliability due to fading memories about 45 years after the event, but detailed statements on the occurrence of ground fissures and sand boils were obtained and these are helpful in understanding the actual conditions at the time of liquefaction-induced permanent ground displacements.

The interviews with eyewitnesses dealt with the following four subjects:

- (i) Damage to Houses and Changes in Land Area
- (ii) Ground Fissures
- (iii) Sand and Water Boils
- (iv) Changes to Wells

4.1 Shimomorita-Sakuramachi Area

Figure 19 has been developed on the basis of reports of ground failures in the vicinity of the Hakusan Shrine at Shimomorita-Sakuramachi, located on the north bank of the Yoshino River.³⁾ A ground fissure 150 m in length and 0.3 m wide occurred in a south-north direction in the grounds of the shrine. The ground east of the fissure subsided by 0.8 m, and moved in a north-northeast direction. The bed of a water channel, about 100 m southeast of the shrine (which can be considered as the Yoshino River), rose about 1 m to almost the same elevation as the road. The area with a higher elevation between the water channel and the Kuzuryu River suffered severe subsidence, and many sand volcanos with a diameter of about 1.0 m were found in the rice fields. The reports of ground failures in Shimomorita-Sakuramachi³⁾ were verified by interviews with the eyewitnesses in the area. Their remarks can be summarized as follows:

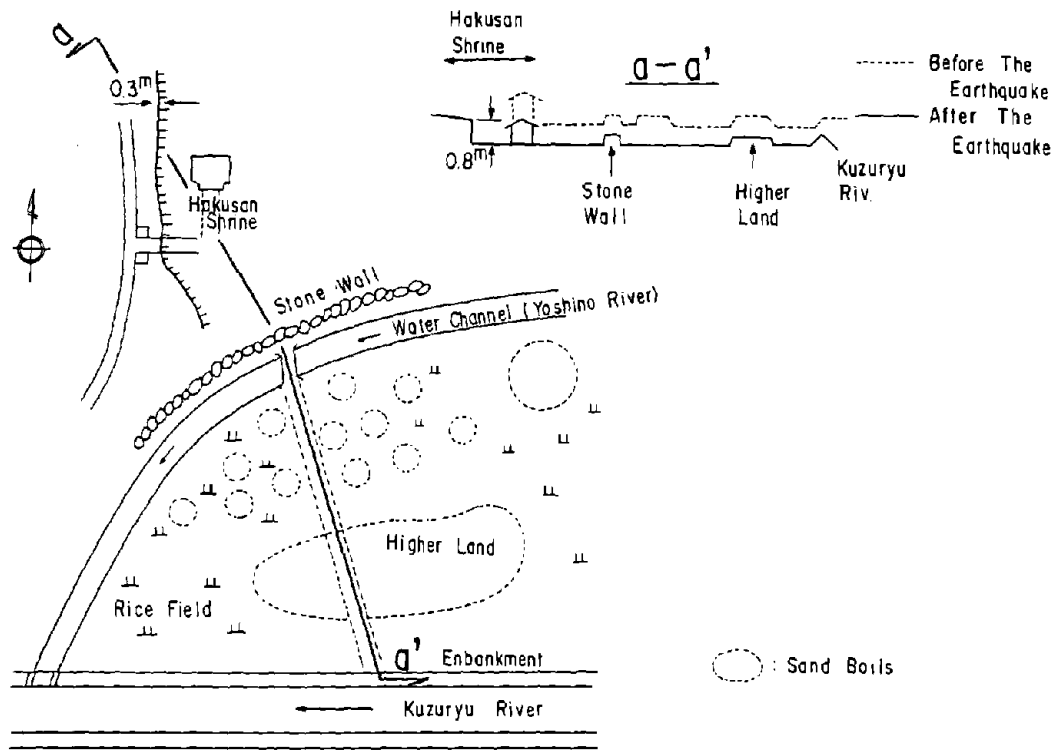


Figure 19. Ground Failures in the Vicinity of Hakusan Shrine

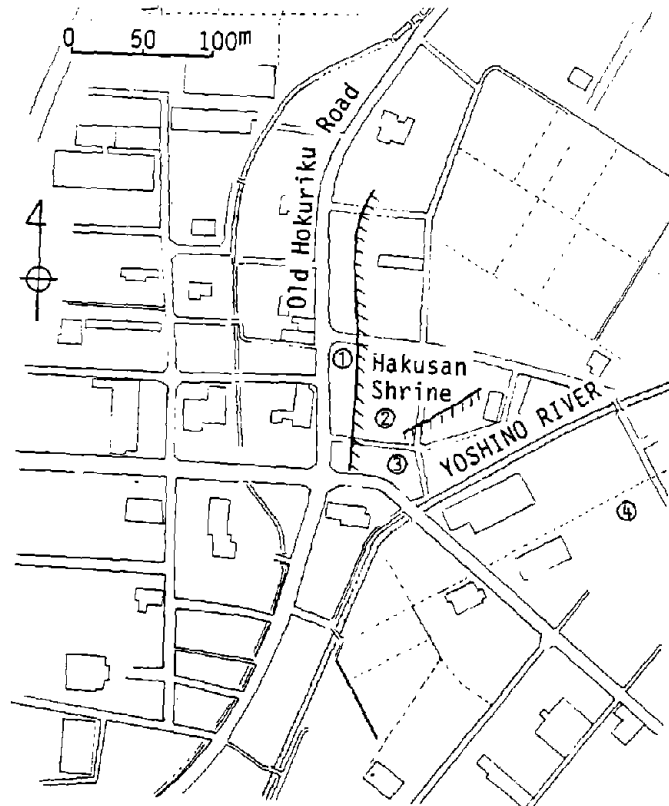


Figure 20. Ground Failures in Shimomorita-Sakuramachi and Vicinity

Point ① in Figure 20: A large ground fissure with a width of 20 to 30 cm occurred in the grounds of Hakusan Shrine almost parallel to the Old Hokurido road (generally in a north-south direction), and the ground to the east of the fissure subsided by 0.5 m to 1.5 m. This fissure continued to the north for about 200 m from the shrine. Between this large fissure and the Yoshino River, small fissures appeared, and fine blue sand and water boiled out. Some eyewitnesses said that the ground surface undulated greatly in the vertical direction during the earthquake.

Point ②: A ground fissure parallel to the Yoshino River appeared under a house. The fissure was 20 to 30 cm wide immediately after the earthquake, but it expanded to 30 to 40 cm by the next morning. Ultimately, it became 1 m wide and over 1.8 m deep. Water and sand boiled out of a well up to 1 m high during the earthquake. The boil action continued for 2 to 3 days after the earthquake. Besides this case, many instances of water and sand boils from wells were reported in the area.

Point ③: From the bed of the Yoshino River, a considerable amount of sand boiled out, and the river bed rose up. Because of the raised river bed, water flowed through the rice fields between the Yoshino and Kuzuryu Rivers.

Point ④: In the rice fields between the Yoshino and Kuzuryu Rivers, many sand and water boils and ground fissures were observed. The heights of the sand and water boils were 0.5 to 2.0 m, and they continued for a long time after the earthquake, but no houses collapsed in this area. On the contrary, on the western side of the large ground fissure (Point ①), on the natural levee, most houses collapsed. Concerning the duration of water and sand boils, most eyewitnesses said that they continued after the earthquake motion ceased, but it should be noted that some stated that the boils ended with the earthquake motion. One eyewitness in this area said that high columns of water were observed in the Kuzuryu River during the earthquake.

4.2 Uenohonmachi Area

Uenohonmachi is located in the area where the Yoshino River turns from south to southwest (Figure 21). There had historically been many floods in this area and seepage of groundwater had been severe. Testimony from eyewitnesses in this area can be summarized as follows:

Point ⑤ and ⑥ in Figure 21: Along both banks of the Yoshino River, ground fissures with widths of 1 to 2 m and lengths of about 300 m occurred. On the west bank, the ground subsided 0.5 to 1.0 m between the fissures and the river. The river was reduced in width and the river bed rose up as a result of extensive sand boils. Residents had to dredge the riverbeds to prevent flooding. On the east side of the Yoshino River, boils of water and sand were particularly severe, and the area was flooded to a depth of 0.5 to 1.0 m. The boundaries of real estate were altered due to lateral movement of the ground, so that many land conflicts arose.

Point ⑤: The width of the ground fissure at this point was about 1.0 m immediately after the earthquake, but it increased to 3 m several hours after the earthquake. A horse fell into the fissure. Ultimately, the fissure filled up with sand a week after the earthquake.

Point ⑥: A stone warehouse at this point sank by a full 6 m, the roof ending up level with the ground surface. On the west side of the Yoshino River, it was reported that the land expanded and that straight roads became curved due to the large displacements of the ground toward the river. Furthermore, many wells had to be abandoned since the well casings were bent.

Point ⑦: Between the Kuzuryu River and the Yoshino River, most of the rice fields were abandoned after being covered by a considerable amount of boiled sand. Most people who saw the boils said that the sand ejected was fine and blue.

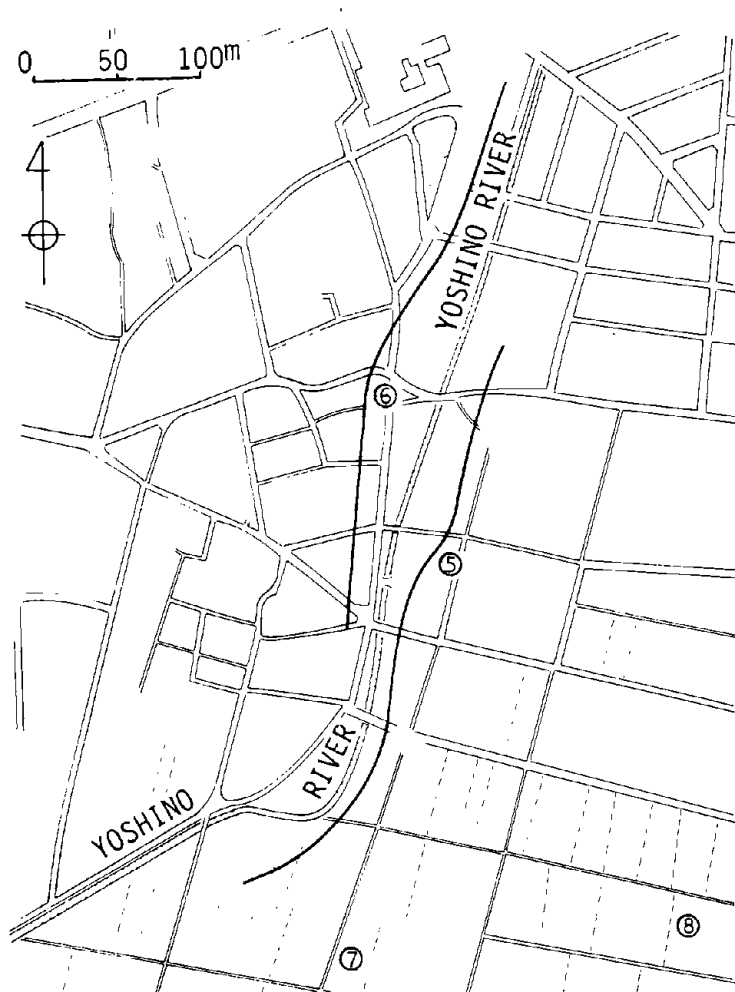
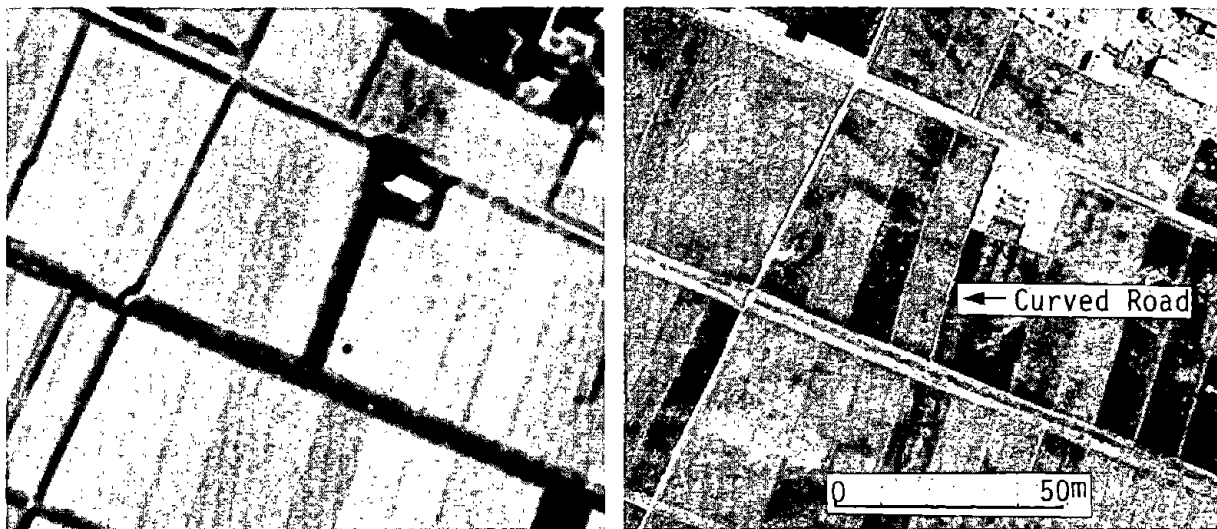


Figure 21. Ground Failures in the Uenohonmachi Area



(a) Before the Earthquake
 (b) After the Earthquake
 Photo 8 Road Curvature due to Permanent Ground Displacement
 (Point ⑧ in Figure 21)

Point ⑧: An agricultural road, which had been straight, was distorted by the earthquake. The maximum displacement at the mid-point of the road was about 4 m. This statement can be verified by aerial photographs taken before and after the earthquake, as shown in Photo 8.

4.3 Summary of Eyewitness Remarks

From the interviews with eyewitnesses of the earthquake, the following instructive information was obtained.

(i) Most of the eyewitnesses said that sand and water boils continued long after the earthquake ended and that fissures, caused by horizontal ground displacements, also continued to expand in width. These statements suggest that the liquefaction-induced ground displacements continued after the earthquake until the pore water pressure dropped.

(ii) Large ground displacements occurred in the direction of the Yoshino River, which was the old bed of the Kuzuryu River, but is now narrower. The river was drastically decreased in width. Furthermore, numerous sand boils were observed in the Yoshino River, and the river bed rose up.

(iii) Large ground fissures formed, mostly parallel to the Yoshino River, and numerous sand and water boils were observed in the low-lying land between the Yoshino and Kuzuryu Rivers. It is worth noting that damage to houses in this area was comparatively light, but the houses on the natural levees were severely damaged although the manifestations of liquefaction were not so severe. This suggests that ground acceleration on the natural levees was higher than that on the liquefied area.

5.0 CONCLUSIONS

The 1948 Fukui earthquake caused severe liquefaction over a vast area of the Fukui Plain along the Kuzuryu River and its tributaries. Many bridges collapsed or were seriously damaged due to liquefaction.

The authors have clarified that the liquefaction also caused large permanent ground displacements through measurements using aerial photographs taken before and after the earthquake. Several characteristics of the permanent ground displacements, ground failures, and their relationship with geological and soil conditions may be summarized as:

- (1) Permanent ground displacements occurred from the natural levees and alluvial fans, which had relatively high elevations, toward the old bed of the Agano River at a lower elevation. In the areas where the ground displacements began, a considerable number of ground fissures opened, whereas numerous sand and water boils were seen in the areas where the ground displacements terminated. The Yoshino River, toward which the ground displacements were directed, was greatly reduced in width and was partially filled.
- (2) Despite the overall ground displacements from the higher land to the lower land, no statistically significant correlation between the magnitude of ground displacements and the gradient of the ground surface was found. The same conclusion was reported in case studies of the 1964 Niigata earthquake¹¹⁾ and the Nihonkai-Chubu earthquake.¹²⁾
- (3) According to a survey of the soil and geological conditions, liquefiable soil, which was sand and sandy gravel, existed over a wide area under the slightly inclined ground surface, but no definite correlation between the gradient of the liquefiable layer and the direction of the permanent ground displacements can be established.
- (4) Interviews with eyewitnesses of the earthquake yielded useful information regarding the occurrence of permanent ground displacements.

Most said that sand and water boils continued and that ground fissures expanded in width for significant periods of time after the earthquake. This means that permanent ground displacements continued after transient earthquake motions had ceased.

REFERENCES

- 1) Office of General Headquarters, Far East Command, The Fukui Earthquake, Hokuriku Region, Japan, 28 June, 1948, Part I Geology and Part II Engineering.
- 2) Japan Science Council, "Report on The 1948 Fukui Earthquake," Committee Report on Damage during The Fukui Earthquake, Tokyo, Japan, March 1949 (in Japanese).
- 3) Japan Meteorological Agency, "The 1948 Fukui Earthquake," Kenshin-Giho No. 14, Tokyo, Japan, March, 1949 (in Japanese).
- 4) Shino, K., "Survey on Damage by The Fukui Earthquake and Aerial Photographs," Report No.6 of Japan Geographical Survey Office, Tokyo, Japan, 1949, pp. 2 to 3 (in Japanese).
- 5) Ogasawara, Y., "The 1948 Fukui Earthquake," Special Report No. 2 of Japan Geographical Survey Office, Tokyo, Japan, 1949 (in Japanese).
- 6) Japan Society of Civil Engineers, "Report on Earthquake Damage in Hokuriku Region (Damage to Civil Engineering Structures)," Research Team on Earthquake Damage in Hokuriku Region by J.S.C.E, Tokyo, Japan, October 1948 (in Japanese).
- 7) Architectural Institute of Japan, "Report on Earthquake Damage in Hokuriku Region (Damage to Buildings)," Journal of Architecture and Building Science No. 63, Research Team on Earthquake Damage in Hokuriku Region By AIJ, Tokyo, Japan, 1948 (in Japanese).
- 8) Fukui Prefectural Government, "Report on the 1948 Fukui Earthquake," Fukui, Japan (in Japanese).
- 9) Public Work Research Institute, "Report on Earthquake Damage in Hokuriku Region," Report No. 78 of P.W.R.I., Tokyo, Japan, 1949 (in Japanese).

- 10) Fukui Prefectural Government, "Report on Disaster by the 1948 Fukui Earthquake" Fukui, Japan, March, 1949 (in Japanese).
- 11) Hamada, M., "Large Ground Deformations and Their Effects on Lifelines: 1964 Niigata Earthquake," This volume.
- 12) Hamada, M., "Large Ground Deformations and Their Effects on Lifelines: The 1983 Nihonkai-Chubu Earthquake," This volume.
- 13) Seed, M.B., Tokimatsu, K., Harder, L.F., and Chung, R.M., "Influence of SPT Procedure in Soil Liquefaction Resistance Evaluation," Journal of Geotechnical Engineering, Vol. 111, No. 12, ASCE, New York, N.Y., 1985, pp. 1425-1445.
- 14) O'Rourke, T.D., Roth, B.L., and Hamada, M., "Large Ground Deformations and Their Effects on Lifeline Facilities: 1971 San Fernando Earthquake," Technical Report NCEER-91-0002, National Center for Earthquake Engineering Research, Buffalo, N.Y., 1992.

Appendix A Accuracy of Permanent Ground Displacement Measurements in
Fukui City

The accuracy of the permanent ground displacement measurements was estimated by the same method as in the case study on the Nihonkai-Chubu earthquake (see Reference 12, Appendix A). A detailed explanation of the photogrammetric analysis is given by O'Rourke, et al.¹⁴⁾ in conjunction with the 1971 San Fernando earthquake in a companion volume.

The accuracy of the permanent ground displacement measurements in Morita-cho, Fukui City was estimated to be ± 1.92 m in the horizontal direction and ± 1.56 m in the vertical direction. The accuracy of the aerial surveys before and after the earthquake was evaluated by a comparison between the coordinates of data points measured by aerial photographs and those taken from topographical maps at a scale of 1/2,500. The relatively large bounds on the estimated accuracy may have resulted in part from errors associated with the topographical maps. Table A-1 summarizes aerial survey accuracies before and after the earthquake, and accuracies of permanent ground displacement measurements.

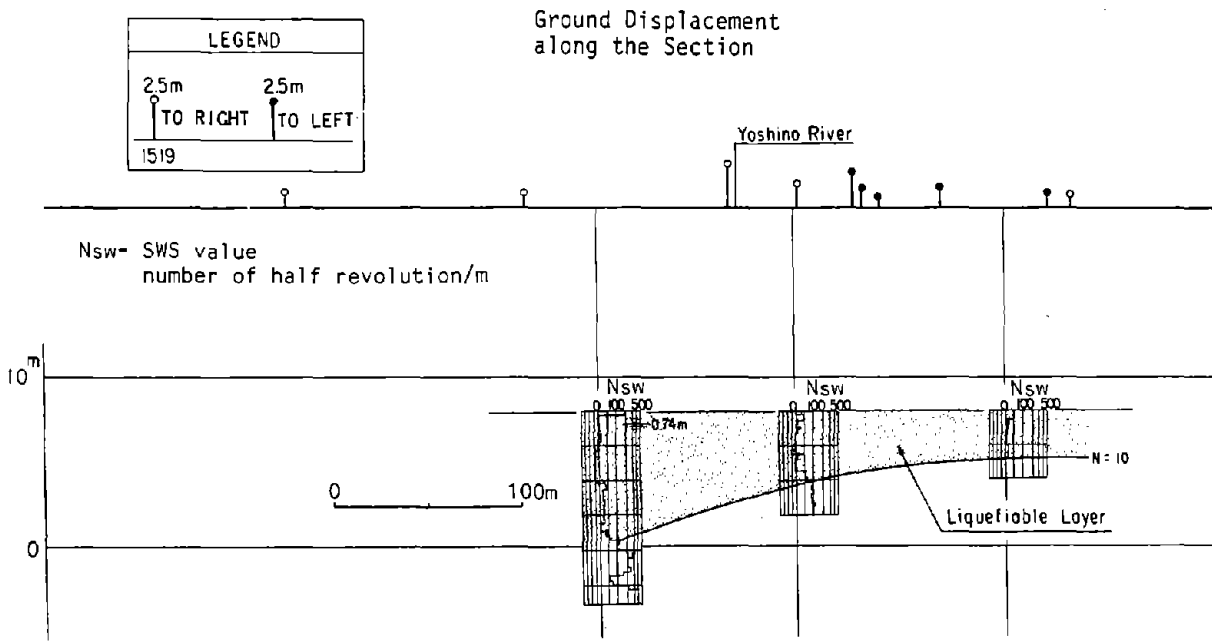
Table A-1 Accuracy of Measurement of Permanent Ground Displacements at Morita-cho in Fukui City

Aerial Survey	Pre-earthquake	Post-earthquake
Total Number of Data Points	15	16
Accuracy of Aerial Survey (Standard deviation of differences of coordinates by 1/2,500 map and aerial surveys)	(m) ± 1.53 (Hori.) ± 1.36 (Vert.)	(m) ± 1.16 (Hori.) ± 0.76 (Vert.)
Accuracy of Measurements Permanent Ground Displacement	$\pm \sqrt{(1.53)^2 + (1.16)^2} = \pm 1.92$ (Hori.) (m) $\pm \sqrt{(1.36)^2 + (0.76)^2} = \pm 1.56$ (Vert.) (m)	

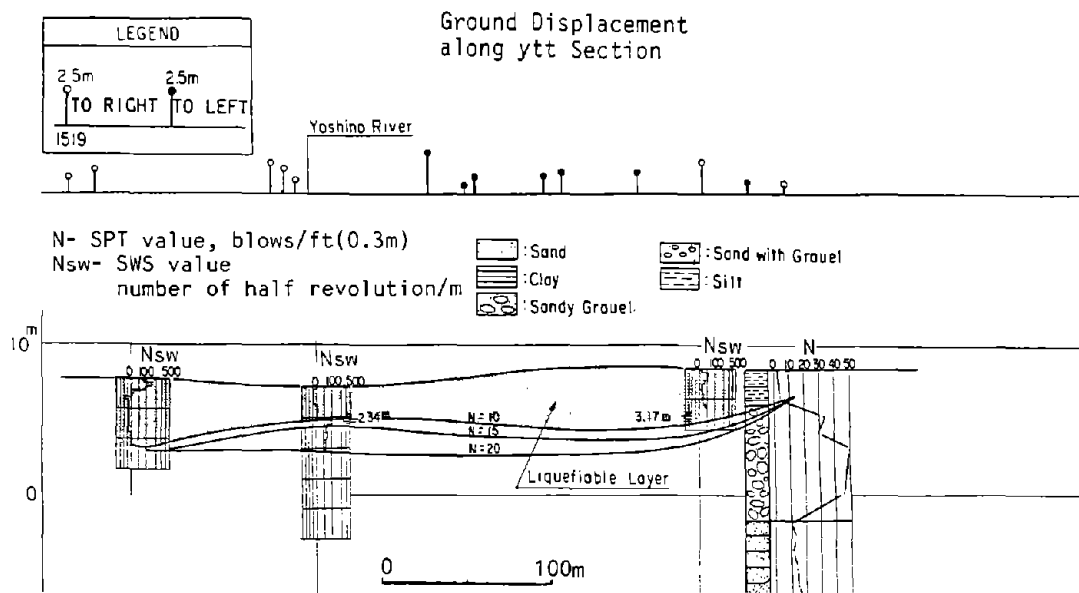
Appendix B Soil Conditions and Evaluation of Soil Layers Susceptible to Liquefaction

Soil conditions and the estimated liquefied soil layers along 5 sections, as marked in Figure 17 in Morita-cho, are shown in Figure B-1. Along sections 1-1', 2-2', and 3-3', most soil data were obtained using the Swedish weight sounding tests (SWS). Standard penetration test (SPT) values were obtained along sections 4-4' and 5-5'.

The SWS values, N_{sw} , expressed in number of half revolutions/m can be estimated as approximately 10 times the SPT value, N , expressed as blows per ft (0.3 m). This approximate relationship appears to be valid for granular soil deposits in the Fukui Plain. Using this relationship, lines of equivalent N are derived from N_{sw} data and superimposed on sections 1-1', 2-2', and 3-3'. In each of these cross-sections, the soils most susceptible to liquefaction are those with equivalent N less than or equal to 10.



(a) Section 1-1'



(b) Section 2-2'

Figure B-1 Soil Conditions and Evaluation of Soil Layers Susceptible to Liquefaction

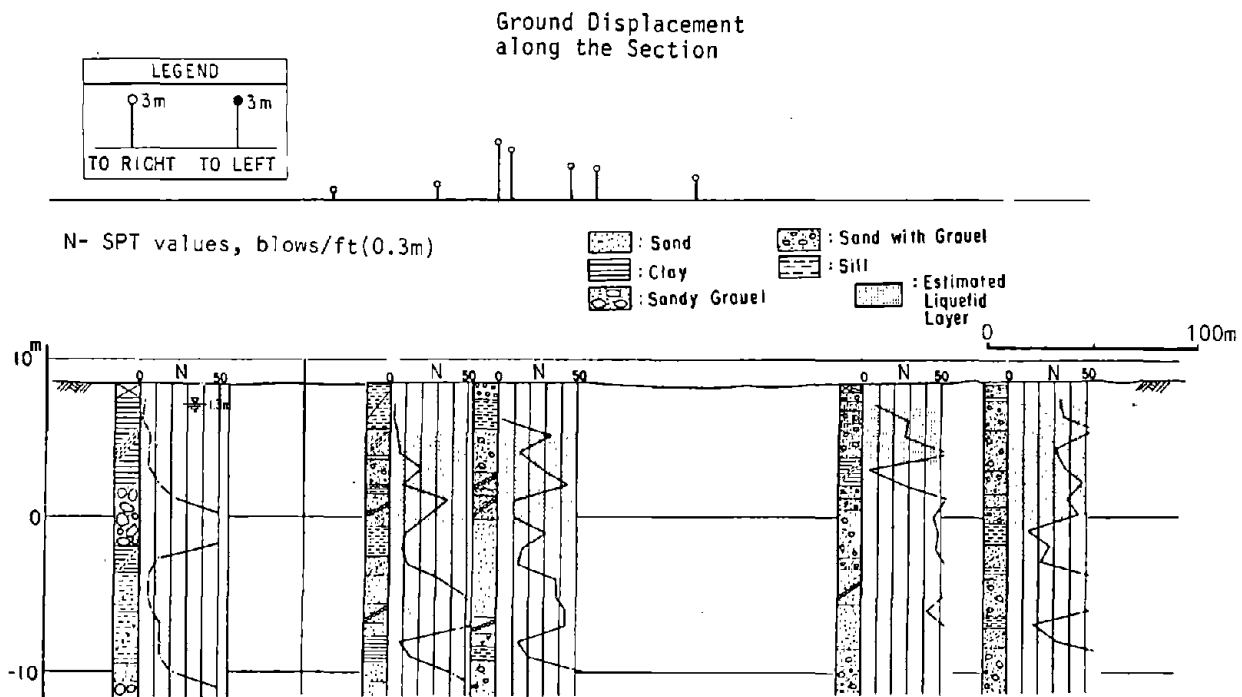
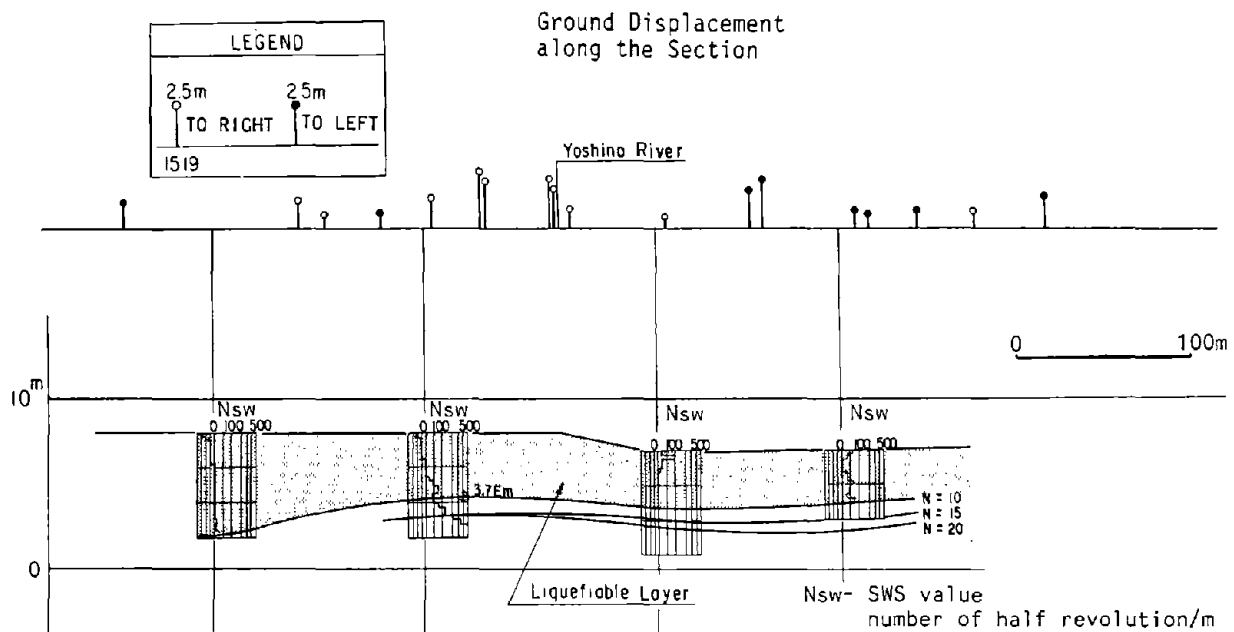
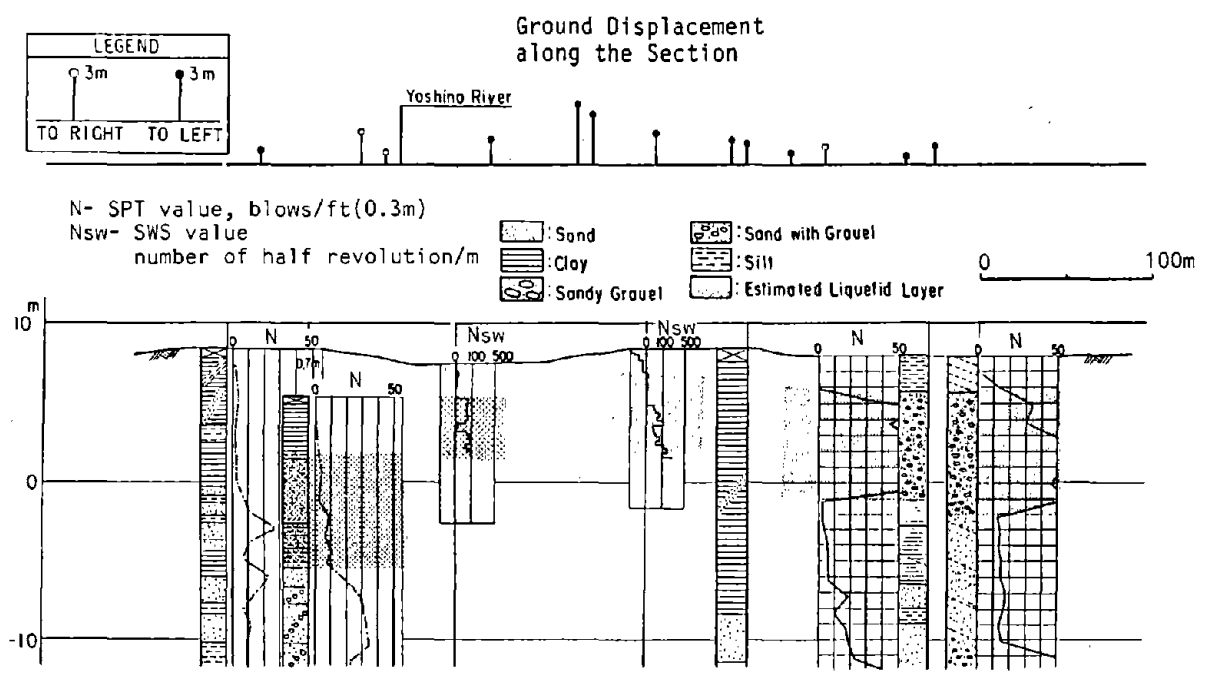


Figure B-1 Soil Conditions and Evaluation of Soil Layers Susceptible to Liquefaction



(e) Section 5-5'

Figure B-1 Soil Conditions and Evaluation of Soil Layers Susceptible to Liquefaction

**Large Ground Deformations and
Their Effects on Lifelines: 1964 Niigata Earthquake**

*M. Hamada, Professor
School of Marine Science and Technology
Tokai University
Shimizu, Shizuoka, Japan*



ACKNOWLEDGEMENTS

This case study of liquefaction-induced ground displacements and the damage caused by them during the 1964 Niigata earthquake was initiated by a research committee on **Earthquake Resistance of Buried Pipelines to Liquefaction** sponsored by the Tokyo Gas Company in 1984. The research committee was organized by the Association for the Development of Earthquake Prediction in Tokyo (ADEP) and was chaired by Professor K. Kubo of Tokai University. The committee continued its research work on the Niigata earthquake until 1987, and collected numerous data about liquefaction-induced permanent ground displacements, soil and geographical conditions, and about the damage to structures and lifeline facilities.

The research was taken over in 1988 by the Japanese team of the U.S.-Japan Cooperative Research on Liquefaction, **Large Ground Deformation and Their Effects on Lifeline Facilities**. This research team conducted additional measurements of liquefaction-induced ground displacements and soil condition survey in Niigata City. Furthermore, the team studied the mechanism of permanent ground displacement by analyzing the collected data and performing numerical analyses. The present report is a compilation of the materials collected by these two research groups and their results.

I wish thank those who have provided assistance in the execution of this research. Particular gratitude is extended to Prof. K. Kubo, who was chairman of the research committee organized by ADEP as well as chairman of the Japanese team in the U.S.-Japan Cooperative Research. Great thanks are also extended to Mr. H. Kobayashi, Mr. R. Osawa, Mr. H. Negishi, Mr. K. Saito, Mr. T. Iwata, and other staff at Tokyo Gas Company, who supported the research activity and gave me continuous encouragement. I also want to thank Mr. I. Yasuda of Hassu Co., Ltd. for performing the measurements of permanent ground displacement using aerial photographs. The collection of data on damage to structures and soil conditions was conducted mainly by the members of the research committee and the faculties and students of Tokai University. My great appreciation to Professor S. Yasuda at Kyushu Institute of Technology, Dr. R. Isoyama at Japan Engineering

Consultants Inc., Mrs. K. Wakamatsu at Waseda University, the late professor K. Emoto at Tokai University, Mr. M. Koshimizu and Mr. Y. Kojima, students at Tokai University, for their great assistance.

Finally, my deepest appreciation to Professor T.D. O'Rourke at Cornell University for his excellent editing of this case study.

Some of the contents of this report have already been published by ADEP in 1986,¹⁾ but for the convenience of readers, the important results are included in this paper, too.

TABLE OF CONTENTS

	<u>Page</u>
Acknowledgements	3-iii
Table of Contents	3-v
List of Figures	3-vii
List of Tables	3-xi
List of Photos	3-xiii
 <u>Section</u>	 <u>Page</u>
1.0 INTRODUCTION	3-1
2.0 OUTLINE OF THE 1964 NIIGATA EARTHQUAKE	3-3
2.1 Epicenter, Magnitude, and Intensity	3-3
2.2 Strong Motion Data	3-3
3.0 COLLECTION AND EVALUATION OF DATA	3-6
3.1 Measurement of Permanent Ground Displacements	3-6
3.2 Location of Large Ground Displacements	3-7
3.3 Surveys of Soil Conditions, and Interviews with Residents	3-9
4.0 PERMANENT GROUND DISPLACEMENTS AND RESULTING DAMAGE DURING THE 1964 NIIGATA EARTHQUAKE	3-10
4.1 Zone I: Upstream Area of Shinano River (Upstream from Bandai Bridge)	3-10
4.1.1 Permanent Ground Displacements	3-10
4.1.2 Soil Conditions	3-18
4.1.3 Damage to Structures	3-22
4.2 Zone II: Downstream Area of Shinano River (Downstream from Bandai Bridge, on the left bank)	3-39
4.2.1 Permanent Ground Displacements	3-39
4.2.2 Soil Conditions	3-39
4.2.3 Damage to Structures	3-44

<u>Section</u>	<u>Page</u>
4.3 Zone III: Niigata Port Area (Bandai Island, Fishery Pier, South Pier, North Pier and Rinko Wharf)	3-45
4.3.1 Permanent Ground Displacements	3-45
4.3.2 Soil Conditions	3-49
4.3.3 Damage to Structures	3-52
4.4 Zone IV: Niigata Station and the Surrounding Area	3-57
4.4.1 Permanent Ground Displacements	3-57
4.4.2 Soil Conditions	3-57
4.4.3 Damage to Structures	3-63
4.5 Zone V: Ebigase and Ohgata Areas	3-73
4.5.1 Permanent Ground Displacements	3-73
4.5.2 Soil Conditions	3-80
4.5.3 Damage to Structures	3-80
4.6 Zone VI: Matsuhama, Shitayama, and Shinkawa Areas	3-81
4.6.1 Permanent Ground Displacements	3-81
4.6.2 Soil Conditions	3-84
4.6.3 Damage Related to Liquefaction Induced Ground Displacements	3-88
5.0 EFFECTS OF THICKNESS OF LIQUEFIED LAYER AND GRADIENT OF GROUND SURFACE ON PERMANENT GROUND DISPLACEMENTS	3-91
6.0 CONCLUSION	3-95
References	3-98
Appendix A Accuracy of Permanent Ground Displacement Measurements in Niigata City	3-101
Appendix B Soil Conditions and Evaluation of Liquefied Layer	3-103
Appendix C Swedish Weight Sounding Test	3-120
Appendix D Factor of Liquefaction Resistance, F_L and Index of Liquefaction Potential, P_L	3-122

LIST OF FIGURES

<u>Figure</u>	<u>Page</u>
1 Epicenter and Seismic Intensity (JMAI) of the 1964 Niigata Earthquake	3-4
2 Strong Motion Recorded at Kawagishi-cho in Niigata City (Acceleration of 4-Storey Building)	3-5
3 Strong Motion Recorded in Niigata City (Meteorological Observatory)	3-5
4 Six Zones for Measurement of Permanent Ground Displacements in Niigata City	3-8
5 Permanent Ground Displacements in the Upstream Area of the Shinano River	
(a) Bandai Bridge to Yachiyo Bridge	3-11
(b) Yachiyo Bridge to Showa Bridge	3-12
(c) Showa Bridge to Echigo Railway Bridge	3-13
(d) Kawagishi-cho	3-14
(e) Kawagishi-cho to Sekiya-cho	3-15
6 Reduced Width of the Shinano River due to the 1964 Niigata Earthquake (m), (-: Reduction of Width)	3-17
7 Change of the Shinano River Course	
(a) Old Water Front circa 1600	3-20
(b) Old Water Front in 1911	3-20
8 Soil Conditions, Estimated Liquefied Layer, and Horizontal Ground Displacements	
(a) Section A-A' (Figure 5(a))	3-20
(b) Section B-B' (Figure 5(b))	3-21
(c) Section C-C' (Figure 5(c))	3-21
9 Damage to Yachiyo Bridge	3-24
10 Damage to a Foundation Pile of Yachiyo Bridge (P ₂)	3-24
11 Collapse of Showa Bridge	3-26
12 Deformation of a Steel Pipe Pile of Pier No. 4 (P ₄)	3-26
13 Movement and Deformation of Meikun High School Buildings, Sand Boils, and Ground Fissures	3-30

<u>Figure</u>	<u>Page</u>	
14	Damage to Hakusan Primary School	3-32
15	Footings and Foundation Beams of Niigata Family Court House	3-35
16	Damage to Piles and SPT-values of the Ground	3-35
17	Permanent Ground Displacement in the Vicinity of Niigata Family Court House	3-35
18	Damage to the Foundation Piles of S-Building	3-38
19	SPT-values at the Site of S-Building	3-38
20	Permanent Ground Displacement in the Downstream Area on the Left Bank of the Shinano River	
	(a) Bandai Bridge to Yanagishima	3-40
	(b) Estuary of the Shinano River	3-41
21	Soil Conditions	
	(a) Section D-D'	3-42
	(b) Section E-E'	3-42
22	Permanent Ground Displacement in Niigata Port Area	
	(a) Bandai Island, Fishery Pier, and South Pier	3-46
	(b) North Pier	3-47
	(c) Rinko Wharf	3-48
23	Bandai Island in 1911 and in 1964 (at the time of the earthquake)	3-50
24	Soil Conditions	
	(a) Section F-F'	3-50
	(b) Section G-G'	3-51
	(c) Section H-H'	3-51
25	Quay Wall of the Fishery Pier	3-54
26	Damage to the Kurinoki River (Point ② in Figure 22(a))	3-55
27	Permanent Ground Displacement at Niigata Station and Its Surroundings	
	(a) North Area	3-58
	(b) South Area	3-59

<u>Figure</u>	<u>Page</u>	
28	Soil Conditions and Estimated Liquefied Layer	
	(a) Section I-I'	3-61
	(b) Section J-J'	3-61
	(c) Section K-K'	3-62
29	Damage to Foundation Piles of the NHK-Building (Point ① in Figure 27(b)) (S. Kawamura et al.)	3-62
30	Permanent Ground Displacement in the Horizontal Direction in the Vicinity of the NHK-Building	3-64
31	Soil Conditions at the Hotel Niigata Site	3-66
32	Horizontal Vectors and Vertical Displacement of Ground in the Vicinity of the Hotel Niigata	3-66
33	Outline of the Hokuriku Building and Arrangement of Foundation Piles (Y. Yoshimi)	3-68
34	Bending Cracks in Concrete Piles of the East Bridge over Railway (Point ④ in Figure 27(b))	3-68
35	Horizontal Ground Displacement in the Vicinity of the East Bridge over Railway	3-70
36	Horizontal Ground Displacement in the Vicinity of Damaged Gas Pipe	3-72
37	Permanent Ground Displacement in Ebigase and Ohgata Areas	
	(a) West Area	3-74
	(b) East Area	3-75
38	Permanent Ground Displacement in the Horizontal Direction on a Contour Map	3-76
39	Change to the Agano River Course	3-77
40	Sand Boils and Ground Fissures in the Vicinity of the Ohgata Primary School	3-79
41	Soil Conditions and Estimated Liquefied Layer	
	(a) Section L-L'	3-82
	(b) Section M-M'	3-82
42	Permanent Ground Displacement in the Matsuhama, Shitayama, and Shinkawa Areas	3-85
43	Permanent Ground Displacement on a Contour Map of the Matsuhama, Shitayama, and Shinkawa Areas	3-86

<u>Figure</u>	<u>Page</u>	
44	Soil Conditions and Estimated Liquefied Layer	
	(a) Section N-N'	3-87
	(b) Section O-O'	3-87
45	Permanent Ground Displacement and Ground Fissures at Shitayama Primary School	3-89
46	Permanent Ground Displacement and Ground Fissures in Shinkawa-cho and Nearby	3-90
47	Correlation between Magnitude of Ground Displacement and Thickness of Estimated Liquefied Layer	3-93
48	Correlation between Magnitude of Ground Displacement and Gradient of Ground Surface	
	(a) Case 1: Horizontal distance is 5 times thickness of estimated liquefied layer	3-94
	(b) Case 2: Horizontal distance is 30 times thickness of estimated liquefied layer	3-94
B-1	Sections for Survey of Soil Condition and Estimation of Liquefied Layer	
	(a) Ebigase-Ohgata	3-104
	(b) Matsuhama-Shitayama-Shinkawa	3-105
	(c) Niigata Station and Its Vicinity	3-106
B-2	Soil Profile and Estimated Liquefied Layer	3-107
		through 3-119
C-1	Apparatus for Swedish Weight Sounding Tests (SWS)	3-121
C-2	Weight for SWS (Unit: mm)	3-121
C-3	Screwpoint for SWS (Unit: mm)	3-121
C-4	Result of SWS	3-121
D-1	Calculation of Index of Liquefaction Potential, P_L	3-123

LIST OF TABLES

<u>Table</u>		<u>Page</u>
A-1	Accuracy in Shinano River, Port Area, and Niigata Station Areas	3-101
A-2	Accuracy in Ebigase-Ohgata and Matsuhama-Shitayama-Shinkawa Areas	3-102



LIST OF PHOTOS

<u>Photo</u>	<u>Page</u>	
1	Aerial Photographs of Vicinity of the Ohgata Primary School (Zone V)	
	(a) Before the Earthquake (1962)	3-8
	(b) After the Earthquake (1964)	3-8
2	Aerial Photographs of the Shinano River	
	(a) Before the Earthquake (1962)	3-17
	(b) After the Earthquake (1971)	3-17
3	Aerial Photographs of the Left Bank of Bandai Bridge	
	(a) Before the Earthquake (1962)	3-23
	(b) Four hours after the Earthquake (1964)	3-23
	(c) Seven years after the Earthquake (1971)	3-23
4	Houses Fallen into the River on the Left Bank of Bandai Bridge	3-24
5	Damage to Yachiyo Bridge	3-24
6	Collapse of Showa Bridge	3-26
7	Aerial Photographs of Kawagishi-cho and Hakusan	
	(a) Before the Earthquake (1962)	3-29
	(b) After the Earthquake (1964)	3-29
8	Aerial Photographs of Meikun High School after the the Earthquake (1964)	3-30
9	Distorted Building at Meikun High School	3-32
10	Sand Volcano in Playground at Meikun High School	3-32
11	Aerial Photographs of Hakusan Primary School	3-32
12	Broken Wall of Swimming Pool	3-32
13	Damage to the Foundation Piles of Niigata Family Court House	
	(a) Upper Part of No. 2 Pile	3-34
	(b) Lower Part of No. 2 Pile (Bending Cracks)	3-34
	(c) Upper Part of No. 1 Pile (Compressive Stress by Bending Moment)	3-34

<u>Photo</u>	<u>Page</u>	
14	Damage to the Foundation Piles of S-Building	3-38
15	Aerial Photographs of Yanagishima-cho of the Downstream Area on the Left Bank of the Shinano River	
	(a) Before the Earthquake (1962)	3-43
	(b) After the Earthquake (1964)	3-43
16	Partially Sunk, Tilting Building in the Downstream Area on the Left Bank of the Shinano River, Point ① in Photo 15	3-43
17	Aerial Photographs of Bandai Island	
	(a) Before the Earthquake (1962)	3-54
	(b) After the Earthquake (1964)	3-54
18	Damage to the Quay Wall at the Fishery Pier (Point ① in Figure 22(a))	3-55
19	Damage to the Quay Wall on the Right Bank of the Old Kurinoki River (Point ② in Figure 22(a))	3-55
20	Damage to the Quay Wall of the North Pier (Point ③ in Figure 22(b))	3-55
21	Damage to the Quay Wall of the North Pier (Point ④ in Figure 22(b))	3-56
22	Damage to the Quay Wall of Rinko Wharf (Point ⑤ in Figure 22(c))	3-56
23	Damage to the Quay Wall of Rinko Wharf (Point ⑥ in Figure 22(c))	3-56
24	Damage to Foundation Piles of the NHK-Building (Point ① in Figure 27(b)) (S. Kawamura et al.)	3-64
25	Damaged Pile of the NHK-Building (S. Kawamura et al.)	3-64
26	Damage to Foundation Piles of the Hotel Niigata Building	3-66
27	Concrete Purification Tank Raised to the Surface at the Hotel Niigata	3-66
28	Collapse of the East Bridge over Railway (Point ④ in Figure 27(b))	3-68
29	Protrusion of a Buried Gas Pipe above the Surface (Point ⑤ in Figure 27)	3-70

<u>Photo</u>	<u>Page</u>
30 Buckling of a Buried Gas Pipe	3-70
31 Buckling of a Buried Gas Pipe	3-72
32 Route 7 after the Earthquake	3-77
33 Risen Portion of the Tsusen River	3-77
34 Ground Fissure in the Playground of the School	3-83
35 A Ground Fissure Underneath a Wooden School Building	3-83
36 Broken Wooden Floor due to Ground Fissure	3-83
37 Separation of Two Buildings	3-83
38 Deformed Road Resulting from the Earthquake	3-83
39 Damage to the School Gymnasium due to Displacement of the Foundations	3-89
40 Separation in a Brick Wall due to the Tensile Strain in the Ground	3-89
41 Ground Fissures in the School Playground	3-89
42 A Shrine Building Which Fell into a Ground Fissure	3-90
43 Ground Fissure with Vertical Displacement of about 1.5 m	3-90

1.0 INTRODUCTION

The Niigata earthquake, magnitude 7.5, occurred on June 16, 1964 and caused extensive soil liquefaction in Niigata City and the surrounding areas. Many buildings, bridges, quay walls, and lifeline systems such as electricity, gas, water, and telecommunications suffered severe damage. This earthquake led to awareness among engineers of the phenomenon of liquefaction in loose, saturated sand, and research was commenced to assess liquefaction and the potential damage it could cause.

The experience of the Niigata earthquake developed awareness of the following types of damage due to liquefaction: 1) Settlement, tilting, and toppling of structures due to reduction in ground bearing capacity; 2) Floating of buried structures such as manholes and tanks due to their buoyancy in the liquefied soil; and 3) Tilting or collapse of retaining walls and quay walls as a result of increased earth pressure and reduction in soil shear strength.

After the Niigata earthquake, research into these types of liquefaction-induced damage progressed. Various kinds of countermeasures to prevent such damage have been developed, and they are being applied in practice.

The author and his co-workers studied liquefaction resulting from the 1983 Nihonkai-Chubu earthquake and the damage caused. A comparison of pre- and post-earthquake aerial photographs clearly showed for the first time that the liquefied soil may induce large permanent displacements of several meters depending on the geographical conditions.

A similar aerial survey was conducted on areas of soil liquefaction caused by the Niigata earthquake, and it was shown that the permanent ground displacements in Niigata City were over 12 m. Besides measurements of permanent ground displacements, the soil and geographical conditions were investigated, and the mechanism of ground displacement was studied.

Furthermore, the damage to bridges, buildings, quay walls, and lifeline facilities in the liquefied area was surveyed, and the relationship between damage and ground displacements was assessed on a quantitative basis.

This paper provides a compilation of materials on the measured permanent ground displacements and soil conditions in Niigata City, as collected by the Japanese research team organized by the Association for the Development of Earthquake Prediction. It also discusses the mechanism of ground displacement and its effect on structures.

Some sections have been excerpted from an existing report, "Study on Liquefaction Induced Permanent Ground Displacement," published in 1986 by ADEP.¹⁾ After this report was published, surveys of permanent ground displacements continued in Niigata. The current paper offers an update on liquefaction-induced ground displacements caused by the 1964 Niigata earthquake and related data.

Detailed permanent ground displacement measurements, original data on soil conditions, and other information that cannot be included in this paper will be published at a later date by ADEP as reference material.

2.0 OUTLINE OF THE 1964 NIIGATA EARTHQUAKE

2.1 Epicenter, Magnitude, and Intensity²⁾

The earthquake occurred on June 16, 1964 at 1:01 p.m. It registered magnitude 7.5 and affected the Japan Sea coast from Niigata through Yamagata and Akita Prefectures. In Niigata City, in particular, which is about 50 km from the epicenter, buildings, bridges, oil storage tanks, lifeline facilities, etc., were extensively damaged. The epicenter was near Awa Island at coordinates $38^{\circ}21'N$, $139^{\circ}11'E$ in the Japan Sea, 22 km off the coast, as shown in Figure 1. The focus of the earthquake was about 40 km deep.

According to seismic measurements on the Japanese Meteorological Agency Scale (JMAI), shown in Figure 1,²⁾ the greatest intensity was V, which is almost equivalent to VII to VIII on the Modified Mercalli Intensity Scale (MMI), and the area of intensity V was comparatively limited. Generally, the maximum acceleration on the ground surface in an area of intensity V is estimated to be within 0.08 to 0.25 g, and so it can be said that the ground motion was not strong considering the severe damage the earthquake caused.

2.2 Strong Motion Data

Earthquake motion data were recorded at two locations in Niigata City. Acceleration data, shown in Figure 2, were recorded in the basement as well as on the roof of a building in Kawagishi-cho.²⁾ The location of the building is shown in Figure 5(e). As described later, an extensive area of Kawagishi-cho was subjected to liquefaction, and other buildings of the same type in the neighborhood toppled over due to liquefaction. However, the damage to the building where the earthquake motion was recorded was very light, except for slight tilting.

The following characteristics can be deduced from the record. During the first part of the record (about 7 sec.), motion with a predominant period of about 0.1 sec. occurred with an amplitude of about 0.05 g. During the second part (7 to 11 sec.) the acceleration reached a maximum of 0.159 g in the

basement and 0.184 g on the roof, and the predominant period drastically increased to about 0.8 sec. After the second part, earthquake motion with a long period of several seconds followed. One of the probable reasons for this drastic change in predominant period of the earthquake motion could be the effect of liquefaction.

Further earthquake motion data was recorded at Niigata Meteorological Observatory on a displacement recorder.²⁾ The location of the observatory is shown in Figure 5(b). Unfortunately, the displacement record in the horizontal direction went off-scale as shown in Figure 3. According to the data in the vertical direction, the main earthquake motion continued for more than 2 minutes.

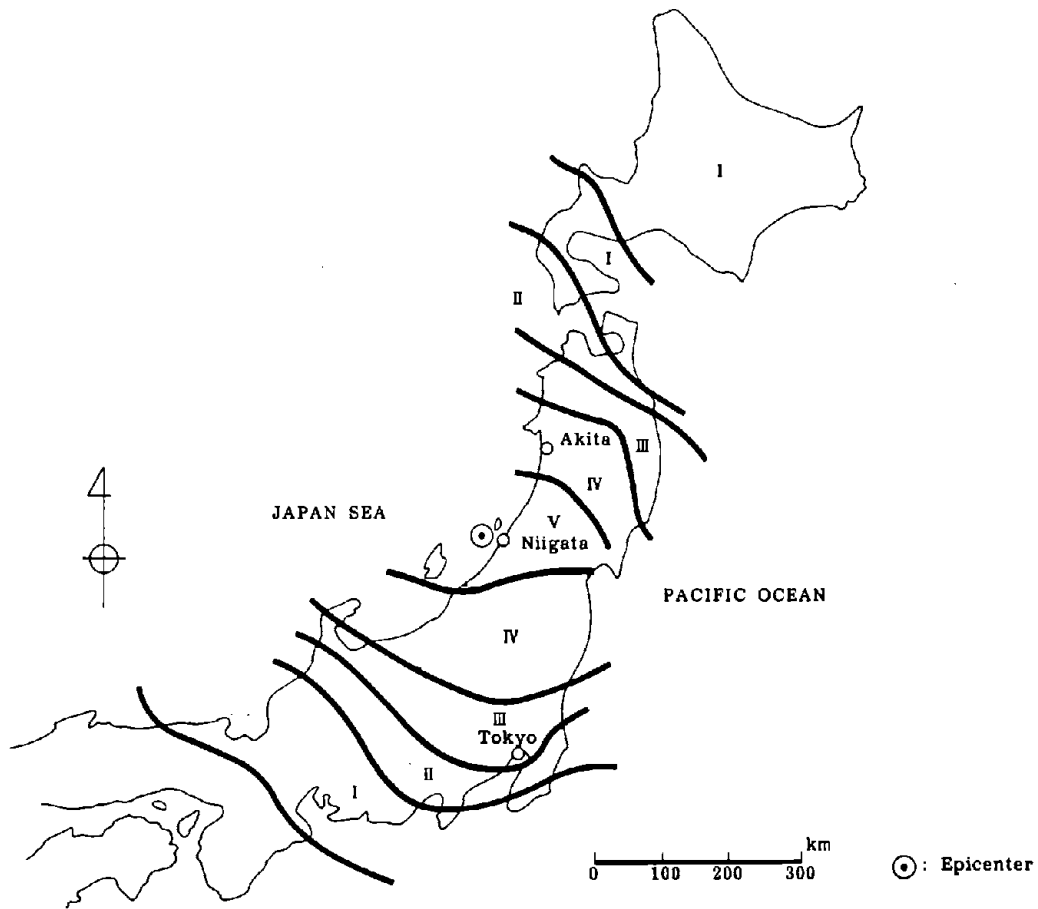
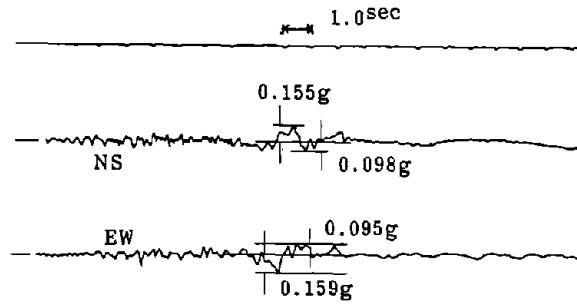
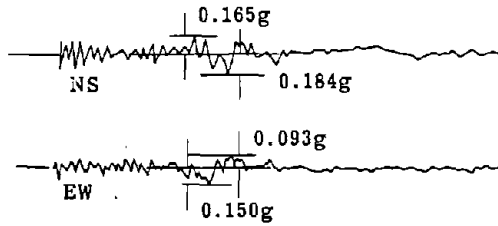


Figure 1. Epicenter and Seismic Intensity (JMAI) of the 1964 Niigata Earthquake²⁾



(a) In The Basement



(b) On The Roof

Figure 2. Strong Motion Recorded at Kawagishi-cho in Niigata City (Acceleration of 4-Storey Building)²⁾

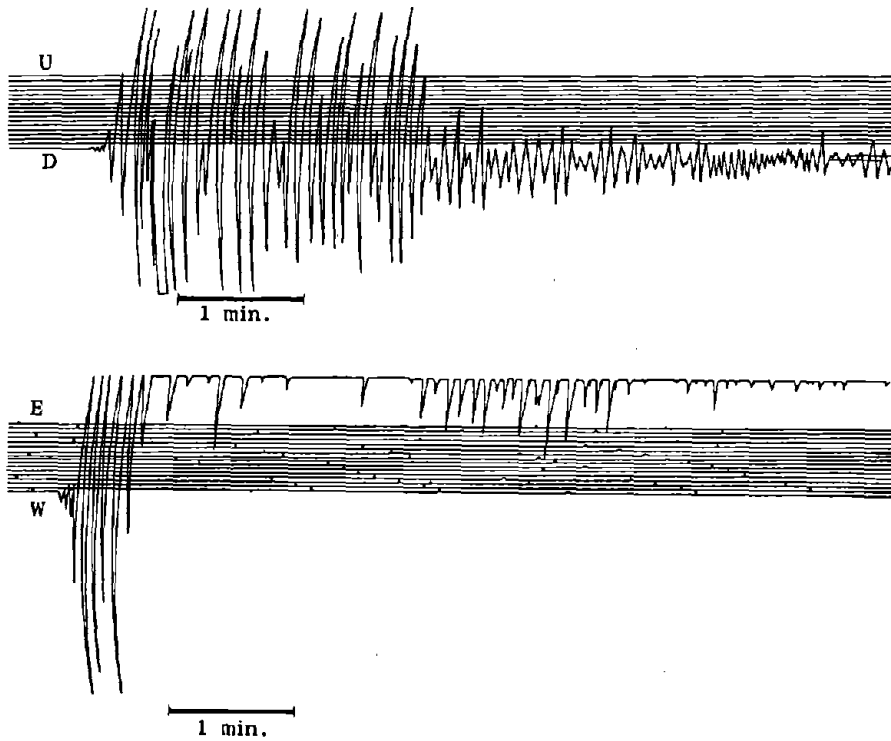


Figure 3. Strong Motion Recorded in Niigata City (Meteorological Observatory)²⁾

3.0 COLLECTION AND EVALUATION OF DATA

3.1 Measurement of Permanent Ground Displacements

In order to measure permanent ground displacements caused by the earthquake, aerial photographs taken before and after the earthquake were used. The permanent ground displacements can be evaluated by subtracting the coordinates of measurement points on the ground surface determined from pre-earthquake photographs from those taken from post-earthquake photographs. Photo 1 is one example of a pair of aerial photographs used for the measurement of permanent ground displacements, showing the vicinity of the Ohgata Primary School. The details of the permanent ground displacement and its related damage are discussed later in 4.5. The pre-earthquake photo was taken two years prior to the earthquake at a scale of 1/11,000. The post-earthquake photo, which shows numerous fissures on the ground surface and deformation of roads, was taken four hours after the earthquake at a scale of 1/12,500.

To measure permanent ground displacements using pre- and post-earthquake aerial photographs, it is necessary to select data points which are considered to be unaffected by the earthquake. In principle, most of the data points in this survey were selected from triangulation points in the periphery of the area to be measured. All the selected triangulation points were located on the stable tops of new sand dunes along the Japan Sea which suffered no ground failures, including liquefaction, and where no damage to structures was found. It can be assumed that no permanent ground displacements were caused by the earthquake in the neighborhood of these triangulation points.

Measurements of permanent ground displacements must be made for points which are fixed to the surface and which can be found in both the pre- and post-earthquake photographs. Manholes, cadastral boundary stones, corners of drainage channels, etc., were selected where possible, but in areas where measurement points such as these could not be found, the roofs of houses

confirmed to have suffered no damage were selected. A total of about 8,000 points was selected in Niigata City.

The accuracy of permanent ground displacement measurements depends on the scales of the pre- and post-earthquake aerial photographs, human error in reading the coordinates of the measurement points, and other factors. The accuracy was estimated to be ± 72 cm horizontally and ± 66 cm vertically along Shinano River areas and in Niigata station area. Furthermore, the accuracy in Ebigase-Ohagata and Matsuhama-Shitayama-Shinkawa areas was estimated to be 99 cm in the horizontal direction and 46 cm in the vertical direction.*

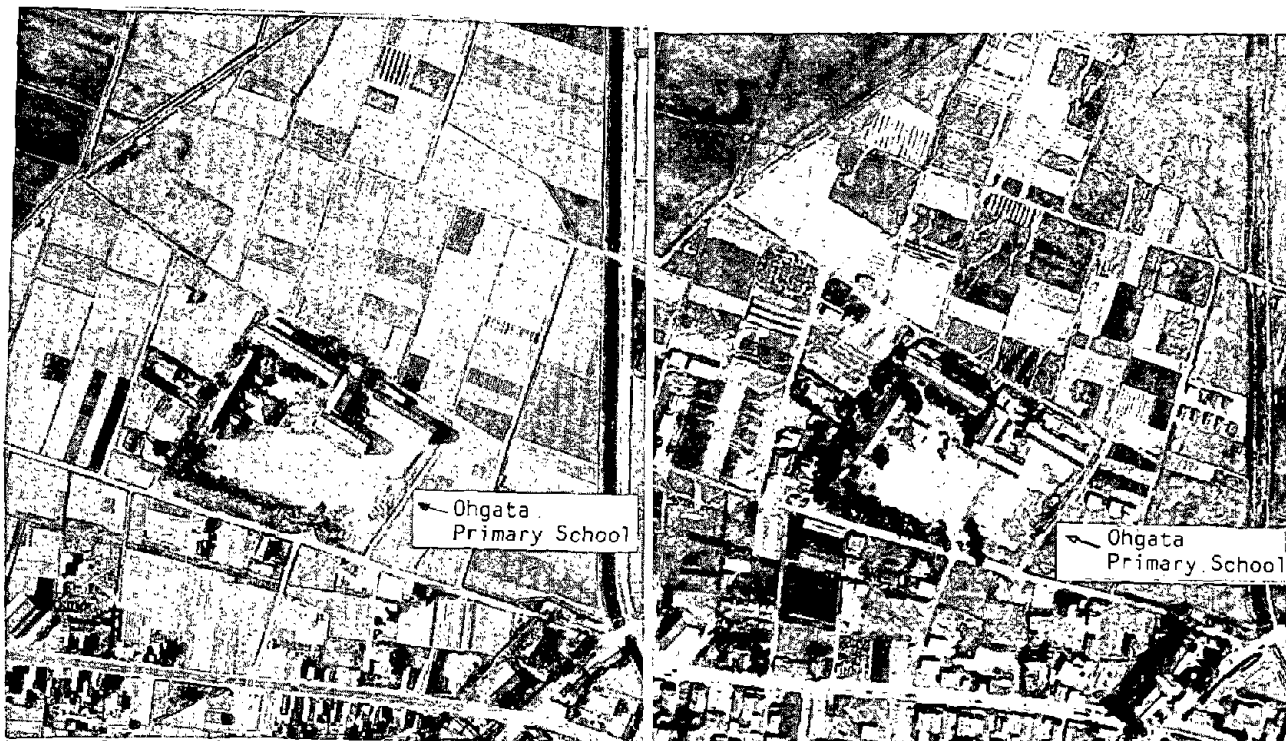
3.2 Location of Large Ground Displacements

Sand boils and ground fissures were observed in extensive areas of Niigata City resulting from liquefaction. Taking damage to structures and ground failures due to liquefaction into consideration, the six zones shown in Figure 4 were selected for the measurement of permanent ground displacements. Besides measurement of ground displacements, data on soil and geological conditions, and damage to structures were collected. Furthermore, the causal relationships between structural damage and ground displacements, as well as the relationship between soil conditions and the magnitude and direction of ground displacements, were investigated.

The six zones are:

- (1) Zone I: Upstream area of Shinano River (upstream from Bandai Bridge)
- (2) Zone II: Downstream area of Shinano River (downstream from Bandai Bridge on the left bank)
- (3) Zone III: Niigata Port area
- (4) Zone IV: Niigata Station and the surrounding areas
- (5) Zone V: Ebigase and Ohgata areas
- (6) Zone VI: Matsuhama, Shitayama, and Shinkawa areas

*See Appendix A.



(a) Before the Earthquake (1962)

(b) After the Earthquake (1964)

Photo 1 Aerial Photographs of Vicinity of Ohgata Primary School (ZONE V)

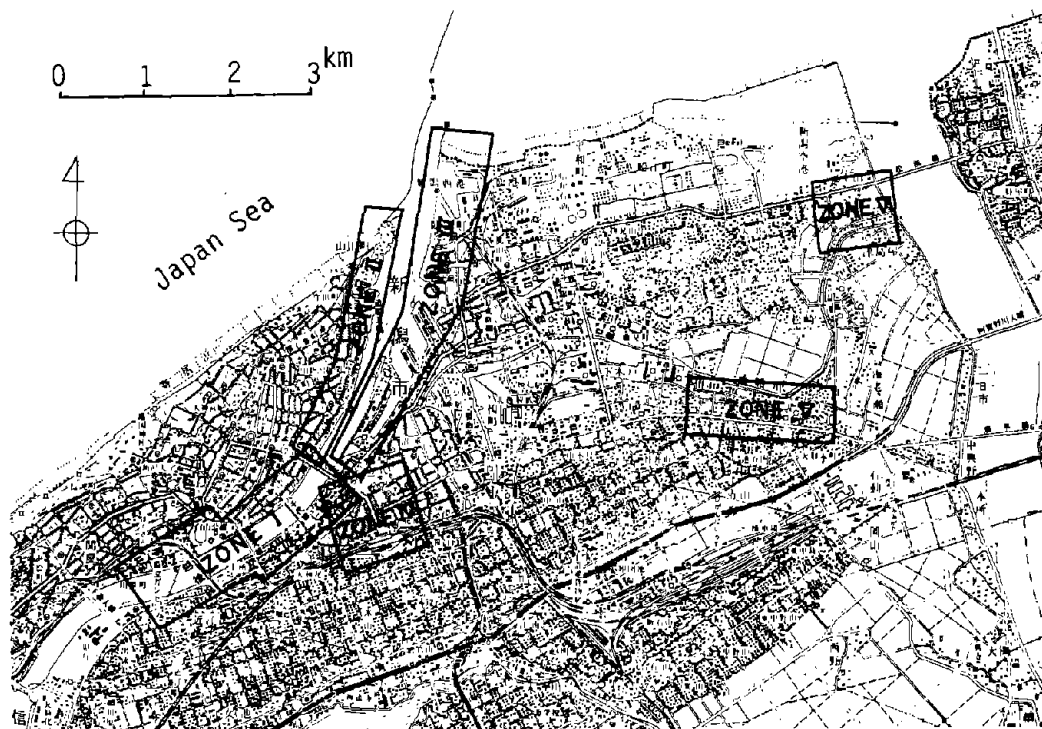


Figure 4. Six Zones for Measurement of Permanent Ground Displacements in Niigata City

3.3 Surveys of Soil Conditions, and Interviews with Residents

In order to clarify the mechanism of permanent ground displacements, a detailed study needs to be conducted on the relationship of both the magnitude and direction of permanent ground displacements, with the soil and geological conditions. Therefore, soil surveys were performed in the six zones, including standard penetration tests (SPT),³⁾* at 20 locations and Swedish weight soundings tests (SWS),** at about 100 locations. Based on the soil survey, soil profiles were drawn along section lines generally parallel to the direction of horizontal displacements of the ground, and the effects of the surface gradient, liquefied layer inclination, the thickness of the liquefied layer, and other factors on the magnitude and direction of the permanent displacements were investigated.

A number of residents, who experienced liquefaction, were interviewed to clarify the occurrence of ground fissures, sand and water boils, and damage to structures. Photographs and other documents showing ground failures and damage to structures were collected from residents.

*Generally, N-values in the U.S. standard are larger than those in the Japanese standard, because of the difference in energy transfer efficiency from the hammer to the rod (see reference 3)).

**See Appendix C.

4.0 PERMANENT GROUND DISPLACEMENTS AND RESULTING DAMAGE DURING THE 1964 NIIGATA EARTHQUAKE

4.1 Zone I: Upstream Area of Shinano River (Upstream from Bandai Bridge)

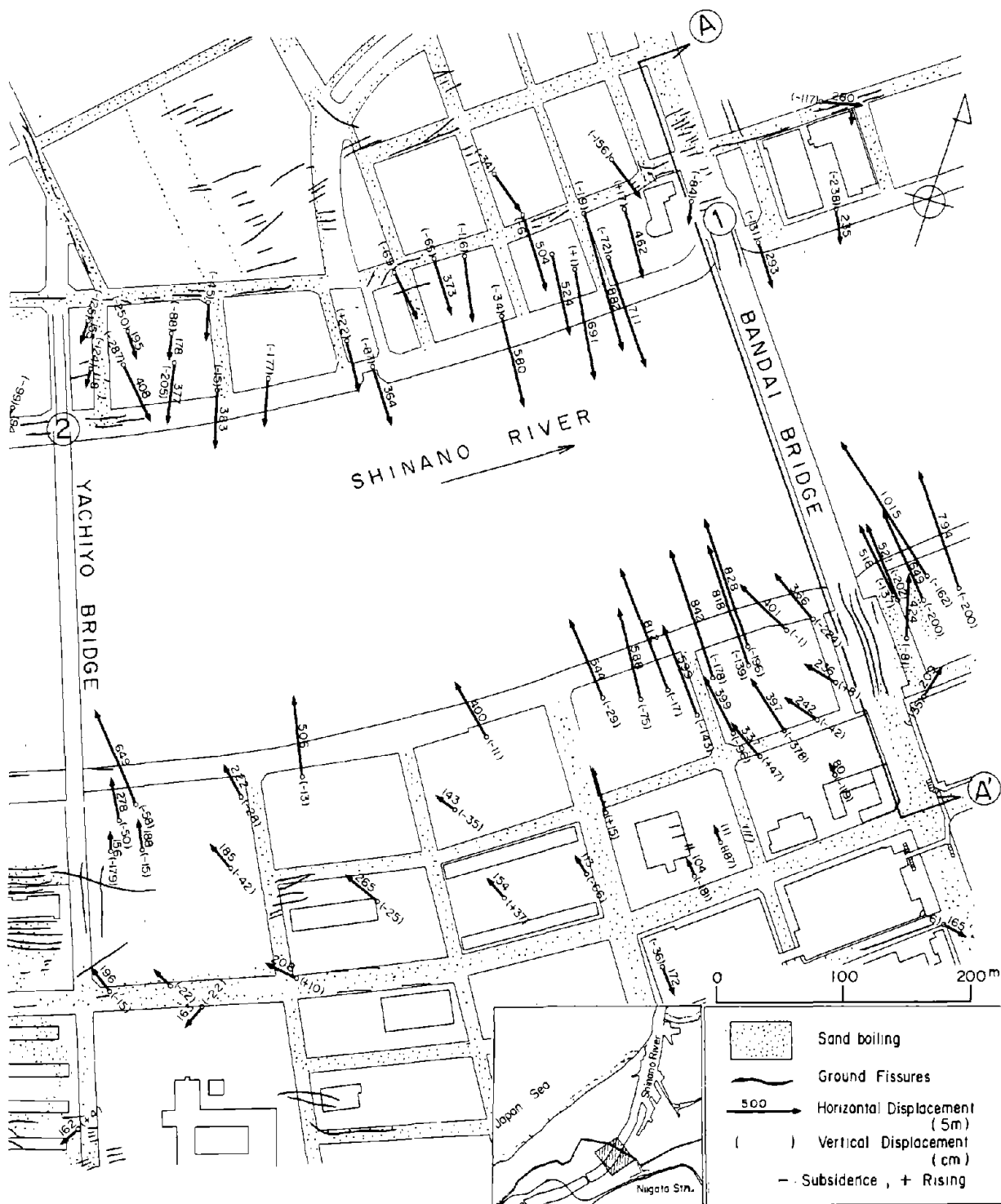
4.1.1 Permanent Ground Displacements

Figures 5(a)-(e) show the permanent ground displacements measured by aerial survey in the upstream reaches of the Shinano River. Figures (a) and (b) are from Bandai Bridge to Showa Bridge, while Figures (c) to (e) are from Showa Bridge to Sekiya-cho. The vectors represent ground displacements in the horizontal direction, each with a number indicating the magnitude of movement (in cm). The numbers in parentheses are displacements in the vertical direction (in cm). The figures also show the locations of ground failures, such as fissures and sand and water boils, which were surveyed by Niigata University immediately after the earthquake.

From these figures, it can be seen that the ground along the Shinano River was displaced mainly toward the river. The horizontal displacements of the ground are mostly perpendicular to the river bank.

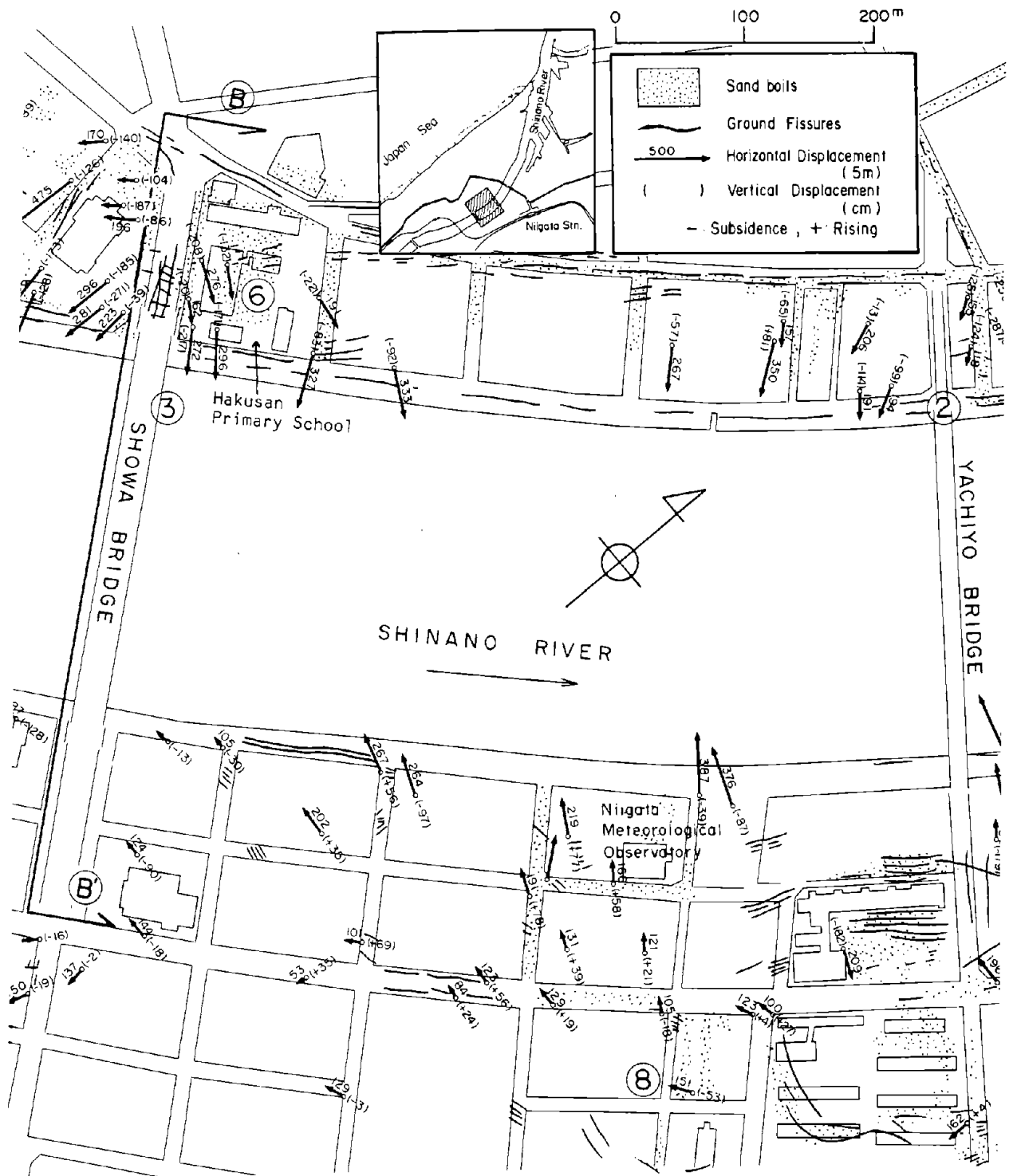
Between Bandai Bridge and Showa Bridge (Figure 5(a) and (b)), both banks moved towards the river. In particular, between Bandai Bridge and Yachiyo Bridge the horizontal displacements towards the river are very large, with the maximum displacement reaching over 8 m. It is notable that the horizontal displacements in the vicinity of the Bandai, Yachiyo, and Showa Bridge abutments were reduced because of the resistance of the structures to ground displacements.

Upstream from the Showa Bridge, ground displacements in the horizontal direction are large on the left bank of the river (Figures 5(c), (d)) but small on the right bank, except in Shinko-cho (Figure 5(e)). As described in 4.1.2, the left bank upstream from Showa Bridge is where the old riverbed was, while most of the right bank is located on a natural levee.



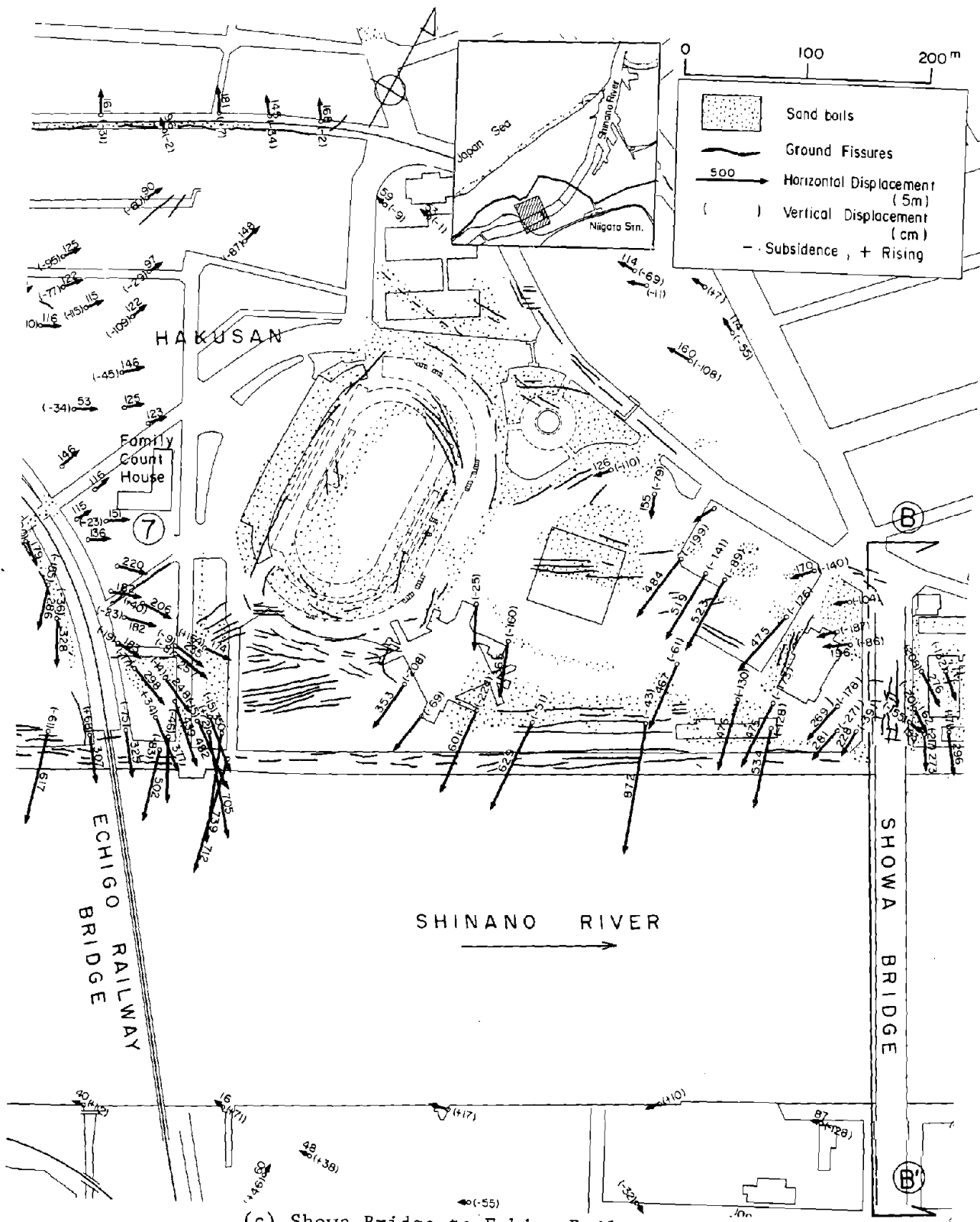
(a) Bandai Bridge to Yachiyo Bridge

Figure 5. Permanent Ground Displacements in the Upstream Area of the Shinano River



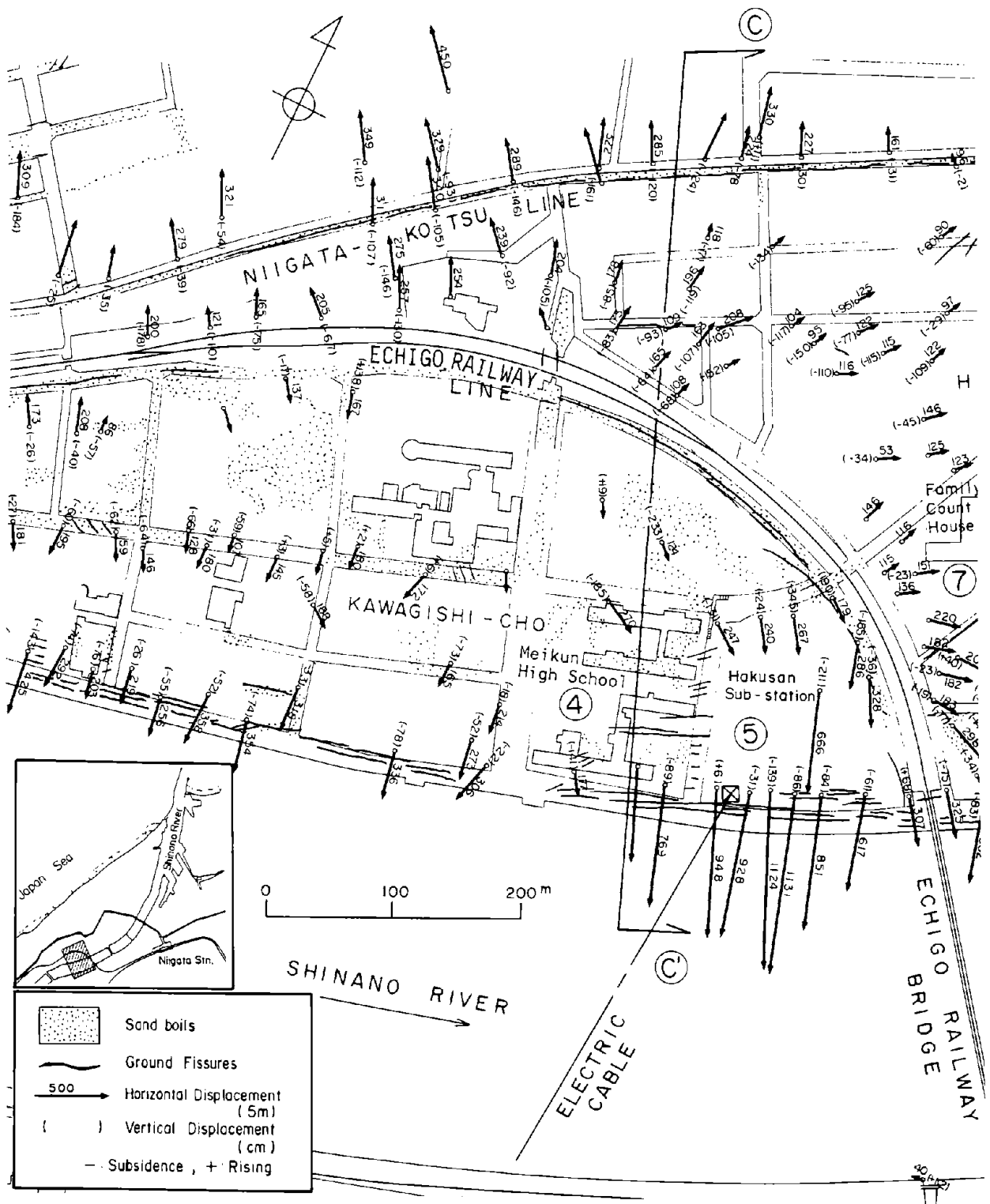
(b) Yachiyo Bridge to Showa Bridge

Figure 5. Permanent Ground Displacements in the Upstream Area of the Shinano River



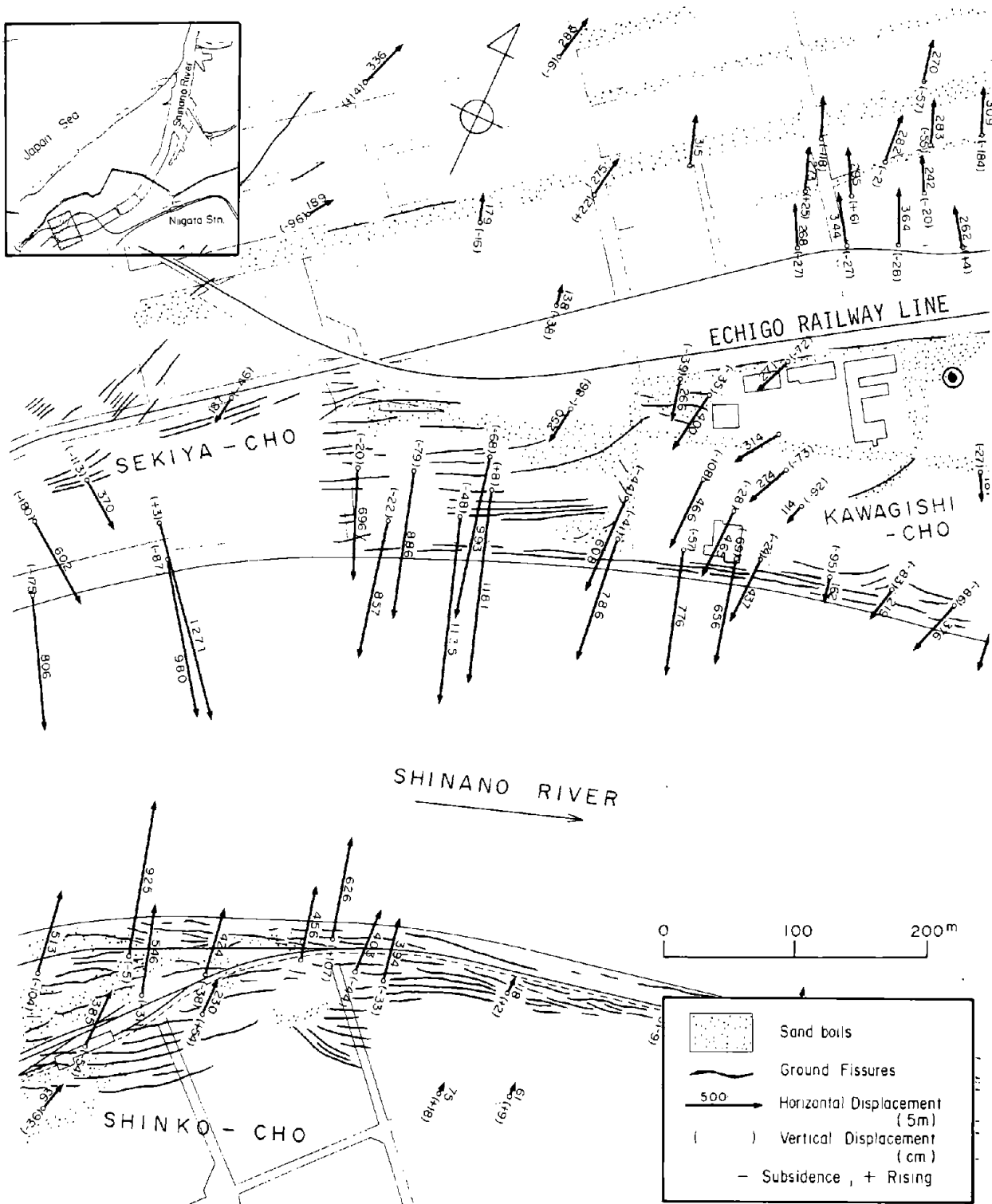
(c) Showa Bridge to Echigo Railway Bridge

Figure 5. Permanent Ground Displacements in the Upstream Area of the Shinano River



(d) Kawagishi-cho

Figure 5. Permanent Ground Displacements in the Upstream Area of the Shinano River



(e) Kawagishi-cho to Sekiya-cho

Figure 5. Permanent Ground Displacements in the Upstream Area of the Shinano River (●: Location of Accelerogram in Figure 2)

Horizontal ground displacements in Kawagishi-cho are extremely large (Figure 5(d)). The maximum displacement in this area is greater than 11 m. Furthermore, in Sekiya-cho, on the left bank, ground displacement was over 12 m (Figure 5(e)), which is the maximum measured displacement in Niigata City. Most ground displacements are toward the river, but it is noteworthy that displacements along the Echigo Railway Line are toward the north, not toward the river (Figure 5(d)). The relationship between direction of ground displacement and the topographic conditions will be discussed in 4.1.2.

Most of the revetments of the Shinano River, which were built of steel sheet piles and wooden piles, collapsed during the earthquake. It can be surmised that the ground near the river moved toward the river after the collapse of the revetments. However, most of the measuring points of permanent ground displacements shown in Figure 5 are located far enough from the revetments to escape the influence of the collapse, and so the results in Figure 5 indeed show that ground over a wide area along the river bank moved toward the river. This means that the river's width was greatly reduced by the earthquake. To verify this fact, an aerial photograph survey was performed, focusing on the change in river width. The change was estimated by subtracting the river width measured on aerial photographs taken two years before the earthquake, from that measured on photographs taken in 1975, by which time the bank revetments had been completely restored. Photo 2 shows the aerial photographs used for these measurements and Figure 6 shows the change in river width. Between Bandai Bridge and Yachiyo Bridge, where permanent ground displacements with a maximum extent greater than 8 m occurred on both banks, the river width was reduced by 16 to 23 m, while between Showa Bridge and Kawagishi-cho, where large permanent ground displacements reaching a maximum of about 11 m occurred only on the left bank, the river width was reduced by 7 to 13 m.

These measured contractions in river width are somewhat larger than the sum of permanent ground displacements, as shown in Figure 5, on both banks of the river. However, taking into account the fact that new revetments were constructed after the earthquake by driving steel sheet piles in front of the



(a) Before the Earthquake (1962)



(b) After the Earthquake (1971)

Photo 2 Aerial Photographs of the Shinano River

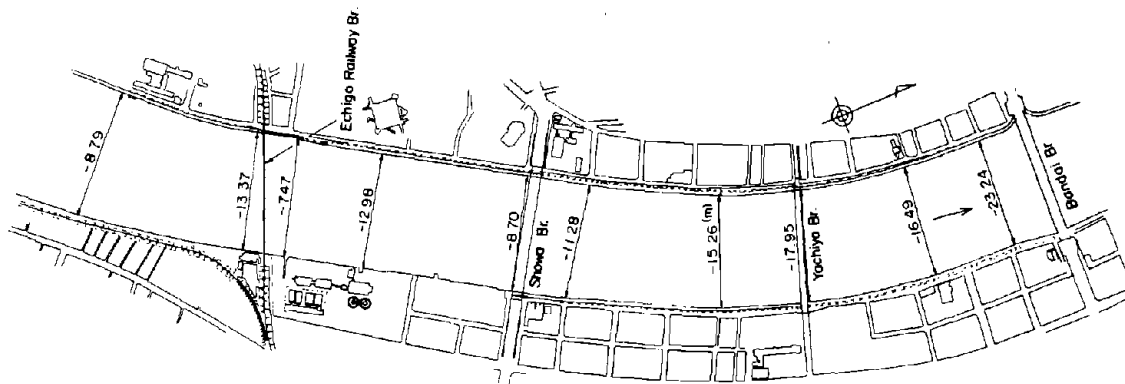


Figure 6. Reduced Width of the Shinano River due to the 1964 Niigata Earthquake (m), (-: Reduction of Width)

collapsed revetments, it can be concluded that reductions in river width, after adjusting for the effects of new construction, coincide quantitatively with the permanent ground displacements measured on the river banks.

The whole area along the Shinano River subsided by 1 to 2 m, as shown by the numbers in parentheses in Figure 5. In Kawagishi-cho ground subsidence greater than 2 m was observed.

Some witnesses who were in the neighborhood of the Shinano River at the time of the earthquake remarked that they saw sand boil above the level of water in the river at numerous places. They noted that the sand boils looked like cacti. These remarks, and the large subsidence of the ground on the river banks, suggest that a considerable amount of sand was carried toward the river.

Many ground fissures, as well as sand and water boils, were also observed along the river. Most of the ground fissures were parallel to the revetments and generally perpendicular to the ground displacements. Areas where ground failures were observed coincide with those where permanent ground displacements occurred.

4.1.2 Soil Conditions

The bed of the Shinano River has moved as shown in Figure 7. By referring to the old line of the river and the coast, circa 1600, it can be concluded that the location of the former river channel roughly coincides with the area where large ground displacements occurred and where ground failures, such as fissures and sand boils, were observed. Namely, the area on the left bank from Showa Bridge to Kawagishi-cho and the area on both banks from Yachiyo Bridge to Bandai Bridge are where the river channel used to be. On the contrary, the area on the right bank from Echigo Railway Bridge to Showa Bridge is on the old natural levee of the river.

Figure 8 shows the soil conditions along 3 section lines crossing the Shinano River and the liquefied layers evaluated using the Factor of Liquefaction

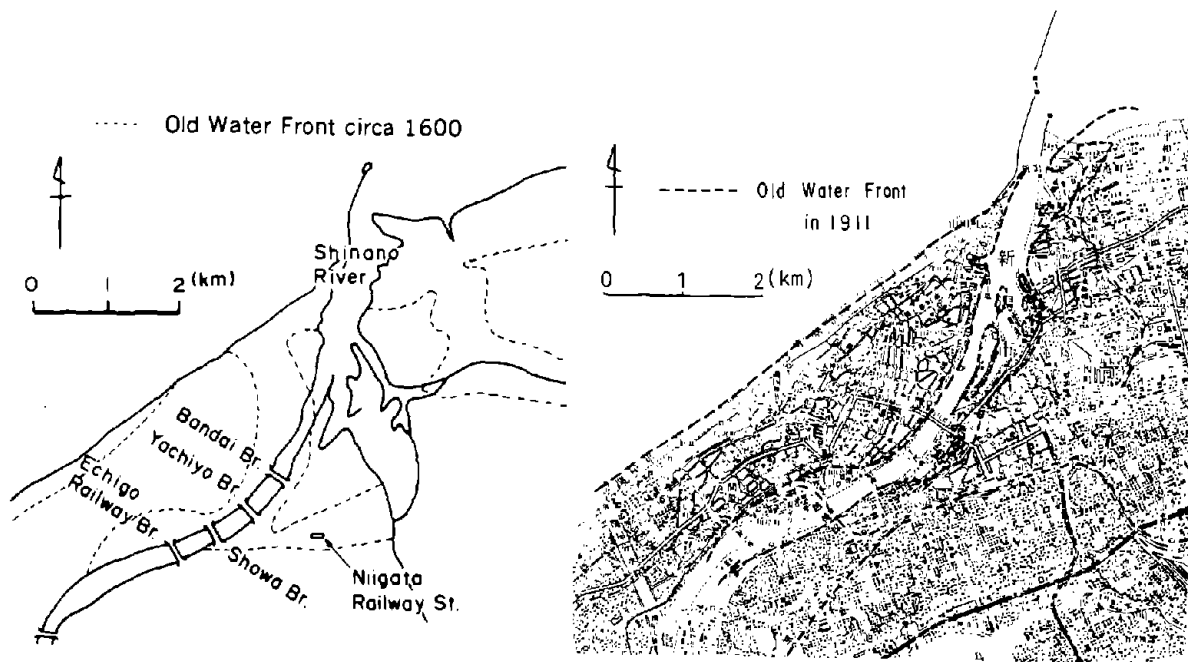
Resistance F_L .⁴⁾* Soil layers with F_L below 1.0 were evaluated to have liquefied during the earthquake. The maximum acceleration at the ground surface, which is required in making an estimate of F_L , was assumed to be about 0.16 g by referring to maximum acceleration recorded in Kawagishi-cho.** The elevation of the ground surface was measured from the aerial photograph taken before the earthquake. Figure 8 also shows the components of the horizontal ground displacements along the section lines.

Section A-A' is along Bandai Bridge as shown in Figure 5(a). Liquefaction was estimated to have occurred in the riverbed as well as in the ground on both banks. The maximum thickness of the liquefied soil is about 10 m at the center of the riverbed. The lower boundary of the liquefied layer was inclined toward the center of the river from both banks. It can be conjectured that the inclination of the boundary had some effect on the occurrence of ground displacements toward the river in addition to vertical difference of ground surface at the revetments of the river.

Section B-B' is along Showa Bridge as shown in Figure 5(b). The simply supported girders of the bridge dropped into the water as a result of the earthquake, as mentioned in 4.1.3 (3). In the neighborhood of the bridge, the ground moved only on the left bank and the maximum displacement was about 4 m. However, the ground displacement on the right bank was very small. Liquefied layers appear to be present in the riverbed and under the left bank, but not under the right bank. As shown in Figure 7, the left bank is underlain by the old riverbed, while the right bank is on the old natural levee. In this case also, the lower boundary of the liquefied layer is inclined toward the river center from the left bank.

*Evaluation of Factor of Liquefaction Resistance, F_L and Index of Liquefaction Potential, P_L is shown in Appendix D.

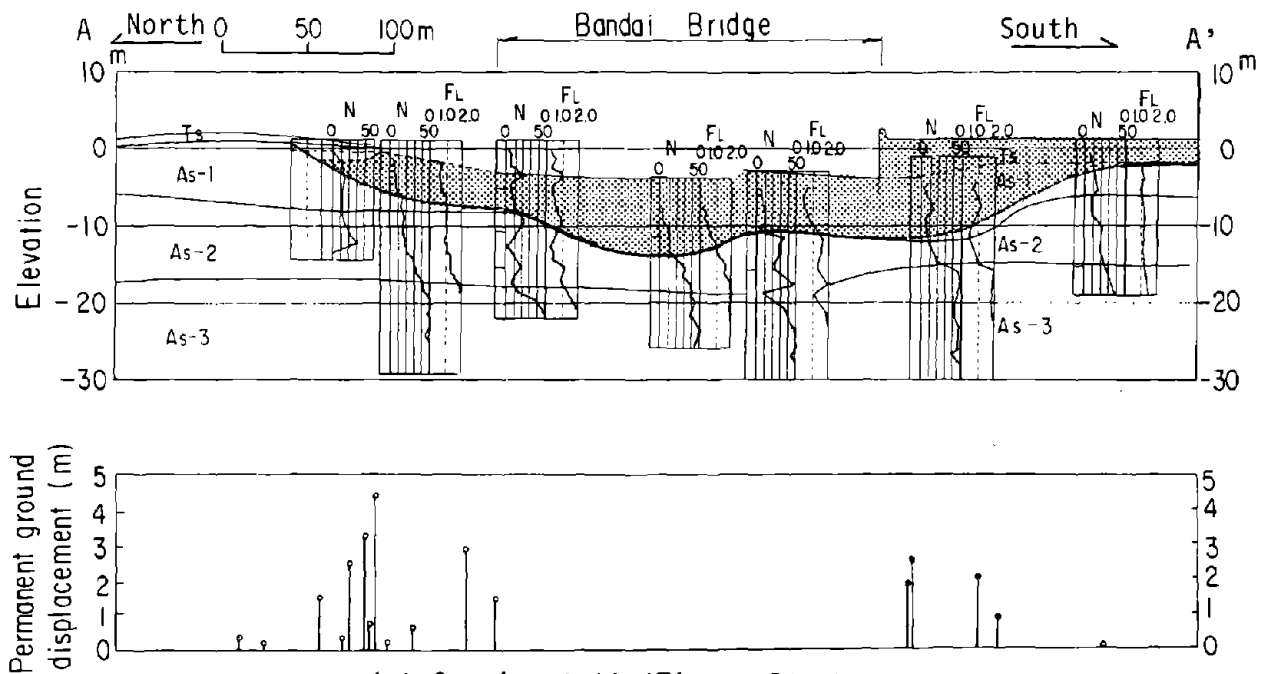
**See 2.2.



(a) Old Water Front circa 1600

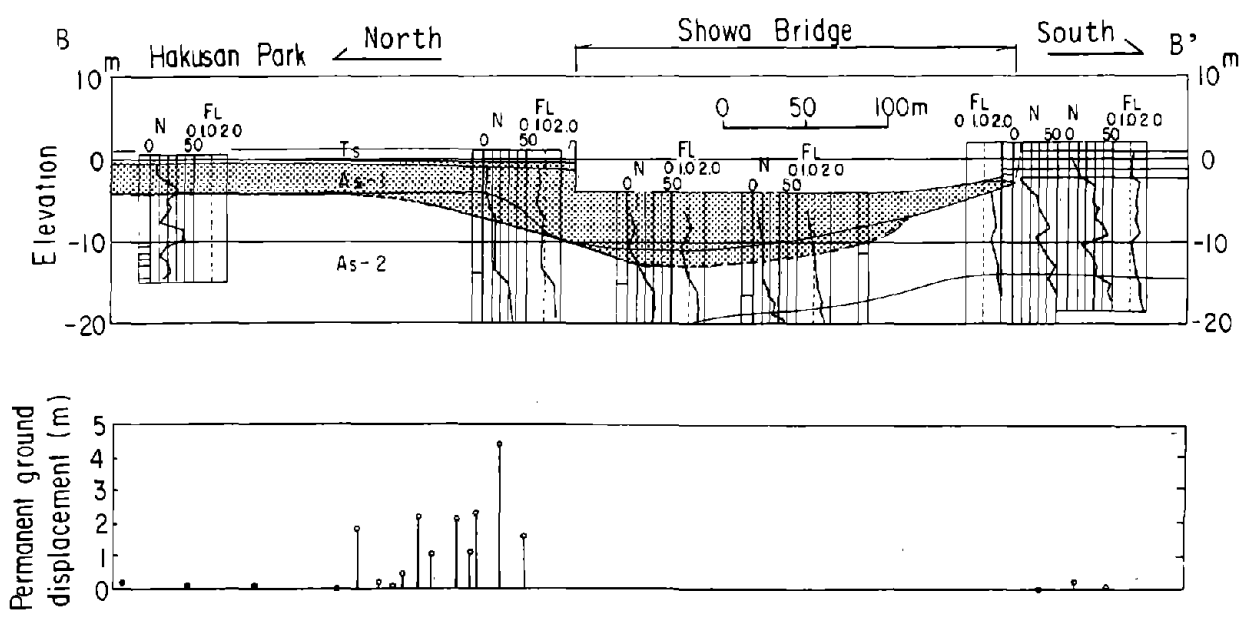
(b) Old Water Front in 1911

Figure 7. Change of the Shinano River Course

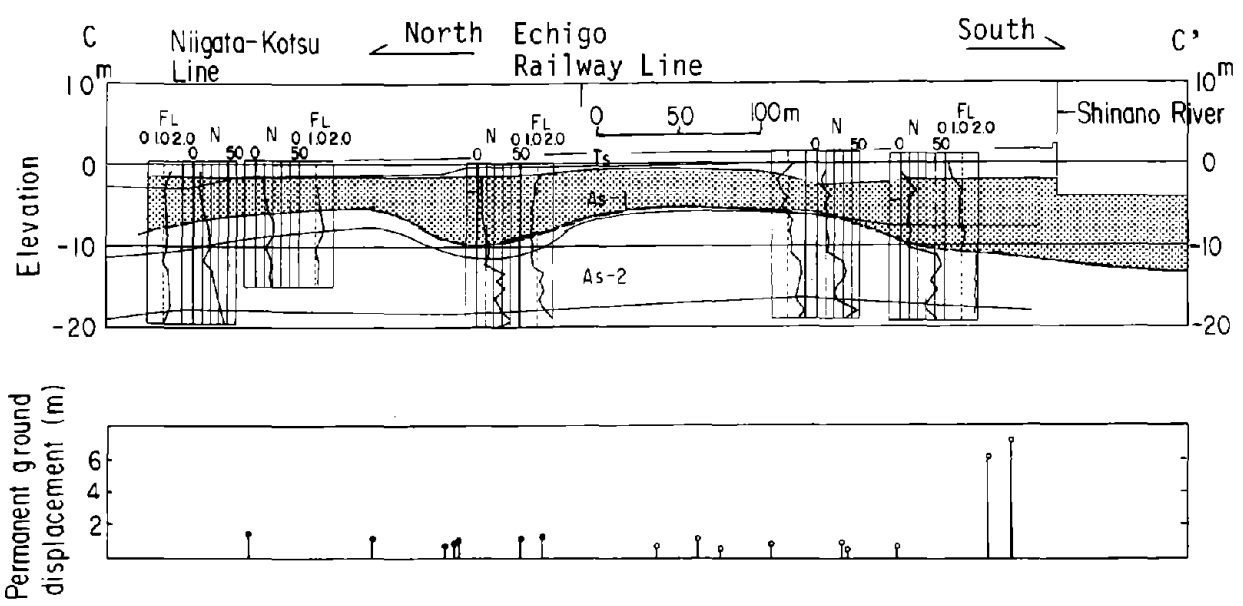


(a) Section A-A' (Figure 5(a))

Figure 8. Soil Conditions, Estimated Liquefied Layer, and Horizontal Ground Displacements



(b) Section B-B' (Figure 5(b))



LEGEND

- | | | | |
|-------------|----------------------|--|-----------------------------------|
| Ts | Surface Soil (Fill) | N : SPT values, blows/ft(0.3m) | |
| As-1 | Alluvial Sandy Soil | FL : Factor of Liquefaction Resistance | ↗ Displacement in Right Direction |
| As-2 | | ▨ : Estimated Liquefied Layer | ↖ Displacement in Left Direction |
| As-3 | | | |
| Ac-1 | Alluvial Clayey Soil | | |
| Ac-2 | | | |

(c) Section C-C' (Figure 5(c))

Figure 8. Soil Conditions, Estimated Liquefied Layer, and Horizontal Ground Displacements

Section C-C' is drawn from the left bank toward the north in Kawagishi-cho (Figure 5(d)). From the south side of the Echigo Railway Line to a point about 100 m from the bank of the Shinano River, the permanent ground displacement is only about 1 m towards the river, but it suddenly increases to as much as 7 m near the bank. The ground surface and the upper surface of the liquefied layer in this area are flat, but the lower boundary of the liquefied layer slopes gently toward the river. The thickness of the liquefied layer is more than 10 m.

North of the Echigo Railway Line, the ground moved toward the north in general, away from the river. Figure 7 shows that this area is located on the old beds of the river. As shown in the soil profile, the estimated thickness of the liquefied layer increases toward the north from the Echigo Railway Line and the lower boundary of the liquefied layer is inclined to the north.

4.1.3 Damage to Structures

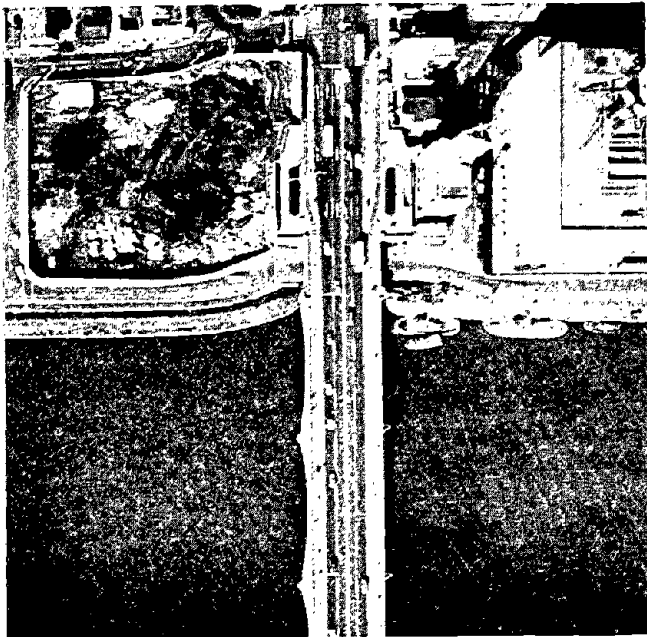
(1) Movement of the river bank (Point ① in Figure 5(a))

Photo 3 shows the left bank of Bandai Bridge two years before the earthquake (a), four hours after the earthquake (b), and seven years after the earthquake (c) by which time the revetment had been restored. Before the earthquake, the revetment had been straight and perpendicular to the bridge axis. The photograph taken four hours after the earthquake shows that the area on the left bank was flooded when the river revetments collapsed. It is notable that the revetment curves greatly in the neighborhood of the abutment of Bandai Bridge in the photograph taken seven years after the earthquake. This indicates that, in the neighborhood of the abutment, the ground displacement was reduced because of the rigidity of the bridge, which is a concrete arch bridge, while the ground further from the abutment moved towards the river freely due to collapse of the revetment. As a result of the large ground displacements toward the river, buildings and houses along the banks slipped into the river. Photo 4 shows an example of houses which slipped into the river on the left bank near Bandai Bridge.



(a) Before the Earthquake (1962)

(b) Four Hours after the Earthquake
(1964)



(c) Seven Years After the Earthquake (1971)

Photo 3 Aerial Photographs of the Left Bank of Bandai Bridge

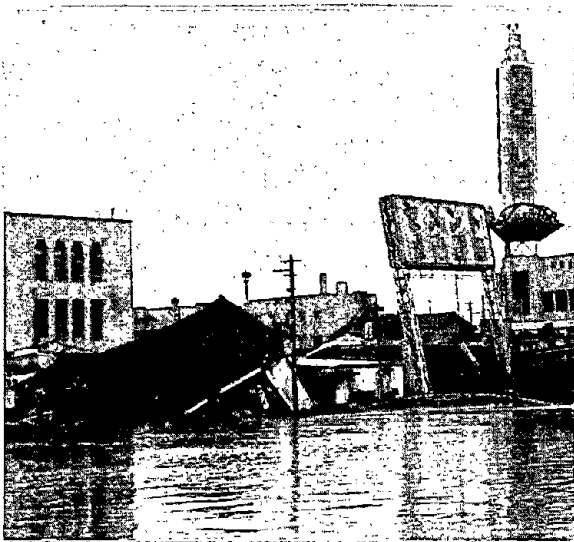


Photo 4 Houses Fallen into the River on the Left Bank of Bandai Bridge

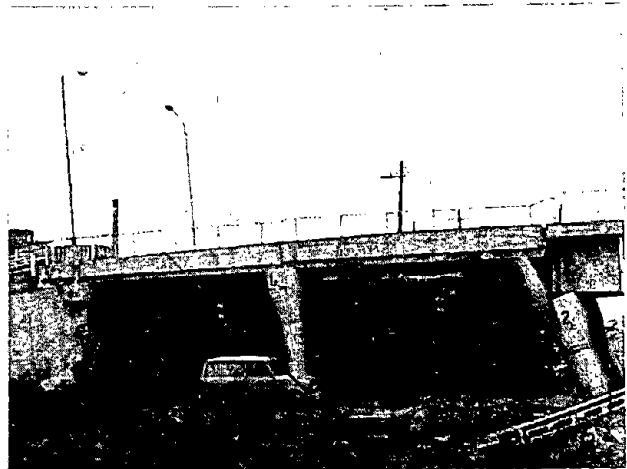


Photo 5 Damage to Yachiyo Bridge

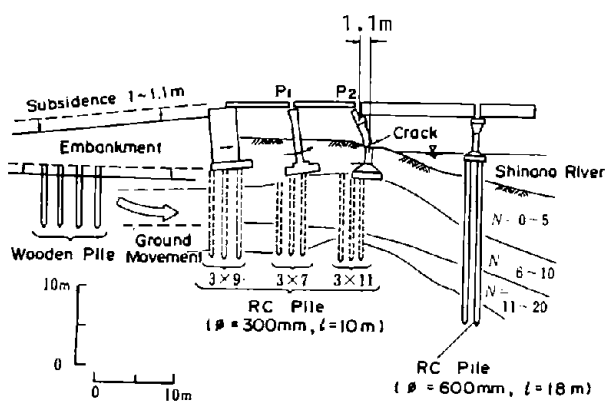


Figure 9. Damage to Yachiyo Bridge(5),6)

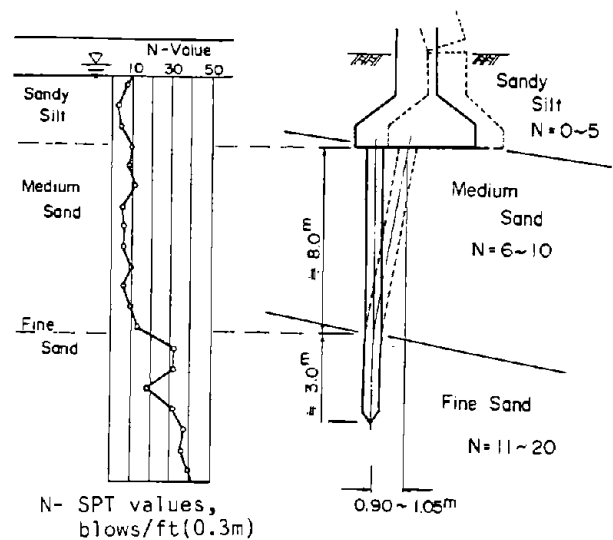


Figure 10. Damage to a Foundation Pile of Yachiyo Bridge(P₂)⁷⁾

(2) Damage to Yachiyo Bridge (Point ② in Figure 5(a))^{5),6)}

Figure 9 and Photo 5 show the damage to the abutment and piers of Yachiyo Bridge. The foundations of the abutment and piers P₁ and P₂ had been constructed on reinforced concrete piles with a diameter of 300 mm and a length of about 10 m. Pier 2 was broken at the level of the ground surface with the permanent deformation between the top of the broken pier and the lower part of the pier being 1.1 m. Figure 10 shows the damage to the pile which was extracted and examined after the earthquake. It was reported that the pile was severely destroyed at a depth of about 8 m from the top of the pile, and horizontal cracks, which could have been caused by the large bending moment, were found through the piles.

Similar damage to the abutment and piers on the right bank was reported. As shown in Figure 5(a) and (b), the permanent ground displacements on both banks were 4 to 6 m toward the river. The reason for the pier failures can be conjectured as follows: the foundations of the piers were pushed toward the river due to large ground displacements while displacement at the top of the piers was restrained because of the resistance of the girders. This caused a large stress concentration in the center of the pier.

(3) Collapse of Showa Bridge^{8),9)} (Point ③ in Figure 5(b))

The collapse of Showa Bridge was one of the worst instances of damage to a structure caused by the Niigata earthquake. The construction of the bridge had been finished only five months before the earthquake. As shown in Photo 6 and Figure 11, five simply supported steel girders between piers P₂ and P₇, each of about 28 m-span, fell into the water. It should be noted that the fallen girders were on the left side of the stream.

The piers were constructed by driving steel pipe piles which had a considerable flexibility in the direction of the bridge longitudinal axis. As shown in Figure 11, the two girders on Pier 6 rested on movable bearings (M in Figure 11). That is, the girders were not fixed to the pier. In contrast, on the other piers, one bearing was movable and the other was fixed (F in

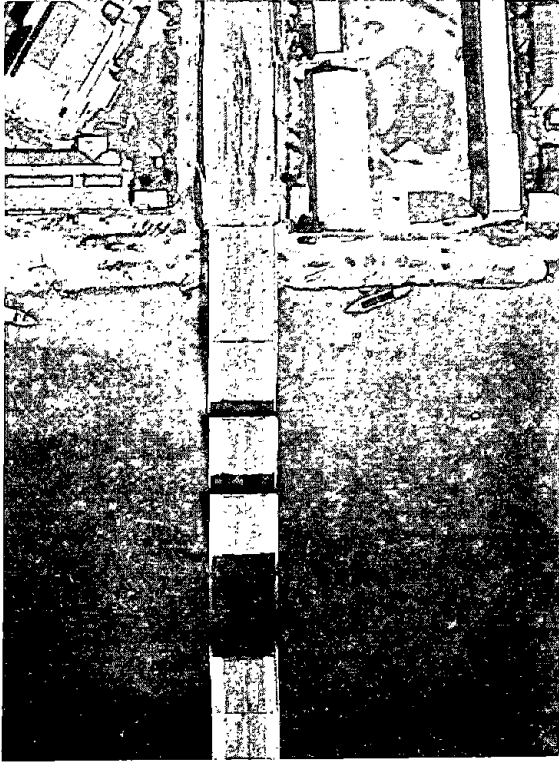


Photo 6 Collapse of Showa Bridge

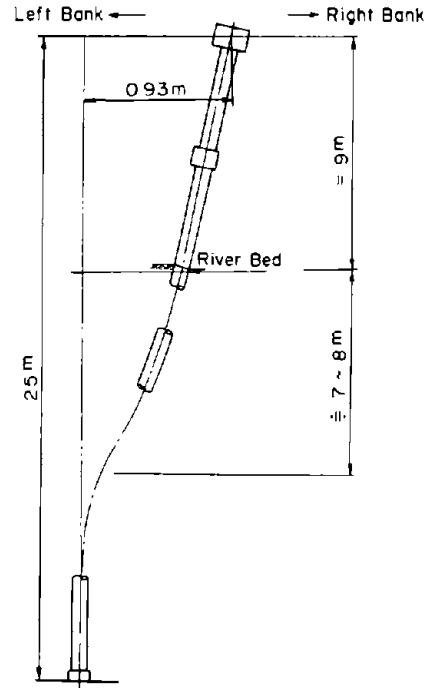


Figure 12 Deformation of a Steel Pipe Pile of Pier No. 4 (P₄)⁸⁾

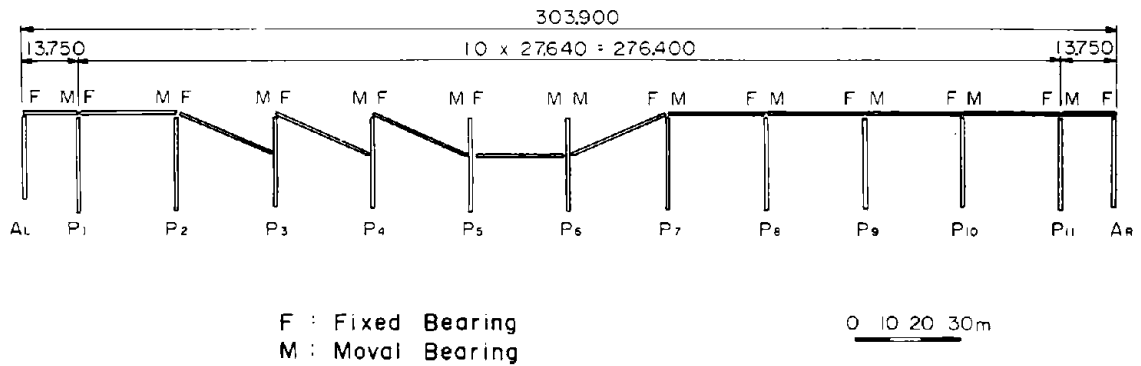


Figure 11. Collapse of Showa Bridge⁸⁾

Figure 11). Therefore, the natural period of Pier 6 was different from that of the other piers due to the lack of additional mass from the girders.

In a previous report,⁸⁾ the collapse of the bridge was explained on the basis of dynamic structural response. Because of the difference in natural periods, relative displacements arose between Pier 6 and the neighboring piers. They exceeded the allowable displacement and triggered the collapse of the bridge. However, this explanation is subject to contradictions, and other causes of failure need to be considered, as mentioned below.

Reliable eyewitnesses reported that the girders began to fall somewhat later, perhaps about 0 to 1 minute after the earthquake motion had ceased. When the earthquake motion started, many people and vehicles were on the bridge, but no lives were lost in spite of the catastrophic collapse. This suggests that there was enough time for people on the bridges to seek refuge on the banks. A taxi driver remarked⁹⁾ that he was driving near the center of the bridge when the earthquake motion started. He immediately stopped his car on the bridge and waited for the motion to cease. After the earthquake motion abated, he ran to the left bank. Another eyewitness on one bank said that damage to the revetment on the left bank of Showa Bridge began after the earthquake.

If the direct cause of the collapse of the girders was relative displacement resulting from the difference in dynamic characteristics of neighboring piers, as described above, the collapse should have occurred during the earthquake itself. However, according to the acceleration measurements taken at Kawagishi-cho, the period for which the acceleration was dominant lasted less than 15 seconds (Figure 2). Therefore, it is not reasonable to consider dynamic relative displacement as the main cause of the collapse.

Figure 12 shows a deformed steel pipe pile from Pier No. 4 (P_4) which was extracted after the earthquake. The pile, with a diameter of 60.9 cm, was bent toward the right bank at a point 7 to 8 m below the riverbed. As shown in Figure 8(b), the left bank, where the liquefied layer was estimated to be

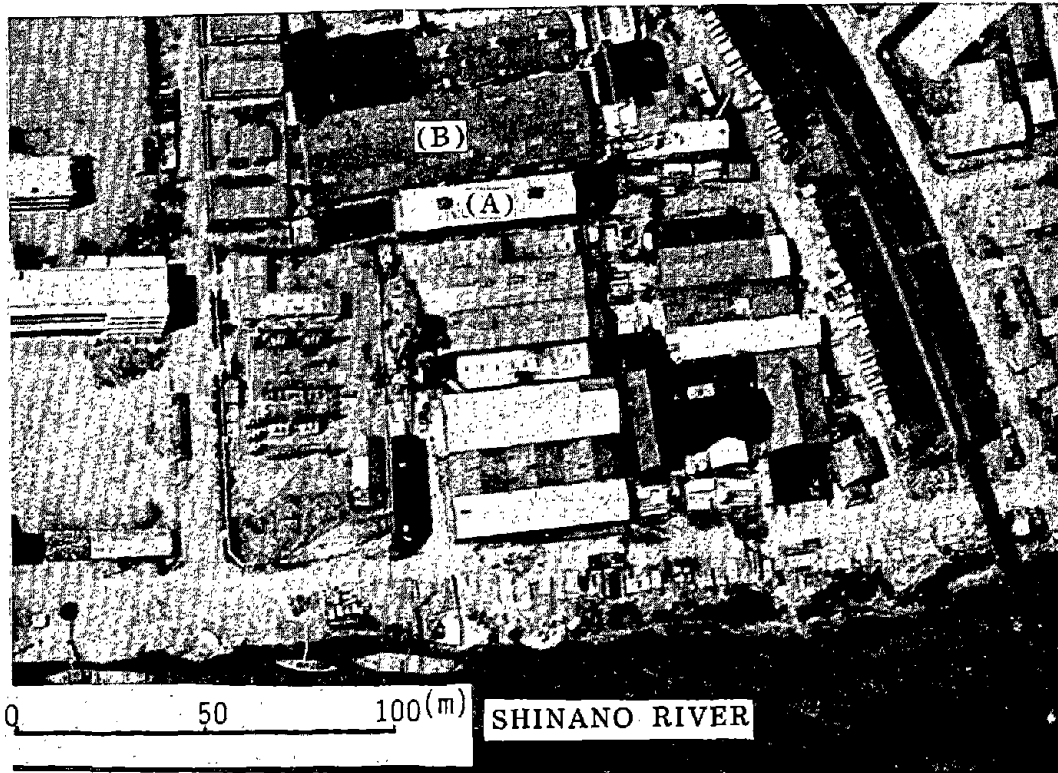
about 10 m thick, slid toward the center of the river by about 5 m. It can be conjectured that the steel pipe pile was bent by this ground displacement.

By taking into consideration the permanent displacements measured on the left bank of Showa Bridge (Figure 5(b)), the damage to the foundation piles, the estimated liquefied layer (Figure 8(b)), and the statements of witnesses, an alternative explanation can be given as a more acceptable reason for the collapse of the girders. The ground on the left bank and in the riverbed liquefied as a result of the earthquake motion and moved toward the river center. The ground displacements continued even after the earthquake motion ceased, until the excess pore water pressure dissipated. The permanent ground displacement on the left bank reached several meters, substantially deforming the foundation piles and causing the girders to fall.

(4) Damage in Kawagishi-cho

In Kawagishi-cho, the ground displacement reached over 11 m as shown in Figure 5(d). Photo 7(a) was taken two years before the earthquake and Photo 7(b), four hours after the earthquake. It is worth noting that the riverbank became more sharply curved after the ground moved towards the river and that the distance between the two buildings (A) and (B) in the photos increased. Building (B) was deformed due to relative displacement between the two sides of the building. In the post-earthquake photograph, numerous sand boils and fissures can be seen.

Meikun High School (Point ④ in Figure 5(d)) is located along the Shinano River in Kawagishi-cho. The buildings of the high school suffered severe liquefaction damage and large ground displacements. Photo 8 shows the school after the earthquake, while Figure 13 shows a schematic drawing of the movement and deformation of the buildings, sand boils, and ground fissures. The building (C), a two-storey reinforced concrete building, which was connected with building (D), a four-storey reinforced concrete building became separated by a distance of 2 m due to the ground displacement toward the river. A school teacher stated that the buildings swayed and moved toward the river like a ship on the ocean.



(a) Before the Earthquake (1962)



(b) After the Earthquake (1964)

Photo 7 Aerial Photographs of Kawagishi-cho and Hakusan (See Figure 5(d))

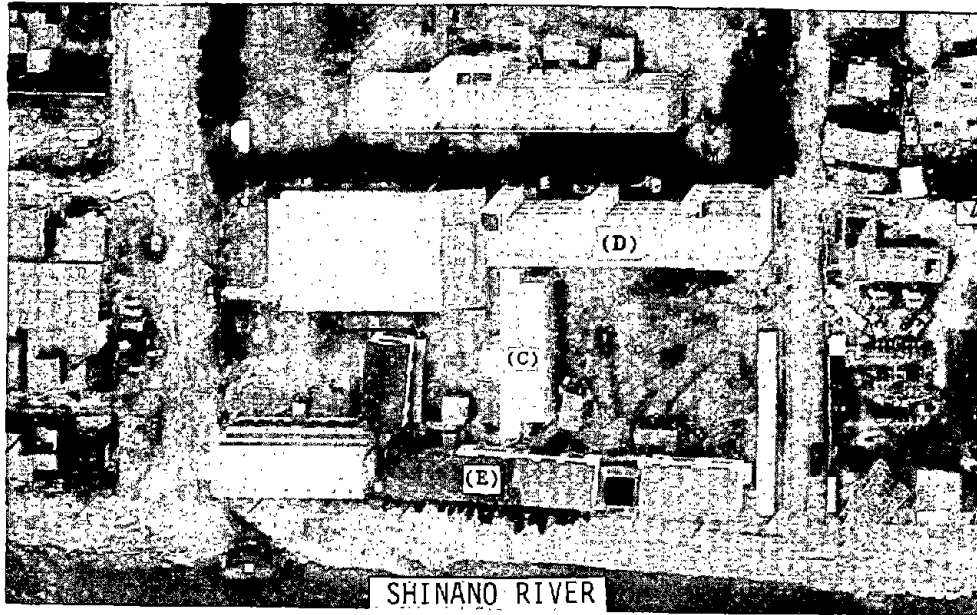


Photo 8 Aerial Photographs of Meikun High School after the Earthquake (1964)

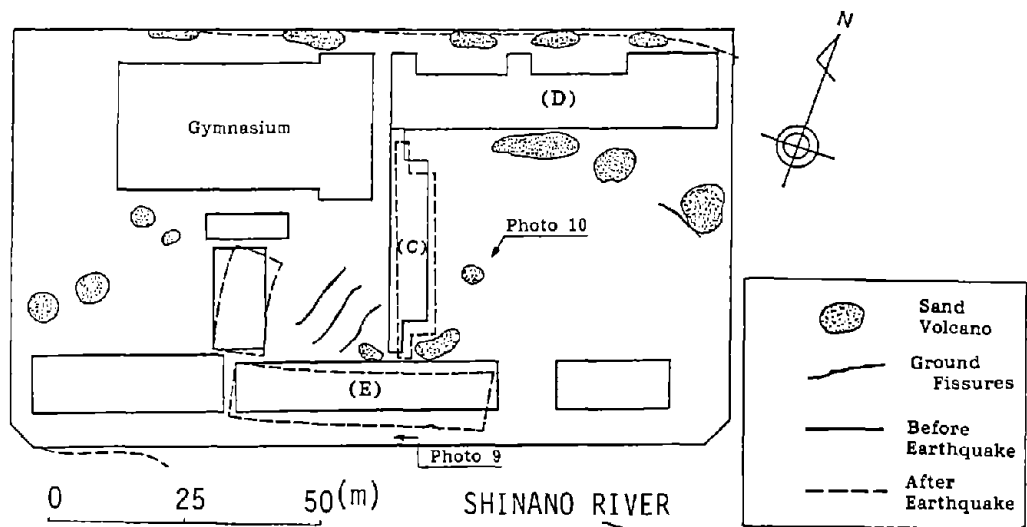


Figure 13. Movement and Deformation of Meikun High School Buildings, Sand Boils, and Ground Fissures

The two-storey wooden building (E) also moved about 3 m towards the river. Due to the relative displacements in the horizontal direction and differential subsidence of the ground, the building was distorted as shown in Photo 9. On the high school playground, numerous sand volcanoes and fissures were observed. Photo 10 is one example of the sand volcanoes.

(5) Damage to the Hakusan power substation (Point ⑤ in Figure 5(d))

According to one source, the Hakusan power substation, located near the river in Kawagishi-cho, "a vast area 300 m wide and 100 m long slid about 7 m toward the Shinano River." It was also reported that a steel tower carrying electric cables into the substation, moved towards the river, slackening the cables crossing the Shinano River. The cables dropped into the water and repairs involved shortening the cables by about 4 m. Since neither liquefaction nor ground displacement was observed on the right bank upstream of Echigo railway bridge, and the cable crosses the river at an angle of about 45° , the shortening is calculated as 5.3 to 6.3 m from the permanent ground displacements of 7 to 9 m in the vicinity of the steel tower, and this roughly coincides with the reported shortening the length of the cable by 4 m.

(6) Damage to Hakusan Primary School (Point ⑥ in Figure 5(b))

The Hakusan Primary School is downstream from the collapsed Showa Bridge on the left bank. It also suffered severe damage as a result of liquefaction. Photo 11 and Figure 14 show post-earthquake aerial picture and sketch, respectively, of the school. A certain amount of sand spouted from the ground, and the fissures can be seen. In the vicinity of the primary school, the magnitude of the permanent ground displacements was 2 to 3 m as shown in Figure 5(b). The side walls of the swimming pool collapsed due to differential displacement in the horizontal direction. Photo 12 shows the broken walls of the swimming pool. A teacher witnessed vertical ground waves with an amplitude of about 1 m, and then the formation of large fissures on the ground surface. After that, sand and water spouted from the fissures.



Photo 9 Distorted Building at Meikun High School



Photo 10 Sand Volcano in Playground at Meikun High School

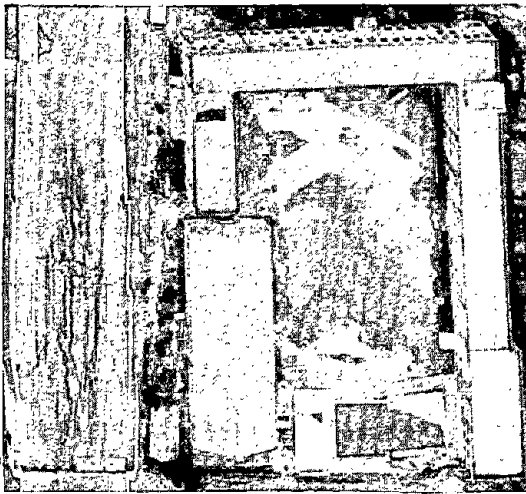


Photo 11 Aerial Photographs of Hakusan Primary School



Photo 12 Broken Wall of Swimming Pool

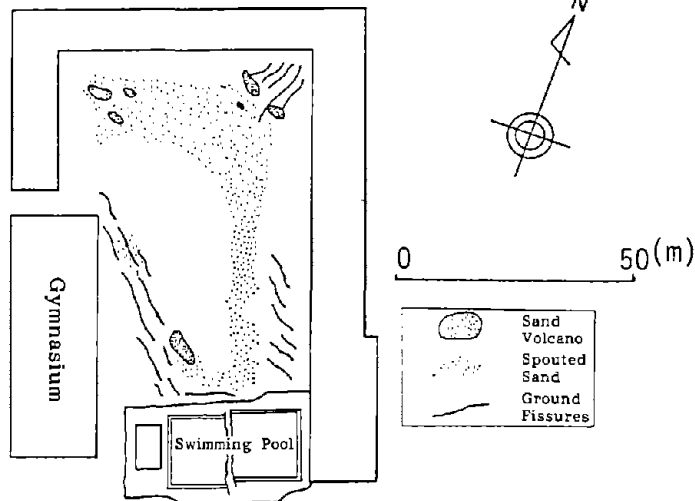


Figure 14. Damage to Hakusan Primary School

(7) Damage to foundation piles of Niigata Family Court House (Point ⑦ in Figure 5 (c))

The Niigata Family Court House, a four-storey reinforced concrete building, was located in the Hakusan area on the left bank of the Shinano River. It was constructed on concrete pile foundations, each with a diameter of 35 cm and a length of 6 to 9 m. After the earthquake, the building inclined about 1 degree due to differential settlement of the ground, and it was conjectured that the foundation piles were damaged. However, after minor repairs were made to the inclined floors, the building was used without additional modification for 25 years. When the building was reconstructed, two foundation piles were excavated. A drawing of the footings and foundation beams is shown in Figure 15.

Figure 16 illustrates the damage to the two piles and the SPT-values of the ground, and Photo 13 shows the damage. Pile No. 2 was damaged at two points. At the upper point the concrete was crushed and the steel reinforcing bars were severely bent as shown in Photo 13(a). At the lower point, there are several horizontal cracks caused by large bending moments (Photo 13(b)).

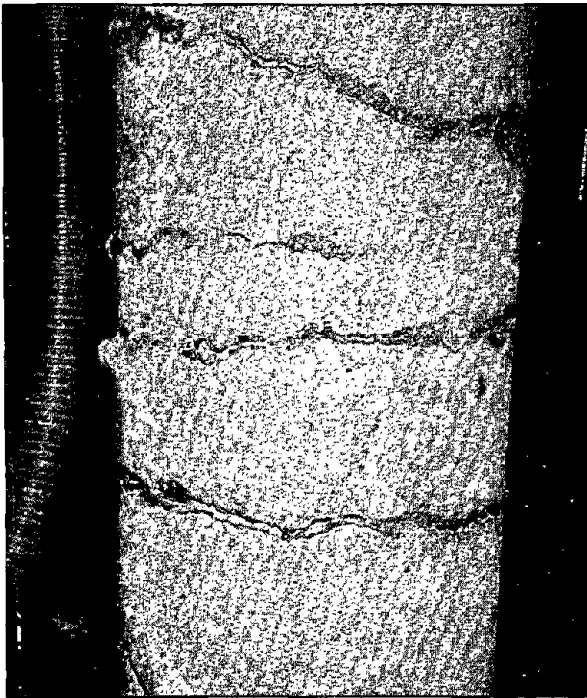
The SPT-values, measured according to SPT procedures down to -8 m, are mostly less than 10, but they increase suddenly below -8 m. It can be assumed that the soil layer below the ground water level (-1.7 m)* and above about -8.5 m liquefied during the earthquake, while the lower layer did not liquefy. It is noteworthy that the two points of damage in the No. 2 pile roughly coincide with the boundaries between the estimated liquefied and non-liquefied layers.

As shown in Photo 13(a), at the upper damage point of Pile No. 2, there is a slight shear displacement of the lower part of the pile relative to the upper part. This suggests that the lower liquefied ground layer moved more than

*It should be noted that the ground water level was measured 25 years after the earthquake.



(a) Upper Part of No. 2 Pile



(b) Lower Part of No. 2 Pile
(Bending Cracks)



(c) Upper Part of No. 1 Pile
(Compressive Stress by
Bending Moment)

Photo 13 Damage to the Foundation Piles of Niigata Family Court House

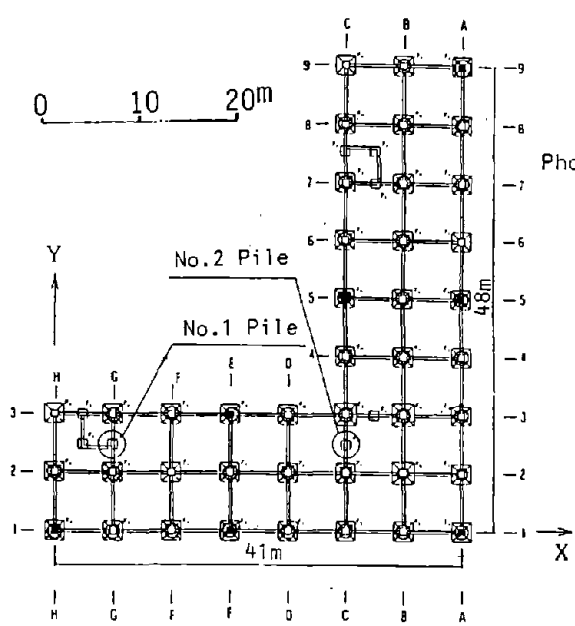


Figure 15. Footings and Foundation Beams of Niigata Family Court House

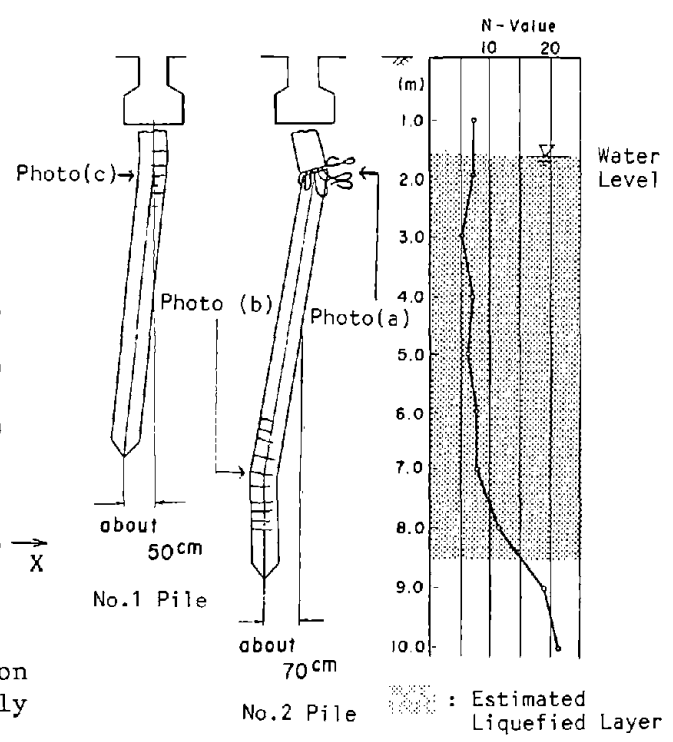


Figure 16. Damage to Piles and SPT-values of the Ground

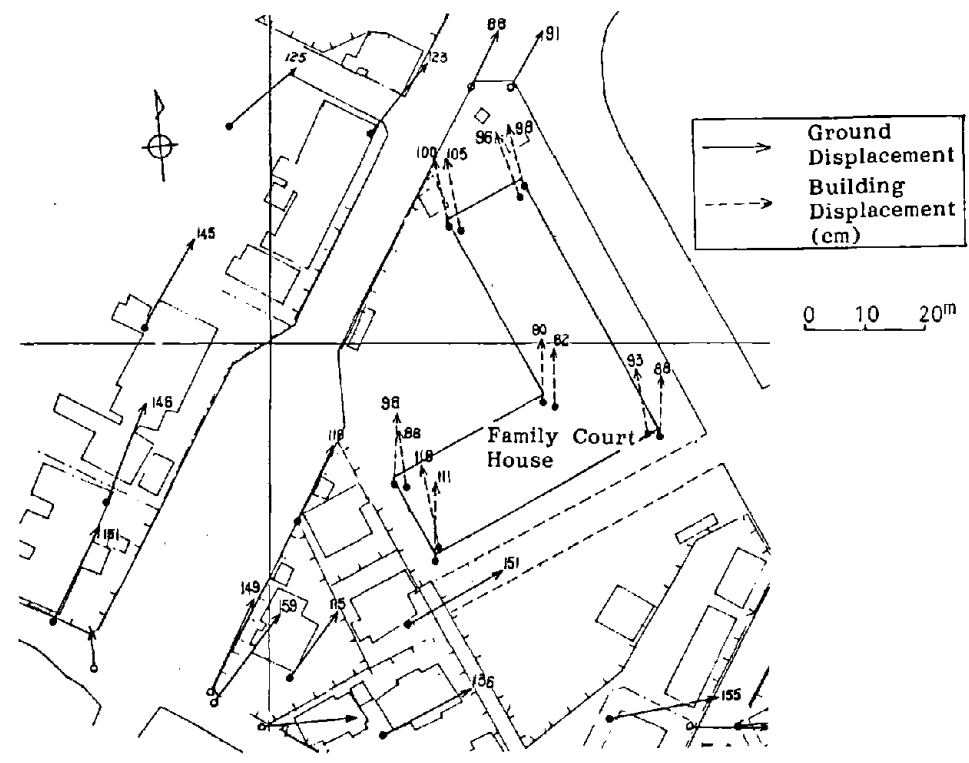


Figure 17. Permanent Ground Displacement in the Vicinity of Niigata Family Court House

the upper non-liquefied ground. It appears, therefore, that slippage occurred between liquefied soil and non-liquefied soil beneath the building.

Compared with the No. 2 pile, the damage to the No. 1 pile was remarkably light. As shown in Figure 16, few horizontal bending cracks were caused in the upper part of the pile. The reason for the light damage to the No. 1 pile is that it did not reach into the basal non-liquefied layer. The tip of the pile was in the liquefied layer. The boundary condition at the tip of the No. 1 pile was more flexible than that of the No. 2 pile.

The permanent ground displacements in the horizontal direction, measured in the vicinity of the building, are shown in Figure 17. The solid vectors shows the displacements on the ground surface around the building as measured from aerial photographs taken before and after the earthquake. The ground moved by 1 to 2 m, mostly in the northeast direction. The dotted vectors are the horizontal movements of the building which were measured by comparing a post-earthquake aerial photograph with a building plan drawn before the earthquake. The building was not included in the pre-earthquake photograph, because it was taken two years before the earthquake, and the building was constructed just one year prior to the earthquake.

The building moved by about 1 m toward the northern direction and some differences in the direction can be observed between the ground displacements and the building displacements. Because the plan was used to determine the coordinates of the building before the earthquake, there may be some errors in the measurement of the building displacements. However, it can be concluded that the foundation piles failed due to the liquefaction-induced ground displacement, shown in Figure 17.

(8) Damage to the foundation piles of the S-building (Point ⑧ in Figure 5(b))

Yoshida et al.¹¹⁾ reported the damage to foundation piles of the S-building. The S-building was a three-storey reinforced concrete building constructed on reinforced-concrete friction piles of 25 cm outer diameter and 13 cm inner

diameter. Three piles were extracted using a water-jet auger during reconstruction of the building, 24 years after the earthquake. Photo 14 shows the extracted piles, and Figure 18 shows the crack pattern schematically.

The No. 1 pile was severely damaged at two points. On the other hand, cracks 5 to 20 mm wide appear with nearly equal spacing in the Nos. 2 and 3 piles. As shown in Figure 19, the SPT-values, N, of the soil to 12 m are around or below 10. So it is thought to have been liquefied during the earthquake. The soil layer below 12 m is considered not to have been liquefied because of its high SPT-values. In the case of the S-building, the tips of the piles, which were designed as friction piles, did not reach into the lower non-liquefied layer. The reason the damage was light is that the piles had more flexible boundary condition compared with the No.2 pile of the Family Court House Building and the piles of NHK-Building mentioned in 4.4.3(1).

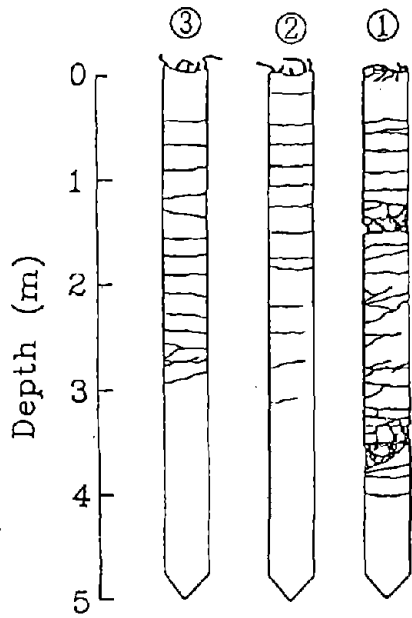


Figure 18. Damage to the Foundation Piles of S-Building¹¹⁾

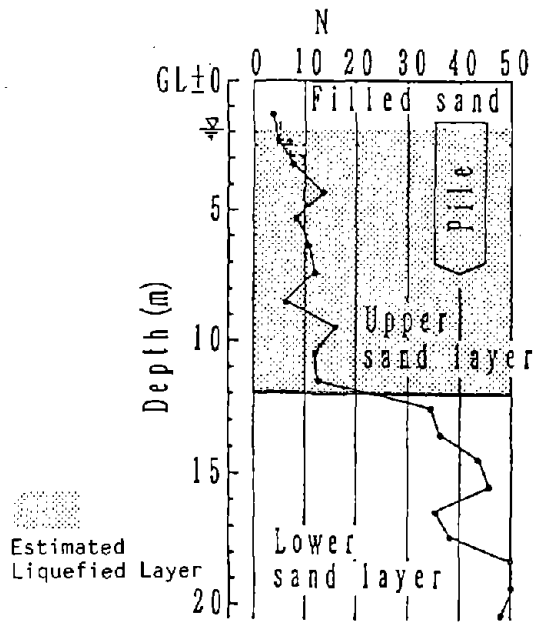


Figure 19. SPT-values at the Site of S-Building¹¹⁾
 N : SPT values, blows/ft(0.3m)

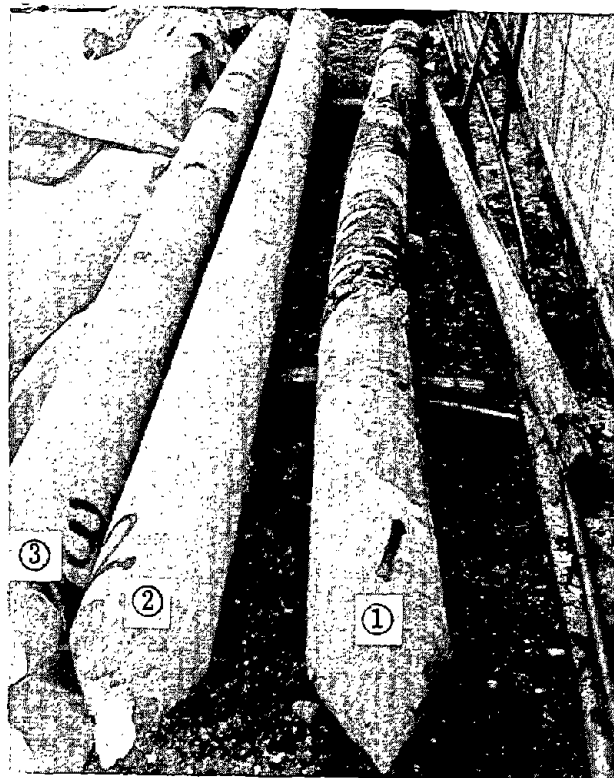


Photo 14 Damage to the Foundation Piles of S-Building¹¹⁾

4.2 Zone II: Downstream Area of Shinano River (Downstream from Bandai Bridge, on the left bank)

4.2.1 Permanent Ground Displacements

The vectors in Figure 20 show the permanent ground displacements in the horizontal direction in the downstream area on the left bank of the Shinano River, while the numbers in parentheses are vertical displacements.

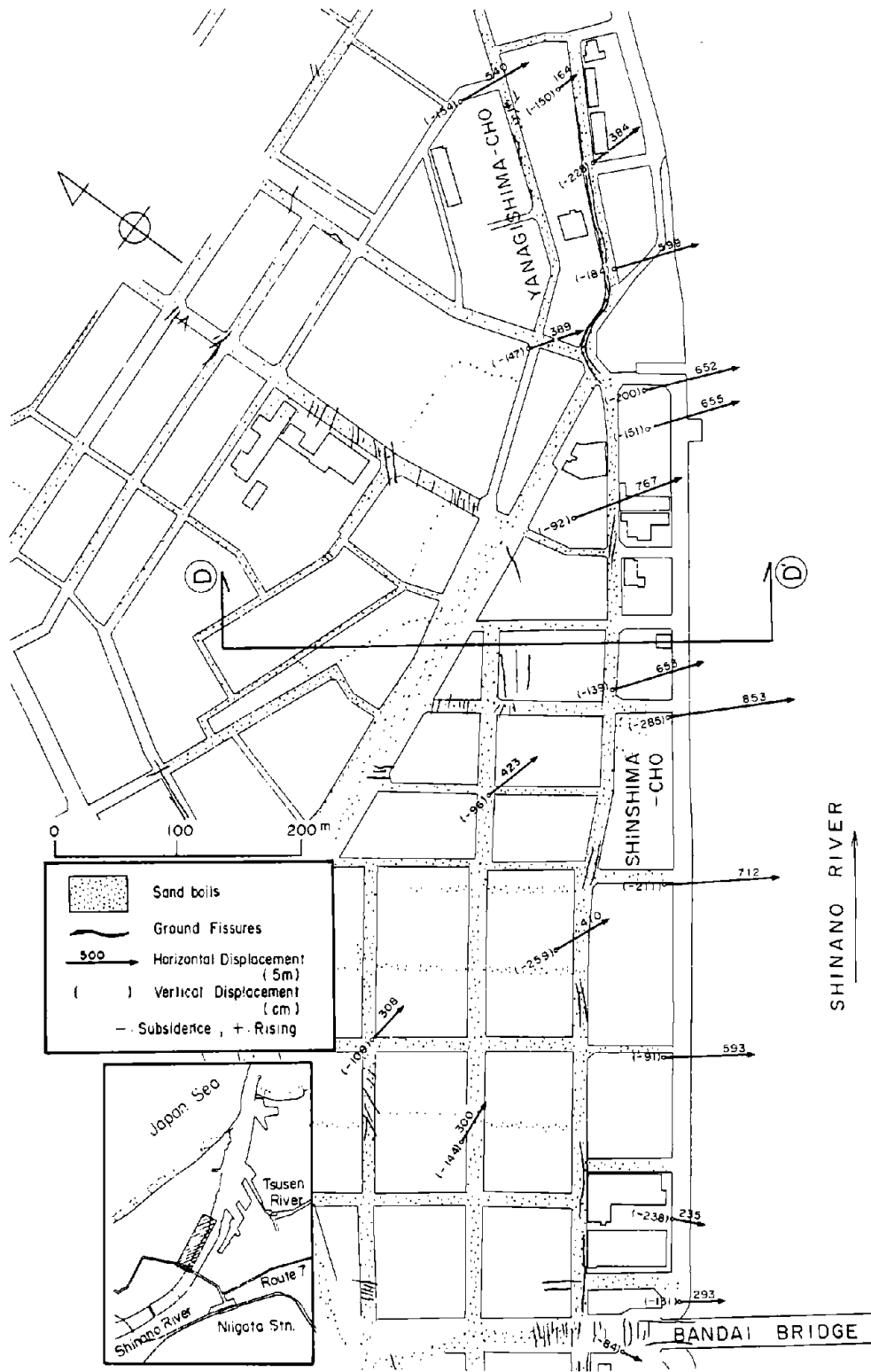
From Bandai Bridge to Yanagishima-cho (Figure 20(a)), the ground moved towards the river by 5 to 8 m. The maximum horizontal displacement in this area is 8.5 m at Shinshima-cho. In the area of Irifune-cho (Figure 20(b)), the horizontal ground displacements were comparatively small at 2 to 3 m.

Around the estuary of the Shinano River, the horizontal displacements toward the river increased again. At the head of the estuary, the displacement reached a maximum of about 11 m. The whole cape on the left bank of the Shinano River was displaced towards the river. In contrast, horizontal displacements toward the sea was not detected.

The ground subsided at all the measuring points by 1 to 2 m. The maximum ground subsidence was measured in Shinshima-cho along the river, where it was about 3 m (Figure 20(a)).

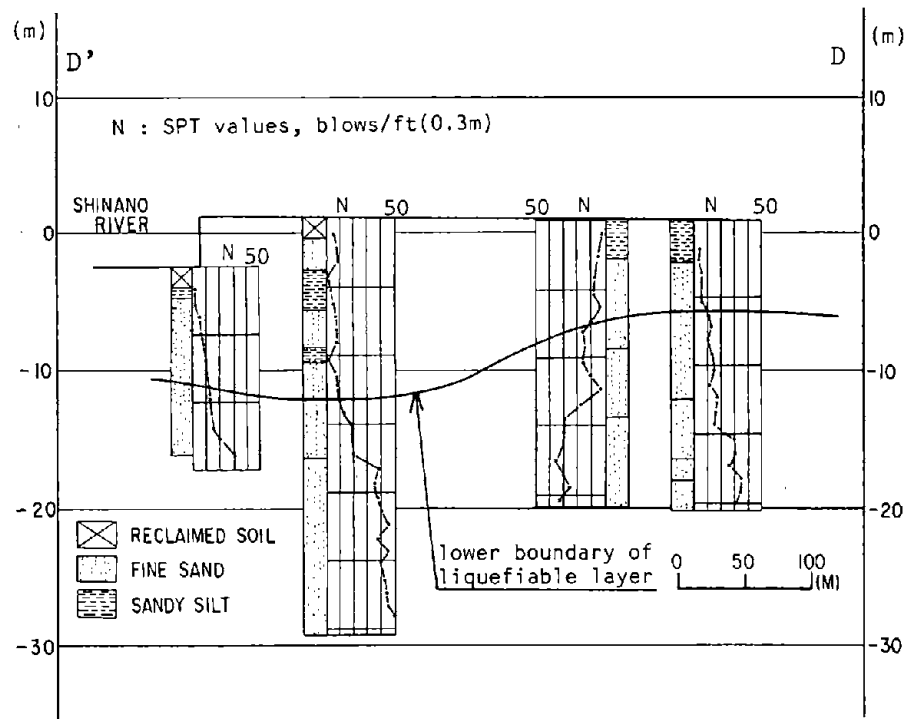
4.2.2 Soil Conditions

The soil conditions along the two sections D-D' and E-E' in Figure 20 are shown in Figure 21. The subsurface soils consist mostly of fine sand and partially sandy silt. The SPT values of the soil layer to about 10 meters below the surface are less than 10. Along these two section lines, no estimate of liquefied layers has been carried out, but sandy layers with low SPT values can be conjectured to have liquefied during the earthquake. Along both sections, the liquefiable layer is thicker around the quay walls of the river than in the inland area. It should be also noted that the boundary between the liquifiable layer and the underlying non-liquefiable layer, which

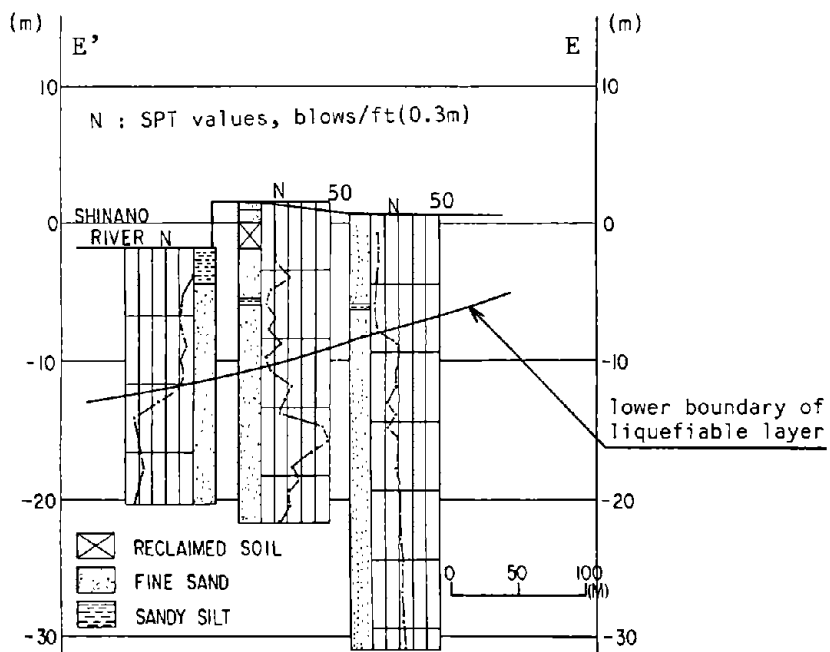


(a) Bandaï Bridge to Yanagishima

Figure 20. Permanent Ground Displacement in the Downstream Area on the Left Bank of the Shinano River

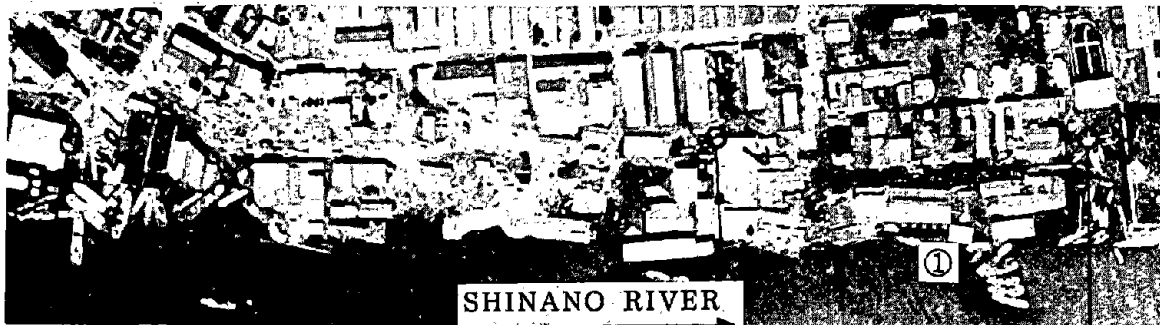
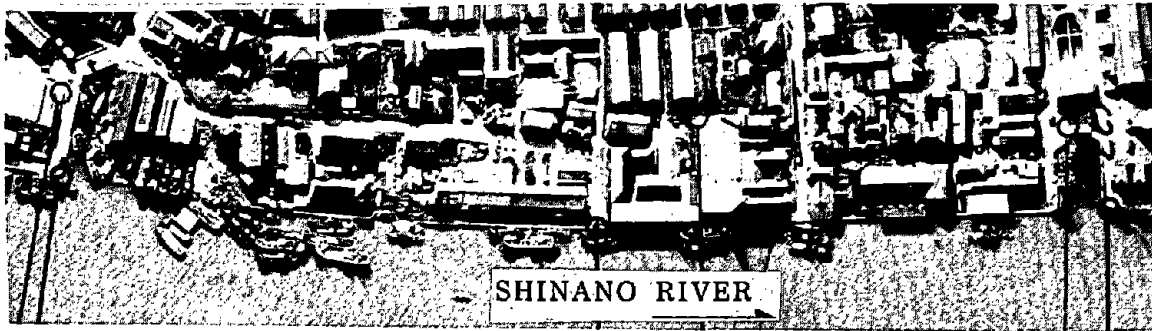


(a) Section D-D'



(b) Section E-E'

Figure 21. Soil Conditions



(b) After the Earthquake (1964)

Photo 15 Aerial Photographs of Yanagishima-cho of the Downstream Area on the Left Bank of the Shinano River



Photo 16 Partially Sunk, Tilting Building in the Downstream Area on the Left Bank of the Shinano River, Point ① in Photo 15¹¹⁾

was approximately estimated as the line of the SPT value of 10, is inclined mostly toward the river.

4.2.3 Damage to Structures¹²⁾

The quay walls on the left bank downstream from Bandai Bridge were constructed mainly of steel sheet piles, with some concrete wall sections. Most of the quay walls collapsed. Large areas were flooded because of the serious subsidence as well as the effects of the tsunami which struck Niigata City after the earthquake. Photo 15 shows aerial photographs of Yanagishima-cho (Figure 20(a)) taken before and after the earthquake. Due to the collapse, many buildings behind the quay walls were inclined severely and/or sunk, as shown Photo 16 (Point ① in Photo 15(b)).

4.3 Zone III: Niigata Port Area (Bandai Island, Fishery Pier, South Pier, North Pier and Rinko Wharf)

4.3.1 Permanent Ground Displacements

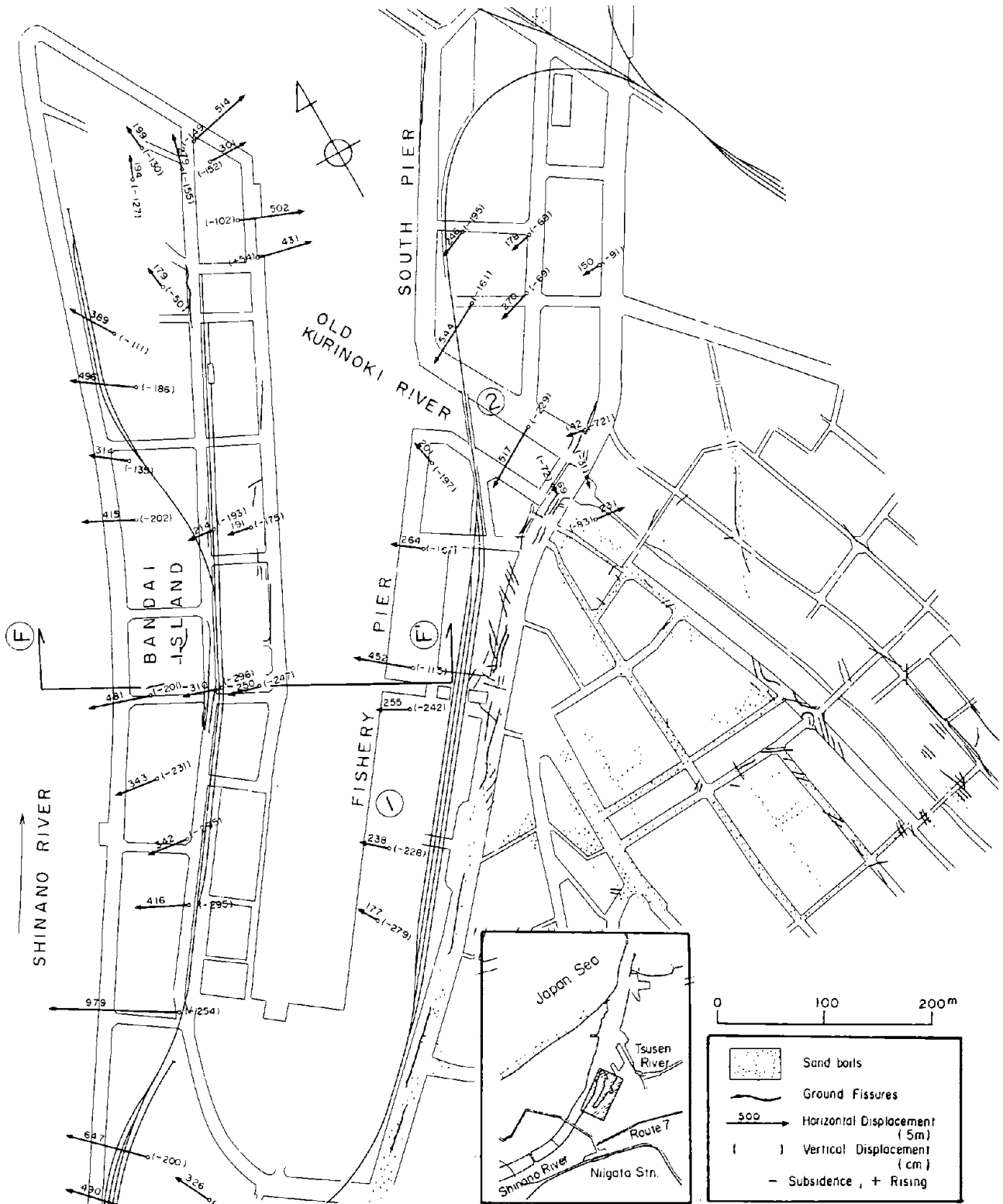
Permanent ground displacements in the Niigata Port area are shown in Figure 22. The horizontal ground displacements on Bandai Island are relatively large, with a maximum of about 10 m (Figure 22(a)). Figure 23 shows an old map of the island in 1911 in comparison with the present one. It can be seen from this old map that Bandai Island and its surrounding consist of two parts. The main part of the island was formed by deposition of the channel bar of the river, while the part connected with the original river shore was formed by reclamation from the river.

In the north part of the island the ground moved toward the water, that is toward the west at the west shore, north at the north shore, and east at the east shore (Figure 22(a)). However, the south part of the island moved toward the west in the direction of the Shinano River. The maximum displacement in the horizontal direction in the south part reached over 9 m. The ground subsided throughout the island. The ground surface settled by about 3 m in the south part of the island, while the subsidence of the ground in the north part was 1 to 2 m.

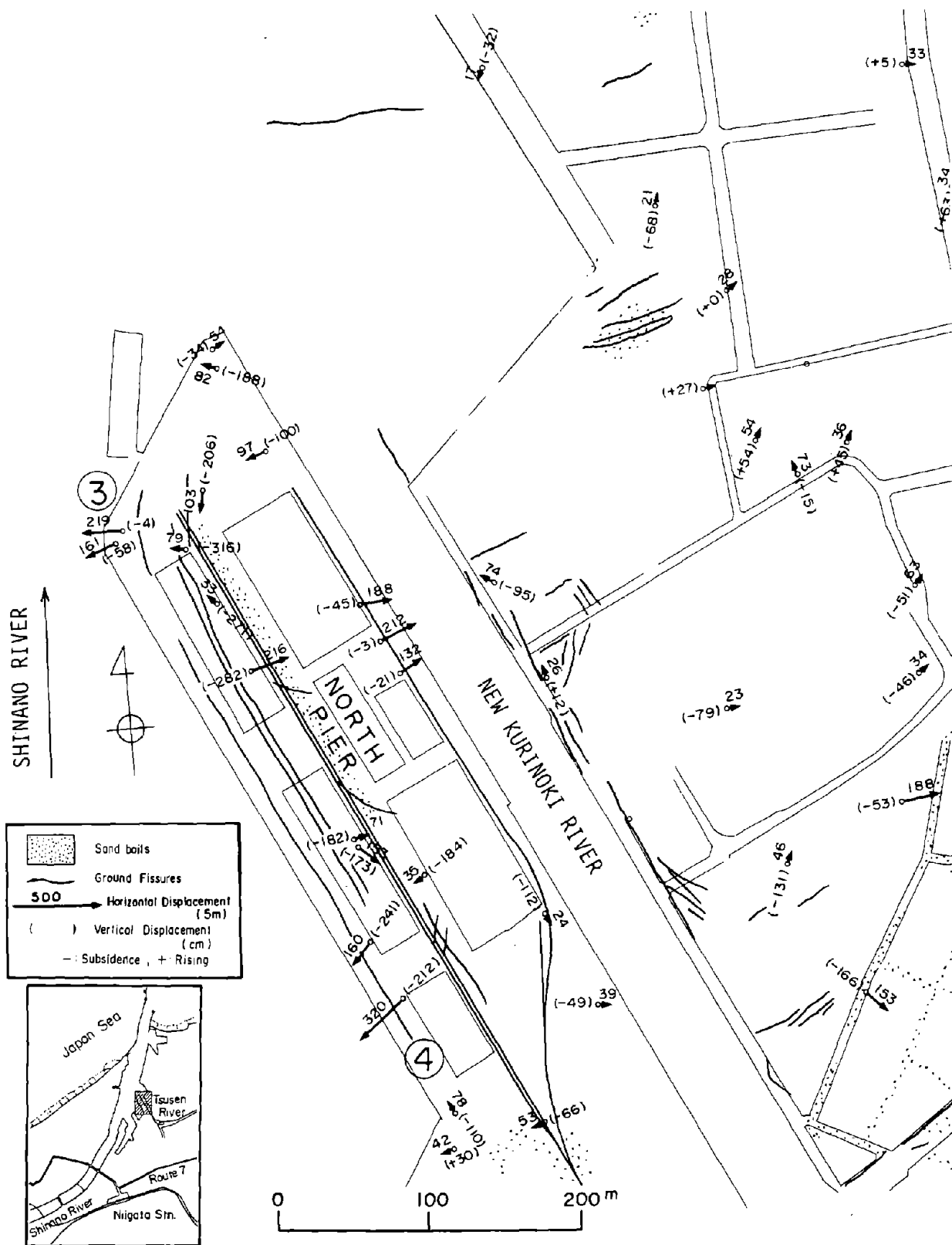
At the Fishery Pier on the right bank of the Shinano River, the ground moved toward the center of the river by 2 to 4 m as shown Figure 22(a). The direction of the horizontal ground displacements was mostly perpendicular to the quay wall. The ground also subsided greatly by 1 to 3 m.

The horizontal ground displacements at the South Pier are in a westerly direction, towards the Old Kurinoki River, with a magnitude of 2 to 5 m. The ground also subsided by 1 to 2 m in this area.

The ground at the North Pier moved toward the water by 2 to 3 m (Figure 22(b)). The west side of the pier was displaced in a westerly direction, toward the Shinano River, while the east side moved toward the waterway (the New Kurinoki River). The pier also subsided by 1 to 2 m.



(a) Bandai Island, Fishery Pier, and South Area
 Figure 22. Permanent Ground Displacement in Niigata Port Area



(b) North Pier

Figure 22. Permanent Ground Displacement in Niigata Port Area

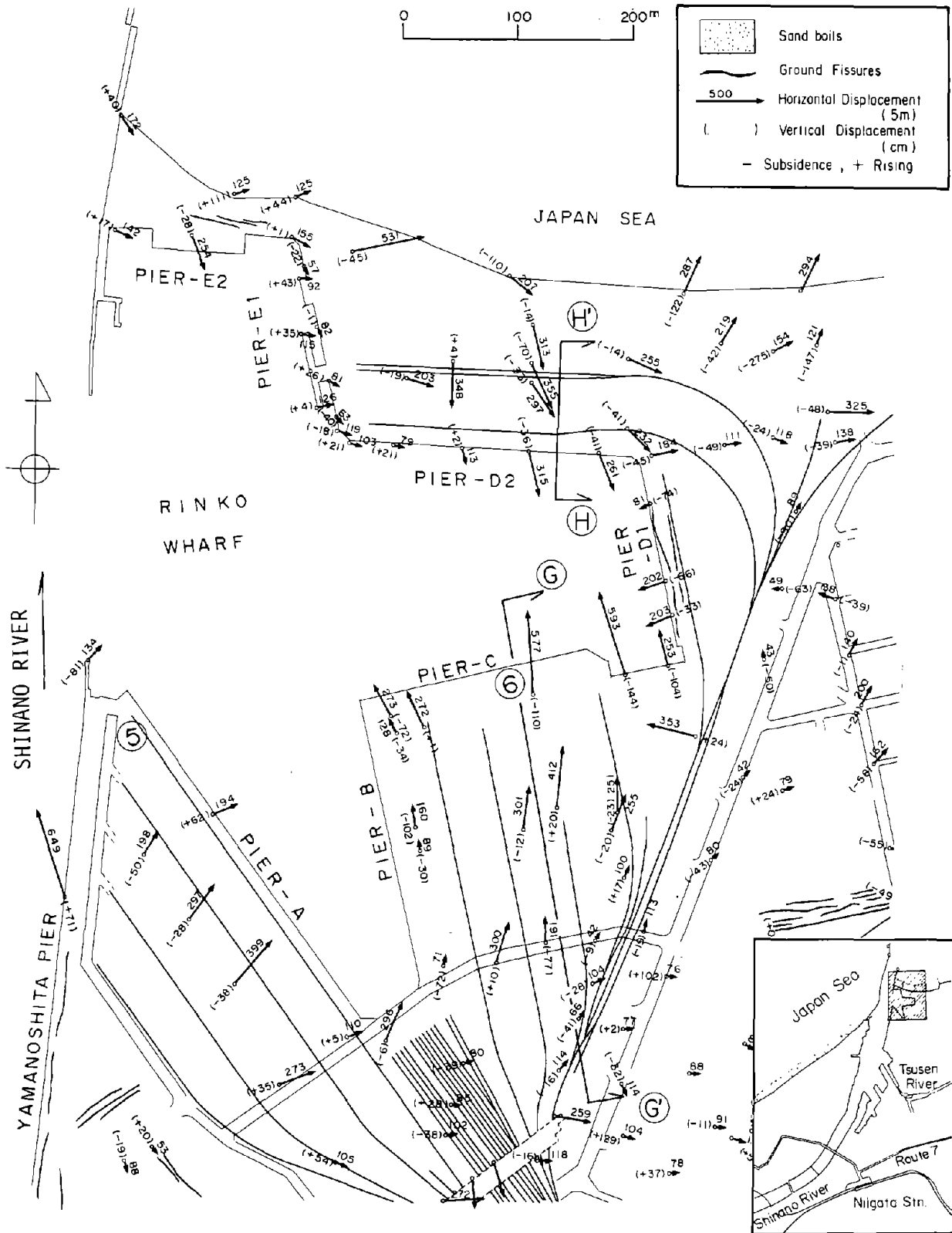


Figure 22. Permanent Ground Displacement in Niigata Port Area

At Rinko Wharf large ground displacements occurred as shown in Figure 22 (c). At Piers A, B, and C, the ground mainly moved toward the northeast or north. The quay wall and the ground behind the wall at Pier C were displaced by a maximum of about 6 m. The ground at Piers D2 and E2 displaced a maximum of about 3 m in a southerly direction. Along the Japan Sea, the shore moved toward the north; that is, into the sea by 1 to 3 meters.

4.3.2 Soil Conditions

Figure 24 shows the soil conditions along three sections, F-F', G-G' and H-H', in the Niigata Port Area. The section F-F' was drawn from the Shinano River through Bandai Island to the Fishery Pier (Figure 22(a)). The subsurface soils along the west side of Bandai Island consist of medium and fine sand with SPT values less than 10 down to about -10 m below the surface. This loose sand, which can be considered to have liquefied during the earthquake, is much deeper on the east side of Bandai Island than on the west side. Along this section, the ground on the island moved towards the Shinano River, leftwards in Figure 24(a). However, the boundary of the liquefiable layer and underlying non-liquefiable layer, which was approximately estimated as the line of the SPT value of 10, is not inclined in the direction of ground displacements towards the Shinano River, but toward the water channel between the Fishery Pier and Bandai Island.

The ground under the Fishery Pier also consists of fine and medium sand, and here, the lower boundary of the liquefiable layer between the Fishery Pier and Bandai Island is inclined toward the water channel, coinciding with the direction of ground movement at the Fishery Pier.

The relationship between the inclination of the boundary between the liquefied and lower non-liquefied soil layers and the direction of the ground displacements, as mentioned above, indicates that the inclination of the boundary does not always show a positive correlation with the direction of ground displacement.

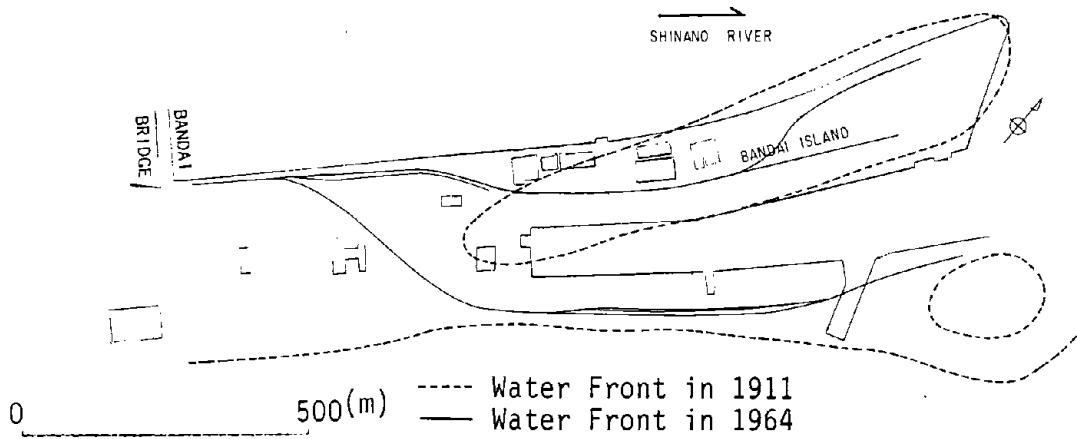
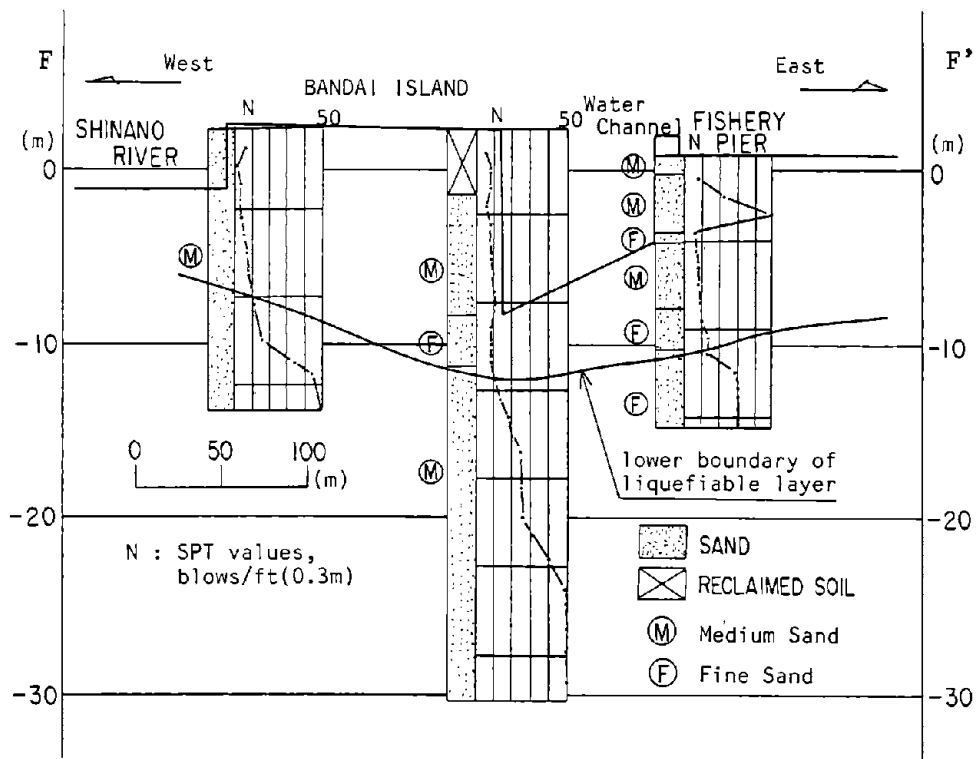
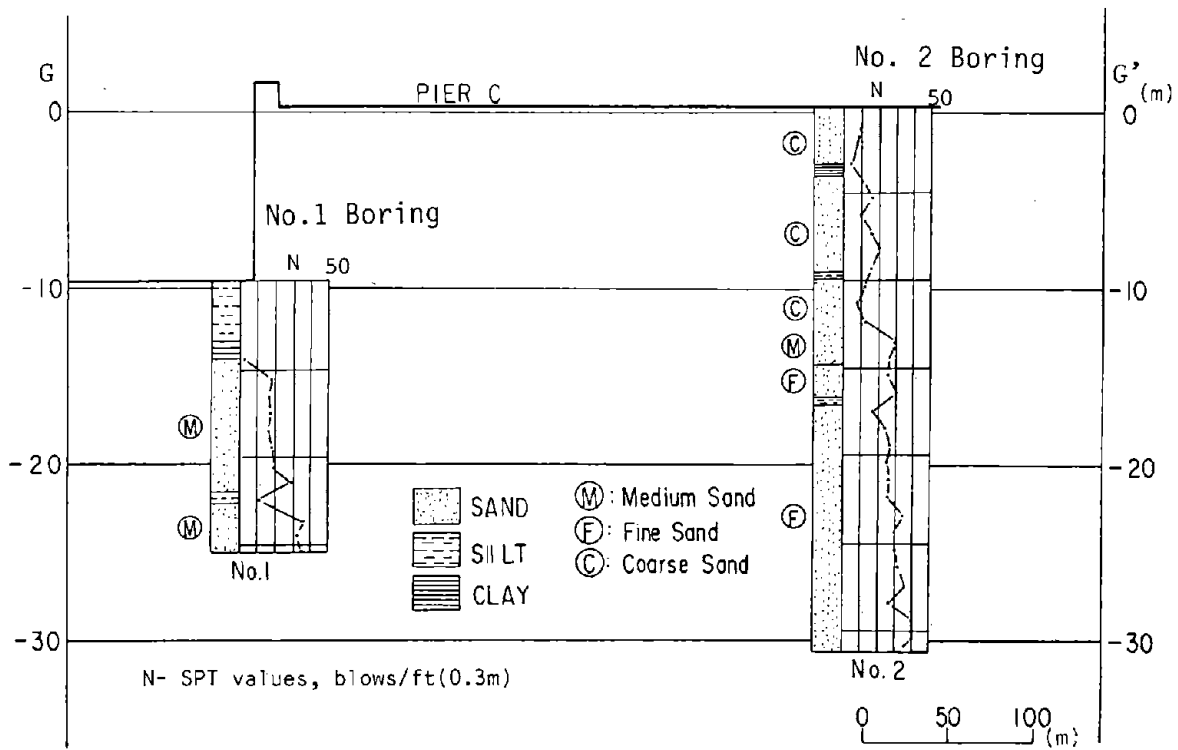


Figure 23. Bandai Island in 1911 and in 1964 (at the time of the earthquake)

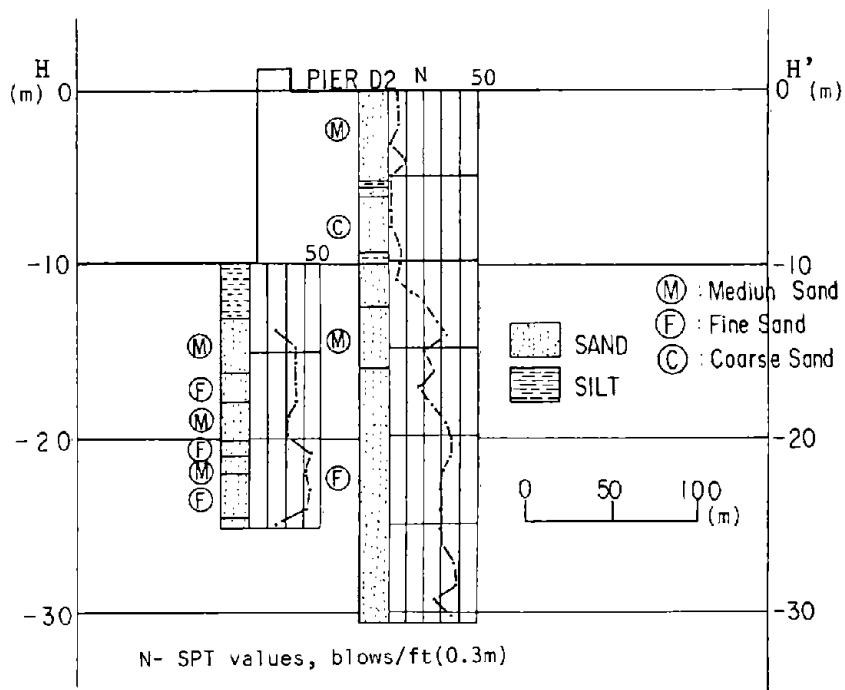


(a) Section F-F'

Figure 24. Soil Conditions



(b) Section G-G'



(c) Section H-H'

Figure 24. Soil Conditions

Section line G-G' through Rinko Wharf is drawn perpendicular to Pier C, where a maximum displacement of about 6 m was observed (Figure 22(c)). The subsurface soils at No. 1 boring consist of medium grain-size sand with relatively high SPT-values of more than 15 below a 5 m-thick silty and clayey layer. The soil under the seabed can be considered to be not especially susceptible to liquefaction. The subsurface soils at No. 2 boring, 300 m away from the quay wall, consist of a loose sand layer down to 5 m, SPT-values of which are less than 10. Although this loose sand can be considered to have liquefied during the earthquake, the No. 2 boring is too far from the quay wall to evaluate adequately the liquefaction of the ground at the quay.

Pier C was reclaimed by pumping up seabed sand from adjacent areas, so the ground behind the quay wall may consist of relatively loose sand. It can be conjectured that this reclaimed sand liquefied and moved toward the sea upon collapse of the quay wall.

This conjecture is substantiated by soil data along the section H-H', which is perpendicular to Pier D2 (Figure 22(c)). The ground behind the quay wall consists of medium and coarse sand with SPT-values below 10, which was also reclaimed with seabed sand. This soil layer can be considered to have liquefied.

4.3.3 Damage to Structures¹²⁾

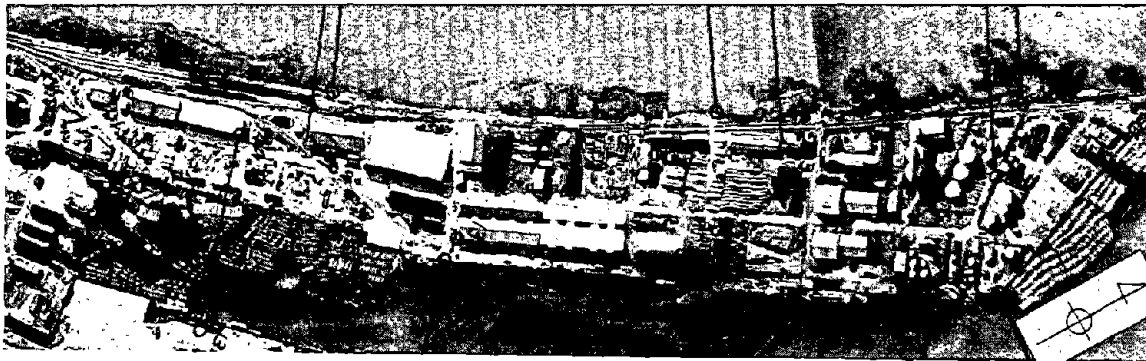
Most of the quay walls on Bandai Island were severely damaged, and a large area of the island, particularly the south area, was flooded, as shown in Photo 17. The quay walls were constructed with steel sheet piles with pile anchorages, but they moved toward the water and collapsed.

The quay walls at Fishery Pier were constructed by driving steel sheet piles in front of existing concrete piers, as shown in Figure 25. The greater part of the quay wall slid toward the water and sank into the water as shown in Photo 18 (Point 1 in Figure 22(a)). The quay wall along the right bank of

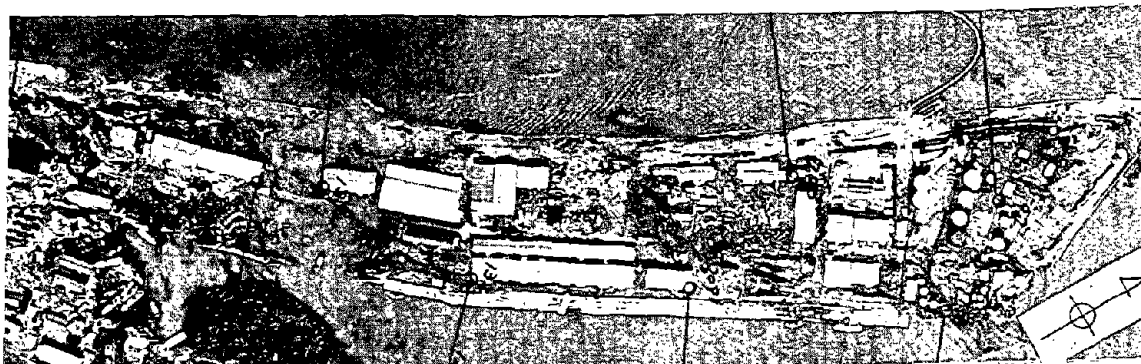
the Old Kurinoki River suffered the most severe damage in this area. The quay wall was constructed of concrete blocks, but it collapsed and sank as shown in Photo 19 and Figure 26 (Point ②).

Photo 20 shows the catastrophic damage to the quay wall at the top of the North Pier (Point ③ in Figure 22(b)). The quay wall, constructed with steel sheet piles, moved about 2 m toward the water and inclined sharply. Photo 21 shows another example of damage to the quay wall of the North Pier (Point ④ in Figure 22(b)). This part of the quay wall was constructed of concrete blocks, and but it moved and inclined severely. The warehouse behind the quay wall also moved and inclined as shown in Photo 21.

The area around Rinko Wharf was also seriously flooded by the collapse of the quay wall and by the tsunami which arrived after the earthquake. The elevation of the ground in this area was very low, almost level with the sea. The quay wall shown in Photo 22 (Point ⑤ in Figure 22(c)), which was built of concrete blocks, moved toward the water, and its top was inclined steeply. The quay wall at Point ⑥ in Figure 22(c) was constructed of steel sheet piles. The ground displaced at a maximum of 6 m at this location, causing settlement and flooding of the warehouse, as shown in Photo 23.



(a) Before the Earthquake (1962)



(b) After the Earthquake (1964)

Photo 17 Aerial Photographs of Bandai Island

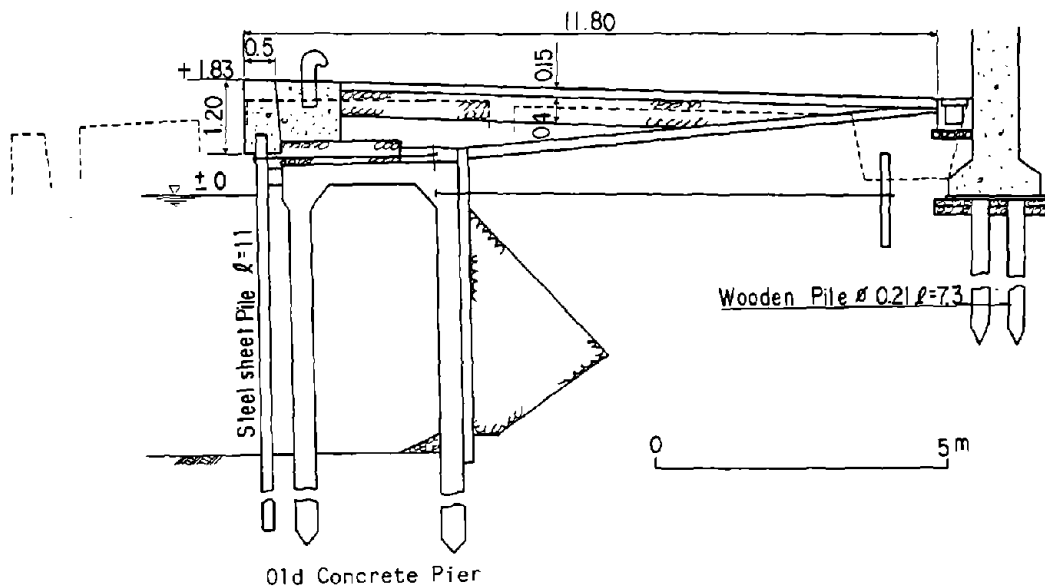


Figure 25. Quay Wall of the Fishery Pier¹²⁾

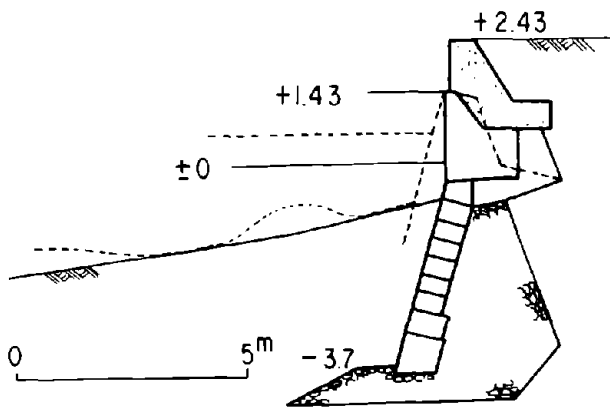


Figure 26. Damage to the Kurinoki River (Point ② in Figure 22(a))12)



Photo 18 Damage to the Quay Wall at the Fishery Pier (Point ① in Figure 22(a))



Photo 19 Damage to the Quay Wall on the Right Bank of the Old Kurinoki River (Point ② in Figure 22(a))12)



Photo 20 Damage to the Quay Wall of the North Pier (Point ③ in Figure 22(b))12)



Photo 21 Damage to the Quay Wall of the North Pier (Point ④ in Figure 22(b))12)



Photo 22 Damage to the Quay Wall of Rinko Wharf (Point ⑤ in Figure 22(c))12)

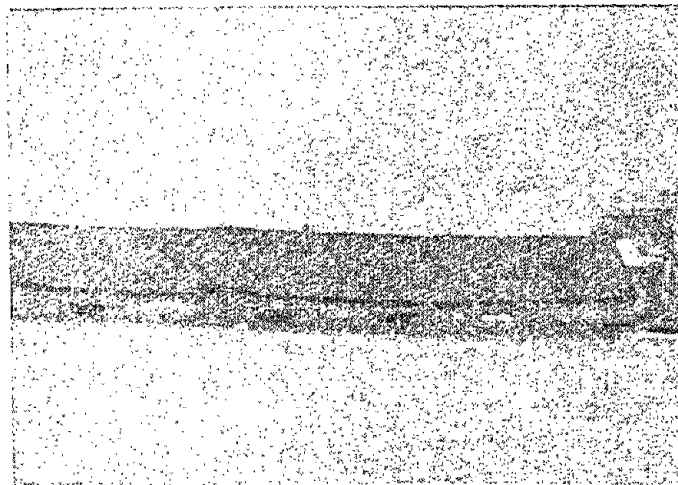


Photo 23 Damage to the Quay Wall of Rinko Wharf (Point ⑥ in Figure 22(c))12)

4.4 Zone IV: Niigata Station and the Surrounding Area

4.4.1 Permanent Ground Displacements

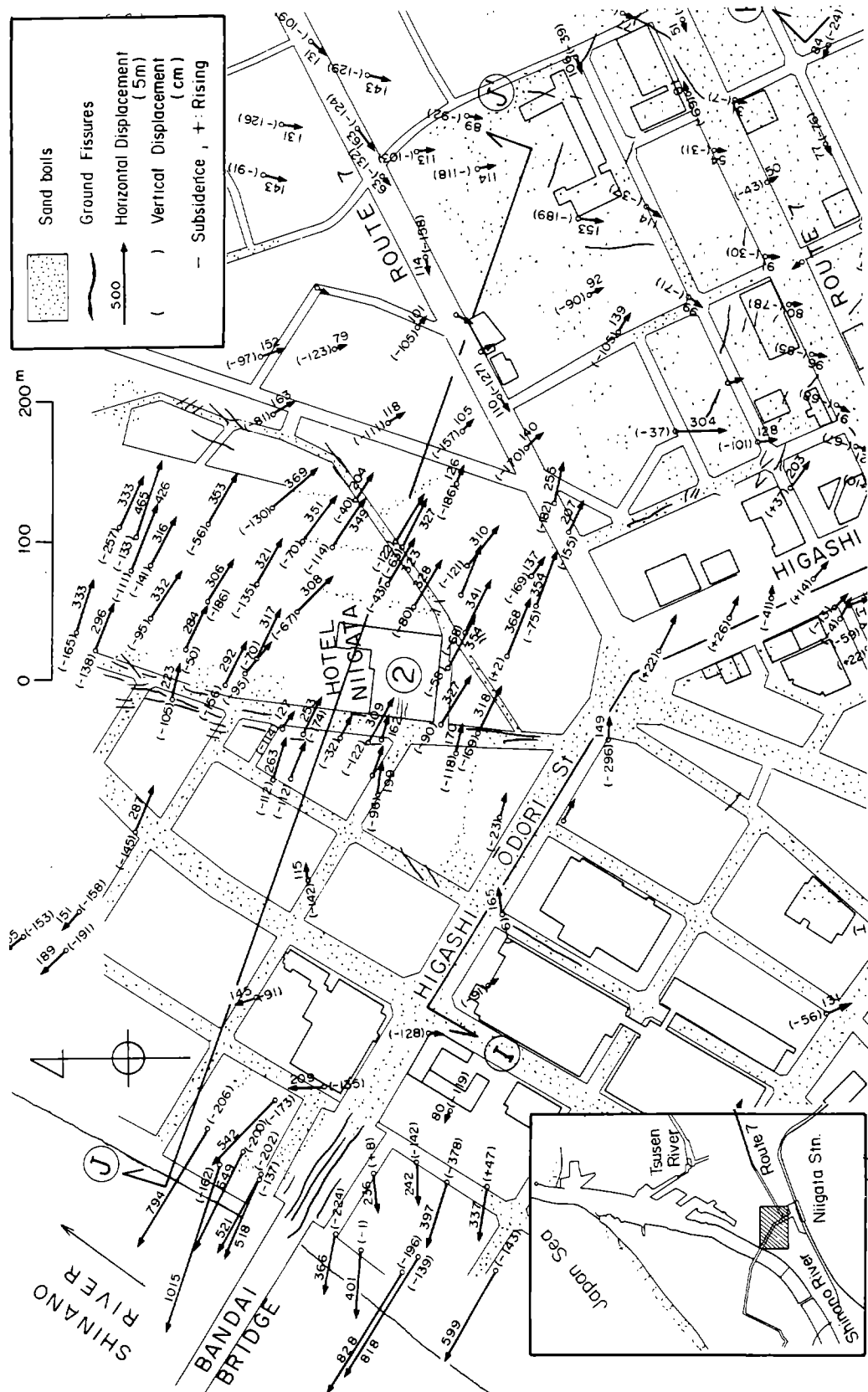
Figure 27 shows the permanent ground displacements in the areas from the Shinano River to Niigata railway station. The vectors represent ground displacements in the horizontal direction, each with a number indicating the magnitude of movement (in cm). The horizontal displacements in this area are comparatively small, less than 4 m, except at the bank of the river. However, the direction of the horizontal displacements is somewhat complex. On the right bank of the Shinano River, the ground moved toward the river in a northwesterly direction, but about 200 m away from the river bank along Higashi-Odori St. (Figure 27(a)), it moved to the southeast, almost opposite that on the river bank. Southeasterly ground displacements occurred along Higashi-Odori St., throughout the neighboring area, and in the vicinity of the railway station (Figure 27(b)).

To the west of the station along the railway, the ground also moved toward the south and southeast (Figure 27(b)), while in the area east of the station and north of the railway, displacements were toward the northwest. These displacements in the northwest direction continued for 200 to 300 m and joined the displacements in the southern direction from the river.

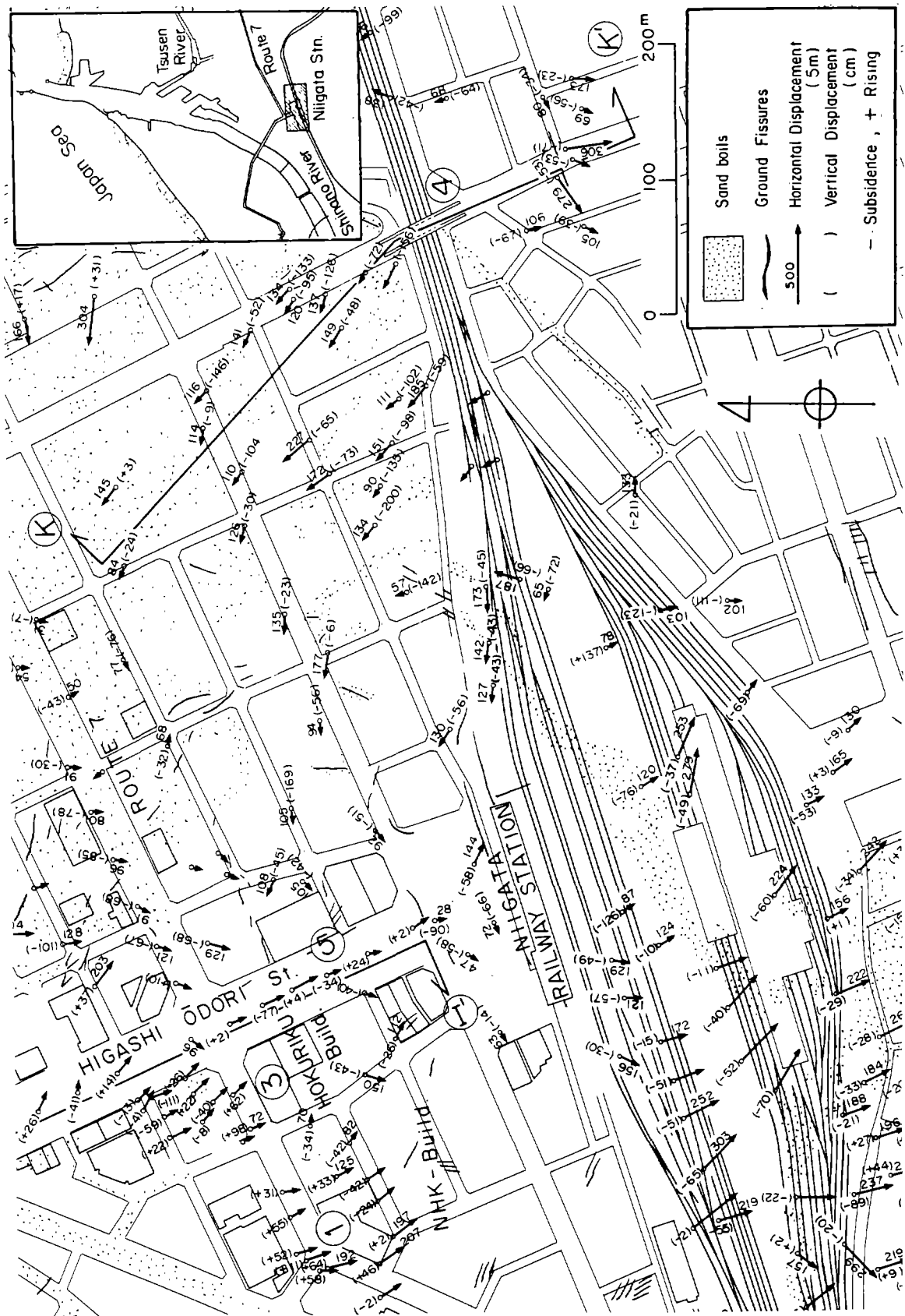
The numbers in parentheses in Figure 27 are the vertical displacements of the ground. The ground subsided at most of the measuring points. Along the Shinano River, the maximum vertical displacement was more than 2 m. In the neighborhood of the station and along the railway, the ground also subsided by about 0.5 to 1.0 m.

4.4.2 Soil Conditions

The soil conditions and liquefied soil layers, which were estimated by the Factor of Liquefaction Resistance F_L ,⁴⁾ along section I-I', from the right bank of Bandai Bridge to Niigata railway station, are shown in Figure 28(a). As shown in the figure, the ground surface is slightly inclined from the



(a) North Area
 Figure 27. Permanent Ground Displacement at Niigata Station and Its Surroundings



(b) South Area

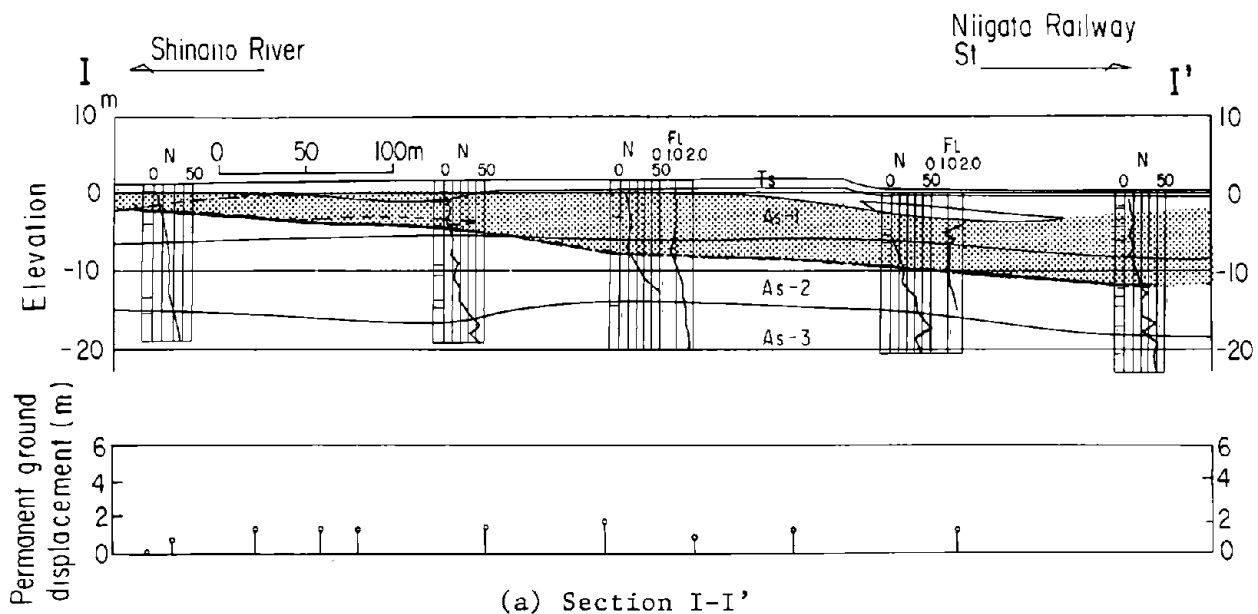
Figure 27. Permanent Ground Displacement at Niigata Station and Its Surroundings

river bank toward the station, but the gradient is very small, less than 0.5%. The elevation of the ground surface was measured from the aerial photographs taken before the earthquake. Along section I-I', the estimated liquefied layer increases in thickness toward the station. The boundary between the liquefied layer and the lower non-liquefied layer is inclined toward the station with a gradient of 2 to 3%.

Along section J-J', the estimated liquefied layer is very thick, at about 10 m, between the river bank and the Hotel Niigata. Its thickness gradually decreases towards the east (toward Route 7). No clear relationship can be found between the direction of ground displacements and the inclination of the boundary between the estimated liquefied layer and the lower non-liquefied layer along section J-J'. Around the hotel and to its west, the boundary is inclined toward the east, coinciding with the direction of ground displacements. However, from the hotel to Route 7, the boundary is inclined toward the west, namely toward the hotel, but the ground moved toward the east, opposite to the inclination.

Furthermore, along section J-J', no clear correlation can be seen between the direction of the ground displacements and the inclination of the surface. The area around Route 7 had the highest elevation along the section, and the ground slopes from there in both directions, but the ground displacement was very small. The area around the Hotel Niigata was a little higher and the ground surface had a slight gradient to the west and east, but the ground displaced only in the easterly direction.

Along section K-K', the estimated liquefied layer is about 7 m thick in the north area of the railway, but this thickness gradually decreases toward the East Bridge over the railway. The girder of this bridge collapsed as a result of liquefaction-induced ground displacements, as described later. To the south of the bridge, the liquefied layer also decreases in thickness and terminates 200 m from the bridge. Along the section, the boundary between the estimated liquefied layer and lower non-liquefied layer is inclined to the north. This inclination coincides with the direction of the ground displacement, although the ground surface is mostly flat in this area. Soil



LEGEND

- | | | | |
|-------------|---------------------|--|---------------------------------|
| Ts | Surface Soil (Fill) | : Estimated Liquefied Layer | Displacement in Right Direction |
| As-1 | Alluvial Sandy Soil | N : SPT values, blows/ft(0.3m) | Displacement in Left Direction |
| As-2 | | FL : Factor of Liquefaction Resistance | |
| As-3 | | | |

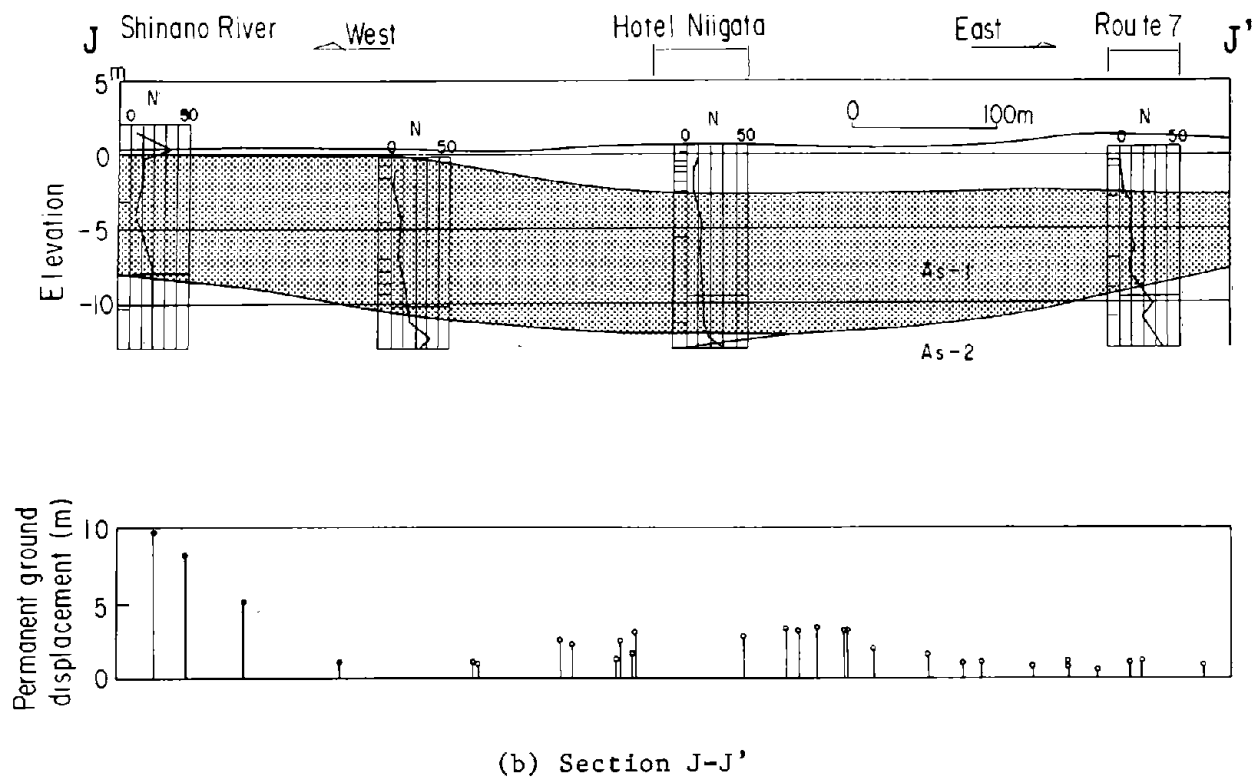
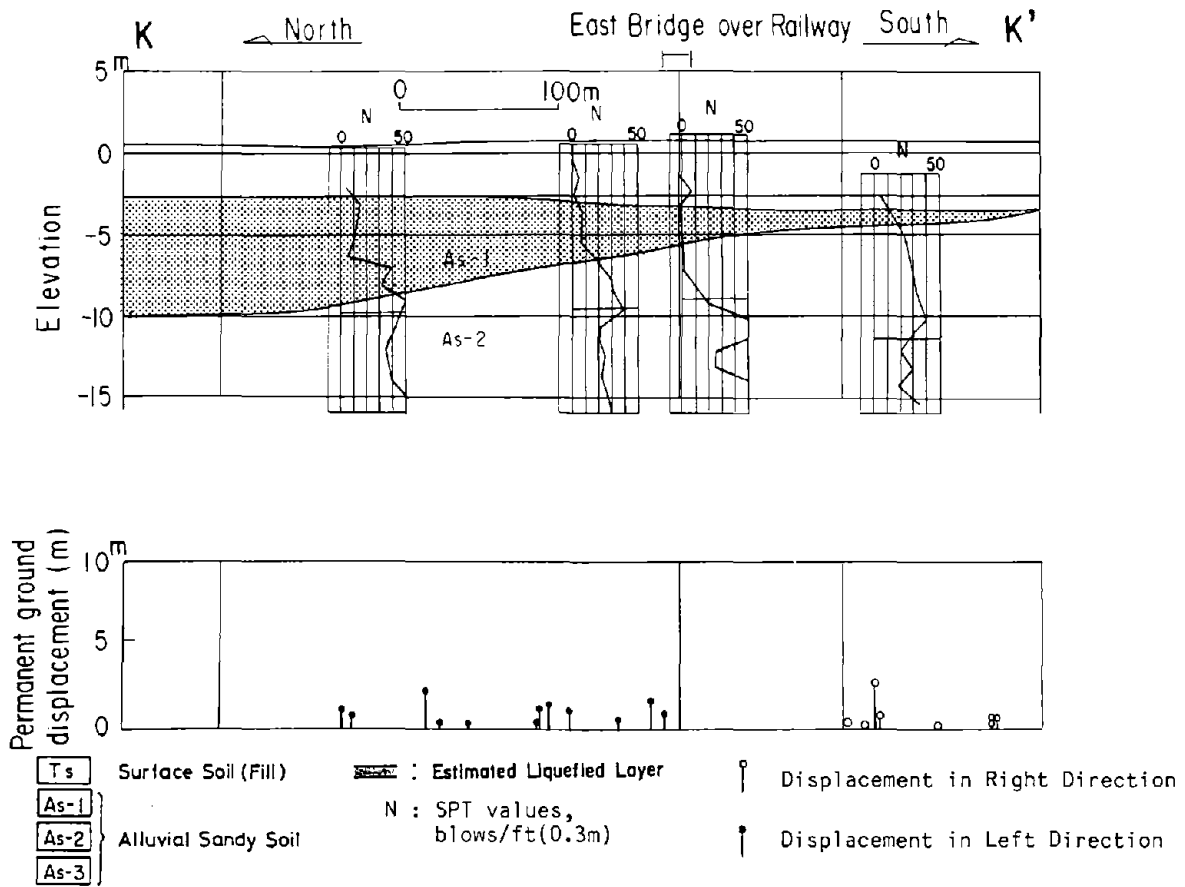


Figure 28. Soil Conditions and Estimated Liquefied Layer



(c) Section K-K'

Figure 28. Soil Conditions and Estimated Liquefied Layer

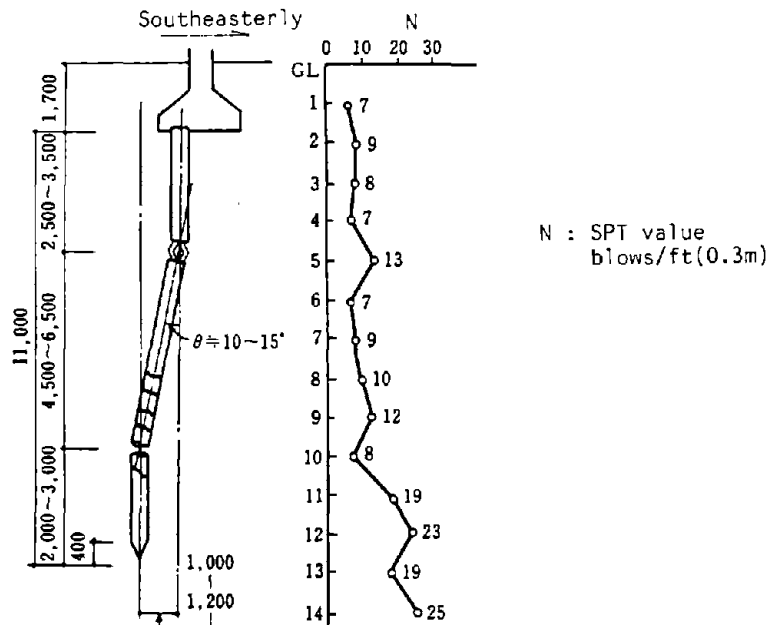


Figure 29. Damage to Foundation Piles of the NHK-Building
(Point ① in Figure 27(b)) (S. Kawamura et al)¹³⁾

profiles for this area in addition to those discussed above may be found in Appendix B.

4.4.3 Damage to Structures

(1) Damage to foundation piles of the NHK Building

The NHK Building, located at Point ① in Figure 27(b), north of Niigata railway station, was a four-storey reinforced concrete building with reinforced concrete pile foundations. When the foundations of the building were excavated for reconstruction in 1985, about twenty years after the earthquake, reinforced concrete piles 35 cm in diameter and 11 to 12 m in length were found to be completely fractured as shown in Photos 24 and 25. This building had been used after basic repairs to the floors without awareness of the failure of the piles. Kawamura et al. reported on the damage to the piles.¹³⁾

As shown in Figure 29 and Photos 24 and 25, the piles were fractured in a similar way to those of the Family Court House shown in Figure 16 and Photo 13. The breakage was discovered at two positions, 2.5 to 3.5 m from the upper end of the piles and 2.0 to 3.0 m from the bottom. Seventy-four of the total of 204 piles were investigated, and it was found that all of them were similarly damaged. From this damage, the horizontal permanent deformation of the piles was estimated to be 1.0 to 1.2 m as shown in Figure 29.

Figure 30 shows details of the permanent ground displacements in the vicinity of the building as measured by the aerial survey. The horizontal displacement vectors are in mostly southeasterly directions, which is the same as that of the pile deformation shown in Figure 29. However, the magnitude of the horizontal ground displacements in the neighborhood of the building are around 2 m, larger than the pile deformation.

The subsurface soils at the building site consist of a loose sandy layer with SPT-values of 5 to 10 down to -10 m, as shown in Figure 29, and this is thought to have liquefied during the earthquake. As is the case for the

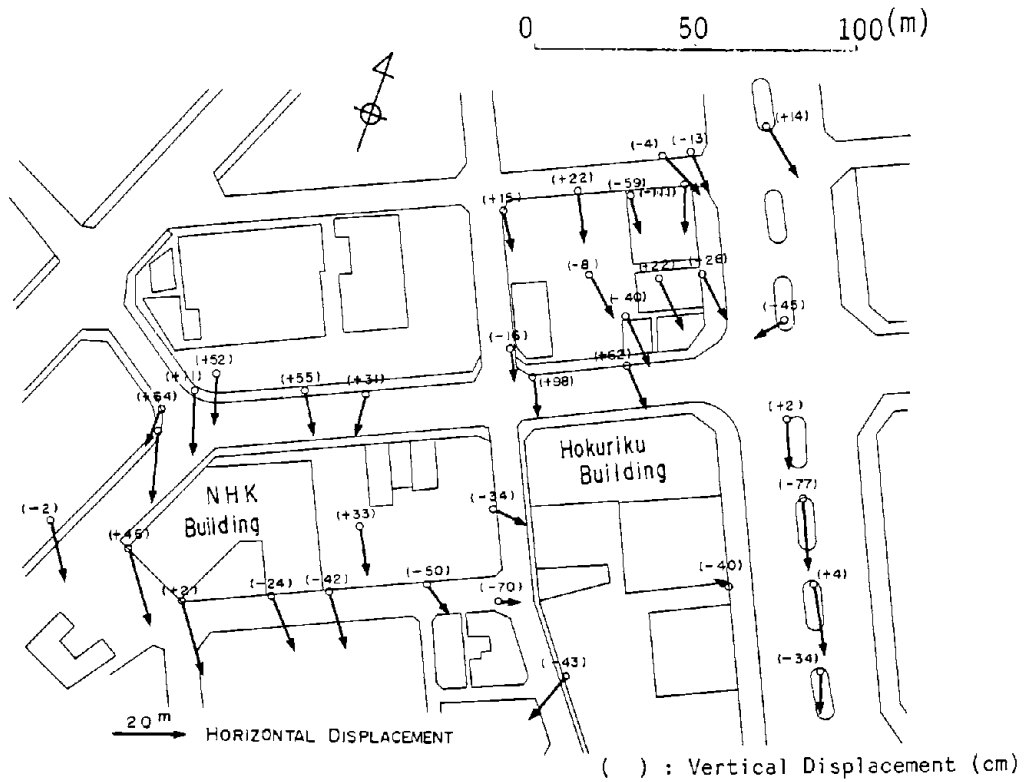


Figure 30. Permanent Ground Displacement in the Horizontal Direction in the Vicinity of the NHK-Building



Photo 24 Damage to Foundation Piles of the NHK-Building (Point ① in Figure 27(b)) (S. Kawamura et al.)¹³



Photo 25 Damaged Pile of the NHK-Building (S. Kawamura et al.)¹³

Family Court House, the lower damaged points generally coincide with the boundary between the estimated liquefied layer and the lower non-liquefied layer. Regarding the failure process of the piles, numerical simulations were conducted, and it was concluded that horizontal permanent displacements of the liquefied ground are the direct cause of the pile failure.^{11),14)}

(2) Damage to the foundation piles of the Hotel Niigata building

Photo 26 shows the damage to the 35 cm diameter reinforced concrete piles of the Hotel Niigata building which is located at Point ② in Figure 27(a). This damage was also found at the time of reconstruction of the building 23 years after the earthquake. The hotel suffered severe damage due to liquefaction. Photo 27 shows that a concrete purification tank at the site was lifted by about 2 m because of its buoyancy in the liquefied soil.

Details of the damage to the foundation piles could not be assessed as clearly for the Hotel Niigata as it could for the NKK Building. Excavation of the foundations was carried out in a short time period by power shovels, thereby preventing direct access by researchers to many of the piles as they were exposed. Nevertheless, it was reported by construction personnel that all the piles were catastrophically broken as shown in Photo 26.

Figure 31 shows that the subsurface soils consist of a loose sand layer with SPT-values of less than 10 down to -13 m. This layer was estimated, using the Factor of Liquefaction Resistance F_L , to have liquefied during the earthquake. The details of horizontal ground displacements in the neighborhood of the building are given in Figure 32. The ground was displaced in the southeasterly direction by 4 to 5 m. An engineer engaged in the excavation of the foundations at the time of the reconstruction remarked that the piles were deformed mostly toward the southeast.

(3) Behavior of the Hokuriku-Building

The 10-storey Hokuriku-Building is located at Point ③ in Figure 27(b) in the neighborhood of the NHK-Building. The Hokuriku-Building was also founded

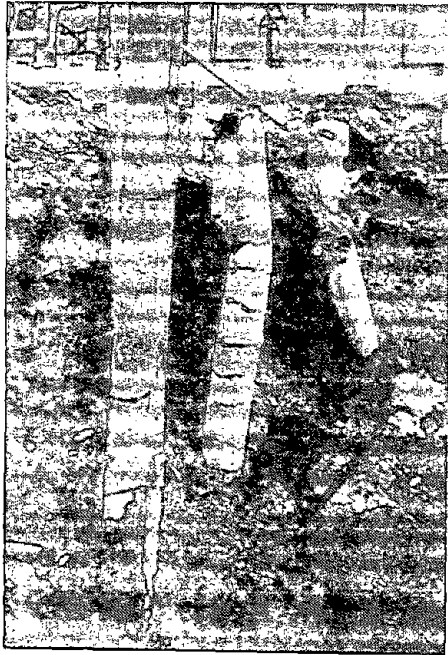


Photo 26 Damage to Foundation Piles of the Hotel Niigata Building

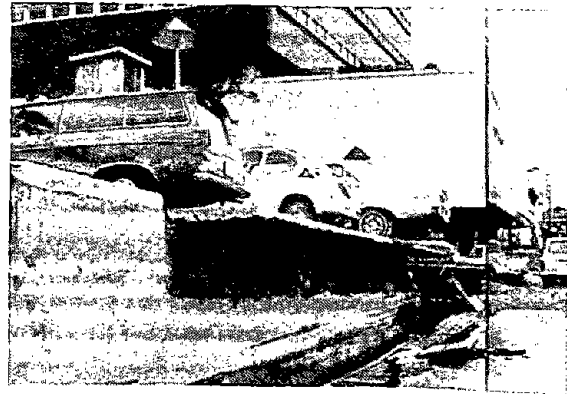
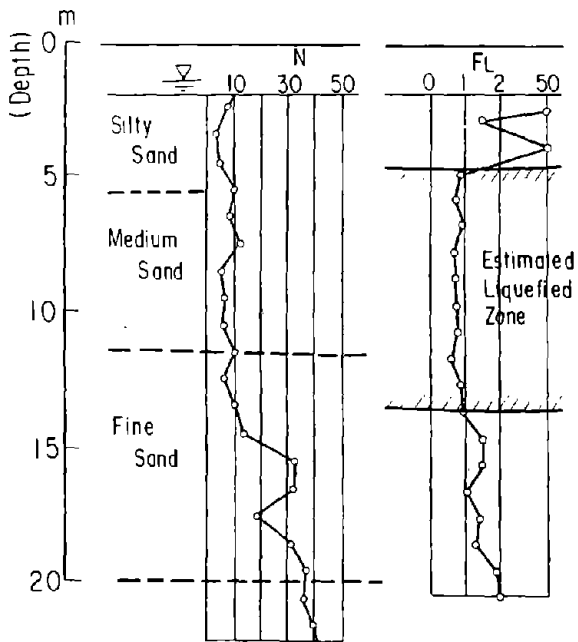


Photo 27 Concrete Purification Tank Raised to the Surface at the Hotel Niigata



N : SPT values, blows/ft(0.3m)
 FL: Factor of Liquefaction Resistance

Figure 31. Soil Conditions at the Hotel Niigata Site

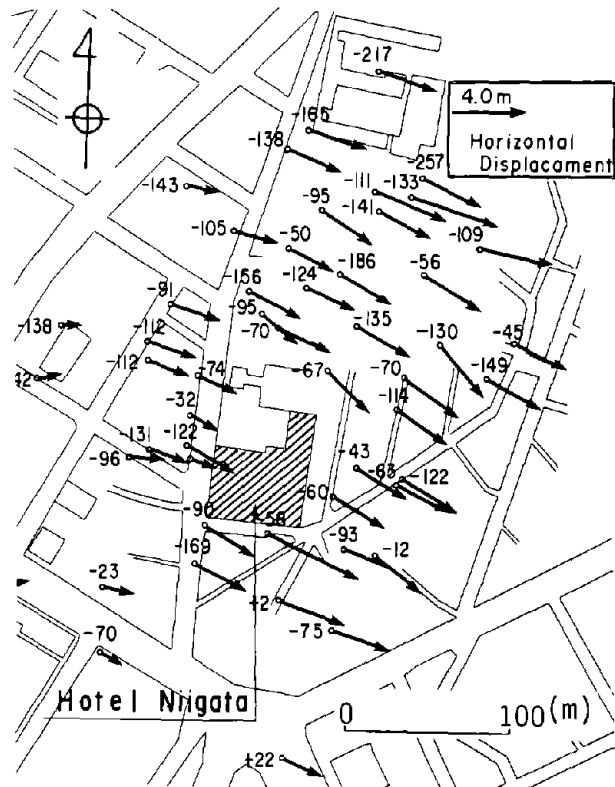


Figure 32. Horizontal Vectors and Vertical Displacement of Ground in the Vicinity of the Hotel Niigata

on reinforced concrete piles with a diameter of 40 cm and a length of 12 m, but no damage was reported to the superstructure after the earthquake. It was reported that no crack appeared in the walls, beams, and columns, and furthermore, that no inclination occurred.

As shown in Figure 30, the ground surface near by this building moved by about 2 m. As probable reasons for lack of damage to the building, the following characteristics of the foundations may be considered:¹⁵⁾

(i) The building has a one-storey basement, which goes 6 to 7 m below the ground surface as shown in Figure 33.

(ii) The foundation piles were driven from the basement floor level into the non-liquefied layer at a depth of about 12 m. The arrangement of foundation piles is shown in Figure 33. The total number of foundation piles in the 10-storey Hokuriku-Building was much more than that in the four-storey NHK-Building. It is conjectured that a large number of piles had a great effect on densification of the soil as well as prevention of ground displacements in the horizontal direction.

(iii) For the excavation of the basement, in-ground walls were constructed using steel sheet piles and cast-in-place concrete piles which were driven in a continuous line at the perimeter of the excavation. It is reported that, after completion of the building, the in-ground walls made of steel sheet piles were removed, but the cast-in-place concrete piles remained.

According to the permanent ground displacements in the vicinity of the building shown in Figure 30, the following characteristics can be pointed out. To the north of the building, the ground moved in a southerly direction mainly toward the buildings, but the displacements were much smaller south of the building, at its rear. Furthermore, along the north side of the building the ground surface rose up 0.6 to 1.0 m, while in the area away from the building it mostly subsided. No decisive conclusion can be drawn because there is a lack of measuring points for ground displacement behind the building, but it may be conjectured that the existence of the basement and the in-ground walls as well as the large number of foundation piles, obstructed the flow of liquefied soil.

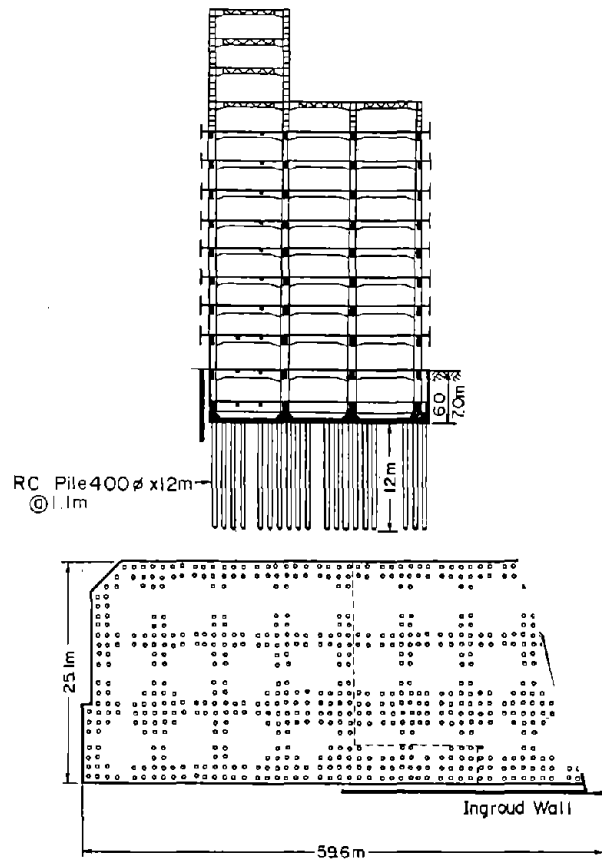


Figure 33. Outline of the Hokuriku Building and Arrangement of Foundation Piles (Y.Yoshimi¹⁵)



Photo 28 Collapse of the East Bridge over Railway (Point ④ in Figure 27(b))¹⁶

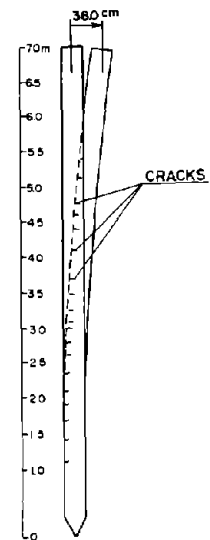


Figure 34. Bending Cracks in Concrete Piles of the East Bridge over Railway (Point ④ in Figure 27(b))¹⁶

The case of the Hokuriku-Building gives an instructive suggestion as to how foundations can be protected against liquefaction-induced permanent ground displacements, as well as how to prevent the occurrence of ground displacements.

(4) Collapse of the East Bridge over the railway¹⁶⁾

The East Bridge over the railway is located to the east of Niigata Railway Station, at Point ④ in Figure 27(b). A simply supported steel girder with a span of 26.6 m fell because of the earthquake, as shown in Photo 28, and crushed a locomotive. The two piers which supported the girder stood on concrete piles of diameter 30 cm and length about 7 m. Figure 34 shows the cracks in a pile extracted after the earthquake. Cracks caused by the bending moment were found not only on the upper portion, but also, towards the bottom. Furthermore, cracks occurred on only one side of the piers. This suggests that the piles were not damaged by repeated inertia force from the superstructure, but by liquefaction-induced ground displacement, which is considered to increase monotonically.

Figure 35 shows the horizontal permanent ground displacements in the area around the collapsed bridge. To the north of the bridge, the ground moved in a northwest direction, mostly parallel to the bridge axis. South of the bridge, however, the ground moved in a southwest direction, perpendicular to the bridge axis. This means that a tensile strain resulted in the ground in the direction of the bridge axis, so that the distance between the two piers of the bridge increased. Figure 35 also shows the ground strain in the horizontal plane, as calculated from the measured displacements.* It can be seen that a significant tensile strain, with a magnitude of about 1.5%, occurred in the direction of the bridge axis.

*See Appendix C of reference 19) about the method of calculation of ground strain.

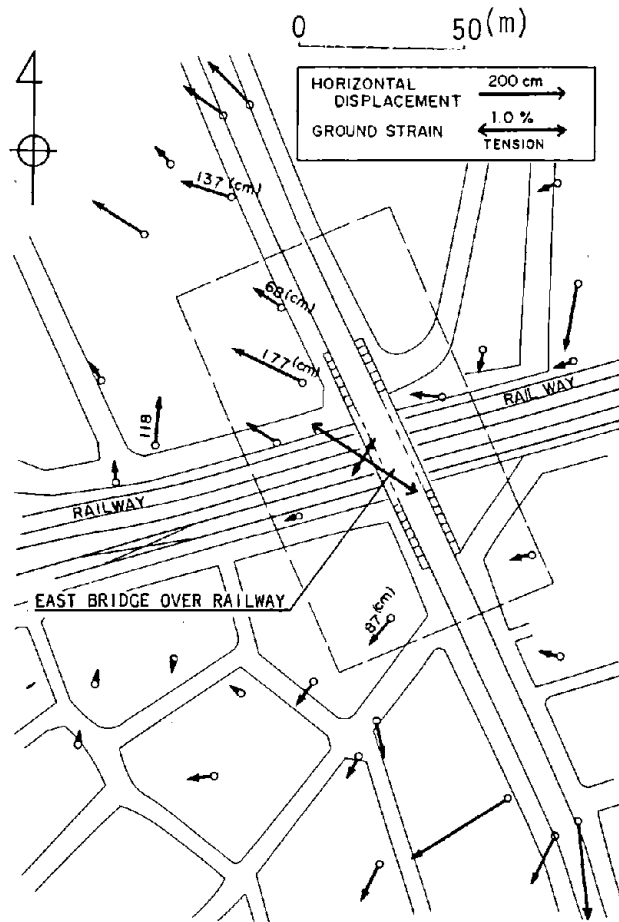


Figure 35. Horizontal Ground Displacement in the Vicinity of the East Bridge over Railway

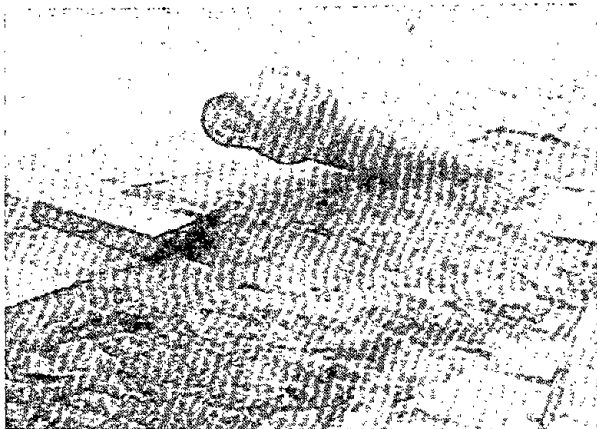


Photo 29 Protrusion of a Buried Gas Pipe above the Surface (Point ⑤ in Figure 27)17)

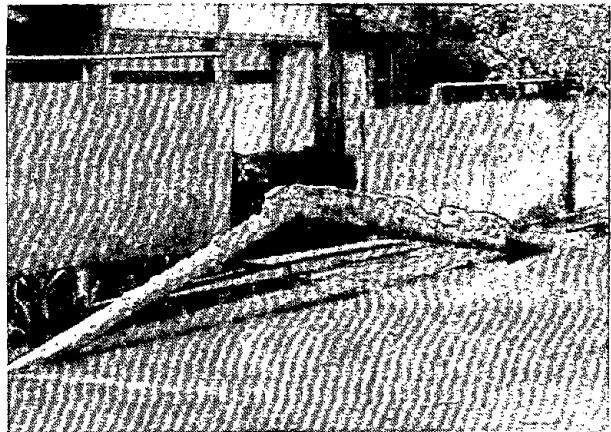


Photo 30 Buckling of a Buried Gas Pipe

(5) Damage to cast-iron gas pipes

In Niigata City, numerous buried pipes were severely damaged by liquefaction and especially by liquefaction-induced ground displacements. Photo 29 shows one example of damage to a cast-iron gas pipe, which was forced out of the ground.¹⁷⁾ The gas pipe had a diameter of 15 cm, and it was connected with mechanical joints. It is well known that buried pipes with a specific gravity less than that of the liquefied soil, such as sewage pipes, can float. However, such abrupt surfacing as seen in Photo 29 is less probable as a result of buoyancy.

Figure 36 shows the permanent ground displacements in the horizontal direction in the vicinity of the damaged gas pipe and the ground strain calculated from the measured displacements. A compressive strain with a magnitude of about 0.2% occurred almost in the direction of the pipe axis. It can be concluded that the pipe was buckled and forced above the surface by the compressive strain when the ground lost much of its stiffness due to liquefaction.

Many similar bucklings of buried pipes were observed. Photos 30 and 31 show other examples of such buckling. These examples were steel pipes for natural gas supply with a diameter of 8 cm.

An engineer with a gas company in Niigata City stated that he found gas pipes underneath the concrete side trenches of the road near the Niigata railway station after the earthquake, which had originally been buried at a distance from the trenches. This instance suggests that the ground at the depth of the pipe moved more than the ground surface during the earthquake.

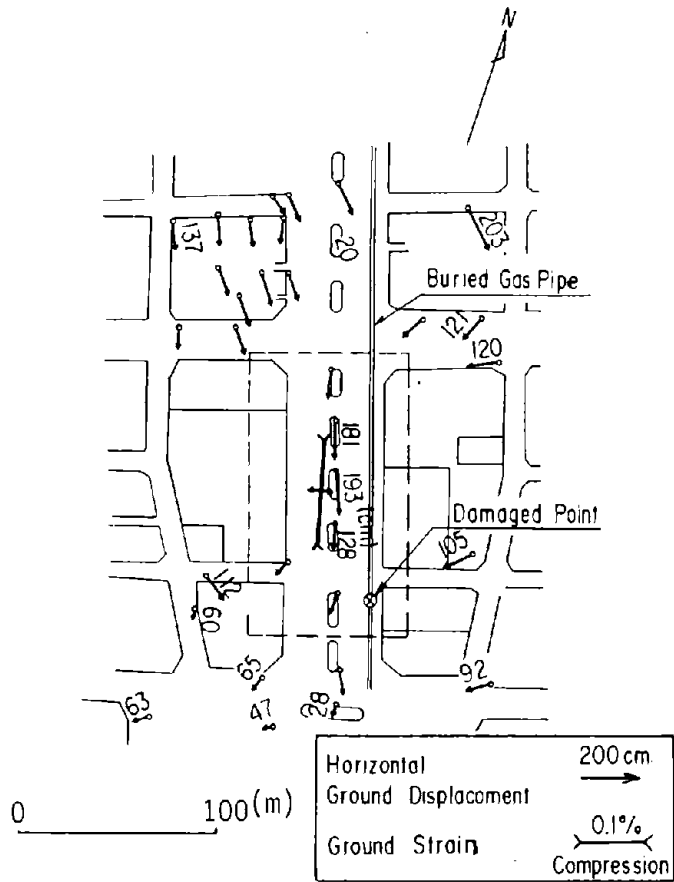


Figure 36. Horizontal Ground Displacement in the Vicinity of Damaged Gas Pipe



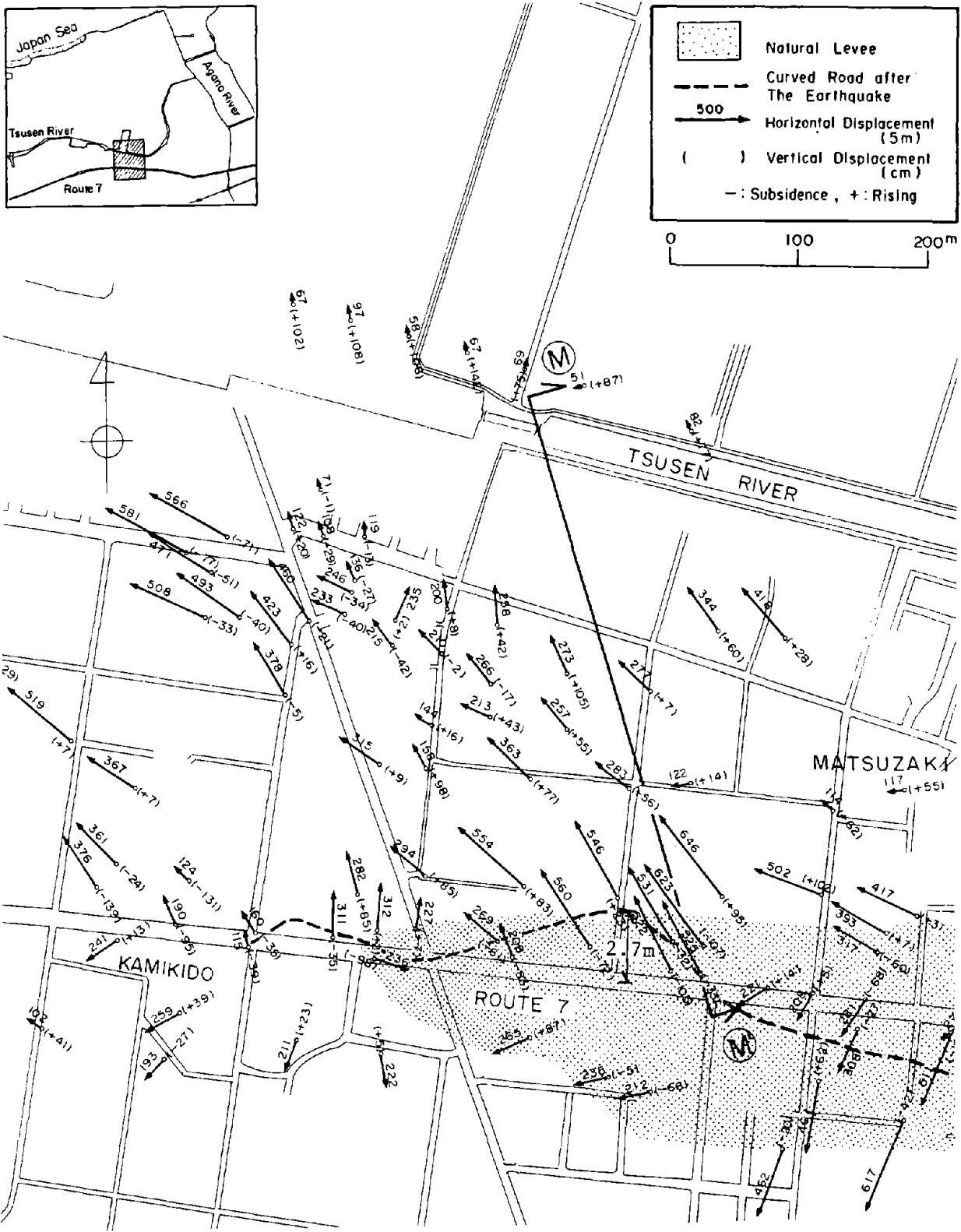
Photo 31 Buckling of a Buried Gas Pipe

4.5 Zone V: Ebigase and Ohgata Areas

4.5.1 Permanent Ground Displacements

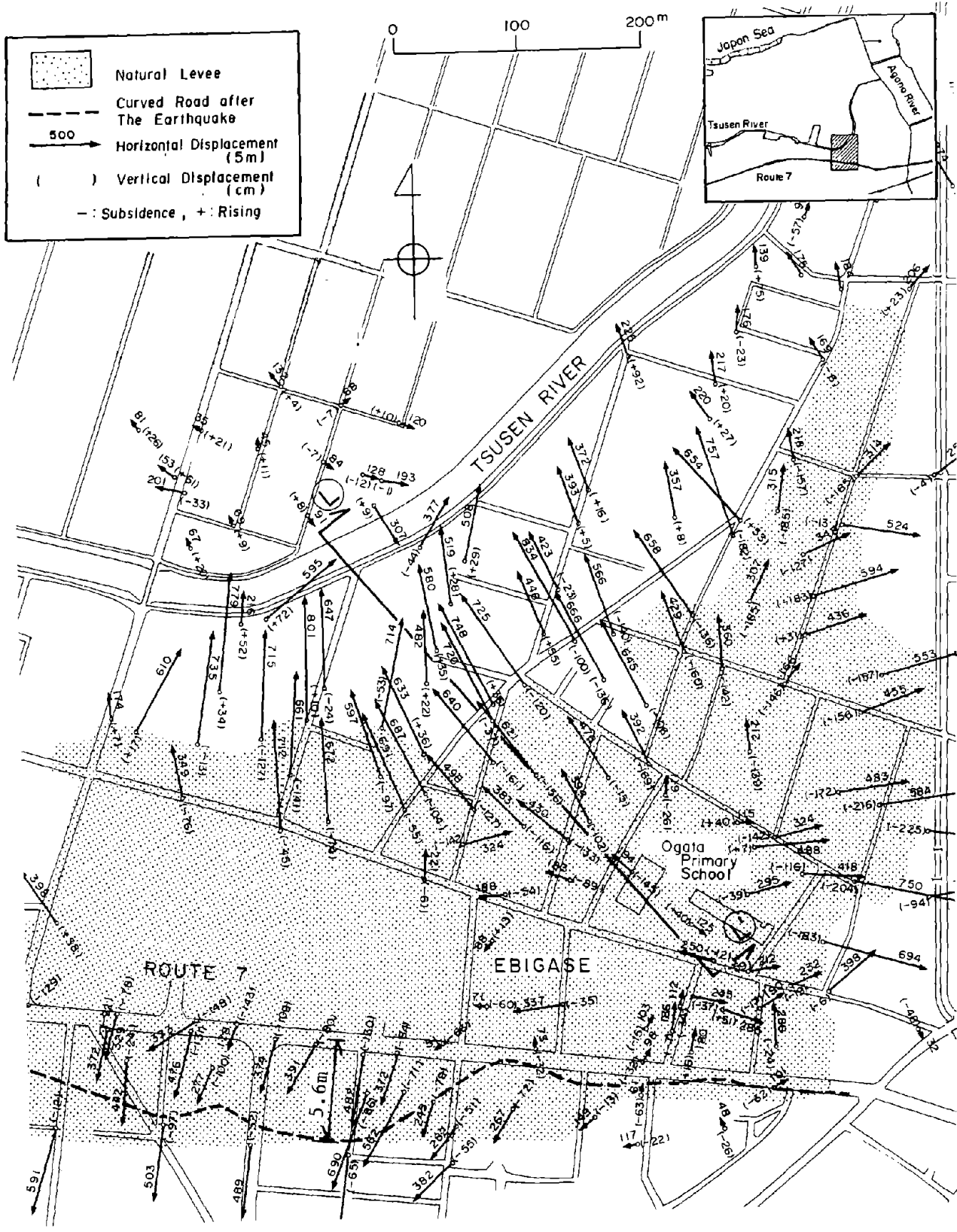
Ebigase and Ohgata, which are located on the left bank of the Agano River, were severely liquefied during the earthquake. The vectors in Figure 37 represent the horizontal ground displacements, and the numbers in the parentheses are the vertical displacements. This area is on the old riverbed and the natural levee of the Anago River. The shadowed area in Figure 37 is the natural levee, while the other area is mostly the old riverbed. Figure 39 shows the old streams of the Tsusen River in 1630. The Tsusen River was about 10 m wide at the time of the earthquake, but it had been the old stream of the Agano River with a large width, as shown in the figure. The horizontal displacements were caused from the natural levee with higher elevation toward the old riverbed with lower elevation. This movement is shown clearly in Figure 38, which shows the horizontal displacement vectors on a contour map of the area. The map was drawn from aerial photographs taken before the earthquake. It must be noted that the mean gradient of these slopes is very small, at less than 1.0%.

The ground to the west along Route 7 moved toward the northwest by a maximum of 6 m (Figure 37(a)), while to the east along Route 7 it was displaced generally toward the south by a maximum of 5 m (Figure 37(b)). This means that Route 7, which had been straight before the earthquake, was greatly distorted by the earthquake. According to a survey of the road after the earthquake conducted by the Ministry of Construction,¹⁸⁾ the road moved toward the north with a maximum displacement of 2.7 m in the western area and toward the south with a maximum of 5.6 m in the eastern area, as shown by the dotted line in Figure 37. The results of this survey coincide well with the results of the aerial survey. Photo 32 shows Route 7 after the earthquake.



(a) West Area

Figure 37. Permanent Ground Displacement in Ebigase and Ohgata Areas



(b) East Area

Figure 37. Permanent Ground Displacement in Ebigase and Ohgata Areas

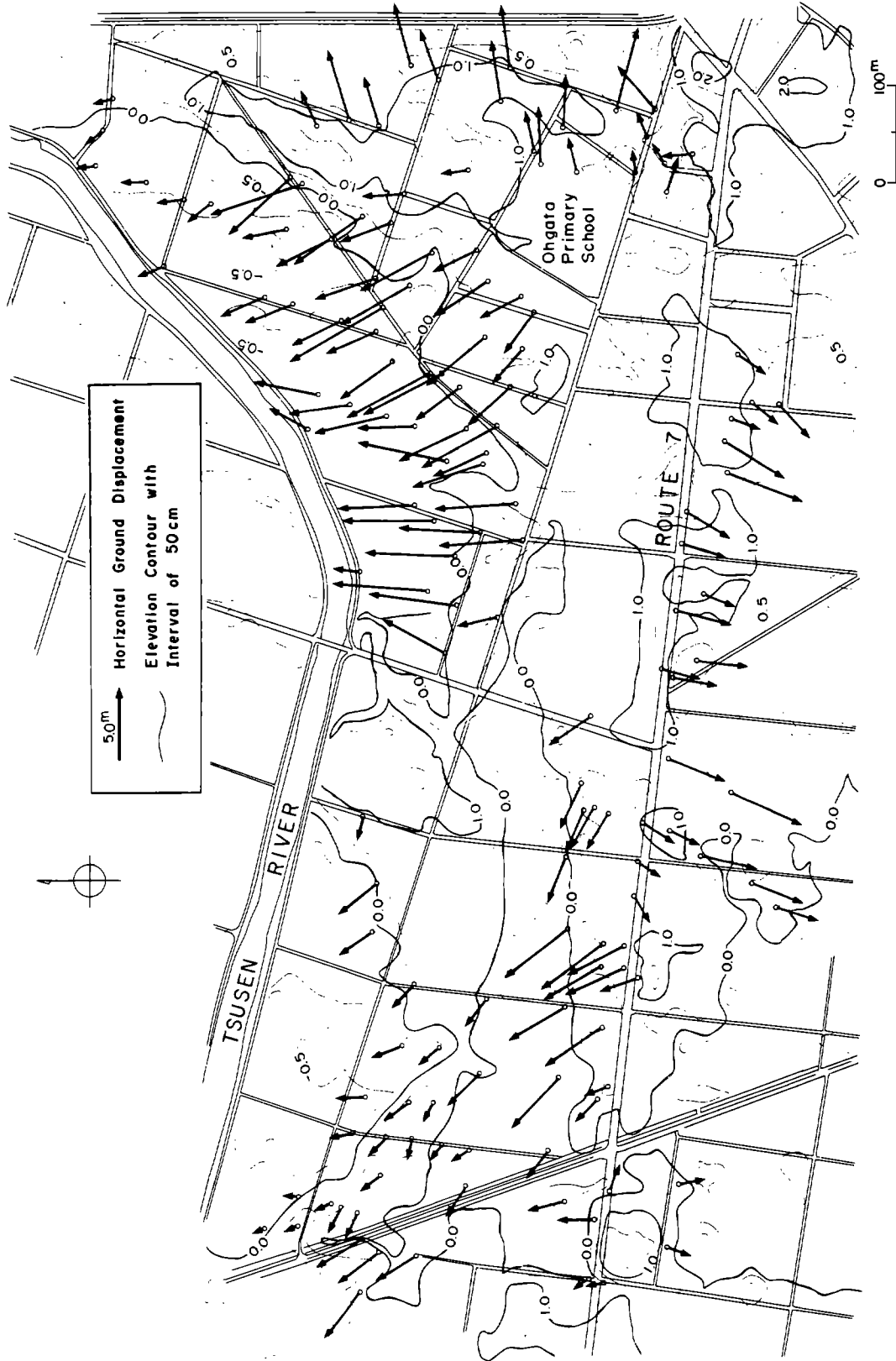


Figure 38. Permanent Ground Displacement in the Horizontal Direction on a Contour Map
 (Numbers on the contours represent elevations above mean sea level, Unit:m)



Photo 32 Route 7 after the Earthquake 18)



Photo 33 Risen Portion of the Tsusen River

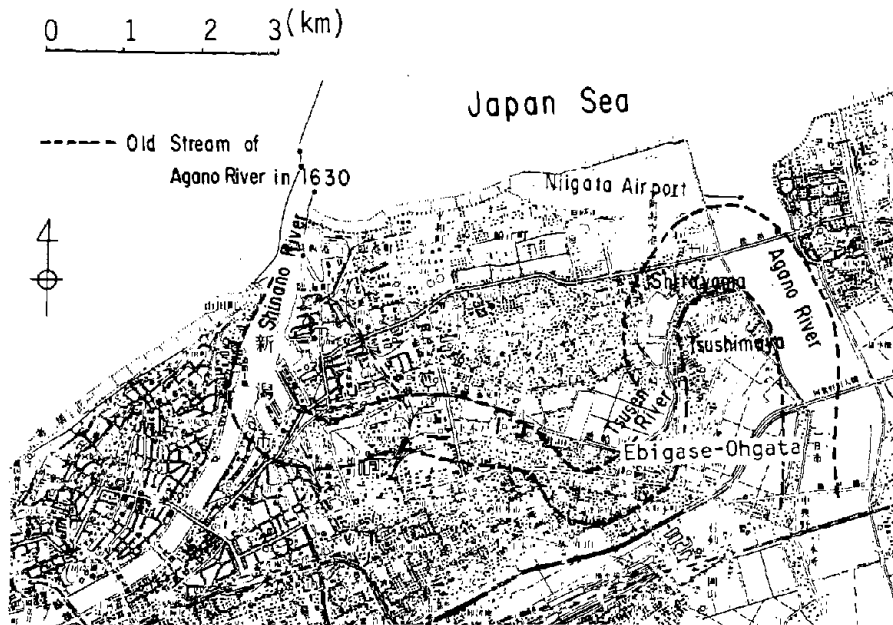


Figure 39. Change to the Agano River Course

As shown in Figure 37, part of Route 7 was built on the natural levee. On the west, the road was built along the northern slopes of the levee, and this is where the ground moved toward the north. On the southern slopes, in the east area, the ground moved toward the south.

The horizontal displacements in a northwest direction along Route 7 to the west (Figure 37(a)) began in the vicinity of the road, continued for about 400 m, and terminated around the Tsusen River. Ground displacements with a remarkable magnitude were also observed at Ohgata Primary School and its vicinity (Figure 37 (b)). From the playground of the school, displacements mostly occurred in radial directions. Displacements in a northwest direction were dominant, and continued for about 300 m towards the Tsusen River. The maximum displacement in this area was over 8 m. Beyond the Tsusen River, the displacements ended.

According to measurements of vertical displacements, shown as numbers in parentheses in Figure 37, most parts of the area subsided due to liquefaction. The primary school and its vicinity, where the horizontal ground displacements began, subsided greatly with a maximum drop of 2.0 m. On the contrary, the ground rose at many points in the neighborhood of the Tsusen River where the horizontal ground displacements ended. Many witnesses remarked that near the Tsusen River a considerable amount of sand and water spouted from the ground, and the riverbed rose above water level in some places, enabling people to cross the river on foot. Photo 33 shows the Tsusen River after the earthquake where the riverbed rose.

Figure 40 shows the location of sand boils and ground fissures, which were identified in aerial photographs taken after the earthquake. Numerous ground fissures were observed in the area of the primary school, where the ground was under tensile strain and where the surface had subsided greatly. Sand boils were seen in the area of the Tsusen River where the horizontal ground displacement ended and the surface rose.

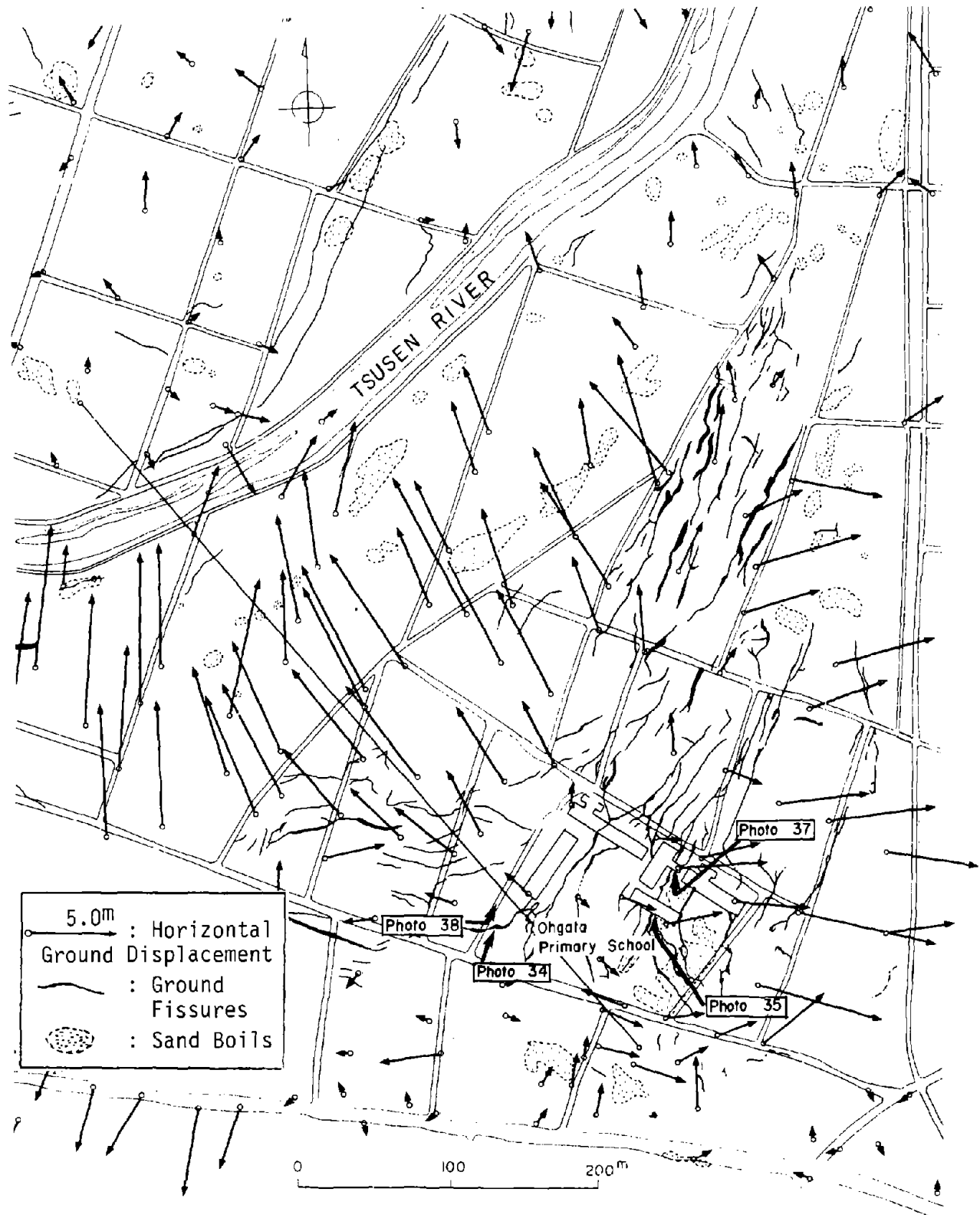


Figure 40. Sand Boils and Ground Fissures in the Vicinity of the Ohgata Primary School

4.5.2 Soil Conditions

Figure 41 shows soil profiles and the liquefied soil layers, which were estimated by the Factor of Liquefaction Resistance F_L ,⁴⁾ along sections L-L' and M-M'. Soil profiles for this area in addition to those discussed below can be found in Appendix B.

The estimated liquefied layer along section L-L' increases in thickness from 4 m to 6 m between the Ohgata Primary School and the Tsusen River. The boundary between the estimated liquefied layer and the lower non-liquefied layer is inclined towards the river with a mean gradient of about 1%, which coincides with the direction of the ground displacements. The ground surface also is inclined toward the river, but with a gradient of about 1.0%.

Along section M-M', the estimated liquefied layer gradually increases in thickness from 5 to 10 m between Route 7 and the area about 100 m distant from the south bank of the Tsusen River. It decreases abruptly at the bank of the river. No liquefied layer was detected on the north bank of the river, where ground displacements were very small. Along section M-M', the ground surface is mostly flat, with a gradient less than 0.2%. The boundary between the estimated liquefied layer and the lower non-liquefied layer is inclined from Route 7 to the river with a mean gradient of about 1.0%.

4.5.3 Damage to Structures

(1) Ohgata Primary School

The Ohgata Primary School is located on a natural levee from where the horizontal displacements originated toward the lower land. Numerous ground fissures were caused in the vicinity of the school due to the tensile strain of the ground, and this resulted in severe damage to the school structures as shown in Photos 34-38. The locations and the orientations of these photographs are shown in Figure 40.

Photo 34 shows one example of a ground fissure in the playground. The grassy ground cracked and liquefied sandy soil can be seen. Witnesses in this area reported that several fissures with a width of about 3 m were formed. A school teacher allegedly fell into a fissure in the playground, and was rescued by neighborhood residents. Photo 35 shows another example of a ground fissure underneath a wooden school building. Photo 36 was taken inside the building. The buildings shown in Photo 37, which were connected before the earthquake, were completely separated by a wide ground fissure over a distance of about 3 m.

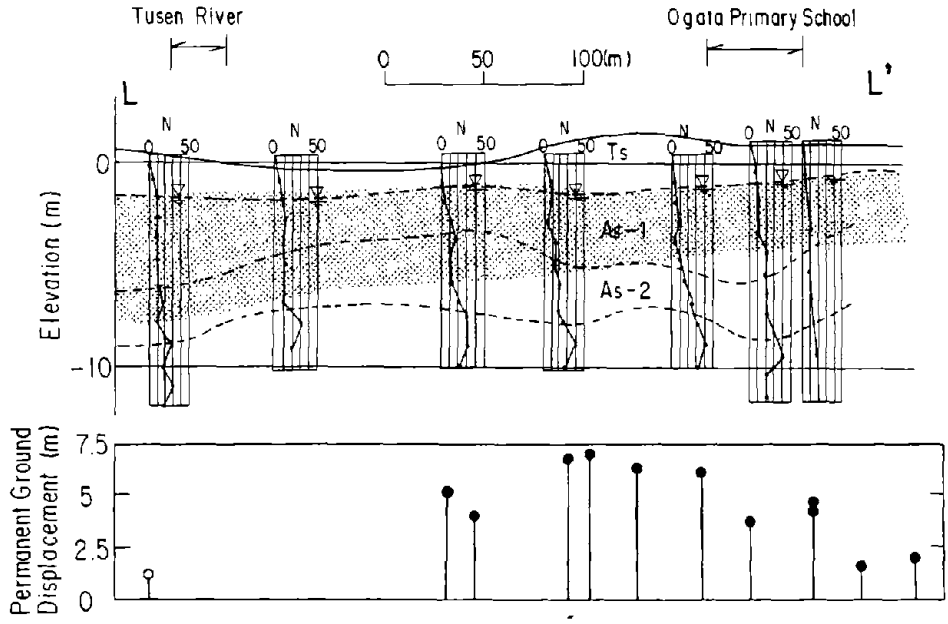
Many statements that the road, which had been straight before the earthquake, was deformed by the earthquake were collected from witnesses in the vicinity of Ohgata Primary School. One example of road deformation is shown in Photo 38, taken at the western boundary of the school playground. One resident along this road remarked that he thought the playground undulated towards his house during the earthquake, and that the road became curved.

In Niigata City, the number of boundary disputes suddenly increased after the earthquake because land boundaries were changed as a result of the large horizontal permanent ground displacements. One housewife in the Ohgata area claimed that she had been defrauded. After the earthquake, a person who introduced himself as a city government official, visited her and asked her to pay some amount of money to the city because of the increased size of her land.

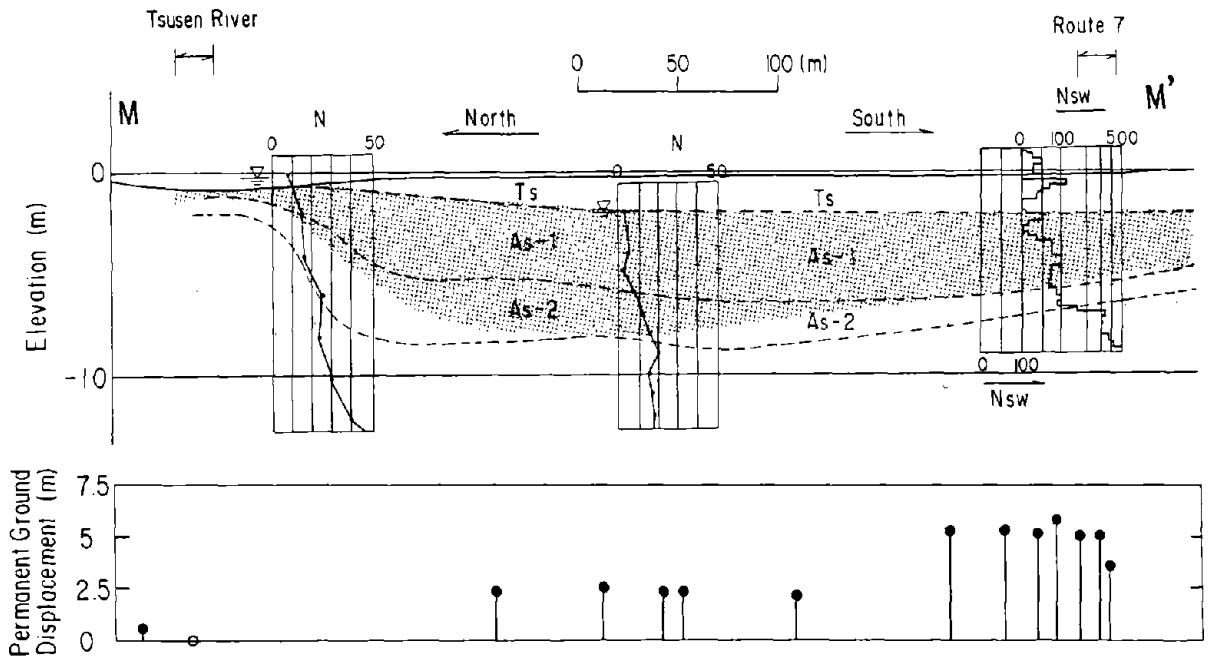
4.6 Zone VI: Matsuhama, Shitayama, and Shinkawa Areas

4.6.1 Permanent Ground Displacements

The Matsuhama, Shitayama, and Shinkawa areas are located on the left bank of the present Agano River where the Tsusen River, the earlier route of the Agano River, flows into it as shown in Figure 39. These areas also suffered extensive damage due to liquefaction during the earthquake. Figure 42 shows the permanent ground displacements, and it can be seen that horizontal displacements occurred from the natural levee, which are marked as shadowed areas in the figure, towards the old riverbed, which are white in the figure.



(a) Section L-L'



LEGEND

- Ts Surface Soil (Fill)
- As-1
- As-2 } Alluvial Sandy Soil
- As-3 }
- : Estimated Liquefied Layer

- N : SPT values, blows/ft(0.3m)
- Nsw : SWS values, number of half revolution/m
- Wsw : SWS values, load in kg
- ⌋ : Displacement toward Right Side on the Cross Section
- ⌋ : Displacement toward Left Side on the Cross Section

(b) Section M-M'

Figure 41. Soil Conditions and Estimated Liquefied Layer



Photo 34 Ground Fissure in the Playground of the School

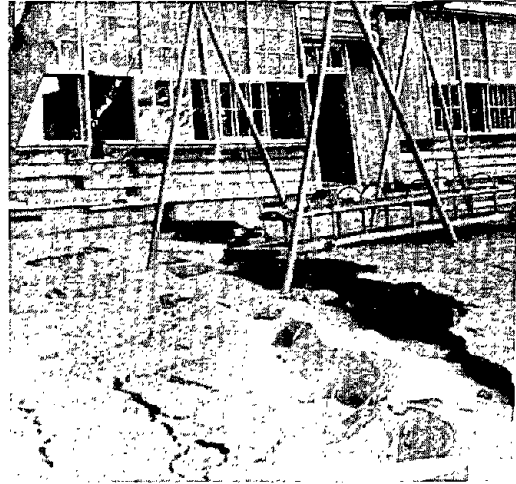


Photo 35 A Ground Fissure Underneath a Wooden School Building



Photo 36 Broken Wooden Floor due to Ground Fissure



Photo 37 Separation of Two Buildings



Photo 38 Deformed Road Resulting from the Earthquake

Figure 43 shows the ground displacements on a contour map of the area which was drawn from the aerial photographs taken before the earthquake. It is clear from the figure that the ground moved from higher land toward lower land. However, it has to be noted that the gradient of the surface is small, less than 3% at maximum.

In Shinkawa-cho, the old natural levee is located on the north bank of the Tsusen River. It is notable that the ground moved towards the lower old riverbed to the north, not towards the Tsusen River to the south. South of the Tsusen River, all the ground displacements were in northwest direction, toward the river. In this area, also, the high land subsided by a maximum of 1.7 m. It was also reported that the riverbed of the Tsusen River rose, and it could be crossed on foot after the earthquake.

4.6.2 Soil Conditions

Figure 44 shows soil profiles along sections N-N' and O-O', which are marked in Figure 42. Estimated liquefied soil layers are shown in the figure along with SPT-values and SWS-values, N_{sw} and W_{sw}. Soil profiles for this area in addition to those discussed below can be found in Appendix B.

Along section N-N', the Shitayama Primary School and Route 345 areas are at a higher elevation, but the gradient of the surface is small, at less than 3%. The estimated liquefied layer has a thickness of about 3 m around the primary school, increasing in both the north and south directions. In the area of Route 345, the thickness of the liquefied layer is about 6 m. The boundary between the estimated liquefied layer and the non-liquefied layer beneath it is inclined from the school to the north and to the south, coinciding with the direction of ground displacements.

In the area of Shitayama along section O-O', the liquefied layer reaches a maximum thickness of 6 m, while around the Tsusen River it is a minimum, at

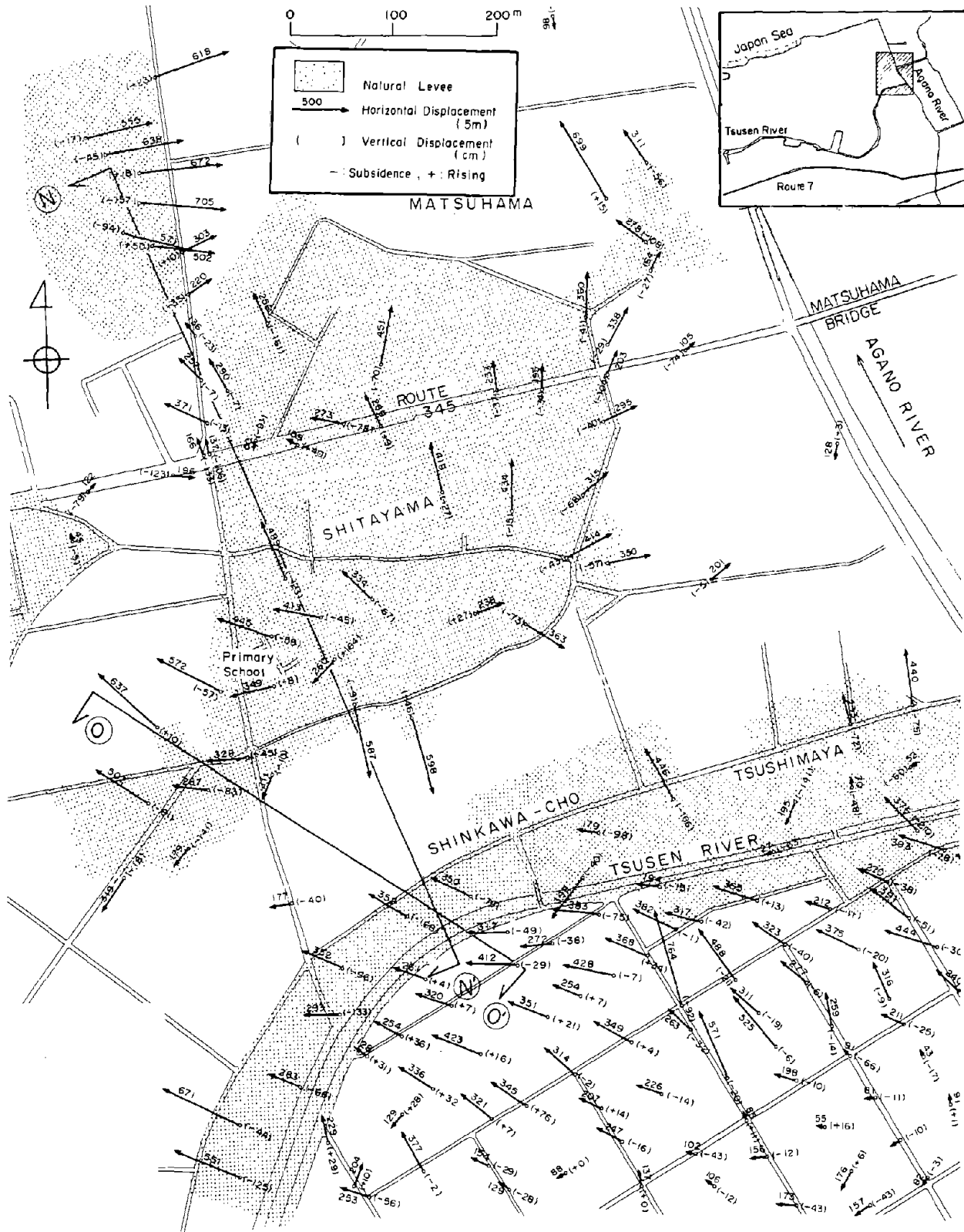


Figure 42. Permanent Ground Displacement in the Matsuhama, Shitayama, and Shinkawa Areas

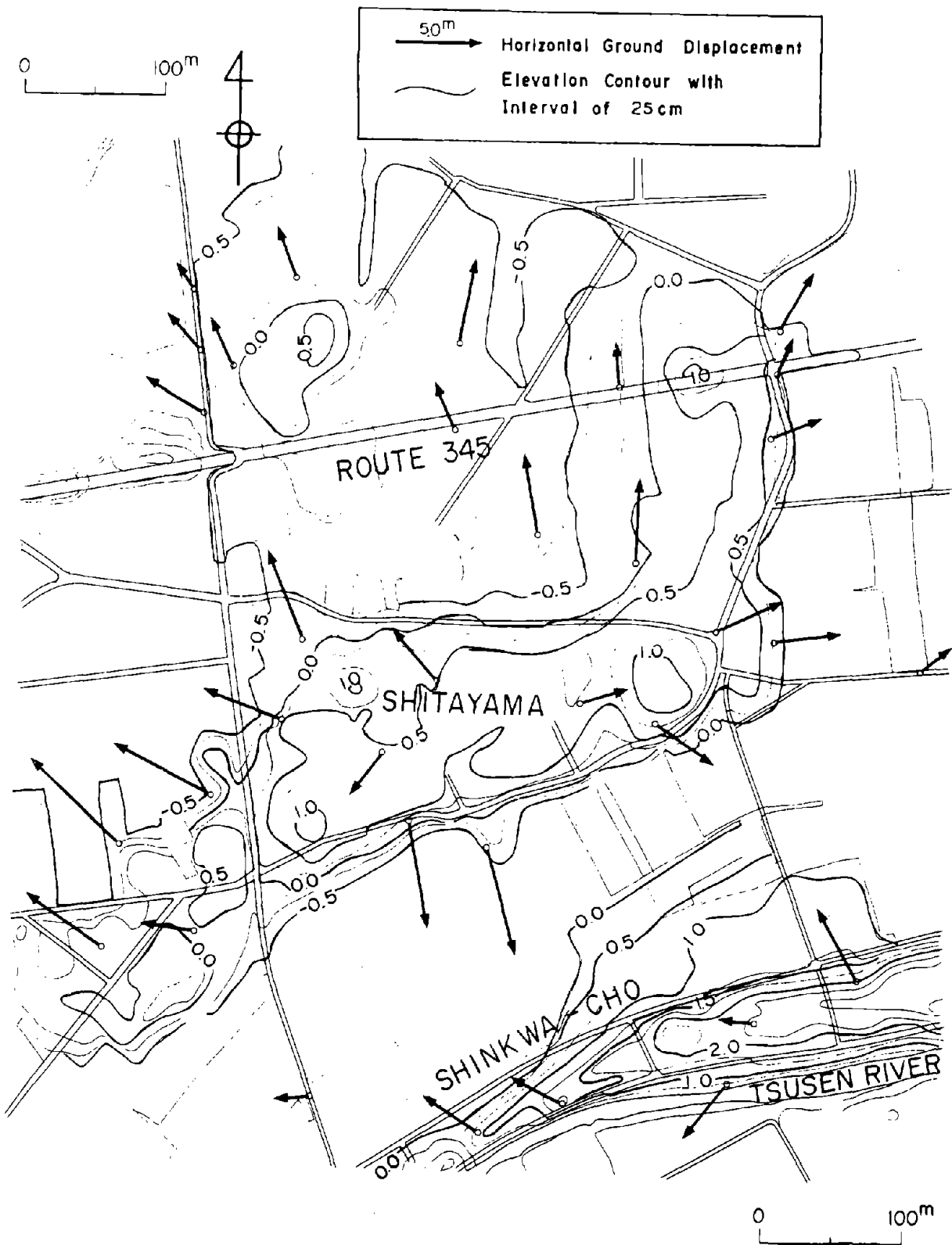
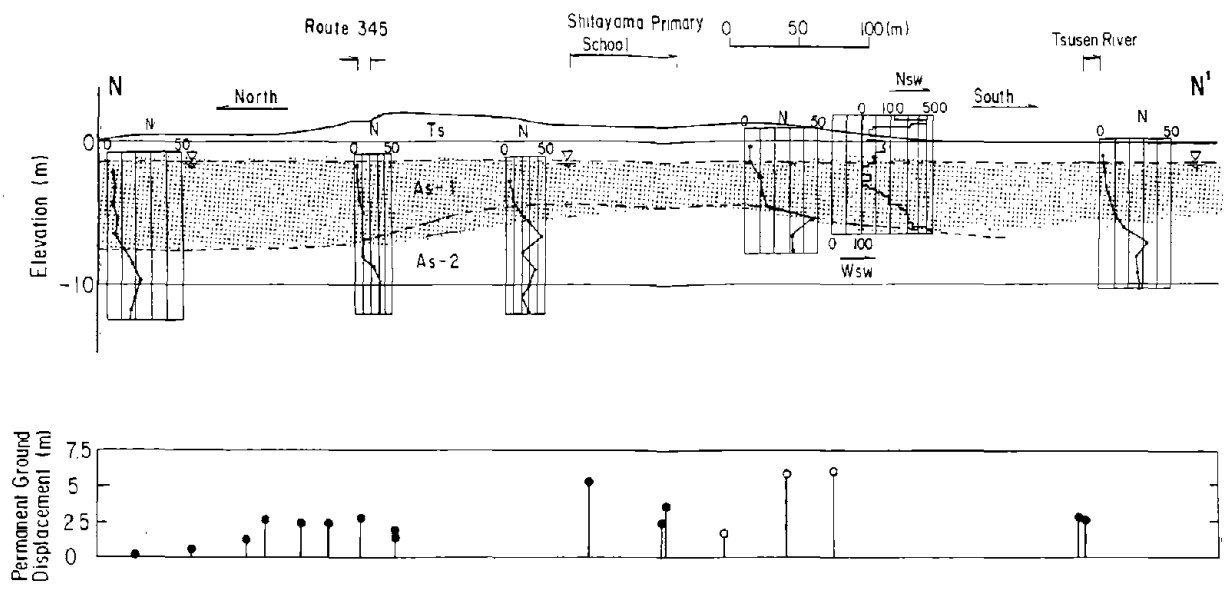
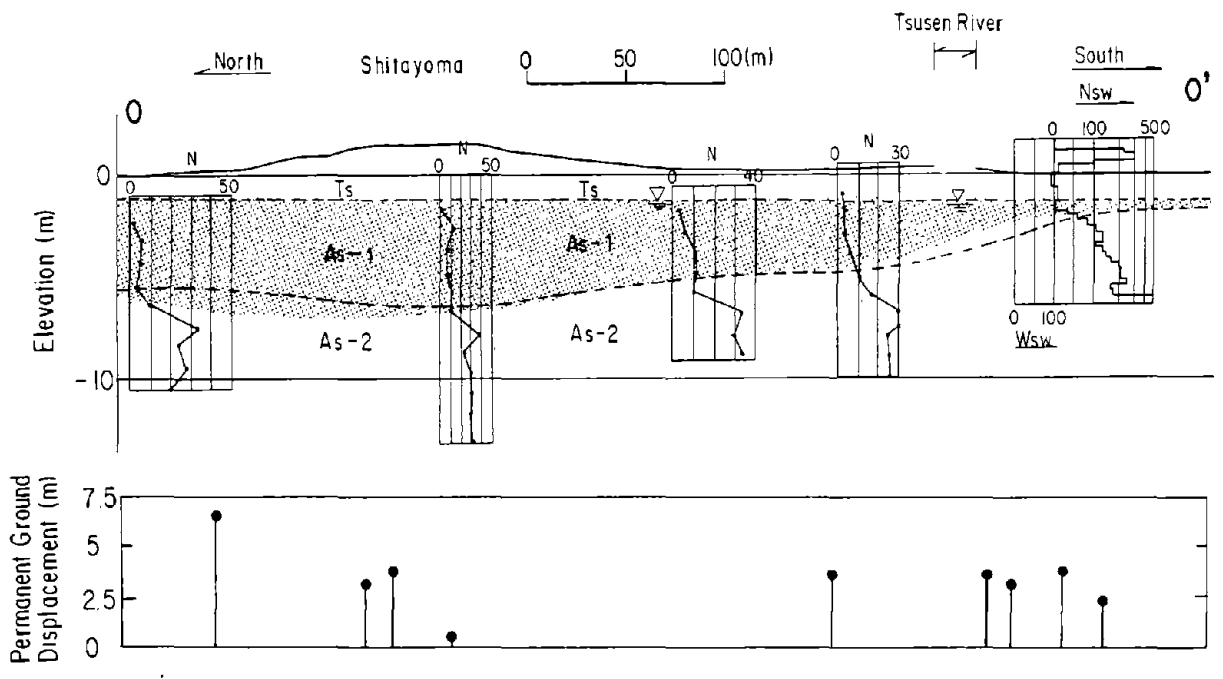


Figure 43. Permanent Ground Displacement on a Contour Map of the Matsuhama, Shitayama, and Shinkawa Areas (Numbers on the contours represent elevations above mean sea level, Unit:m)



(a) Section N-N'



LEGEND

Ts	Surface Soil (Fill)	N :	SPT values, blows/ft(0.3m)
As-1	Alluvial Sandy Soil	Nsw :	SWS values, number of half revolution/m
As-2		Wsw :	SWS values, load in kg
As-3			
 			
 	Estimated Liquefied Layer		Displacement toward Right Side on the Cross Section
			Displacement toward Left Side on the Cross Section

(b) Section O-O'

Figure 44. Soil Conditions and Estimated Liquefied Layer

1 m. From the Tsusen River toward the north, the boundary between the estimated liquefied layer and the lower non-liquefied layer is inclined towards the north, and this coincides with the direction of the ground movements, which developed in a northward direction from the Tsusen River. However, north of Shitayama, the boundary is slightly inclined toward the south in the opposite direction to the ground displacements.

As mentioned above, no clear and consistent relationship between the direction of the horizontal ground displacements and the inclination of the boundary between the liquefied layer and the non-liquefied layer can be determined.

4.6.3 Damage Related to Liquefaction Induced Ground Displacements

(1) Shitayama Primary School and vicinity

Shitayama Primary School is located on the top of the natural levee, from where most permanent ground displacements in the horizontal direction spread out in a radial direction. Figure 45 shows details of the ground displacements and ground fissures in this area. The wooden buildings of the school suffered severe damage due to the ground displacements. Photo 39 shows damage to the gymnasium at the primary school, which was caused by displacement of the foundations due to tensile strain in the ground. Photo 40 is another example of damage resulting from tensile strain in the ground, in which brick wall was pulled apart. In the playground of the primary school, numerous ground fissures resulted from the ground tensile strain as the ground moved in radial directions. Photo 41 shows one example of a ground fissure in the playground.

(2) Shinkawa-cho and vicinity

Along the Tsusen River in Shinkawa-cho and nearby, the ground moved toward the north a maximum of about 5 m, and ground fissures parallel to the river were dominant on the north bank of the river as shown in Figure 46. Photo 42 shows a shrine building, which fell into a ground fissure about 3 m wide, and Photo 43 is another example of a ground fissure with a vertical differential displacement of about 1.5 m.

(2) Shinkawa-cho and vicinity

Along the Tsusen River in Shinkawa-cho and nearby, the ground moved toward the north by a maximum of about 5 m, and ground fissures parallel to the river were dominant on the north bank of the river as shown in Figure 46. Photo 42 shows a shrine building, which collapsed into a ground fissure about 3 m wide, and Photo 43 is another example of a ground fissure with a vertical differential displacement of about 1.5 m.

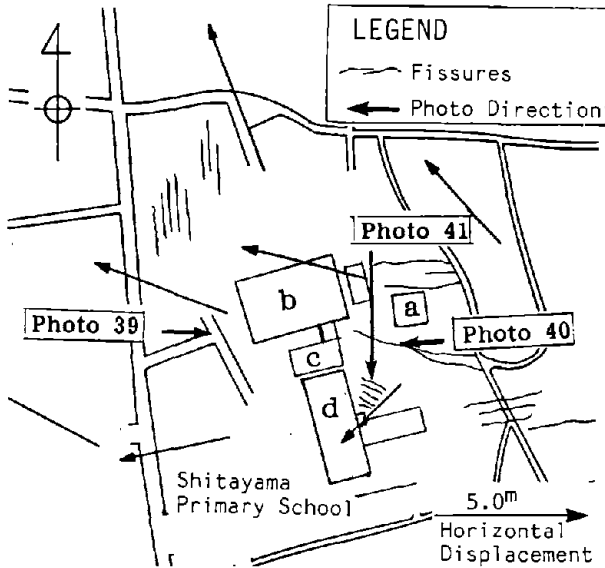


Figure 45. Permanent Ground Displacement and Ground Fissures at Shitayama Primary School



Photo 39 Damage to the School Gymnasium due to Displacement of the Foundations



Photo 40 Separation in a Brick Wall due to the Tensile Strain in the Ground



Photo 41 Ground Fissures in the School Playground

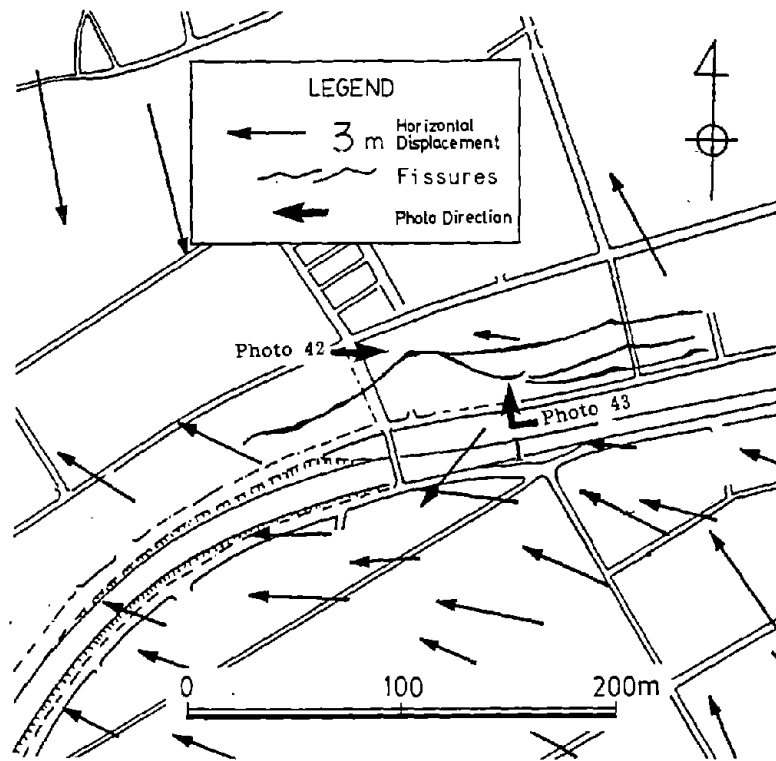


Figure 46. Permanent Ground Displacement and Ground Fissures in Shinkawa-cho and Nearby



Photo 42 A Shrine Building Which Fell into a Ground Fissure

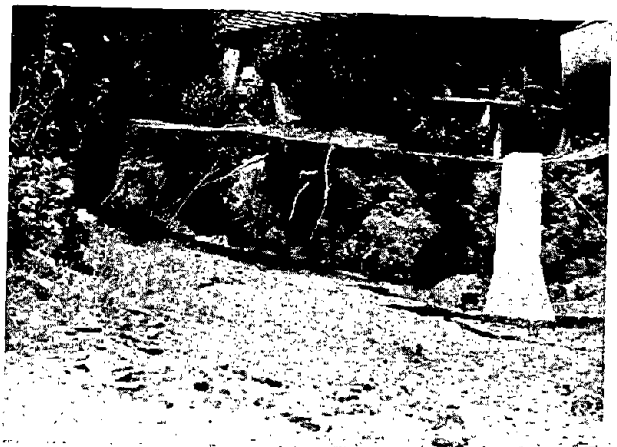


Photo 43 Ground Fissure with Vertical Displacement of about 1.5 m

5.0 EFFECTS OF THICKNESS OF LIQUEFIED LAYER AND GRADIENT OF GROUND SURFACE ON PERMANENT GROUND DISPLACEMENTS

Regression analyses were conducted by Hamada et al.¹⁾ to investigate if there is any relationship between the magnitude of permanent ground displacements and the thickness of the liquefied layer and the gradient of the ground surface. On the basis of this study, the following empirical formula was proposed:

$$D \approx 0.75 \sqrt[2]{H} \cdot \sqrt[3]{\theta} \dots\dots\dots (1)$$

D: Magnitude of permanent ground displacement in horizontal direction (m)

H: Thickness of liquefied layer (m)

θ : The greater gradient of ground surface or lower boundary of liquefied layer (%)

The proposed correlation given by Equation (1) only provides an approximate fit with the field data. The measured ground displacements are actually scattered between values half and twice the values given by the above formula. In particular, the correlation with the gradient of the lower boundary of the liquefied layer is comparatively poor. In the present report also, no definite correlation could be found between the direction of the permanent ground displacements and the gradient of the liquefied layer.*

The following can be considered probable factors for this poor correlation.

- (i) Soil data for points far from the ground displacement measurement points (sometimes more than 100 m) were used in the correlation analysis.

*See 4.5.2 and 4.6.2.

- (ii) In the past correlation analyses, the gradients of the ground surface and liquefied layer were taken as mean values over the entire length of slopes, some of which are greater than several hundreds meters. The horizontal distance over which the gradient is measured has a great influence on the result.
- (iii) It is difficult to estimate precisely the gradient of the lower boundary of the liquefied layer, usually below 2-3%, since the estimation of the liquefied layer itself is difficult.

In this report, therefore, the correlation was re-examined by using data carefully selected as follows:

- (i) Only borehole data with SPT-values and grain size distributions within 25 m of the ground displacement measuring points were used.
- (ii) Data for ground displacements, less than 1.0 m, were discarded in consideration of the accuracy of the measurements.
- (iii) The horizontal distance over which the surface gradient was estimated was chosen to be 5 times to 30 times the thickness of the estimated liquefied layer.

Figures 47 and 48 show the effects of the thickness of the liquefied layer and the gradient of the ground surface on the magnitude of the ground displacements, respectively. A comparatively good correlation between the magnitude of the ground displacements and the thickness of the liquefied layer can be seen in Figure 47. However, no significant correlation could be found with the gradient of the surface, as shown in Figure 48. Although the horizontal distances over which the gradients were estimated were varied from 5 times to 30 times the thickness of the liquefied layer in Figure 48 (a) and (b), respectively, the correlation improved only by a marginal amount.

The lack of correlation between the magnitude of the ground displacement and the gradient of the ground surface appears to contradict the fact that the ground moved from higher to lower elevations, as mentioned in 4.5.1 and 4.6.1. However, this contradiction can be resolved if it is assumed that ground displacements were caused by fluid behavior of the liquefied soil. The gradient of the liquid surface has little influence on the magnitude of

the movement of the liquid, but does affect its velocity. If the liquefied soil tends to behave as a fluid, the ground at higher elevations will sink and spread laterally as the fluid tries to achieve a uniform elevation. The ground surface will rise up where lateral movements terminate.

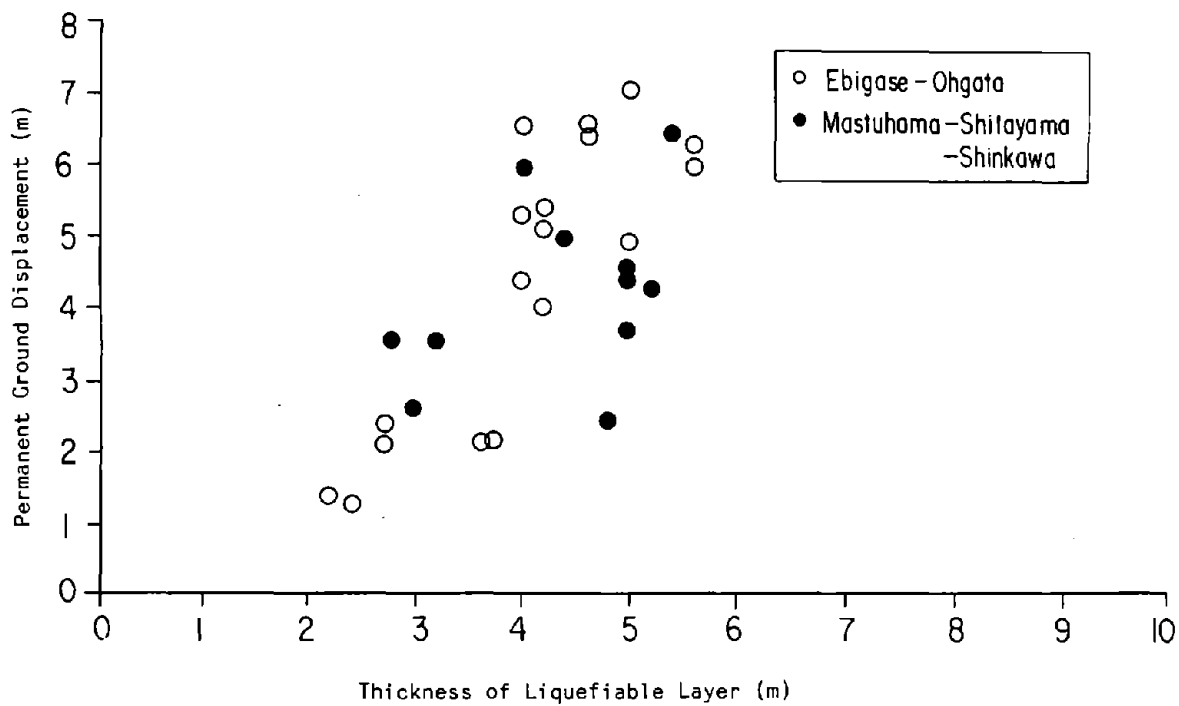
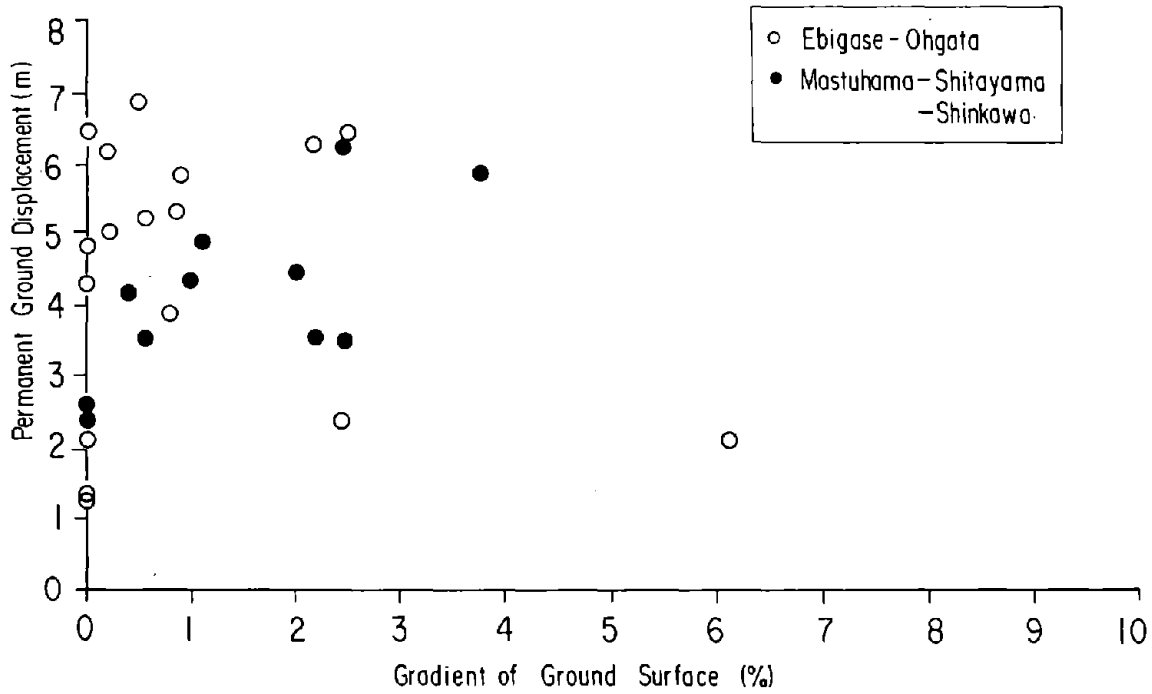
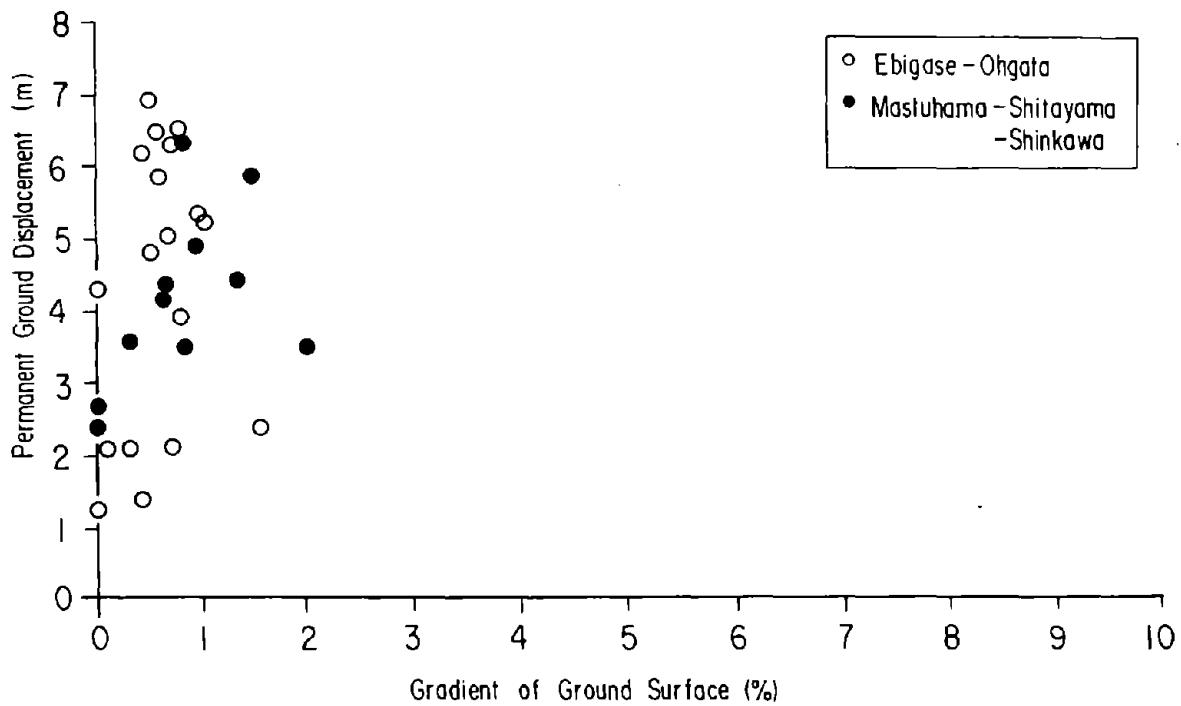


Figure 47 Correlation between Magnitude of Ground Displacement and Thickness of Estimated Liquefied Layer



(a) Case 1: Horizontal distance is 5 times thickness of estimated liquefied layer



(b) Case 2: Horizontal distance is 30 times thickness of estimated liquefied layer

Figure 48. Correlation between Magnitude of Ground Displacement and Gradient of Ground Surface

6.0 CONCLUSION

Several important characteristics of liquefaction-induced ground displacement and its related damage to structures can be summarized from the case studies of the 1964 Niigata earthquake:

(1) Along the banks of the Shinano River, ground displacements as large as 12 m occurred mostly toward the river. The collapse of river quay walls was partially responsible for the large ground displacements. However, in areas away from the river (for instance, the northern area of Echigo Railway Line in Kawagishi-cho and the northern area of Niigata Railway station), the ground did not necessarily move toward the river. The direction of ground displacements is complex, and is affected by the geological and geographical conditions of the areas.

(2) In the areas of Ebigase-Ohgata and Matsuhama-Shitayama-Shinkawa the ground displaced from higher to lower elevation. From the viewpoint of the geological conditions, ground displacements were caused from old sand dunes and/or old natural levees toward the old streams of big rivers.

(3) In areas where horizontal ground displacements occurred, the ground surface subsided and many ground fissures were caused due to the tensile strain of the ground. In contrast, in areas where the horizontal ground displacements terminated, the ground surface sometimes rose and numerous sand and water boils were observed. A large part of the Tsusen River was filled by materials ejected from the riverbed, and an eyewitness near the Showa Bridge stated that the sand and water boils were seen above the level of water in the river. The fact mentioned above suggests that the ground displacements were caused by the volumetric transfer of liquefied soil.

(4) The relationship between the magnitude of permanent ground displacements and the thickness of the liquefied layer and the gradient of ground surface was studied by using the data from Ebigase-Ohgata and Matsuhama-Shitayama-Shinkawa areas in Niigata City. A comparatively good correlation between the magnitude of the ground displacements and the thickness of the

liquefied layer was found. However, no clear and consistent correlation between the magnitude of the ground displacements and the gradient of ground surface could be found. This lack of correlation appears to contradict the fact that the ground moved from higher to lower elevations, as mentioned in above (2). This contradiction can be resolved if it is assumed that the ground displacements were caused by fluid behavior of the liquefied soil. The gradient of the liquid surface has little influence on the magnitude of the movement of the liquid, but does affect its velocity. If the liquefied soil tends to behave as a fluid, the ground at higher elevations will subside and spread laterally as the fluid tries to achieve a uniform elevation. The ground surface will rise up where lateral movements terminate.

(5) No statistically significant correlation could be found between the direction of the ground displacements and the inclination of the liquefied layer, particularly the inclination of the lower boundary of the liquefied layer.

(6) Liquefaction-induced ground displacements are more probable cause for the collapse of Showa Bridge than relative displacements by dynamic response of the piers. This conclusion was reached by taking into consideration the permanent ground displacements measured on the left bank, the damage to the foundation piles, the estimated liquefied layer, and the statements of eyewitnesses. In the case of the collapse of Showa Bridge, everyone on the bridge had enough time to evacuate the bridge, so no lives were lost. This fact suggests that the liquefaction-induced ground displacements were caused gradually and continued a long time after the earthquake motion ceased until the excess pore water pressures were dissipated.

(7) At the Niigata Family Court House and NHK buildings, reinforced concrete piles were severely broken at two positions. These positions roughly coincide with the boundaries between the estimated liquefied layer and on-liquefied layer. It can be concluded that the piles were broken at the boundaries due to stress concentration resulting from liquefaction-induced ground displacements.

(8) At the East Bridge over the railway near Niigata Station the concrete piles were cracked only on one side of the pile. This means that the cracks were not caused by the repetitious inertial force, but by monotonically increasing load due to liquefaction-induced displacements.

(9) Numerous buried pipes were severely damaged because of liquefaction and associated ground deformations in Niigata City. In particular, many buried pipes were forced out of the ground due to buckling by compressive straining of the ground.

(10) No structural damage was reported at the Hokuriku-Building, while the neighboring NHK-Building suffered severe damage to its foundation piles. The lack of damage to the Hokuriku Building is most likely related to the following characteristics:

- (i) The building has a one-story basement which is 6-7 m deep from the ground surface.
- (ii) The total number of the foundation piles of the Hokuriku-Building with ten stories was much more than that of NHK-Building with four stories. It is conjectured that a large number of piles had a great effect on densification of the soil as well as prevention of ground displacements in the horizontal direction.
- (iii) Some part of temporary in-ground walls for the excavation of the basement had not been removed after construction and existed at the time of the earthquake.

REFERENCES

- 1) Hamada, M., Yasuda, S., Isoyama, R., and Emoto, K., "Study on Liquefaction-Induced Ground Displacements," A Report by Research Committee, Association for the Development of Earthquake Prediction, Tokyo, Japan, Nov., 1986, pp. 20-35.
- 2) Japan Society of Civil Engineers, "Report on the 1964 Niigata Earthquake," Research Committee on the 1964 Niigata Earthquake, Tokyo, Japan, 1966, pp. 8-9 (in Japanese).
- 3) Seed, H.B., Tokimatsu, K., Harder, L.F., and Chung, R.M., "Influence of SPT Procedure in Soil Liquefaction Resistance Evaluation," Journal of Geotechnical Engineering, Vol. 111, No. 12, ASCE, New York, N.Y., 1985, pp. 1425-1445.
- 4) Iwasaki, T., Tatsuoka, F., Tokida, K., and Yasuda, S., "A Practical Method for Assessing Soil Liquefaction Potential Based on Case Studies at Various Sites in Japan," Proceedings, Fifth Japan Earthquake Symposium, Tokyo, Japan, 1978, pp. 641-648 (in Japanese).
- 5) Tatsuoka, F. and Adachi, T., "New Series on Civil Engineering," Gihodo, No. 18, Tokyo, Japan, 1981 pp. 258-262 (in Japanese).
- 6) Japan Society of Civil Engineers, "Report on the 1964 Niigata Earthquake," Research Committee on the 1964 Niigata Earthquake, Tokyo, Japan, 1966, pp. 395-405 (in Japanese).
- 7) Yoshida, I., "Damage to R.C. Concrete Pile during the 1964 Niigata Earthquake," Proceedings, Eighth Earthquake Engineering Conference, Japan Society of Civil Engineers, Tokyo, Japan, 1965, pp. 25-28 (in Japanese).
- 8) Japan Society of Civil Engineers, "Report on the 1964 Niigata Earthquake," Research Committee on the 1964 Niigata Earthquake, Tokyo, Japan, 1966, pp. 376-393 (in Japanese).

- 9) Public Work Research Institute, Ministry of Construction, "Report on the 1964 Niigata Earthquake," Report No. 125, Session V, Public Work Research Institute, Tokyo, Japan, 1965, pp. 54-62 (in Japanese).
- 10) Horii, K. and Miyahara, M., "Bridges Spanning Over the Lower Course of the River Shinano," Bulletin of Science and Engineering Research Laboratory, No. 34, Special Issue on the Niigata Earthquake, Waseda University, Tokyo, Japan, 1966, pp. 151-170 (in Japanese).
- 11) Yoshida, N., and Hamada, M., "Damage to Foundation Piles and Deformation Pattern of Ground due to Liquefaction-Induced Permanent Ground Deformations," Proceedings, Third Japan-U.S. Workshop on Earthquake Resistant Design of Lifeline Facilities and Countermeasures for Soil Liquefaction, Technical Report NCEER-91-000-1, National Center for Earthquake Engineering Research, Buffalo, N.Y., U.S.A., 1991, pp. 147-162.
- 12) Port and Harbor Research Institute, Ministry of Transportation, "Report on Damage to Port and Harbor Facilities during the 1964 Niigata Earthquake," Yokosuka, Japan, 1965, pp. 24-83 (in Japanese).
- 13) Kawamura, S., Nishizawa, T., and Wada, T., "Damage to Piles due to Liquefaction Found by Excavation Twenty Years after Earthquake," Nikkei Architecture, Tokyo, Japan, 1985, pp. 130-134 (in Japanese).
- 14) Association for the Development of Earthquake Prediction, "Numerical Analysis on Foundation Piles of N-Building," A Report by Japanese Research Team for U.S.-Japan Cooperative Research on Liquefaction, Large Ground Deformation and Their Effects on Lifeline, Tokyo, Japan, 1988, pp. 646-683 (in Japanese).
- 15) Yoshimi, Y., "Liquefaction of Sandy Ground, Second Version," Gihodo, Tokyo, Japan, 1990, pp. 118-119 (in Japanese).

- 16) Japan Society of Civil Engineers, "Report on the 1964 Niigata Earthquake," Research Committee on the 1964 Niigata Earthquake, Tokyo, Japan, 1966, pp. 409-420 (in Japanese).
- 17) Japan Gas Association, "Effects of the 1964 Niigata Earthquake on Urban Gas Facilities," Tokyo, Japan, 1965, p. 195 (in Japanese).
- 18) Ministry of Construction, Hokuriku Regional Construction Office, "Damage to National Roads by the 1964 Niigata Earthquake," Niigata, Japan, 1964, pp. 41-42 (in Japanese).
- 19) Hamada, M., "Large Ground Deformation and Their Effects on Lifelines, The 1983 Nihonkai-Chubu Earthquake," This volume.
- 20) O'Rourke, T.D., Roth, B.L., and Hamada, M., "Large Ground Deformation and Their Effects on Lifeline Facilities: 1971 San Fernando Earthquake," Technical Report NCEER-91-0002, National Center for Earthquake Engineering Research, Buffalo, N.Y., 1992.

Appendix A Accuracy of Permanent Ground Displacement Measurements in Niigata City

The accuracy of the permanent ground displacement measurements was estimated by the same method as it was for the case study on the Nihonkai-Chubu earthquake (see Reference 19, Appendix A). A detailed explanation of the photogrammetric analysis is also given by O'Rourke et al.²⁰⁾ in conjunction with the 1971 San Fernando earthquake in a companion volume. Tables A-1 and A-2 summarize the total number of pre- and post-earthquake data points, aerial survey accuracies, and accuracies of permanent ground displacement measurements. The accuracy along the Shinano River, in the Niigata Port area and Niigata railway station was estimated to be ± 72 cm in the horizontal direction and ± 66 cm in the vertical direction, while in the Ebigase-Ohgata and Matsuhama-Shitayama-Shinkawa areas, it was ± 99 cm in the horizontal direction and ± 46 cm in the vertical direction.

Table A-1 Accuracy in Shinano River, Port Area, and Niigata Station Areas

Aerial Survey	Pre-earthquake	Post-earthquake
Total Number of Data Points	11	11
Accuracy of Aerial Survey (Standard deviation of differences of coordinates by 1/25,000 map and aerial surveys)	± 0.49 (Hori.) (m) ± 0.50 (Vert.)	± 0.51 (Hori.) (m) ± 0.43 (Vert.)
Accuracy of Measurement of Permanent Ground Displacement	$\pm \sqrt{(0.49)^2 + (0.51)^2} = \pm 0.72$ (Hori.) (m) $\pm \sqrt{(0.50)^2 + (0.43)^2} = \pm 0.66$ (Vert.) (m)	

Table A-2 Accuracy in Ebigase-Ohgata and Matsuhama-Shitayama-Shinkawa Areas

Aerial Survey	Pre-earthquake	Post-earthquake
Total Number of Data Points	11	11
Accuracy of Aerial Survey (Standard deviation of differences of coordinates by 1/25,000 map and aerial surveys)	± 0.66 (Hori.) (m) ± 0.30 (Vert.)	± 0.74 (Hori.) (m) ± 0.33 (Vert.)
Accuracy of Measurement of Permanent Ground Displacement	$\pm \sqrt{(0.66)^2 + (0.74)^2} = \pm 0.99$ (Hori.) (m) $\pm \sqrt{(0.30)^2 + (0.33)^2} = \pm 0.46$ (Vert.) (m)	

Appendix B Soil Conditions and Evaluation of Liquefied Layer

Twenty SPT-borings and about 100 Swedish weight sounding tests (SWS) were performed in Niigata City. Additional data were collected on eighty existing borehole records. Based on these data, soil conditions were examined and the soil which liquefied during the earthquake was estimated by calculating the Factor of Liquefaction Resistance F_L .⁴⁾*. Basically, soil with an F_L value less than 1.0 was estimated to have liquefied. However, in areas where soil data were not adequate, engineering judgment was sometimes introduced in order to classify the soil and to evaluate soil strength. The Index of Liquefaction Potential, P_L .⁴⁾*, which represent the intensity of liquefaction was also calculated at the points of SPT-borings and Swedish weight sounding tests.

Soil conditions at 15 sections from a total of 28 were already shown in the main text. This appendix summarizes the soil conditions, as interpreted from SPT borings and Swedish weight sounding tests, for the remaining 13 sections. The locations and the directions of the remaining 13 sections are shown in Figure B-1. The soil conditions and the estimated liquefied layer are summarized for these sections in Figure B-2.

Nomenclatures in Figure B-2 are as follows:

T_S :	Surface Soil
A_S-1 } A_S-2 } A_S-3 }	: Alluvial Sandy Soil
A_C-1 } A_C-2 }	: Alluvial Clayey Soil
N :	SPT value, blows/ft (0.3 m)
N_{SW} :	Swedish weight sounding value, number of half revolution/m
W_{SW} :	Swedish weight sounding values, load in kg
F_L :	Factor of Liquefaction Resistance (See Appendix D)
P_L :	Index of Liquefaction Potential (See Appendix D)

*See Appendix D.

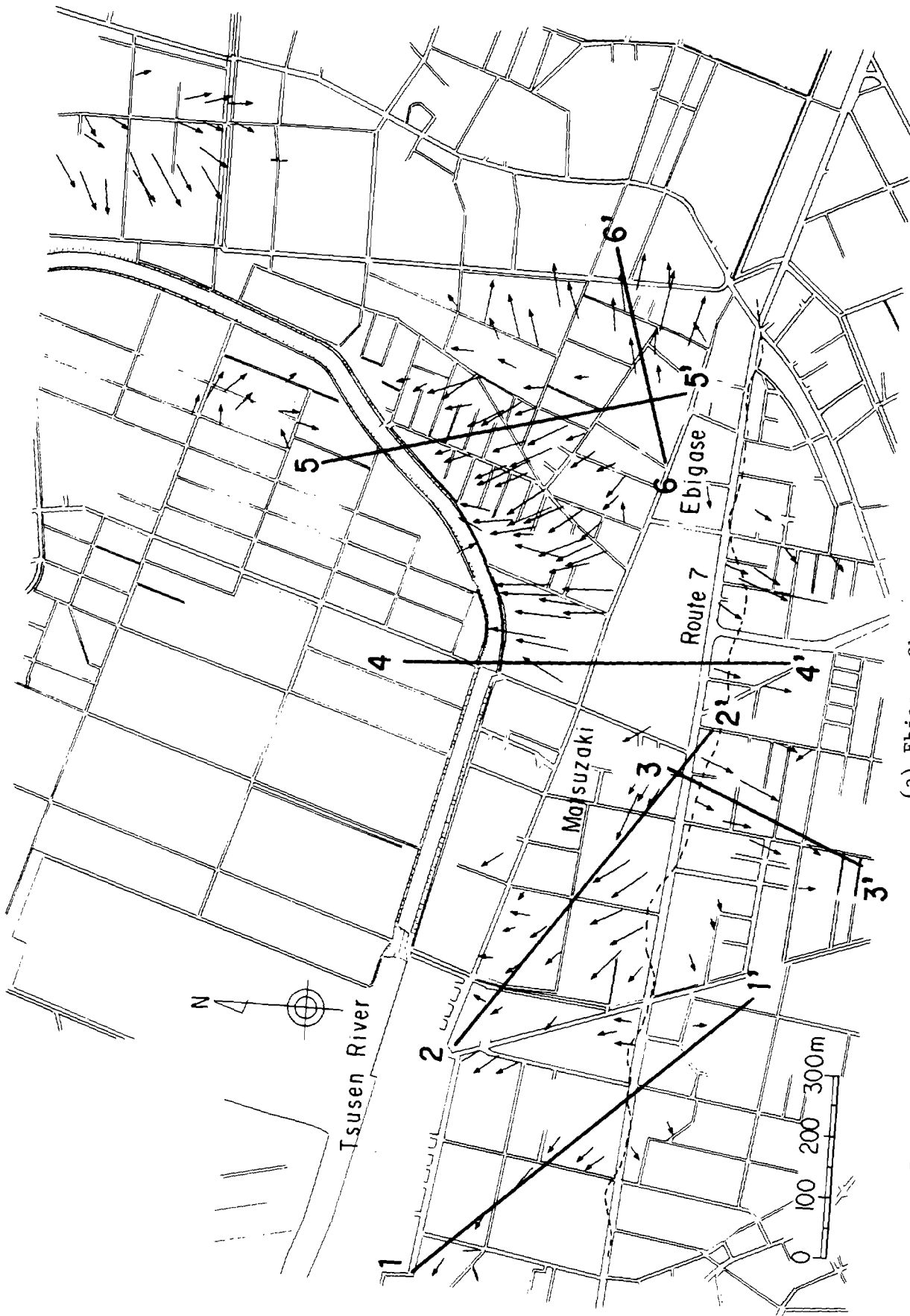
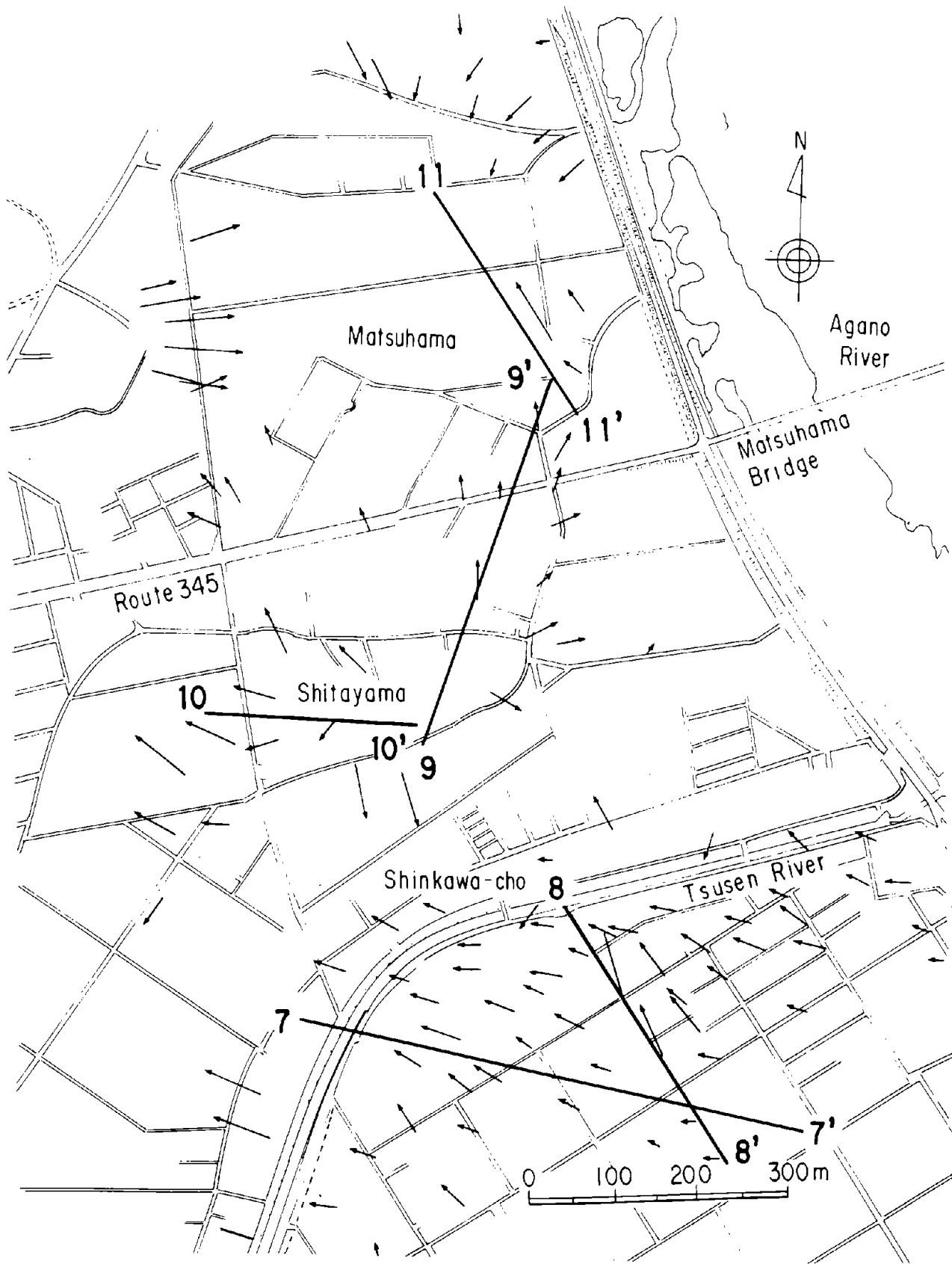


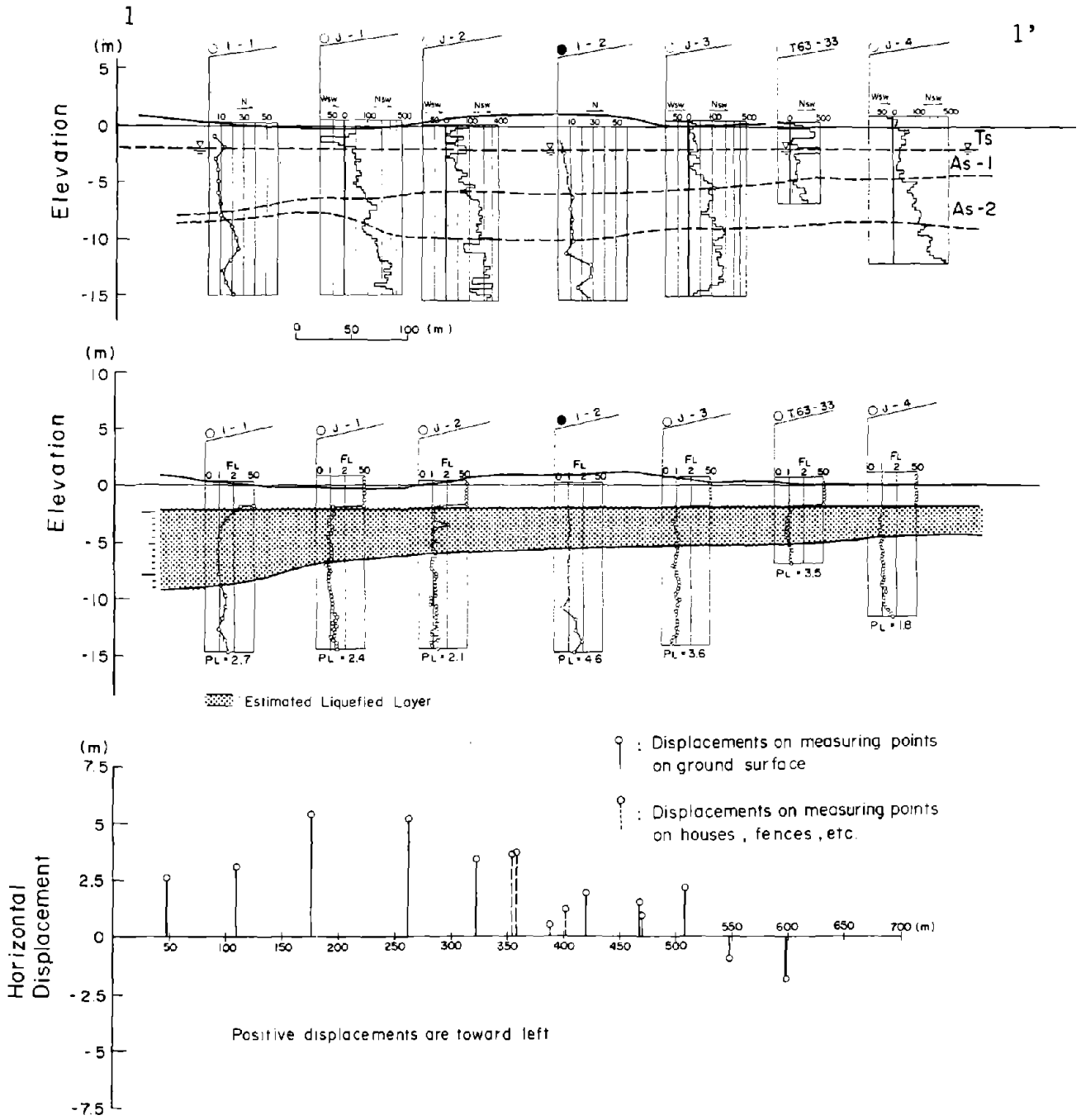
Figure B-1 Sections for Survey of Soil Condition and Estimation of Liquefied Layer
 (a) Ebigase-Ohgata



(b) Matsuhama-Shitayama-Shinkawa
 Figure B-1 Sections for Survey of Soil Condition and Estimation of Liquefied Layer



(c) Niigata Station and Its Vicinity
 Figure B-1 Sections for Survey of Soil Condition and Estimation of Liquefied Layer



Section 1-1'

Figure B-2 Soil Profile and Estimated Liquefied Layer

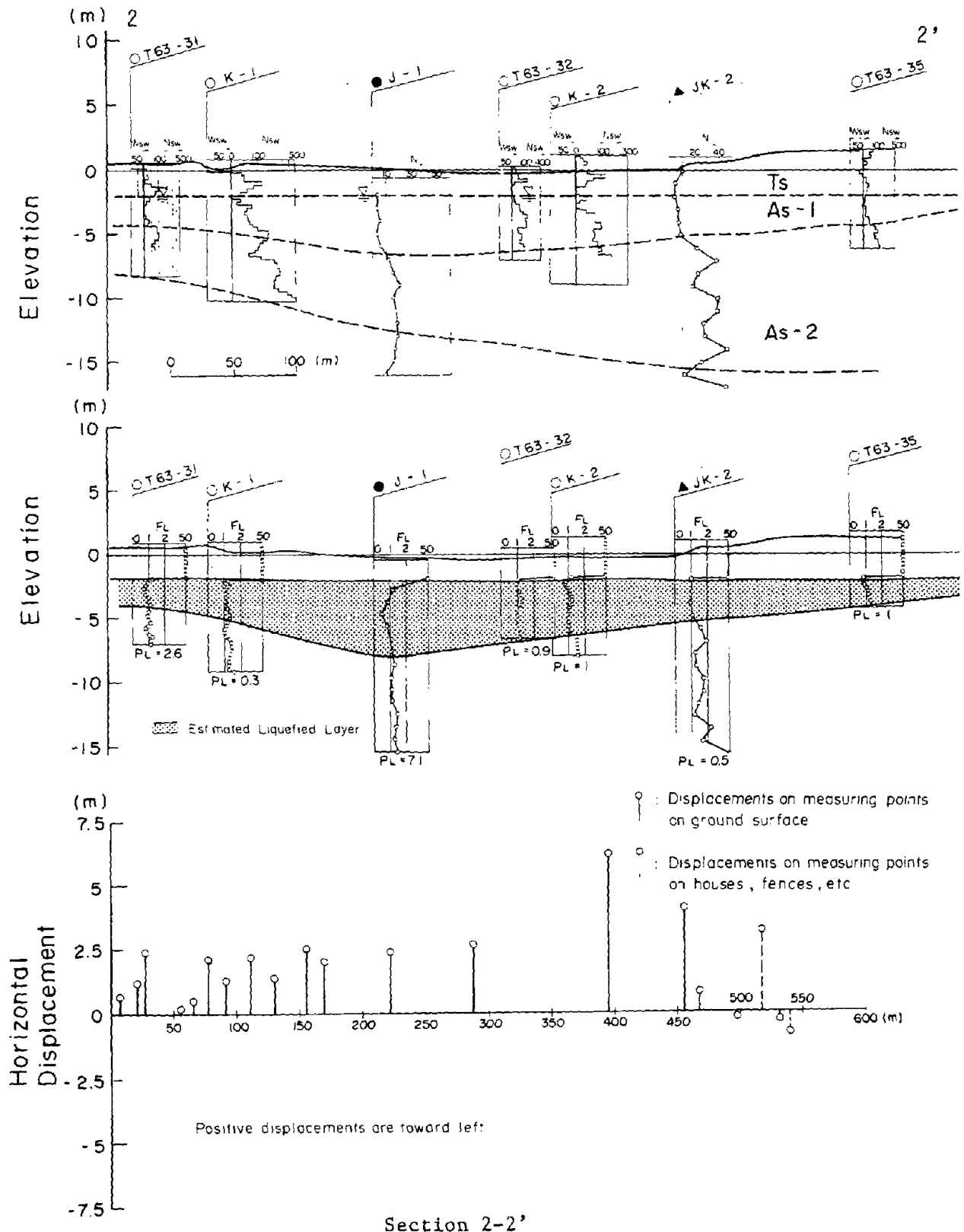
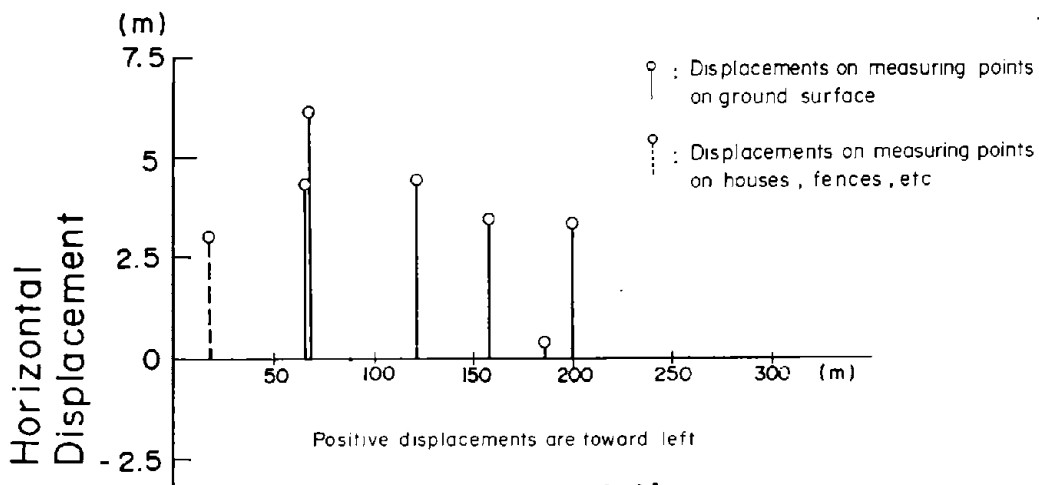
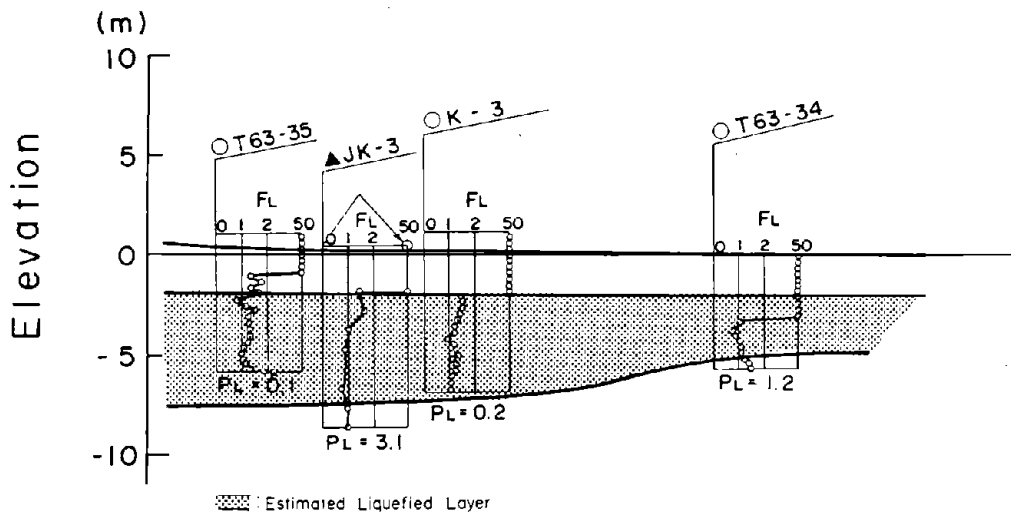
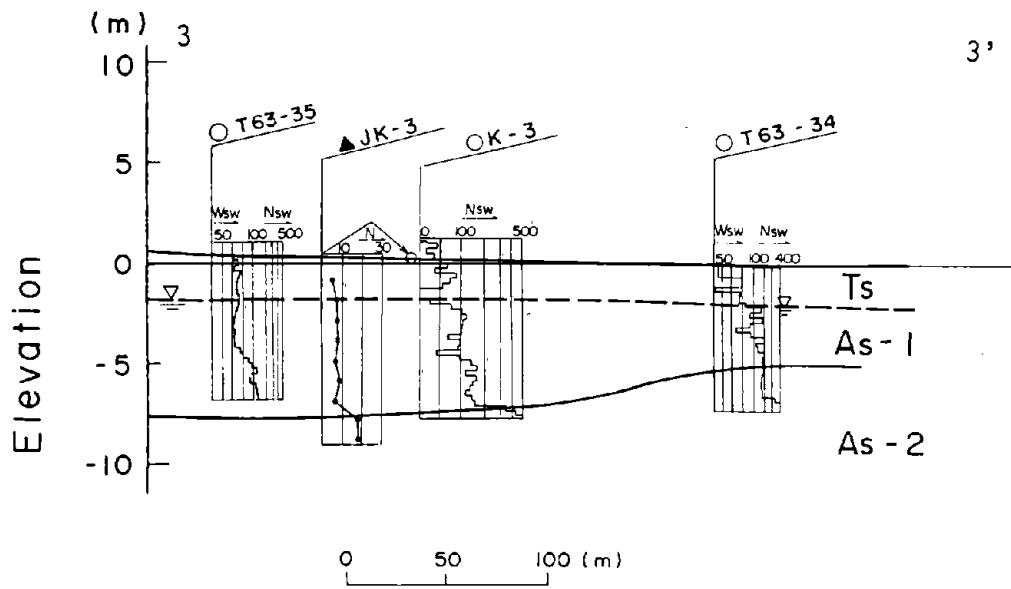
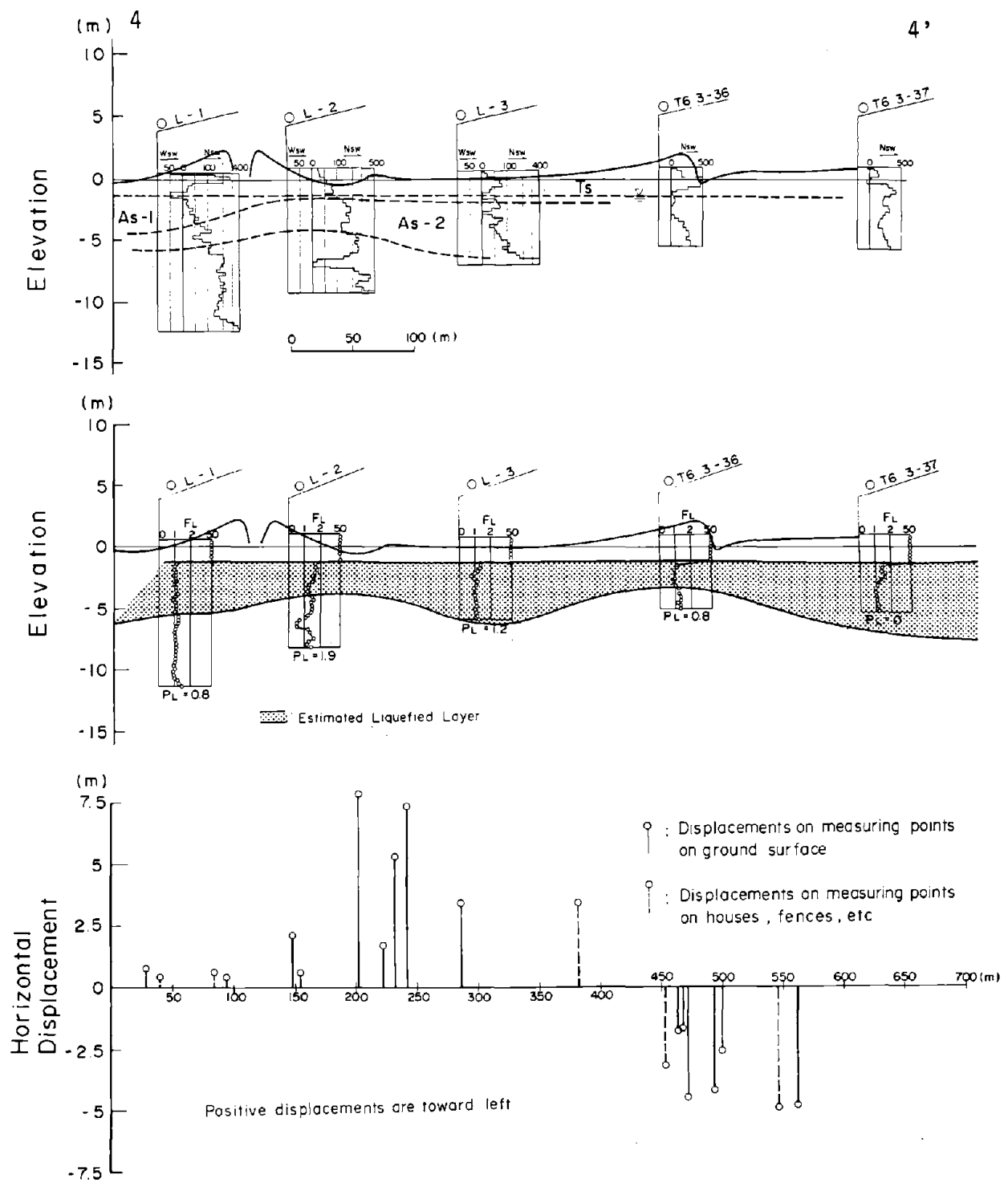


Figure B-2 Soil Profile and Estimated Liquefied Layer



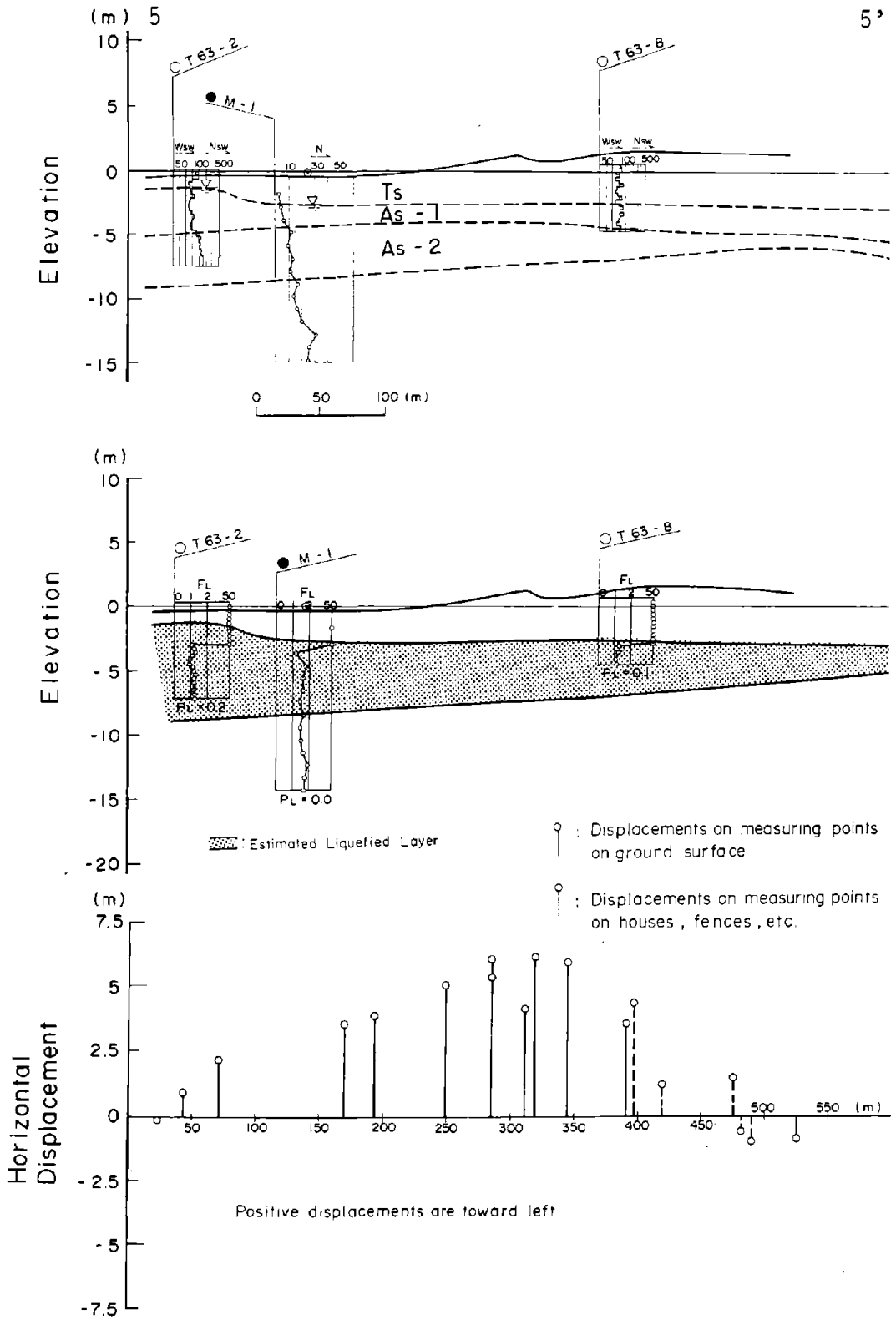
Section 3-3'

Figure B-2 Soil Profile and Estimated Liquefied Layer



Section 4-4'

Figure B-2 Soil Profile and Estimated Liquefied Layer



Section 5-5'

Figure B-2 Soil Profile and Estimated Liquefied Layer

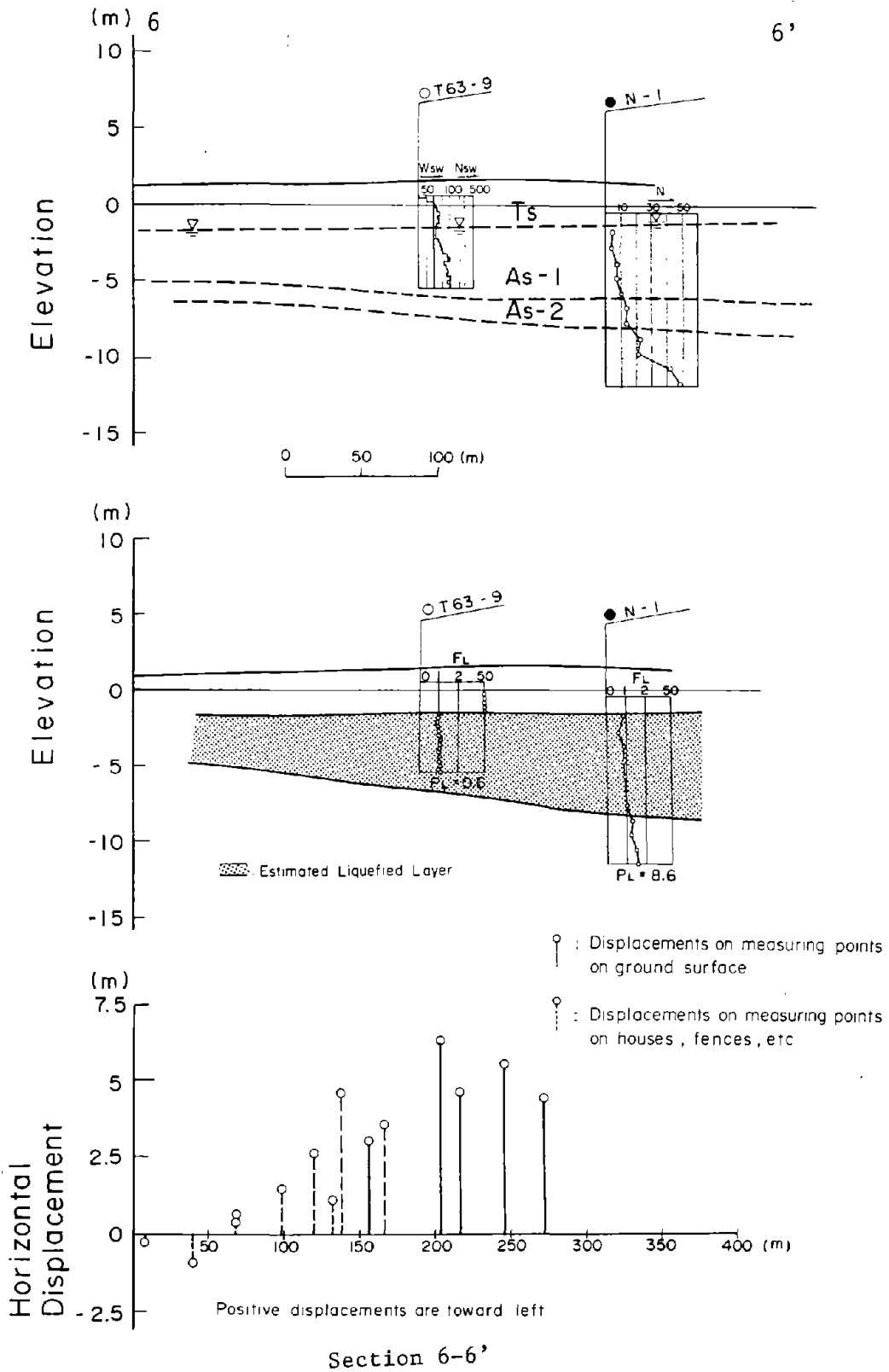
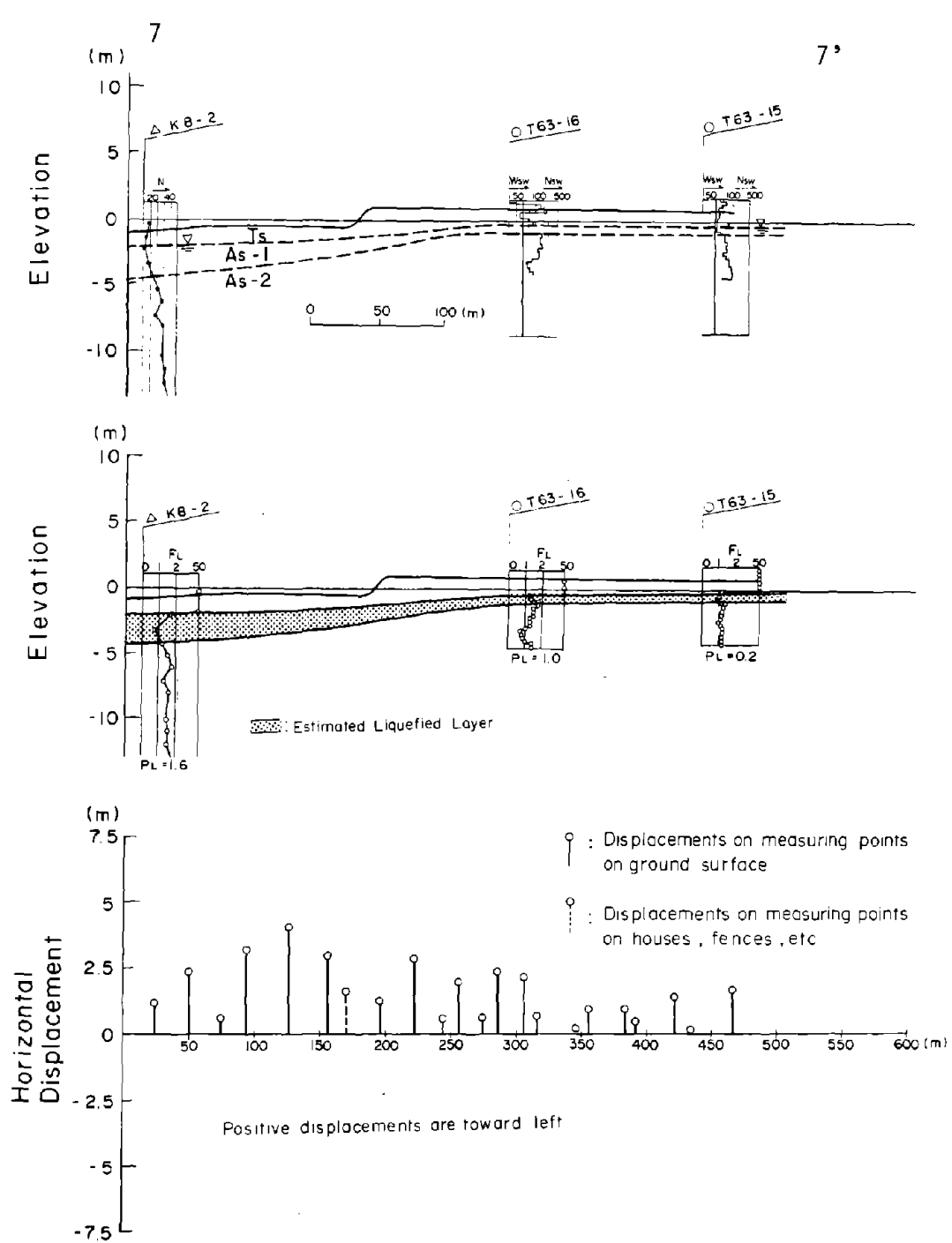


Figure B-2 Soil Profile and Estimated Liquefied Layer



Section 7-7'

Figure B-2 Soil Profile and Estimated Liquefied Layer

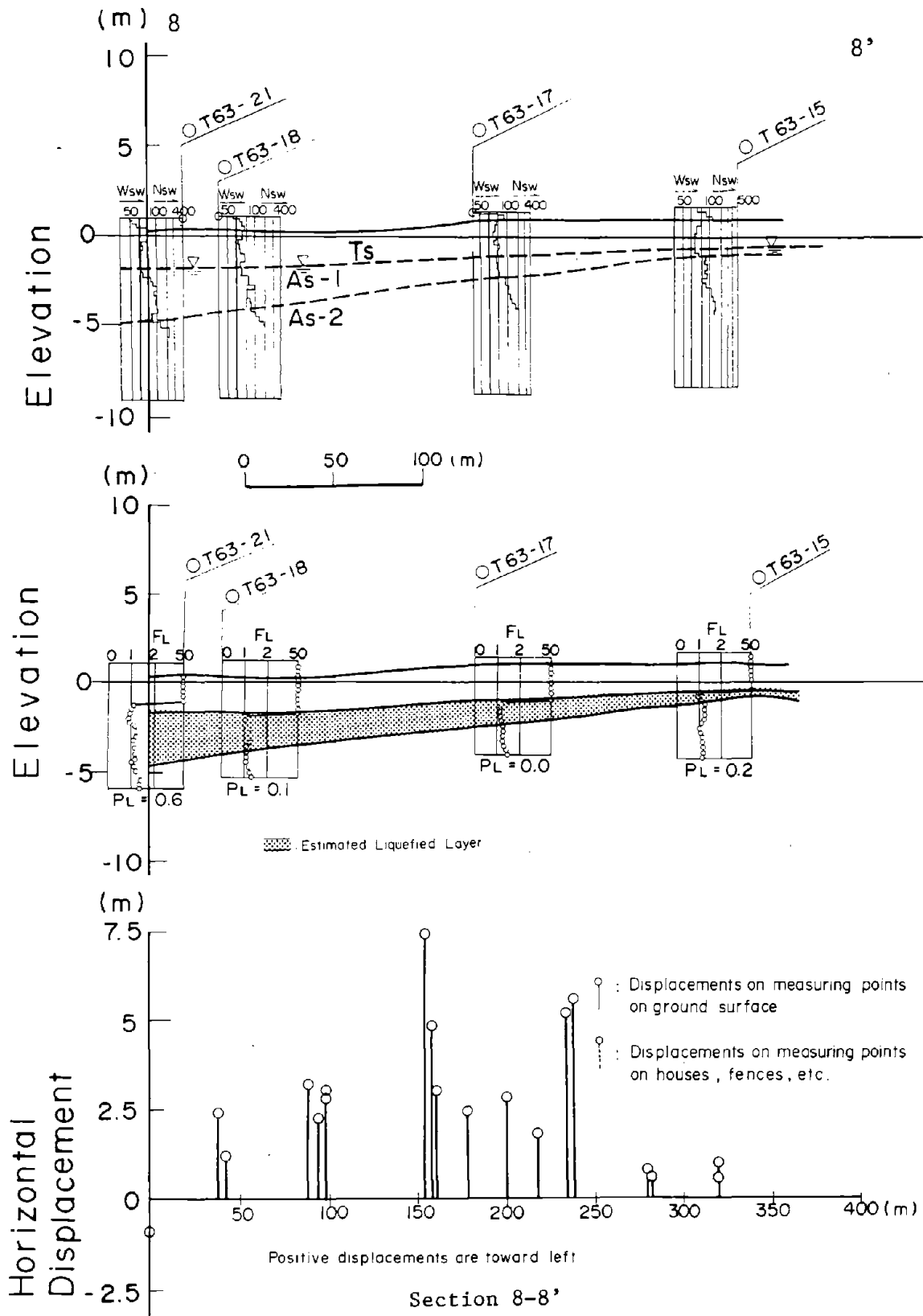


Figure B-2 Soil Profile and Estimated Liquefied Layer

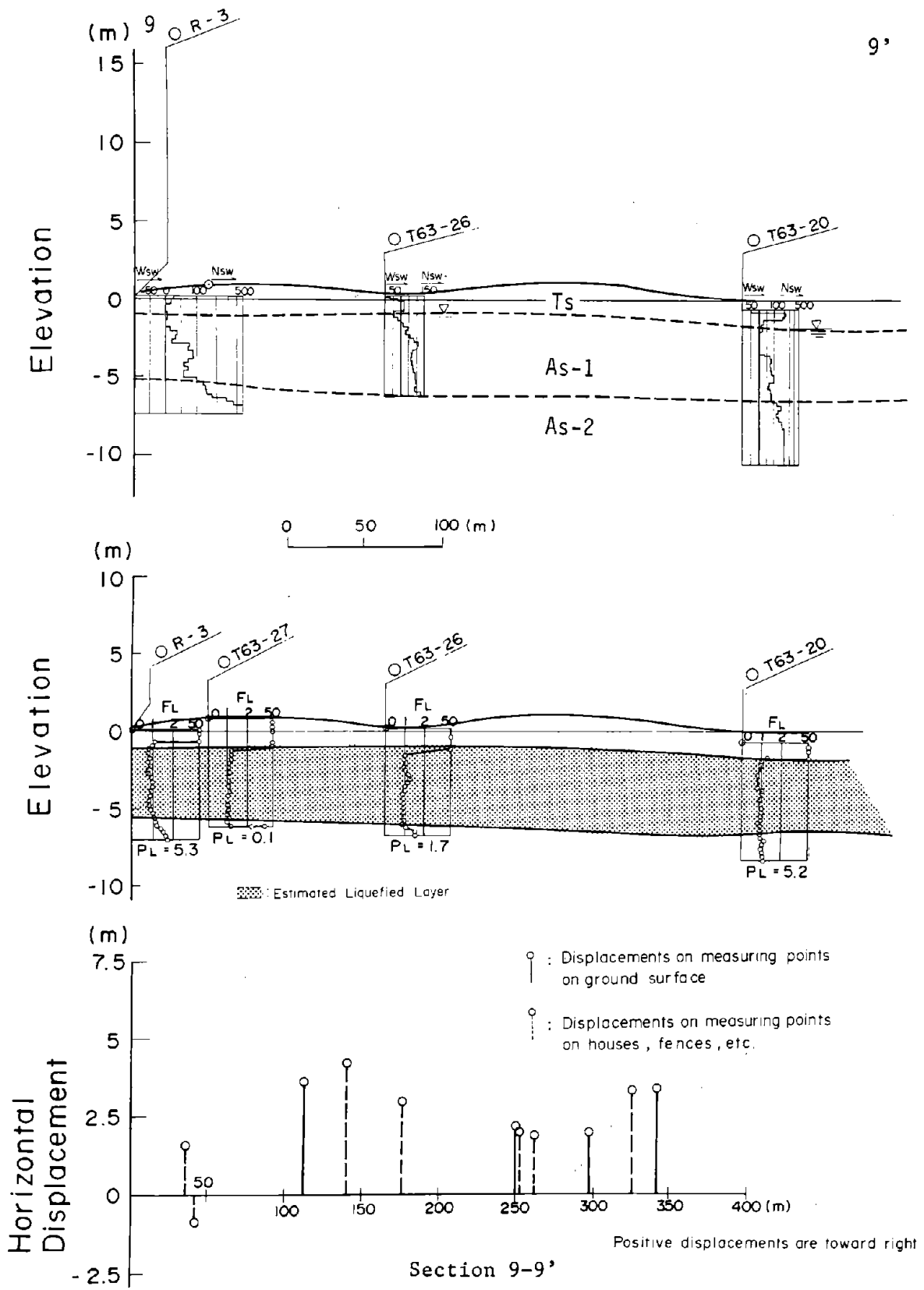


Figure B-2 Soil Profile and Estimated Liquefied Layer

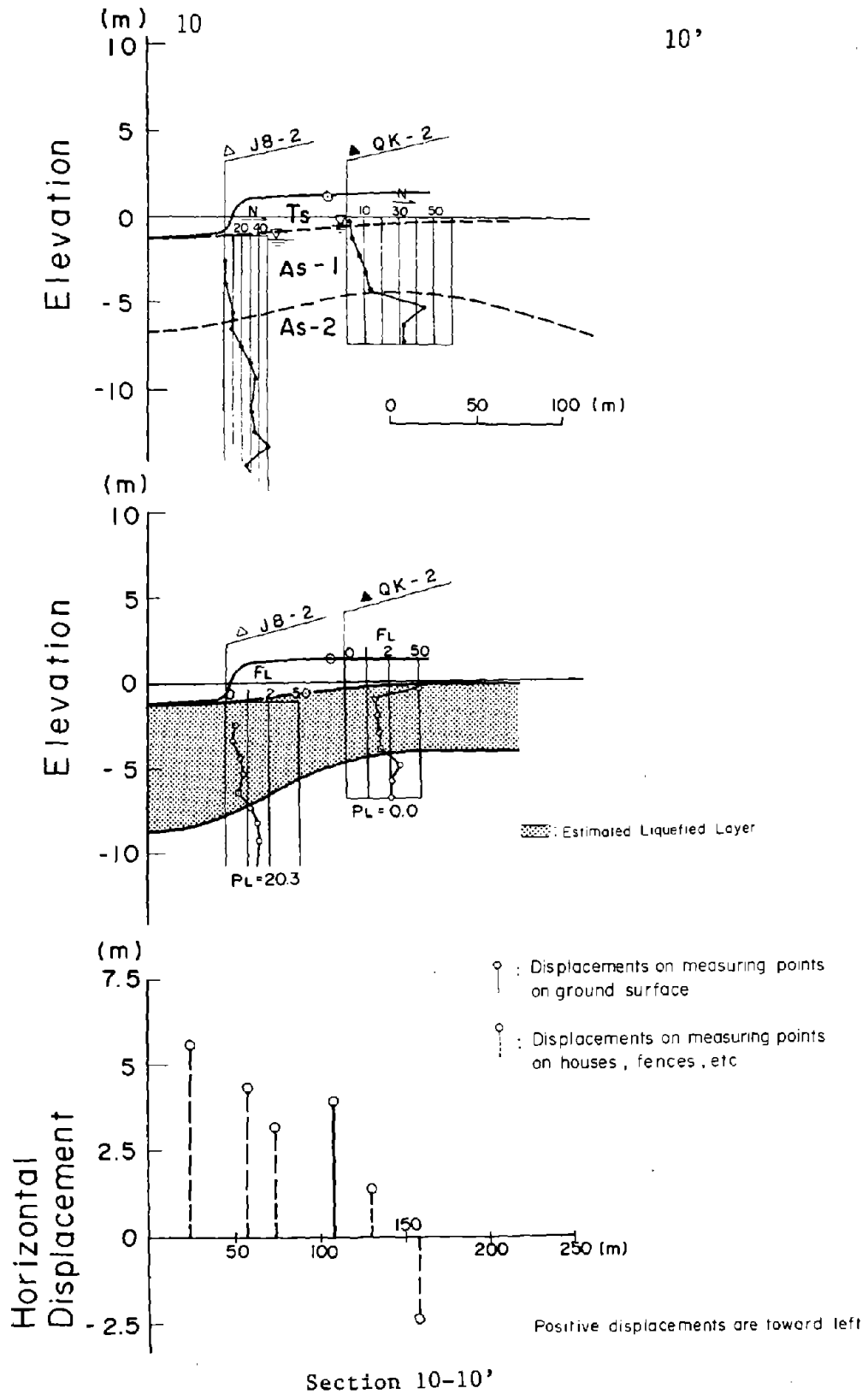
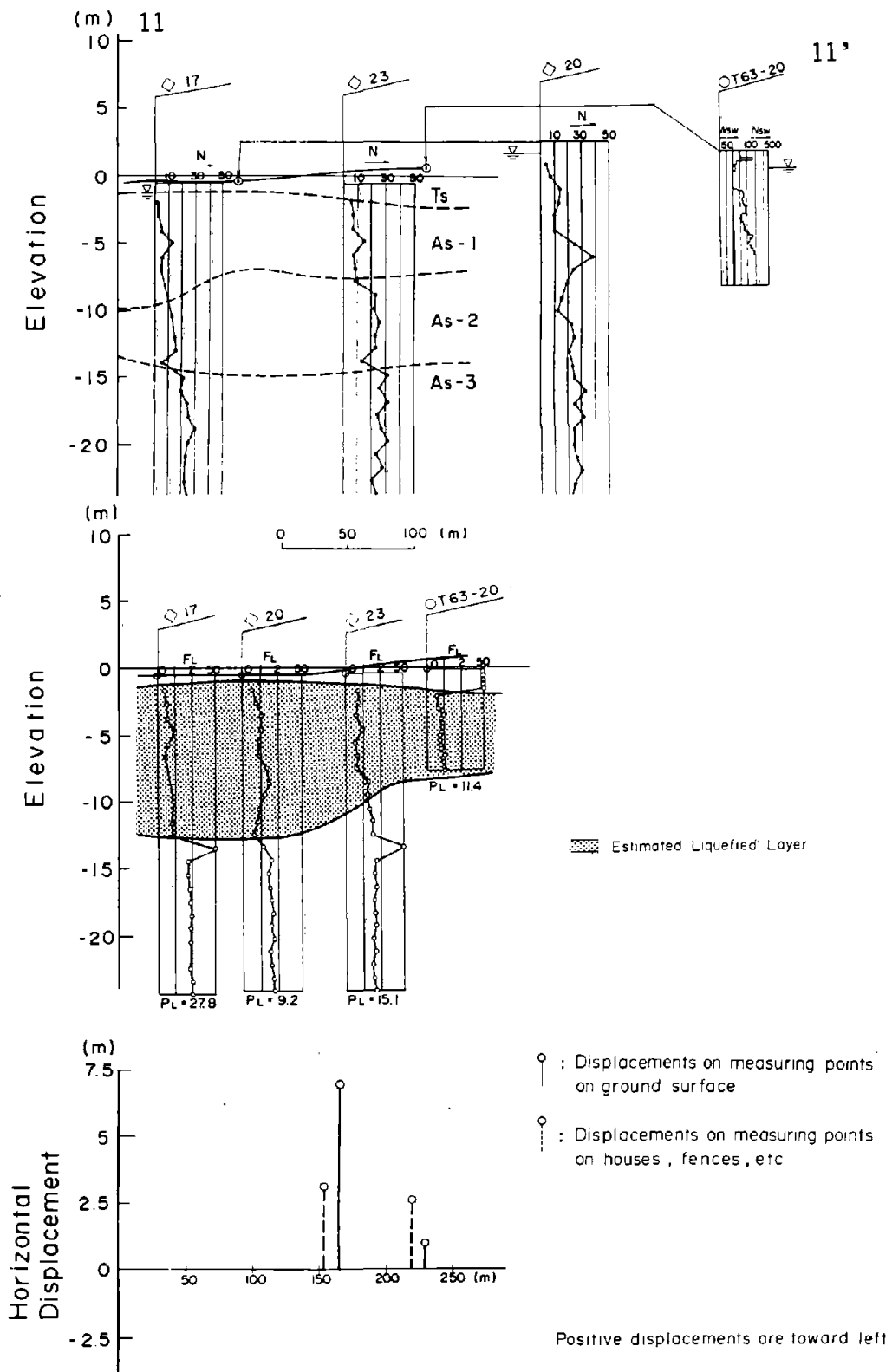
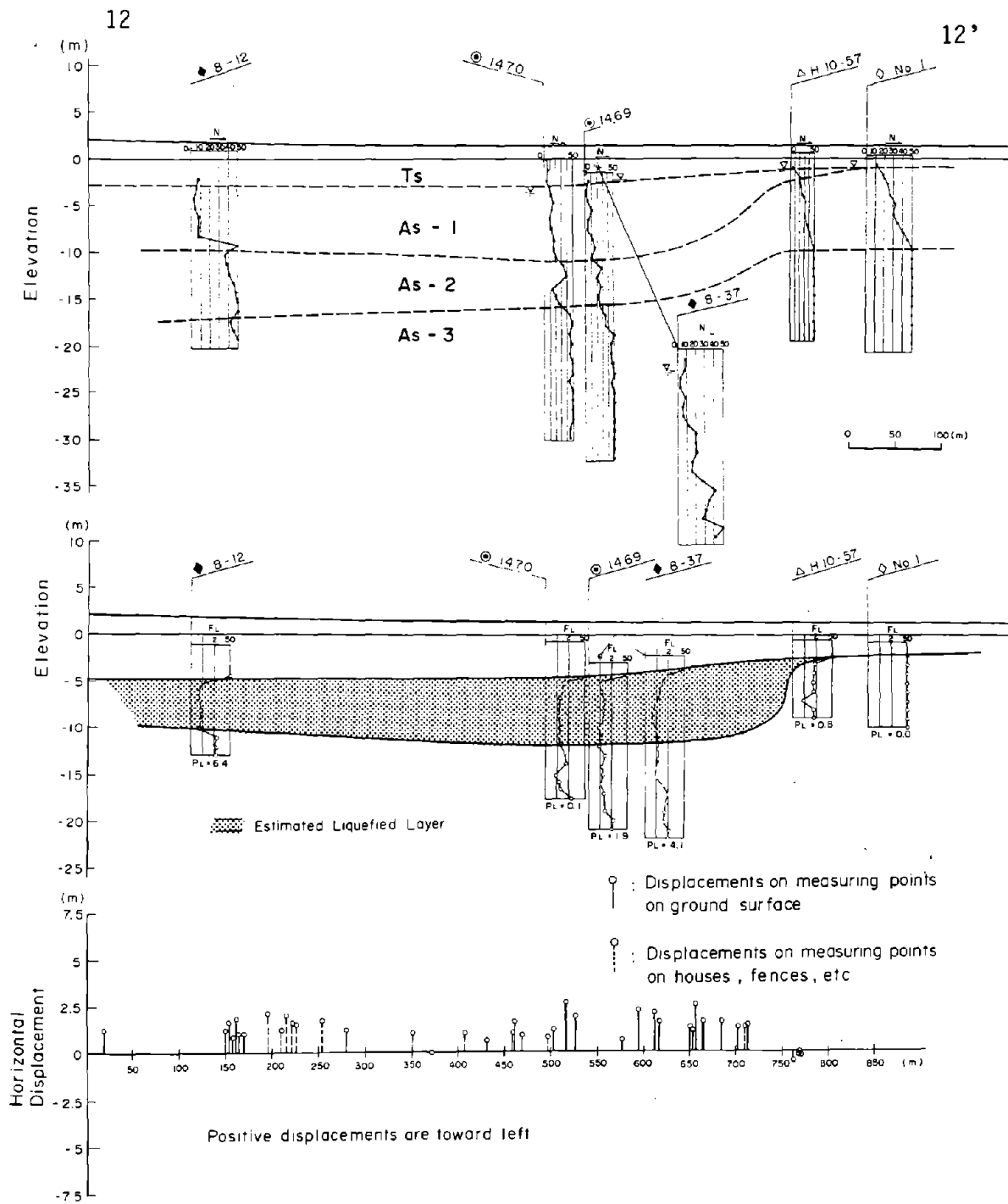


Figure B-2 Soil Profile and Estimated Liquefied Layer



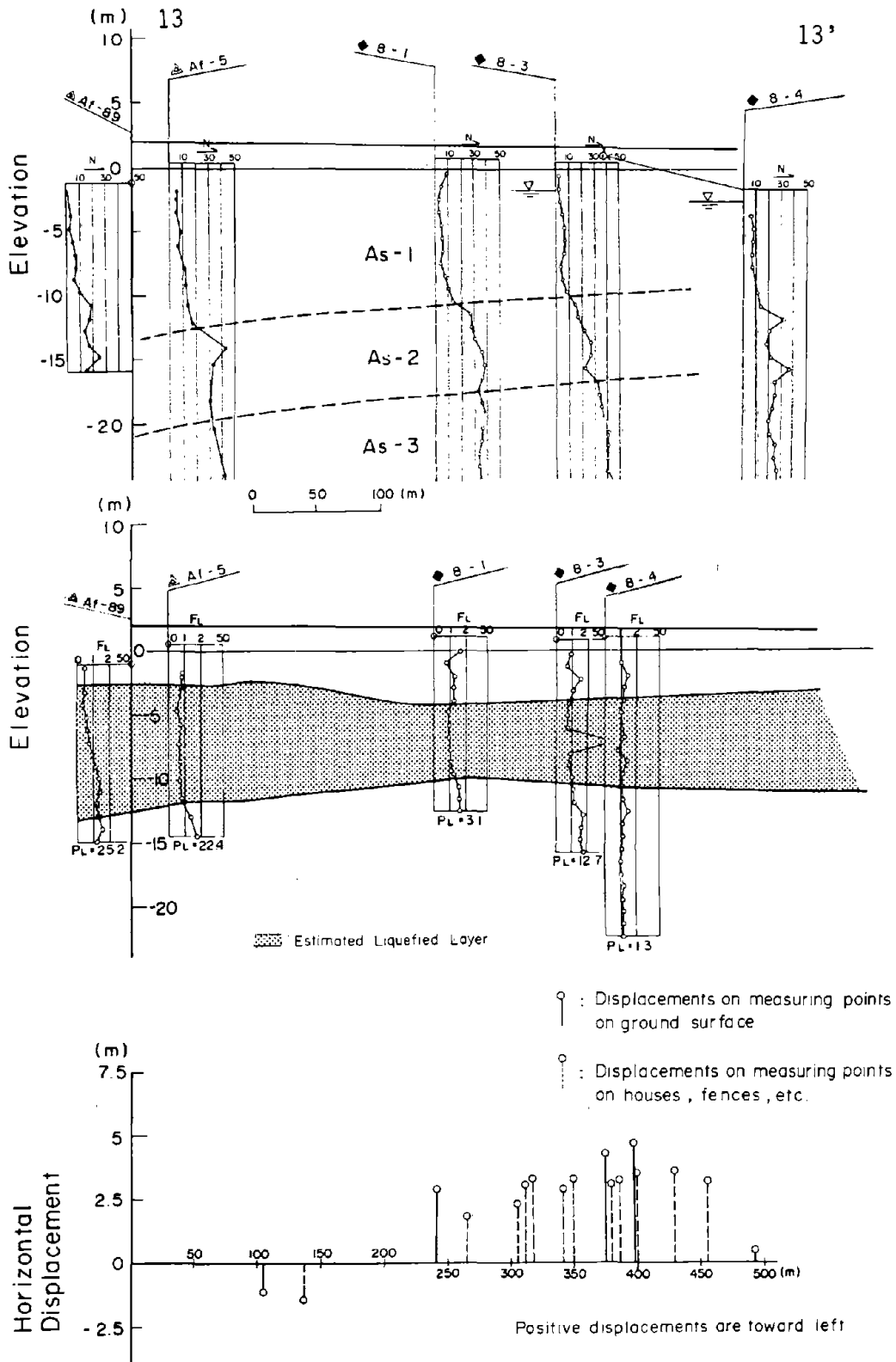
Section 11-11'

Figure B-2 Soil Profile and Estimated Liquefied Layer



Section 12-12'

Figure B-2 Soil Profile and Estimated Liquefied Layer



Section 13-13'

Figure B-2 Soil Profile and Estimated Liquefied Layer

Appendix C Swedish Weight Sounding Test

The Swedish weight sounding method is used for in-situ tests of soil penetration resistance. According to Japan Industrial Standard (JIS) A1221-1976, the apparatus and the procedure of the test are defined as follows:

C-1 Apparatus

The apparatus for the Swedish weight sounding test is shown in Figures C-1, C-2 and C-3, and consists of the following parts:

- (1) Handle
- (2) Weight: The weights shall be of cast steel, as shown in Figure C-2 with steel handles. There should be two weights of 10 kg and three weights of 25 kg.
- (3) Loading clamp: The loading clamp shall be such that it can be fixed anywhere along the rod. The weight of the loading clamp is 5 kg.
- (4) Base plate
- (5), (6) Rod: The diameters are 10 mm and 19 mm.
- (7) Screw point: The screwpoint shall be of a special, highly abrasive-resistant steel and of the shape shown in Figure C-3.

C-2 Testing Method and Recording of Results

Swedish weight sounding test is conducted according to the following procedure:

- (1) Gradually increase the load to be 5, 15, 25, 50, 75, and 100 kg, gradually and record total depths of the penetration with reference to the load W_{sw} (kg).
- (2) At the point where the penetration of the rod stops under a loading of 100 kg, revolve the rod halfway such that no vertical force is applied. Record the number of half revolutions, which is required for the penetration of 1.0 m (N_{sw}). The result of Swedish weight sounding is shown as Figure C-4 by the values W_{sw} and N_{sw} at each elevation.

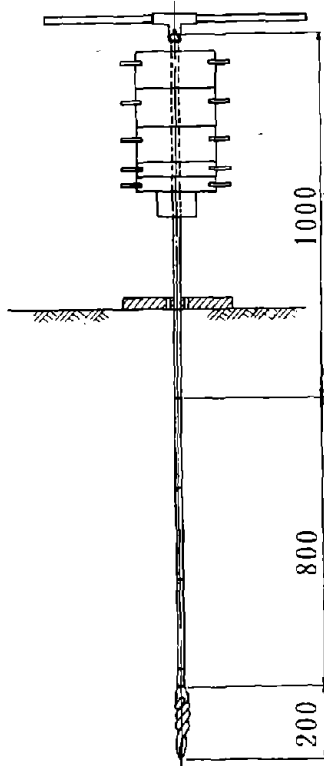


Figure C-1 Apparatus for Swedish Weight Sounding Test (SWS) (Unit: mm)

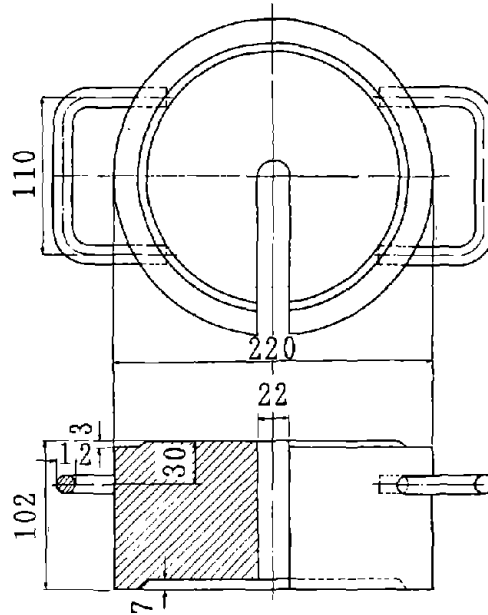


Figure C-2 Weight for SWS (Unit: mm)

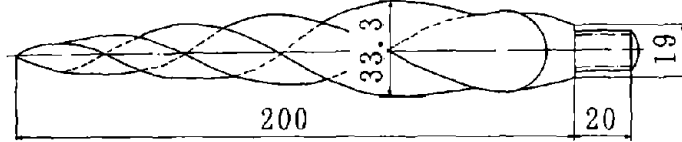


Figure C-3 Screwpoint for SWS (Unit: mm)

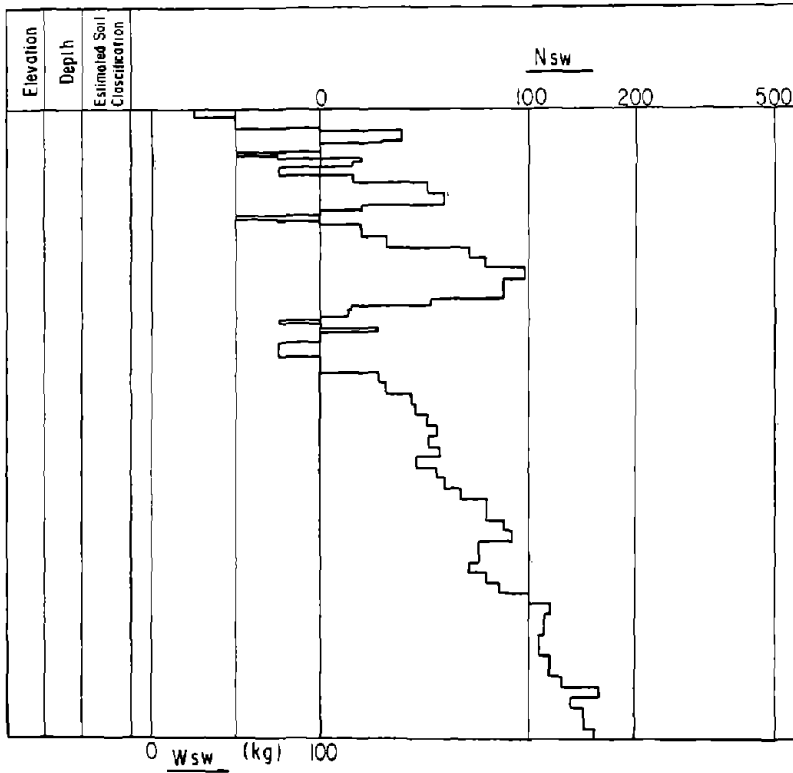


Figure C-4 Result of SWS

Appendix D Factor of Liquefaction Resistance, F_L and Index of Liquefaction Potential, P_L ⁴⁾

The ability of a soil element at an arbitrary depth to resist liquefaction can be expressed by the Factor of Liquefaction Resistance, F_L , as follows:

$$F_L = \frac{R}{L} \quad (D-1)$$

In which R is the in-situ resistance of the soil element to dynamic loads and can be simply evaluated, based on undrained cyclic shear test results, as follows:

$$R = 0.882 \sqrt{\frac{N}{\sigma_v' + 0.7}} + 0.19, \quad \text{for } 0.02 \text{ mm} \leq D_{50} \leq 0.05 \text{ mm} \quad (D-2)$$

$$R = 0.882 \sqrt{\frac{N}{\sigma_v' + 0.7}} + 0.225 \log_{10} \frac{0.35}{D_{50}} \quad \text{for } 0.05 \text{ mm} \leq D_{50} \leq 0.6 \text{ mm} \quad (D-3)$$

$$R = 0.882 \sqrt{\frac{N}{\sigma_v' + 0.7}} - 0.05, \quad \text{for } 0.6 \text{ mm} \leq D_{50} \leq 1.5 \text{ mm} \quad (D-4)$$

in which N is the number of blows in the standard penetration test, σ_v' is the effective overburden pressure (in kg/cm^2), and D_{50} is the mean particle diameter (in mm). The value of L in Equation (D-1) is the dynamic load induced in the soil element by earthquake motion, and can be estimated by

$$L = \frac{\tau_{\max}}{\sigma_v'} = \frac{\alpha_{s\max}}{g} \frac{\sigma_v}{\sigma_v'} \quad d = k_s \frac{\sigma_v}{\sigma_v'} \quad d \quad (D-5)$$

Where τ_{\max} is the maximum shear stress (in kg/cm^2), $\alpha_{s\max}$ is the maximum acceleration at ground surface (in cm/sec^2), g is the acceleration of gravity ($= 980 \text{ cm/sec}^2$), σ_v is the total overburden pressure (in kg/cm^2), k_s

is the seismic coefficient, and γ_d , the reduction factor for dynamic shear stress, is as follows:

$$\gamma_d = 1 - 0.015 z \quad (D-6)$$

in which z is the depth in meters.

The Index of Liquefaction Potential P_L can be introduced to express the severity of liquefaction as,

$$P_L = \int_0^{20} F \cdot \omega(z) dz \quad (D-7)$$

in which $F = 1 - F_L$ for $F_L \leq 1.0$ and $F = 0$ for $F_L > 1.0$, and $\omega(z) = 10 - 0.5Z$ (z in meters), as illustrated in Figure D-1. For the case of $F_L = 0.0$ for the entire range from $z = 0$ to $z = 20$ m, P_L becomes 100, and for the case of $F_L \geq 1.0$ for the entire range from $z = 0$ to $z = 20$ m, P_L becomes 0.0.

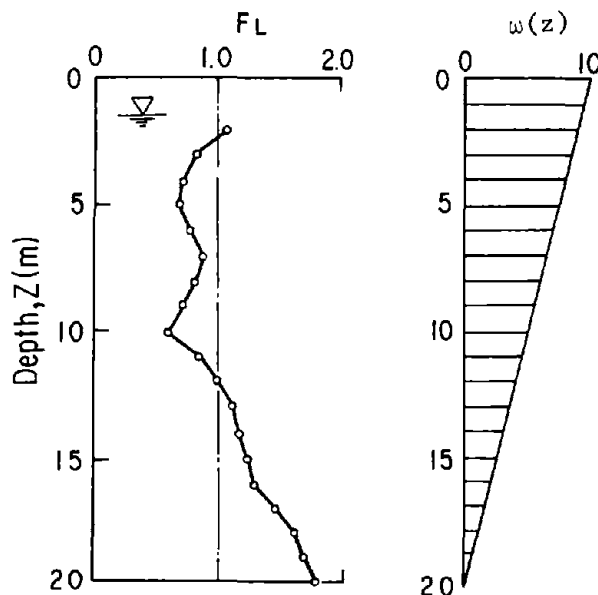
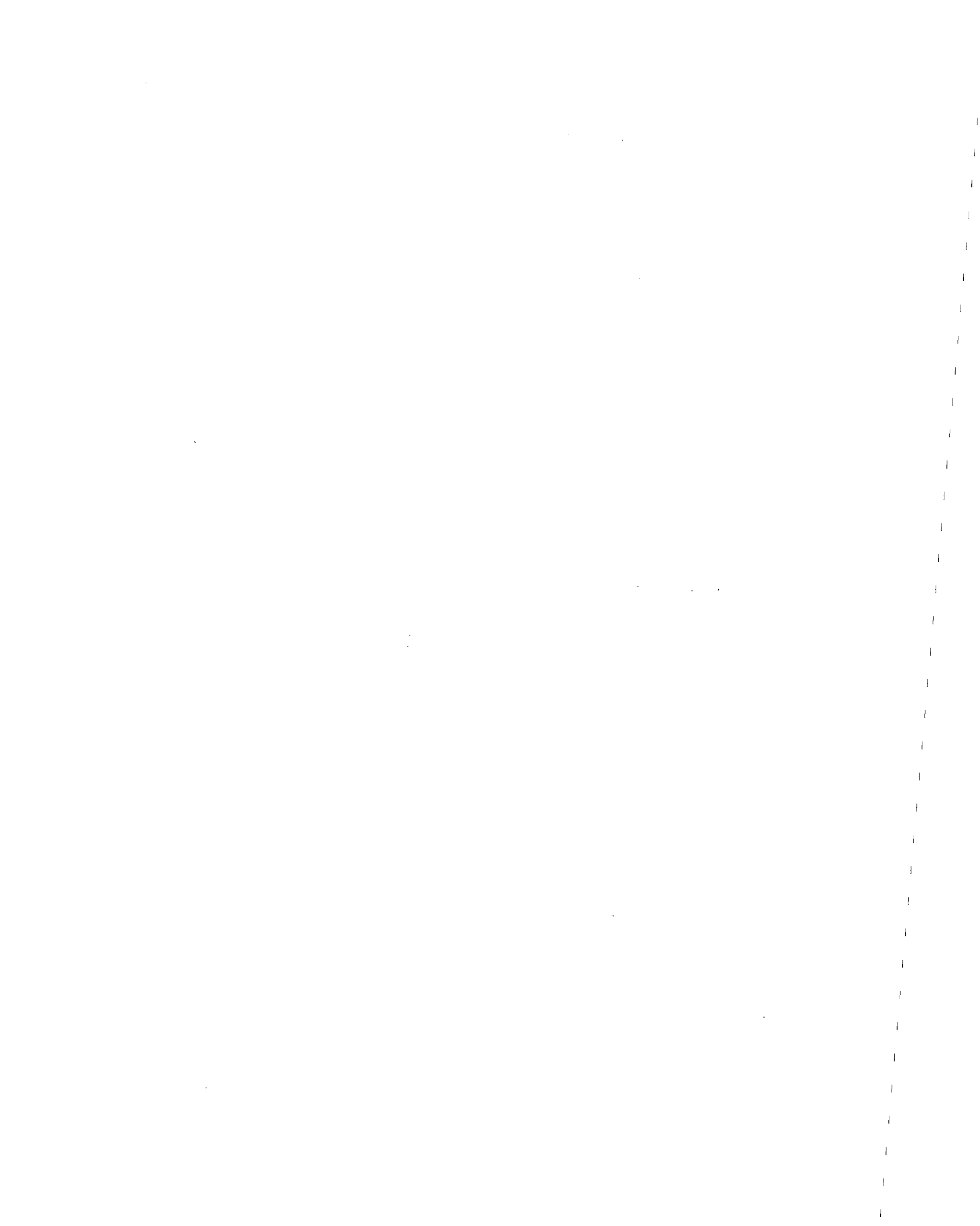
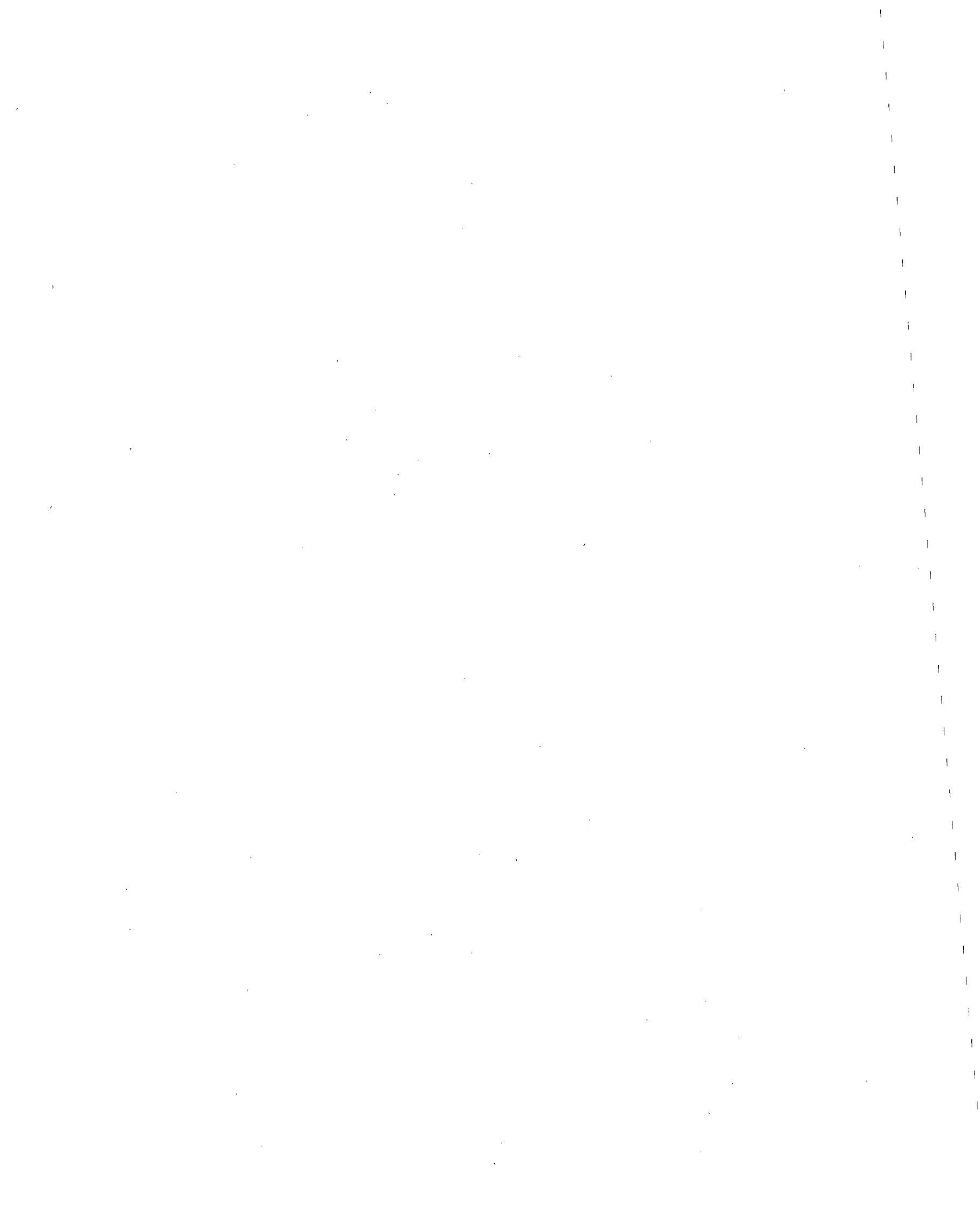


Fig. D-1 Calculation of Index of Liquefaction Potential, P_L



**Large Ground Deformations and
Their Effects on Lifelines:
1983 Nihonkai-Chubu Earthquake**

*M. Hamada, Professor
School of Marine Science and Technology
Tokai University
Shimizu, Shizuoka, Japan*



ACKNOWLEDGEMENT

This case study of the 1983 Nihonkai-Chubu earthquake was the first memorable achievement for researchers working on liquefaction-induced ground displacements and the damage they cause to structures. Two engineers from Tokyo Gas Co. and I visited Noshiro City immediately after the earthquake to investigate the damage to buried gas pipes. At a meeting with city officials, one interesting example of damage to a welded gas pipe was examined. The pipe was ruptured at a 45° elbow, and the two ruptured ends were about 70 cm apart. It appeared the damage was not caused by the earthquake tremor, but by large, permanent ground displacements. In the vicinity of the damaged pipe, large ground fissures were observed, and the houses and the walls were reported to have moved considerably during the earthquake. Therefore, my co-researchers and I tried to measure ground displacements and to examine the relationship between pipe damage and ground displacements. This study became the starting point for a series of investigations into liquefaction-induced permanent ground displacements.

The case study of the 1983 Nihonkai-Chubu earthquake was conducted by a committee researching the "Earthquake Resistance of Buried Pipelines to Liquefaction," sponsored by the Tokyo Gas Company. The research committee was organized by the Association for the Development of Earthquake Prediction in Tokyo.

I wish to express my great appreciation to Prof. K. Kubo, who was chairman of the research committee and who consistently encouraged the research activity. Thanks should also be extended to members of the research committee and the engineers from Tokyo Gas Company who fully supported the research. I also want to thank Mr. I. Yasuda at Hassu Co., Ltd. for measuring the permanent ground displacements from aerial photographs. Furthermore, my deep appreciation to Dr. R. Isoyama at Japan Engineering Consultants and Prof. S. Yasuda at Kyushu Institute of Technology for their cooperation, and to Prof. T.D. O'Rourke at Cornell University for his excellent editing of this case study.

K. Emoto, late assistant professor at Tokai University made a large contribution to this case study. However, he passed away just after completion of the case study - a victim of cancer of the large intestine. I dedicate this report to his memory and pray that he may rest in peace.

TABLE OF CONTENTS

	<u>Page</u>
Acknowledgements	4-iii
Table of Contents	4-v
List of Figures	4-vii
List of Tables	4-xi
List of Photos	4-xiii
 <u>Section</u>	
1.0 INTRODUCTION	4-1
2.0 OUTLINE OF THE 1983 NIHONKAI-CHUBU EARTHQUAKE	4-2
2.1 Epicenter, Magnitude, and Intensity	4-2
2.2 Strong Motion Data	4-2
3.0 COLLECTION AND EVALUATION OF DATA	4-4
3.1 Measurement of Permanent Ground Displacements	4-4
3.2 Location of Large Ground Displacements	4-5
3.3 Surveys of Soil Conditions and Interviews with with Residents	4-5
4.0 PERMANENT GROUND DISPLACEMENTS AND RESULTING DAMAGE IN NOSHIRO CITY	4-8
4.1 Zone I: Southern Area of Noshiro City	4-8
4.1.1 Permanent Ground Displacements and Ground Failures	4-8
4.1.2 Soil Conditions and Estimated Liquefied Layer	4-14
4.1.3 Damage to Buried Gas Pipes and Well Casings	4-18
4.2 Zone II: Northern Part of Noshiro City	4-27
4.2.1 Permanent Ground Displacements and Ground Failures	4-27
4.2.2 Soil Conditions and Estimated Liquefied Layer	4-35
4.2.3 Damage to Buried Pipes	4-39

<u>Section</u>	<u>Page</u>
5.0 CORRELATION ANALYSIS OF RATE OF DAMAGE TO HOUSES AND BURIED PIPES WITH PERMANENT GROUND DISPLACEMENTS AND STRAINS	4-46
5.1 Correlation of Rate of Damage to Houses and Buried Pipes with the Magnitude of Permanent Ground Displacements	4-46
5.2 Correlation of Rate of Damage to Buried Pipes with Permanent Ground Strains	4-49
6.0 EFFECTS OF THICKNESS OF LIQUEFIED LAYER AND GRADIENT OF GROUND SURFACE ON PERMANENT GROUND DISPLACEMENTS	4-52
7.0 PERMANENT GROUND DISPLACEMENTS AND RESULTING DAMAGE AT AKITA HARBOR	4-56
7.1 Zone III: Gaiko Wharf at Akita Harbor	4-56
7.1.1 Permanent Ground Displacements and Ground Failures	4-56
7.1.2 Soil Conditions	4-59
7.1.3 Damage to Quay Wall and Foundation Piles	4-59
8.0 CONCLUSION	4-63
References	4-65
Appendix A Accuracy of the Measurement of Permanent Ground Displacements in Noshiro City and Akita Harbor	4-67
Appendix B Soil Conditions along 27 Sections in Noshiro City, and Evaluation of the Liquefied Zone	4-71
Appendix C Calculation of Permanent Ground Strains	4-85

LIST OF FIGURES

<u>Figure</u>		<u>Page</u>
1	Epicenter, Fault Zone and Maximum Acceleration	4-3
2	Seismic Intensity (JMAI)	4-3
3	Accelerograph at Akita Harbor	4-3
4	Survey Area of Permanent Ground Displacements and Their Related Damage in Noshiro City and Akita Harbour	
	(a) Noshiro City (ZONES I and II)	4-6
	(b) Akita Harbour (ZONE III)	4-6
5	Permanent Ground Displacements in the Southern Part of Noshiro City (ZONE I)	
	(a) ZONE I-1	4-9
	(b) ZONE I-2	4-10
6	Details of the Permanent Ground Displacements, and Ground Fissures on the Northern Slope of Maeyama	4-12
7	Section Lines for the Study of Soil Conditions (ZONE I)	4-15
8	Soil Conditions and the Estimated Liquefied layer	
	(a) Section S-5	4-16
	(b) Section S-10	4-16
	(c) Section S-13	4-17
	(d) Section S-17	4-17
9	Locations of Damaged Gas Pipes	4-19
10	Damage to the Gas Pipe at Point No.1	4-20
11	Permanent Ground Displacements in the Vicinity of the Damaged Gas Pipe (Point No.1)	4-20
12	Damage to the Gas Pipe at Point No.2	4-21
13	Permanent Ground Displacements in the Vicinity of the Damaged Gas Pipe (Point No.2)	4-21
14	Damage to the Gas Pipe at Point No.3	4-23
15	Permanent Ground Displacements in the Vicinity of the Damaged Gas Pipe (Point No.3)	4-23
16	Permanent Ground Displacements in the Vicinity of the Damaged Gas Pipe (Point No.4)	4-24

<u>Figure</u>		<u>Page</u>
17	Movement of the Two Broken Ends of the Pipe	4-24
18	Damage to Well Casing	
	(a) Damage to Well Casing	4-26
	(b) Result of Swedish Cone Penetration Test and Liquefiable Soil	4-26
19	Permanent Ground Displacements in the Northern Part of Noshiro City (ZONE II)	
	(a) ZONE II-1	4-28
	(b) ZONE II-2	4-29
20	Permanent Ground Displacements and Ground Failures in Aoba-cho and Shonan-cho	4-30
21	Permanent Ground Strains in Noshiro City	4-32
22	Permanent Ground Displacements and Strains in the Vicinity of the Split Tree	4-34
23	Section Lines for Survey on Soil Conditions (ZONE II)	4-36
24	Soil Conditions and Estimated Liquefied Layer	
	(a) Section N-1	4-37
	(b) Section N-3	4-38
	(c) Section N-7	4-37
25	Permanent Ground Displacements and Strains in the Vicinity of the Damaged Telecommunications Cable	4-40
26	Measurement of Movement of Wastewater Pipe	4-40
27	Movement of Wastewater Pipe and Ground Displacements (Shinyanagi-cho Route)	
	(a) Manholes No.1-No.2	4-42
	(b) Manholes No.2-No.4	4-42
28	Movement of Wastewater Pipe and Ground Displacements in Cross-Section a-a'	4-43
29	Movement of Wastewater Pipe and Ground Displacements (Haginodai Route)	4-43
30	Movement of Wastewater Pipe and Ground Displacements in Cross-Section b-b'	4-45

<u>Figure</u>	<u>Page</u>
31 Square Cells for Analysis of Quantitative Relationship between Permanent Ground Displacements and Damage Rates to Houses and Buried Pipes	4-48
32 Relationship between the Damage Rate to Houses and the Permanent Ground Displacements	4-48
33 Relationship between the Damage Rate to Buried Gas Pipes (diameter = 75 to 150 mm) and Permanent Ground Displacements	
(a) Cast Iron Gas Pipes	4-48
(b) Steel Pipes	4-48
34 Relationship between the Damage Rate to Buried Gas Pipes and the Permanent Ground Displacements (steel pipes, diameter = 32 to 50 mm)	4-50
35 Relationship between the Damage Rate to Buried Water Pipes and the Permanent Ground Displacements (asbestos cement pipes, diameter = 100 to 200 mm)	4-50
36 Relationship between the Damage Rate to Buried Gas Pipes (diameter = 75 to 150 mm) and the Permanent Ground Strains	
(a) Cast Iron Gas Pipes	4-51
(b) Steel Pipes	4-51
37 Correlation between Magnitude of Ground Displacements and Thickness of Estimated Liquefied Layer	4-53
38 Correlation between Magnitude of Ground Displacements and Gradient of Ground Surface	
(a) Case 1: Horizontal distance is 5 times the thickness of the liquefied layer	4-54
(b) Case 2: Horizontal distance is 60 times the thickness of the liquefied layer	4-54
39 Locations of Damage to Quay Walls and Liquefaction at Akita Harbor	4-57
40 Permanent Ground Displacements, Ground Fissures and Sand Boil at Gaiko Wharf	4-58
41 Soil Conditions at Gaiko Wharf	
(a) Boring No.1	4-60
(b) Boring No.2	4-60

<u>Figure</u>		<u>Page</u>
42	Quay Wall of Pier C	4-61
43	Movement and Inclination of Caissons of Pier C at Gaiko Wharf	4-61
44	Damage to Prestressed Concrete Pile of Gaiko Warehouse	4-62
Appendix		
A-1	Data Points for Aerial Survey in Northern Area of Noshiro City (ZONE II)	4-68
B-1	Soil Profile and Estimated Liquefied Layers	4-72 through 4-84

LIST OF TABLES

<u>Table</u>		<u>Page</u>
A-1	Accuracy of the Permanent Ground Displacement Measurements	
	(a) South Area (ZONE I)	4-69
	(b) North Area (ZONE II)	4-69
A-2	Accuracy of the Permanent Ground Displacement Measurements at Akita Harbor (ZONE III)	4-70

LIST OF PHOTOS

<u>Photo</u>	<u>Page</u>
1 Aerial Photograph for Measurements of Permanent Ground Displacements	4-7
2 Aerial View of Noshiro City	4-7
3 Undulating Ground Surface on the Northern Slope of Maeyama	4-13
4 Fissure with Subsidence on the Northern Slope of Maeyama	4-13
5 Fissure with Subsidence on the Northern Slope of Maeyama	4-13
6 Damage to the Gas Pipe at Point No.1	4-20
7 Damage to the Gas Pipe at Point No.2	4-21
8 Damage to the Gas Pipe at Point No.3	4-23
9 Damage to the Gas Pipe at Point No.4	4-24
10 Damage to Well Casing	4-26
11 Ground Fissure in the Aoba-cho Graveyard	4-33
12 Sand Boil in Shonan-cho	4-33
13 A Tree Split by Liquefaction	4-33
14 Ground Fissure in the Vicinity of the Split Tree	4-33
15 Bulking of Telecommunications Conduit	4-40
16 Protrusion of Telecommunications Conduits into Manholes	
(a) Manhole No.1	4-40
(b) Manhole No.2	4-40
17 Damage to Sheet Pile Quay Wall (Nakajima Pier)	4-57
18 Ground Fissure at Gaiko Wharf	4-60

1.0 INTRODUCTION

The Nihonkai-Chubu earthquake, with a magnitude of 7.7, occurred in the Japan Sea about 90 km west of Aomori Prefecture on May 26, 1983, causing severe damage to the coastal areas of the Tohoku region. In particular, liquefaction resulted in severe damage to houses, buildings, and lifeline facilities in cities such as Noshiro and Akita along the Japan Sea. Liquefaction-caused damage, including the subsidence and floating of structures, was also experienced during the 1964 Niigata earthquake, and many countermeasures against a recurrence of such kinds of damage have been developed and adopted in practice. However, it was through the experience of the Nihonkai-Chubu earthquake that permanent ground displacements induced by liquefaction were first recognized.

Permanent ground displacements were measured by surveys based on aerial photographs taken before and after the earthquake. In addition to the measurement of permanent ground displacements, the authors conducted geological surveys and soil soundings, and investigated the effects of these factors on the occurrence of permanent ground displacements. Furthermore, the authors investigated the damage to houses, quay walls, and lifeline facilities, which could be attributed to permanent ground displacements. Data were collected on the damage, and people were interviewed about their experience during and after the earthquake.

Some parts of this report related to displacements and the damage they caused in Noshiro City have been excerpted from the report "Study on Liquefaction-Induced Permanent Ground Displacement," published in 1986 by the Association for the Development of Earthquake Prediction.¹⁾ Since the publication of that report, investigations have continued in Noshiro and Akita cities. The current paper presents up-to-date results of the research and includes recently collected data.

2.0 OUTLINE OF THE 1983 NIHONKAI-CHUBU EARTHQUAKE

2.1 Epicenter, Magnitude, and Intensity

The earthquake occurred on May 26, 1983 at 12:00 a.m. It registered a magnitude 7.7, and struck areas along the Japan Sea coast in Akita and Aomori Prefectures. In the cities of Noshiro and Akita in particular, which were located about 100 km and 150 km, respectively, from the epicenter, houses, quay walls, and lifeline facilities were damaged extensively by liquefaction.

The epicenter of the main shock was located on the bed of the Japan Sea, 100 km from the main island of Japan at $40^{\circ}21.4'N$, $139^{\circ}4.6'E$, as shown in Figure 1. The focal depth of the earthquake was about 15 km.

According to the Japanese Meteorological Agency Scale (JMAI) (Figure 2),²⁾ the highest seismic intensity was V, which is roughly equivalent to VII-VIII on the Modified Mercalli Intensity Scale (MMI). The liquefaction-induced permanent ground displacements in Noshiro and Akita cities, which are discussed in the present report, occurred where the intensity was in the V range.

The two main characteristics of this earthquake that caused property damage and loss of life were the liquefaction and the tsunami. The tsunami which hit the coast of the Japan Sea immediately after the earthquake was particularly destructive, killing about 100 people.

2.2 Strong Motion Data

Strong earthquake tremors were recorded at many locations in northern Japan. The maximum recorded horizontal acceleration was 0.399 g at a bridge site on Hokkaido Island, about 200 km from the epicenter. In the area where liquefaction was extensive, as will be discussed later in this report, several accelerographs were recorded. Figure 3 shows the acceleration recorded in Akita Harbor, with a maximum horizontal acceleration of 0.235 g.²⁾ The quay wall of Akita Harbor was severely damaged by liquefaction.

No accelerograph recording of this strong earthquake was obtained in Noshiro City, where damage due to liquefaction was most severe. By taking into consideration the seismic intensity reading of V (JMAI) and the city's epicentral distance of about 100 km, less than that of Akita City where maximum horizontal acceleration was 0.235 g, it can be roughly estimated that the maximum horizontal acceleration in Noshiro City was around 0.25 g.

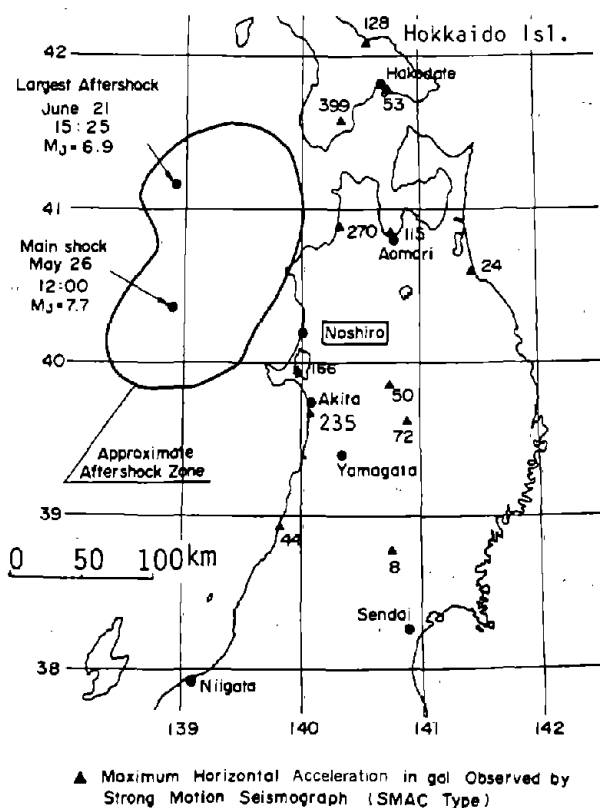


Figure 1. Epicenter, Fault Zone and Maximum Acceleration

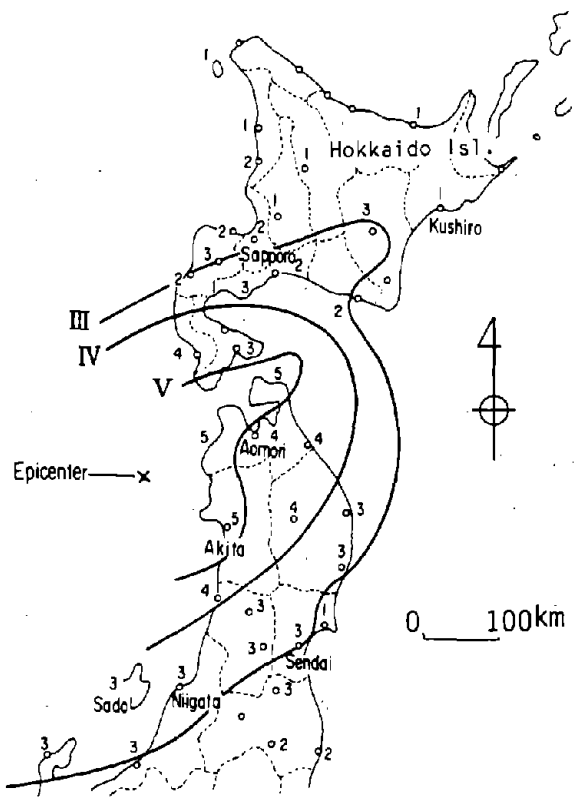


Figure 2. Seismic Intensity (JMAI)²⁾

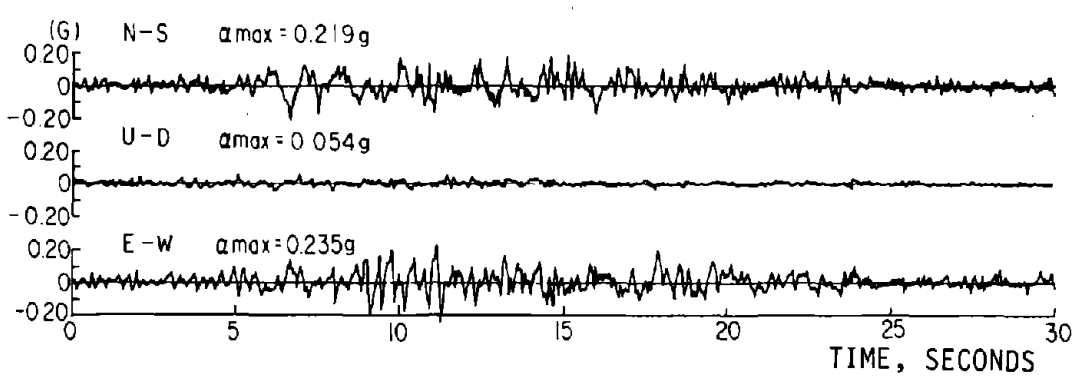


Figure 3. Accelerograph at Akita Harbor²⁾

3.0 COLLECTION AND EVALUATION OF DATA

3.1 Measurement of Permanent Ground Displacements

In order to measure permanent ground displacements caused by the earthquake, aerial photographs taken before and after the earthquake were used. The ground displacement was evaluated by subtracting the coordinates of measuring points on the ground surface determined from pre-earthquake aerial photographs from those of post-earthquake photographs.* The pre-earthquake photograph was taken in 1981, two years before the earthquake, and the post-earthquake photograph was taken a week after its occurrence. The scale of both photographs is 1:8000. Photo 1 is an example of pre-earthquake photograph of the southern part of Noshiro City used for measurement, where white circles show measurement points on the ground surface.

The datum points necessary for measurement were selected triangulation points located on the stable tops of hills or on sand dunes where no ground failures, including liquefaction and sliding, were found. It can be assumed that no permanent ground displacements were caused by the earthquake at these locations. The measurement points selected were objects fixed to the ground surface, such as manhole covers and corners of drainage channels. There were about 2,000 measurement points in Noshiro and Akita cities.

The accuracy with which permanent ground displacements are measured depends on the scale of the aerial photographs, etc., allowing for human error. The accuracy of the measurements was estimated to be ± 16 cm horizontally and ± 20 cm vertically in the southern area of Noshiro City, and ± 17 cm horizontally and ± 28 cm vertically in the northern area. In the area of Akita Harbor, the accuracy was estimated to be ± 13 cm horizontally and ± 20 cm vertically.

3.2 Location of Large Ground Displacements

Liquefaction and the damage it caused to structures were observed over a wide area of the Japan Sea coast, in places such as Noshiro City, Hachirogata, Wakami-cho, Oga City, and Akita City. Liquefaction-caused damage was particularly severe in Noshiro City and Akita City. In Noshiro, houses, buildings, and buried tanks and pipes were extensively damaged. In Akita City the quay walls of the harbor were seriously damaged.

Permanent ground displacements were measured in the following three zones which are shown in Figure 4(a) and (b).

- (1) ZONE I : Southern area of Noshiro City
- (2) ZONE II : Northern area of Noshiro City
- (3) ZONE III: Gaiko wharf at Akita Harbor

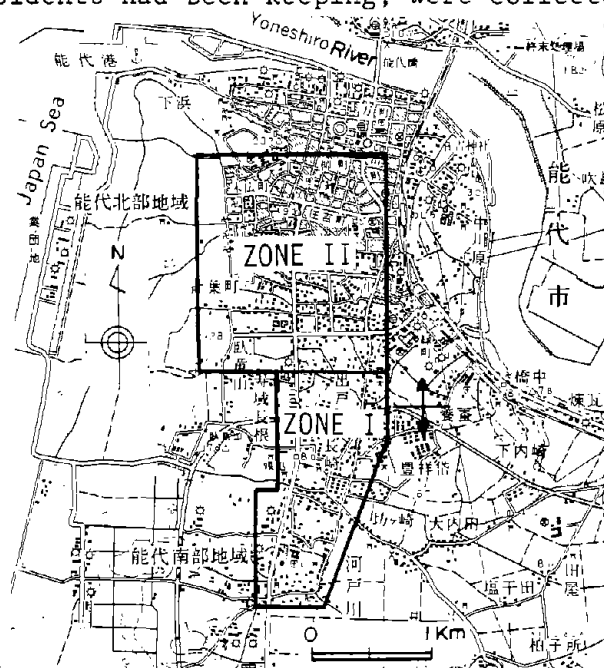
3.3 Surveys of Soil Conditions and Interviews with Residents

In order to examine the relationship between the occurrence of permanent ground displacements and soil and geological conditions, 12 standard penetration tests (SPT)⁴⁾,* and 134 Swedish weight sounding tests (SWS)³⁾** were conducted in Noshiro City. In addition, 50 existing bore-hole records were collected. In Akita City as well, about 20 existing bore-hole records were collected. Based on these soil and geological surveys, soil profiles were drawn along section lines, which were mostly parallel to the direction of the ground displacements, and soil layers, which most likely liquefied during the earthquake, were estimated. The effects of influential factors, such as the thickness and inclination of the estimated liquefied layer and the ground surface gradient, on the occurrence of permanent ground displacements were examined.

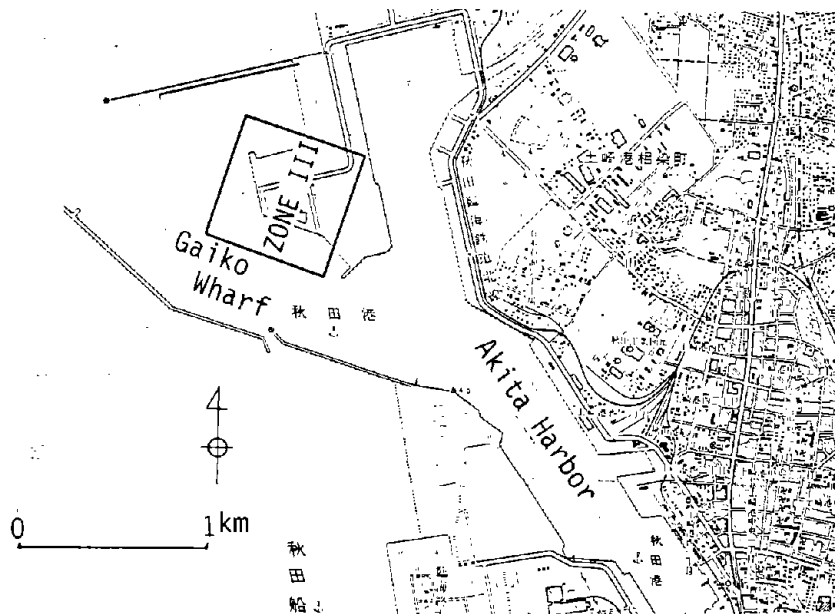
*Generally, SPT values in U.S. standard are larger than those in Japanese standard, because of the difference in energy transfer efficiency from the hammer to the rod (See reference 4)).

**See Appendix C of reference 3).

A number of residents of Noshiro City, who saw the liquefaction and its related ground failures, were interviewed to clarify the actual situation surrounding the occurrence of the ground displacements. Furthermore, photographs and other documents concerning the liquefaction and ground failures, which residents had been keeping, were collected.



(a) Noshiro City (ZONES I and II)



(b) Akita Harbor (ZONE III)

Figure 4. Survey Area of Permanent Ground Displacements and Their Related Damage in Noshiro City and Akita Harbor

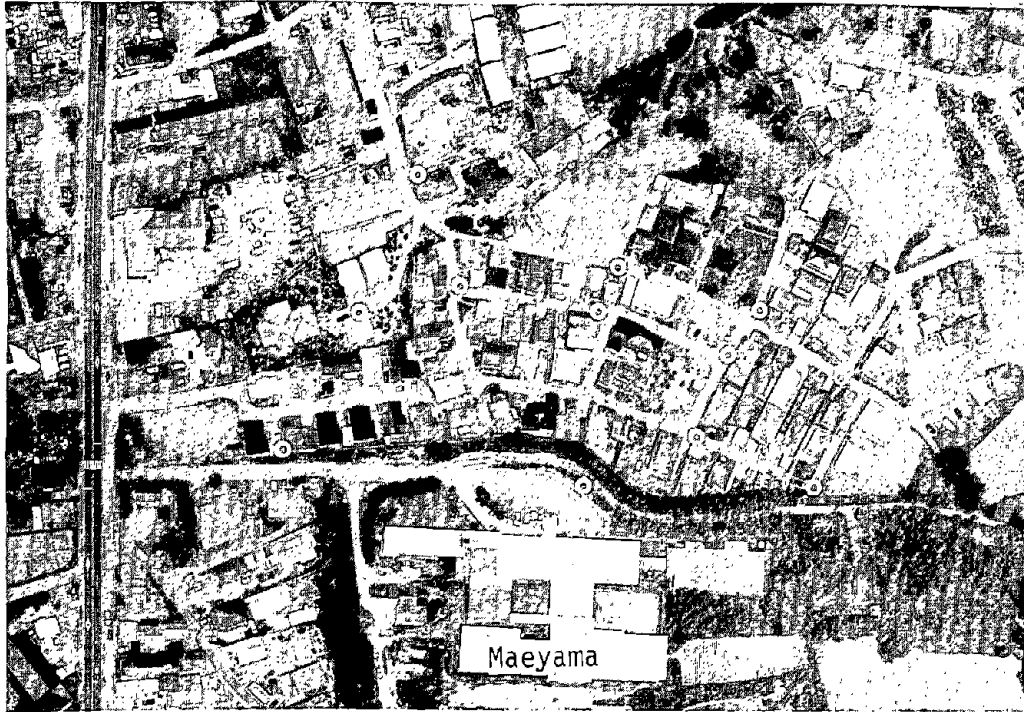


Photo 1 Aerial Photograph for Measurements of Permanent Ground Displacements

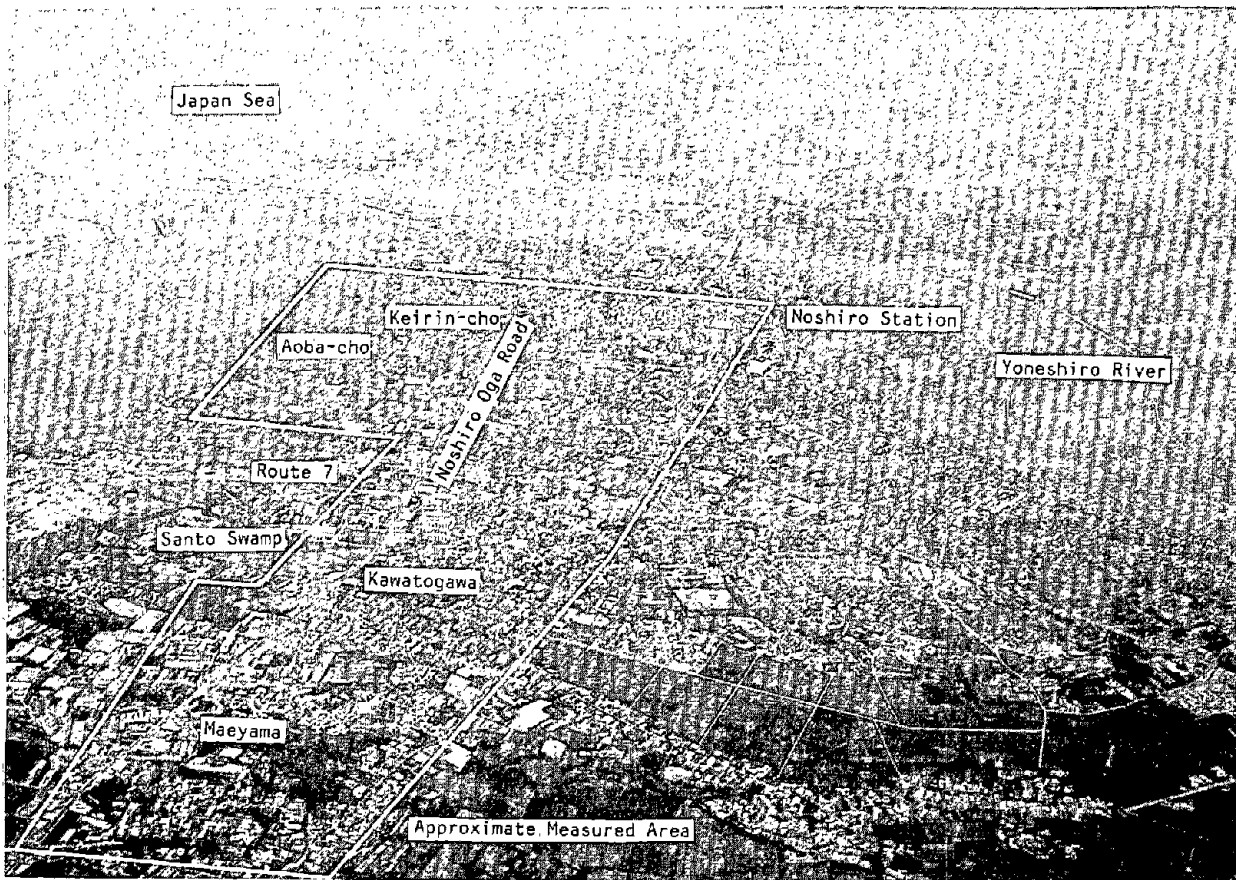


Photo 2 Aerial View of Noshiro City

4.0 PERMANENT GROUND DISPLACEMENTS AND RESULTING DAMAGE IN NOSHIRO CITY

Figure 4(a) and Photo 2 show the area over which permanent ground displacements were measured in Noshiro City. The area surrounded by the solid line in Photo 2, where damage to houses and buried pipes due to liquefaction and ground fissures was observed, is located between the sand dunes along the Japan Sea and the alluvial plain along the Yoneshiro River. As mentioned later in this report, the ground surface in this area has a slight gradient.

4.1 Zone I: Southern Area of Noshiro City

4.1.1 Permanent Ground Displacements and Ground Failures

Figure 5(a) and (b) show the permanent horizontal ground displacements measured in the southern part of Noshiro City. Contour lines in the figure represent elevations of ground surface above mean sea level, which were measured two years before the earthquake. It can be seen that a large area suffered ground displacements along the gentle slopes of the sand dunes. This area had recently been developed as a residential area.

A particularly large displacement occurred on the slopes of Maeyama, a sand hill about 10 m higher than the surrounding area (Figure 5(b)). On the northern slope of the hill, displacements began near the top and extended horizontally for more than 300 m in a northerly direction. The maximum horizontal displacement exceeded 5.0 m, and the direction of the displacements was almost parallel to that of the slope (perpendicular to contour lines).

The displacements on the southern slope of Maeyama extended horizontally for about 200 m from the top to a location near the road running east-west at the toe of the slope. The displacements on the eastern slope also extended to a location near the north-south road, where the ground surface was mostly flat.

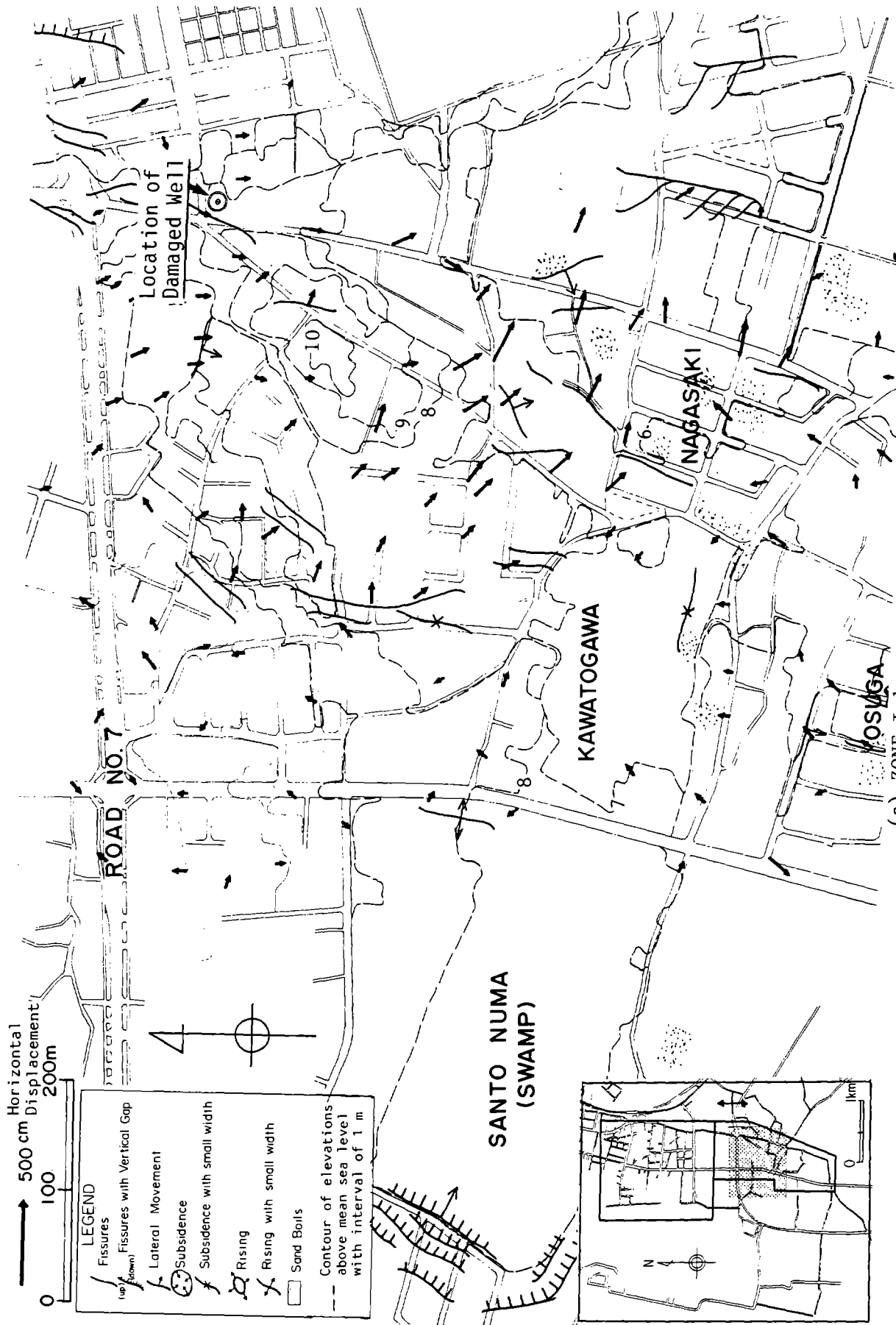
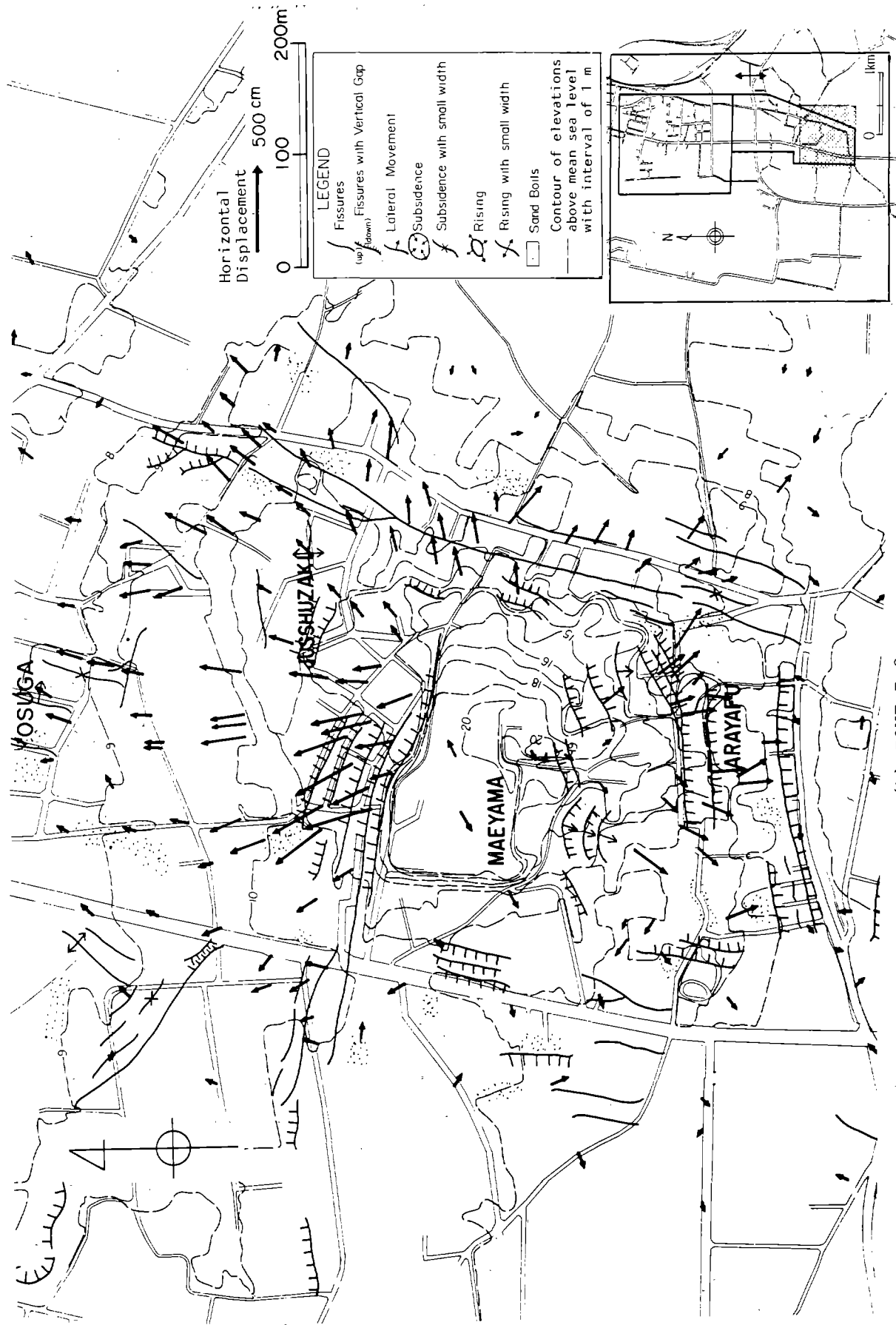


Figure 5. Permanent Ground Displacements in the Southern Part of Noshiro City (ZONE I)



(b) ZONE I-2
 Figure 5. Permanent Ground Displacements in the Southern Part of Noshiro City (ZONE I)

Figure 5 shows ground failures such as sand boils, fissures, subsidence and uplift, as investigated by the University of Akita. A considerable number of ground fissures and large areas of subsidence were found on the gentle slopes of Maeyama, and these caused serious damage to the residential area. In particular, many ground fissures were found on the upper part of the northern slope of the hill, where large tensile ground strains occurred because of the horizontal ground displacements. Details of permanent ground displacements and ground failures on the northern slope of the hill are shown in Figure 6. The numbers at the foot of the horizontal vectors show the vertical displacements of the ground. Photos 3, 4, and 5 are examples of the ground fissures and subsidence, showing the damage they caused to the residential area. The locations and the orientations of the photographs are shown in Figure 6. From Photo 3, which was taken in an easterly direction looking toward Maeyama, it can be seen that the ground surface had an undulating appearance. Most of the houses in this area were severely damaged, making them uninhabitable. Photos 4 and 5 show examples of the fissures along with the subsidence found in this area. The fissures were parallel to the retaining wall, which is shown in Figure 6.

It is notable in Figure 6 that the ground surface subsided by a maximum of about 1 m near the top of the sand dune slope where the horizontal ground displacements started, while the ground heaved at locations midway and at the foot of the slope. At these locations the ground displacements decreased in magnitude. Near the top of the slope, the number of sand and water boils was much less in spite of the many ground fissures. In contrast, sand and water boils were observed at locations midway and at the foot of the slope. These observations suggest that a considerable volume of liquefied soil shifted from the upper to lower portions of the slope, resulting in large ground displacement in the horizontal direction.

Interviews with residents of this area were conducted to gain information about the permanent ground displacements. A resident of the northern slope responded to a question about the duration of the earthquake by saying that she felt that the tremors continued for about 30 minutes because that was how long her house made noises. This witness suggested that the permanent ground



Photo 3 Undulating Ground Surface on the Northern Slope of Maeyama



Photo 5 Fissure with Subsidence on the Northern Slope of Maeyama

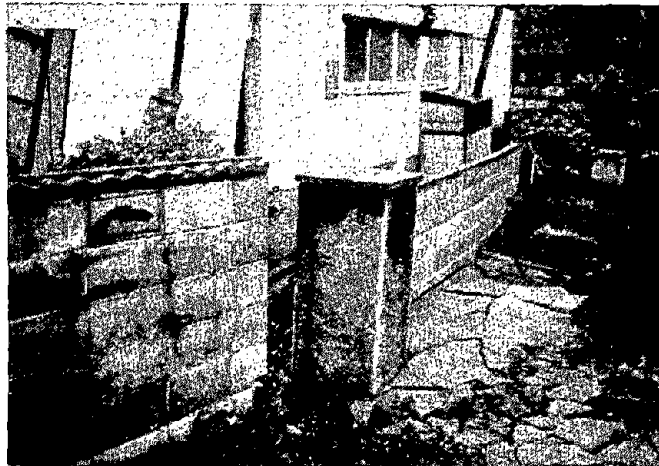
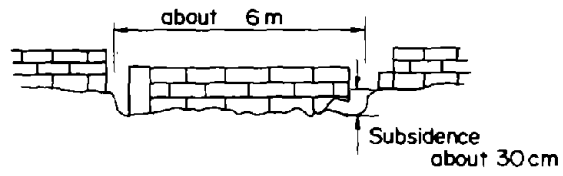


Photo 4 Fissure with Subsidence on the Northern Slope of Maeyama

displacements continued to occur for a long time after the tremors ceased; that is, until the excess pore water pressure was dispersed. Another resident of the area stated that the boundaries of real estate became unclear and many conflicts arose.

4.1.2 Soil Conditions and Estimated Liquefied Layer

Subsurface soil conditions were investigated to look into the causes of the permanent ground displacements. Standard penetration tests (SPT)⁴⁾ were conducted at 12 locations and Swedish weight sounding (SWS) tests were made at 134 locations in Noshiro City. In addition, the existing record of 50 SPT borings were collected to supplement the above soil investigations.

Based on these data, soil profiles along the section lines shown in Figure 7 were drawn. The layer of soil most susceptible to liquefaction along each section was evaluated by calculation of the Factor of Liquefaction Resistance F_L .⁵⁾ Soil with an F_L value less than 1.0 was considered to have liquefied.*

Figure 8 shows the subsurface soil conditions and the estimated liquefied layer along section lines S-5, 10, 13 on the slope of Maeyama, and one section line 17 at Nagasaki.** The horizontal displacements given in the figure are the components of the displacement vectors in the direction of the section. The subsurface consists of filled sand, natural levee, sand dune, alluvial sand, and alluvial clay. Some alluvial peat also appears along line S-17.

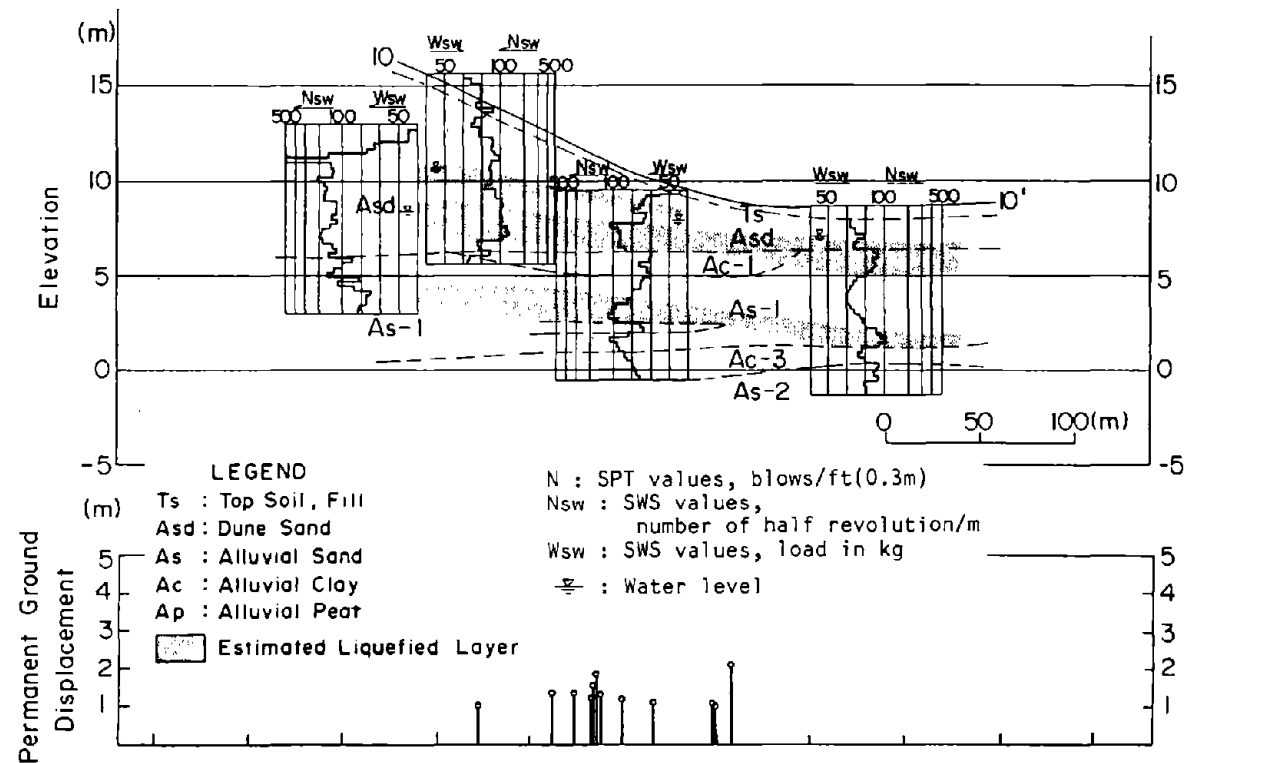
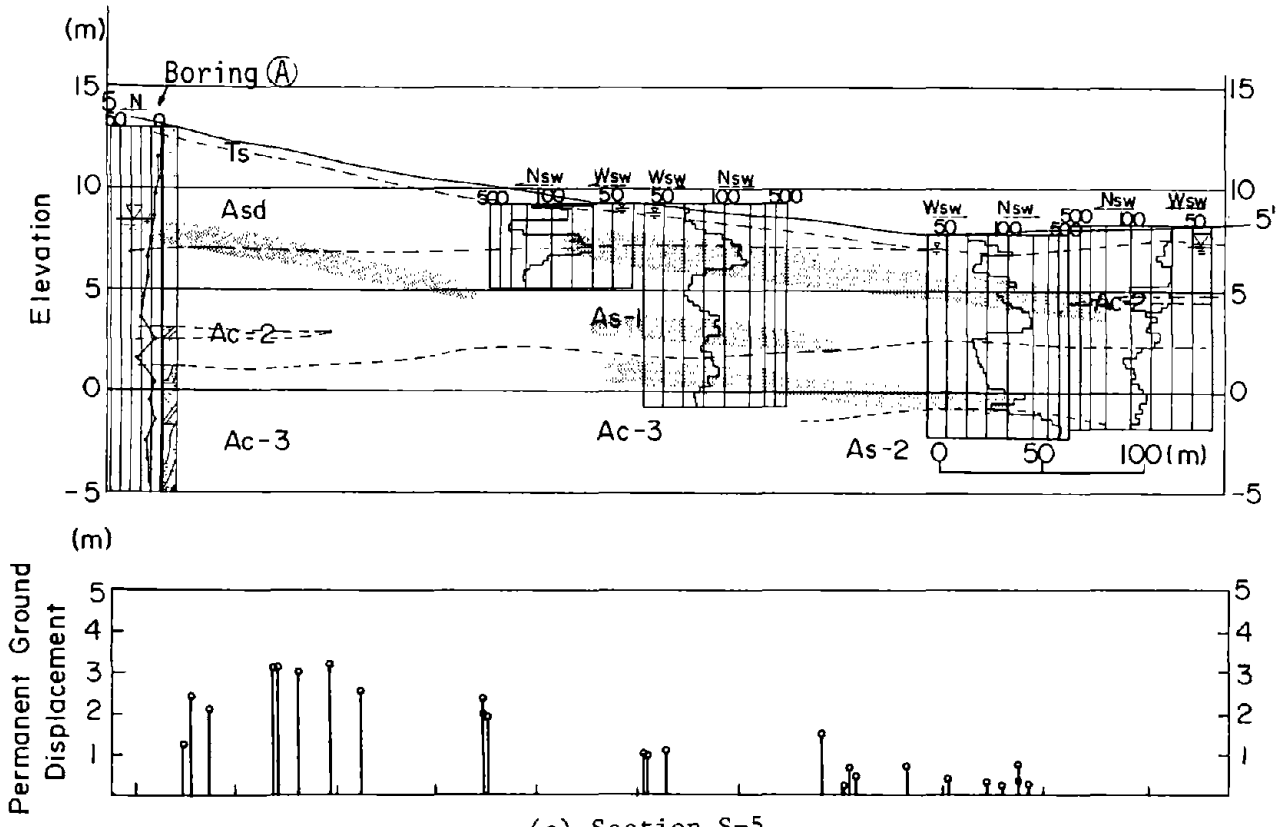
Along the section lines on the slope of Maeyama, the gradient of the ground surface is about 1 to 5%, but along section line S-17, the gradient is much less - below 0.5%. The estimated liquefied layers consist of two or three layers, some of which are separated, because silty layers, which are less

*See Appendix D of reference 5). The maximum acceleration on the ground surface, which is necessary for calculating F_L , was assumed to be 0.25 g with reference to the information summarized in Figures 1 and 3.

**Subsurface profiles along other sections are shown in Appendix B.



Figure 7. Section Lines for the Study of Soil Conditions (ZONE I)



LEGEND

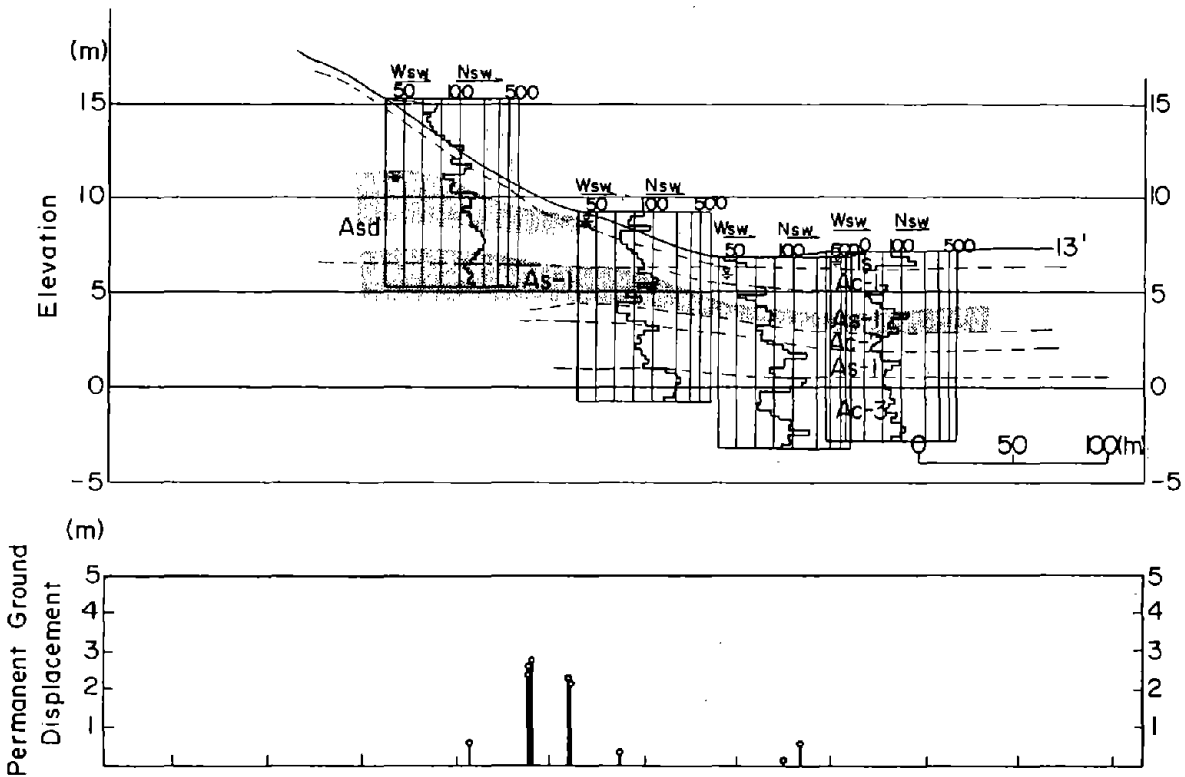
Ts : Top Soil, Fill
 Asd: Dune Sand
 As : Alluvial Sand
 Ac : Alluvial Clay
 Ap : Alluvial Peat

N : SPT values, blows/ft(0.3m)
 Nsw : SWS values, number of half revolution/m
 Wsw : SWS values, load in kg

☐ Estimated Liquefied Layer

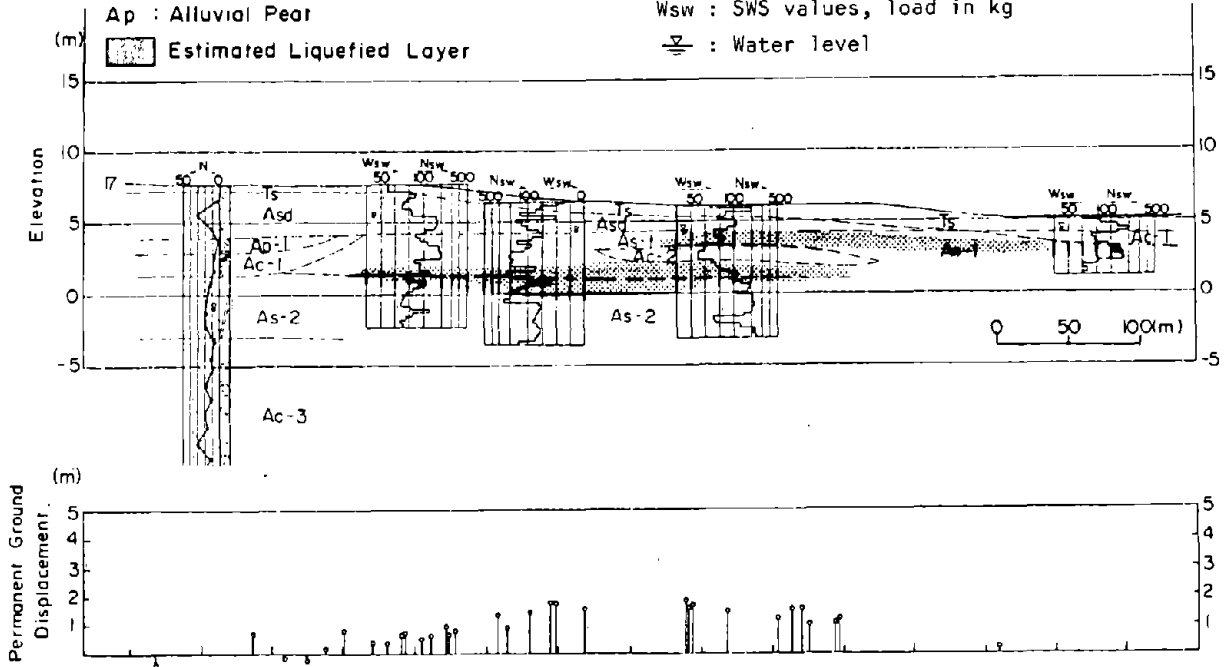
☉ : Water level

Figure 8. Soil Conditions and the Estimated Liquefied Layer



(c) Section S-13

- LEGEND**
- Ts : Top Soil, Fill
 - Asd : Dune Sand
 - As : Alluvial Sand
 - Ac : Alluvial Clay
 - Ap : Alluvial Pear
 - Estimated Liquefied Layer
 - N : SPT values, blows/ft(0.3m)
 - Nsw : SWS values, number of half revolution/m
 - Wsw : SWS values, load in kg
 - Water level



(d) Section S-17

Figure 8. Soil Conditions and the Estimated Liquefied Layer

prone to liquefaction, lie between the sandy layers. Along all the sections, liquefied soil layers with a total thickness of 2 to 5 m underlie the gently sloping ground surface where the gradient is less than 5%.

Generally speaking, the magnitude of the permanent ground displacement is larger where the surface gradient is large and/or the liquefied soil layer is thick. Therefore, the gradient of the ground surface and the thickness of the liquefied layer can be considered as influential factors affecting the magnitude of the displacement. However, at the top of the slope along section line S-5, the permanent ground displacement was over 3 m, but the estimated liquefied layer is not very thick. The ground water level, which considerably affects the estimation of the liquefied layer, was measured about one year after the earthquake at a point about 50 m away from section line S-5. There is a possibility that the water level was much higher just along the section line during the earthquake.

Correlations involving the magnitude of ground displacement, gradient of the ground surface, and thickness of the estimated liquefied layer are discussed in section 6.0 of this work.

4.1.3 Damage to Buried Gas Pipes and Well Casings

(1) Damage to Welded Steel Gas Pipes⁶⁾

A welded steel gas pipe with a diameter of 80 mm was damaged at four locations, as shown in Figure 9. The relationship between damage to the buried gas pipes and permanent ground displacements is discussed according to location with reference to the four points shown in the figure.

Point ① The pipe was damaged at a 22° elbow, as shown in Figure 10. Photo 6 and Figure 10 show that a bending crack occurred on the inside of the elbow. As shown in Figure 11, the ground south of the damaged point moved toward the south and southeast. It can be concluded that this ground displacement caused a tensile strain in the pipe and an excessive bending moment at the

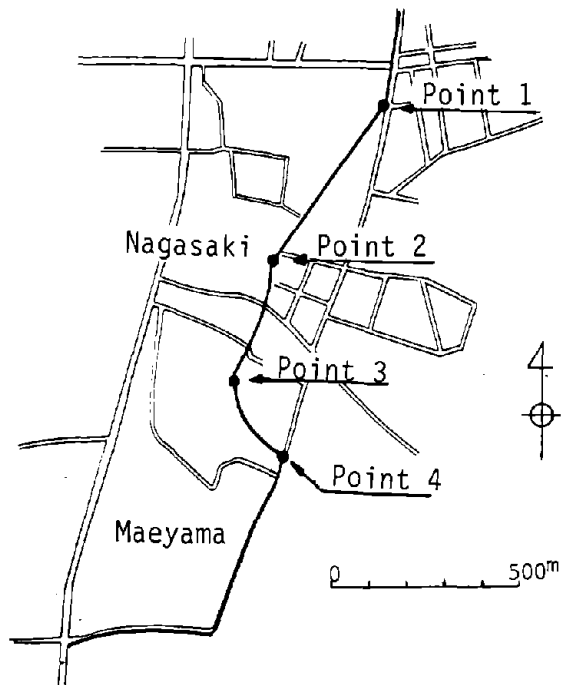


Figure 9. Locations of Damaged Gas Pipes

elbow portion, resulting in the crack.

Point ② The pipe was torn in the axial direction as shown in Photo 7. The two broken ends were driven into each other as shown in Figure 12. This failure was found at a small-angle bend portion (Figure 13). As for the engaged ends of the broken pipe, it may be conjectured that there were two stages to the failure process. The first stage was the severing of the pipe and its separation. The second was the driving together of the two broken ends under an excessive compressive load.

As shown in Figure 13, the ground moved northwest to the north of the damaged point, primarily perpendicular to the pipe axis. To the south, the ground moved north in the direction of the pipe axis. First, the pipe could have been broken by bending moment due to the lateral displacement of the ground to the north. Later, the pipe could have been compressed due to the axial displacement of the ground to the south, and the two broken ends then were driven into each other. If this hypothesis is correct, it can be concluded that there was a time lag in the occurrence of the two permanent ground displacements.

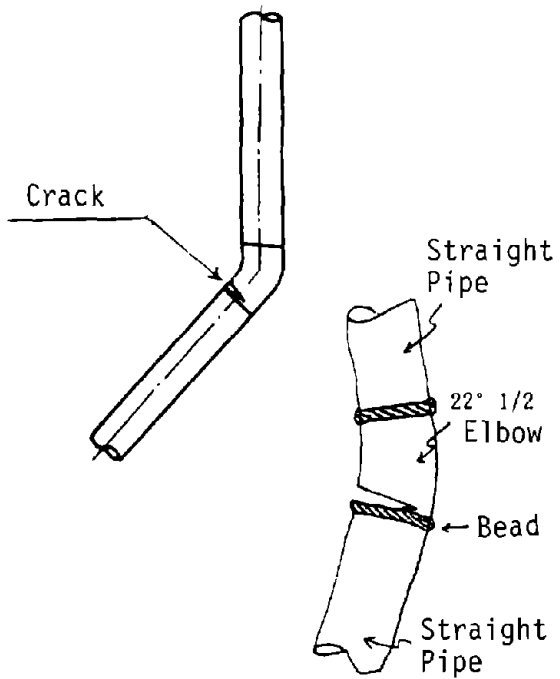


Figure 10. Damage to the Gas Pipe at Point No.1



Photo 6 Damage to the Gas Pipe at Point No.1

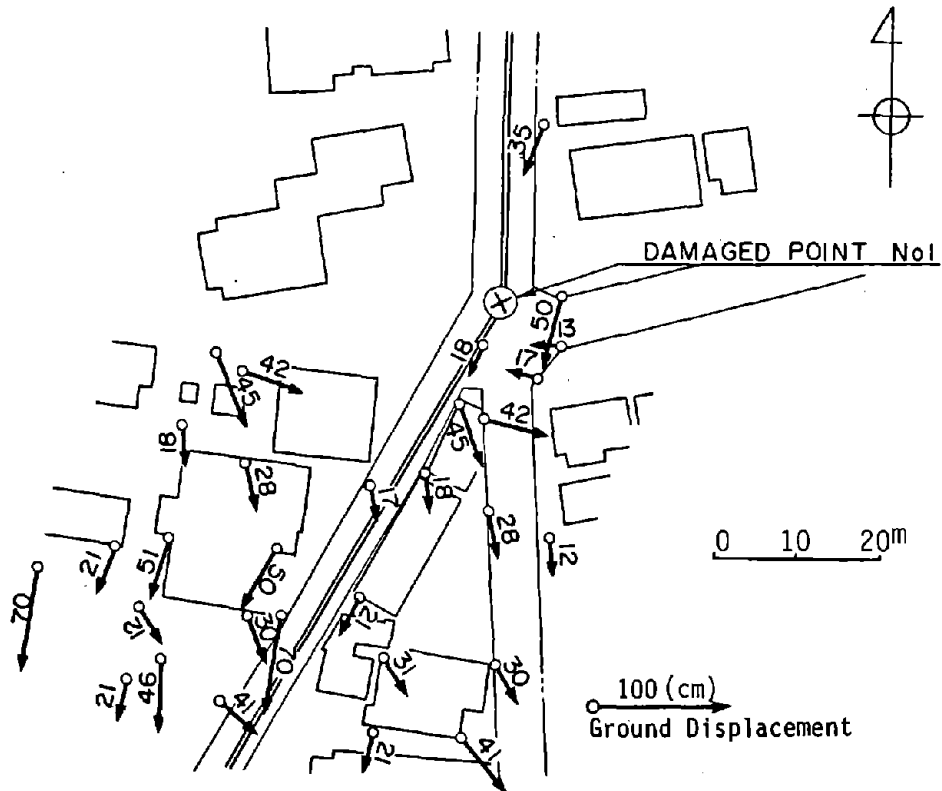


Figure 11. Permanent Ground Displacements in the Vicinity of the Damaged Gas Pipe (Point No.1)

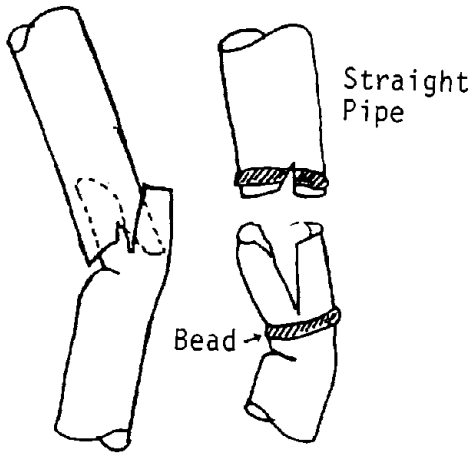


Figure 12. Damage to the Gas Pipe at Point No.2

Photo 7 Damage to the Gas Pipe at Point No. 2

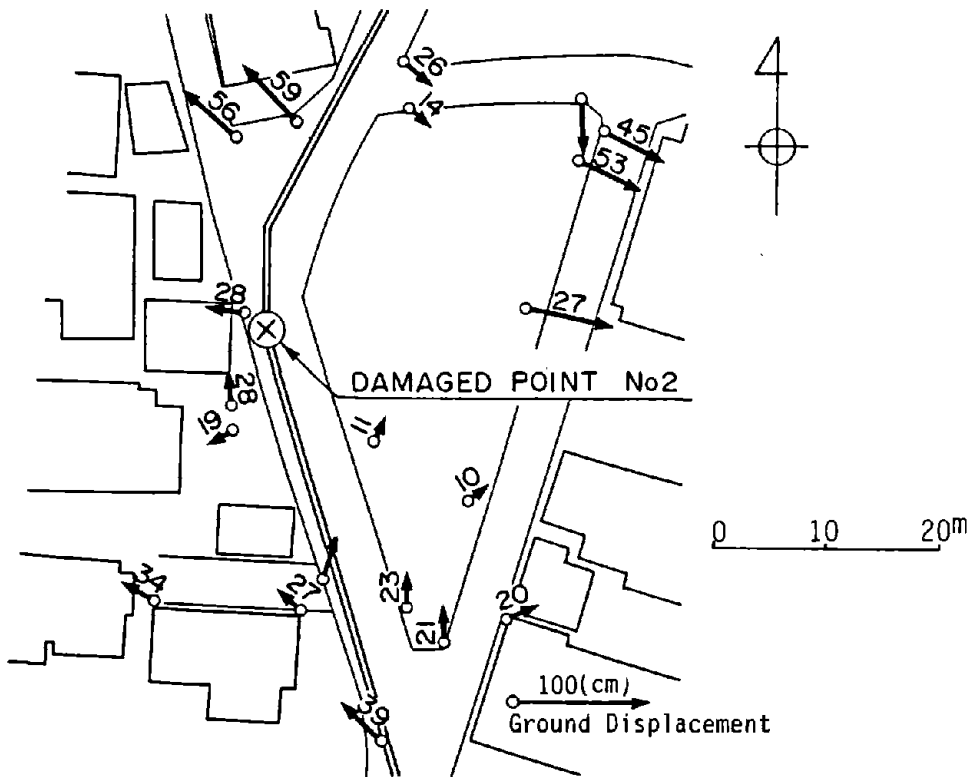


Figure 13. Permanent Ground Displacements in the Vicinity of the Damaged Gas Pipe (Point No.2)

Point ③ The pipe was found to have been severed by a tensile strain as shown Photo 8. The elliptical deformation of the pipe cross section, however, indicates that the pipe was compressed and bent at the elbow by a compressive force applied through the straight portion before separation. The separation of the severed ends was very slight, and the ends were mostly in contact with each other. This damage assessment shows that the pipe was first compressed and then put under tensile strain. As shown in Figure 15, the ground to the south of the damage point moved northwest, in the direction of the pipe axis, causing compressive strain in the pipe. However, ground displacement which could have caused tensile strain in the pipe apparently did not occur in the vicinity of the pipe.

As mentioned later, at Point ④, which is about 250 m southeast of Point ③, a large tensile force due to ground displacement was caused in the pipe. This force was enough to separate the pipe. It is probable that this tensile force affected the pipe at Point ③ also under the condition that the soil surrounding the pipe lost its stiffness due to the liquefaction. In this case, it is also necessary to assume that there was a time lag between the occurrence of the ground displacements in the vicinity of Point ③ and the ones at Point ④. However, in the case of Point ③, the possibility cannot be ruled out that the pipe was not fractured by the permanent ground displacements, but by the ground vibration, namely by a repetitious force.

Point ④ The pipe failed at the welded joint of a 45° elbow. It was discovered upon excavation that the two broken ends were separated by about 70 cm, as shown in Photo 9. A large bending moment at the elbow, due to tensile force applied from the straight portion of the pipe, caused the breakage. The permanent ground displacements along the damaged pipe were over 2.0 m to the north of the damaged point, and it was generally oriented outwards from the pipe axis, as shown in Figure 16. These ground displacements caused tensile stress in the pipe resulting in a large bending moment in the direction shown in Figure 16. Accordingly, the pipe was severed at the elbow by both a bending moment and tensile force. After that, the two severed ends moved separately, as illustrated by the solid line shown in Figure 17 due to slippage between the pipe and the ground caused by the release of the tensile force in the pipe.

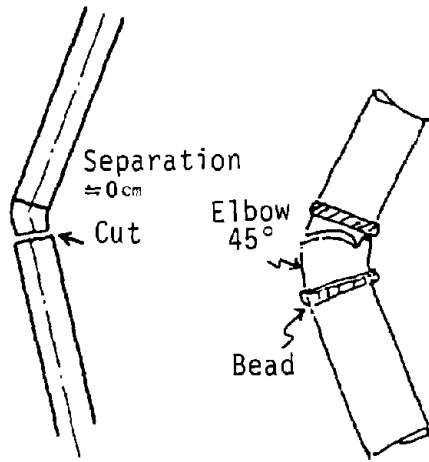


Figure 14. Damage to the Gas Pipe at Point No.3

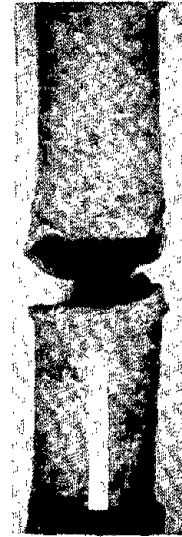


Photo 8 Damage to the Gas Pipe at Point No.3

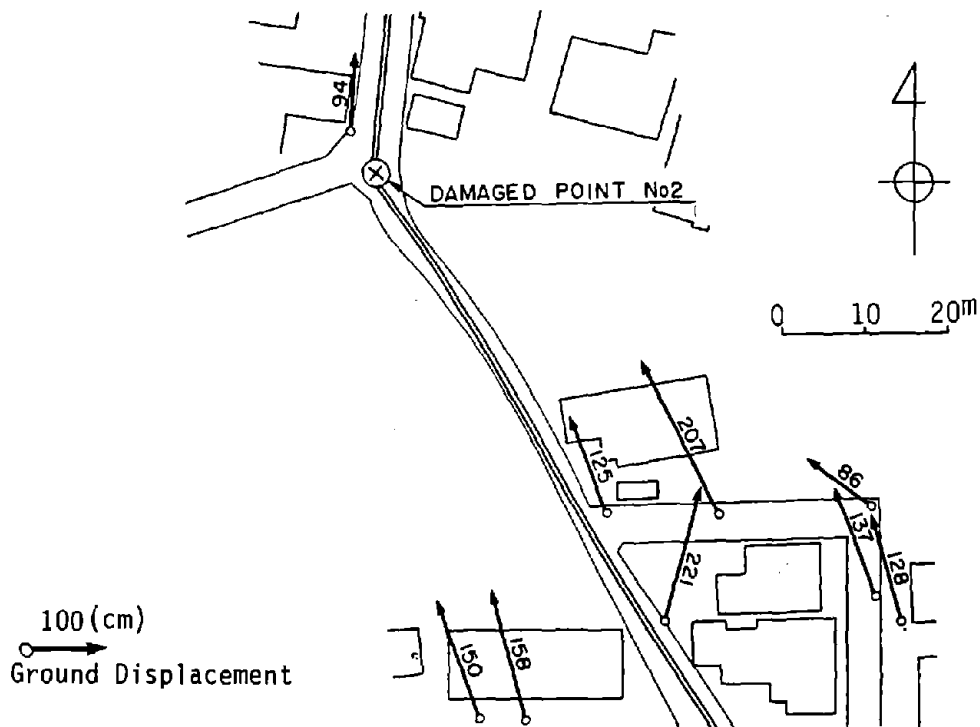


Figure 15. Permanent Ground Displacements in the Vicinity of the Damaged Gas Pipe (Point No.3)

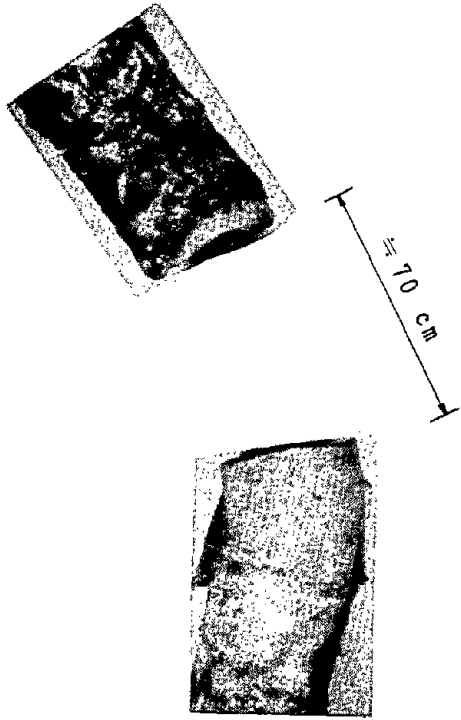


Photo 9 Damage to the Gas Pipe at Point No.4

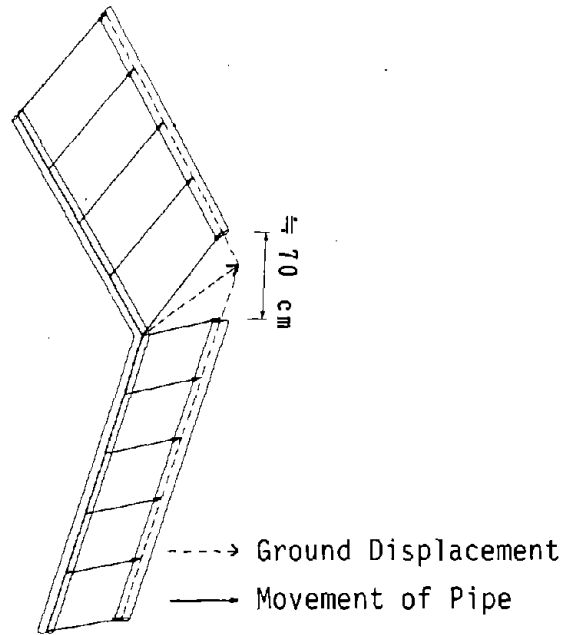


Figure 17. Movement of the two Broken Ends of the Pipe

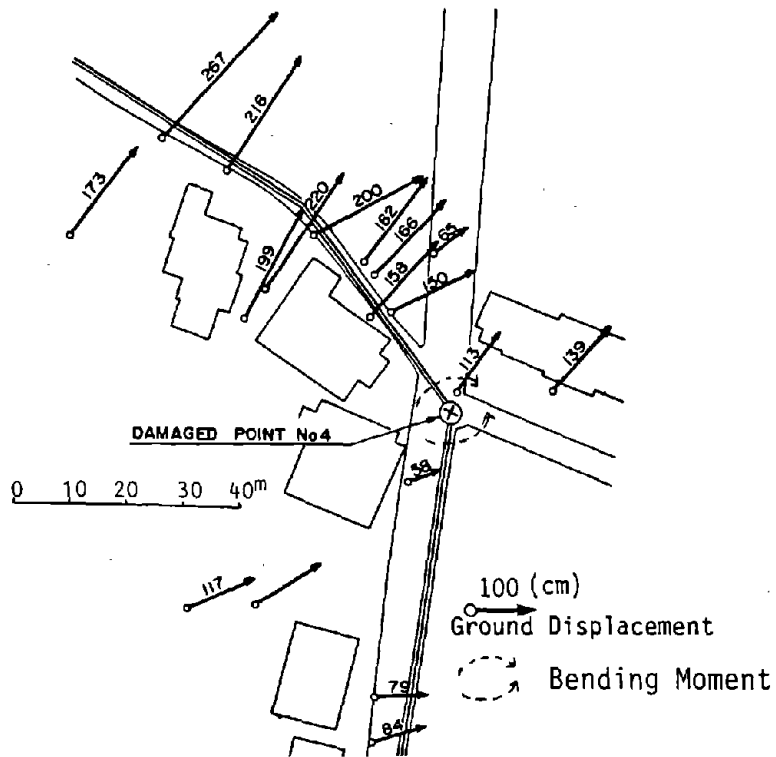


Figure 16. Permanent Ground Displacements in the Vicinity of the Damaged Gas Pipe (Point No.4)

As described above, the process by which gas pipes were damaged can be explained by taking into the consideration the effects of permanent ground displacements. However, it should be noted that other explanations are tenable, including one based on the dynamic forces caused by the earthquake motion itself.

(2) Damage to Well Casings

Many wells were damaged due to liquefaction and became unusable in Noshiro City. A typical example of damage to a well casing is shown in Photo 10, and illustrated in Figure 18(a). The location of the well is shown in Figure 5(a). The casing was bent at two positions. The upper one just about at the groundwater level and the lower one about 1.0 m below water level. There is no data from SPT borings nor Swedish weight sounding tests (SWS) in the vicinity of the damaged well. Figure 18(b) shows the data from the nearest SWS, which is about 100 m northwest of the well.

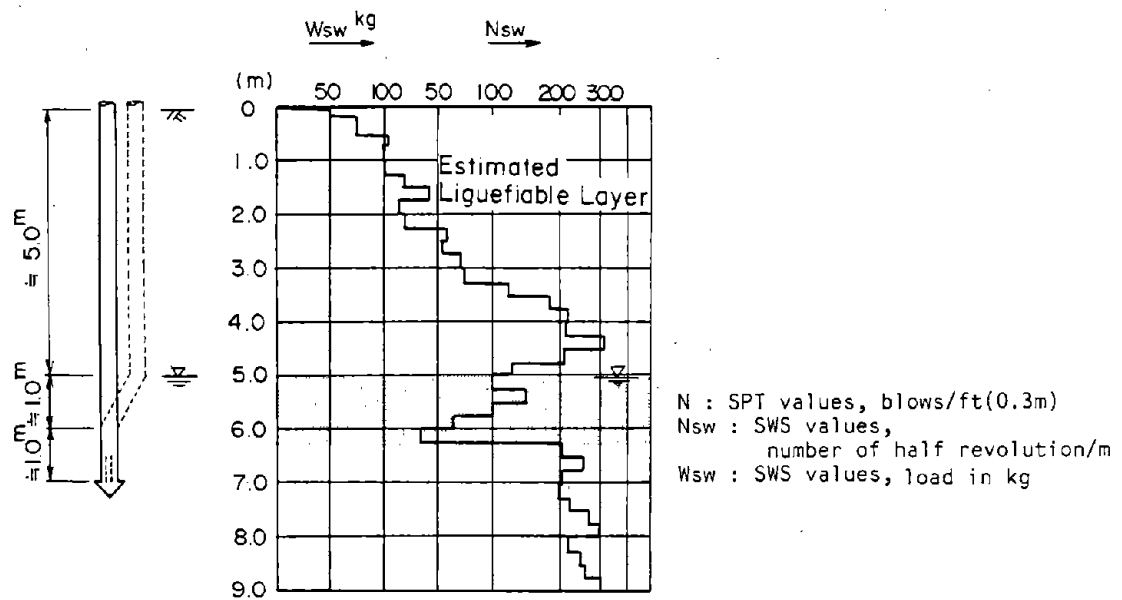
As mentioned previously, data from more than 100 Swedish weight sounding tests and about 60 standard penetration tests, including existing data, were collected in Noshiro City. According to these data the SWS value, N_{sw} , is found to be roughly ten times the SPT value, N . Figure 18(b) shows that a liquefiable layer exists between -5.0 m and -6.2 m. The upper boundary of the liquefiable layer, which is at ground water level,* coincides with the upper bend in the casing, while the lower boundary roughly coincides with the location of the lower bend.

The deformation pattern of well casings in Noshiro City is almost the same as the damage to foundation piles in Niigata City.³⁾ Through an investigation of the damage to piles and the soil condition in Niigata, it was concluded that liquefaction-induced ground displacements were the direct cause of the damage. As shown in Figure 5(a) the ground surface was displaced by about 1.0 m in a mostly southern direction. It also can be concluded that liquefaction-induced ground displacements bent the well casings.

*It should be noted that the ground water level was measured two years after the earthquake.



Photo 10 Damage to Well Casing



(a) Damage to Well Casing

(b) Result of Swedish Cone Penetration Test and Liquefiable Soil

Figure 18. Damage to Well Casing

4.2 Zone II: Northern Part of Noshiro City

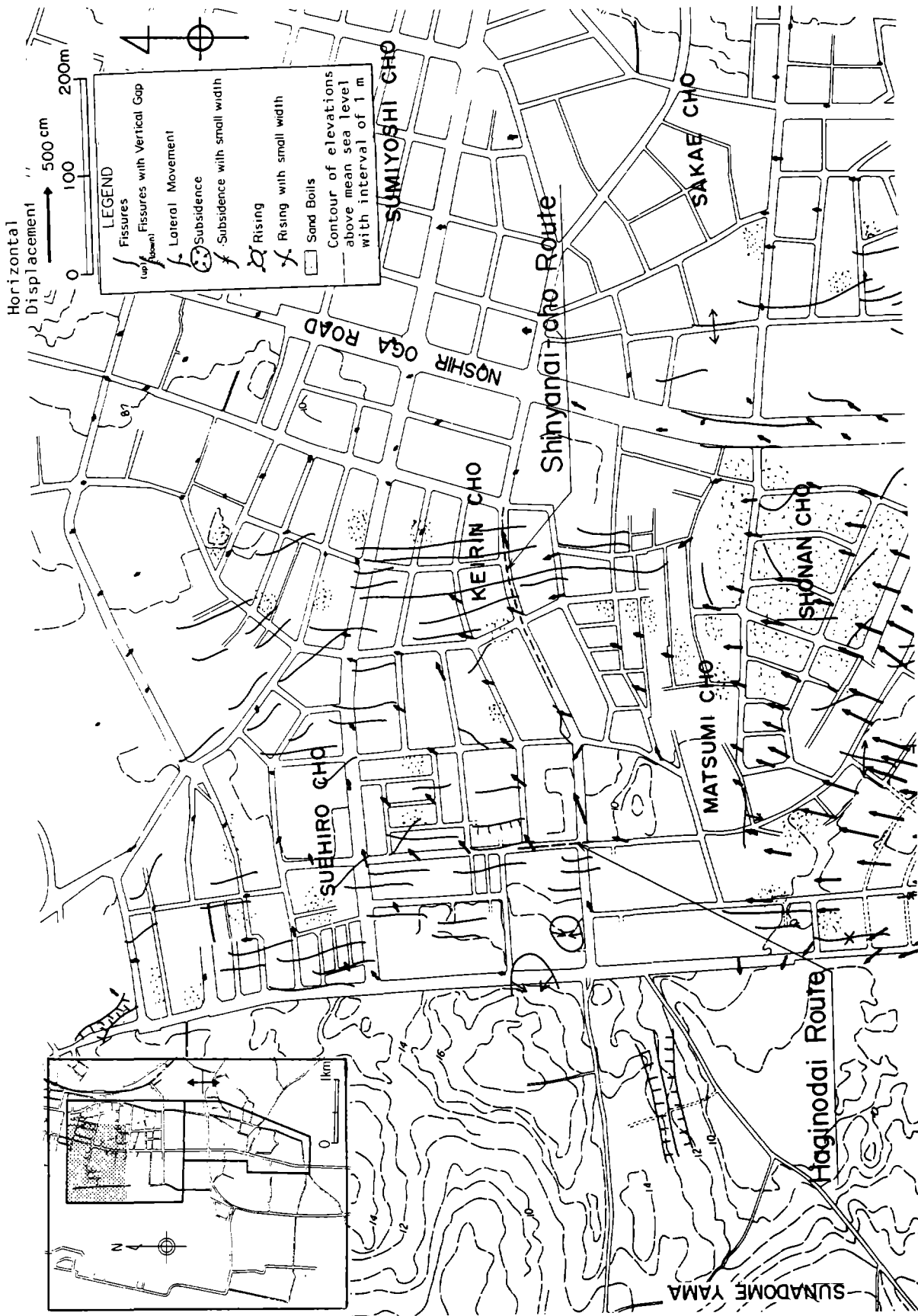
4.2.1 Permanent Ground Displacements and Ground Failures

The horizontal vectors of permanent ground displacements in the northern part of Noshiro City are shown in Figure 19. Contour lines in the figure represent elevations of ground surface above mean sea level, which were measured two years before the earthquake. Ground displacements were prominent on the west side of the Noshiro-Oga Road, which has a gentle gradient and forms the transition area between the sand dunes along the Japan Sea and the alluvial plain along the Yoneshiro River. The displacements began halfway down the sand dune, Sunadomeyama, and extended for about 800 m in a northerly and northeasterly direction. The maximum horizontal displacement was about 3 m on the slopes of Aoba-cho (Figure 19(b)). On the other hand, permanent ground displacements in the eastern area, on the east side of the Noshiro-Oga Road, an area mostly on the alluvial plain, were very small - less than 0.5 m.

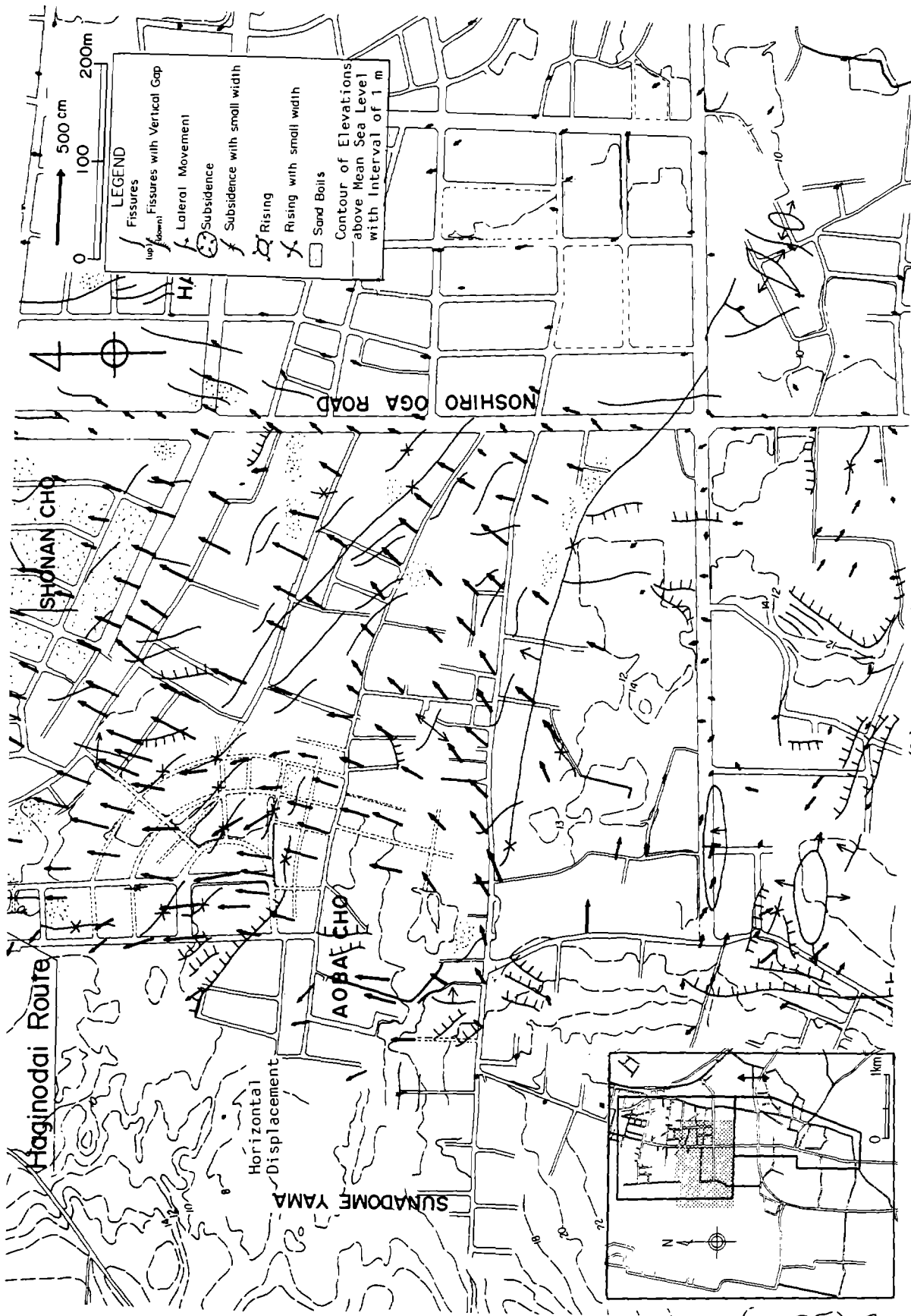
In the Aoba-cho and Shonan-cho areas, ground fissures running northwest-southeast were dominant (Figure 19(b)) and were generally perpendicular to the ground displacements. In the Suehiro-cho and Keirin-cho areas the ground fissures observed ran north-south (Figure 19(a)).

Figure 20 gives details of the permanent ground displacements from Aoba-cho to Shonan-cho. Many ground fissures occurred in the areas where the horizontal ground displacements began, while sand and water boils were observed in the area where the ground displacements decreased in magnitude. Photos 11 and 12 shows typical examples of ground fissures in the graveyard at Aoba-cho and the sand boils in Shonan-cho, respectively. The locations and the orientations of the photos are shown in Figure 20.

In the area upstream of the ground displacements, the ground surface subsided by a maximum of about 1 m (Figure 20). The subsidence of the ground surface downstream of the displacement was less, and at some measuring points, the ground surface rose up. These results mentioned above suggest that a certain



(a) ZONE II-1
 Figure 19. Permanent Ground Displacements in the Northern Part of Noshiro City (ZONE II)



(b) ZONE II-2

Figure 19. Permanent Ground Displacements in the Northern Part of Noshiro City (ZONE II)



Figutr 20. Permanent Ground Displacements and Ground Failures in Aoba-cho and Shonan-cho

amount of liquefied soil was transported from upper to lower elevations, resulting in large ground displacements.

These ground displacements caused large ground strains. Figure 21 shows the ground strains in the horizontal plane, as calculated from the measured ground displacements by the least squares approximation under the assumption that the ground strains were constant within each square cell (200m x 200m).*

The figure also includes results for the southern part of the city. On the northeastern slope of Sunadomeyama in the northern part of the city, large tensile strains occurred approximately in the direction of the slope. In the area near Shonan-cho and Matsumi-cho at the toe of the slope, compressive strains occurred. The maximum tensile and compressive strains in these areas were 1.7% and 1.5%, respectively. It should be noted that the ground strains are a mean value in a 200 m x 200m square cell. Similar results can be found on the slopes of Maeyama in the south. The upper sections of the slopes have dominant tensile strains, while compressive strains are notable on the lower slopes.

Photo 13 shows one interesting piece of evidence of the occurrence of large ground strain. The photo shows a tree split by the ground displacements in Aoba-cho.⁷⁾ The location and orientation of the picture are shown in Figure 22, along with the horizontal vectors of the permanent ground displacements in the surrounding area. Figure 22 also shows the permanent ground strains as calculated from the measured displacements. A large tensile strain of about 2% occurred in the vicinity of the tree, and the direction of the tensile strain coincides with that of the split. It can be conjectured that the tensile strain parted the roots of the tree, and the fracture extended to the trunk. Photo 14 shows another example of a large ground tensile strain, a wide fissure in the neighborhood of the split tree.

*See Appendix C.

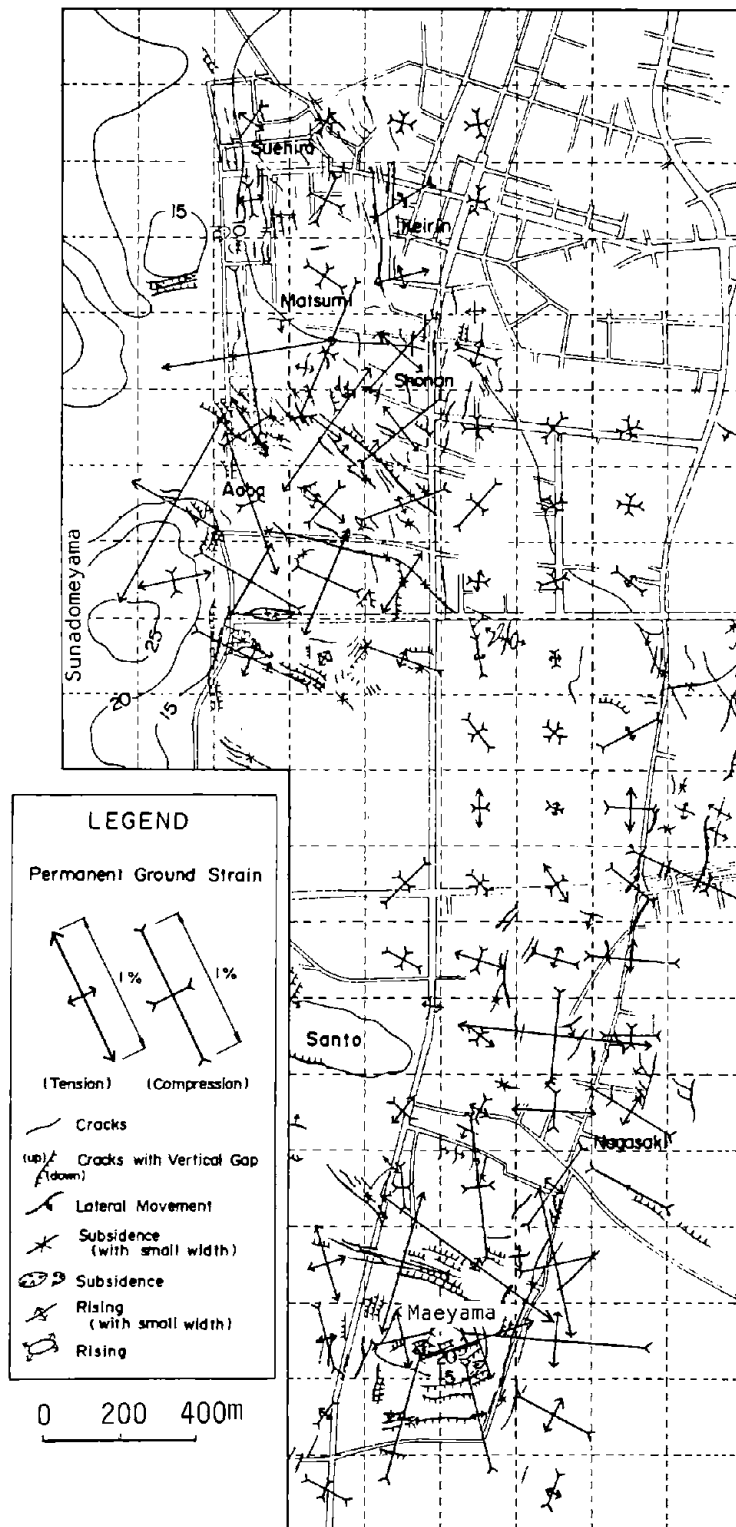


Figure 21. Permanent Ground Strains in Noshiro City



Photo 11 Ground Fissure in the Aoba-cho Graveyard

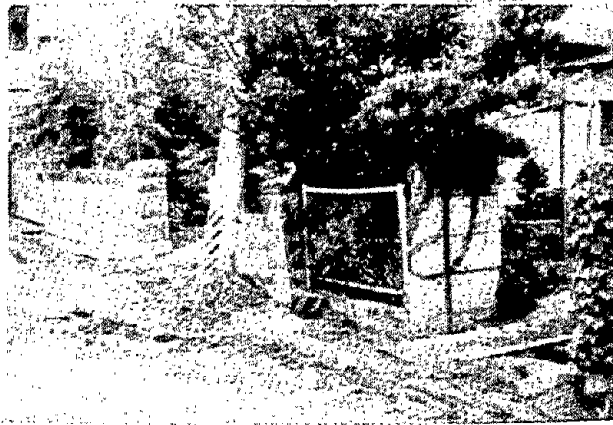


Photo 12 Sand Boil in Shonan-cho

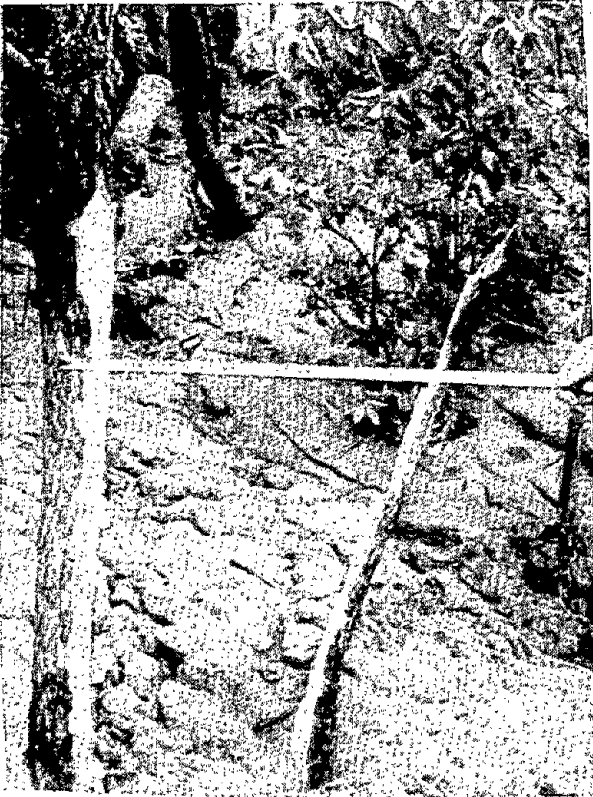


Photo 13 A Tree Split by Liquefaction



Photo 14 Ground Fissure in the Vicinity of the Split Tree

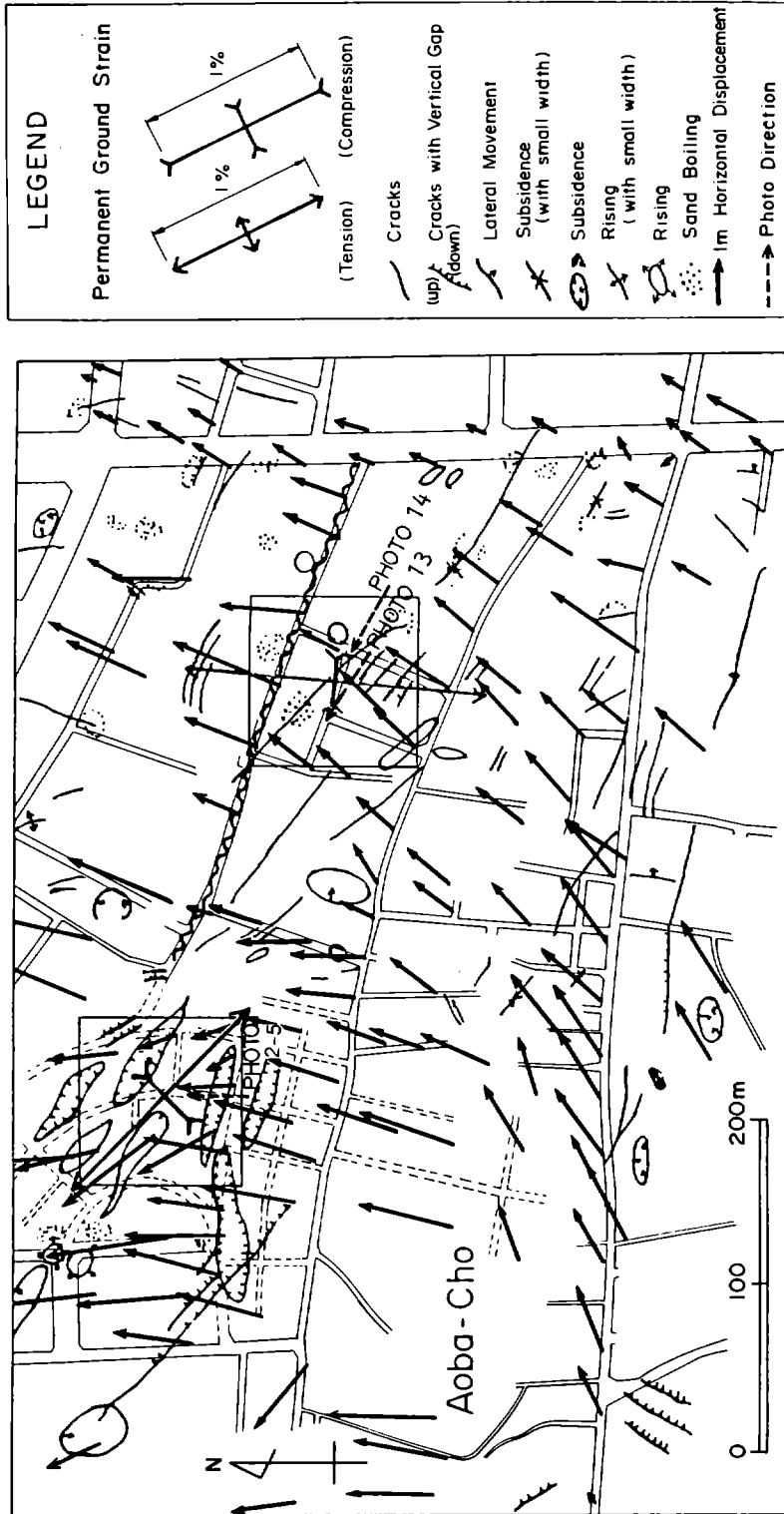


Figure 22. Permanent Ground Displacements and Strains in the Vicinity of the Split Tree

4.2.2 Soil Conditions and Estimated Liquefied Layer

Soil and geological conditions were investigated to study the factors which influenced the occurrence of permanent ground displacements. In-situ measurements with SPT and SWS were conducted, and existing borehole data were collected.

Soil profiles along the section lines shown in Figure 23 were drawn, and the liquefied layer was estimated by means of F_L .⁵⁾ Figure 24 shows the soil profiles and the estimated liquefied soil layer along section lines N-1, N-3, and N-7. Soil profiles along other section lines are shown in Appendix B. The subsurface soils consist of sandy fill, dune sand, alluvial sand and alluvial clay. The displacements shown in the figure are components of the horizontal vectors in the direction of the sections. The dune sand and the alluvial sand were estimated to have partially liquefied. The thickness of the liquefied layer was 1 to 5 m. The surface gradient in the northern area of the city is much less than that in the southern area, being less than 1.0%.

Along section N-7, the ground displacements are large in two areas. One is the upper slope, where the thickness of the estimated liquefied layer is comparatively large - about 4 m. The second is halfway up the slope where the surface gradient increases. Along section N-3, the maximum ground displacement occurred halfway up the slope at a location where the liquefied layer is thick and the ground surface gradient increases abruptly. However, the correlation between ground displacement, thickness of the liquefied layer, and surface gradient is not consistent. Along section N-1, the ground displacements are large at the top of the slope where the liquefied layer was comparatively thin and the surface gradient very small. At the halfway point up the slope along section N-1, the thickness of the estimated liquefied layer was over 5 m, but the ground displacement was less than 1.0 m.

A quantitative examination of the correlation between ground displacements and factors such as gradient of the ground surface, etc. is given in section 6.0.

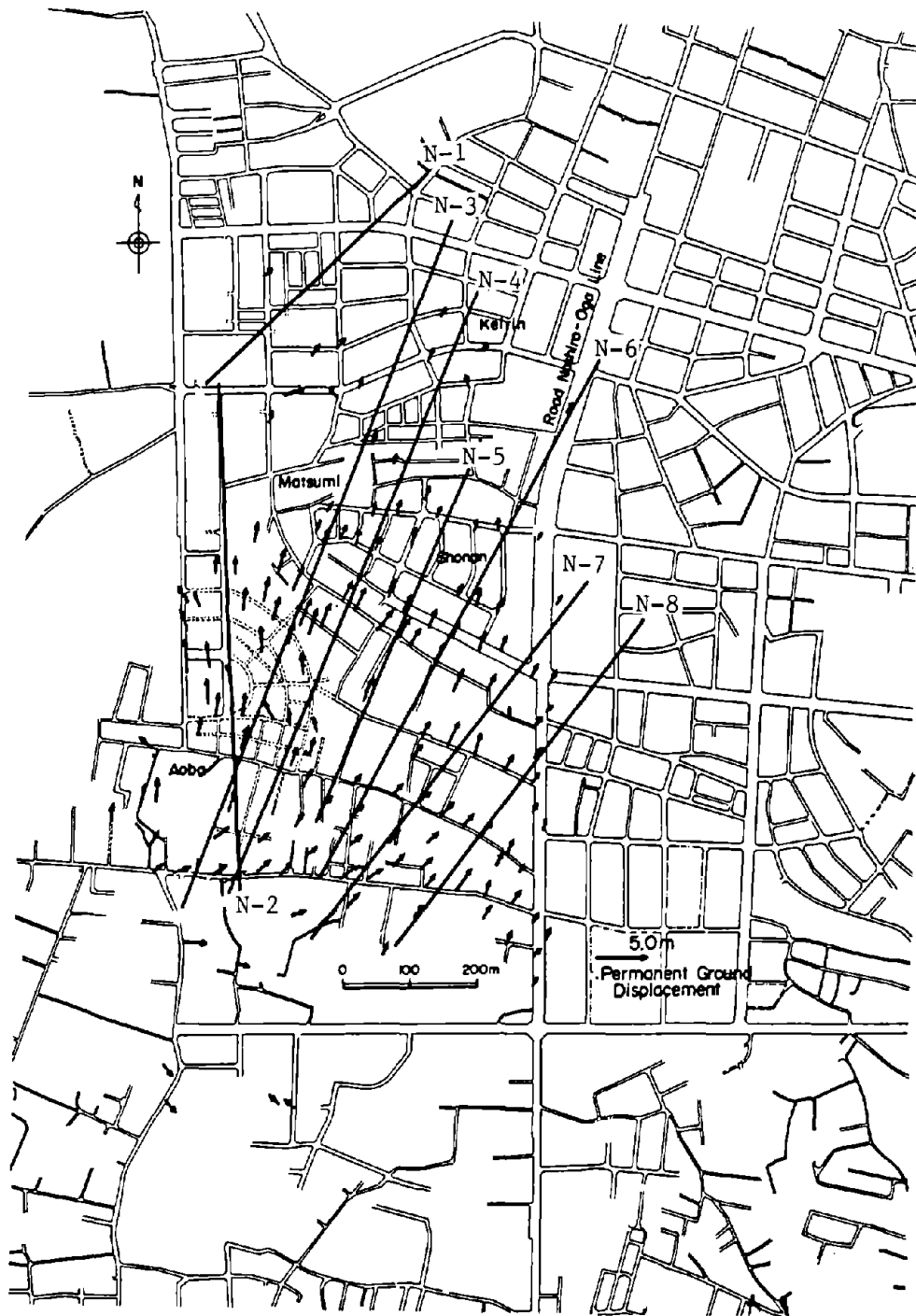
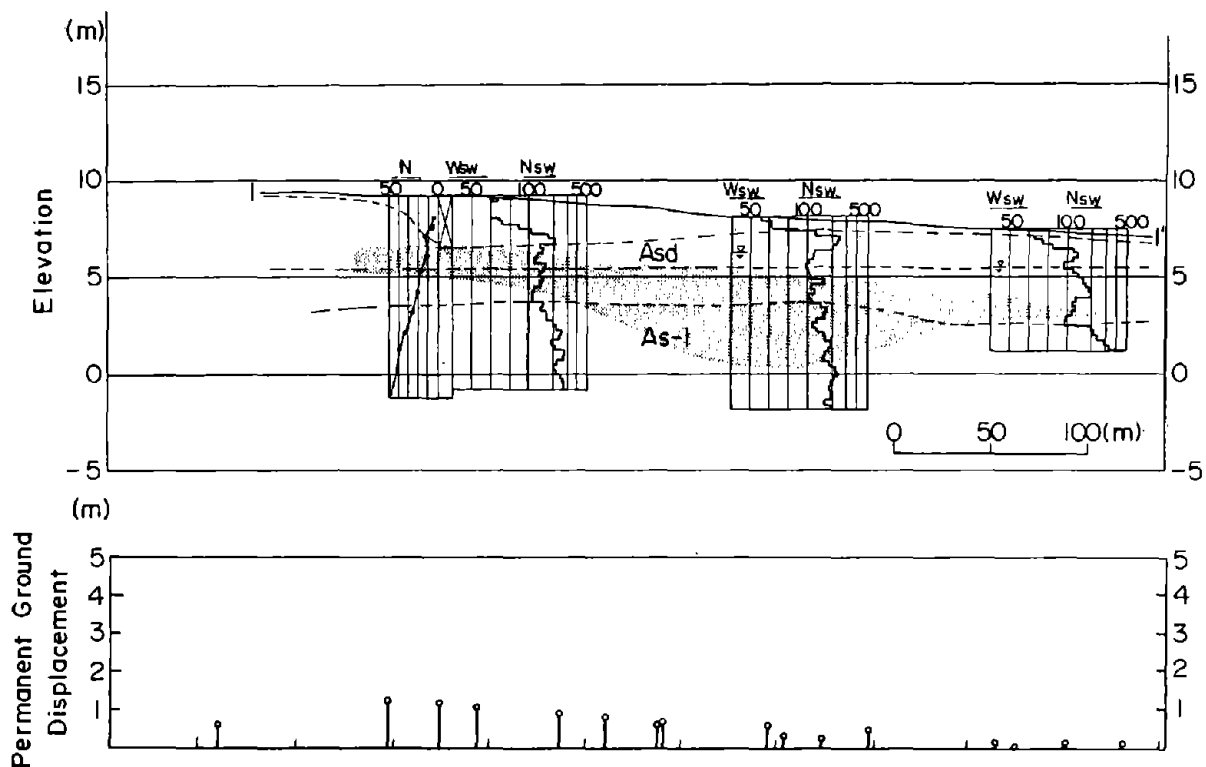


Figure 23. Section Lines for Survey on Soil Conditions (ZONE II)



LEGEND

- Ts : Top Soil, Fill
- Asd: Dune Sand
- As : Alluvial Sand
- Ac : Alluvial Clay
- Ap : Alluvial Pear

- N : SPT values, blows/ft(0.3m)
- Nsw : SWS values, number of half revolution/m
- Wsw : SWS values, load in kg
- ▽ : Water level

Estimated Liquefied Layer

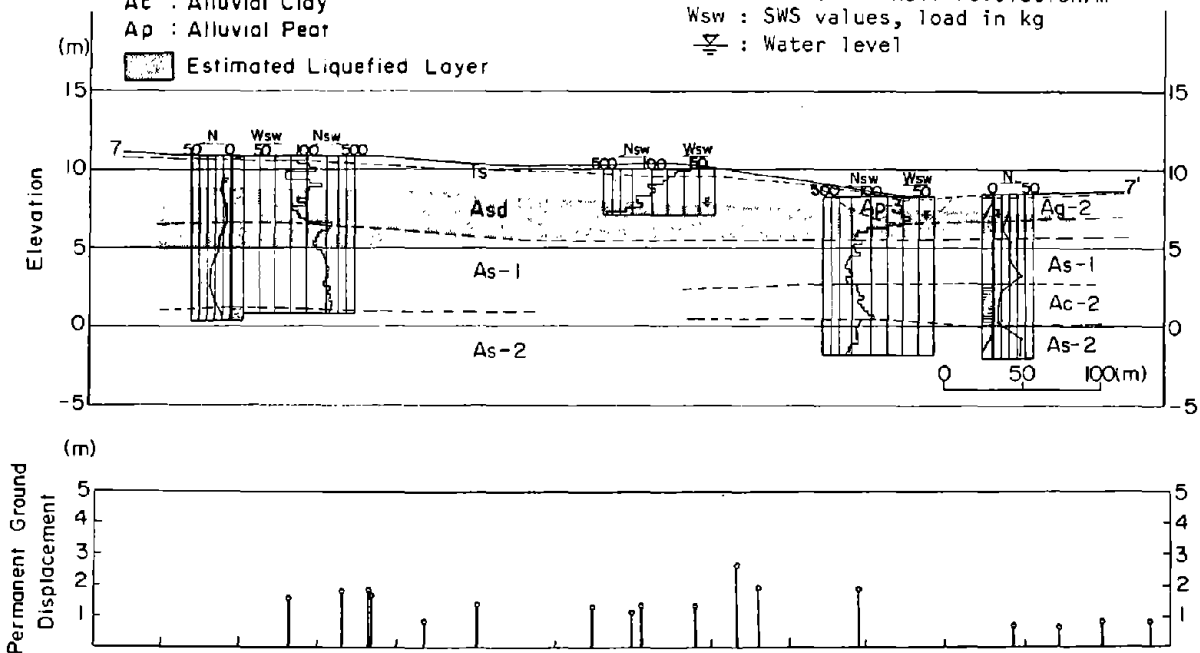
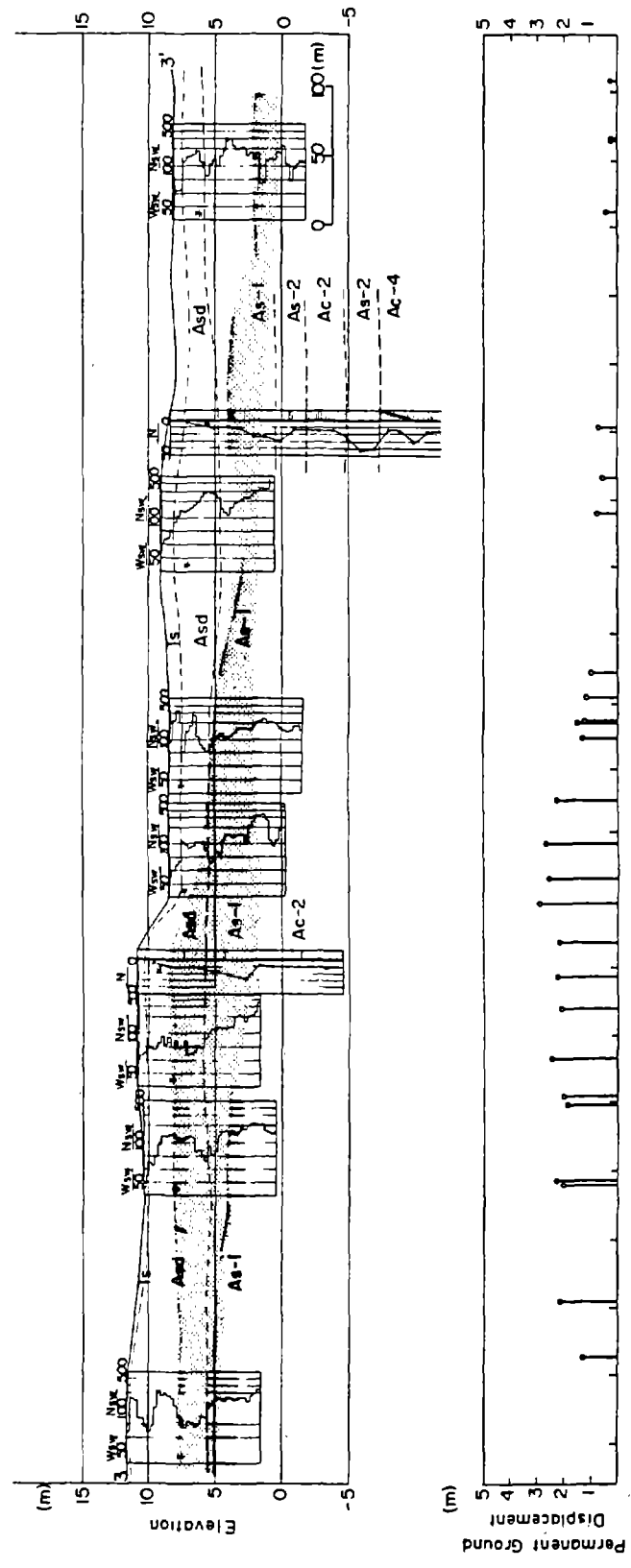


Figure 24. Soil Conditions and Estimated Liquefied Layer

N : SPT values, blows/ft(0.3m)
 Nsw : SWS values,
 number of half revolution/m
 Wsw : SWS values, load in kg
 -▽- : Water level

LEGEND
 Ts : Top Soil, Fill
 Asd : Dune Sand
 As : Alluvial Sand
 Ac : Alluvial Clay
 Ap : Alluvial Peat
 [Hatched Box] : Estimated Liquefied Layer



(b) Section N-3
 Figure 24. Soil Conditions and Estimated Liquefied Layer

4.2.3 Damage to Buried Pipes

(1) Damage to Telecommunications Conduits

Photo 15 shows the buckling of a steel conduit in which a telecommunications cable was severed. The diameter and thickness of the steel conduit with screw joints are 89 mm and 4 mm, respectively, while the diameter of the cable inside the conduit is 42 mm. The breakage occurred at the location shown in Figure 25, between the two manholes separated by a distance of about 250 m. In the vicinity of manhole No. 2, the ground was displaced to the right by about 1.5 m, predominantly in the axial direction. In the area of manhole No. 1, however, the ground displacements were nearly perpendicular to the direction of the conduit axis. This means that a compressive strain was caused along the conduit. Figure 25 also shows the strain as calculated from the measured ground displacements. This strain is compressive and has a magnitude of about 0.5%. It is conjectured that the conduit was easily buckled by such a compressive strain, given that the surrounding ground lost its strength due to the liquefaction.* Photo 16 shows the protrusion of the conduits at the two manholes No. 1 and No. 2, as a result of the compressive strain.

(2) Movement of Wastewater Pipes

Movement of wastewater pipes caused by the earthquake was measured along two routes, Shinyanagi-cho Route No. 1 and Haginodai Route No. 2 in Noshiro City at the time of reconstruction⁹⁾. The locations and orientations of the two routes are shown in Figure 19(a). As shown in Figure 26, the lateral distances between the straight line connecting two neighboring manholes and the pipe axis were measured. The pipes had been laid in a straight line between manholes before the earthquake. Therefore, the measured distances

*This conduit-buckling process was quantitatively simulated by using a beam model by T. Suzuki⁸⁾.

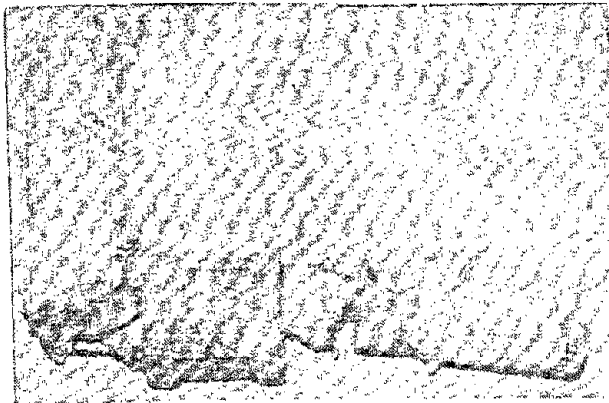


Photo 15 Bulking of Telecommunications Conduit

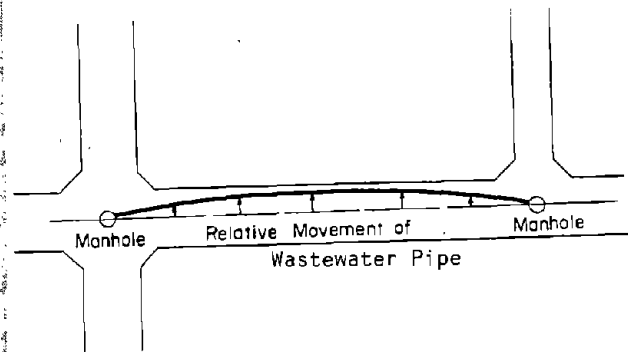


Figure 26. Measurement of Movement of Wastewater pipe

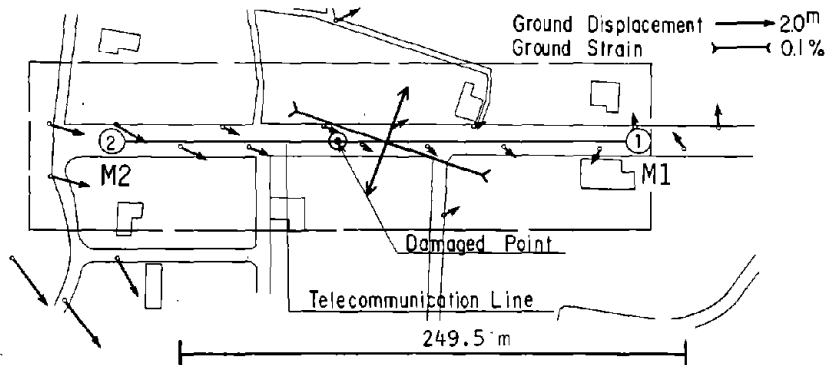
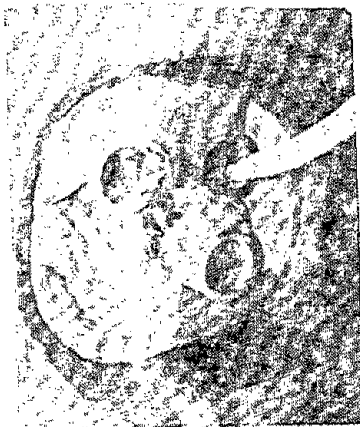
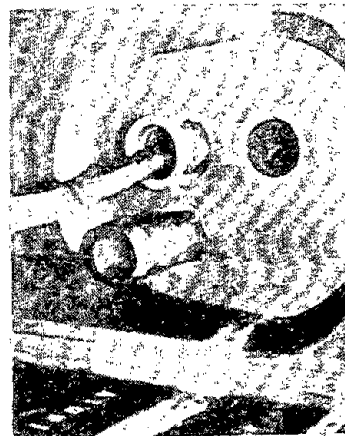


Figure 25. Permanent Ground Displacements and Strains in the Vicinity of the Damaged Telecommunications Cable



(a) Manhole No.1



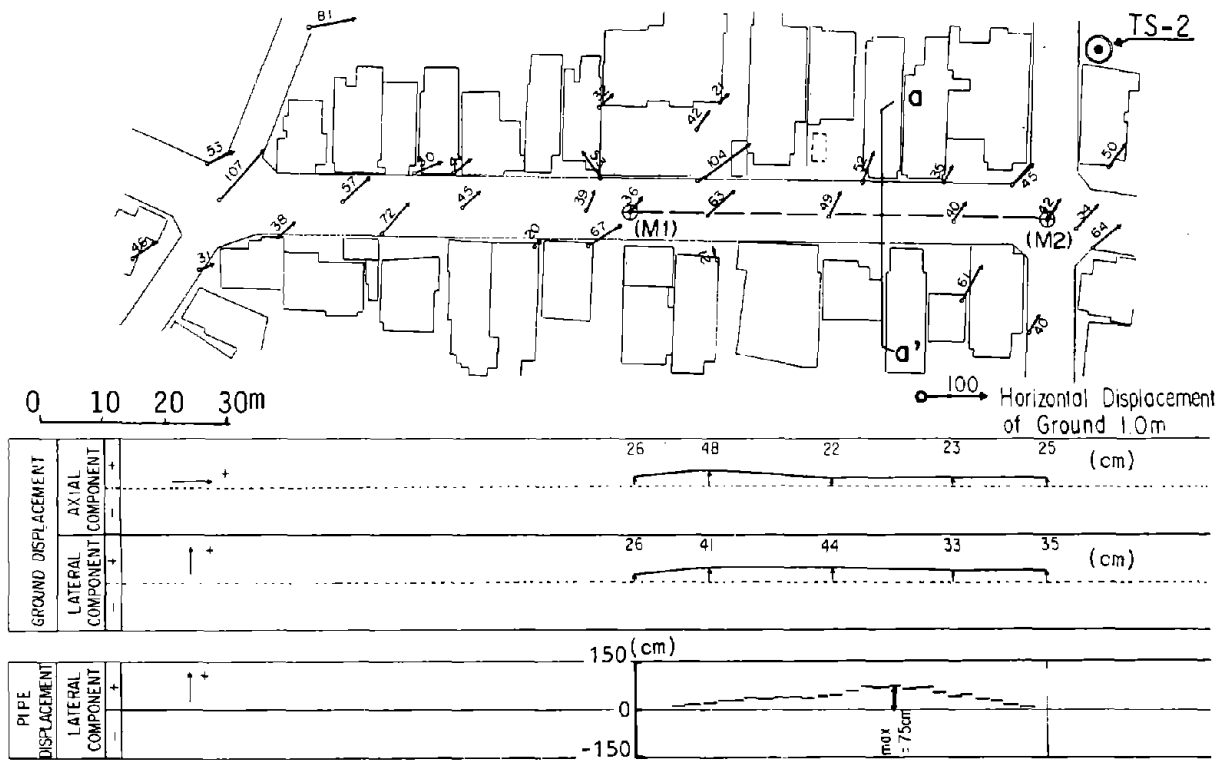
(b) Manhole No.2

Photo 16 Protrusion of Telecommunications Conduits into Manholes

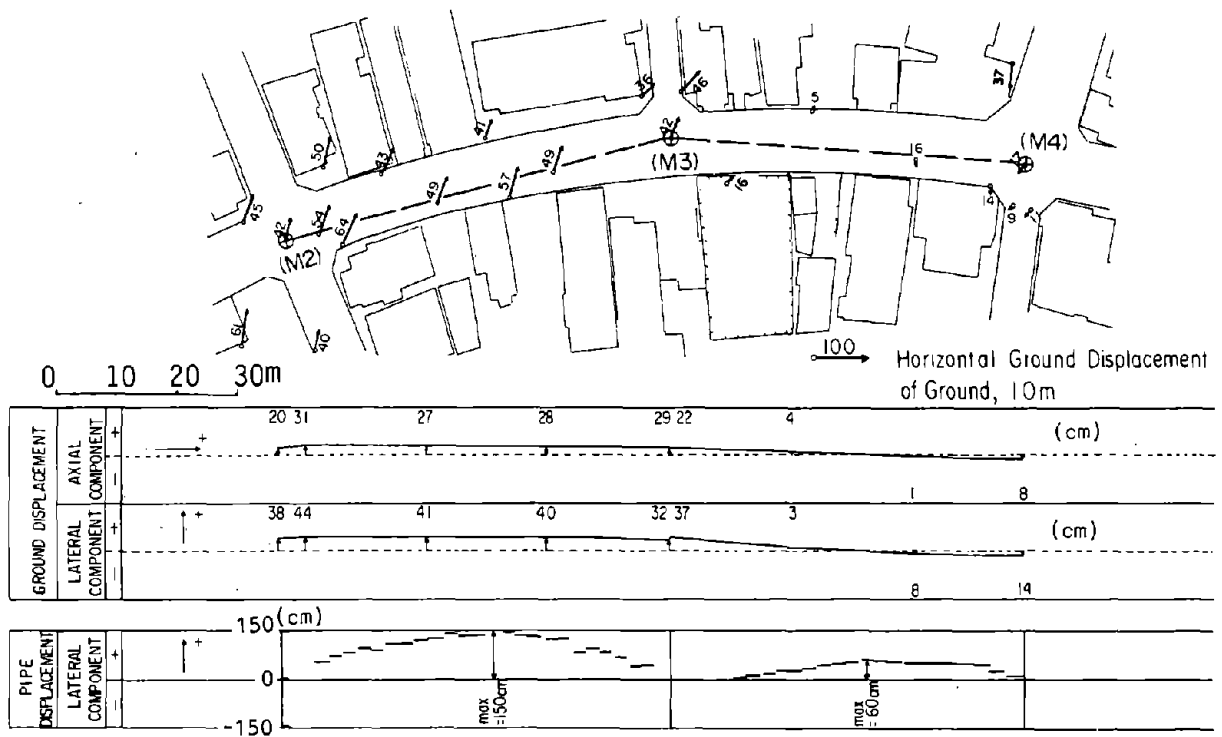
are the relative displacements of the pipes with respect to the manholes. Along the two routes, the displacements at the ground surface were also measured by aerial survey. The pipes were asbestos-cement pipes with diameters of 60 cm in Shinyanagi-cho Route and 30 cm in Haginodai Route.

Figure 27 shows the movement of the pipe along the Shinyanagi-cho Route in comparison with the permanent ground displacements at the ground surface. The figure shows the components of the ground displacements in the axial and the lateral directions. Between manholes No.1 and No.2 (Figure 27(a)), the lateral components of the displacements at the ground surface are 26 to 44 cm, but the maximum displacement of the pipes reached 75 cm. Here, it should be noted that the movements of the pipe were measured as relative displacements with respect to the two neighboring manholes. That means that the absolute displacement of the pipe was more than 75 cm. The results outlined in Figure 27(a) show that the pipes moved much more than the ground surface. Similar results were obtained between manholes No.2 and No.3 as well as between No.3 and No.4 (Figure 27(b)). Between No.2 and No.3, the maximum movement of the pipe reached 150 cm, but the displacements at the ground surface were about 40 cm. Figure 28 illustrates the pipe movement and the displacement at the ground surface in the cross section along line a-a' in Figure 27(a), where movement of the pipe was a maximum. The absolute displacement of the pipe is calculated to be 105 cm by adding the maximum relative displacement of 75 cm to the mean displacement of the two manholes, 30 cm. However, along line a-a' the displacement at the ground surface was measured to be only 38 cm.

A SWS test, the location of which is shown in Figure 27(a) as TS-2, was conducted in the neighborhood of the damaged wastewater pipes two years after the earthquake. The result is shown in Figure 28 along with the displacement of the pipe in the cross section. The subsurface mostly consists of dune sand. As mentioned previously, the SWS values, N_{sw} , is about ten times the N-value obtained from SPT borings. The results of the SWS in Figure 28 show that a liquefiable layer exists between -2.0 m and -6.5 m. The upper boundary of the estimated liquefied layer is at the groundwater level. The wastewater pipe was not in the estimated liquefied layer, but in the



(a) Manhole No.1-No.2



(b) Manhole No.2-No.4

Figure 27. Movement of Wastewater Pipe and Ground Displacements (Shinyanagi-cho Route)

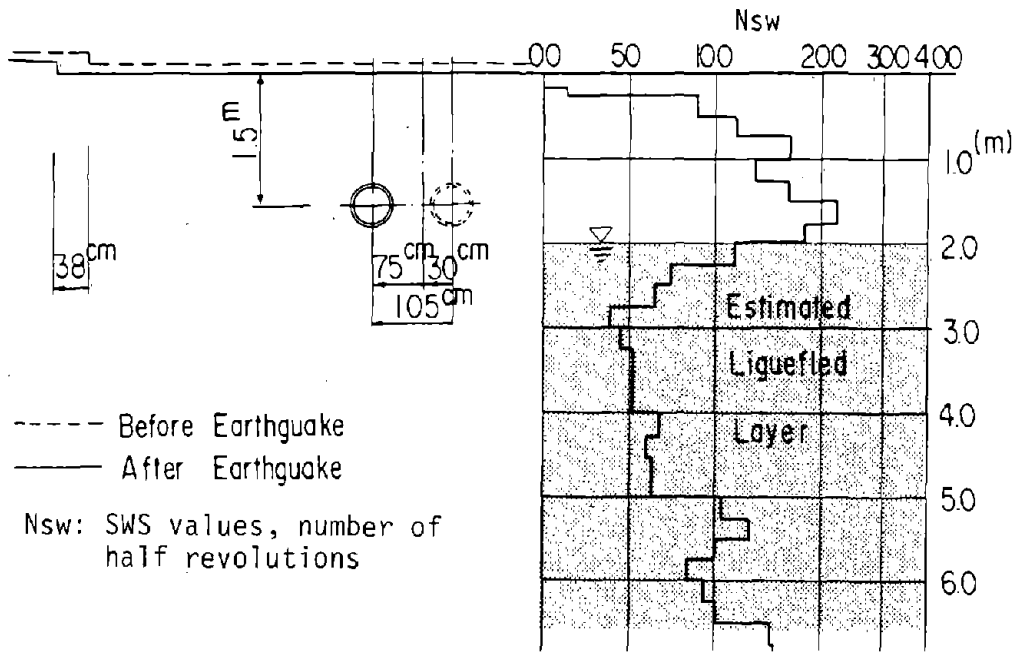


Figure 28. Movement of Wastewater Pipe and Ground Displacements in Cross-Section a-a'

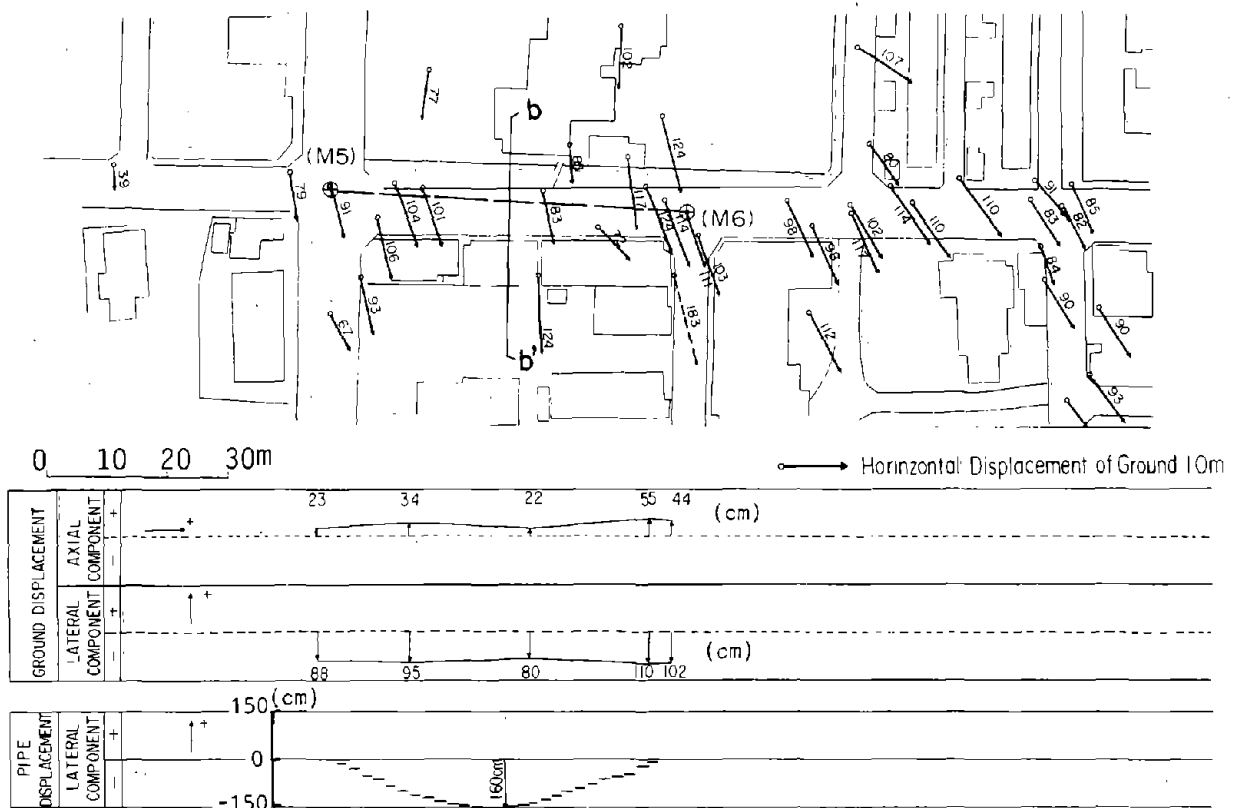


Figure 29. Movement of Wastewater Pipe and Ground Displacements (Haginodai Route)

overlying non-liquefied layer. It should be noted that the groundwater level was measured at the end of July, which was in dry season, two years after the earthquake. The earthquake occurred at the end of May. A possibility cannot be denied that the groundwater was at a higher level during the earthquake. Furthermore, it is probable that some of the soil above the groundwater liquefied due to the upward permeation of the groundwater. If this hypothesis is correct, the results shown in Figures 27 and 28 suggest that the liquefied layer moved much more than the non-liquefied layer nearer the ground surface.

Similar results were observed along Haginodai Route, as shown in Figures 29 and 30. Figure 29 shows that the maximum movement of the pipe was 160 cm, but the ground displacements in the lateral direction were limited to 80 to 110 cm. Figure 30 shows the pipe movement in cross section b-b' in comparison with the displacement of the ground surface. The total displacement of the pipe is estimated to have been 255 cm, a figure arrived at by adding the relative displacement between the manholes and the pipe, 160 cm, to the mean displacement of the manholes, 95 cm. On the contrary, the displacement at the ground surface was limited to only 82 cm. Figure 30 also shows the soil profile with N-values at a site about 50 m north of the wastewater pipes. The subsurface consists of sandy fill and the sand dune. The groundwater is located at -1.7 m below the ground surface, and the soil layer between -1.7 m and around 4.2 m can be judged to have liquefied.* The wastewater pipe was located in this liquefiable layer.

Phenomena similar to the above were reported in the case study on the 1964 Niigata earthquake³⁾. The reinforced concrete foundation piles of the Niigata Family Court House Building were severed at two depths. At the upper breakage point, which roughly coincided with the boundary between the estimated liquefied layer and the upper non-liquefied layer, the piles were completely parted and separated into blocks. The lower block moved more

*It should be noted that since the groundwater level was measured two years after the earthquake, the upper boundary of the liquefiable layer may have altered.

than the upper block. This suggests that the liquefied layer was displaced more than the upper non-liquefied layer. Furthermore, a gas company engineer in Niigata City found gas pipes underneath the drainage ditches along the road after the earthquake. These pipes had been laid away from the ditches.

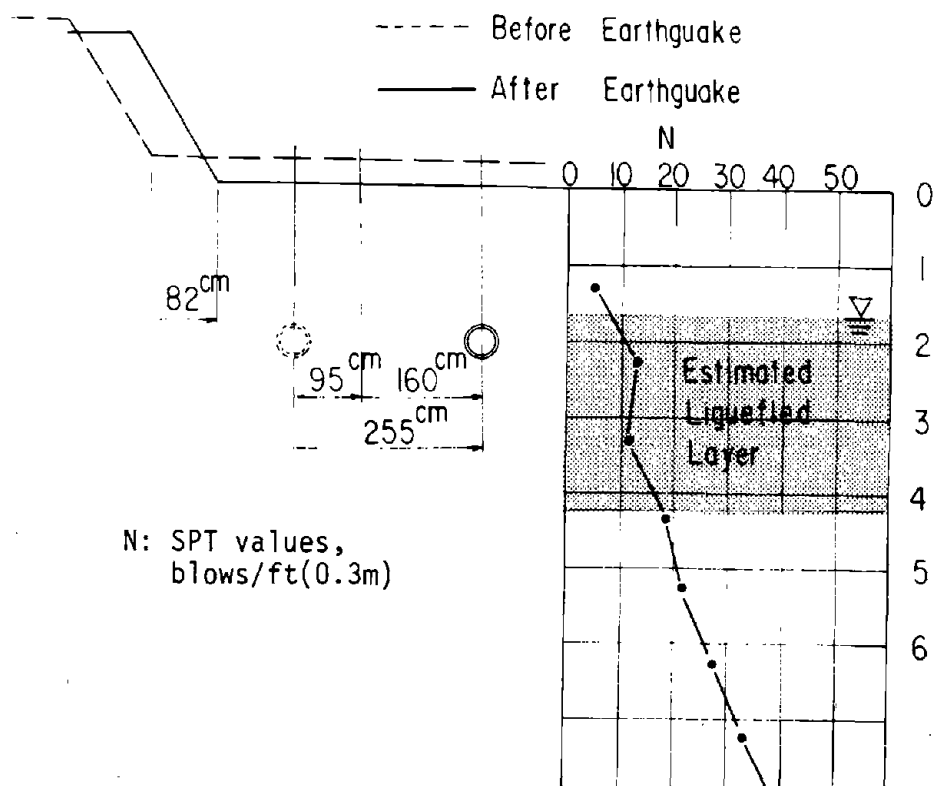


Figure 30. Movement of Wastewater Pipe and Ground Displacements in Cross-Section b-b'

5.0 CORRELATION ANALYSIS OF RATE OF DAMAGE TO HOUSES AND BURIED PIPES WITH PERMANENT GROUND DISPLACEMENTS AND STRAINS

In this section, the correlation between the damage rate to houses and buried pipes, and the permanent ground displacements and the permanent ground strains, as calculated from the measured displacements, is discussed.

5.1 Correlation of Rate of Damage to Houses and Buried Pipes with the Magnitude of Permanent Ground Displacements

As mentioned previously, houses and buried pipes in Noshiro City sustained severe damage during the 1983 Nihonkai-Chubu earthquake. In this section, the correlation between the magnitude of the permanent ground displacements and the damage rate to houses and buried pipes is examined.

Permanent horizontal ground displacements were measured at about 2,000 points in Noshiro City, and the damage to houses and buried pipelines was thoroughly investigated by the city government.⁷⁾ These data were analyzed for the correlation study using the following procedure:

(i) The area of Noshiro City, where the permanent ground displacements were measured, was divided into 100 m-square cells, as shown in Figure 31. The mean value of the permanent ground displacements measured within each cell was calculated, disregarding the directions of the displacement vectors.

(ii) In cases where the amplitudes and directions of displacement vectors in adjacent cells are similar, they were combined to form one block, from which one mean value of the ground displacement was calculated. The reason for doing this was to increase the number of samples of damage to houses and buried pipes in one block, thereby improving the reliability of the results of the correlative analysis between the damage rate and the permanent ground displacement.

(iii) The rate of damage to buried pipes was calculated as the number of damage points per kilometer in each cell or block, and the rate of damage to houses was obtained as a ratio of the number of damaged houses to the total number of houses, as shown below:

$$\text{Rate of damage to houses} = \frac{n_1 + 0.5n_2}{m}$$

where,

- m : Total number of houses in each cell or block
- n_1 : Number of totally destroyed houses in each cell or block
- n_2 : Number of partially destroyed houses in each cell or block

The relationship between the rate of damage to houses and the magnitudes of the permanent ground displacements is shown in Figure 32. To ensure the reliability of these results, any data for blocks or cells containing less than 75 houses were excluded. A relatively good correlation can be seen between the magnitude of the displacement and the damage rate to houses. However, it should be noted that in some areas, even though the permanent displacement was small, the damage rate is comparatively high.

For example, the asterisk in Figure 32 shows the damage rate at Keirin-cho in the northern part of the city (Figure 19(a)). In this area, the permanent ground displacement was small, but ground failures such as fissures and sand boils were found. This means that houses could have been damaged by local failures of the foundation ground - fissures, subsidence, and bulging - without large ground displacements due to liquefaction over a wide area.

Figure 33 shows rate of damage to cast iron gas pipes (CIP) and steel gas pipes (SP) with diameters of 75 to 150 mm. No definite conclusion could be reached because the amount of data was insufficient, but it is clear that the damage rates to both types of pipe have some proportional relationship with the magnitude of the permanent ground displacements. It can also be seen from the figures that the damage rate to CIPs, is much more than that to SPs.

It should be noted that in some areas where the permanent ground displacements were small, the rate of damage to CIPs is very high. For example, the asterisk in Figure 33(a) shows the results for the Suehiro-cho area, which is also in the northern part of the city, as shown in Figure 19(a). In this area, although the permanent ground displacements were very

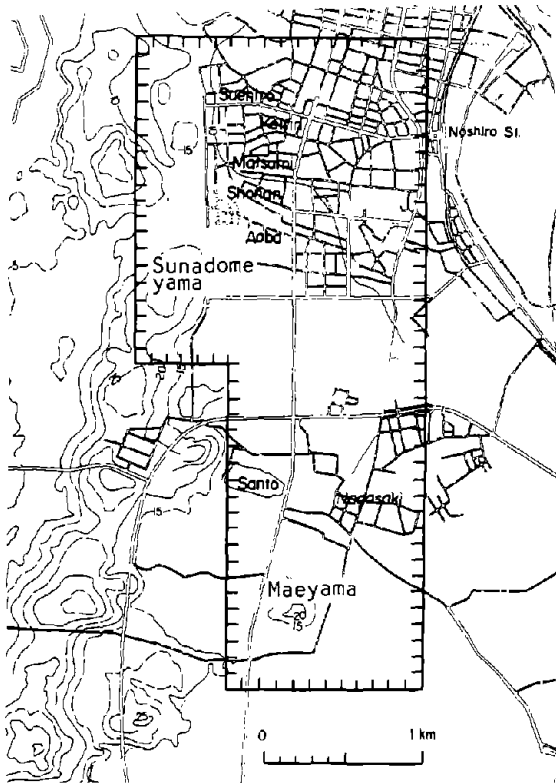


Figure 31. Square Cells for Analysis of Quantitative Relationship between Permanent Ground Displacements and Damage Rates to Houses and Buried Pipes

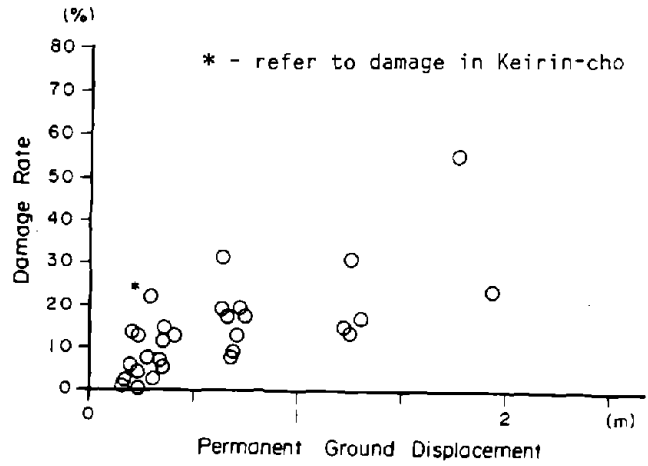
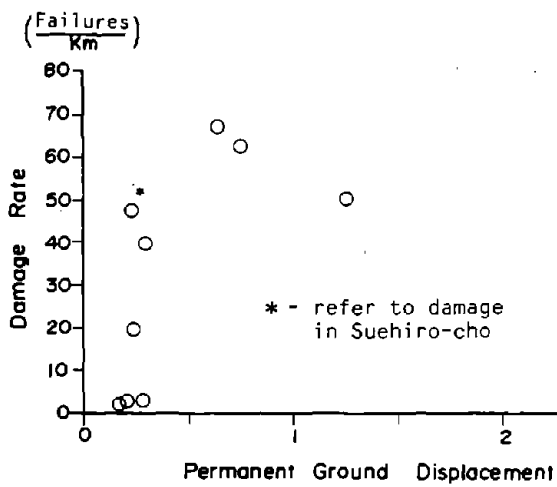
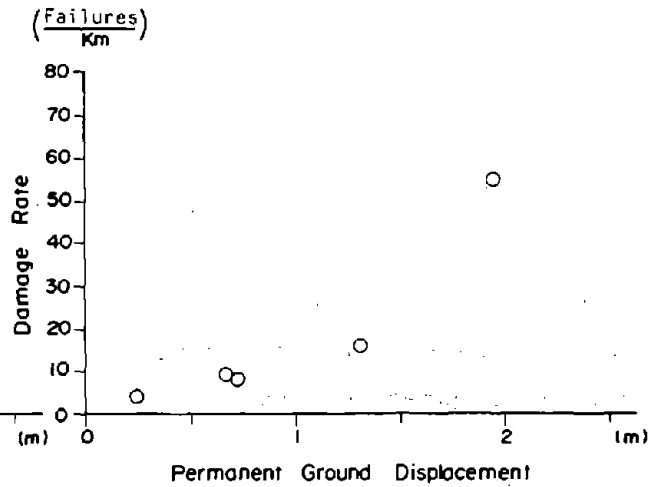


Figure 32. Relationship between the Damage Rate to Houses and the Permanent Ground Displacements



(a) Cast-Iron Gas Pipes



(b) Steel Pipes

Figure 33. Relationship between the Damage Rate to Buried Gas Pipes (diameter=75 to 150 mm) and the Permanent Ground Displacements

small (less than 25 cm) the damage rate was very high, at about 50 instances per kilometer. As previously mentioned in the case of the damage rate to houses, the permanent ground displacements in this area were small, but ground failures due to liquefaction were observed as shown in Figure 19(a). This indicates that because the strength of cast iron pipes is generally low, the damage was caused instead by local ground failures induced by liquefaction, and/or by relative displacements resulting from wave propagation.

As shown in Figure 34, there is no clear correlation between rate of damage to small-diameter (32 to 50 mm) gas pipes and the magnitude of the permanent ground displacements. Most of the damage to small diameter gas pipes occurred at screw joints and T-shape joints. Since the strength of these joints is generally low, damage may result from factors other than the permanent ground displacements, as in the case of the cast iron pipes. These results show that permanent ground displacements are not necessarily the only factor contributing to damage to small-diameter pipes.

A similar result was obtained in the case of asbestos-cement water pipes, between 100 and 200 mm in diameter. As shown in Figure 35, no clear correlation can be made between the rate of damage to these water pipes and the permanent ground displacements. It is also possible that these pipes may have been damaged by causes other than permanent ground displacements because of their low strength.*

5.2 Correlation of Rate of Damage to Buried Pipes with Permanent Ground Strains

As described in 4.2.1, permanent ground strains were calculated from the

*The damage rate for asbestos-cement water pipes, as shown in Figure 35, was lower than that for the 75 to 150 mm dia. cast iron gas pipes shown in Figure 33(a), although the water pipes were comparatively weaker than the gas pipes. This may be due to the fact that damage to the gas pipes was measured much more accurately.

measured displacements in Noshiro City.* Figure 21 shows the ground strains in the horizontal plane. Correlations of the rate of damage to cast iron and steel gas pipes (diameters of 75 to 150 mm) with ground strain are shown in Figure 36. In this figure, the abscissa is the maximum absolute value of the two principal ground strains. The correlation with ground strain is not much higher than that for the displacements, as shown in Figure 33. This weak correlation may be the result of insufficient accuracy in calculating the ground strain. Furthermore, there may be other reasons for damage to buried pipes besides permanent ground displacements, as previously mentioned.

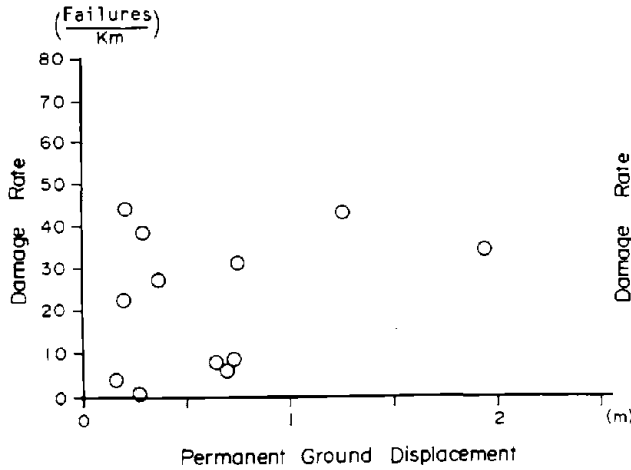


Figure 34. Relationship between the Damage Rate to Buried Gas Pipes and the Permanent Ground Displacements (steel pipes, diameter = 32 to 50 mm)

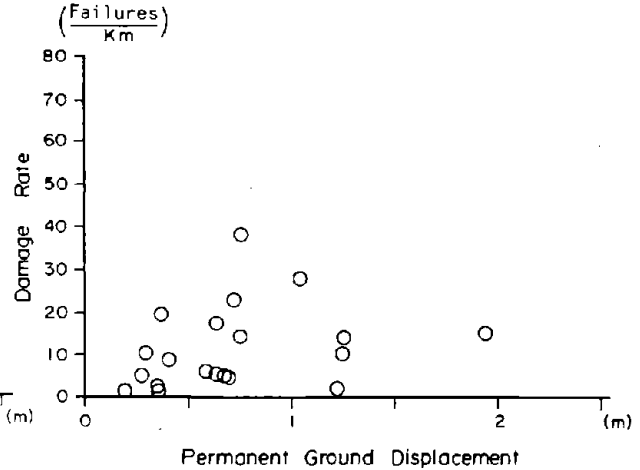
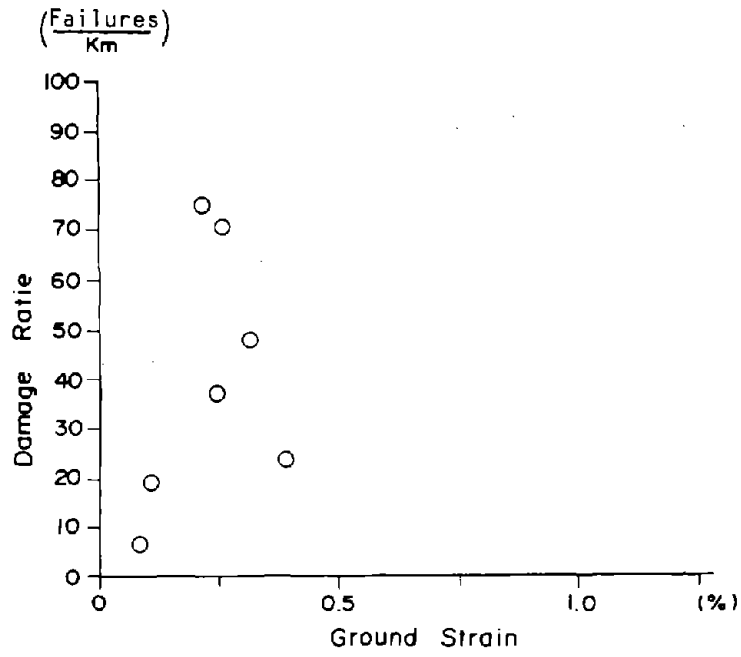
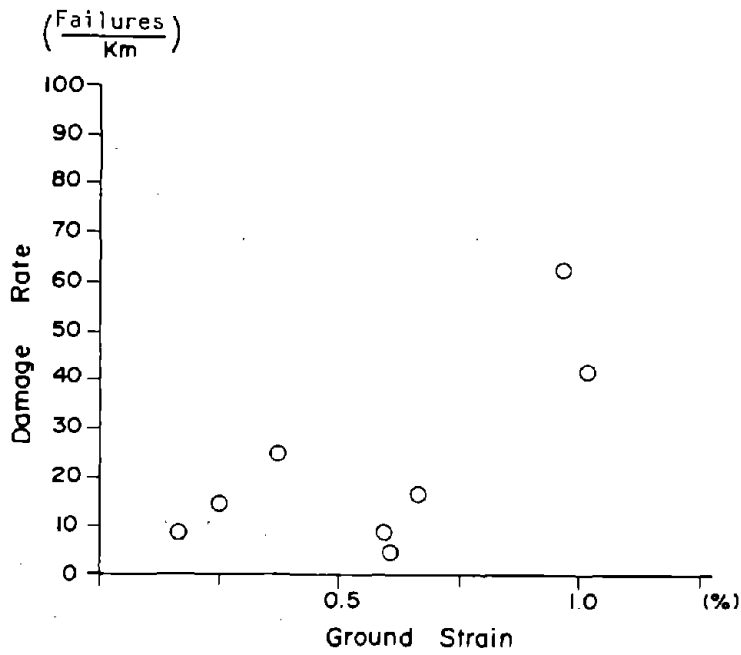


Figure 35. Relationship between the Damage Rate to Buried Water Pipes and the Permanent Ground Displacements (asbestos cement pipes, diameter = 100 to 200 mm)

*See Appendix C.



(a) Cast Iron Gas Pipes



(b) Steel Pipes

Figure 36. Relationship between the Damage Rate to Buried Gas Pipes (diameter=75 to 150 mm) and the Permanent Ground Strains

6.0 EFFECTS OF THICKNESS OF LIQUEFIED LAYER AND GRADIENT OF GROUND SURFACE ON PERMANENT GROUND DISPLACEMENTS

Regression analyses were conducted by Hamada et al.¹⁾ to investigate which relationships may exist between the magnitude of permanent ground displacements and thickness of liquefied layer and gradient of ground surface. On the basis of this study, the following empirical formula was proposed:

$$D \approx 0.75^2 \sqrt{H} \cdot \sqrt[3]{\theta} \dots\dots\dots (1)$$

D: Magnitude of permanent ground displacement in horizontal direction (m)

H: Thickness of liquefied layer (m)

θ : The greater gradient of the ground surface or the lower boundary of liquefied layer (%)

The proposed correlation given by Equation (1) only provides an approximate fit with the field data. Ground displacements are actually scattered between values half and twice the values given by the above formula. In particular, the correlation between the gradient of the ground surface and the lower boundary of the liquefied layer is comparatively poor. The following factors can be considered probable reasons for this poor correlation:

- (i) Soil data far from the measurement points of ground displacements (sometimes more than 100 m) were used in the correlation analysis.
- (ii) In the correlation analysis, the surface gradients were taken as mean values over slopes of lengths greater than several hundred meters. The horizontal distance over which the gradient is measured has a great influence on the result of the correlation analysis.
- (iii) In general, it is difficult to estimate the gradient of the lower boundary of the liquefied layer, usually below 2-3%, since a clear identification of the liquefied layer itself is difficult.

In this report, therefore, the correlation was re-examined by using data carefully selected as follows:

- (i) Only borehole data with SPT-values and grain size distributions within 25 m of the ground displacement measuring points were used.
- (ii) Data for ground displacements, less than 1.0 m, were discarded in consideration of the accuracy of the measurements.
- (iii) The horizontal distance over which the surface gradient was estimated was chosen to be 5 times to 60 times the thickness of the estimated liquefied layer.

Figure 37 shows a clear correlation between the ground displacements and the thickness of the liquefied layer. However, no significant correlation could be found between the ground displacements and the gradient of the surface, as shown in Figure 38. Although the horizontal distances over which the gradients were estimated are 5 times and 60 times the thickness of the liquefied layer in Figures (a) and (b), respectively, the correlation barely improved.

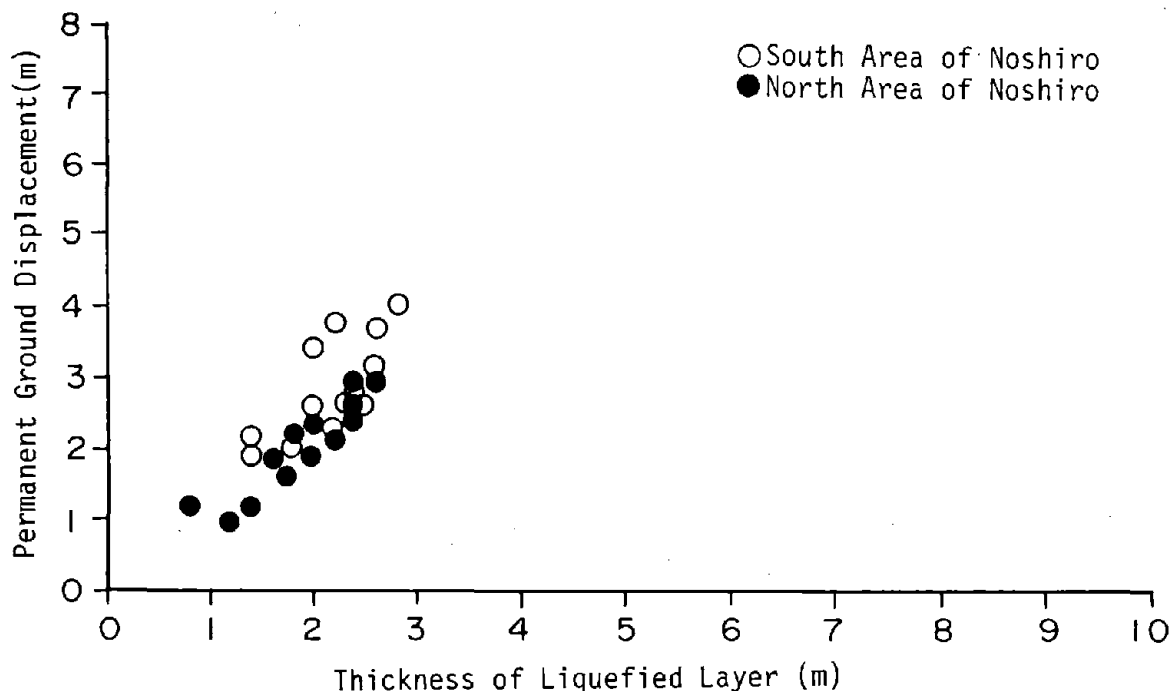
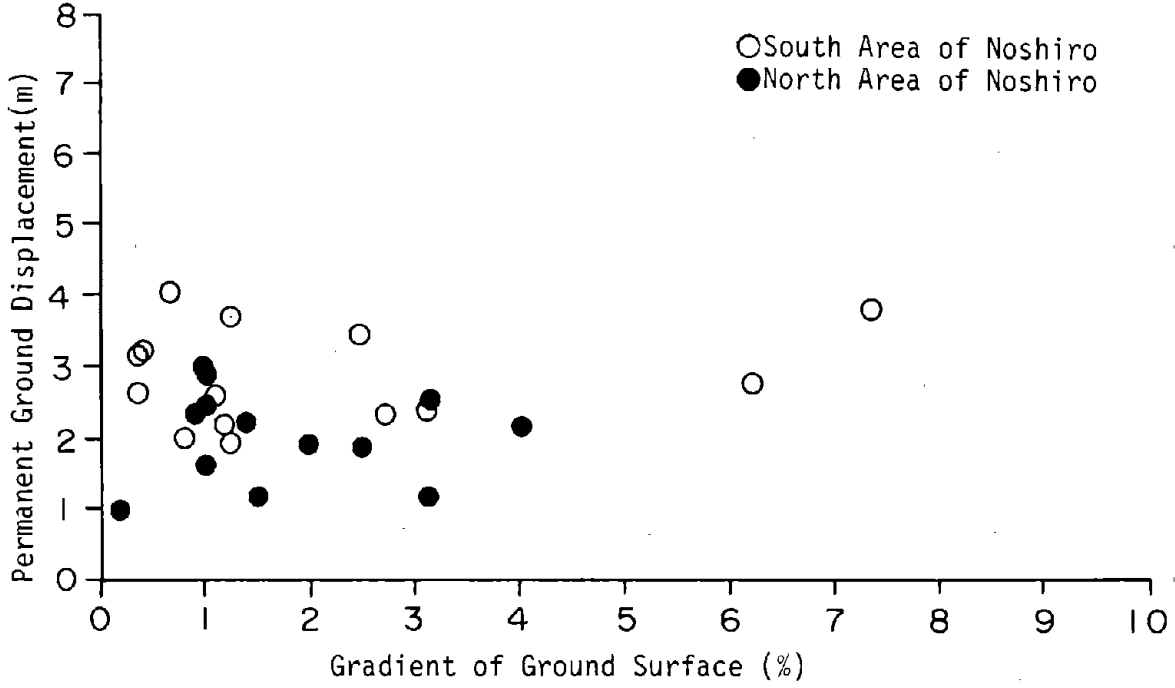
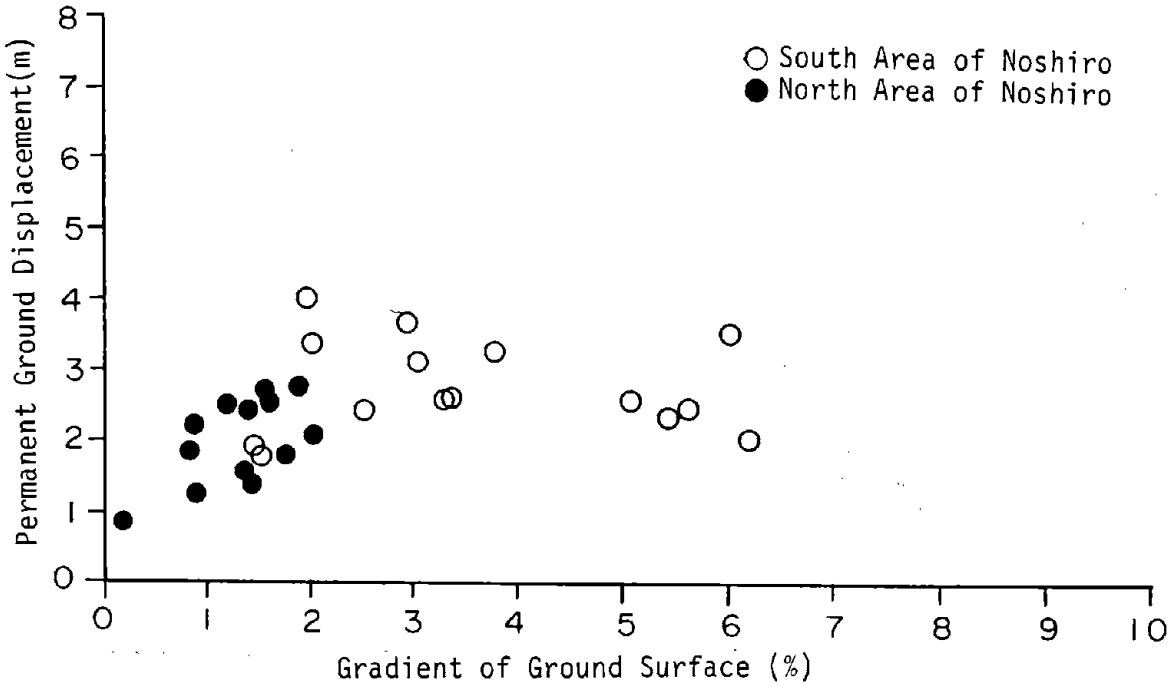


Figure 37. Correlation between Magnitude of Ground Displacements and Thickness of Estimated Liquefied Layer



(a) Case 1: Horizontal distance is 5 times the thickness of the liquefied layer



(b) Case 2: Horizontal distance is 60 times the thickness of the liquefied layer

Figure 38. Correlation between Magnitude of Ground Displacements and Gradient of Ground Surface

The lack of correlation between the magnitude of the ground displacements and the gradient of the ground surface appears to contradict the fact that the ground displaced from higher to lower elevations, as mentioned in 4.1.1 and 4.2.1. However, this contradiction can be resolved if it is assumed that ground displacements were caused by fluid behavior of the liquefied soil. In this case, the gradient of the liquid surface has little influence on the magnitude of movement, but does affect its velocity. If the liquefied soil tends to behave as a fluid, ground with higher elevations will sink and spread laterally as the fluid tries to achieve a uniform elevation. Under these conditions, the ground will rise up where lateral movements terminate.

7.0 PERMANENT GROUND DISPLACEMENTS AND RESULTING DAMAGE AT AKITA HARBOR

Akita Harbor suffered severe damage to its quay walls due to liquefaction during the 1983 Nihonkai-Chubu earthquake. Most of the damage consisted of the collapse and large inclination of steel sheet pile quay walls, collapse of concrete-block quay walls and the movement of caisson quay walls. Figure 39 outlines the locations of liquefaction in the Akita Harbor area.¹⁰⁾ In particular, Gaiko, the South Pier, the North Pier and Nakajima Pier were severely damaged due to liquefaction. Photo 17 shows one example of the damage to a quay wall made of steel sheet piles at Nakajima Pier. The quay wall was severely tilted and the concrete slab behind the quay wall sank significantly.

At Gaiko, which is an area newly reclaimed from the sea, liquefaction-induced ground displacements were observed. The quay wall, which is made of concrete caissons, moved about 1.5 m and was inclined to a maximum of 3 degrees.

7.1 Zone III: Gaiko Wharf at Akita Harbor

7.1.1 Permanent Ground Displacements and Ground Failures

Figure 40 shows the permanent ground displacements, locations of ground fissures and sand boils. The Gaiko Warehouse and the ground around it moved seaward with a maximum displacement of about 2 m. In front of the warehouse (facing away from the sea), ground fissures 30 to 50 cm wide were observed. The permanent ground displacements are generally perpendicular to the ground fissures. It is noteworthy that the ground surface slopes slightly in a southerly direction toward Pier C at a gradient of about 0.5%.

Near the corner of Road A and Road B, the ground surface was displaced to the northwest. Behind the ground displacement, large ground fissures with a maximum width of about 1.0 m were observed. Photo 18 shows one example of these ground fissures, the location and orientation of which is shown in Figure 38. It is also noteworthy that the ground surface is inclined

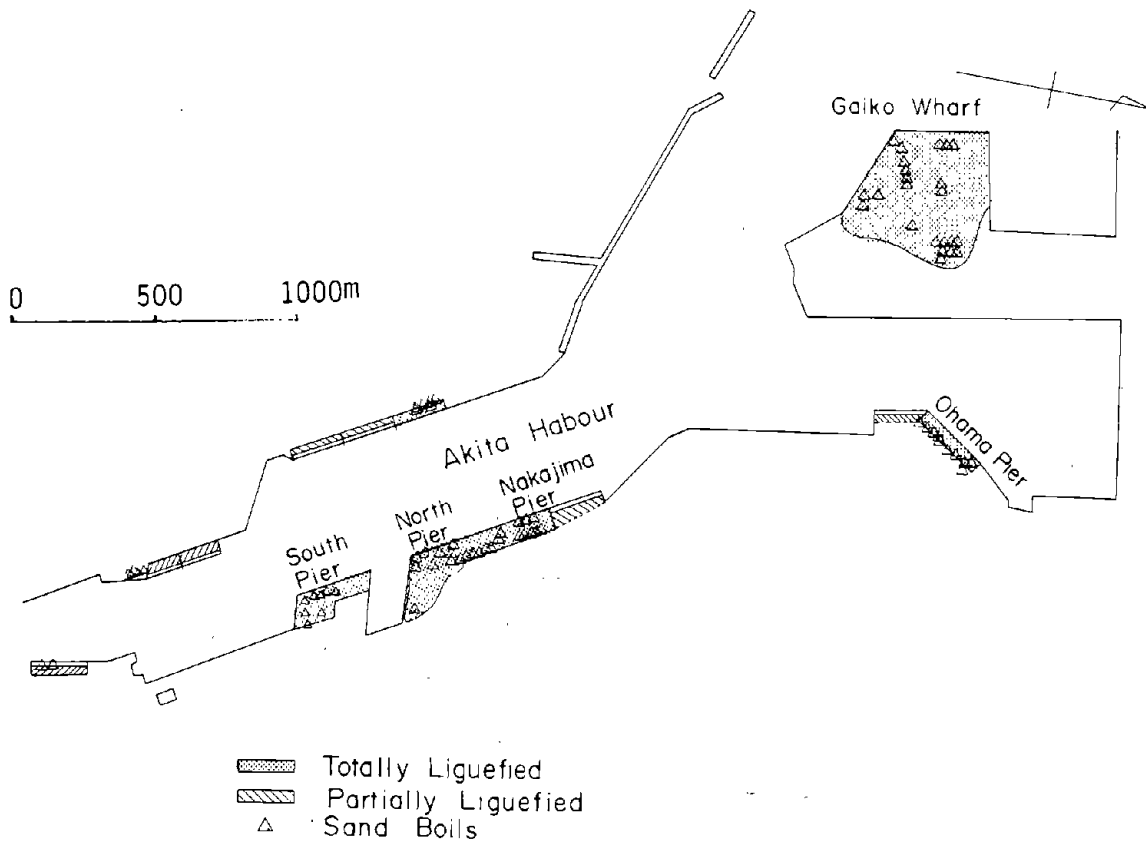


Figure 39. Locations of Damage to Quay Walls and Liquefaction at Akita Harbor(1)

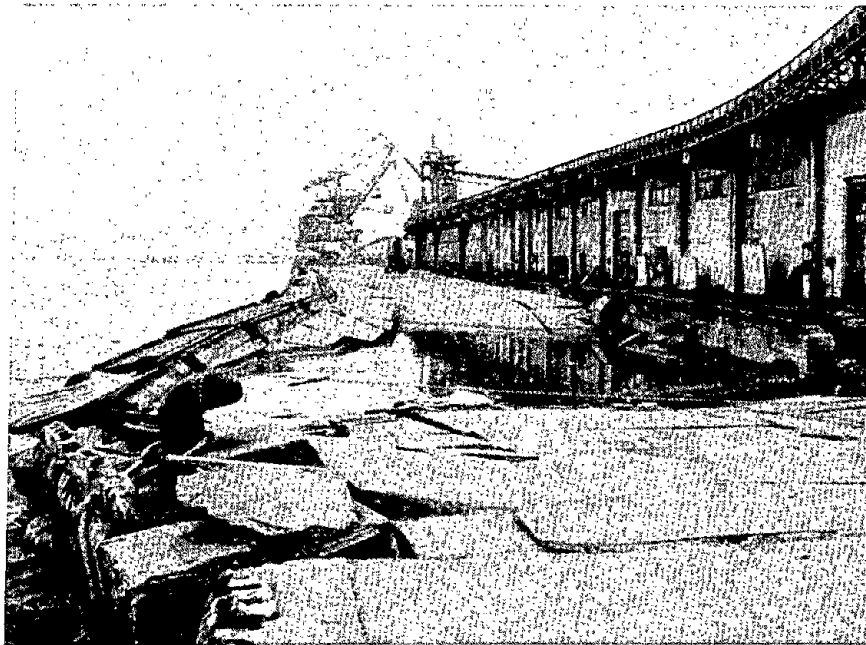


Photo 17 Damage to Sheet Pile Quay Wall (Nakajima Pier)

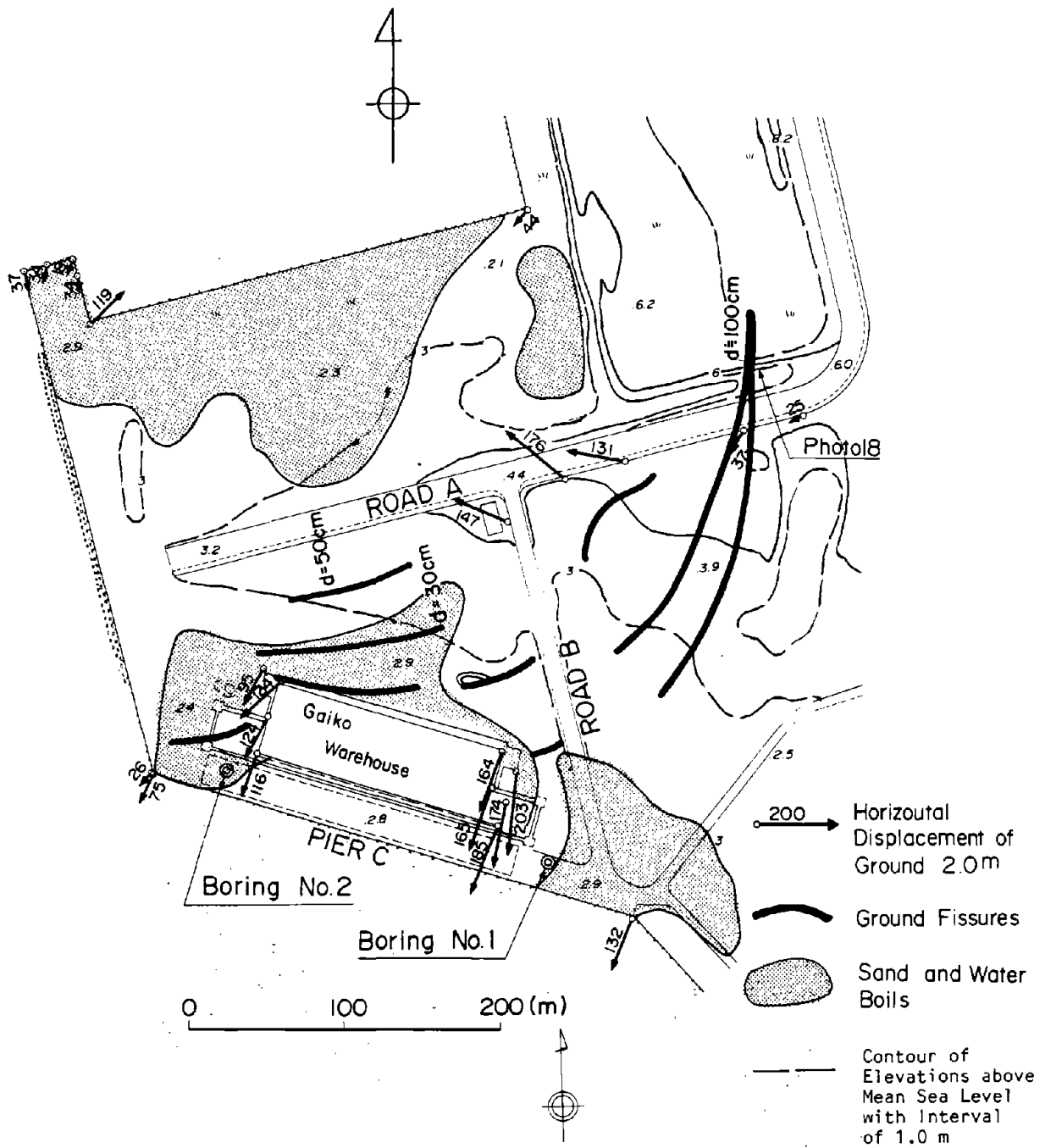


Figure 40. Permanent Ground Displacements, Ground Fissures and Sand Boil at Gaiko Wharf

slightly northwest in this area, mostly in the direction of the ground displacements and with a gradient of about 0.5%.

7.1.2 Soil Conditions

Figure 41 shows the soil profiles measured at Boreholes No.1 and No.2 in the vicinity of the Gaiko Warehouse, the locations of which are shown in Figure 38. The subsurface consists of a medium sand with SPT-values, N, less than 10 to a depth of about -14 m. The groundwater is mostly at the same depth as the sea level. Below -14.0 m, the ground consists of a thin layer of gravel and fine sand with an N-value of over 20. The ground below groundwater level to a depth of -14.0 m can be considered to have liquefied during the earthquake.

7.1.3. Damage to Quay Wall and Foundation Piles

(1) The Quay Wall of Pier C at Gaiko Wharf

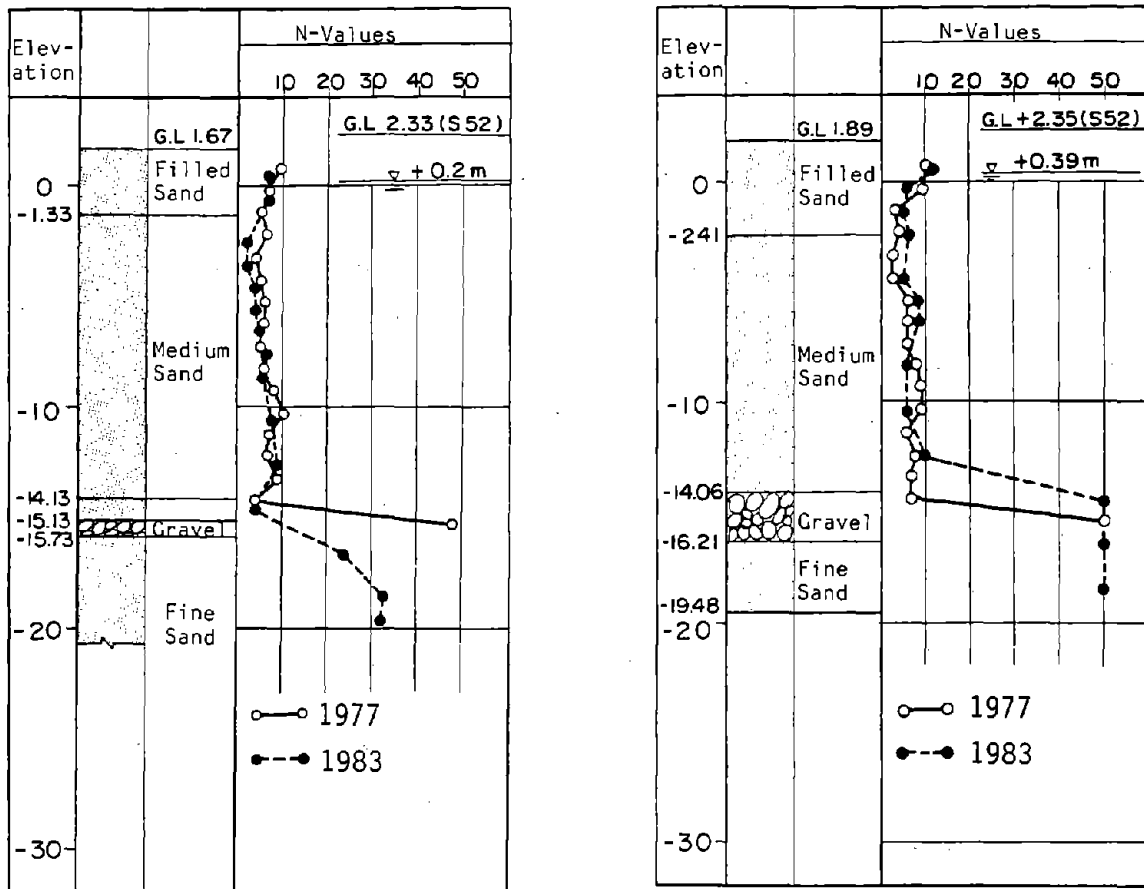
The quay wall of Pier C was built of concrete caissons 16.0 m long, 13.0 m wide, and 14.5 m high, as shown in Figure 42. Figure 43 shows the horizontal displacement at the top of the caissons and their inclinations.¹¹⁾ The caissons moved seaward with a maximum displacement of about 1.5 m. They were inclined by about 3 degrees. The magnitude of the displacement of the caissons mostly coincides with that of the surrounding ground measured by aerial survey.

(2) Foundation Piles of the Gaiko Landing Warehouse

The Gaiko Warehouse was built on prestressed concrete piles 60 cm in outer diameter and about 18 m long. After the earthquake, the floor slab was removed and the ground was excavated to a depth of -5.5 m. Horizontal cracks which could have been caused by a bending moment were found at a depth of -4.9 m. Below -5.5 m, damage to the piles was inspected by inserting an inclinometer into the inner space of the pile. During this inspection, it was found that the inclinometer could not be inserted deeper than about



Photo 18 Ground Fissure at Gaiko Wharf



(a) Boring No.1

(b) Boring No.2

Figure 41. Soil Conditions at Gaiko Wharf

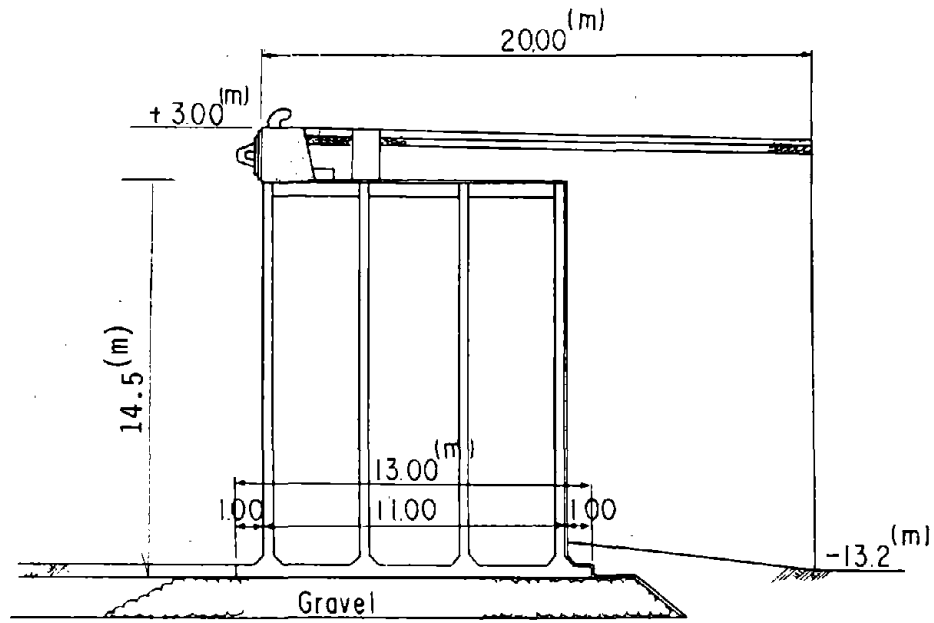
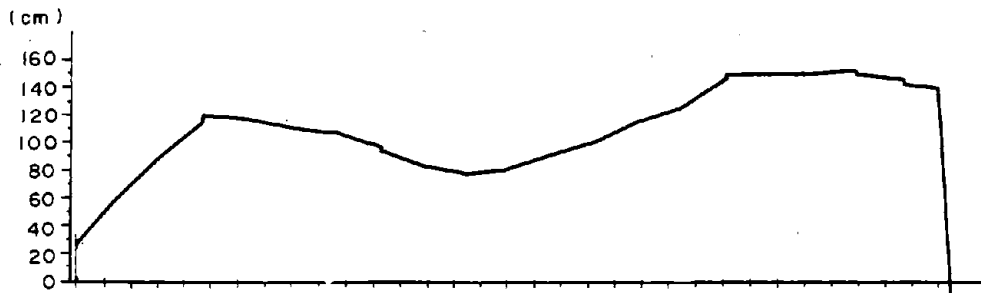


Figure 42. Quay Wall of Pier C 11)



(a) Displacement at Top of Caissons



(b) Inclination of Caissons

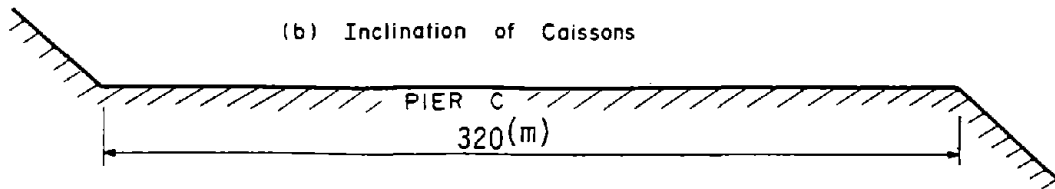


Figure 43. Movement and Inclination of Caissons of Pier C at Gaiko Wharf 11)

-14.9 m and that the inclination of the piles changed at a depth of -7.5 m.

From these findings, it is likely that the piles were damaged at levels of -7.5 m and around -15 m. The damage at -7.5 m is comparatively light because the inclinometer could be inserted deeper than this. The damage at about -15 m, however, was much more severe, indicating that the concrete might have been crushed, closing up the hollow pile. This depth basically coincides with the boundary between the liquefiable layer and the lower non-liquefiable layer, described in 6.1.2 and shown in Figure 41.

It should be noted that similar damage to piles occurred in Niigata City during the 1964 Niigata Earthquake.³⁾ At the NHK Building, the concrete foundation piles failed at two positions, and the lower position coincided with the boundary between the estimated liquefied layer and the lower non-liquefied layer. Similar damage to the concrete piles of the Family Court House Building in Niigata City was also reported.

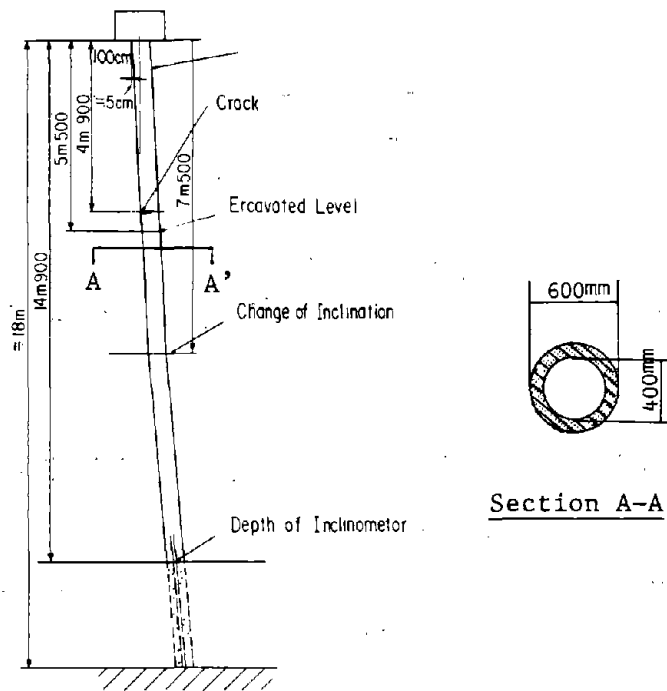


Figure 44. Damage to Prestressed Concrete Pile of Gaiko Warehouse

8.0 CONCLUSION

A summary of the main observations from this case study about liquefaction-induced ground displacements and their related damage associated with the 1983 Nihonkai-Chubu earthquake is given below:

- (1) In Noshiro City, permanent ground displacements with a maximum magnitude of 5 m occurred on gently sloping sand dunes with a mean gradient of less than 5%. In the flat areas of the alluvial plains along the Yoneshiro River, no ground displacements of more than 0.5 m could be found.
- (2) Around the top of the slopes, where the permanent ground displacements began, the ground surface subsided and ground fissures resulted. Lower down the slopes, however, heave of the ground surface was observed, and sand and water boils were found. This suggests that the large horizontal ground displacements were caused by the volumetric transport of liquefied soil.
- (3) It can be conjectured that the gradient of the ground surface and the thickness of the liquefied layer affected the magnitude of the ground displacements. However, it is difficult to draw a definite quantitative correlation between the magnitude of the permanent ground displacements and the gradient of the ground surface. The maximum displacement did not necessarily occur at the location with the maximum ground surface inclination.
- (4) Tensile strain occurred in the ground in the area where the ground displacements started, while compressive strains occurred in the area where the ground displacements ended. The maximum tensile and compressive strains, which were calculated from the measured ground displacements as mean values in 200 m x 200 m cells in Noshiro City, were 1.7% and 1.5%, respectively.

- (5) In the northern part of Noshiro City, wastewater pipes which were laid in the liquefied layer were displaced more than the ground surface. This means that the liquefied layer moved more than the non-liquefied layer above it.
- (6) Most of the damage to welded steel gas pipes in the southern area of Noshiro City can be explained by considering the permanent ground displacements in the vicinity as the direct cause.
- (7) A good correlation was found between the magnitudes of the permanent ground displacements and rate of damage to houses. However, it should be noted that there were some cases where the rate of damage was high, even though the displacement was small. This may be because the houses were damaged by local failures of the foundation ground, such as fissures and subsidence arising from liquefaction without large displacements.
- (8) A correlation between the magnitudes of the ground displacements and rate of damage to larger-diameter (75 to 150 mm) steel and cast iron gas pipes was recognized, but this was not true for smaller-diameter (32 to 50 mm) steel gas pipes and 100 to 200 mm diameter asbestos-cement water pipes. Most of the damage to small-diameter gas pipes occurred at screw joints and T-shape joints. This indicates that, because the strength of these smaller diameter pipes was generally low, the damage could have resulted from other causes such as local ground failures induced by liquefaction and relative displacements due to wave propagation, rather than from permanent ground displacements.

REFERENCES

- 1) Hamada, M., Yasuda, S., Isoyama, R., and Emoto, K., "Study on Liquefaction Induced Ground Displacements," report of Research Committee, Association for the Development of Earthquake Prediction, Tokyo, Japan, Nov., 1986, pp. 3-19.
- 2) Japan Society of Civil Engineers, "Report on the 1983 Nihonkai-Chubu Earthquake," report of Earthquake Engineering Committee, Tokyo, Japan 1986, pp. 18-19, pp. 54-55 (in Japanese).
- 3) Hamada, M., "Large Ground Deformations and Their Effects on Lifelines, 1964 Niigata Earthquake," This volume.
- 4) Seed, H.B., Tokimatsu, K., Harder, L.F., and Chung, R.M., "Influence of SPT Procedure in Soil Liquefaction Resistance Evaluation," Journal of Geotechnical Engineering, Vol. 111, No. 12, ASCE, New York, N.Y., 1985, pp. 1425-1445.
- 5) Iwasaki, T., Tatsuoka, F., Tokida, K., and Yasuda, S., "A Practical Method for Assessing Soil Liquefaction Potential Based on Case Studies at Various Sites in Japan," Proceedings, Fifth Japan Earthquake Symposium, Tokyo, Japan, 1978, pp. 641-648 (in Japanese).
- 6) Japan Gas Association, "The 1983 Nihonkai-Chubu Earthquake and Damage to Gas Facilities," Tokyo, Japan, 1984, pp. 38-48 (in Japanese).
- 7) Noshiro City Government, "The 1983 (May 26) Nihonkai-Chubu Earthquake, A Document of Experiences of Earthquake Hazard in Noshiro City," Noshiro, Japan, 1984 (in Japanese).

- 8) Suzuki, T., "Damage to Telecommunication Facilities during the 1983 Nihonkai-Chubu Earthquake," report of Research Committee on Large Ground Deformations and Their Effects on Lifeline Facilities, Association for the Development of Earthquake Prediction, Tokyo, Japan, 1990, pp. 243-270 (in Japanese).
- 9) Kawashima, K., Sugita, H., Kono, N., Isoyama, R., and Taguchi, Y., "Damage to Wastewater Pipes and Permanent Ground Displacements during the 1983 Nihonkai-Chubu Earthquake," Proceedings, Earthquake Engineering Conference, 1989, Japan Society of Civil Engineers, Tokyo, Japan, 1989, pp. 97-100 (in Japanese).
- 10) Japan Society of Civil Engineers, "Report on the 1983 Nihonkai-Chubu Earthquake," report of Earthquake Engineering Committee, Tokyo, Japan 1986, pp. 314-321 (in Japanese).
- 11) Port and Harbor Institute, Ministry of Transportation, "Report on the 1983 Nihonkai-Chubu Earthquake, Damage to Port and Harbor Facilities," Technical Report No. 511, Port and Harbor Institute, Yokosuka, Japan, 1985, pp. 10-27.
- 12) Hamada, M., Yasuda, S., and Wakamatsu, K., "Case Studies on Liquefaction-Induced Permanent Ground Displacements," Proceedings, 1st Japan-U.S. Workshop on Liquefaction, Large Ground Deformations, and Their Effects on Lifeline Facilities, Association for the Development of Earthquake Prediction, Tokyo, Japan, 1988, pp. 3-21.
- 13) Fujii, Y., Hatanaka, M., Shiomi, T., and Tanaka, Y., "Liquefaction Analysis of Seawalls during 1983 Nihonkai-Chubu Earthquake," Technical Report NCEER-89-0032, Proceedings of the 2nd U.S.-Japan Workshop on Liquefaction, Large Ground Deformations, and Their Effects on Lifelines, National Center for Earthquake Engineering Research, Buffalo, NY, 1989, pp. 322-335.

Appendix A Accuracy of the Measurements of Permanent Ground Displacements in Noshiro City and Akita Harbor

The accuracy of the permanent ground displacement measurements was evaluated on the basis of the following procedure:

Step 1: Several data points were selected in the area of the measurement including the triangulation points. Figure A-1 shows one example of a set of data points in the northern area of Noshiro City in the case of the pre-earthquake survey.

Step 2: The coordinates of the data points were measured independently by two methods, a survey on the ground surface using transits and a geodimeter, and an aerial photographic survey.

Step 3: Under the assumption that the coordinates measured by the on-ground survey were correct, the error in the coordinates measured by the aerial survey were distributed over all data points to minimize the mean value of the squares of the differences in the coordinates by the two surveys. This distribution of the error was conducted by an adjustment of the location and the angle of the aerial photographs.

Step 4: The accuracy of the aerial survey was determined as a standard deviation of the differences between the coordinates by the on-ground survey and the corrected aerial survey coordinates.

Step 5: The accuracy of the permanent ground displacement measurements was calculated as the square root of the sum of squared accuracy of the two aerial surveys, before and after the earthquake.

The accuracy of the permanent ground displacements in Noshiro City and Akita Harbor, estimated using the five steps above is shown in Tables A-1 and A-2.

Naturally, the accuracy of the permanent ground displacements using this procedure depends heavily on the accuracy of the on-ground survey. However, in the present case, the accuracy of the on-ground survey in Noshiro City was

better, ± 8.1 cm in the horizontal direction, than that of the aerial surveys, so its effects were neglected.

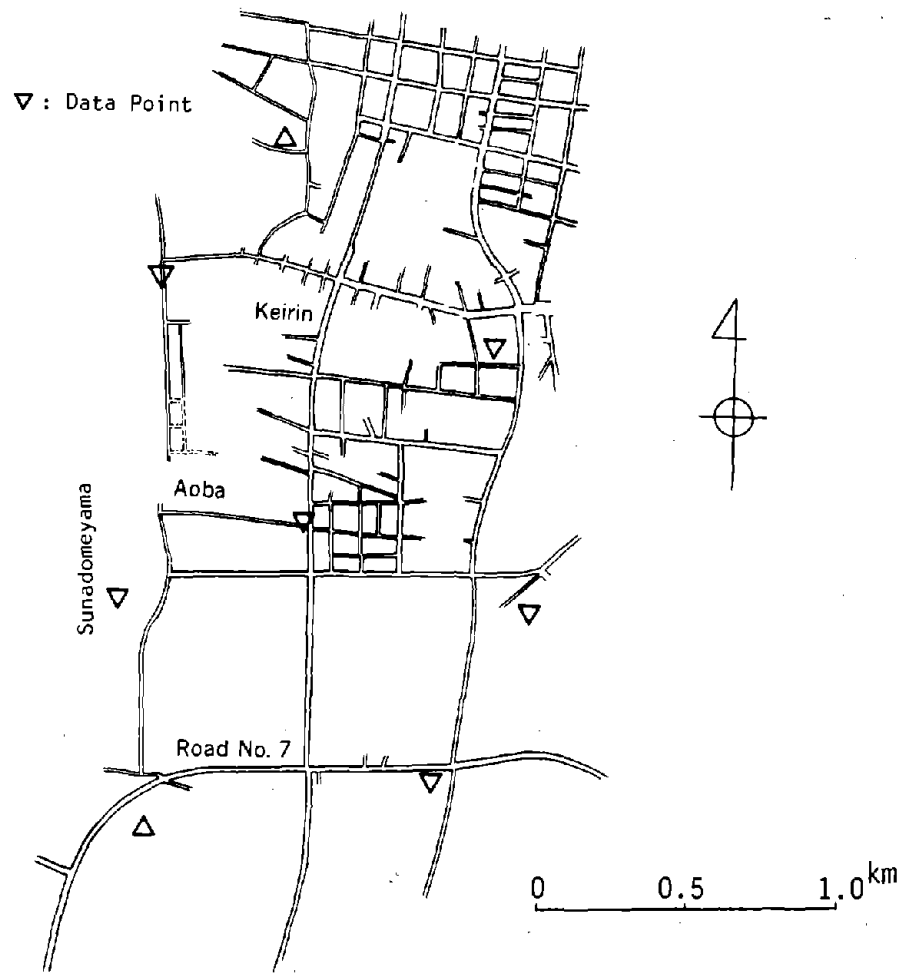


Figure A-1. Data Points for Aerial Survey in Northern Area of Noshiro City (ZONE II)

Table A-1 Accuracy of the Permanent Ground Displacement Measurements

(a) South Area (ZONE I)

Aerial Survey	Pre-earthquake	Post-earthquake
Total Number of Data Points	21	5
Accuracy of Aerial Survey (Standard deviation of differences of coordinates by on-ground and aerial surveys)	(m) ± 0.08 (Hori.) ± 0.16 (Vert.)	(m) ± 0.14 (Hori.) ± 0.12 (Vert.)
Accuracy of Permanent Ground Displacement Measurements	$\pm \sqrt{(0.08)^2 + (0.14)^2} = \pm 0.16$ (Hori.) (m) $\pm \sqrt{(0.16)^2 + (0.12)^2} = \pm 0.20$ (Vert.) (m)	

(b) North Area (ZONE II)

Aerial Survey	Pre-earthquake	Post-earthquake
Total Number of Data Points	8	9
Accuracy of Aerial Survey (Standard deviation of differences of coordinates by on-ground and aerial surveys)	(m) ± 0.14 (Hori.) ± 0.26 (Vert.)	(m) ± 0.10 (Hori.) ± 0.12 (Vert.)
Accuracy of Permanent Ground Displacement Measurements	$\pm \sqrt{(0.14)^2 + (0.10)^2} = \pm 0.17$ (Hori.) (m) $\pm \sqrt{(0.26)^2 + (0.12)^2} = \pm 0.28$ (Vert.) (m)	

Table A-2 Accuracy of the Permanent Ground Displacement Measurements at Akita Harbor (ZONE III)

Aerial Survey	Pre-earthquake	Post-earthquake
Total Number of Data Points	11	12
Accuracy of Aerial Survey (Standard deviation of differences of coordinates by geographical maps with a scale of 1/2500.*)	(m) ± 0.10 (Hori.) ± 0.14 (Vert.)	(m) ± 0.09 (Hori.) ± 0.14 (Vert.)
Accuracy of Permanent Ground Displacement Measurements	$\pm \sqrt{(0.10)^2 + (0.09)^2} = \pm 0.13$ (Hori.)(m) $\pm \sqrt{(0.14)^2 + (0.14)^2} = \pm 0.20$ (Vert.)(m)	

*) The accuracy of aerial survey at Akita Harbor was examined by comparing the coordinates from the aerial photographs with those from the geographical maps with a scale of 1/2500 instead of on-ground survey.

Appendix B Soil Conditions along 27 Sections in Noshiro City, and
Evaluation of the Liquefied Zone

Twelve SPT borings and 134 SWS tests were conducted in Noshiro City, and existing data on 50 SPT borings were also collected. Based on these results, soil profiles were investigated along 27 section lines in the city, which are shown in Figures 7 and 23, and estimations were made of the soil which liquefied during the earthquake. These estimations were performed by calculating the Factor of Liquefaction Resistance F_L .⁵⁾ Soil with an F_L value of less than 1.0 was considered to have liquefied. However, in areas where the amount and the quality of soil data were not adequate, some engineering judgment was used on a supplemental basis to classify the soil and evaluate its strength.

Figure B-1 summarizes the soil profiles along 27 different section lines shown in Figures 7 and 23. Estimated liquefied soil layers, which are shadowed in the figure, are shown in conjunction with SPT values, N , and SWS values, N_{sw} and W_{sw} .

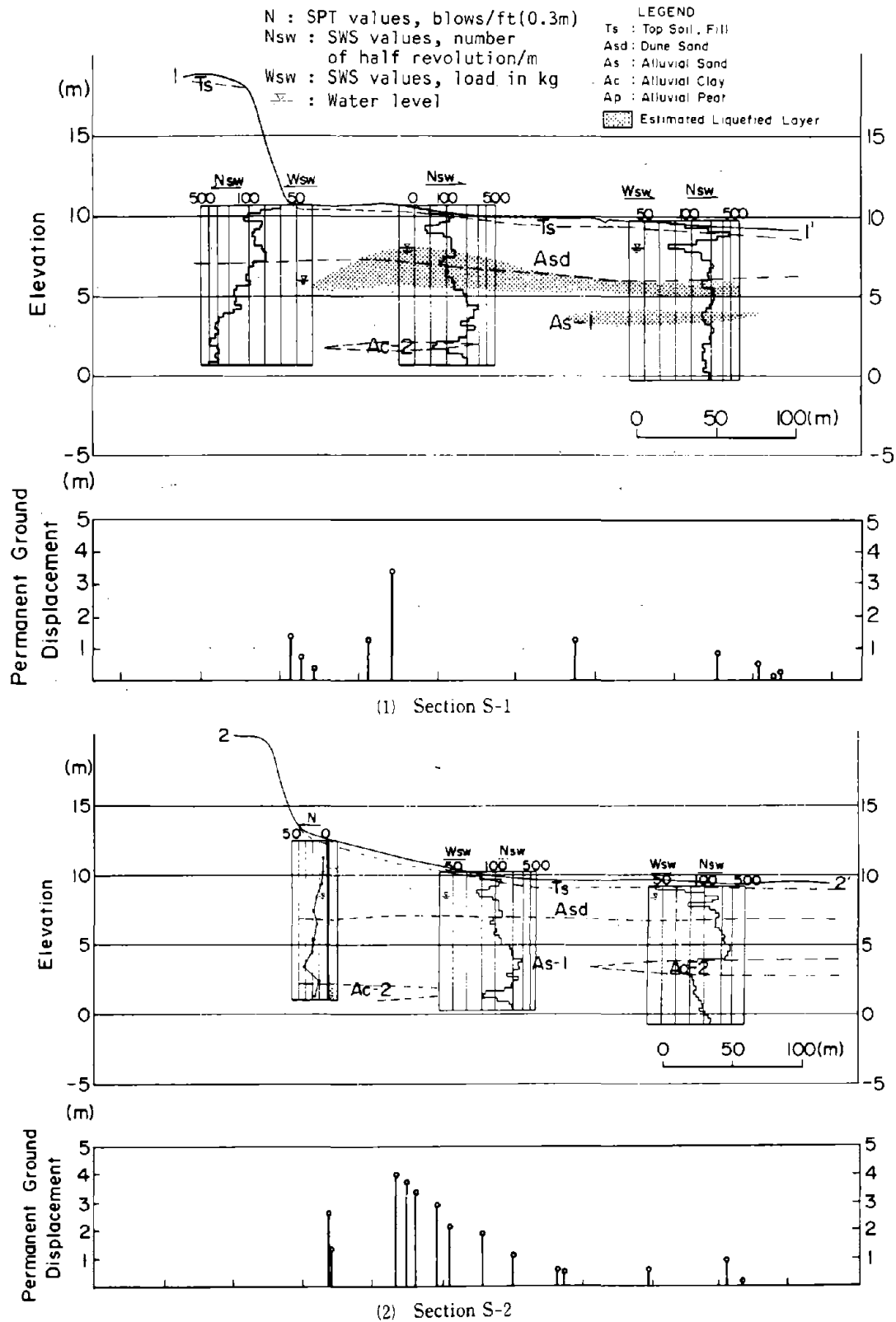


Figure B-1 Soil Profile and Estimated Liquefied Layers

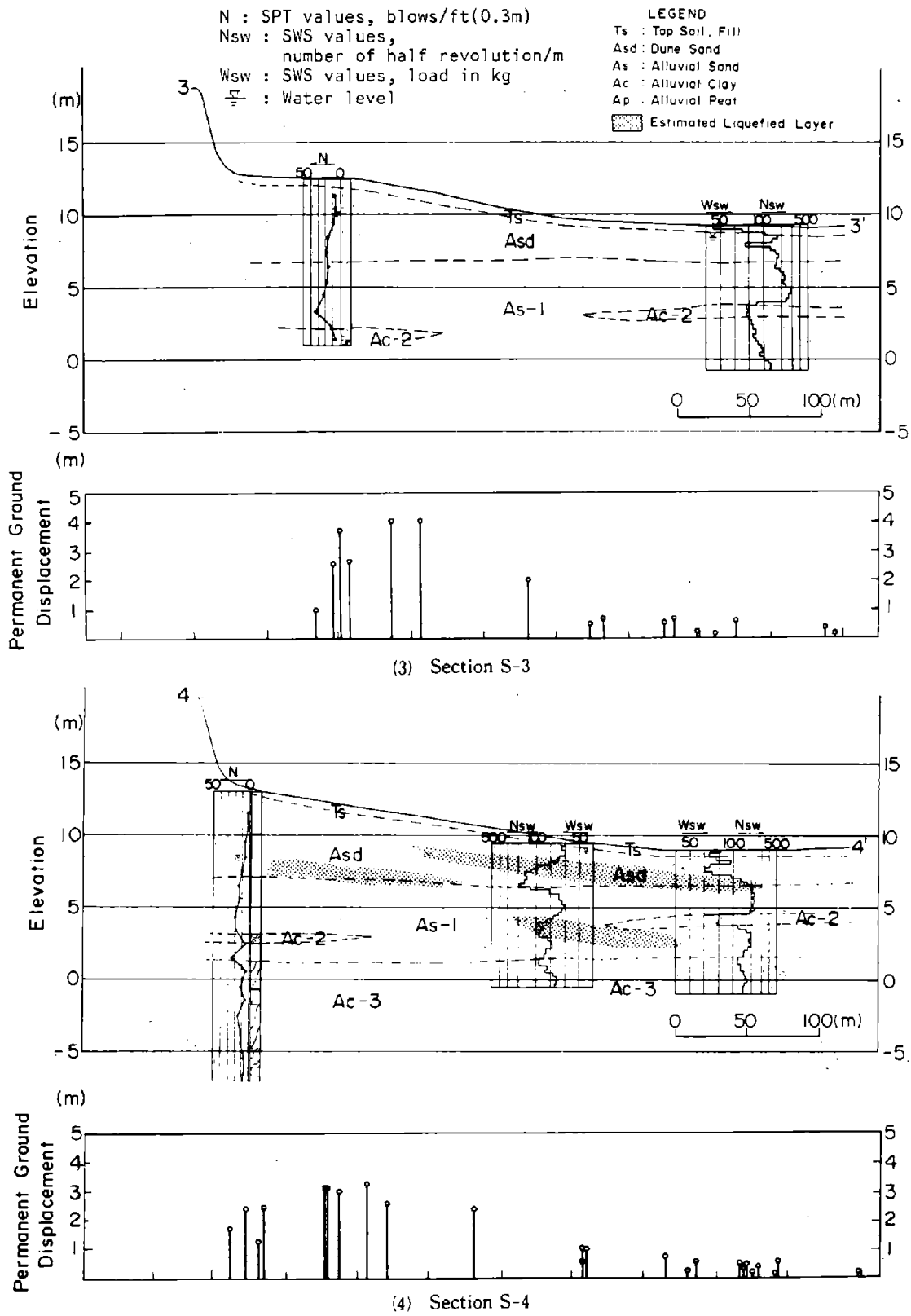


Figure B-1 Soil Profile and Estimated Liquefied Layers

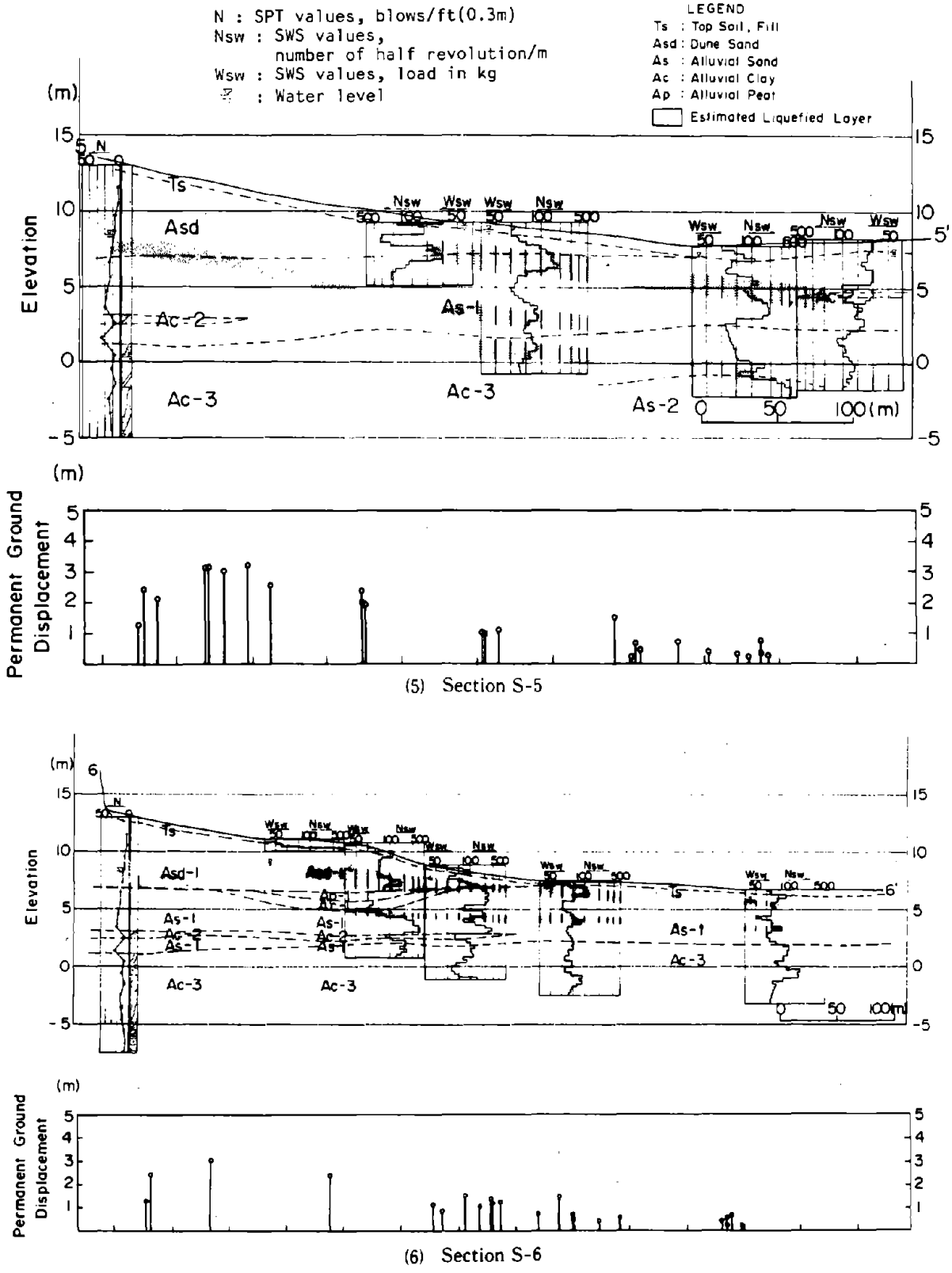


Figure B-1 Soil Profile and Estimated Liquefied Layers

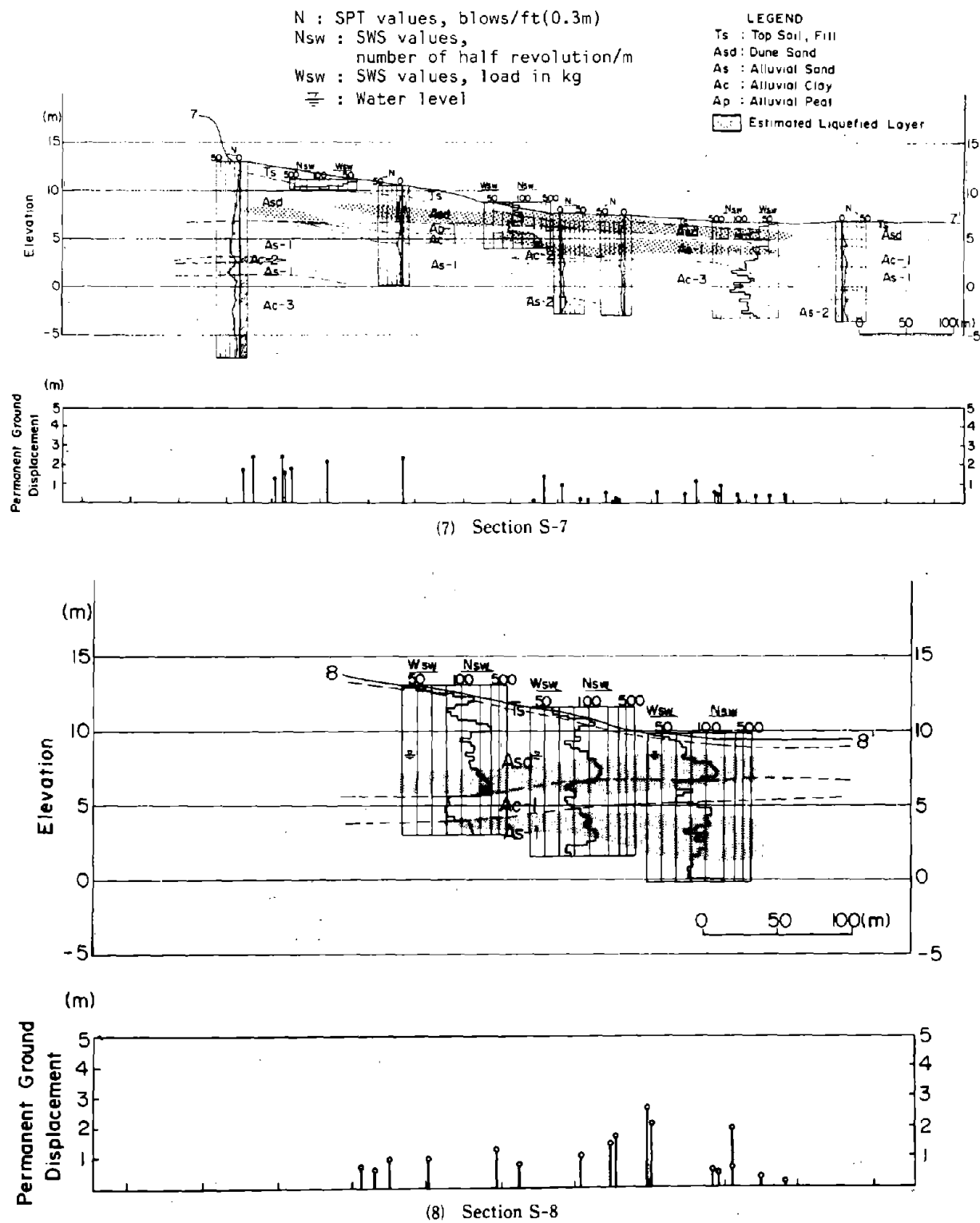


Figure B-1 Soil Profile and Estimated Liquefied Layers

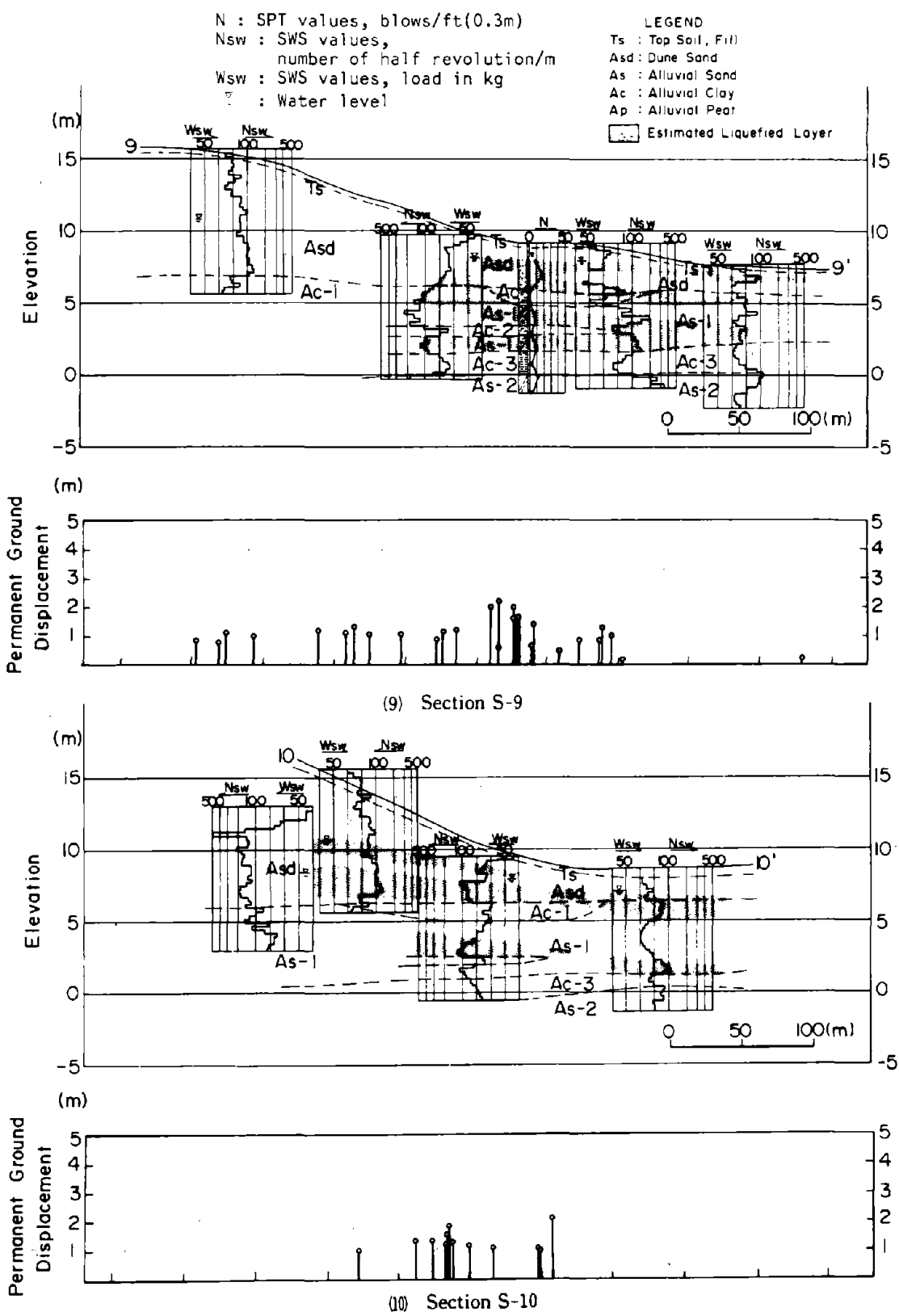


Figure B-1 Soil Profile and Estimated Liquefied Layers

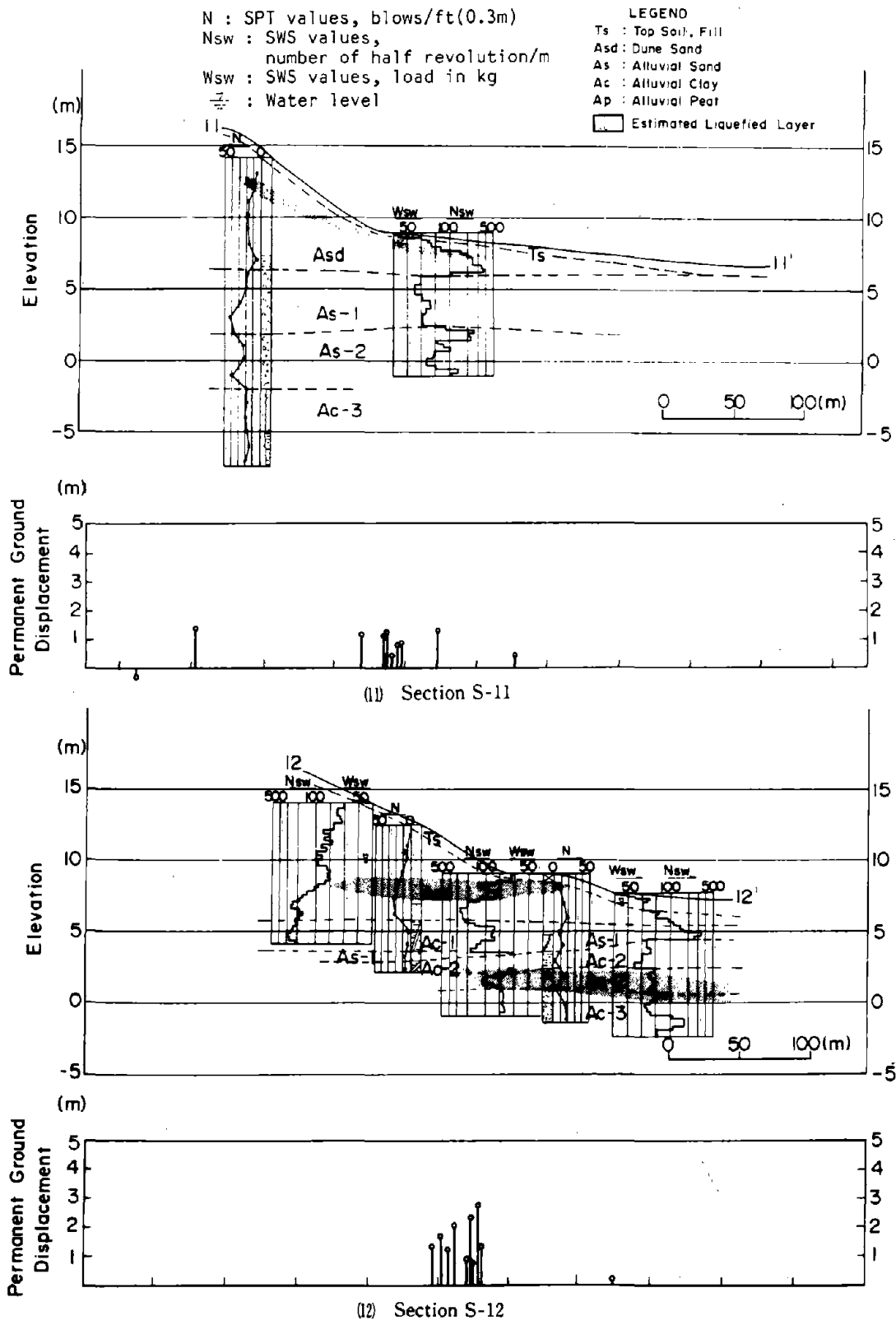


Figure B-1 Soil Profile and Estimated Liquefied Layers

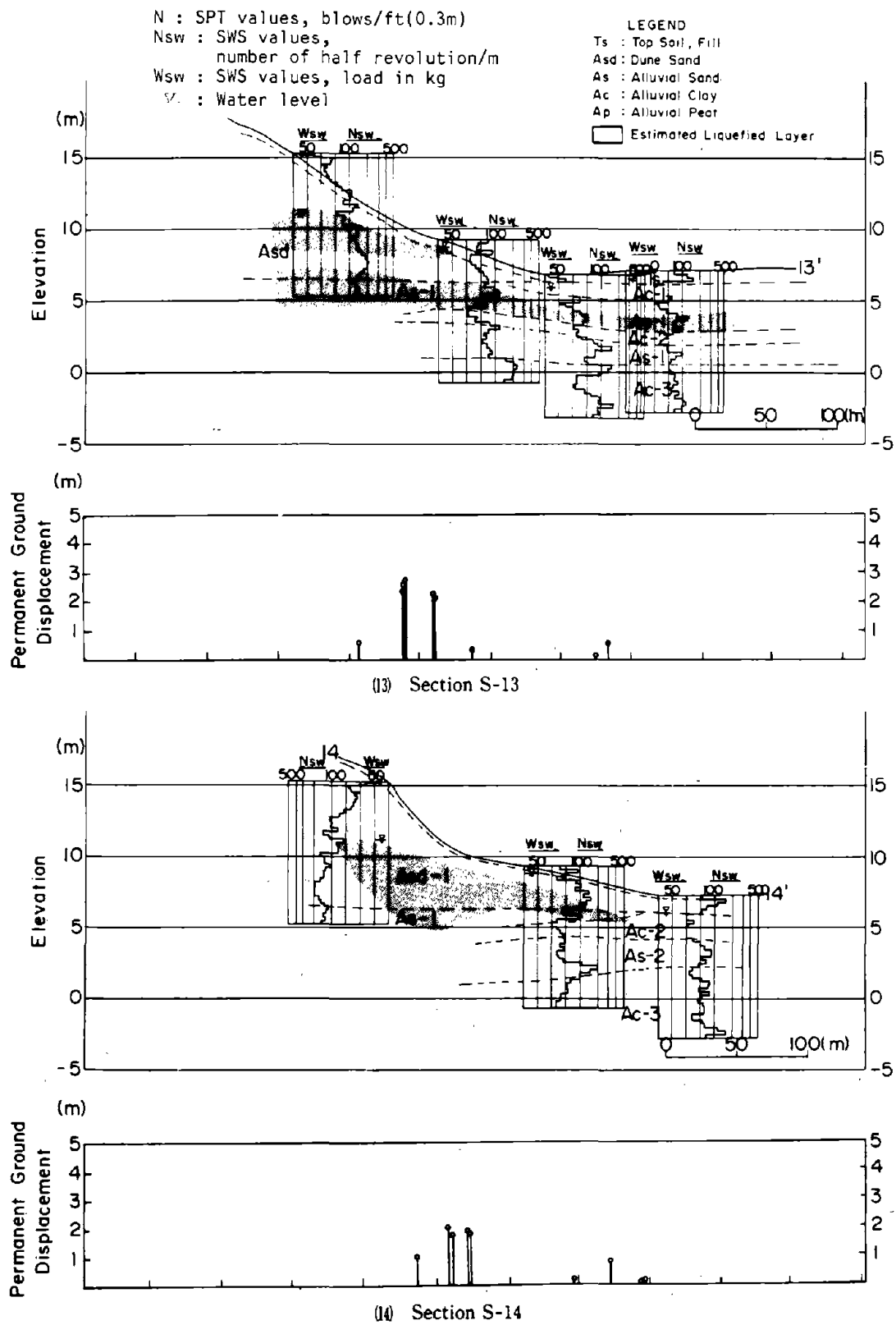


Figure B-1 Soil Profile and Estimated Liquefied Layers

N : SPT values, blows/ft(0.3m)
 Nsw : SWS values, number of half revolution/m
 Wsw : SWS values, load in kg
 ☉ : Water level

LEGEND
 Ts : Top Soil, Fill
 Asd : Dune Sand
 As : Alluvial Sand
 Ac : Alluvial Clay
 Ap : Alluvial Peat
 □ Estimated Liquefied Layer

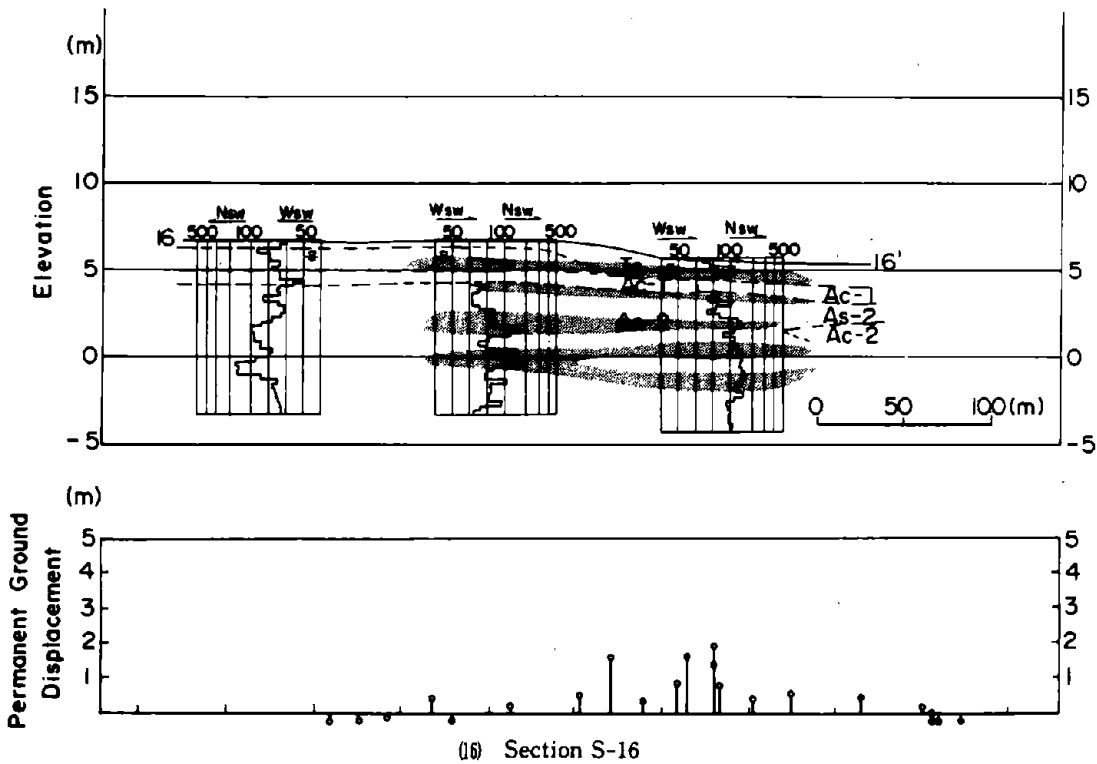
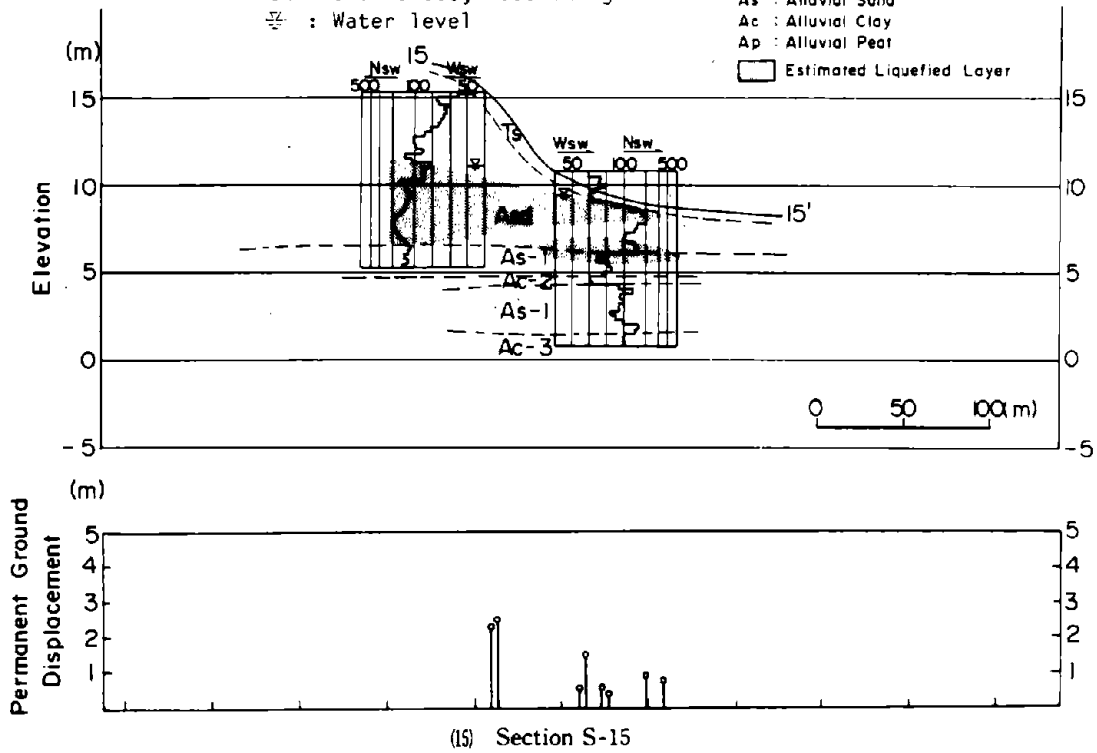




Figure B-1 Soil Profile and Estimated Liquefied Layers

N : SPT values, blows/ft(0.3m)
 Nsw : SWS values,
 number of half revolution/m
 Wsw : SWS values, load in kg
 : Water level

LEGEND
 Ts : Top Soil, Fill
 Asd : Dune Sand
 As : Alluvial Sand
 Ac : Alluvial Clay
 Ap : Alluvial Peat
 Estimated Liquefied Layer

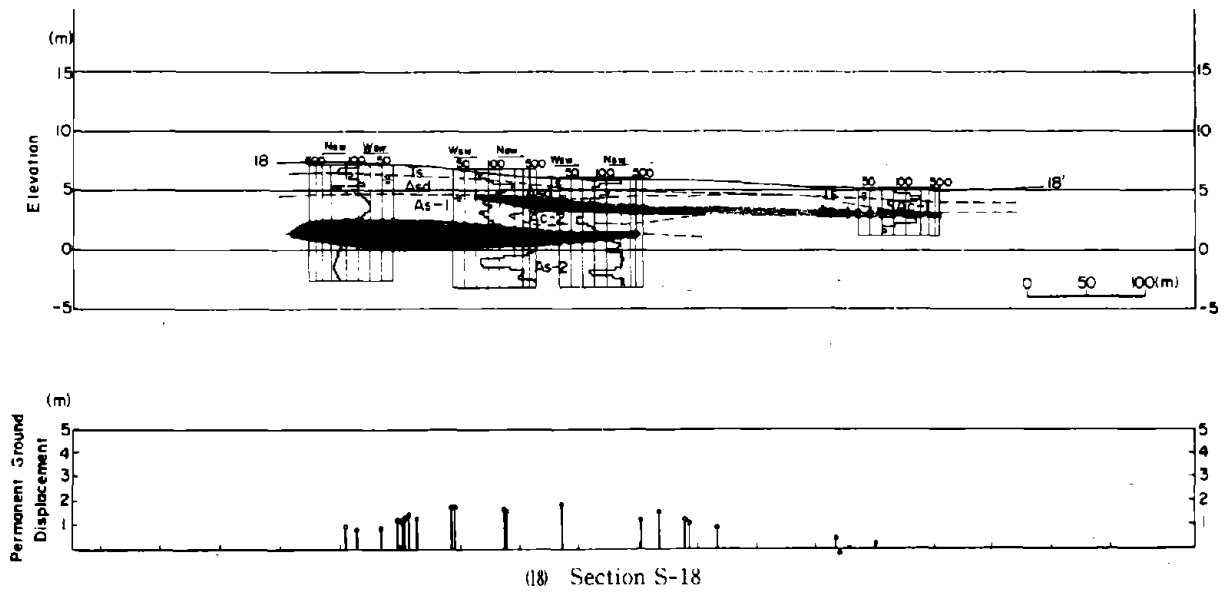
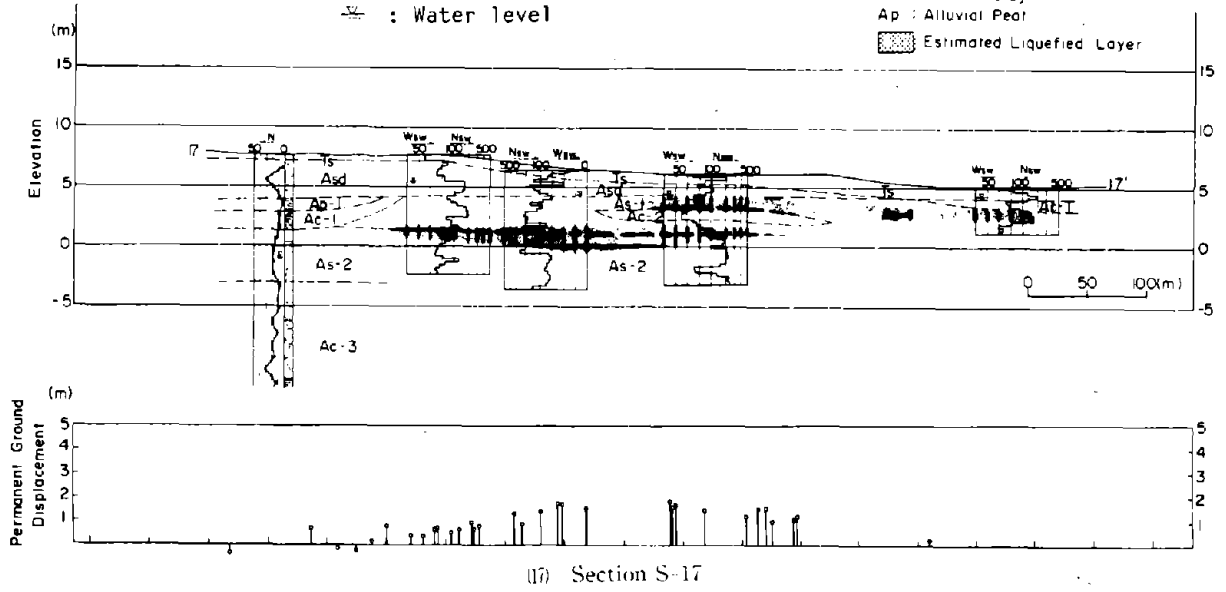


Figure B-1 Soil Profile and Estimated Liquefied Layers

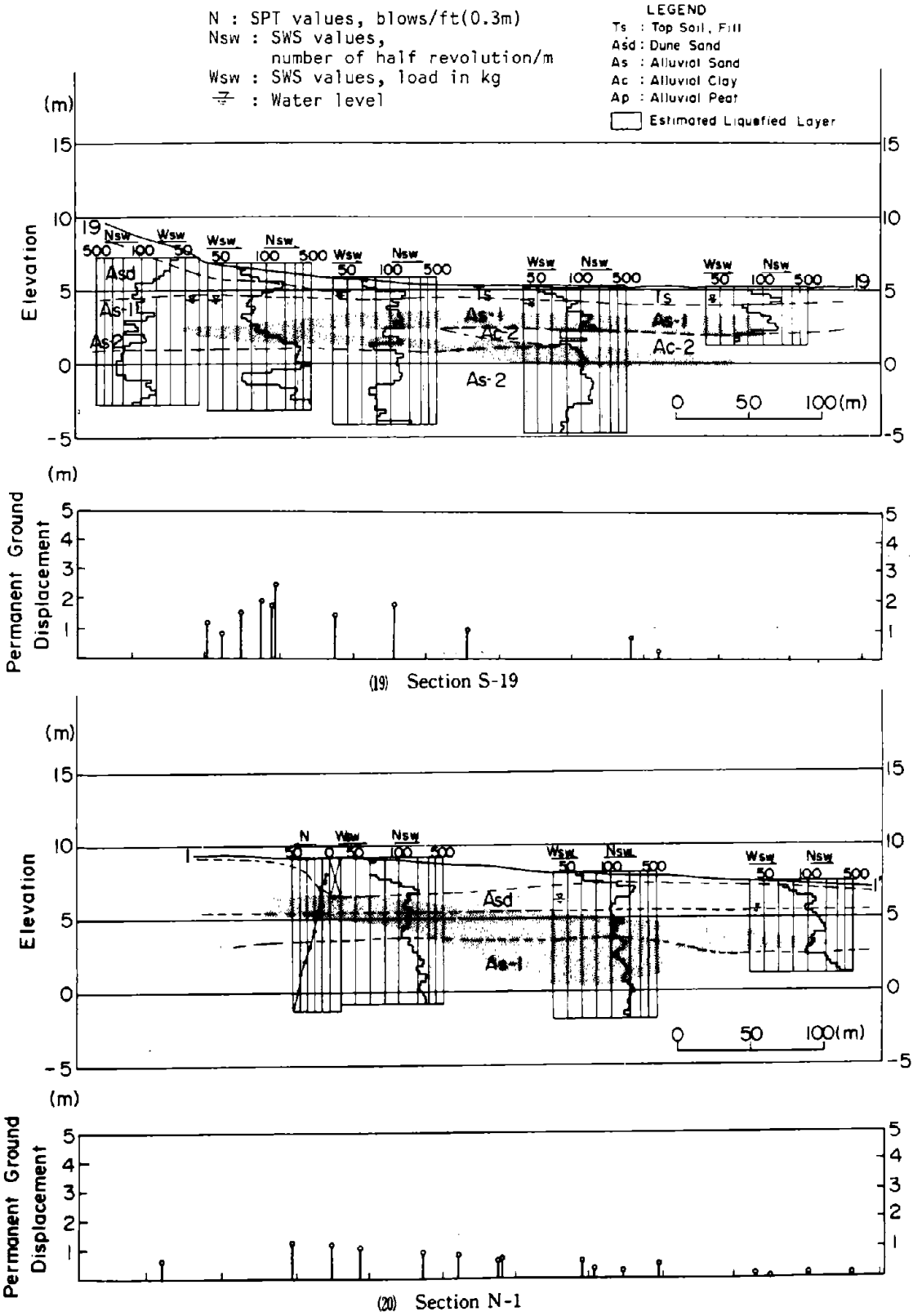
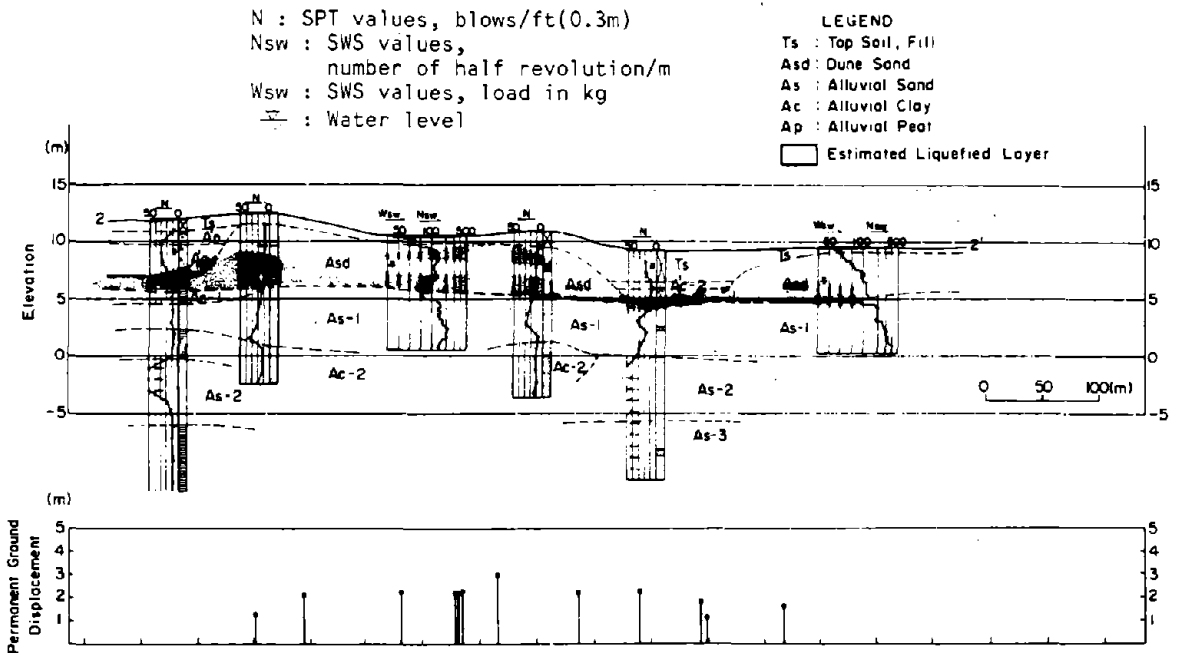
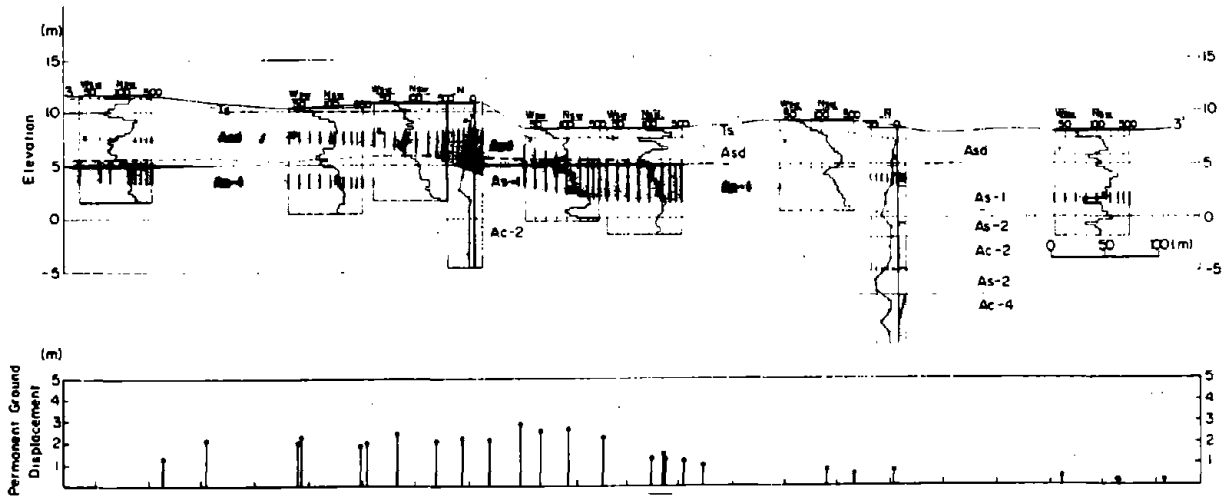


Figure B-1 Soil Profile and Estimated Liquefied Layers

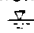



(21) Section N-2

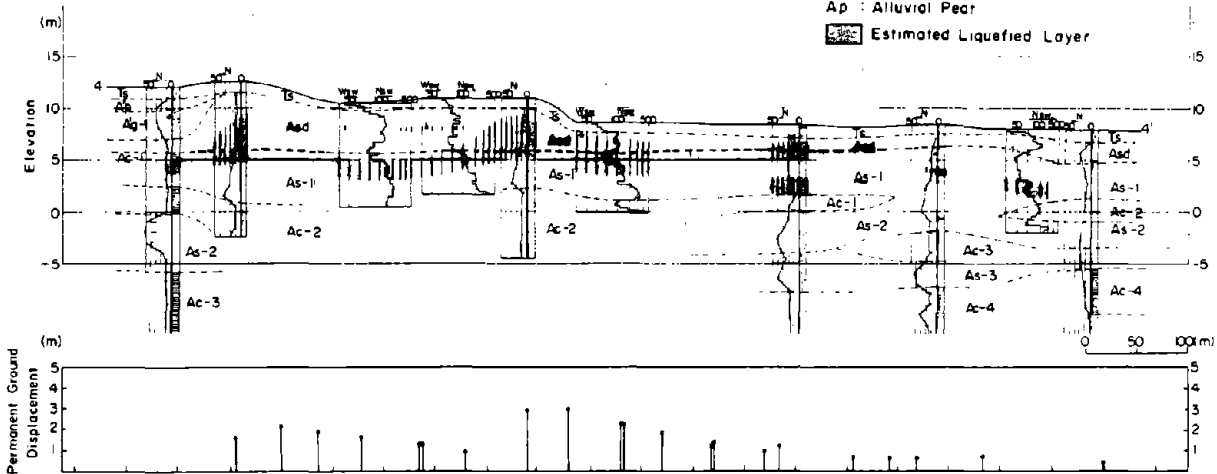


(22) Section N-3

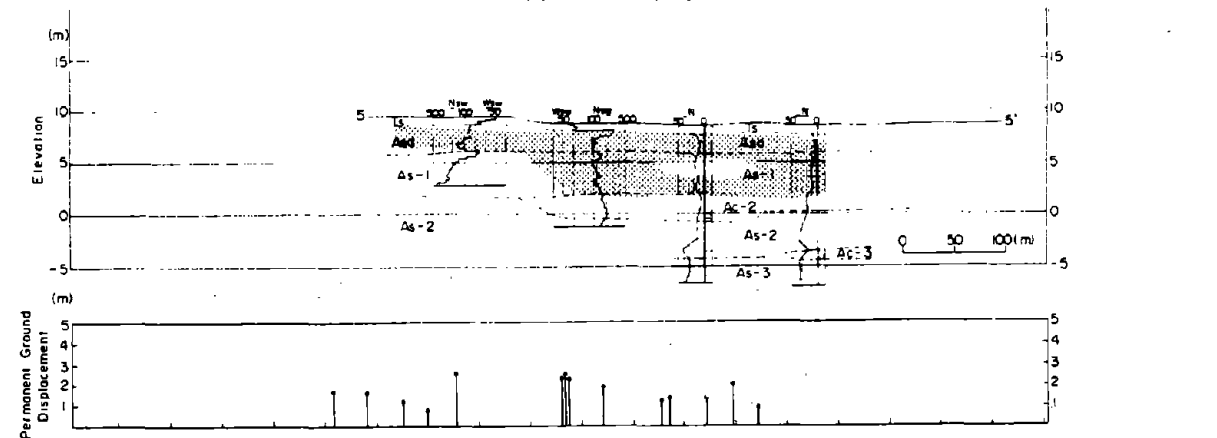
Figure B-1 Soil Profile and Estimated Liquefied Layers

N : SPT values, blows/ft(0.3m)
 Nsw : SWS values, number of half revolution/m
 Wsw : SWS values, load in kg
 : Water level

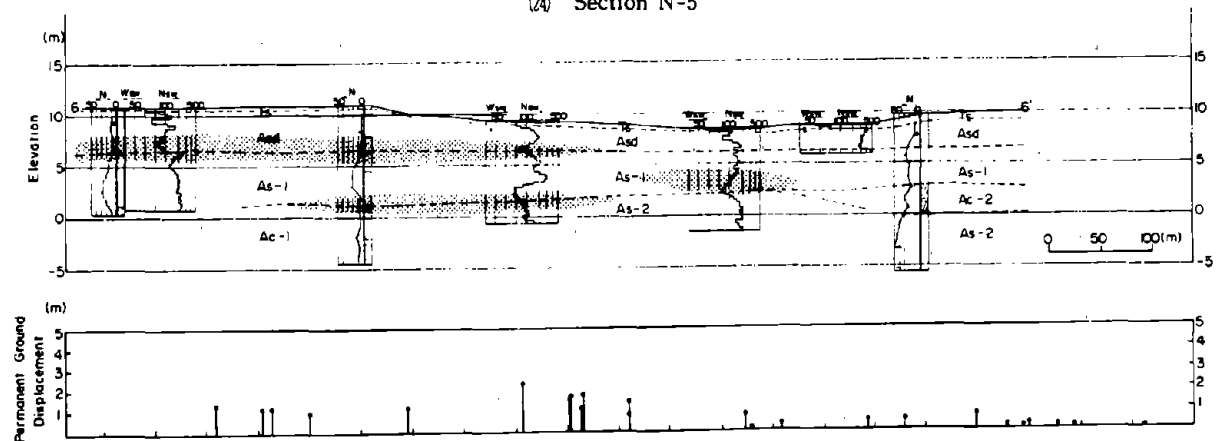
LEGEND
 Ts : Top Soil, Fill
 Asd : Dune Sand
 As : Alluvial Sand
 Ac : Alluvial Clay
 Ap : Alluvial Peat
 Estimated Liquefied Layer



(23) Section N-4



(24) Section N-5



(25) Section N-6

Figure B-1 Soil Profile and Estimated Liquefied Layers

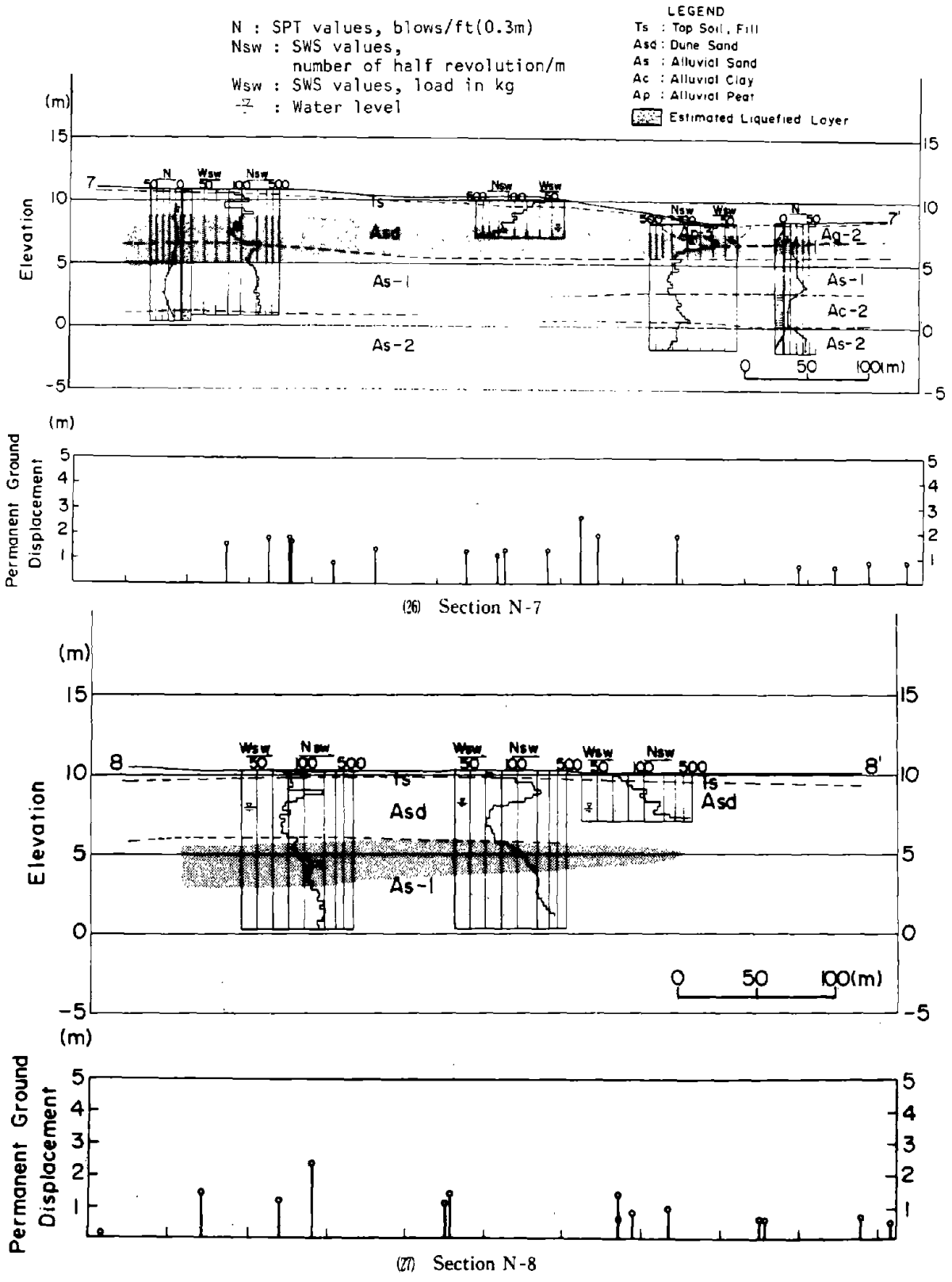


Figure B-1 Soil Profile and Estimated Liquefied Layers

Appendix C Calculation of Permanent Ground Strains

The permanent ground strain in the horizontal plane is calculated from permanent ground displacements using the following procedure:

- (i) The displacement function in each square cell (200m x 200m, see Figure 21 in main text) is assumed to be linear, that is, the strain in a cell is assumed to be constant, as follows:

$$\begin{aligned} u &= \alpha_1 x + \beta_1 y + \gamma_1 \\ v &= \alpha_2 x + \beta_2 y + \gamma_2 \end{aligned} \dots\dots\dots (C-1)$$

where,

- x, y : Coordinates in the east-west and south-north directions
- u, v : Components of ground displacements in the respective directions

- (ii) The six coefficients, α_1 , α_2 , β_1 , β_2 , γ_1 , and γ_2 , are determined from the permanent ground displacements measured in a square cell using the least squares approximation. For the determination of ground strains, at least three displacement vectors are necessary in each square cell. The permanent ground strains in the horizontal plane are obtained as follows:

$$\begin{aligned} \epsilon_x &= \frac{\partial u}{\partial x} = \alpha_1 \\ \epsilon_y &= \frac{\partial v}{\partial y} = \beta_2 \\ \gamma_{xy} &= \frac{\partial v}{\partial x} + \frac{\partial u}{\partial y} = \beta_1 + \alpha_2 \end{aligned} \dots\dots\dots (C-2)$$

where,

- ϵ_x, ϵ_y : Normal strain in x and y directions in horizontal plane, respectively.
- γ_{xy} : Shear strain in horizontal plane

**Liquefaction-Induced Large Ground Deformations
and Their Effects on Lifelines
During the 1990 Luzon, Philippines Earthquake**

*K. Wakamatsu, Research Associate
Science and Engineering Research Laboratory
Waseda University
Tokyo, Japan*

*N. Yoshida, Head of Research
Engineering Research Institute
Sato Kogyo Co., Ltd.
Tokyo, Japan*

*N. Suzuki, Senior Research Engineer
Engineering Research Center
NKK Corporation
Tokyo, Japan*

*T. Tazoh, Senior Research Engineer
Institute of Technology
Shimizu Corporation
Tokyo, Japan*



ACKNOWLEDGEMENTS

Most of the research on liquefaction-induced large ground deformations and related damage during the 1990 Luzon, Philippines earthquake was conducted by a reconnaissance team dispatched by the Association for the Development of Earthquake Prediction, Tokyo, Japan.

The authors express their great appreciation to Prof. M. Hamada, head of the reconnaissance team, other Japanese team members, Mr. A.A. Acacio of the University of the Philippines, and researchers at the Technological University of the Philippines headed by Mr. J.C. Manalastas for their assistance during the reconnaissance work. Thanks are extended to Mr. K. Sakai and Mr. I. Morimoto of Kiso Jiban Consultants, Dr. S. Yasuda of Kyushu Institute of Technology, and Dr. R. Isoyama for providing valuable information.

TABLE OF CONTENTS

	<u>Page</u>
Acknowledgments	5-iii
Table of Contents	5-v
List of Figures	5-vii
List of Photos	5-ix

<u>Section</u>	<u>Page</u>
1.0 INTRODUCTION	5-1
2.0 TECTONIC SETTING, INTENSITY, AND EFFECTS EXPERIENCED	5-2
3.0 DISTRIBUTION OF LIQUEFACTION-INDUCED GROUND FAILURES	5-3
4.0 LOCATIONS OF LARGE GROUND DEFORMATION AND THEIR GEOGRAPHICAL SETTINGS	5-5
5.0 GROUND DEFORMATIONS AND RELATED DAMAGE IN DAGUPAN CITY	5-7
5.1 Overview of Ground Deformation	5-7
5.2 Ground Deformation along Perez Boulevard	5-7
5.3 Ground Deformation along Angel Fernandez Avenue	5-16
5.4 Ground Deformation along Fernandez Street	5-19
5.5 Ground Deformation along Rivera Street	5-19
5.6 Ground Deformation along Rizal Street	5-20
5.7 Ground Deformation along Galvan, Zamora, and Burgos Streets	5-21
5.8 Ground Deformation in Pantal District	5-22
5.9 Ground Deformation in Pogo Chico District	5-23
5.10 Ground Deformation in Southern Residential Areas	5-24
5.11 Ground Deformation in the Area along the Lingayen Gulf	5-25

6.0	DAMAGE TO BUILDINGS AND HOUSES IN DAGUPAN CITY	5-26
6.1	Overview of Damage	5-26
6.2	Damage Pattern	5-27
7.0	DAMAGE TO LIFELINE FACILITIES IN DAGUPAN CITY	5-31
7.1	Water Supply System	5-31
7.2	Other Buried Structures and Electricity Distribution Lines	5-33
7.3	Electricity Distribution Lines	5-34
8.0	SUBSURFACE CONDITIONS AND ESTIMATION OF LIQUEFIED LAYERS IN DAGUPAN CITY	5-37
8.1	Subsurface Conditions	5-37
8.2	Estimation of Liquefied Layers	5-42
8.3	Geotechnical and Geomorphological Conditions at Large Deformation Sites	5-43
9.0	GROUND DEFORMATION IN BARRIO NARVACAN, SANTO TOMAS	5-46
10.0	CONCLUSION	5-49
	REFERENCES	5-51

LIST OF FIGURES

<u>Figure</u>		<u>Page</u>
1	Summary Map of the Luzon, Philippines Earthquake of July 16, 1990 (Modified from Punongbayan and Torres, 1991 and Sato, 1990)	5-2
2	Map Showing the Liquefied Sites during the Luzon, Philippines Earthquake of July 16, 1990	5-4
3	Map Showing Liquefied Sites along the Lingayen Gulf and Areas of Large Ground Deformations	5-6
4	Approximate Extent of Liquefaction in Dagupan City	5-8
5	Extent of Liquefaction-induced Ground Failures in Central Dagupan	5-8
6	Damage in the Vicinity of Magsaysay Bridge	5-11
7	Sketch of Damage to Magsaysay Bridge (after Iemura ¹²)	5-11
8	Damage in the Central Section of Perez Boulevard	5-13
9	Damage around the Bus Terminal	5-18
10	Damage in the Central Section of Rizal Street	5-21
11	Damage to Buildings and Liquefied Area in Central Dagupan	5-27
12	Water Supply System in Dagupan City	5-32
13	Damaged Lines in the Water Supply System	5-32
14	Damage to Well Casings	5-35
15	New Water Supply System under Contemplation	5-35
16	Sewage Mains	5-36
17	Locations of Gas Stations	5-36
18	Damaged Electricity Distribution Lines	5-36
19	Map Showing the Distribution of Abandoned Meanders of the Pantal River and Locations of Soil Boreholes and Soundings in Central Dagupan	5-38
20	Cross Section of Sediments along Section A-A' Showing Geotechnical Features and Estimated Liquefied Layers	5-38

<u>Figure</u>	<u>Page</u>
21 Cross Section of Sediments along Section B-B' Showing Geotechnical Features and Estimated Liquefied Layers	5-39
22 Cross Section of Sediments along Section C-C' Showing Geotechnical Features and Estimated Liquefied Layers	5-39
23 Cross Section of Sediments along Section D-D' Showing Geotechnical Features and Estimated Liquefied Layers	5-40
24 Cross Section of Sediments along Section E-E' Showing Geotechnical Features and Estimated Liquefied Layers	5-40
25 Cross Section of Sediments along Section F-F' Showing Geotechnical Features and Estimated Liquefied Layers	5-41
26 Grain Size Distribution Curves for Soils Near Magsaysay Bridge	5-41
27 Relationship between the Thickness of the Liquefied Layer and the Thickness of the Non-Liquefied Layer above it in Areas where Liquefaction Effects Were Observed and Not Observed	5-44
28 Records of Swedish Cone Penetration Tests in Barrio Narvacan	5-44

LIST OF PHOTOS

<u>Photo</u>		<u>Page</u>
1	This kind of fish pond is seen throughout Dagupan City. Cultivation of fish is one of the chief industries of Dagupan.	5-6
2	Settlement and tilting of buildings along Perez Boulevard. Note the height of the eaves.	5-9
3	Damage near Magsaysay Bridge looking from upstream. Lateral spreading and submergence of the ground along both riverbanks are clearly seen (Courtesy of Dr. G. F. Wieczorek).	5-10
4	Perez Market, at the right bank of the Pantal River. The foundation of the building was pulled toward the river (to the left) by lateral spreading of the ground.	5-10
5	Riverbank behind Perez Market. The fence broke and collapsed into the river. Magsaysay Bridge is seen in the distance.	5-10
6	The Asia Career building comprised a 5-story portion and 1-story portion. The high rise portion sank by about 1.5 meters at maximum (Courtesy of Dr. I. Towhata).	5-12
7	The Asia Career building. The low rise portion was dragged down by the settlement of the high rise portion. (Courtesy of Dr. I. Towhata).	5-12
8	Lateral spreading of the right bank along the Pantal River to the north of the building in Photos 8 and 7. A wooden house was carried into the river and completely destroyed.	5-12
9	Damage to a hospital due to lateral spreading. To the right is the Pantal River.	5-12
10	A creek flows from west to east to the north of Perez Boulevard. It is presumed to be an old channel of the Pantal River.	5-14
11	Backyard of the building next to the Fernandez Building to the east. Concrete slabs and the fence cracked and broke because the foundation ground moved toward the creek (to the left) in Photo 10.	5-14
12	A 4-story RC building tilted significantly due to liquefaction. The store next to this building was struck and damaged by this building. Both were condemned.	5-15

<u>Photo</u>	<u>Page</u>	
13	Damage of Luzon College due to liquefaction. The handrail was as high as the man's hand before the earthquake.	5-15
14	Floating of an underground septic tank at Luzon College.	5-16
15	Damage along Angel Fernandez Avenue. The road was cracked by 1 meter on the north side of the street (right side). An electric pole was snapped and the buildings subsided by about 1 meter.	5-16
16	Philippine National Bank looking from Angel Fernandez Avenue. The buildings seem to have settled a little but no damage could be found on the exterior wall.	5-17
17	Damage to the exterior wall of the Philippine National Bank looking from the rear. The building was pulled by a lateral ground movement toward the Pantal River (to the left).	5-17
18	Damage to an RC house in the north of central Dagupan. The northern part of the site (left side of the photo) faces the Pantal River. Since the foundation ground moved toward the river, the building separated at several points. Many sand boils and cracks parallel to the river were seen around this point.	5-19
19	A 5-story RC building in the middle of Fernandez Street. It settled by more than half of the height of the first floor.	5-20
20	A house located at the left bank of the Pantal River. Since the foundation ground moved toward the river, the building tilted severely toward the river and its foundations failed.	5-20
21	Collapse of tower of an old Catholic church facing Zamora Street, thought to have been caused by ground shaking (Courtesy of Mr. T. Nakajima).	5-22
22	Sand boils in the residential area along the Pantal River in Pantal district. Almost all houses settled by several tens of centimeters.	5-22
23	Damage to a gate on the right bank of the Pantal River in the Pantal District, a result of lateral spreading of the ground.	5-23
24	Fish pond north of Central Dagupan filled with sand boils.	5-23

<u>Photo</u>	<u>Page</u>	
25	Damage on the right bank of the Pantal River in the Pogo Chico District. The revetment moved by about 10 meters toward the river center (Courtesy of T. Nakajima).	5-24
26	Nine-meter-long RC wall segments with 25 cm x 60 cm cross Section. They were supported by tie beams every three meters, but moved toward the river center due to lateral spreading.	5-24
27	Cracks on a concrete slab due to lateral movement of the ground on the left bank of the Pantal River flowing through the south of Central Dagupan. The revetment moved by about 5 meters toward the river center.	5-25
28	Misalignment and vertical undulation of the roadway on the bank of the Pantal River in the Lasip Grande District. This side is the Pantal River (Courtesy of Mr. T. Nakajima).	5-25
29	Head scarp of lateral spreading on the roadway in the Lasip Chico District. A branch of the Pantal River is to the right (Courtesy of Mr. T. Nakajima).	5-26
30	The Dagupan-San Fabian Road was straight before the earthquake, but was displaced by about 2 meters to the inland side (right). Electric poles tilted due to the lateral ground movement.	5-26
31	An aerial view of Central Dagupan. Magsaysay Bridge is seen in the center and Perez Boulevard runs from the lower center to the right (Courtesy of Dr. G. F. Wiczorek).	5-28
32	Differential settlement of a building due to liquefaction along Perez Boulevard.	5-28
33	Heaving of the earth floor slab due to settlement of the structure.	5-29
34	Building displaced and damaged due settlement of the adjacent building along Angel Fernandez Avenue (Courtesy of Kiso Jiban Consultants).	5-29
35	Building displaced and damaged due settlement of the adjacent building along Fernandez Street (Courtesy of Kiso Jiban Consultants).	5-30
36	Settlement and tilting of a house due to liquefaction.	5-30

<u>Photo</u>	<u>Page</u>
37 The Insular Life building, one of two buildings constructed with pile foundations in Dagupan City. The building is located in the non-liquefied area. Several small cracks were observed on the non-structural exterior walls and these were caused by ground shaking.	5-31
38 Excavated main sewage pipe cracked by the earthquake.	5-35
39 A partly empty underground oil tank buoyantly rose up to the surface. Photo shows the excavated tank.	5-35
40 An electric pole wired to a house was severed due to lateral movement of the house.	5-35
41 Barrio Narvacan was submerged. Water reaches eaves height at high tide.	5-47
42 Damage in Barrio Narvacan. Land re-appears at low tide in some places. Sand and water boiled up everywhere during the earthquake, and the village gradually sank under the sea.	5-47
43 Damage in Barrio Narvacan. Traces of water at high tide are seen on the eaves (Courtesy of Dr. M. Hakuno)	5-47
44 Well settled due to liquefaction. Sand nearby is thought to have boiled out (Courtesy of Dr. M. Hakuno)	5-47

1.0 INTRODUCTION

An earthquake of magnitude 7.8 occurred in the town of Rizal on Luzon Island in the Philippines at 4:26 local time on July 16, 1990. Another major shock followed three minutes later, with an epicenter northwest of that of the main shock (Figure 1). A 125 km-long ground rupture was consequently found along the Philippine Fault and the Digdig Fault.

Over 1,600 people were killed and at least 3,000 were seriously injured. The earthquake inflicted damage over an area of about 20,000 km², extending from Manila through the Central Plains and into the mountainous regions in the north of Luzon Island. Landslides and liquefaction occurred widely in the affected area. Landslides directly caused by the earthquake and those induced later by monsoon rains cut highways at numerous points, delaying rescue and recovery efforts.

Low-lying areas in Central Luzon, which experienced a ground motion of M.M. Intensity VIII or greater, suffered greatly from liquefaction-related effects. The damage was especially severe in the case of roads, bridges, buildings, and lifeline systems. Most permanent ground deformations were concentrated in two areas: Dagupan City and other areas along the Lingayen Gulf, and inland flood plains along the Agno River and its tributaries.

This case history focuses on liquefaction-induced deformations and related structural damage in Dagupan City and Barrio Narvacan on the Lingayen Gulf. By way of introduction, ground motion intensity, regional seismicity, and an overview of the damage caused by this event are described. Characteristics of the large ground deformations are discussed based on a reconnaissance investigation and measurements performed by the authors. Further descriptions are given of site conditions, subsurface soils, and groundwater, along with the results of liquefaction analysis. Information is presented on damaged structures, including buildings, bridges, roads and lifeline facilities, and relationships are examined between the large ground deformations and this structural damage.

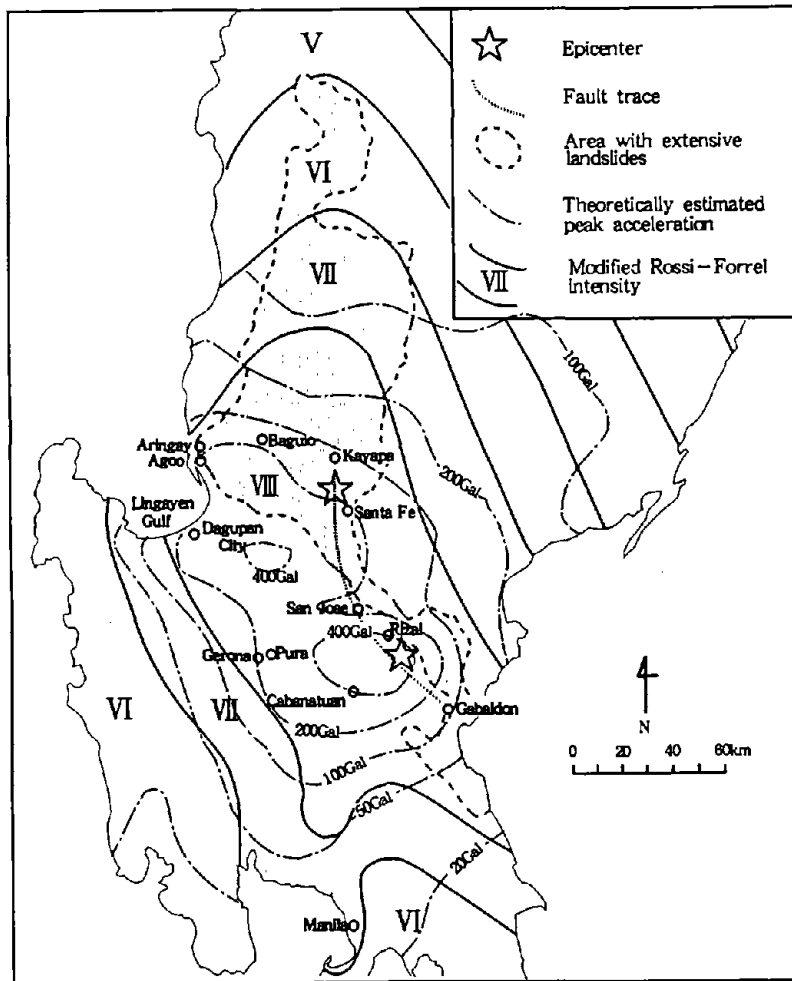


Figure 1. Summary Map of the Luzon, Philippines Earthquake of July 16, 1990 (Modified from Punongbayan and Torres, 1991 and Sato, 1990)

2.0 TECTONIC SETTING, INTENSITY, AND EFFECTS EXPERIENCED

The Philippines lie at the interface of two major tectonic plates, namely the Philippine Sea plate and the Eurasian plate. The Philippine Sea plate moves northeast towards and sinks at the Philippine trench. On the other hand, the Eurasian plate moves toward the southeast and sinks at the Manila, Negros, Sulu and Cotabato trenches. The Luzon, Philippines earthquake of July 16, 1990 occurred as a result of relative movement between these two tectonic plates. The general features of the main shock were as follows:

Origin time: 16:26'34.4" (local time)

Epicenter: 15.658°N, 121.227°E

Depth: 25 km

Ms: 7.8

Mw: 7.6¹⁾ (Moment Magnitude)

According to Punongbayan and Torres,²⁾ two separate seismic events are visible in the seismograms of the main shock. The first earthquake occurred on the Philippine Fault and the second one occurred about 3 minutes later on the Digdig Fault, one of the branches of the Philippine Fault. The epicenters of these earthquakes were located in Rizal and Kayapa, which are shown in Figure 1. The fault trace, with a mapped length of about 125 km, also is shown in the figure. The horizontal slippage along this fault reached 6.2 m at maximum. In addition, a third fault extending from Agoo City to Baguio City might have moved, according to measurements of the aftershocks.

The regional distribution of the modified Rossi-Forrel intensity resulting from this earthquake is shown in Figure 1. No strong-motion accelerogram was recorded in the Philippines at the time of the main event. Sato³⁾ estimated the distribution of the peak ground acceleration theoretically by considering the extent of the fault, and these results are also shown in Figure 1.

3.0 DISTRIBUTION OF LIQUEFACTION-INDUCED GROUND FAILURES

Figure 2 shows the locations of liquefied sites found by several reconnaissance teams⁴⁾⁻¹¹⁾ as well as by the authors. Ground failures and damage to structures attributable to liquefaction occurred in many locations along a 216 km (346 miles) long zone that stretched from Manila to the coastal region on the Lingayen Gulf. The most distant liquefied site from the epicenter is located in Bauang (Site 1 in Figure 2), the epicentral distance of which is about 140 km. The area in which severe liquefaction occurred can be classified into three regions: the coastal region on the Lingayen Gulf, the interior along the Agno River, and the eastern region along the fault. Damage due to liquefaction was notable in Dagupan City, which faces the southern shore of the Lingayen Gulf. Liquefaction is

presumed to have occurred at more sites than shown in Figure 2, but because of political and transportation conditions, confirmed liquefied sites are limited to those along major roads.

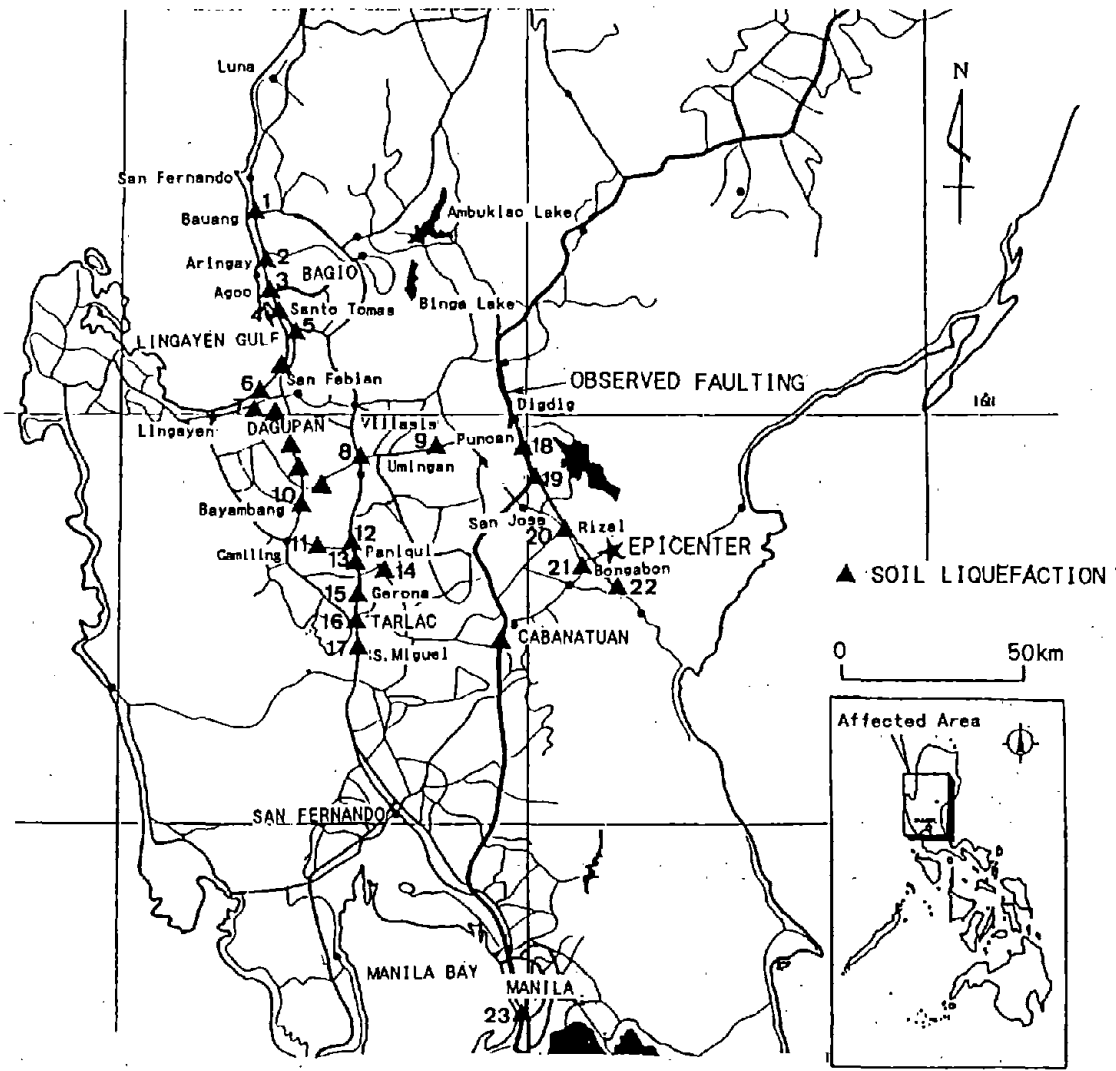


Figure 2. Map Showing the Liquefied Sites During the Luzon, Philippines Earthquake of July 16, 1990

4.0 LOCATIONS OF LARGE GROUND DEFORMATION AND THEIR GEOGRAPHICAL SETTINGS

Figure 3 shows the two areas of large ground deformation, which are the principal zones of interest in this case history. The locations are Dagupan City and Barrio Narvacan on the Lingayen Gulf.

Dagupan City, a city with a population of about 110,000, is located about 200 km north-northwest of Manila, on the southern shores of the Lingayen Gulf. Many sand bars and dunes have formed around the coastline of the Lingayen Gulf, and numerous fish ponds have been built in the marsh as between the bars and/or dunes (Photo 1). Central Dagupan is located behind this marsh, where the Pantal River, a branch of the larger Agno River, flows through to the east and north. Central Dagupan is thought to have been only 1 m above sea level before the earthquake. According to Punongbayan and Torres,²⁾ the development of Dagupan as a commercial center was firmly established in 1891, when the Manila-Dagupan railway was completed. Until the 1900s, the site of the present public market was still a swamp, waist-deep in water. Much of the present downtown area along A.B. Fernandez Avenue (formerly Torres Bugallon Avenue) was marsh land. Travel by boat along the Agno River was still the most practical means of transport. In 1908, the commercial center extended beyond the Quintos Bridge on the other side of the Pantal River. Continuing growth of the city necessitated the construction of Perez Blvd. and Magsaysay Bridge in 1948 to create more space for commercial activities. This was achieved by the usual practice of reclaiming the swamps and less productive fishponds and building on them.

Barrio Narvacan is located at the tip of a sand spit southwest of Santo Tomas. This area comprises grasslands and paddy fields, and is dotted with fish-ponds and small villages.

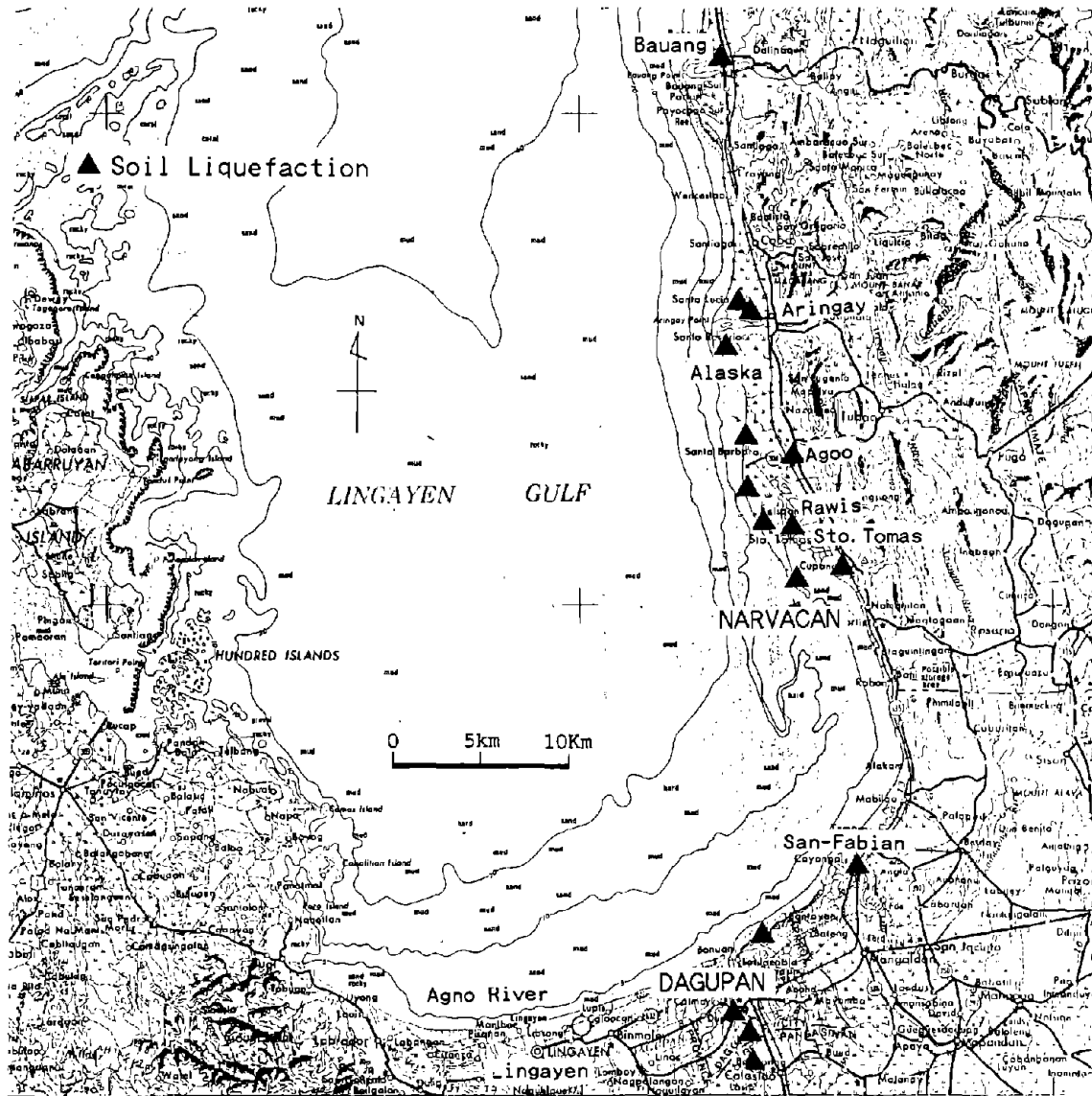


Figure 3. Map Showing Liquefied Sites along the Lingayen Gulf and Areas of Large Ground Deformations



Photo 1. This kind of fish pond is seen throughout Dagupan City. Cultivation of fish is one of the chief industries of Dagupan.

5.0 GROUND DEFORMATIONS AND RELATED DAMAGE IN DAGUPAN CITY

5.1 Overview of Ground Deformation

Figures 4 and 5 show the areas where sand boils were observed and the areas where no liquefaction-effects were observed. The direction and magnitude of the lateral spreading is also shown in the figure. These values were estimated based entirely on observations and interviews with residents. No aerial photographs taken before or after the earthquake are available at present because of government security considerations.

Dugupan City suffered various types of liquefaction-associated damage such as building settlement, bridge collapse, breakage and/or buckling of buried pipelines, electric pole settlement, and lateral spreading of river banks. Damage to structures in Dagupan City was reported as follows:

- 47 buildings condemned by the city government
- 1230 houses totally destroyed
(including reinforced concrete [RC] buildings)
- 6235 houses partially destroyed (including RC buildings)
- 80% of city roads damaged
- 2 bridges collapsed
- 1 supermarket condemned

Ground deformations and damage to the structures are described with reference to notations A to G and a to w in Figures 4 and 5, respectively. These notations are used to identify the various locations of interest.

5.2 Ground Deformation along Perez Boulevard

The buildings along Perez Boulevard suffered the most severe damage in the city, as shown in Photo 2.

(1) Magsaysay Bridge and Vicinity

Large lateral ground movements occurred toward the Pantal River near the

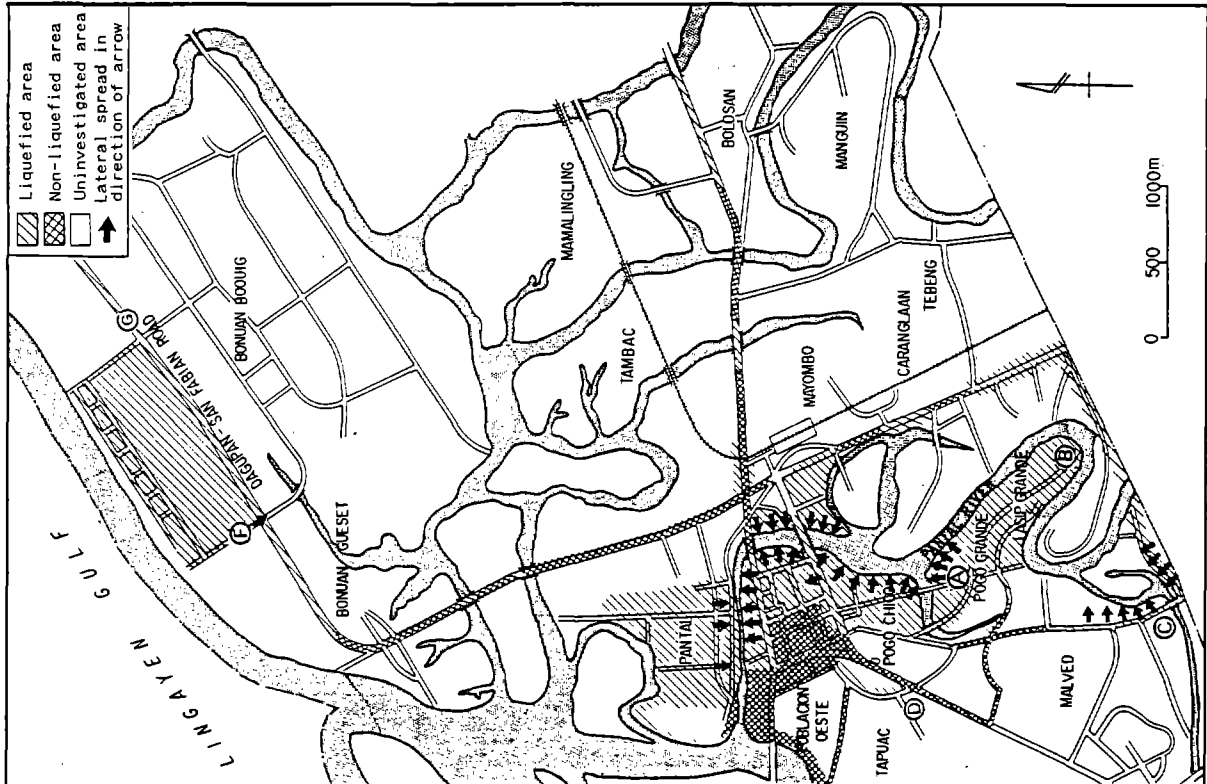


Figure 4. Approximate Extent of Liquefaction in Dagupan City

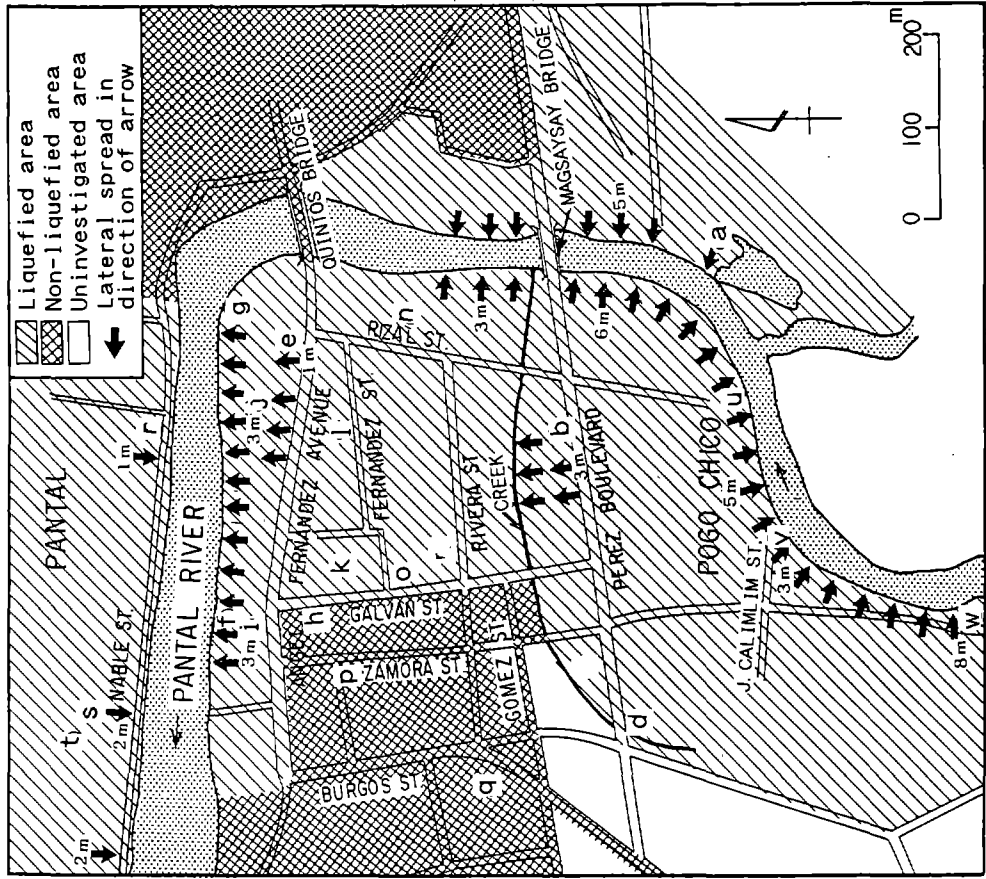


Figure 5. Extent of Liquefaction-induced Ground Failures in Central Dagupan

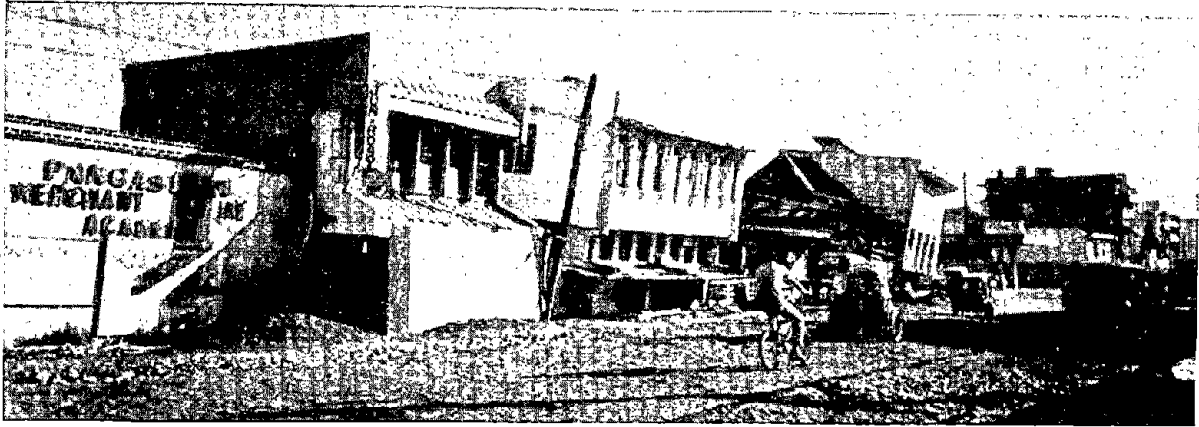


Photo 2. Settlement and tilting of buildings along Perez Boulevard. Note the height of the eaves.

Magsaysay Bridge, and caused serious damage to structures as shown in Figure 6. The Magsaysay Bridge, a 7-span reinforced concrete (RC) bridge on Perez Blvd., suffered the collapse of three spans of concrete plate girders. Two piers toppled because of liquefaction-induced loss of bearing capacity and lateral spreading of the riverbank (Figure 7, Photo 3). The foundations of Perez Market, a one-story RC building located southeast of the Magsaysay Bridge, was pulled about 1 to 2 m toward the river center, causing serious inclination of the building as shown in Photo 4. In this area, numerous sand boils were observed even two months after the earthquake. The riverbank was estimated to have moved by at least 5 m toward the river center, thus splitting apart the concrete fence shown in Photo 5. According to a resident, who was present at the time of the earthquake, the ground began to move during the ground shaking and stopped when the shaking stopped. Nipa houses made of palms to the north of Perez Market were carried into the river and were knocked down.

The Asia Career Building, a 5-story RC building with a one-story section, located northeast of Magsaysay Bridge, subsided by more than 1 m, but was hardly damaged as regards the structural elements of the high-rise portion. The one story section was forced into the ground as a result of settlement of the high-rise portion and was extensively damaged as shown in Photos 6 and 7. According to the design drawings, the foundation consists of a 40 cm thick continuous footing embedded at a depth of 80 cm. A one-story wooden house to

the north of the Asia Career Building moved by about 3 m toward the river and completely collapsed (Photo 8). Sand boils were found in the vacant lot between the wooden houses and the Asia Career Building. Several cracks, about 10 cm wide and 1 to 2 m long, appeared in the lot northeast of the wooden houses located about 30 m from the river, so this point is presumed to be the head scarp of the lateral spreading. According to one resident, the ground began to slide slowly just after the earthquake and soon stopped moving.



Photo 3. Damage near Magsaysay Bridge looking from upstream. Lateral spreading and submergence of the ground along both riverbanks are clearly seen (Courtesy of Dr. G. F. Wiczorek).



Photo 4. Perez Market, at the right bank of the Pantal River. The foundation of the building was pulled toward the river (to the left) by lateral spreading of the ground.



Photo 5. Riverbank behind Perez Market. The fence broke and collapsed into the river. Magsaysay Bridge is seen in the distance.

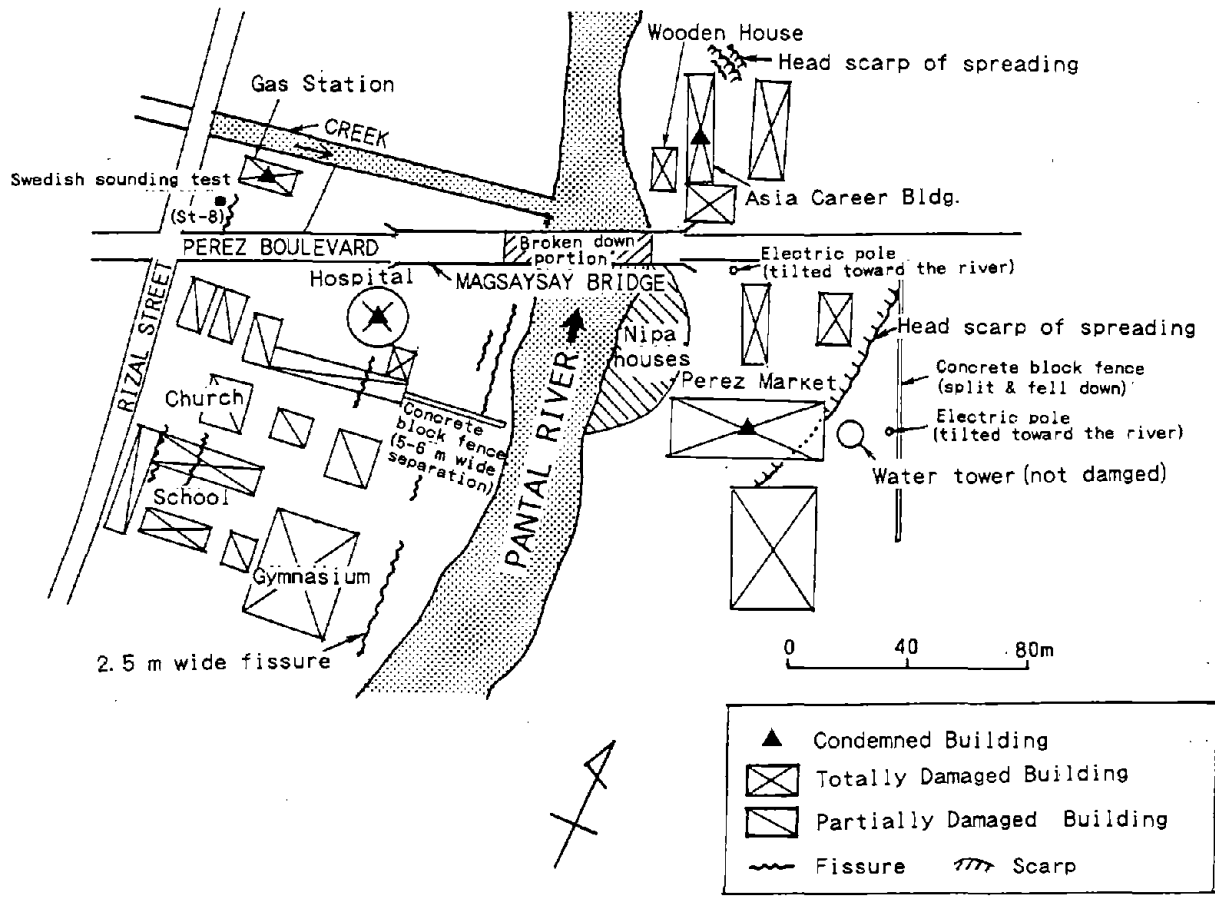


Figure 6. Damage in the Vicinity of Magsaysay Bridge

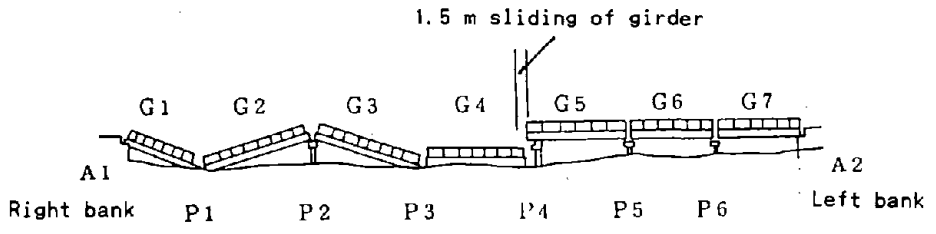


Figure 7. Sketch of Damage to Magsaysay Bridge (after Iemura¹²)

Southwest of the bridge, fissures about 2.5 m wide were found parallel to the river in places, and the area bounded by the fissures and the riverbank was submerged into the river. Nazareth General Hospital, a 3-story RC building circular in plan, tilted over as its foundations were shifted by ground movement, resulting in severe damage to the structure (Photo 9). To the south of this building, a 2-story RC building slipped toward the river and was split apart near the river bank. The concrete-block fence originally attached to this building was separated where it joined the building due to the lateral movement of the ground, which reached a separation of more than 5 m.

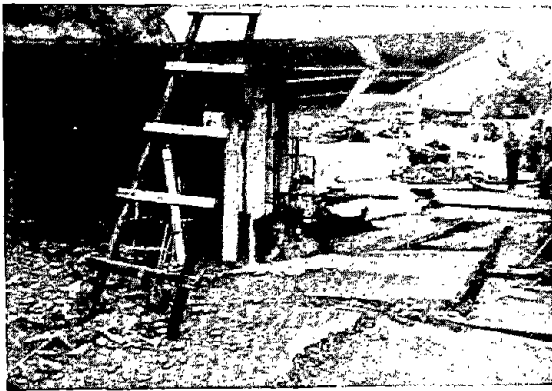


Photo 6. The Asia Career building comprised a 5-story portion and 1-story portion. The high rise portion sank by about 1.5 meters at maximum (Courtesy of Dr. I. Towhata)



Photo 7. The Asia Career building. The low rise portion was dragged down by the settlement of the high rise portion (Courtesy of Dr. I. Towhata).



Photo 8. Lateral spreading of the right bank along the Pantal River to the north of the building in Photos 6 and 7. A wooden house was carried into the river and completely destroyed.



Photo 9. Damage to a hospital due to lateral spreading. To the right is the Pantal River.

(2) Central Part of Perez Boulevard (site b in Figure 5)

Figure 8 shows a sketch of the damage around the central part of Perez Boulevard. Settlements of buildings were the largest in the area between site 1 and site 5 in Figure 8; the buildings sank about 1.5 m at maximum, relative to the street. The owners of the Fiesta Marketing Corporation building (site 1 in Figure 8), a 4-story RC building constructed in 1976, told of the situation during the earthquake as follows:

"The building sank 2 m into the ground and hot water spouted up around the building. Wide fissures appeared on both sides of Perez Boulevard, with widths ranging from 1.5 to 2 m on the north side and from 1 to 1.5 m on the south side. The Fernandez Building (Far East Bank) (site 2 in Figure 8) and Quanzon Building (site 3 in Figure 8) were found displaced by 3 m the north. A crack, 50 to 70 cm wide and parallel to the street, was formed between the building at site 2 and a concrete block fence to the north. The land nearby

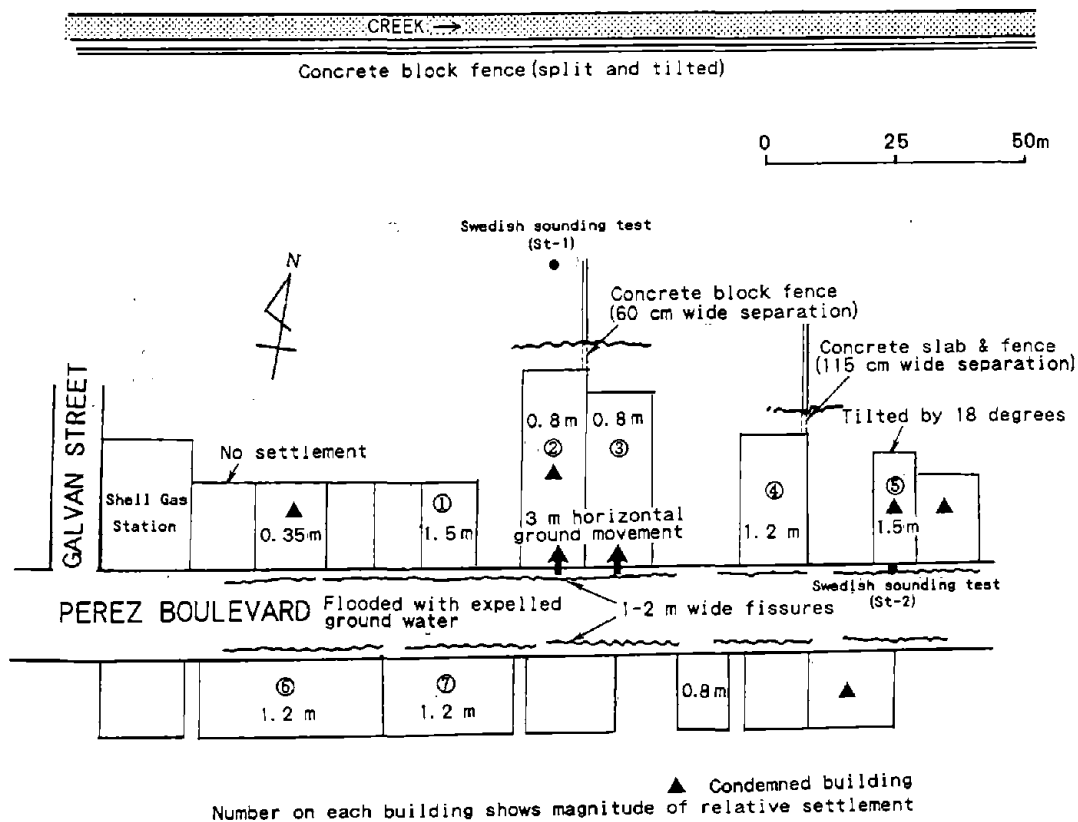


Figure 8. Damage in the Central Section of Perez Boulevard

had been reclaimed from a fish pond using coconut leaves in around 1950 and then filled with beach sand in 1960. There was a creek at the back (to the north) of the site, the width of which was reduced to 2.5 to 3 m after the earthquake from its pre-earthquake width of 5 m (Photo 10)." According to a visual survey conducted by the authors, the pavements were separated by about 3 m from the roadway.

The concrete block fence leading from north to south and the concrete slab collapsed completely in the service yard behind the 4-story RC building located at site 4 in Figure 8. The fence and slab were separated from the building by about 115 cm (Photo 11). The fissures filled with sand boils, which indicates that liquefaction-induced lateral movement of the ground had taken place. The floor heaved by about 75 cm in the north and sank by 20 cm in the south relative to the floor. A resident said, "I went out when I felt the earthquake, but I could do nothing except sit down because of the strong ground motion. I saw the block fence crack. The crack opened up during the vibration and stopped as the vibration diminished."



Photo 10. A creek flows from west to east to the north of Perez Boulevard. It is presumed to be an old channel of the Pantar River.



Photo 11. Backyard of the building next to the Fernandez Building to the east. Concrete slabs and the fence cracked and broke because the foundation ground moved toward the creek (to the left) in Photo 10.

The 4-story RC Lam Wai Nam Building, located at site 4 in Figure 8, tilted over by 18 degrees from the vertical (Photo 12). This was the largest tilt observed in the city. The tilting was restrained upon contact with the neighboring Felipe Siapno Building (Marketmix) which caused damage to the Felipe Siapno Building. The Lam Wai Nam Building was being demolished at the time of our survey (at the end of September, 1990). The foundation ground was covered with bad-smelling water and methane gas was bubbling up from the water. This gas was presumed to come from the humus soil which had formed from the coconut leaves used for reclamation.

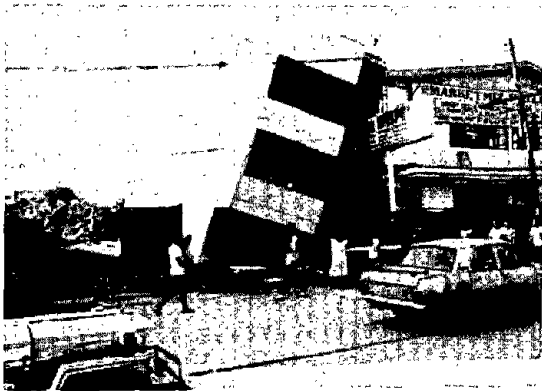


Photo 12. A 4-story RC building tilted significantly due to liquefaction. The store next to this building was struck and damaged by this building. Both were condemned.



Photo 13. Damage of Luzon College due to liquefaction. The handrail was as high as the man's hand before the earthquake.

(3) Luzon College (site c in Figure 5)

Luzon College was established in 1950, and has about 1,000 students. As shown in Figure 5, the site is located between Perez Boulevard and a creek to the north. No liquefaction effects were found to the north of the creek. The boundary between the liquefied and nonliquefied areas seems to be this creek. Sand boils and cracks were abundant on the site. A 5-story RC school building supported by a continuous-footing foundation subsided by about 1 meter at maximum. Settlement was larger near the creek. Photograph 13 shows the damage inside the school building and a stairway handrail that settled by about 50 cm. In addition, two underground septic tanks floated up under buoyancy by about 40 cm due to liquefaction (Photo 14).

5.3 Ground Deformation along Angel Fernandez Avenue

Although Magsaysay Bridge on Perez Boulevard collapsed, Quintos Bridge on the same river was not damaged. The effects of liquefaction and lateral spreading began to appear about 10 m from the western end of the bridge, and almost all buildings in the section between the intersections with Rizal Street and Galvan Street subsided by about 50 cm relative to the street. Subsidence reached 1 m at maximum. The northern sidewalk twisted by 1 m at maximum toward the river due to lateral spreading, and a crack, 1 m wide, opened (Photo 15). According to a resident, a 2-story RC building (site e in Figure 5) moved by 1 m to the north. The sidewalk in front of this building separated by about 70 cm from the roadway. The crack opened a little during the main shock, and opened further during the subsequent after shock. The ground motion was less severe during the aftershock than during the main shock.

The riverbank north of the Pantal River in the section between site f and site g in Figure 5 sank severely and sandbags had been placed at this location by the time of inspection. According to a resident, "The ground flooded with expelled water up to knee level until 1 hour after the earthquake. The street along the riverbank could not be used because the ground subsided by more than half a meter below the water". Damage was not observed at the City Hall (site h in Figure 5), but what appeared to be sand boils were found in the area.



Photo 14. Floating of an underground septic tank at Luzon College.

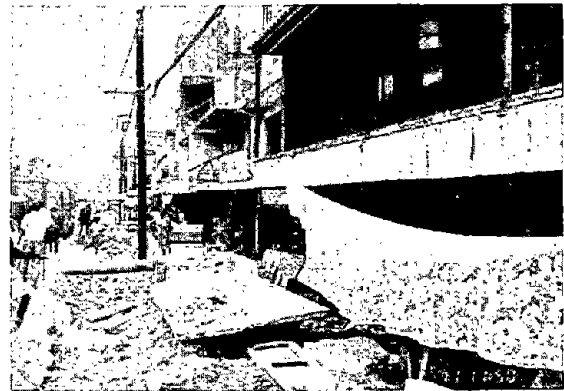


Photo 15. Damage along Angel Fernandez Avenue. The road was cracked by 1 meter on the north side of the street (right side). An electric pole was snapped and the buildings subsided by about 1 meter.

The Philippine National Bank (site i in Figure 5) faces Angel Fernandez Avenue to the south and the Pantal River to the north. The building is a one-story RC building with modern facade (Photo 16). The damage seemed minor when seen from the outside. A small amount of settlement was visible, but no cracks could be seen in the exterior wall. Inside the building, however, the concrete floor slab was cracked and buckled, load bearing columns had settled into the ground, and boiled sand was observed around the columns. The damage was more severe to the north, i.e. in the direction of the river, where differential settlement, cracks, and buckling of the walls and floor, and deformation of furniture and interior walls were observed. Wide fissures parallel to the river were observed on the concrete slab in the rear yard, indicating that the site had moved towards the river. The exterior wall was cracked, indicating that the foundations were dragged toward the river (Photo 17).



Photo 16. Philippine National Bank looking from Angel Fernandez Avenue. The buildings seems to have settled a little but no damage could be found on the exterior wall.



Photo 17. Damage to the exterior wall of the Philippine National Bank looking from the rear. The building was pulled by a lateral ground movement toward the Pantal River (to the left).

Figure 9 shows a sketch of the area around the bus terminal (site j in Figure 5). East of the vacant lot, three structures lining the river, namely, a one-story block house, a 2-story RC building, and a one-story RC building, were found to have tilted significantly in response to ground displacement into the river (Photo 18). Several houses on the river bank to the north of the vacant lot had settled. A resident who has lived in the area for 6 years said, "The ground surface used to be horizontal before the earthquake, but it

was inclined toward the river after the earthquake. The concrete slab of the house had a crack 70 cm wide. I was outside at the time of the earthquake. The ground cracked first, and then sand boiled up in the crack next. Afterwards, the house began to move. The movement was slow at the beginning, and became fast later on. It continued even after the earthquake. I can feel settlement continuing even now, although the amount is very small." Another resident living next to the previous one said, "Fissures appeared during the earthquake at the front yard, then, dark, bad-smelling mud blew up there and covered the ground up to the knee. The ground motion was strong, and the ground moved by about 3 meters toward the river. I felt the movement begin during the earthquake, and it continued even after the earthquake."

North of the bus terminal, the riverbank was distorted by 3 m at maximum over a length of about 50 m. Sand boiled up widely near the riverbank. Several cracks were found oriented parallel to the river in the vacant lot north of the bus terminal. Three of these fissures were remarkably wide, ranging from 1.5 to 2 m in width, and a maximum of 30 cm vertical movement was observed in the ground surface across them.

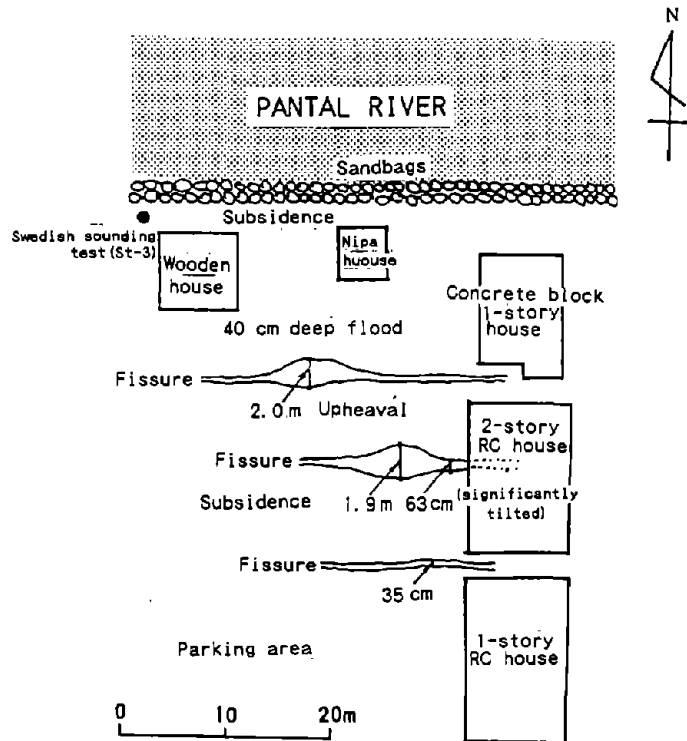


Figure 9. Damage around the Bus Terminal
5-18

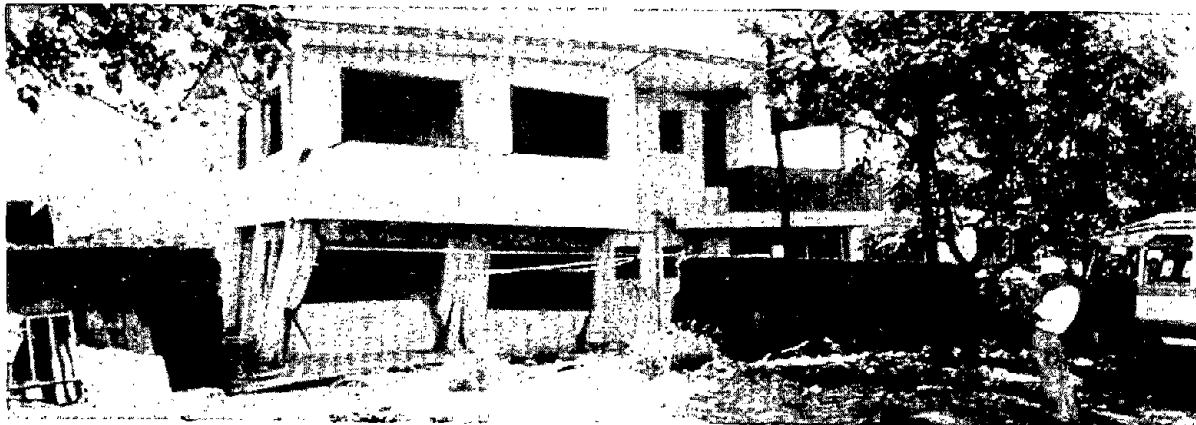


Photo 18. Damage to an RC house in the north of central Dagupan. The northern part of the site (left side of the photo) faces the Pantal River. Since the foundation ground moved toward the river, the building separated at several points. Many sand boils and cracks parallel to the river were seen around this point.

5.4 Ground Deformation along Fernandez Street

Almost all the buildings along this street were damaged as a consequence of liquefaction. The buildings settled by several tens of centimeters to 1 m relative to the street, but no lateral spreading effect was observed in this area. A large amount of a sand/water mixture boiled out at site k in Figure 5, where the Old Public Market collapsed completely. It had already been demolished by the time of the investigation (2 months after the earthquake). Photograph 19 shows a 5-story RC building, located at site l in Figure 5, which sank by more than half the height of its first story. This was the largest settlement along the street.

5.5 Ground Deformation along Rivera Street

The intersection of Rivera and Galvan Streets formed the boundary between liquefied and nonliquefied regions along this street. West of Galvan Street, roofs and exterior walls collapsed in some places, and this is presumed to be damage caused by ground shaking rather than liquefaction. East of Galvan Street, abundant liquefaction effects were noted. The Chinese Baptist Church at site m in Figure 5 suffered cracking and buckling of its interior concrete floor and settled differentially. According to a resident, "Sand/water mixture boiled from the cracks both inside and outside the building during the earthquake, and it accumulated to knee-level to the north. The water was

black and hot, and gave off a foul smell. This was an old residential area, and not land reclaimed from fish ponds, unlike Perez Boulevard."

5.6 Ground Deformation along Rizal Street

As with the previous four streets, the buildings on both sides of this street were damaged due to liquefaction, but the settlement was smaller, being limited to several tens of centimeters. Figure 10 is an enlarged view of the area around site n in Figure 6. The construction manager for a new 4-story RC building said, "The frame was just about to be completed at the time of the earthquake. The building settled by about 30 cm at the southeast corner and rotated slightly in a clockwise direction. The foundations are of a continuous footing construction. Several cracks 40 cm wide and extending parallel to the river appeared to the east of the building. A sand/water mixture boiled up and water covered the ground to a depth of about 20 cm." A 2-story wooden house northeast of the building tilted severely toward the river. Both this house and the block fence were pulled apart due to the lateral ground movement toward the river (Photo 20). The river bank at this site forms a swamp which appears to be an abandoned channel, and the ground failure described was especially severe within this former channel.

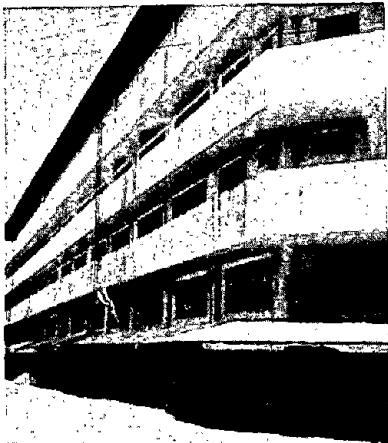


Photo 19. A 5-story RC building in the middle of Fernandez Street. It settled by more than half of the height of the first floor.



Photo 20. A house located at the left bank of the Pantal River. Since the foundation ground moved toward the river, the building tilted severely toward the river and its foundations failed.

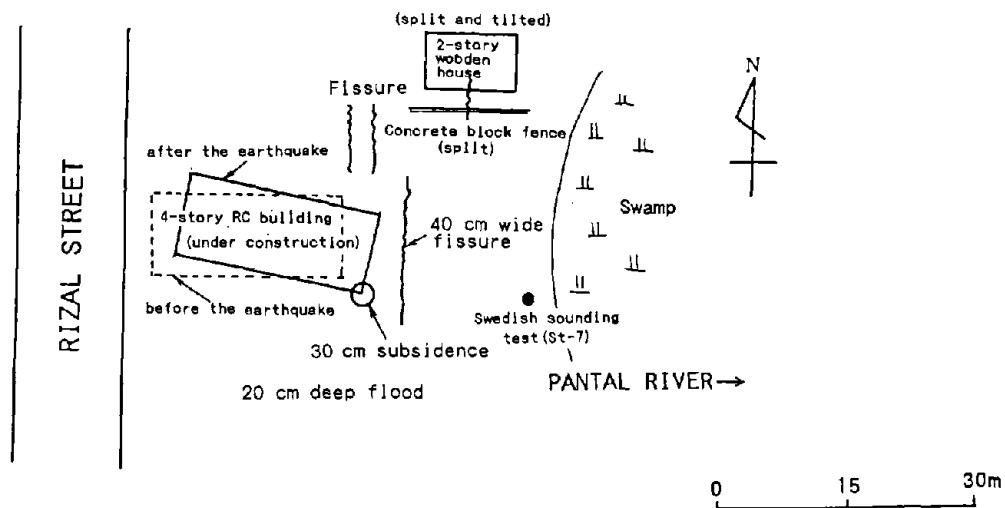


Figure 10. Damage in the Central Section of Rizal Street

5.7 Ground Deformation along Galvan, Zamora, and Burgos Streets

As shown in Figure 5, significant liquefaction effects were observed east of Galvan Street, but no evidence of liquefaction was found to the west except along Perez Boulevard. The floor cracked and heaved slightly in many places inside the Philippine Independent Church, which was built in 1950 (site o in Figure 5). According to a resident, "Sand/water boiled up in large amounts. The expelled water was hot and covered the ground to knee level. The base of a saint's statue in the church collapsed. The area east of Galvan Street was hardly damaged. This area was not used as a fish pond in the past."

Along Zamora Street, damage was light in the northern section bounded by the creek which flows to the north of Luzon College, but liquefaction-induced damage was extensive to the south. The upper structure of the brick Catholic church at site p in Figure 5 collapsed (Photo 21). The damage is thought to have been due to vibration because no evidence of liquefaction, such as sand boils, ground cracks, or subsidence, was found.

5.8 Ground Deformation in Pantal District

In the residential zone along Nable Street located north of the Pantal River, large numbers of sand boils were observed in house yards. The wooden houses settled by about 50 cm (Photo 22). The concrete protection structures along the riverbank were distorted by about 1 m toward the river, apparently a smaller movement than on the opposite bank of the river. A 59-year old man who lived at site r in Figure 5 in a 2-story Spanish style wooden house built at the end of the 19th century said: "The ground vibrated in the horizontal direction at first and later in the vertical direction. The ground cracked and bluish, bad-smelling sand boiled up all over the place. The water covered the ground to knee level. An outhouse sank by about 50 cm, and a masonry wall suffered cracking, 20 cm wide, running from east to west. The ground then began to move slowly. It began to move during the earthquake and continued after the earthquake. According to my parents, a big earthquake occurred here in 1892 and a 1-m-wide crack formed parallel to the river, but they did not say whether sand boils occurred or not."

A resident living to the east of the previous house said that his house had settled by about 60 cm as a result of the earthquake, and boiled sand had piled up to about 30 cm. The gate tilted toward the river, and a fence running perpendicular to the river split apart by about 1 m (Photo 23). At



Photo 21. Collapse of tower of an old Catholic church facing Zamora Street, thought to have been caused by ground shaking (Courtesy of Mr. T. Nakajima).



Photo 22. Sand boils in the residential area along the Pantal River in Pantal district. Almost all houses settled by several tens of centimeters.

sites in Figure 5, many cracks were found on perimeter fences perpendicular to the river, and the cumulative width of the cracks, amounted to about 2 m. Cracks could be observed even as far as 70 m from the river.

North of the residential area were fish ponds. Ground cracks and sand boils were abundant in the uncultivated fields around the ponds. Almost all the cracks at this location ran from east to west, and their maximum width was 1.3 m. According to some residents, "The area used to be a rice field until 1972, and was developed into fish ponds because of salination. The depth of the fish pond was about 1.3 meters. Sand boiled from the bottom of the pond, continuing for about 1 minute and 20 seconds. Sand was deposited to a depth of more than 40 cm." (Photo 24)

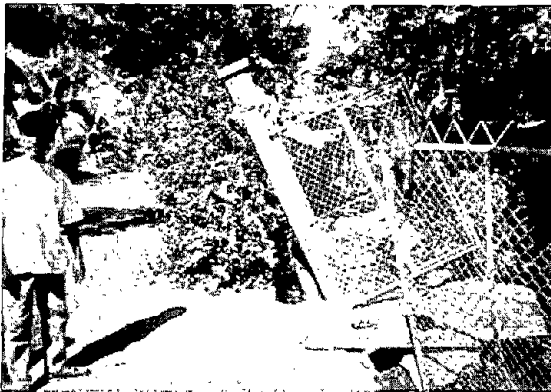


Photo 23. Damage to a gate on the right bank of the Pantal River in the Pantal District, a result of lateral spreading of the ground.



Photo 24. Fish pond north of Central Dagupan filled with sand boils.

5.9 Ground Deformation in Pogo Chico District

A concrete wall along Calimlim Street sank, moved, and was destroyed. A river protection structure was pushed toward the center of the river by about 10 m between u and v in Figure 5 (Photo 25) as a consequence of liquefaction-induced vertical and lateral movements of the ground. According to a resident, the revetment was constructed recently using 9-meter-long RC wall segments, supported with tie rods. Houses along the Pantal River tilted toward the river, and some homes were washed away. The ground cracked along the street, and sand boiled out from the cracks. The temperature of the

expelled water was about 60°C. The RC wall segments have a 25 cm x 60 cm cross-section (Photo 26). Since they project about 1.5 m above the ground surface, the length under the ground is estimated to be 7.5 m. The tie rods were attached every 3 m (5 wall segments).

Photograph 27 shows large fissures in a concrete slab at the Carlesberg Beer Company located at site w in Figure 5 which had a maximum width of 290 cm. The width of the ground fissure under the slab reached 350 cm. Several fissures, similar to those in Photo 27 were observed extending parallel to the river on this site. Those nearer the river are wider. The cumulative horizontal displacement across these fissures amounted to at least 8 m toward the river. Two warehouses collapsed almost completely. The presence of open ground fissures beneath these buildings and nearby sand boils indicates that liquefaction-induced ground failure was the primary cause of the damage. According to employees, "Black sand/water mixture boiled up and flowed to a depth of 1.5 m, and this continued for about 30 minutes. The river protection began to move during the ground motion, ending up 5 m into the river."

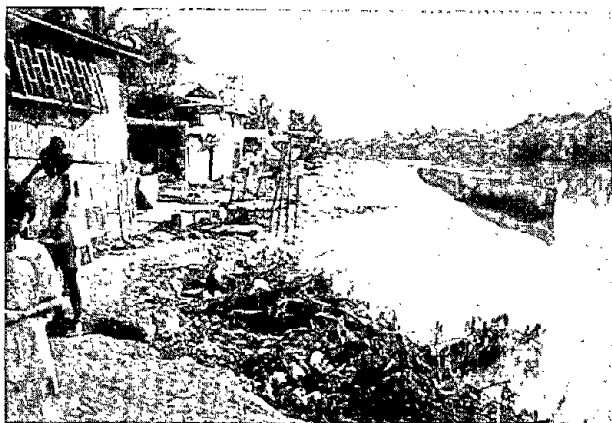


Photo 25. Damage on the right bank of the Pantal River in the Pogo Chico District. The revetment moved by about 10 meters toward the river center (Courtesy of T. Nakajima).

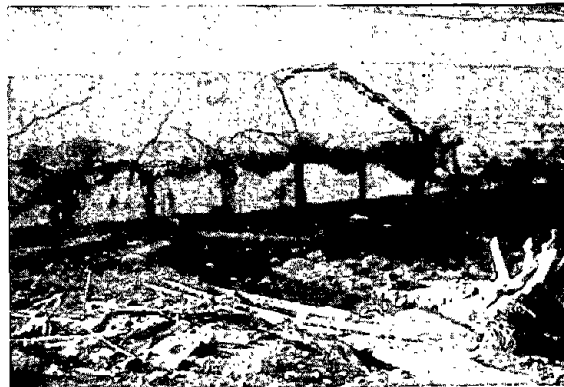


Photo 26. Nine-meter-long RC wall segment with 25cm x 60cm cross section. They were supported by tie beams every 3 m, but moved toward the river center due to lateral spreading.

5.10 Ground Deformation in Southern Residential Areas

Numerous sand boils and lateral spreading of the ground occurred in the areas south of Central Dagupan, including the Pogo Grande, Lasip Grande, and Lasip

Chico districts (see Figure 4). At an elementary school located at A in Figure 4, the riverbank moved about 2 m toward the river due to lateral spreading of the ground, and five classrooms were washed away. A sand boil, 1.5 x 2.4 m in area, and a tree displaced by about 2 m were evident at the site 2 months after the earthquake. The roadway had sunk by 30 cm.

At site B in Figure 4, misalignment and vertical undulation of the roadway occurred due to lateral movement of the ground (Photo 28). At site C in Figure 4, the ground cracked and slipped due to lateral spreading toward the river (Photo 29).



Photo 27. Cracks on a concrete slab due to lateral movement of the ground on the left bank of the Pantal River flowing through the south of Central Dagupan. The revetment moved by about 5 m toward the river center.

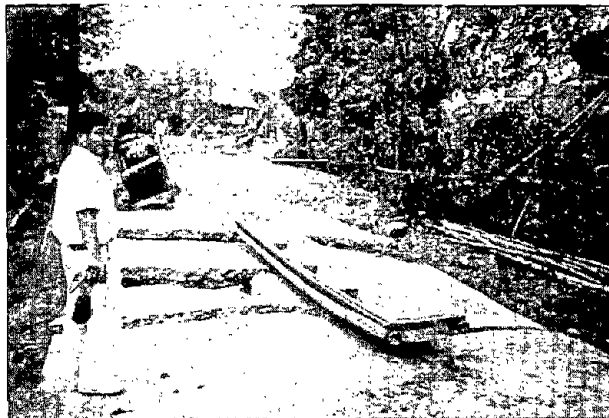


Photo 28. Misalignment and vertical undulation of the roadway on the bank of the Pantal River in the Lasip Grande District. This side is the Pantal River (Courtesy of Mr. T. Nakajima).

5.11 Ground Deformation in the Area along the Lingayen Gulf

Along the Dagupan-San Fabian Road, running to Agoo from Dagupan on the Lingayen Gulf Shore, liquefaction effects were noted in some places. Site E in Figure 4 is a new residential area which is thought to have been developed by leveling sand dunes. Sand boils and ground cracks were observed in several places. Only a few houses had been built, but some of them collapsed.

At site F in Figure 4, the road assumed a curved shape as shown in Photo 30, with a maximum lateral displacement of about 2 m inland. The road used to be straight before the earthquake according to a resident. The site is the

boundary between sand dunes and the marshy lowland. The ground movement occurred from the dunes in the direction of the lowland.

A 1-m-wide fissure about 500 m long, was observed along the road at site G in Figure 4. The road runs along the boundary between the dune sand and the lowland. Liquefaction-related effects such as breakage and differential settlement of fences were observed in some places on the lowland side.

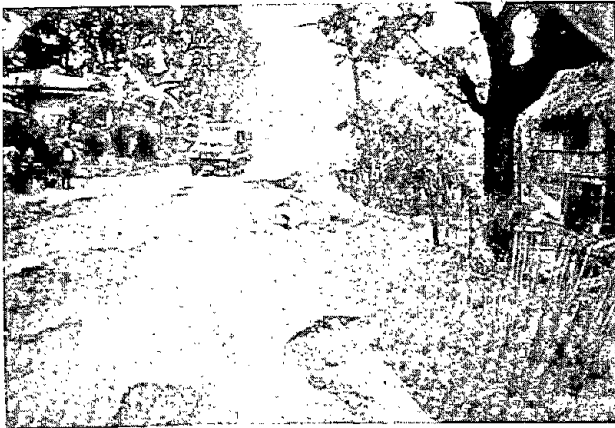


Photo 29. Head scarp of lateral spreading on the roadway in the Lasip Chico District. A branch of the Pantar River is to the right (Courtesy of Mr. T. Nakajima).

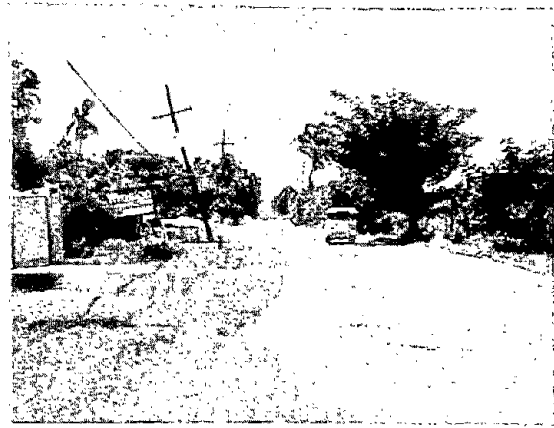


Photo 30. The Dagupan-San Fabian Road was straight before the earthquake, but was displaced by about 2 meters to the inland side (right). Electric poles tilted due to the lateral ground movement.

6.0 DAMAGE TO BUILDINGS AND HOUSES IN DAGUPAN CITY

6.1 Overview of Damage

Little structural damage was evident in areas of the city where liquefaction was not observed. Numerous buildings were severely damaged, including 47 buildings condemned for demolition in central Dagupan, where liquefaction-induced ground failure occurred. Most of these buildings were reinforced-concrete and 2- to 5-stories high without pile foundations. Photo 31 is an aerial view of Central Dagupan, and Figure 11 shows the distribution of damaged buildings as well as the estimated liquefied area. Many examples of liquefaction-induced damage to individual buildings were described in the preceding section, so only the general pattern of damage to buildings and houses will be described in this section.

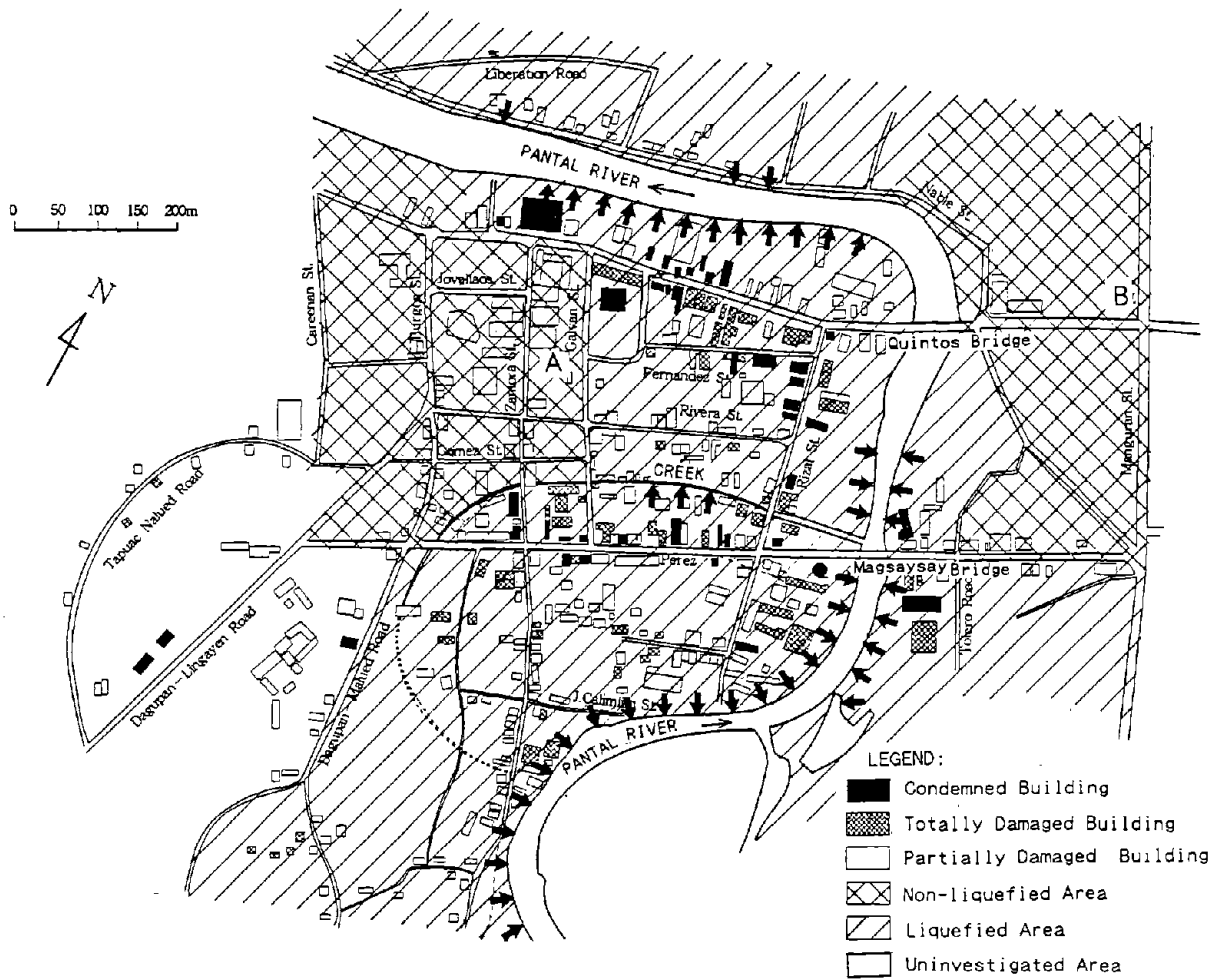


Figure 11. Damage to Buildings and Liquefied Area in Central Dagupan

6.2 Damage Pattern

Damage to the structures in Dagupan City can be classified into the following five patterns:

(1) Settlement due to Loss of Bearing Capacity

As described earlier, RC buildings were abundant in Central Dagupan, and most of them were affected by ground subsidence. Damage was severe along Perez Boulevard and Angel Fernandez Avenue, which coincide with the area where significant liquefaction-induced ground failures were observed. The settlement of the buildings ranged from 50 cm to 1.5 m relative to the

roadway. Tokimatsu, et al.⁹⁾ pointed out that this subsidence is a little less than that observed at the time of the 1964 Niigata, Japan earthquake. However, since the roadway itself sank, no absolute amount of settlement for the buildings is known at present. Techniques using aerial photographs taken before and after the earthquake, for example, can be employed to measure absolute displacements of the ground, but this type of investigation could not be carried out because of the difficulty in getting aerial photographs.

Differential settlement was also abundant. Typical damage due to differential settlement is shown in Photo 32. In addition, Photos 2, 12, 13, 15, and 19 are examples of affected buildings. More than half of the buildings in Central Dagupan tilted by more than 1 degree from the vertical.⁹⁾ The building shown in Photo 12 tilted by 18 degrees, the largest angle measured in Central Dagupan. An adjacent building prevented it from overturning completely.

Settlement of buildings also caused great damage to non-structural elements. Floors, for example, heaved up because the surrounding ground beneath load bearing walls and columns suffered relative settlement, as exemplified in Photo 33. Many examples of damage to exterior walls were also observed.



Photo 31. An aerial view of Central Dagupan. Magsaysay Bridge is seen in the center and Perez Boulevard runs from the lower center to the right (Courtesy of Dr. G. F. Wiczorek).

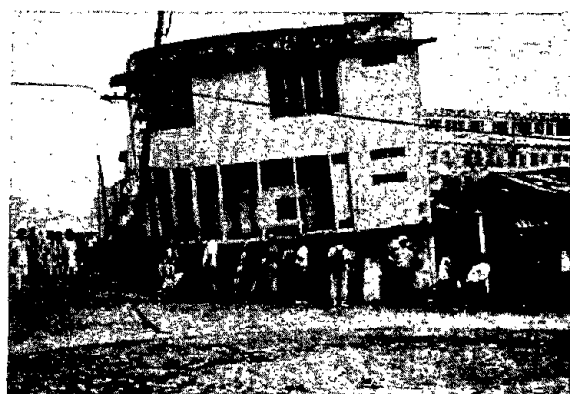


Photo 32. Differential settlement of a building due to liquefaction along Perez Boulevard.

(2) Damage Associated with Adjacent Buildings

Structural damage associated with the settlement or tilting of adjacent buildings was also observed. One typical case of this type is shown in Photos 34 and 35, in which the settled building dragged down the neighboring structure. If two buildings were directly connected or in contact with each other, and one building settled more than the other building, for example, it pulled the adjacent building down. This type of damage occurred even in a building consisting of quite different structural portions. Photos 6 and 7 are an example of this type, in which the one-story portion was dragged and damaged by the settlement of the 5-story portion. The house shown in Photo 12 (on the right) was damaged because the neighboring building tilted over and struck it.



Photo 33. Heaving of the earth floor slab due to settlement of the structure.



Photo 34. Building displaced and damaged due to settlement of the adjacent building along Angel Fernandez Avenue (Courtesy of Kiso Jiban Consultants).

(3) Damage Caused by Lateral Spreading

Damage caused by lateral spreading of the ground was also abundant. If movements of the ground in contact with a foundation vary with location, then structural elements are subjected to displacement forces and damage. Photos 4, 9, 11, 17, 18, and 20 are examples of damage due to lateral spreading.

(4) Damage due to Local Ground Deformation

Liquefaction also occurred over a widespread area outside Central Dagupan where most of the structures are one- or two-story wooden houses. Little large-scale settlement and differential settlement of houses occurred because these houses are not as heavy as the RC buildings in Central Dagupan. However, local ground deformations, such as ground cracks, relative subsidence, and ground undulations, caused severe structural damage to some of these houses (Photos 22 and 36).



Photo 35. Building displaced and damaged due to settlement of the adjacent building along Fernandez Street (Courtesy of Kiso Jiban Consultants).



Photo 36. Settlement and tilting of a house due to liquefaction.

(5) Damage due to Ground Motion

Some damage to structures occurred in non-liquefied areas. Such damage appeared to have been caused by ground motion. Photograph 21 shows an example of damage due to ground motion. Only two buildings had been built with pile foundations. Both were located in nonliquefied areas. No damage was observed to the Macador Hotel building at site A in Figure 11. Several cracks due to ground motion were observed on the nonstructural walls of the Insular Life building located at site B in Figure 11 (photo.37).



Photo 37. The Insular Life building, one of two buildings constructed with pile foundations in Dagupan City. The building is located in the non-liquefied area. Several small cracks were observed on the non-structural exterior walls and these were caused by ground shaking.

7.0 DAMAGE TO LIFELINE FACILITIES IN DAGUPAN CITY

7.1 Water Supply System

(1) Network Description

Figure 12 shows the water supply system in Dagupan City. Water is supplied from 10 wells through a distribution network consisting of various pipe materials. These materials are cast iron pipes (CIP) of 200 mm in diameter, asbestos cement pipes (ACP) of 75 to 100 mm, and polyvinyl chloride pipes (PVC) of less than 100 mm in diameter. All were buried approximately 2 m deep.

It is estimated that cast iron pipes represent 20% of the total length of the network, asbestos cement pipes 50%, and polyvinyl chloride pipes 30%. The 200-mm-diameter cast iron pipes, connected with lead caulked joints, are the oldest and the largest of the pipes in active service. They were laid about 55 years ago. The joints of the asbestos cement pipes are sealed with rubber rings, and the polyvinyl chloride pipes are joined with rubber rings or adhesive materials.

(2) Damage to Buried Pipes and Wells

Figure 13 represents the damaged lines which the city water department decided to abandon after the earthquake. The actual location of the damage was not investigated because the pipes were considered too old to repair and too deep to excavate. The spatial extent of the liquefied area is also illustrated in the figure. The abandoned lines include all kinds of pipe materials and are distributed over the liquefied area as shown in Figure 13.

Damage to buried pipes was concentrated at branches or junctions between trunk pipes and distribution pipes. Other typical locations of failure were at service pipe connections to houses and buildings. This damage is considered to have been caused by excessive shear forces, which might have been due to relative displacements between the pipes and the ground or the houses. A number of polyvinyl chloride branch pipes were damaged in the liquefied area.

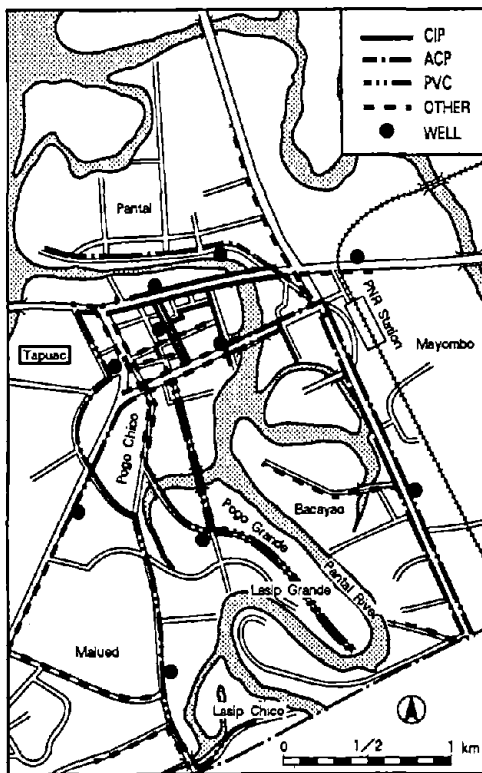


Figure 12. Water Supply System in Dagupan City

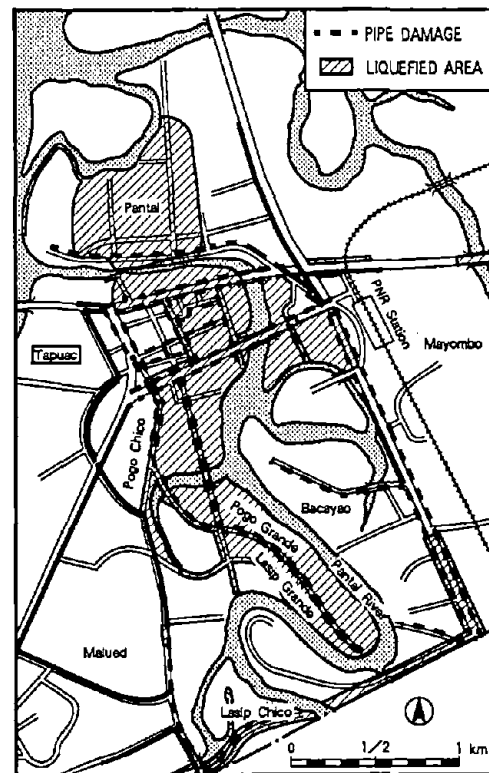


Figure 13. Damaged lines in the Water Supply System

Damage to pipes occurred mainly in the liquefied area, except in the Tapuac District where failures of polyvinyl chloride pipes were reported. Neither sand boils nor any other liquefaction-induced phenomena were observed on the ground surface, so this damage is considered a dynamic effect of the ground motion.

Besides the damage to buried pipes, some well casings were distorted by shear deformation at a depth of 1.5 to 3.0 m as shown in Figure 14. These deformations are thought to have been induced by lateral spreading of the surface layer in the liquefied area. These wells were abandoned because greater damage at lower levels in the casings was suspected. It should be mentioned that the distribution pipes were buried at the same depth as some of the observed damage to well casings.

(3) Restoration of Water Supplies

Restoration work on non-damaged wells was completed within two days of the earthquake because the Dagupan Power Corporation gave priority to repairing distribution lines to pumping stations. These wells, and certain other wells for private use, were very effective as emergency water supplies immediately following the disaster and before the buried pipes were repaired.

The Dagupan City Water Department began a renovation program for the water supply system several years ago. Figure 15 schematically illustrates the planned new water supply system including, fifteen new wells located outside the city. New distribution lines also will be constructed along the damaged pipe routes as shown in the figure.

7.2 Other Buried Structures and Electricity Distribution Lines

(1) Sewage Pipes

Reinforced concrete pipes, with diameters varying from 600 to 800 mm, were used as sewage mains which discharged into the Pantal River. The sewage mains under the main streets of the city were severed during the earthquake.

Figure 16 shows the locations of heavily damaged sewage mains along major streets in the city. Photo 38 shows an excavated sewage pipe.

At the time of the investigations, the wastewater did not drain well in most areas of the city because restoration of the damaged sewage pipes only started two months after the earthquake. As mentioned earlier, the water supply system depends on ground water drawn from wells in an aquifer beneath the city. A malfunctioning waste drainage system lead to contamination of this source.

(2) Buried Oil Tanks

Buried oil tanks at five of eight gas stations in the liquefied area floated to the surface as shown in Figure 17. Photo 39 shows a risen tank resting on the ground. Similar damage to tanks was reported during the 1964 Niigata earthquake and the 1983 Nihonkai Chubu earthquake in Japan.

7.3 Electricity Distribution Lines

Most of the electric poles in the distribution system either sank, inclined, or collapsed in the liquefied area. The maximum vertical displacement of the poles amounted to 2 m, in a case where a heavy transformer was fitted to the pole. Figure 18 shows the damaged distribution lines along which damaged poles were noted. Other damage included leakage of insulating oil from transformers on 30 poles.

Photo 40 shows very unusual damage to a reinforced concrete pole behind a wooden pole erected after the earthquake. The concrete pole was severed near the top and pulled to the left because the top of the pole was connected to a house through a wire. The house moved to the left horizontally as a result of lateral spreading of the liquefied ground. Electricity supplies to 20,000 houses were cut off due to the damage of the poles and the distribution lines during the earthquake. It was possible, however, to restore services to approximately 70% of these houses within three days after the earthquake.

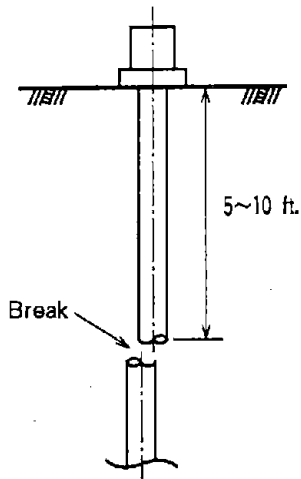


Figure 14. Damage to Well Casings

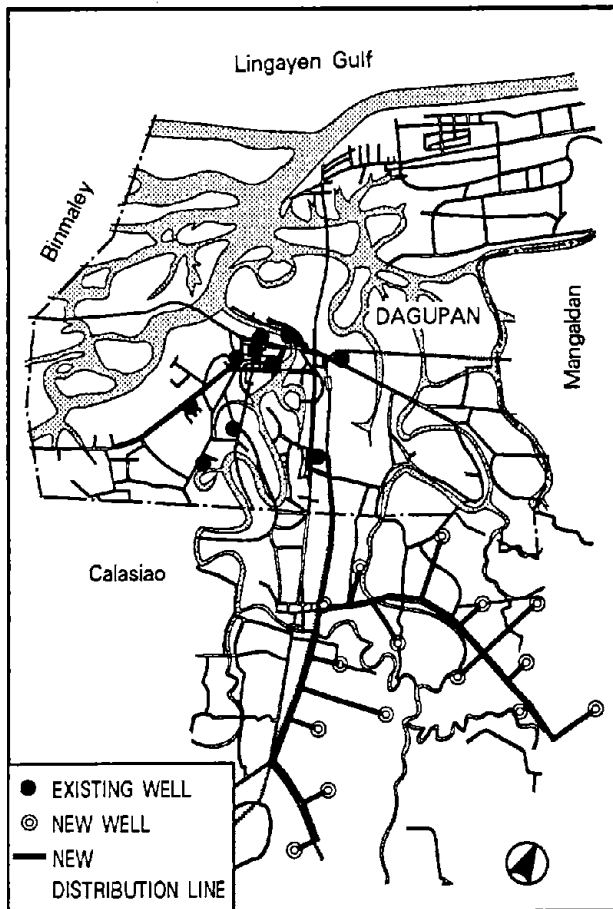


Figure 15. New Water Supply System Under Contemplation



Photo 38. Excavated main sewage pipe cracked by the earthquake.

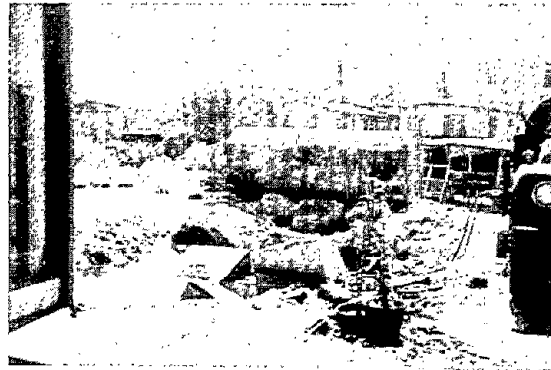


Photo 39. A partly empty underground oil tank buoyantly rose up to the surface. Photo shows the excavated tank.



Photo 40. An electric pole wired to a house was severed due to lateral movement of the house.

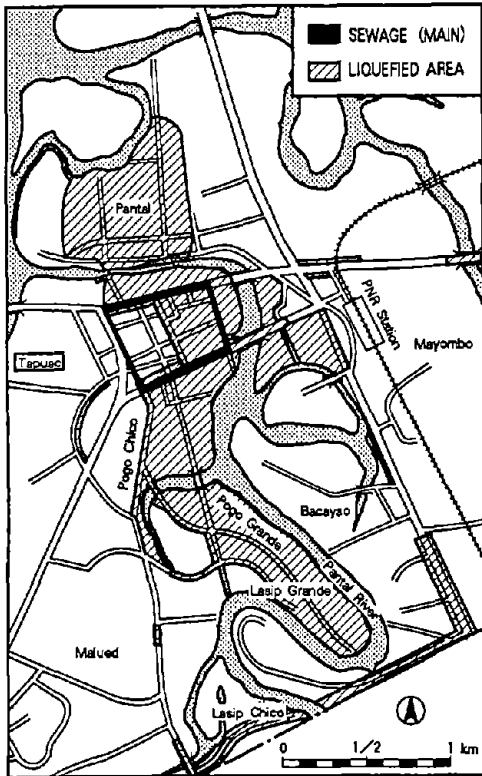


Figure 16. Sewage Mains

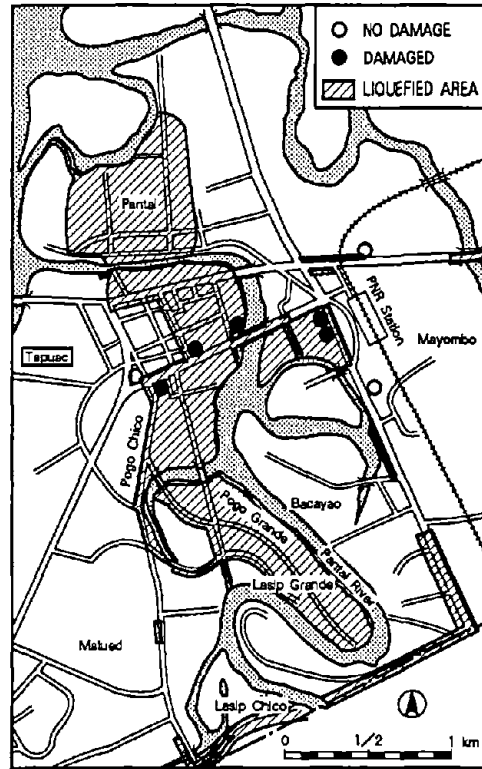


Figure 17. Locations of Gas Stations

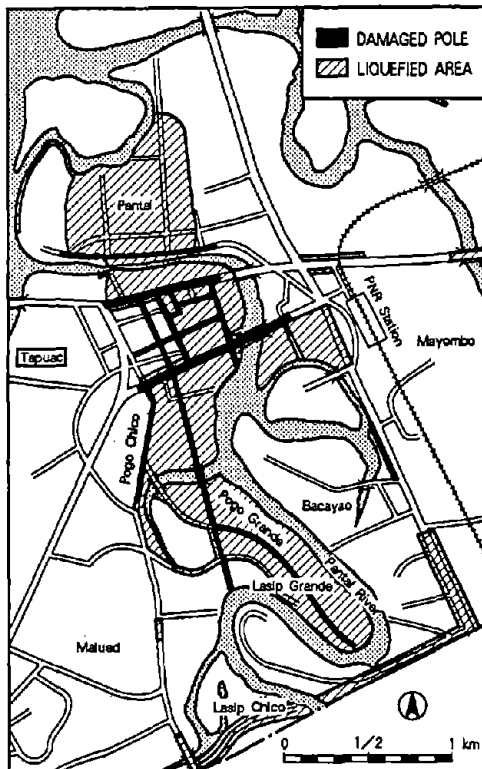


Figure 18. Damaged Electricity Distribution Lines

8.0 SUBSURFACE CONDITIONS AND ESTIMATION OF LIQUEFIED LAYERS IN DUGUPAN CITY

8.1 Subsurface Conditions

Dagupan City conducted borehole investigations with standard penetration tests (SPTs) at 21 sites in the city after the earthquake. In addition, the authors together with Kiso Jiban Consultants Co., Ltd.⁷⁾ conducted Swedish cone penetration tests (see Appendix C of reference 16) at 12 sites in Central Dagupan after the earthquake. Soil profiles along 6 sections, which are shown in Figure 19, were drawn on the basis of these investigations. The soil profiles are presented in Figures 20 to 25. A fine sand layer (As), with SPT-values between 10 and 40, exists near the ground surface or several meters below it. Under this layer, there exists a sand layer containing silt (Asc) and a clayey layer (Ac). The ground surface is composed of sandy soil, which is thought to be fill (B), as well as natural levee and/or point-bar deposits (Ts), or clayey soil from back marsh or swamp deposits (Tc).

According to a topographic map compiled in 1921, the area bounded by the Pantal River and the creek running to the north of Perez Boulevard used to be marshland supporting coconut trees. Moreover, as mentioned earlier, there were fish ponds along Perez Boulevard in the area between Galvan Street and Rizal Street, as shown in Figure 19. These ponds were filled originally with coconut leaves, and later with beach sand. Settlement and tilting of the buildings in this filled area were especially significant. Both banks of the Pantal River near the Magsaysay Bridge and the area to the north of Perez Boulevard are thought to be abandoned meanders of the Pantal River based on our visual survey (Figure 19). The fish ponds were probably built in the swamp of the abandoned channel. No SPT borehole investigation was conducted in the filled area. However, according to an SWS test conducted by the authors, there exists a very soft humus layer of coconut leaves of about 50 cm thick at a level roughly 2 to 3 m below the surface. This implies that the old fish ponds were 2 to 3 m deep and that the thickness of fill is also 2 to 3 m.

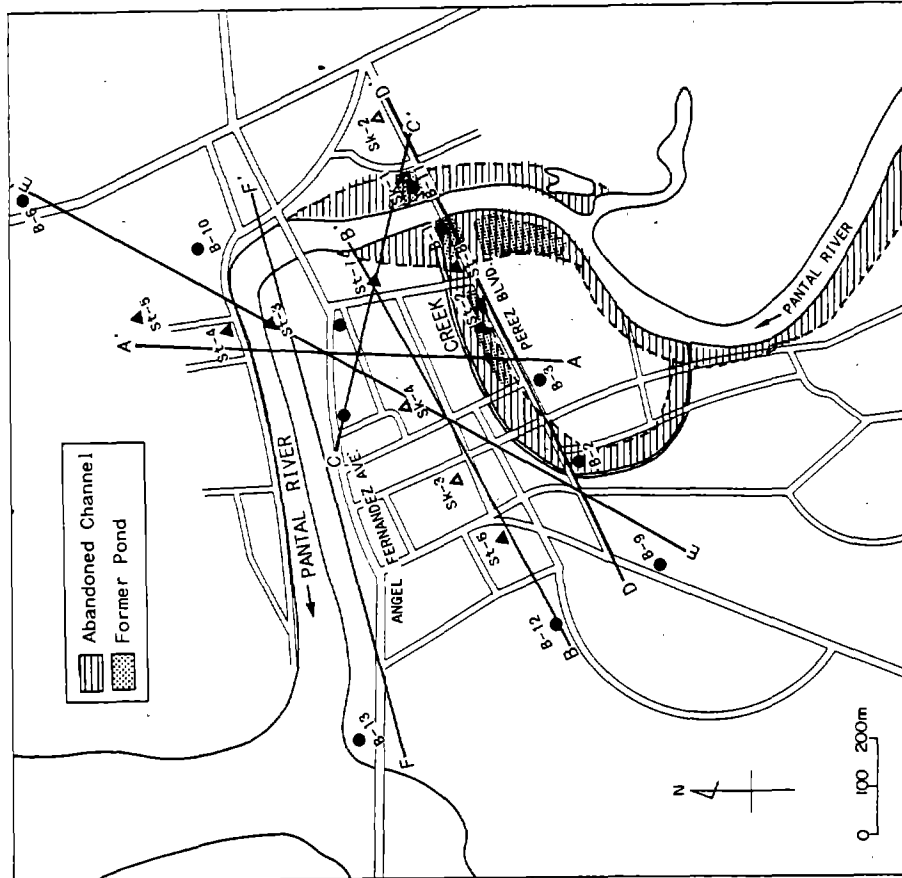


Figure 19. Map Showing the Distribution of Abandoned Meanders of the Pantanal River and Locations of Soil Boreholes and Soundings in Central Dagupan

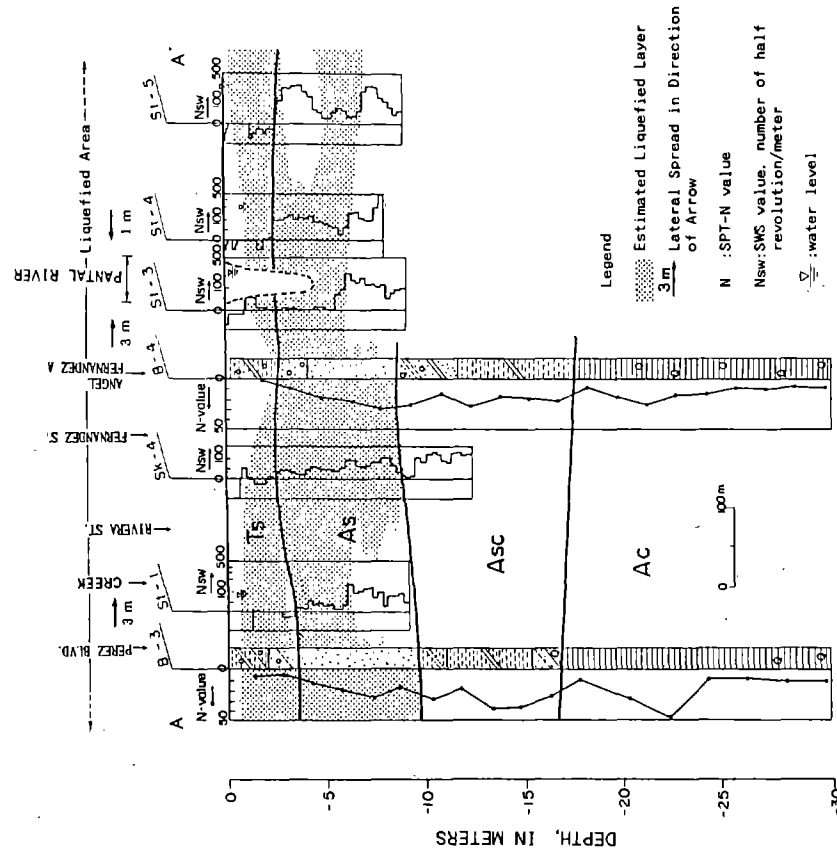


Figure 20. Cross Section of Sediments along Section A-A' Showing Geotechnical Features and Estimated Liquefied Layers

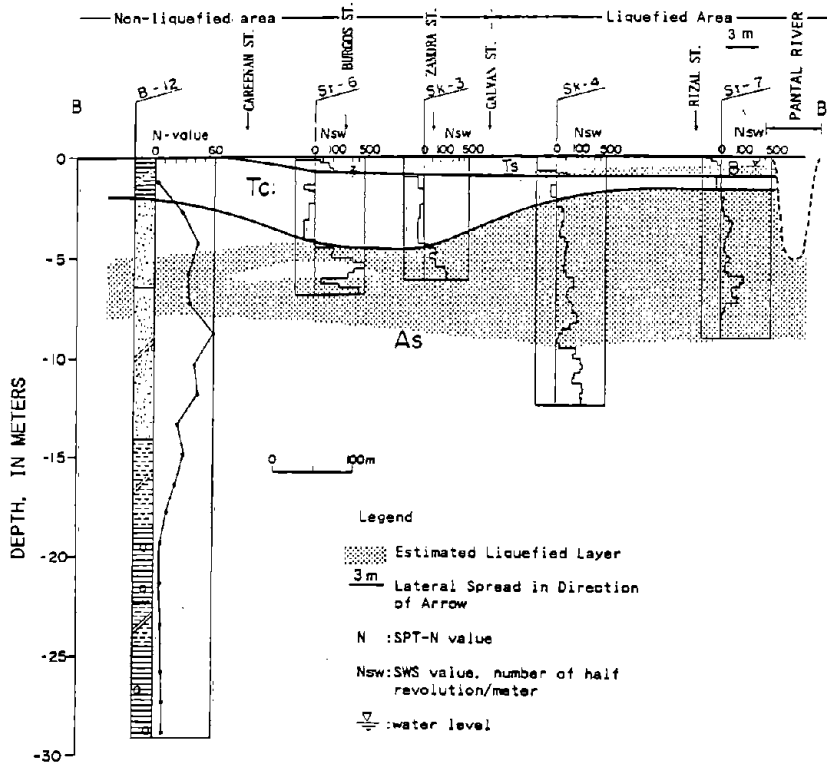


Figure 21. Cross Section of Sediments along Section B-B' Showing Geotechnical Features and Estimated Liquefied Layers

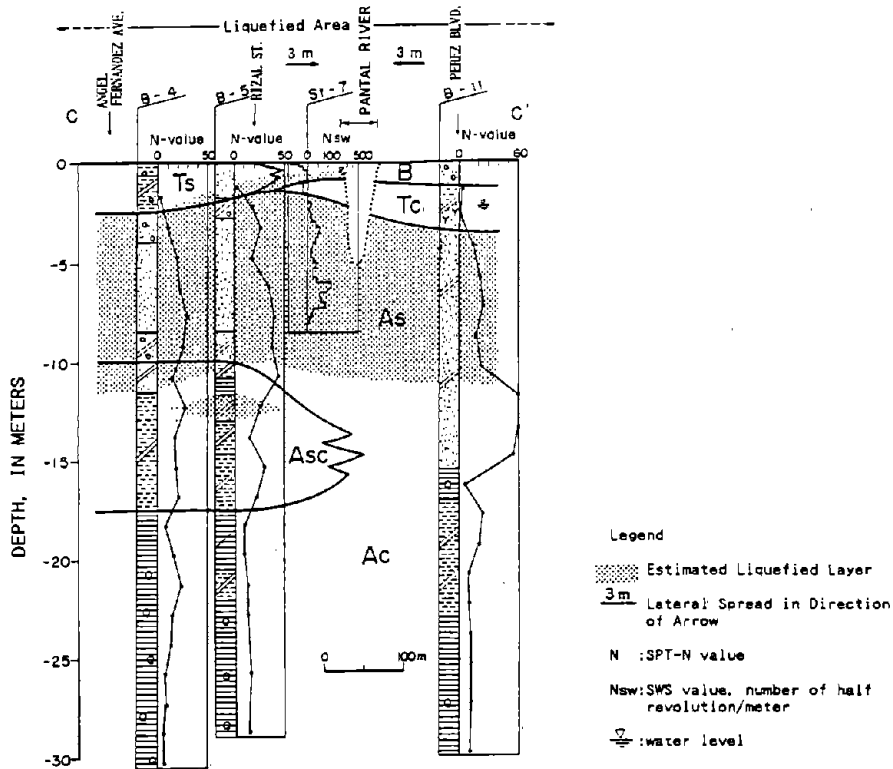


Figure 22. Cross Section of Sediments along Section C-C' Showing Geotechnical Features and Estimated Liquefied Layers.

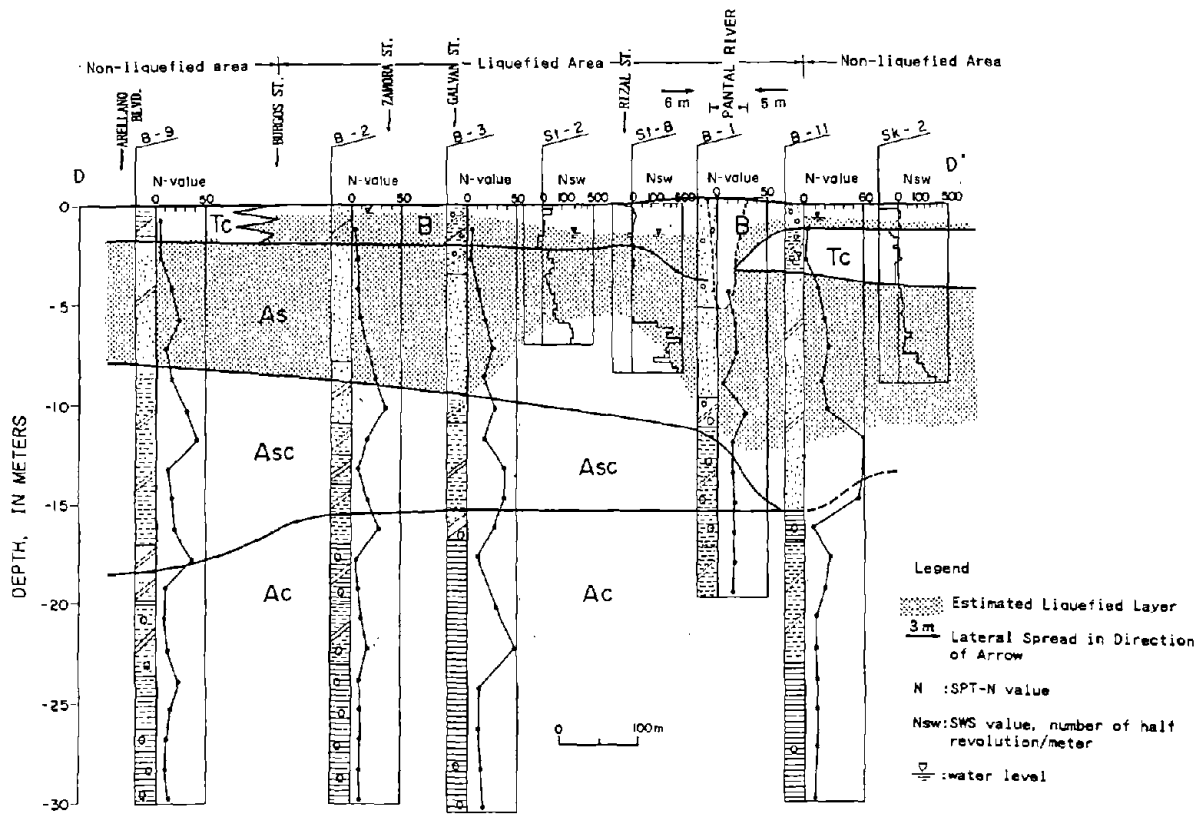


Figure 23. Cross Section of Sediments along Section D-D' Showing Geotechnical Features and Estimated Liquefied Layers

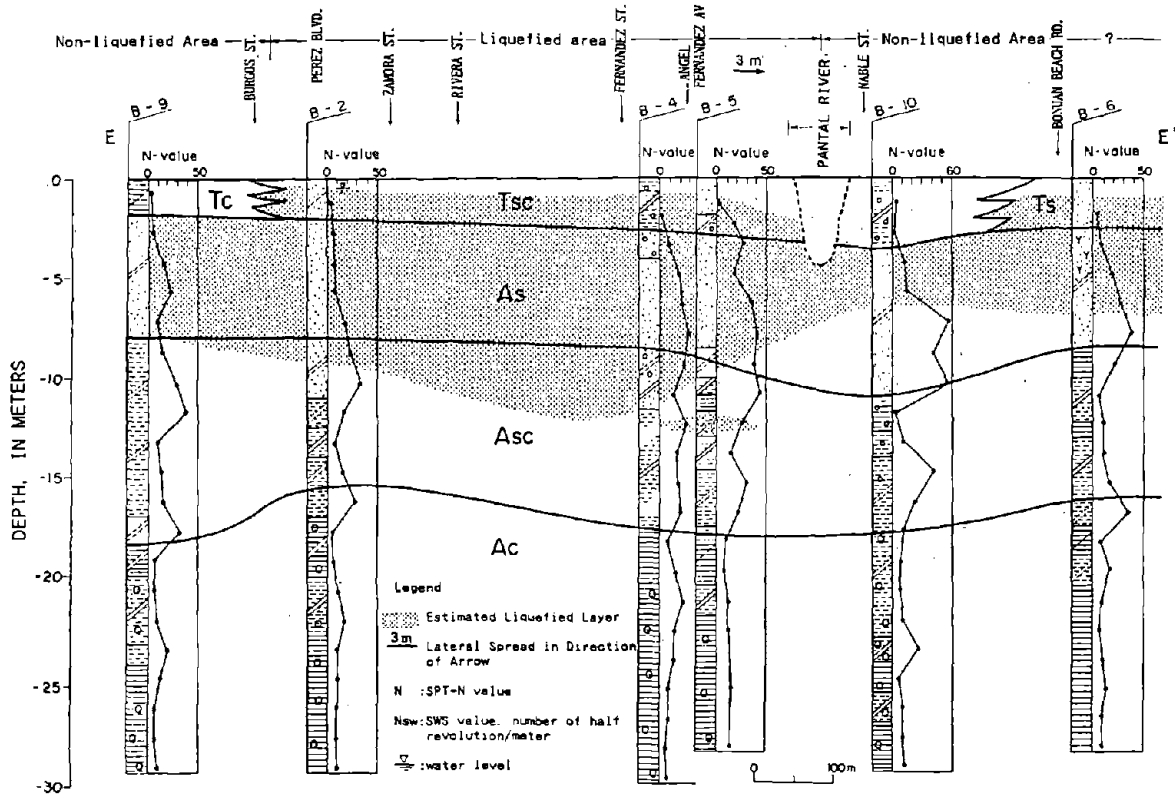


Figure 24. Cross Section of Sediments along Section E-E' Showing Geotechnical Features and Estimated Liquefied Layers

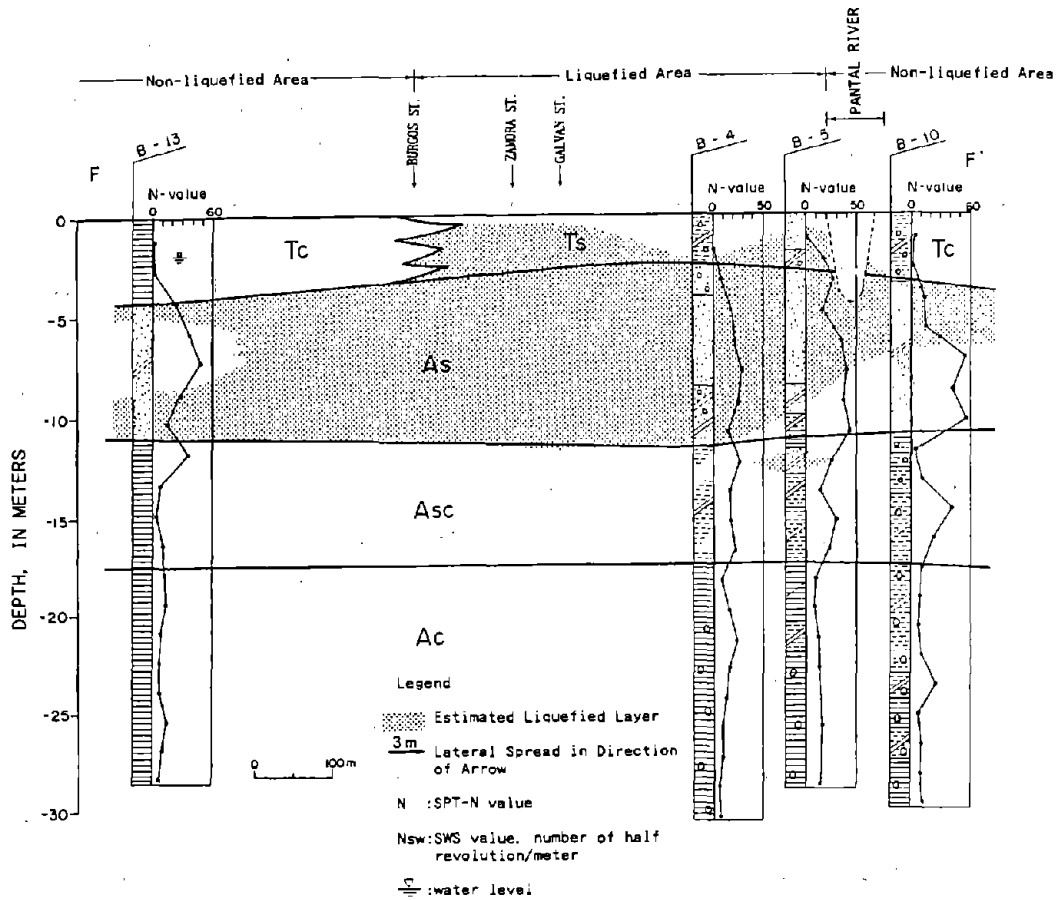


Figure 25. Cross Section of Sediments along Section F-F' Showing Geotechnical Features and Estimated Liquefied Layers

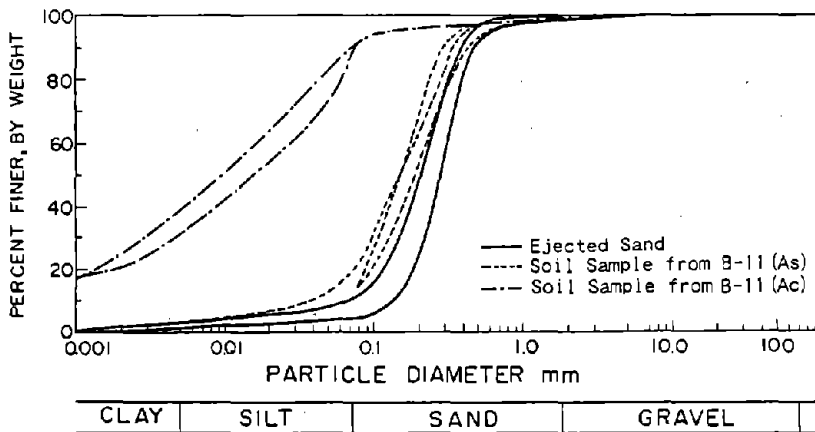


Figure 26. Grain Size Distribution Curves for Soils near Magsaysay Bridge

It should be noted that the efficiency of energy transmission by hammer in the simple penetration test used in the Philippines is different from that of the rope-pulley method used in Japan.* In other words, the SPT-value obtained in the Philippines is not equivalent to that in Japan. According to Kiso Jiban Consultants Co., Ltd.,⁷⁾ which made a comparison between the winch method used in the Philippines and the rope-pulley method, the energy transmission ratio in the winch method is about half that of the rope-pulley method. In other words, the observed SPT-values are about twice the Japanese SPT-values. Consequently, the SPT-values of sandy soils would lie between 5 and 20 and those of clayey soil would be about 5, if the rope-pulley method were employed. Judging from these SPT-values and inclusions, such as the shells and humus soil given in sample descriptions during the borehole investigations, the upper Ac layer consists of marine sediments deposited during a sea transgression several to ten thousand years ago. The Asc layer, lying above the Ac layer, consists of blackish water-deposited sediments, dating from a minor regression following the transgression. Sand layers, with relatively high SPT-values below the As layer, have the same origin as the Asc layer, and are formed of beach and sand bar deposits. The upper loose As layer is thought to consist of deposits from the Pantal River.

8.2 Estimation of Liquefied Layers

The liquefied layer, estimated on the basis of the Japanese Highway Bridge Code [Japan Road Association¹³⁾], is shown by shading in Figures 20 to 25. When calculating F_L values, the SPT-values obtained in the borehole investigation were modified by reducing them by 50%. The SPT-values at the site where SWS tests were conducted are estimated using N_{sw} - N relationships [Kiso Jiban Consultants Co., Ltd.⁷⁾]. Since no strong motion record was obtained during this earthquake, an estimated peak acceleration of 200 gal [Sato³⁾] was assumed in the calculations. As shown in Figures 20 to 25, liquefaction is thought to have occurred in the deposits from the Pantal

*Generally, SPT-values in U.S. standard are larger than in Japanese standard, because of the difference in energy transfer efficiency from the hammer to the rod (see reference 19).

River at the top of the fine sand layer (As), in the sandy fill (B), and in the natural levee and/or point bar deposits (Ts) below the water table.

Figure 26 is a comparison of the grain size distribution curves of sand in the As layer and the clay in the Ac layer near Magsaysay Bridge. The data are taken from borehole B-11, as well as from soil sampled at sand boils near the borehole site. Fines contents are larger than 90% and clayey contents are larger than 30% in the Ac layer, so the probability that liquefaction occurred in this deposit is very small. On the contrary, the sand in the As layer has a nearly uniform grain size, with a mean grain size, $D_{50} = 0.2$ mm. Hence, it could liquefy easily in a loose state. The sand boil material had similar grain size characteristics as the sand in the As layer, although the fines content may have been lost due to, for example, rainfall. The similarity in grain size distributions between the As layer and ejected sand implies that the source of liquefied material was the As layer.

8.3 Geotechnical and Geomorphological Conditions at Large Deformation Sites

Looking at Figures 20 to 25, it is clear that in areas where liquefaction effects were observed on the ground, the thickness of the liquefied layer is on the order of 5 to 10 m. In addition, the unliquefied layer above it is thin, being less than 3 m deep near the St-2 site in Figure 23 where tilting and settlement of the buildings were extreme. Furthermore, the thickness of the liquefied layer reached about 10 m in areas where damage due to lateral spreading was seen, including the area near Magsaysay Bridge (B-1 and B-11 in Figure 23). On the contrary, where the liquefied layer was thinner than 3 m, and where there exists a fairly thick non-liquefied layer above the liquefied layer, no liquefaction effects were observed.

The relationship between the thickness of the liquefied layer and the thickness of the overlying nonliquefied layer in Dagupan City is shown in Figure 27. The boundary which distinguishes the occurrence of damage due to liquefaction under the peak acceleration of 200 gals, as proposed by Ishihara,¹⁴) is also shown in the figure. The situation in Dagupan City generally agrees with Ishihara's proposal.

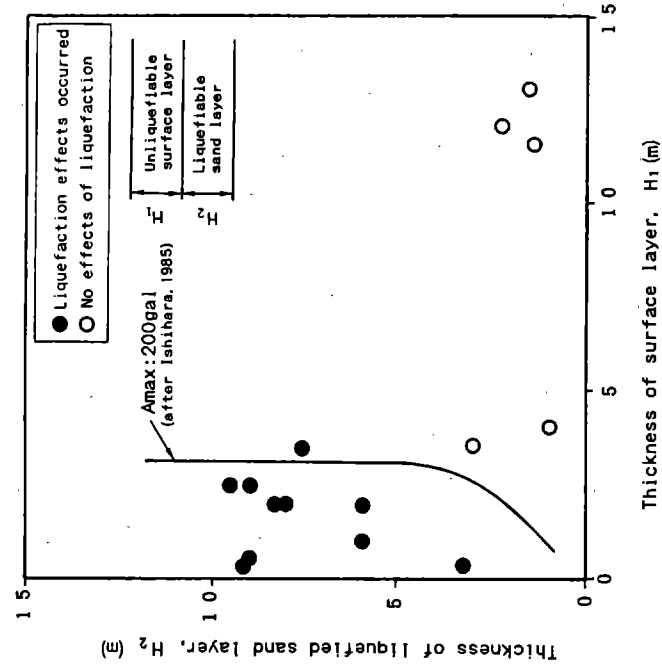


Figure 27. Relationship between the Thickness of the Liquefied Layer and the Thickness of the Non-liquefied Layer above it in Areas Where Liquefaction Effects Were Observed and Not Observed

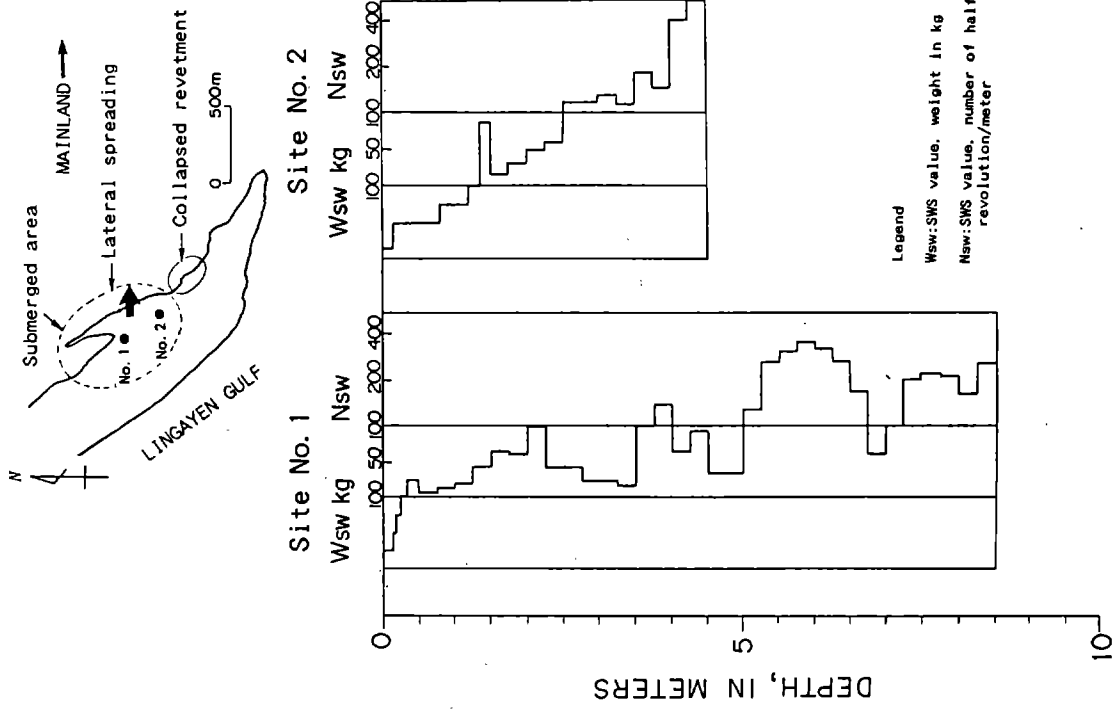


Figure 28. Records of Swedish Cone Penetration Tests in Barrio Narvacan

Lateral spreading occurred in the area along the Pantar River and nearby creek, and the ground movements were in a direction perpendicular to the water flow. Furthermore, by looking at Figure 19, it is seen that the areas, where large ground displacements occurred, were abandoned meanders of the Pantar River. Lateral spreading toward the center of the river along the Pantar River is similar to that which occurred along the Shinano River during the 1964 Niigata earthquake, described by Hamada et al.¹⁵⁾ Lateral spreading toward the small creek is similar to ground deformation in the Ohgata district of Niigata City during the 1964 Niigata earthquake [Hamada¹⁶⁾], the Morita district of Fukui City during the 1948 Fukui earthquake [Hamada et al.¹⁷⁾], and the Nishi-kameari district of Tokyo during the 1923 Kanto earthquake [Hamada et al.¹⁸⁾]. Geomorphological ground conditions at these sites have the following common features:

- 1) The ground surface is nearly flat, but is inclined slightly in the direction of ground movement.
- 2) The ground movements were in a direction perpendicular to the river or creek. These watercourses were only several meters wide at the time of the earthquake, but had been much wider a few centuries before the earthquake.
- 3) There are thick river deposits near the ground surface, and these are thought to have liquefied.

Lateral spreading in Dagupan most likely was the result of mechanisms similar to those identified for the earlier earthquakes [Hamada et al.¹⁵⁾]. Sand boiled from abandoned meanders and flowed toward the river center. As a result, the whole area near the riverbank moved. The ground sank due to volume change caused by the transported materials. The existence of a thick liquefied layer and thin nonliquefied layer above it, in addition to the lack of rigid river bank protection, is the major reason why significant lateral displacement occurred.

9.0 GROUND DEFORMATION IN BARRIO NARVACAN, SANTO TOMAS

A small village, named Barrio Narvacan, is located at the tip of a sand spit to the southwest of Santo Tomas. Large scale subsidence and lateral displacements caused by the liquefaction occurred in Barrio Narvacan (Figure 3, Photos 41 to 44). This is a fishing village with a population of about 1,000 consisting of 360 families and about 150 houses. The following paragraph is a summary of an account given by the 50-year old village head, Mr. Federico Ramirez:

This village was developed by people who migrated from Narvacan in Ilocos Sur Province about 100 years ago. Most houses are made of wood with high floors, and only a few houses are of concrete blocks. In addition to houses, there was a church and a school which were also wooden buildings. The earthquake struck at low tide. The ground motion during the earthquake was very severe. Vertical motion was followed by horizontal motion which continued for about 50 seconds. When he left the house, hot water was boiling up everywhere in the village. The boiled sand was black in color and contained oil. There is an oil reservoir in the area, which was known because trial boreholes had been drilled. Oil, however, had never risen to the surface before the earthquake. The ground became covered with water 5 minutes later, so the duration of the sand boiling is not known. Water spouts were also seen in the sea. Everyone felt that the ground sank gradually after the earthquake. It sank quickly by about 1 meter at first, and after that it sank more slowly. This continued for about 30 minutes. Finally, the water rose to chest level. The submerged area is about 400 x 200 meters, and it subsided by 3 meters at maximum. A 24-year old woman was killed under a fallen roof. Villagers spent several days on boats and then moved to temporary houses on the opposite shore on the main island or to higher ground. The area had been nearly level before the earthquake. The surface soil in the western part of the area consists of slightly hard sandy soil, but in the eastern part, where sand boils and subsidence occurred,

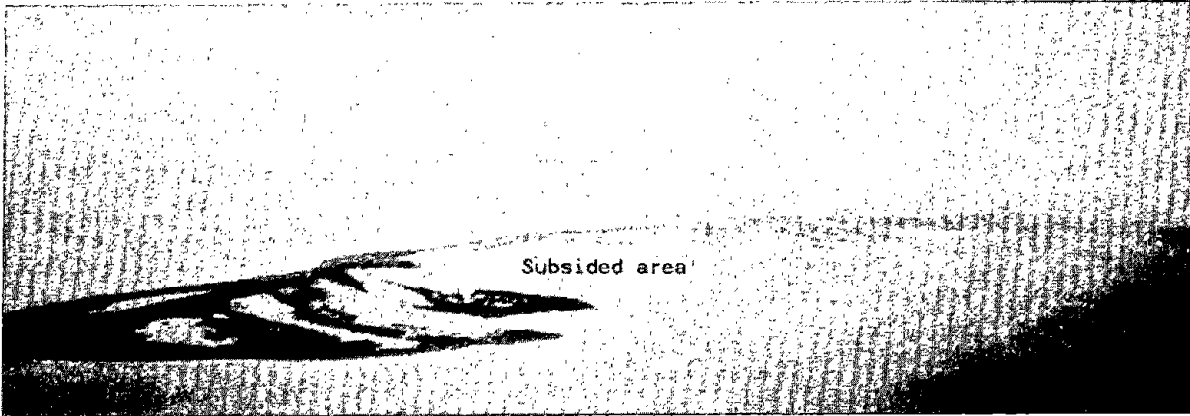


Photo 41. Barrio Narvacan was submerged. Water reaches eaves height at high tide. (Courtesy of Dr. M. Hamada.)



Photo 42. Damage in Barrio Narvacan. Land re-appears at low tide in some places. Sand and water boiled up everywhere during the earthquake, and the village gradually sank under the sea.



Photo 43. Damage in Barrio Narvacan. Traces of water at high tide are seen on the eaves. (Courtesy of Dr. M. Hakuno).



Photo 44. Well settled due to liquefaction. Sand nearby is thought to have boiled out. (Courtesy of Dr. M. Hakuno).

it is soft silty soil. The eastern area expanded by about 10 meters toward the mainland as a result of the earthquake.

Photos 43 and 44 show the village at low tide. There were sea walls protected by boulders on the shore to the south of the village facing the main island, and these slipped and sank due to liquefaction. Figure 28 shows the records of SWS testings conducted by the authors at two sites in the village. The soil to a depth of 2.3 to 3.5 m below the surface is a loose deposit (N_{sw} is less than 60), with an estimated SPT-value of about 10.

Based on these observations, it can be seen that subsidence and lateral displacement occurred due to liquefaction in the eastern part of the area, resulting in the village sinking under the sea. The lack of shore-protection or dikes is possibly one reason for this, for it allowed horizontal displacements of the order of 10 m. Similar submergence of small villages has also been observed in Alaska and Rawis (see Figure 3 for locations).

10.0 CONCLUSION

A summary of the principal characteristics of soil liquefaction, large ground deformation, resulting damage, and subsurface conditions associated with the 1990 Luzon, Philippines earthquake is given below:

- (1) Liquefaction-induced ground failures developed in many locations within a zone 216 km long and 100 km wide on the Central Plain of Luzon Island during the earthquake of July 16, 1990. The zone extended from Manila to the coast of the Lingayen Gulf.
- (2) The most damaging type of ground failure resulting from liquefaction was loss of bearing capacity and lateral spreading. The landforms found to be most vulnerable to these types of failure were recent alluvial deposits along rivers and beaches and loose sand fills. Major damage included destruction of bridges, buildings, roadways, and the river banks and submergence of a village near the shore.
- (3) Dagupan City suffered its most serious damage to public infrastructure and private property due to liquefaction. Major damage to the structures included destruction of bridges, buildings, houses, pavements, and pipelines in riverside areas of the city.
- (4) Based on the results of post-earthquake ground investigations, including 21 SPT borehole logs and 12 SWS testings, the relationship between the liquefaction-induced damage and ground conditions in Dagupan City can be summarized as follows:
 - Damage to ground and structures in Dagupan City was mainly caused by liquefaction and lateral spreading of the loose, fine sand deposits underlying the areas near the Pantal River.
 - Liquefaction effects were observed in areas where the estimated liquefied layer was between 5 and 10 m thick and was overlaid by more than 3 m of non-liquefied material. On the contrary, liquefaction effects were not manifested in areas where the estimated liquefied layer was less than 3 m thick and was overlaid by a non-liquefied surface layer more than 3 m thick.
 - Lands reclaimed from fishponds about 40 years ago were included in the areas where damage due to liquefaction was significant. In these areas, the liquefaction of loose sand fill overlaying the natural sand deposits accelerated damage to structures.

- Lateral spreading occurred in zones along the Pantal River and abandoned meanders. The displacements were estimated to be as large as several meters and oriented perpendicular to the adjacent river.
- (5) In the coastal areas along the Lingayen Gulf, large scale subsidence and lateral spreading accompanied liquefaction. At least three small villages subsided by 0.5 to 3 m below the high-tide mark.

REFERENCES

- 1) Abe, K. and Yoshida, N., "Mechanism of the Luzon Earthquake of July 16, 1990," Programme and Abstracts, Meeting of the Seismological Society of Japan, No. 2, Hokkaido, 1990, p.63.
- 2) Punongbayan, R.S. and Torres, R.C., "Correlation of River Channel Reclamation and Liquefaction Damage of the 16 July 1990 Luzon Earthquake in Dagupan City, Philippines," Final Report of the Training Course in Japan, 1990, for the First Phase of the Training Program on Earthquake Engineering and Disaster Management for Establishing Building Administration System in Philippines, October 7 to December 7, Nagoya, Japan, United Nations Center for Regional Development, 1991 (in press).
- 3) Sato, T., "Damage in Cabanatuan - Estimation of Peak Acceleration, Preliminary Report on the Philippine Earthquake of July 16, 1990," Japan Society of Civil Engineers, Tokyo, Japan, October, 1990, pp.6-7 (in Japanese).
- 4) Japan Society of Civil Engineering, "Preliminary Report of Japan Society of Civil Engineers Reconnaissance Team on July 16, 1990 Luzon Earthquake," 1990.
- 5) Architectural Institute of Japan Reconnaissance Team, "Preliminary Report on the Philippines Earthquake," Architectural Institute of Japan, Tokyo, Japan, 1990, p.56 (in Japanese).
- 6) EQE Engineering, "The July 16, Philippines Earthquake, Preliminary Report," San Francisco, U.S.A., 1990, p.47.
- 7) Kiso Jiban Consultants Co., Ltd., "Report on the July 16, 1990 Luzon Earthquake," Tokyo, Japan, 1990, p.87 (in Japanese).
- 8) Sato, T., Private communication, Disaster Prevention Research Institute, Kyoto University.
- 9) Tokimatsu, K., Midorikawa, S., Tamura, S., Kuwayama, K. and Abe, A., "Preliminary Report on the Geotechnical Aspects of the Philippine Earthquake of July 16, 1990," Proceedings, 2nd Int. Conf. on Recent Advances in Geotechnical Earthquake Engineering and Soil Dynamics, St. Louis, Vol. II, 1991, pp.1693-1700.

B29
9

- 10) Wieczorek, G.F., Arbolera, R., and Tubianosa, B., "Liquefaction and Landsliding from the July 16, 1990 Luzon, Philippines Earthquake," Technical Report NCEER-91-0001, Proceedings of the Third Japan-U.S. Workshop on Earthquake Resistant Design of Lifeline Facilities and Countermeasures for Soil Liquefaction, 1991, pp.39-66.
- 11) Miwa, S., Private communication, Tobishima Corporation, Tokyo, Japan.
- 12) Iemura, H., "Summary of the Damage to Bridges Caused by the July 16, 1990 Luzon, Philippines Earthquake," Preliminary Report on the Philippine Earthquake of July 16, 1990, Japan Society of Civil Engineers, October, 1990, pp.18-19 (in Japanese).
- 13) Japan Road Association, "Specifications for Highway Bridges," Part V Earthquake Resistant Design, 1991 (in Japanese).
- 14) Ishihara, K., "Stability of Natural Deposits during Earthquakes," Proceedings, 11th International Conference on Soil Mechanics and Foundation Engineering, San Francisco, Vol.1, 1985, pp.321-376.
- 15) Hamada, M., Yasuda, S., Isoyama, R., and Emoto, K., "Study on Liquefaction-induced Permanent Ground Displacements," Association for The Development of Earthquake Prediction, Tokyo, Japan, 1986.
- 16) Hamada, M., "Large Ground Deformations and Their Effects on Lifelines - The 1964 Niigata Earthquake," This volume.
- 17) Hamada, M., Yasuda, S., and Wakamatsu, K., "Large Ground Deformations and Their Effects on Lifelines - The 1948 Fukui Earthquake," This volume.
- 18) Hamada, M., Wakamatsu, K., and Yasuda, S., "Liquefaction-induced Ground Deformation during the 1923 Kanto Earthquake," This volume.
- 19) Seed, H.B., Tokimatsu, K., Harder, L.F. and Chung, R.M., "Influence of SPT Procedure in Soil Liquefaction Resistance Evaluation," Journal of Geotechnical Engineering, Vol. 111, No. 12, ASCE, New York, N.Y., 1985, pp.1425-1435.